

EVALUATION OF A NOVEL DESIGN OF MASONRY STRUCTURES SUBJECT  
TO GROUND MOVEMENT

by

Sharief Ramsis Nasief Mansour  
B.Sc.(Eng.), M.Sc., DIC

A Thesis submitted for the degree of  
Doctor of Philosophy of the University of London

Department of Civil Engineering  
Imperial College of Science & Technology  
London SW7 2BU  
August 1988

## ABSTRACT

This thesis describes theoretical and experimental work undertaken to study the behaviour of simple masonry structures subjected to ground movement. Five structures were tested, each comprising an articulated reinforced concrete ring beam, supporting a masonry core wall, 2250x1828 mm in plan and up to 1828 mm high. The structures were designed in accordance with a novel procedure known as the "Four-Point-Support-System" (FPSS).

Most, if not all, of existing design concepts, require special treatment of both the foundations and the structures; the FPSS however, uses traditional inexpensive design methodology so as to tolerate some differential movement, while also, permitting repairs to be effected before the structure becomes unserviceable. Differential movement was induced using a settlement simulation test rig, so as to determine the deformation response and the degree of damage of the FPSS. Results are compared to the allowable deflection limits described in the literature and recommended by previous research. The deformation pattern was measured in both inplane and out-of-plane directions, while the wall strain distribution was monitored using a specially developed electronic Demec gauge. A load cell and jacking system were used to simulate progressive ground movement, and a load control phase was employed to restore the deformed structure.

Test results are presented in the form of load-deflection relationships, out-of-plane deformation and rotation of supports, influence of the aspect ratio of the walls and articulation of the ring beam. The effect of cyclic settlement and restoration on the structural response was also monitored with respect to the degree of degradation of structural stiffness. Strain contours of the walls, in addition to monitoring the damage pattern, were used to define the level of cracking of the FPSS.

Theoretical modelling of the FPSS, using the finite element method, is used to analyse the structural response in both the elastic state and at the post-cracking range, and for comparison with experimental behaviour. Additionally, most pertinent to warping and torsional behaviour of the box core structure, a 3-dimensional elastic model was introduced.

The test results are considered sufficiently promising to warrant the undertaking of full-scale prototype tests of low-rise structures. Finally, assessment of the FPSS is carried out to determine preliminary design formula for the limiting deformation as an interim design guideline for flexible structures subject to differential ground movement.

To my Mother and Father

The Lord is my strength and my shield.

Psalm 28:7



## ACKNOWLEDGEMENTS

This work was conducted in the Concrete Structures Section of the Department of Civil Engineering of Imperial College. It gives me pleasure to express my profound indebtedness to my supervisor Professor S.H. Perry, for all his advice; his friendship and constant encouragement throughout my study, involving a large portion of his leisure time, has been of great value and unforgotten appreciation. I wish to express my sincere gratitude to Professor J.B. Burland for his generous assistance, careful and close guidance throughout the work undertaken in this project, and for helping me to have a better understanding of the structure and the soil. My thanks go also to the Head of Concrete Section, Dr. J.B. Newman, for his valuable comments.

Financial support was provided by a grant from the R.E.Co.(Sudan), B.A.C. Scholarship and the ORS Awards Scheme for Overseas Research Students; all are gratefully acknowledged.

I also wish to thank Mr. D. Hitchings for his inestimable assistance during the development of the finite element package, Dr. M.D. Kotsovos for his advice and consistent help on the non-linear program, Campbell Middleton and Angus Low of Ove Arup and Partners for their assistance during the development of the theoretical model and Andy Pullen for help in the design of the electronic circuits. I also wish to express my gratitude and appreciation for the vehement help offered by the members of the Concrete Laboratories under the direction of Mr. P. Jellis, in particular, Tony Boxall, Les Clark for the test rig fabrication, Robby Wilson, Andrew Hearnshaw for the preparation of the test models, and Jeff Mires for the help during testing. I wish also to thank my fellow colleagues, especially, Peter Bischoff, Zaki El-Hassan and John Holmyard for the useful advice and discussions.

Lastly, but in no way least, I am deeply thankful to Christine, whose understanding, encouragement and care have helped in so many ways in getting this research through. I would like also to express my sincere thanks to my parents, Ramsis and Ragaa, for having been the inexhaustible source of support and inspiration in all aspects of my life and without whom I would not have reached this stage in life.

## TABLE OF CONTENTS

TITLE PAGE	1
ABSTRACT	2
DEDICATIONS	3
ACKNOWLEDGEMENTS	5
TABLE OF CONTENTS	6
LIST OF FIGURES	11
LIST OF TABLES	18
PRINCIPAL NOTATIONS	20
ABBREVIATIONS	23
UNITS OF MEASUREMENT	23
<b>CHAPTER 1 INTRODUCTION</b>	<b>24</b>
1.1 THE PROBLEM OF GROUND MOVEMENT AND ASSOCIATED DAMAGE	24
1.2 THE PROBLEM OF DESIGN ON MOVING GROUND	25
1.3 THE PRESENT RESEARCH	26
<b>CHAPTER 2 GENERAL BACKGROUND TO THE PROBLEM OF GROUND MOVEMENT AND STRUCTURES</b>	<b>30</b>
2.1 INTRODUCTION	30
2.2 FORMS OF GROUND MOVEMENT	30
2.2.1 Edge deformation	31
2.2.2 Centre deformation	32
2.3 FORMS OF STRUCTURAL MOVEMENT	33
2.3.1 Hogging mode	33
2.3.2 Sagging mode	33
2.3.3 Large-differential vertical mode	34
2.3.4 Horizontal mode	34
2.4 FORMS OF STRUCTURAL DAMAGE	35
2.5 STRUCTURAL DESIGN AND SOIL STRUCTURE INTERACTION	36
2.6 BASIS OF DESIGN EVALUATION	38
2.7 BASIS OF STRUCTURAL DESIGN	40
2.7.1 Importance of the structure	40
2.7.2 Economic considerations	40
2.7.3 Subjective criteria	40
2.8 STRUCTURAL DESIGN IN AREAS OF GROUND MOVEMENT	42
2.9 REVIEW OF PREVIOUS DESIGNS	45
2.9.1 Separate rooms or blocks	45
2.9.2 Prefabricated panels on flexible frame	46
2.9.3 Flexible building material	47
2.9.4 Open joint or split design	47
2.9.5 Soil contact	48
2.9.6 Rigid box system	49
2.9.7 Stiff structures	49
<b>CHAPTER 3 ASSESSMENT OF DAMAGE CRITERIA FOR STRUCTURES SUBJECT TO GROUND MOVEMENT</b>	<b>55</b>
3.1 INTRODUCTION	55
3.2 CLASSIFICATION OF DAMAGE DEPENDING UPON THE EXTENT OF BUILDING DEFORMATION	56
3.3 CLASSIFICATION OF DAMAGE DEPENDING UPON THE OVERALL STRUCTURAL BEHAVIOUR	57
3.4 REVIEW OF DAMAGE CRITERIA	59
3.4.1 Empirical methods	60

	Terzaghi (1935)	60
	Short and Simms (1949)	61
	Rigby and DeKema (1952)	61
	Capper (1953)	61
	Meyerhof (1953)	61
	Rausch (1955)	62
	Skempton and MacDonald (1956)	63
	Polshin and Tokar (1957)	65
	Bjerrum (1963)	66
	Mayer and Rusch (1967)	68
	Centre Scientifique et Technique de la Construction (CSTC) (1967)	69
	Building Research Advisory Board (BRAB) (1968)	71
	Pfeffermann (1968)	71
	Horn and Lambe (1964)	72
	Comite Europeen du Beton (CEB) (1973)	72
	Grant, Christian and Vanmarcke (1974)	73
	Walsh (1975,1978) and Holland (1981)	73
	Starzweski (1974)	73
	Leonards (1975)	74
	Bally (1975)	75
	O'Rourke, Cording and Boscardin (1976)	75
	Post Tensioning Institute (PTI) (1978) and Wray (1978)	76
	Alexander and Lawson (1981)	76
	Yokel, Salomone and Gray (1982)	77
3.4.2	Theoretical methods	78
	Rosenhaupt (1964)	78
	National Coal Board (NCB) (1975)	79
	Burland and Wroth (1974)	81
	MacLeod and Abu-El-Magd (1980)	84
	Hooper (1982) and Driscoll (1985,1986)	85
3.5	COMPARISON OF CRITERIA OF DAMAGE	86
3.5.1	Correlation between damage and structure deformation	87
3.5.2	Parameters affecting damage criteria	93
3.5.3	Basis of criteria for the onset of damage	95
3.6	OUT-OF-PLANE SERVICEABILITY LIMIT	99
3.6.1	Boundary conditions of walls	100
3.6.2	Geometry of walls	101
3.6.3	Limiting serviceability criteria	102
	<b>CHAPTER 4 REVIEW OF DESIGNS FOR ACCOMMODATING GROUND MOVEMENT AND METHODS OF REPAIR</b>	<b>104</b>
4.1	INTRODUCTION	104
4.2	DESIGN BY PARTIAL PROTECTION	105
4.3	DESIGN BY PERMITTING MOVEMENT	106
4.3.1	Design based on energy absorption devices	108
4.3.2	Design based on occurrence of permanent deformation	111
4.4	METHODS OF REPAIR FOR STRUCTURES IN AREAS OF GROUND MOVEMENT	112
4.5	TECHNIQUES FOR REINSTATEMENT OF STRUCTURES	114
4.5.1	Method of injection of cement grout	116
4.5.2	Underpinning	117
4.5.3	Jacking method	118
4.5.4	Heave recovery by watering	120
	<b>CHAPTER 5 DESCRIPTION OF A NOVEL DESIGN METHOD — THE FOUR-POINT-SUPPORT-SYSTEM</b>	<b>121</b>
5.1	INTRODUCTION	121

5.2	FLEXIBLE STRUCTURAL SYSTEM	121
5.3	STRUCTURAL FORM OF THE FPSS	124
	5.3.1 Slab or articulated ring beam	125
	5.3.2 Walls	127
	5.3.3 Repairability measures	129
	5.3.4 Roof structure	130
5.4	MODELLING OF THE FPSS	131
<b>CHAPTER 6 DESCRIPTION OF TEST RIG, FABRICATION AND TESTING OF MODELS</b>		<b>133</b>
6.1	INTRODUCTION	133
6.2	EXPERIMENTAL PROGRAMME	135
6.3	TEST MODELS	135
	6.3.1 Choice of model	135
	6.3.2 Geometry	138
6.4	MATERIALS	141
	6.4.1 Reinforcement steel	141
	6.4.2 Concrete	141
	6.4.3 Bricks	142
	6.4.4 Mortar	143
6.5	MATERIAL QUALITY CONTROL	144
	6.5.1 Concrete	144
	6.5.2 Brickwork	146
	6.5.3 Assessment of moduli of elasticity and rupture for brickwork	146
6.6	EXPERIMENTAL EQUIPMENT AND SET-UP	149
	6.6.1 Test rig	149
	6.6.2 Load arrangement	149
	6.6.3 Support system	153
	6.6.4 Jacking and load cell system	156
	6.6.5 Concrete and steel strain measurements	158
	6.6.6 Brickwork-wall strain measurement	159
	6.6.7 Deflection measurements during settlement	164
	6.6.8 Data logging and data retrieval systems	165
6.7	TESTING PROCEDURE	166
6.8	PROBLEMS ENCOUNTERED DURING TESTING	169
<b>CHAPTER 7 THEORETICAL BACKGROUND AND MATHEMATICAL MODELLING</b>		<b>172</b>
7.1	INTRODUCTION	172
7.2	BEAMS ON ELASTIC FOUNDATIONS	172
	7.2.1 Winkler model using matrices	172
	7.2.2 Winkler model using numerical methods	175
7.3	FRAME ANALYSIS OF STRUCTURES	176
	7.3.1 Conventional techniques	176
	7.3.2 Stiffness matrix technique	178
7.4	FINITE ELEMENT ANALYSIS METHOD	180
7.5	SLABS ON ELASTIC GROUND METHOD	180
7.6	MODELLING OF THE FPSS - ELASTIC MODEL	184
7.7	MODELLING OF THE FPSS - FINITE ELEMENT MODEL	189
	7.7.1 Three dimensional linear analysis of FPSS	190
	7.7.2 Linear stress distribution of the FPSS	193
	7.7.3 Review of the biaxial failure envelop of brickwork masonry	199
	7.7.4 Two dimensional finite element non-linear analysis of masonry walls of FPSS	200
	7.7.5 Comparison of the biaxial failure envelopes of brickwork and concrete	201

7.7.6	Representation of boundary conditions of FPSS	204
7.7.7	Non-linear stress distribution of the FPSS	205
7.8	THEORETICAL MODELLING OF THE FPSS	215
7.8.1	Introduction	215
7.8.2	Non-uniform torsion and warping	216
7.8.3	Stiffness matrix of a thin walled beam element subjected to non-uniform torsion	219
7.8.4	Theoretical investigation of the deformation response of the FPSS	220
	<b>CHAPTER 8 EXPERIMENTAL OBSERVATIONS AND TEST RESULTS</b>	<b>224</b>
8.1	INTRODUCTION	224
8.2	DISTRIBUTION OF STRAIN IN THE RING BEAM STEEL	224
8.3	DEFLECTIONS	227
8.3.1	Wall-beam structure	227
8.3.2	Core wall Deflection	234
8.3.3	Out-of-plane warping and lateral distortion of walls	244
8.3.4	Angular rotation and tilt of ring beam	245
8.4	WALL STRAIN	252
8.4.1	Vertical strain distribution	252
8.4.2	Horizontal strain distribution	253
8.4.3	Principal strain distribution	254
8.5	DAMAGE CAUSED DURING TESTING	257
8.6	PHOTOGRAPHS OF WALLS	279
	<b>CHAPTER 9 GENERAL DISCUSSION AND ASSESSMENT OF THE FOUR-POINT-SUPPORT-SYSTEM</b>	<b>283</b>
9.1	INTRODUCTION	283
9.2	STRUCTURAL BEHAVIOUR OF FPSS	283
9.2.1	Differential movement of supports	283
9.2.2	Deformation of walls	284
9.3	CYCLIC BEHAVIOUR OF FPSS	285
9.4	STRUCTURE DETERIORATION AND STIFFNESS DEGRADATION	288
9.5	REINSTATEMENT OF THE STRUCTURE	292
9.6	COMPARISON OF EXPERIMENTAL RESULTS WITH PREDICTIONS OF THEORETICAL MODELS	294
9.7	LIMITING DEFORMATION OF THE FPSS	299
9.8	INTERIM GUIDANCE FOR DESIGN OF FPSS	301
9.8.1	Allowable deflection ratio	301
9.8.2	Reinstatement of the structure	304
9.8.3	Ring beam	305
	<b>CHAPTER 10 CONCLUSIONS AND RECOMMENDATIONS FOR FUTURE WORK</b>	<b>308</b>
10.1	CONCLUSIONS	308
10.1.1	Review of literature of design of structures	308
10.1.2	Present investigation	309
10.2	RECOMMENDATIONS FOR FUTURE RESEARCH	313
	<b>REFERENCES</b>	<b>315</b>
	<b>APPENDIX 1 TERMINOLOGY FOR THE DEFORMATION OF STRUCTURES UNDER SETTLEMENT</b>	<b>331</b>
	<b>APPENDIX 2 DESIGN OF FPSS MODELS</b>	<b>333</b>
	<b>APPENDIX 3 IN-HOUSE DEVELOPMENT OF ELECTRONIC DEMEC GAUGE</b>	<b>336</b>

APPENDIX 4	THEORETICAL INVESTIGATION OF THE MAXIMUM VERTICAL DEFLECTION OF THE FPSS	338
APPENDIX 5	WALL STRAIN CONTOURS	341
APPENDIX 6	EXPERIMENTAL RESULTS AND DATA	342

## LIST OF FIGURES

2.1	Edge deformation caused by movement of expansive soils (adapted after Holland,1981).	31
2.2	Edge deformation caused by movement due to ground subsidence (adapted after Lacey and Swain,1957).	32
2.3	Centre deformation caused by movement of expansive soils (adapted after Holland, Pitt and Lawrance,1980).	32
2.4	Centre deformation caused by ground subsidence.	32
2.5	Form of damage due to hogging mode of ground deformation (after BRE,1981).	33
2.6	Form of damage due to sagging mode of deformation (after BRE,1981).	34
2.7	Form of damage due to vertical ground subsidence (after Barber,1969).	35
2.8	Form of damage due to horizontal straining of the ground.	35
2.9	Damage evaluation of structures subject to differential movement (adapted after Chan <u>et al.</u> ,1979).	39
2.10	Use of flexible panels and frames to accommodate ground movement.	46
2.11	Location of joints in split design of Masonry Buildings (after Webb,1969).	47
2.12	Structure separator used to reduce the effect of ground movement by cushioning on a layer of gravel (after Agib,1983).	49
2.13	Stiff design to prevent differential movement of structures (adapted after Carrillo-Gil,1980 ; Agib,1983 ; Jones,1985).	50
2.14	Typical design of raft slabs (after Tomlinson, Driscoll and Burland,1978).	51
2.15	Critical design parameters of slab-on-ground (after Holland,1981).	52
2.16	Design detail of piles (after BRE,1980 ; Webb,1969).	54
3.1	Distortion of wall with openings under sagging (after Rausch,1955).	62
3.2	Defintions of building settlement with and without tilt (adapted after Skempton and MacDonald,1956).	64
3.3	Relation between relative deflection of brickwalls and aspect ratio of walls (after Polshin and Tokar,1957).	66
3.4	Limiting deformation of partition walls (after Mayer and Rusch,1967).	69
3.5	Application of radius of curvature of the ground profile to define relative strain in buildings.	80
3.6	Idealization of a building as a rectangular beam (adapted after Burland and Wroth,1974).	82
3.7	Types of building deformation caused by settlement.	87
3.8	Types of deformation of separate footing foundations.	91
3.9	Comparison of criteria of damage for inplane deformation of buildings.	92
3.10	Relationship between the ratio of cracking strength to ultimate strength and the wall return ratio (adapted after Anderson,1985).	101
3.11	Variation of lateral pressure with respect to aspect ratio of masonry walls.	102
3.12	Comparison of criteria of damage for lateral deformation of masonry walls.	103
4.1	Design of structures by partial protection against ground movement.	106

4.2	Limiting differential settlement by load control devices (after Clark <u>et al.</u> ,1973).	109
4.3	Energy absorption device to allow sway of building frames (after Anagnostides, Hagreaves and Wyatt,1988).	110
4.4	Effect of embedded springs on the bracings of building frames subject to a subsidence wave (after Lacey and Swain,1957 ; Heathcote,1965).	111
4.5	Design by permitting movement with no induced secondary stresses.	112
4.6	Grouting of foundations to compensate settlement of structures (after Tomlinson,1984).	116
4.7	Levelling of structures by underpinning techniques (after Tomlinson,1984).	117
4.8	Levelling of structures using jacking techniques (after Tomlinson,1984).	119
5.1	Deformation of an open box structure subject to lateral or longitudinal load and displacement.	122
5.2	Deformation of FPSS walls at three horizontal sections shown in Figure 5.1(b) (Deflection is exaggerated for clarity).	123
5.3	Three- and four-point-support-systems.	124
5.4	Problems arising from excessive tilting of buildings (after Attewel <u>et al.</u> ,1986).	125
5.5	Deformed shape of walls and suspended slab of the four-point-support-system (FPSS).	126
5.6	Effect of tilt of the supports on the total settlement of the FPSS.	127
5.7	Effect of cross walls in increasing deformability of the FPSS.	127
5.8	Warping of walls of the FPSS (in plan view) due to shortening and lengthening of diagonals $D_2$ and $D_1$ , respectively.	128
5.9	Equilibrium of end forces at the settling wall corner B-B'.	129
5.10	Detail of sliding roof to accommodate vertical and transverse movement.	131
6.1	General arrangement of FPSS walls.	139
6.2	General arrangement of reinforcement for FPSS ring beam.	140
6.3	Typical stress-strain relationship for reinforcement bars.	142
6.4	Formwork of FPSS ring beam.	145
6.5	Typical compressive test for brickwork prisms.	147
6.6	Stress-strain relationship of brickwork prisms for each model.	147
6.7	Typical testing of brickwork wallets in indirect tension.	148
6.8	Test rig arrangement for the short and high walls.	150
6.9(a)	General layout of test rig.	151
6.9(b)	Plan of test rig at various levels.	152
6.10	Superimposed loading on top of the walls.	153
6.11	General arrangement of support system.	154
6.12	General arrangement of scaffolding platforms.	155
6.13	Jack and load cell arrangement.	156
6.14	Calibration of jacking system.	158
6.15	Calibration of load cell.	158
6.16	Electronic Demec gauge.	161
6.17	Calibration of electronic Demec gauge.	161
6.18	Logic circuit of electronic Demec gauge.	162
6.19	Position of strain rosettes in the wall.	163
6.20	Vertical and horizontal measurements of wall deflections of two L-shaped wall tests.	164
7.1	Interactive response of ground and structure based on a Winkler ground model.	173



7.2	Simulation of ground deformation in frameless buildings using vertical and horizontal springs (after Kleipkov <u>et al.</u> ,1980).	174
7.3	Simulation of ground deformation in 3-dimensions using vertical and lateral springs (after Klepivov <u>et al.</u> ,1980).	175
7.4	Deformation of a frame structure on flexible subgrade (after Lee and Harrison,1970).	177
7.5	Rotation of semi-rigid frames due to settlement beneath a single footing.	178
7.6	Settlement of a multi-bay multi-storey structure with single footing foundation (after Attewel <u>et al.</u> ,1986).	178
7.7	General ground mounds (after Lytton and Woodburn,1973).	181
7.8	Loading condition of a slab on a subgrade of deformable soil.	182
7.9	Wall C or D subject to system of edge moments.	185
7.10	Representation of edge reactions on wall C or D by an equivalent system of forces applied at the corners.	186
7.11	Deformation pattern of main walls A or B on settlement of the FPSS.	187
7.12	Representation of an equivalent system of edge moments applied on wall A or B.	188
7.13	Finite element mesh of the FPSS.	190
7.14	Representation of FPSS as 4-quarter finite element meshes.	192
7.15	Stress distribution along the top horizontal section of main walls.	195
7.16	Stress distribution along middle height of the horizontal section of main walls.	195
7.17	Stress distribution along the soffit horizontal section of main walls.	196
7.18	Stress distribution at vertical section of main walls at the settling corner.	196
7.19	Stress distribution at vertical section of main walls at the fixed corner.	197
7.20	Stress distribution at vertical section of adjacent walls at an opposite corner to the settling one.	197
7.21	Stress distribution along the top horizontal section of adjacent walls.	198
7.22	Stress distribution along middle height of the horizontal section of adjacent walls.	198
7.23	Biaxial envelop for concrete and brickwork under compression-compression stresses (adapted after Kotsovos,1979).	203
7.24	Biaxial envelop for concrete and brickwork under compression-tension stresses (adapted after Kotsovos,1979).	203
7.25	Biaxial envelop for concrete and brickwork under tension-tension stresses (adapted after Kotsovos,1979).	203
7.26	Cases of loading of main walls of FPSS subject to settlement.	207
7.27	Stages of loading of main walls of FPSS subject to load case(1).	208
7.28	Stages of loading of main walls of FPSS subject to load case(2).	209
7.29	Stages of loading of main walls of FPSS subject to load case(3).	211
7.30(a)	Variation of deflection ratio with relative stiffness of the FPSS - Load case(1).	212
7.30(b)	Variation of deflection ratio with relative stiffness of the FPSS - Load case(2).	212
7.30(c)	Variation of deflection ratio with relative stiffness of the FPSS - Load case(3).	213
7.31(a)	Variation of maximum induced stress with relative stiffness of the FPSS - Load case(1).	213
7.31(b)	Variation of maximum induced stress with relative stiffness of the FPSS - Load case(2).	213
7.31(c)	Variation of maximum induced stress with relative stiffness	

of the FPSS - Load case(3).	214
7.32(a) Variation of maximum induced strain with relative stiffness of the FPSS - Load case(1).	214
7.32(b) Variation of maximum induced strain with relative stiffness of the FPSS - Load case(2).	214
7.32(c) Variation of maximum induced strain with relative stiffness of the FPSS - Load case(3).	215
7.33 A closed section box (a), with an elemental section (b).	216
7.34 A differential element represented as a thin plate (after Mallick and Dungar,1977).	217
7.35 A closed section beam element subjected to two degrees of freedom at each node (after Mallick and Dungar,1977).	219
7.36 Representation of a system of body forces simulating settlement of the FPSS.	221
8.1 Effect of cyclic settlement on steel strain of ring beam (Test W1A).	228
8.2 Effect of cyclic settlement on steel strain of ring beam (Test W1B).	228
8.3 Effect of cyclic settlement on steel strain of ring beam (Test W2A).	229
8.4 Effect of cyclic settlement on steel strain of ring beam (Test W2B).	229
8.5 Effect of cyclic settlement on steel strain of ring beam (Test W3A).	230
8.6 Effect of cyclic settlement on steel strain of ring beam (Test W3B).	230
8.7 Effect of cyclic settlement on steel strain of ring beam (Test W4A).	231
8.8 Effect of cyclic settlement on steel strain of ring beam (Test W4B).	231
8.9 Effect of cyclic settlement on steel strain of ring beam (Test W5A).	232
8.10 Effect of cyclic settlement on steel strain of ring beam (Test W5B).	232
8.11 Relation between reduction in support load and corner deflection (Test W1A).	235
8.12 Relation between reduction in support load and corner deflection (Test W1B).	235
8.13 Relation between reduction in support load and corner deflection (Test W2A).	235
8.14 Relation between reduction in support load and corner deflection (Test W2B).	236
8.15 Relation between reduction in support load and corner deflection (Test W3A).	236
8.16 Relation between reduction in support load and corner deflection (Test W3B).	236
8.17 Relation between reduction in support load and corner deflection (Test W4A).	237
8.18 Relation between reduction in support load and corner deflection (Test W4B).	237
8.19 Relation between reduction in support load and corner deflection (Test W5A).	237
8.20 Relation between reduction in support load and corner deflection (Test W5B).	238
8.21 Effect of cyclic settlement on the vertical deformation of the wall (Test W2A).	239
8.22 Effect of cyclic settlement on the vertical deformation of the wall (Test W3A).	240

8.23	Effect of cyclic settlement on the vertical deformation of the wall (Test W3B).	241
8.24	Effect of cyclic settlement on the vertical deformation of the wall (Test W4A).	242
8.25	Effect of cyclic settlement on the vertical deformation of the wall (Test W5B).	243
8.26	Effect of cyclic settlement on the lateral distortion of the wall (Test W1).	246
8.27	Effect of cyclic settlement on the lateral distortion of the wall (Test W2).	246
8.28	Effect of cyclic settlement on the lateral distortion of the wall (Test W3).	247
8.29	Effect of cyclic settlement on the lateral distortion of the wall (Test W4).	247
8.30	Effect of cyclic settlement on the lateral distortion of the wall (Test W5).	248
8.31	Effect of cyclic settlement on the out-of-plane warping of the wall (Test W1).	248
8.32	Effect of cyclic settlement on the out-of-plane warping of the wall (Test W2).	248
8.33	Effect of cyclic settlement on the out-of-plane warping of the wall (Test W3).	249
8.34	Effect of cyclic settlement on the out-of-plane warping of the wall (Test W4).	249
8.35	Effect of cyclic settlement on the out-of-plane warping of the wall (Test W5).	249
8.36	Effect of cyclic settlement on angular rotation of ring beam (Test W3).	250
8.37	Effect of cyclic settlement on angular rotation of ring beam (Test W4).	251
8.38	Effect of cyclic settlement on angular rotation of ring beam (Test W5).	251
8.39	Position of neutral axis before and after settlement.	254
8.40	Maximum principal strain distribution of wall (Test W1AA).	258
8.41	Maximum principal strain distribution of wall (Test W1AB).	259
8.42	Maximum principal strain distribution of wall (Test W3AA).	260
8.43	Maximum principal strain distribution of wall (Test W4AB).	261
8.44	Maximum principal strain distribution of wall (Test W5AA).	263
8.45	Distribution of maximum and minimum principal strain (Test W1AA).	266
8.46	Distribution of maximum and minimum principal strain (Test W1AB).	267
8.47	Distribution of maximum and minimum principal strain (Test W3AA).	268
8.48	Distribution of maximum and minimum principal strain (Test W3BA).	269
8.49	Distribution of maximum and minimum principal strain (Test W4BA).	270
8.50	Distribution of maximum and minimum principal strain (Test W5AA).	272
8.51	Distribution of maximum and minimum principal strain (Test W5BB).	273
8.52	Crack propagation during settlement (Test W1).	276
8.53	Crack propagation during settlement (Test W2).	276

8.54	Crack propagation during settlement (Test W3).	277
8.55	Crack propagation during settlement (Test W4).	277
8.56	Crack propagation during settlement (Test W5).	278
8.57	Diagonal cracking of FPSS wall after settlement (Test W1).	280
8.58	Vertical cracking along edge of wall (Test W2).	280
8.59	Repairs of vertical crack (Test W2).	280
8.60	Rotation of point support on settlement (Test W3).	281
8.61	Tilting of settling support due to rotation of ball joint (Test W3).	281
8.62	Vertical splitting crack along edge of adjacent wall (Test W4).	281
8.63	Vertical edge crack at the intersection of main and adjacent walls (Test W4).	282
8.64	Diagonal cracking at lower courses of wall during settlement (Test W4).	282
9.1	Variation of the energy ratio with the maximum vertical deflection of the FPSS model.	287
9.2	Variation of the damping ratio with the maximum vertical deflection of the FPSS model.	288
9.3	Stiffness degradation at first cycle of settlement.	291
9.4	Stiffness degradation at last cycle of settlement.	291
9.5	Comparison of experimental results with theoretical predictions of the vertical deflection of the FPSS supports.	296
9.6	Comparison of experimental results with theoretical predictions of lateral displacement of the FPSS walls.	297
9.7	Allowable deflection ratio of structures relative to the limiting tensile strain.	299
9.8	Allowable tilt ratio of structures relative to the limiting tensile strain.	300
9.9	Comparison of experimental results with predictions of equations(9.2 & 9.3).	304
9.10	Typical deformation of the ring beam during settlement.	306
A1.1	Definitions of settlement terms (after Burland and Wroth,1974).	331
A1.2	Definition of tilt and out-of-plane warping.	332
A3.1	External signal requirements.	336
A3.2	Upright signal of Demec gauge.	337
A4.1	Principal sectorial area of a closed rectangular section.	338
A6.1	Effect of cyclic settlement on the vertical deformation of the wall (Test W2B).	343
A6.2	Effect of cyclic settlement on the vertical deformation of the wall (Test W4B).	344
A6.3	Effect of cyclic settlement on the vertical deformation of the wall (Test W5A).	345
A6.4	Distribution of vertical strain along wall (Test W1).	346
A6.5	Distribution of vertical strain along wall (Test W2).	347
A6.6	Distribution of vertical strain along wall (Test W3).	348
A6.7	Distribution of vertical strain along wall (Test W4).	350
A6.8	Distribution of vertical strain along wall (Test W5).	351
A6.9	Distribution of horizontal strain along wall (Test W1).	353
A6.10	Distribution of horizontal strain along wall (Test W2).	354
A6.11	Distribution of horizontal strain along wall (Test W3).	355
A6.12	Distribution of horizontal strain along wall (Test W4).	357
A6.13	Distribution of horizontal strain along wall (Test W5).	358
A6.14	Maximum principal strain distribution of wall (Test W1BA).	360
A6.15	Maximum principal strain distribution of wall (Test W1BB).	361

A6.16	Maximum principal strain distribution of wall (Test W2BA).	362
A6.17	Maximum principal strain distribution of wall (Test W3AB).	363
A6.18	Maximum principal strain distribution of wall (Test W3BB).	364
A6.19	Maximum principal strain distribution of wall (Test W4BA).	365
A6.20	Maximum principal strain distribution of wall (Test W5AB).	368
A6.21	Maximum principal strain distribution of wall (Test W5BA).	370

## LIST OF TABLES

2.1	Comparison of the cost of preventive designs (adapted from Williams, Pidgeon and Day,1985).	40
2.2	Summary of traditional methods of design for ground movement.	44
2.3	Summary of general design details of slabs-on-ground (after Holland,1981).	52
3.1	Classification of damage (after I.Struct.E.,1978).	58
3.2	Values of k and corresponding values of $f_{max}$ for the damage limits, when $\Delta/L = 1/300$ (collated after Skempton and MacDonald,1956).	65
3.3	Limiting damage criteria with respect to the angular distortion as proportion of span (after Bjerrum,1963).	67
3.4	Summary of limits of damage (collated after CSTC,1967).	69
3.5	Allowable deflection ratio (after BRAB,1968).	71
3.6	Allowable deformation of rigid partitions (collated after CEB,1973).	73
3.7	Allowable curvature deflection ratio (collated after Walsh,1975 and Holland,1981).	74
3.8	Classification of damage according to the structural form (collated after Starzweski,1974).	74
3.9	Limiting tilt, rotation and maximum settlement for rigid buildings (after Bally,1975).	75
3.10	Recommended relative deflection ratio for no damage (collated after PTI,1978 and Wray,1978).	77
3.11	Comparison of criteria of damage for structures subject to ground movement.	88
3.12	Permissible shrinkage strain of building materials (collated after BRE,1979 ; Alexander and Lawson,1981 ; Fenton and Suter,1986).	97
3.13	Summary of limiting tensile strain at visible damage.	96
3.14	Limiting tensile and shear stresses for masonry.	98
3.15	Limiting stresses at the onset of visible cracking (collated after West, Hodgkinson and Haseltine,1978 ; Drysdale and Essawy,1988).	100
3.16	Allowable limiting curvature at visible cracking (collated after Furler and Thurlimann,1978 ; Baker,1978).	103
4.1	Summary of traditional methods for reinstatement of structures.	115
6.1	Symbols designating tests.	134
6.2	Properties of reinforcement bars.	142
6.3	Properties of concrete.	143
6.4	Properties of bricks.	143
6.5	Properties of mortar.	144
6.6	Results of control tests for concrete ring beam.	145
6.7	Results of control tests for brickwork prisms and mortar cubes.	148
6.8	Properties of strain gauges.	159
6.9	Properties of electronic Demec gauge.	160
6.10	Test schedule of FPSS models.	167
6.11	Test programme for different types of supports.	170
6.12	Test programme for beam and column joints.	170
7.1	Maximum stresses and strains induced in the FPSS F.E. model.	193
7.2	Resultant forces and moments for loading cases(1,2,3).	222
8.1	Summary of steel reinforcement strains.	225

8.2	Description of damage of FPSS models.	275
9.1	Summary of limiting deformation of experimental testing of models.	289
9.2	Summary of stiffness degradation and restoring force of experimental tests.	293
9.3	Experimental results for the maximum vertical deflection and lateral displacement of the FPSS models.	294
9.4	Theoretical predictions of maximum vertical deflection of the FPSS supports.	295
9.5	Theoretical predictions of lateral displacement of the FPSS models.	295
9.6	Comparison of calculated allowable deflection ratio of empirical formula with experimental results.	302

## PRINCIPAL NOTATIONS

$A_S$	area of steel reinforcement
$A^H, A^S$	differentiation constants for hard and soft mounds
$B^H, B^S$	differentiation constants for hard and soft mounds
$B_z$	bimoment at a section
$d_f$	vector of foundation displacements
$d_g$	vector of ground displacements from the datum of free-ground displacements
$d_s$	vector of absolute structural displacements
$D, \phi$	diameter
$D$	flexural rigidity of the slab of thickness, $h$
$e$	edge distance of mound
$E_s, E_c$	elastic modulus of steel and concrete
$E_w$	elastic modulus of brickwork
$f_{cu}$	compressive cube strength
$f_c'$	compressive cylinder strength
$G$	shear modulus
$H$	height or depth of beam or wall
$I$	moment of inertia about neutral axis
$I_J$	polar moment of inertia of the cross section
$I_p$	tangential second moment of area
$I_s$	St.Venant torsional stiffness factor
$I_w$	principal sectorial moment of inertia of cross section
$K_g, K_{gd}$	stiffness matrix of the ground
$K_s$	stiffness matrix of the structure
$L$	span length of wall or beam
$M$	bending moment
$M_i$	bending moments at node $i$
$M_u$	ultimate design moment (Appendix 2)
$M_z$	external torque applied at any section along the $Z$ axis
$M_{FAB}$	fixed bending moments of beam $AB$
$N_i$	axial forces at node $i$
$P$	applied point load
$P_e$	equivalent load vector
$P_g$	vector of interface nodal forces acting upon the ground
$P_s$	vector of interface nodal forces acting on the structure
$q$	shear flow per unit length



$Q$	shear force
$Q_i$	shear forces at node $i$
$r_x, r_y$	curvature of a thin plate in $x$ and $y$ directions
$R\phi 4\text{mm}$	mild steel reinforcement of 4 mm diameter
$S_i$	Winkler spring stiffness at point $i$
$T$	applied torque at the end of an element
$u$	horizontal displacement parallel to the $x$ -axis
$v$	vertical displacement parallel to the $y$ -axis
$w$	tilt or rigid body rotation
$w_i$	ground settlement at footing $i$
$W_w$	applied load on wall
$W_{wm}$	ultimate design load on wall
$x, y, z$	cartesian coordinates
$y_o^{H, S}$	initial mound shape for the hard and soft mounds
$Y_m$	mound differential heave or settlement
$\beta$	angular distortion
$\beta_m$	$m\pi x/a$ , of length $a$
$\gamma_L, \gamma_R$	relative rotation per unit moment, $M$ at left and right supports
$\gamma_m$	$m\pi y/b$ , of length $b$
$\delta$	differential settlement (Chapter 3)
$\delta, t$	wall thickness of the section (Chapters 6,7, Appendix 4)
$\nabla^4 w$	fourth partial differentiation of settlement $w$ , with respect to $x$ and $y$ coordinates $(\frac{d^4}{dx^4} + \frac{2d^4}{dx^2dy^2} + \frac{d^4}{dy^4})w$
$\Delta$	total settlement
$\epsilon$	strain
$\epsilon_b$	critical direct tensile strain
$\epsilon_{crit}$	critical tensile strain
$\epsilon_d$	critical diagonal tensile strain
$\epsilon_1, \epsilon_2$	maximum and minimum principal strain
$\theta$	angle of rotation per unit length
$\theta_A, \theta_B$	rotation of beam at nodes $A$ and $B$
$\lambda(z)$	warping function
$\mu_w$	coefficient of warping
$\nu$	Poisson's ratio
$\sigma$	stress
$\sigma_c$	critical stress
$\sigma_{ii}$	stresses along $x$ - $x$ , $y$ - $y$ and $z$ - $z$ directions
$\sigma_1, \sigma_2$	maximum and minimum principal stress
$\sigma_{z, s}$	longitudinal direct stress associated with the restrained warping

or the flexure twist of the member

- $\rho$  perpendicular distance from the shear centre to the tangent at the section
- $\phi$  angular displacement of the section
- $\phi_0$  angular displacement of the end section at  $z=0$
- $\tau$  tangential shearing stress
- $w(s)$  sectorial coordinate of a point  $s$  measured from a pole  $P$  with initial radius  $P_0$  and is equal to the double area enclosed by the lines  $P_0, P_s$  and the curve  $s$  of the cross-section
- $\bar{w}(s)$  principal sectorial area of the cross section
- $\Omega$  double area enclosed by middle line of the section (Chapter 7)  
closed integration along the middle line of the thin walled cross section
- $\sum_{i=1}^m$  summation of elemental terms from  $i=1$  to  $i=m$

## ABBREVIATIONS

ACI	American Concrete Institute
ASTM	American Society of Testing and Materials
BRE	Building Research Establishment
BS	British Standard
CEB	Comite Europeen Du Beton
CSTC	Centre Scientifique et Technique de la Construction
FEA	Finite element analysis
FPSS	Four point support system
ICE	Institution of Civil Engineers
IStructE	Institution of Structural Engineers
LVDT	Linear variable differential transformer
NCB	National Coal Board (England)
2-D	Two dimensional
3-D	Three dimensional

## UNITS OF MEASUREMENT

ft.	foot
in.	inch
kg	kilograms
KN	kilonewton
lb	pounds weight
m	metre
mm	millimetre
MN	meganewton
MPa	megapascal (= 1 N/mm <sup>2</sup> )
Ω	ohm
μsec	microsecond

## CHAPTER 1 INTRODUCTION

### 1.1 THE PROBLEM OF GROUND MOVEMENT AND ASSOCIATED DAMAGE

Ground movement is caused either by volume change of clay soils (that is, expansive soils), or by local relaxation of existing stress within an adjacent area of ground (that is, tunnelling, nearby excavation or mining subsidence). The ground disturbance triggers a chain of movements on the ground surface that frequently result in severe damage to man-made structures. The scale of damage is alarming; for example in the United States the annual repair bill for buildings and roads damaged by expansive soils amounts to approximately \$6 to \$8 billion (Holtz,1983). The situation is yet more serious in developing countries where damage bills impose a proportionally larger financial burden (Osman and Charlie,1984). Documented studies of ground movement date back to 1333, when one of the first observed studies of settlement was conducted on the Cathedral of Koenigsberg, Germany which settled 72 in. between 1333 and 1833. Also, the Tower of Pisa, constructed between 1174 and 1350 (Krynine,1947), and St. Paul's Cathedral built between 1677 and 1710 are reported to have settled during their construction and, indeed, the process is still continuing at present (Thomas and Fisher,1974). However, the rationale behind the prevention of movement was, in most cases, to ensure the design of a strong rigid substructure (Terzaghi,1935). From the turn of the century, increasing attention has been focussed on the estimation of ground movement and settlement of buildings (Glick,1936 ; Tschebotarioff,1951). Extensive work on correlating the magnitude of settlement necessary to cause structural distress on different types of building was first collated by Meyerhof (1947) and Skempton and MacDonald (1956).

Although the nature of the superstructure influences the magnitude of ground movement and the amount of distortion that different types of construction can withstand (Terzaghi,1935), the effect of flexible structures has only been investigated since 1930 (Tschebotarioff,1951).

Observations and experimental studies of ground movement on structures, especially in England, Germany and France, started after the Second World War. These studies investigated the safety of buildings

after the war (Short and Simms,1949). Moreover, with the surge of mining in the 1940's, the problem of ground movement on buildings caused by subsidence became particularly acute (Mautner,1948 ; Rausch,1955 ; Littlejohn,1974 ; NCB,1975).

The significance of expansive soils was recognized in the early 1940's and is now well demonstrated by the many case histories of damage to and failures of buildings and roads.

Later, in the 1960's, after the introduction of the ultimate theory as a design philosophy, excessive deflection and differential movement of slender structures caused some severe damage to structural parts and partition walls. Several reporters, then, collected data of damage where there was a requirement to define safe limits of building deformation for the structural design codes (Mayer and Rusch,1967; CEB,1973).

With the accumulation of knowledge concerning ground movement and its effects on structures, many problems regarding the design of structures on moving ground remain under investigation.

## **1.2 THE PROBLEM OF DESIGN ON MOVING GROUND**

Various types of structures behave differently when subjected to ground movement and, consequently, their function is affected by the resulting damage. Some structures, for example load-bearing buildings, can accommodate a certain amount of differential movement within their structural members without the risk of cracking or failure, whereas framed structures have a tendency to resist the movement. Hence the simplest classification is to distinguish between "flexible structures" and "rigid structures", which are designed either to allow for or to prevent differential movements, thereby minimizing the risk of damage to buildings. The choice depends on many factors, among which are the amount of movement to cater for function of the building, practical construction factors, and economic considerations, both as part of the design process and maintenance.

Since the possibility of tall buildings and bridges being subjected to damage caused by moving ground becomes more distant with the increasing rigidity of the structure and the corresponding deep foundations, the present research is focussing more on low-rise buildings, which are more vulnerable to damage. Although several foundation designs exist that are able to prevent differential movement,

the requirements of design for low-rise structures, in particular houses, present a problem especially in developing countries. This is due to the following reasons (Donaldson,1975 ; Burland,1984):

- 1) foundation treatment must be relatively inexpensive compared to the total cost of the dwellings,
- 2) construction of the foundation and the superstructure must be simple so that it can be carried out without resorting to the use of sophisticated procedures and elaborate equipment,
- 3) the superstructure of the building must not suffer undue damage due to differential movement, and
- 4) maintenance of the superstructure must be relatively inexpensive compared to the cost of a more sophisticated structural design.

Although the choice of the foundation-structure system is dependent upon the economic consequences, discussed in reasons 1 & 2, the degree of rigidity of the structural system and the extent of damage is governed by serviceability criteria (see 3 above). Generally, the degree of damage should not exceed an allowable value; however, this value is based on a subjective criteria (described in Section 2.5) that is reliant upon the user's judgement. The variability of adopting a design that is influenced by uncertainties of the amount of movement to be designed for and the expected damage presents a problem for assessing the effective cost of the design. This is covered by 4 above, namely, maintenance of a deformed structure. Taking into consideration these problems, a novel design method was mooted.

### **1.3 THE PRESENT RESEARCH**

The main aims of the work described in this thesis are to assess and to develop the potential of a new structural masonry design, namely the four-point-support-system for low-rise buildings, in areas of ground movement. These objectives were achieved by:

- undertaking a review study of the characteristics of ground movement and its effect on structures,
- reviewing critically the available methods of design of structures subject to ground movement,
- assessing the evaluation of damage criteria cited by investigations, together with establishing an out-of-plane damage criteria for a 3-dimensional review of structures,

- developing an integrated maintenance system for the design,
- experimental investigation of the economic feasibility of the four-point-support-system (FPSS),
- determining safe working limits of the FPSS, and
- formulating a practical preliminary guideline for the design of FPSS.

In Chapter 2, the effects of different ground movements on various types of structures are investigated. The main factors that influence the choice of the type of structure are discussed, together with the design philosophy. The majority of the Chapter is devoted to a review of the existing literature on types of solutions relating to structures on moving ground. In addition, the different philosophies of design are reviewed with reference made to appropriate design analysis procedures.

Different damage criteria are reported in the literature. Chapter 3 discusses the evaluation and assessment of building damage from observations made during the past century. Various criteria of damage have been reviewed, dependent upon the type of structure, its characteristic factors and theoretical background. Development of an out-of-plane criteria for masonry walls from observations of tests conducted in the literature was performed. For the purpose of defining the allowable limit of deformation of a building before cracking, comparison of the existing techniques was conducted.

From the point of view of structural efficiency, ground movement may be absorbed by the foundation-structure system without incurring excessive damage. A review of the methods of design for permitting movement is conducted in Chapter 4, together with the different techniques for the structural reinstatement of buildings.

The four-point-support-system (FPSS) is introduced in Chapter 5 as a design methodology that would allow movement to occur differentially between its four supports. The choice of the design is discussed with particular reference made to the walling system, roof-wall connection and the type of supports. Maintainability of the structural system was also considered during the early stages of the FPSS promotion. Preliminary investigation of the FPSS to be able both to deform elastically and to accept (absorb) damage within its structural elements was studied.

The experimental investigations and testing of the four-point-support-system are reported in Chapter 6. Half-scale models simulating

structural modules (described in Section 5.4) were tested, firstly, to monitor the behaviour of the FPSS under settlement. Secondly, the tests set out to examine the influence of different structural parameters in defining the safe operating limits of relative deflection and damage. The third purpose of the tests was to investigate the capacity of each structural part, that is, the ring beam, the wall system and the flexible roof-wall joist joint in absorbing differential movement. The investigation did not include the influence of rate of ground movement on the behaviour of the structure.

Test models were loaded, prior to settlement tests, to resemble the self-weight condition by using dead weights; settlement loading was performed at one of the supports, this also represented the worst case of loading, that is, the hogging mode. The experimental investigation involved measurement of:

- the maximum settlement and supporting load during settlement,
- deformation of the wall-beam structure, both vertically and horizontally,
- warping deformation of the adjacent walls,
- rotation of beam supports during settlement,
- steel strain in the ring beam, and
- wall strain during settlement.

The experimental investigation examined the effects of the following variables:

- increased articulation of the ring beam, this was provided by:
  1. introduction of a weak beam-short column joint, and
  2. providing a point support,
- benefit of a larger reinforcement area in the ring beam,
- aspect ratio of the walls, and
- effect of reinstatement of the structure by jacking.

These tests recognized some of the factors which influence the general structural response of FPSS to settlement, and helped the identification of the capacity of the system to absorb differential movement. However, due to limitations of the test rig and adherent test programmes, they cannot be viewed as a complete guide for the design. This set of tests did not study the influence of window or door openings, which would normally be incorporated in a typical structure using the FPSS. Results of the tests and observation of damage are



given in Chapter 8.

The theoretical background and the evaluation of design concepts are presented in Chapter 7. A finite element method was used to model the behaviour of the FPSS under settlement, through 3-dimensional elastic simulation and, also, 2-dimensional non-linear representation. Assessment of the four-point-support-system as a novel design for masonry structures is carried out in Chapters 7, 9 and 10. Limitations of the system are compared with observations of existing structures and empirical criteria of damage in order to define the working range of the FPSS under settlement. Preliminary design formulae are proposed as an initial contribution to a design procedure for flexible structures subject to ground movement.

## CHAPTER 2 GENERAL BACKGROUND TO THE PROBLEM OF GROUND MOVEMENT AND STRUCTURES

### 2.1 INTRODUCTION

Problems associated with differential ground movement have been reported from many parts of the world. A large majority of buildings, especially lightly loaded structures founded on areas undergoing ground movement, have experienced a wide range of cracking and damage. Since usually, the ground movement occurs over a long period of time, although only a fraction of the lifetime of the building, the structure is being subjected, in effect, to static loading. This form of loading is different from the superimposed type of static loading, and is often neglected when designing a structure. It occurs due to the change or withdrawal of subsurface support, caused by the local relaxation of, or increase of, existing stresses underneath the bearing foundation.

A thorough understanding of possible ground movement, and the consequent movement of the structure, is necessary for two reasons. Firstly, to predict the possible extent of damage and take appropriate measures to allow for this in design and construction of the foundation and the superstructure. Secondly, to achieve a building which if subjected to tolerable amounts of damage, would not have its function impaired or prove difficult and expensive to repair.

There are several ways of designing structures likely to be subject to ground or soil problems. The various techniques differ both in cost and degree of effectiveness. Thus, an optimum design would conform to certain cost restrictions but might suffer a tolerable degree of distortion and cracking.

### 2.2 FORMS OF GROUND MOVEMENT

Displacement of the ground, or soil movement, underneath a building affects the structure in two modes, direct and indirect. The direct mode results from movement of ground immediately below the building, and may be caused by a number of reasons, the most common being swelling and shrinking of expansive soils or, freezing and thawing of the ground. Foundation settlement also occurs due to water leakage

below the foundation, or to excess surcharged weight of the building, or it may be caused by landslides, method of construction, or by continuous vibration and compaction, for example, power-generation houses. The indirect mode of movement is a result of earth activity adjacent to the building and is divided into two classes. The first class is subsidence waves that propagate from deep in the earth and go through the ground towards the building, as for example, mining subsidence, driving of piles near existing buildings and vibration in tunnels. The other class is caused by stress dissipation in the ground around the vicinity of the structure due to relief of the confining bodies. Some of the cases reported are due to opencuts and unbraced excavations adjacent to buildings, tunnel excavation and construction, landslides, and depressions adjacent to building sites.

Difficulties are encountered when endeavouring to correlate the stiffness of the structure with its deformation. These are due to soil-structure interaction, leading to redistribution of the stresses within the deformed structure. Thus, it is necessary to relate the deformation of the structure with that of the ground, that is, the different forms of ground mounds (Lytton,1970 ; Meyer and Lytton,1966).

### 2.2.1 Edge deformation

Edge deformation is caused by either swelling or shrinking of part of the ground at the edges of the structure, or migration of moisture due to adjacent vegetation, refer to Figure 2.1. Settlement of foundations at the middle of the building can also cause edge deformation. A trough of subsidence occurring at some distance away from the structure can cause parts of the ground to slide in relation to the edge of the building, refer to Figure 2.2.

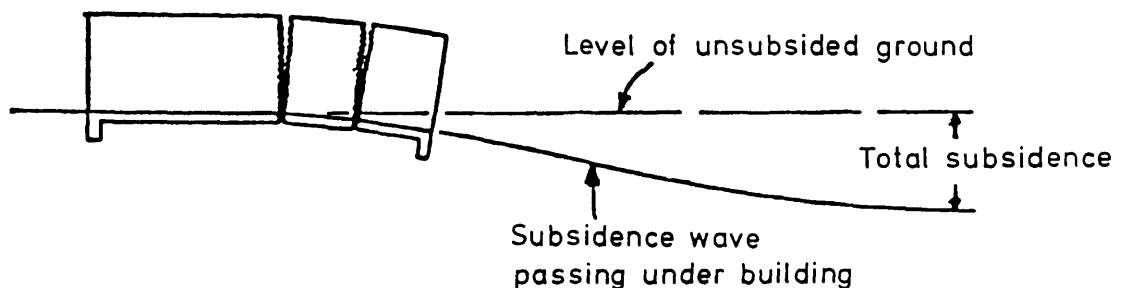


Figure 2.1 Edge deformation caused by movement due to ground subsidence (adapted after Lacey and Swain,1957).

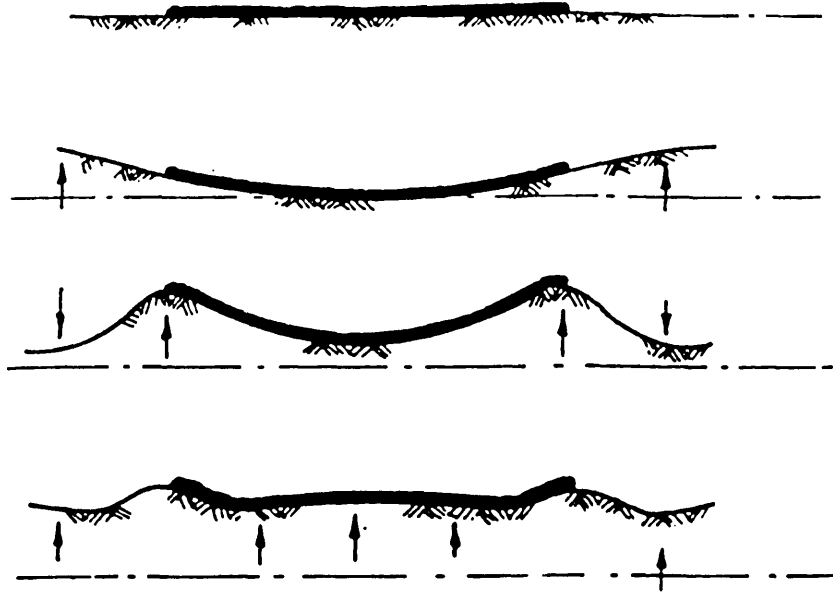


Figure 2.2 Edge deformation caused by movement of expansive soils (adapted after Holland,1981).

**2.2.2 Centre deformation**

Centre deformation is caused when the edge deformation conditions occur at the centre of the structure, refer to Figure 2.3. A trough of subsidence causing differential settlement of the ground relative to the centre of the structure would give rise to a central mound; refer to Figure 2.4.

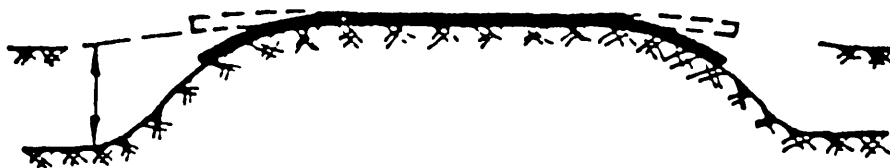


Figure 2.3 Centre deformation caused by movement of expansive soils (adapted after Holland, Pitt and Lawrance,1980).

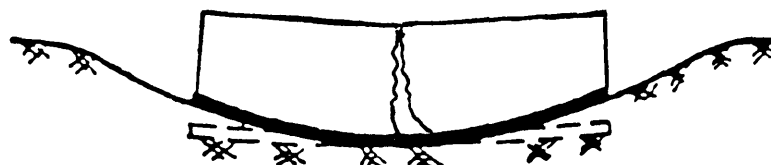


Figure 2.4 Centre deformation caused by ground subsidence.

## 2.3 FORMS OF STRUCTURAL MOVEMENT

It is necessary to define the different forms of structural movement that can occur, both to assess the behaviour of the deformed structure and to calculate the design load on the critical sections. The forms of structural movement are classified according to the ground deformation mounds. Holland (1981) and Walsh (1975) defined several forms of movement.

Movements caused by general heave (swelling and shrinking soils, freezing and thawing of ground) are hogging and sagging. Other modes of movement and damage to buildings occur in the form of differential vertical and horizontal movements associated with mining subsidence, opencut excavations, and tunnelling.

### 2.3.1 Hogging mode

Swelling and shrinkage of the ground often leads to a mode of structure distortion resulting in corners down and centres up, refer to Figure 2.5. These movements of the structure give rise to diagonal cracks which are wider at the top and narrow at the bottom. In other instances, where vegetation exists near buildings, such a mode occurs on one side of the building only.

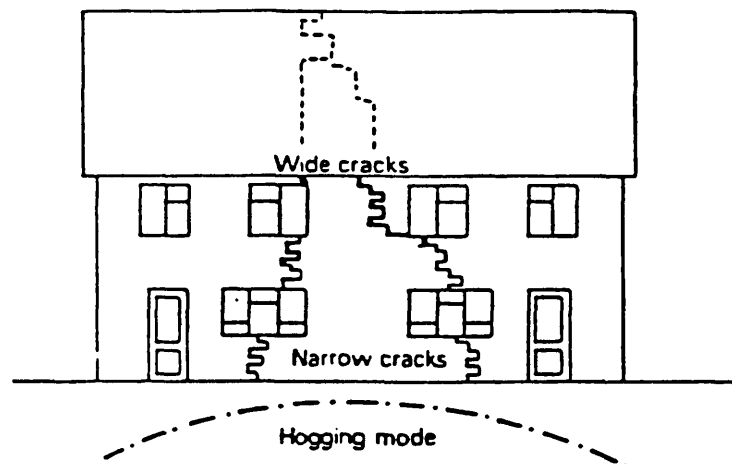


Figure 2.5 Form of damage due to hogging mode of ground deformation (after BRE,1981).

### 2.3.2 Sagging mode

A downward movement or a drop of support at the centre of the building would initiate this mode. It is characterized by much narrower

cracks than the hogging mode, with wider cracks at the bottom of the building, refer to Figure 2.6.

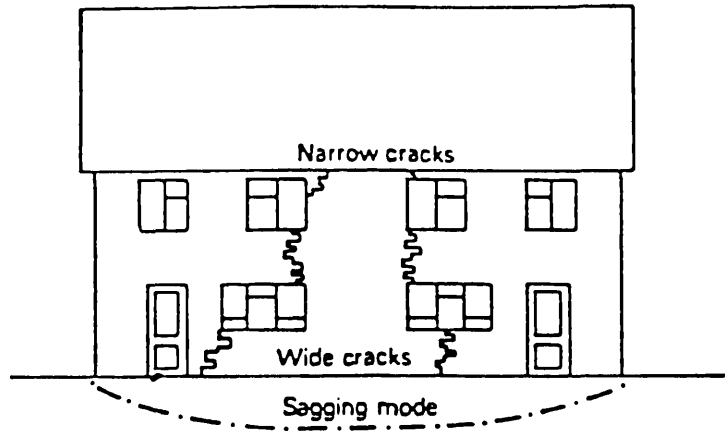


Figure 2.6 Form of damage due to sagging mode of deformation (after BRE, 1981).

### 2.3.3 Large-differential vertical mode

Ground disturbances triggered by a trough of subsidence close to the ground surface or vibration due to underground tunnelling can cause a sudden depression of the ground surface. Generally, the change of ground profile exhibits large differential vertical movement of adjacent points. This may result in either vertical shearing of the building, or sharp curving of the structure in a vertical plane. This also causes disruption of drainage and overall tilting of the structure, particularly to tall buildings (O'Rourke, Cording and Boscardin, 1976 ; Tugaenko, Matus and Stoyanova, 1984), refer to Figure 2.7.

### 2.3.4 Horizontal mode

The effect of subsidence on adjacent points on the ground is to induce horizontal strains at the ground surface. This is attributed to the location of the epicentre of the subsidence wave, and its distance relative to the ground points. This results in horizontal extension or contraction of different parts of the ground, leading to tensile or compressive horizontal strains respectively, along the building.

The degree of damage suffered by a structure is not only dependent on the intensity of tension and compression which it undergoes, but also on the type of building and construction materials (Lacey and Swain, 1956 ; Barber, 1969), refer to Figure 2.8.

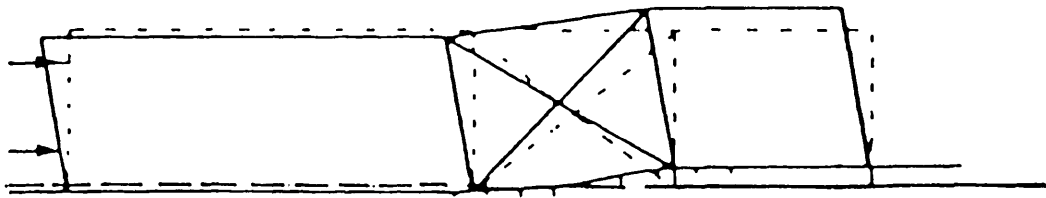


Figure 2.7 Form of damage due to vertical ground subsidence (after Barber,1969).

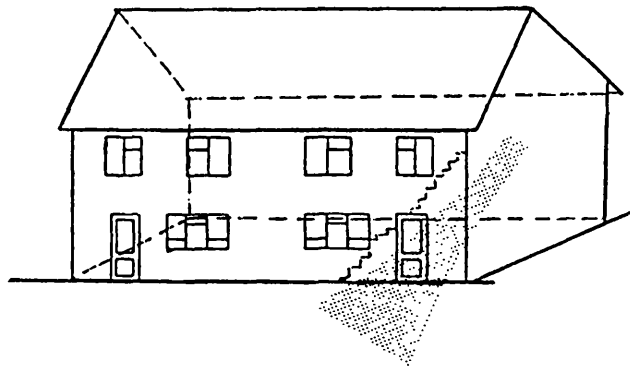


Figure 2.8 Form of damage due to horizontal straining of the ground.

#### 2.4 FORMS OF STRUCTURAL DAMAGE

Probably a majority of all buildings experience some form of cracking and damage due to foundation settlement (Terzaghi and Peck,1967). An understanding of the structural response to ground movement is required in order to classify the form of cracking and to assess the extent of damage with respect to each form of structural movement. Based on site observations, various classifications of ground movement and building damage have been reported (Skempton and MacDonald,1956 ; Meyerhof,1956 ; Feld,1965 ; Burland and Wroth,1974). These will be discussed in more detail in Chapter 3. The following are the most commonly observed effects of structural damage:

(a) In mining subsidence, differential horizontal movements induce horizontal ground strains, that is, both compressive and tensile, which occur in two forms, "travelling" and "residual" (Rodin,1969). An inclined crack tends to initiate from the foundation level to the full height of the building (Lacey and Swain,1956 ; Barber,1969). NCB(1975) recommended the division of buildings into independent units, therefore avoiding any linkage. Severe cracking is often observed at connecting

wing walls, outbuildings or concrete drives, or where flexible foundations are deep.

(b) Differential vertical movement induces two modes of structural response, sagging and hogging, which result in vertical or diagonal cracks throughout the building. At weak points in the building near openings such as doors and windows, distortion can occur. Heaving of ground slabs and change in slope of ground floors are detrimental to both sensitive machinery and drainage systems (Barber,1969 ; Rodin,1969).

(c) Tilting of structures as a result of differential vertical movement of the ground is characterized by vertical cracking throughout the height of the building. For slender structures, such as cooling towers and chimneys, severe tilting affects stability of the structure (Rodin,1969 ; O'Rourke et al.,1976 ; Tugaenko et al.,1984).

(d) Vertical subsidence of the ground and changes in gradient of the surface profile inflict damage to drainage systems and buried pipelines, thus seriously affecting their operation. Joint leakages are common in the case of buried pipelines, which are often affected by transverse fracture of pipes (Attewel, Yeates and Selby,1986). Similarly, vertical movement causing longitudinal cracks spanning several metres can occur near the edges in roads and pavements (Burland,1984). However, large ground depressions alongside roads characterize the effects of subsidence.

(e) Poorly detailed joints such as wall joints and roof-wall joints, seriously jeopardize the safety of the building. Instability of the entire building and roof sliding leading to subsequent collapse, have also been reported (Simms and Bridle,1966 ; Cassie,1969 ; O'Rourke et al.,1976).

## **2.5 STRUCTURAL DESIGN AND SOIL STRUCTURE INTERACTION**

Movement of the ground is resisted by overburden pressure resulting from both the overlying structure and the applied loads on the structure. Different types of foundations have different load concentrations on the ground, and this will affect the amount of



potential movement likely to be experienced. The movement likely to be encountered by the structure is affected by the rate of settlement of the ground, which is a property of the type of the underlying soil. Loading on the foundations also depends on the resistance of the structure's members to differential settlement. As a result, the redistributed load on the foundation varies with the rigidity of the structure and the manner of settlement of the ground. Thus, there is an effect of coupling or interaction between the building members and the different ground mounds, this study is known as soil-structure interaction. The parameters affecting the soil-structure interaction are as follows (Burland,1984):

- 1) Type of soil,
- 2) Differential movement of ground, and
- 3) Contact pressures, which are due to
  - a) type of foundations, and
  - b) type of structure.

Burland, Broms and De Mello (1977) have pointed out that no matter how sophisticated the analytical method used in design, it is only as good as the idealizations, and these are far from certain. Idealizations can be divided into three broad types for both the ground and the structure:

- 1) The geometry,
- 2) The loading, and
- 3) The material properties.

Difficulty arises in defining these parameters, which in most cases leads to gross assumptions (Burland,1984 ; Attewel et al.,1986). A rational design method for foundation-structure interaction is required which takes into consideration the soil structure interaction by adopting a representative model (Burland et al.,1977). The problem of defining a proper mathematical model to represent the behaviour of the ground, and its implications to design, has long been the concern of many investigators (Richard and Zia,1962 ; Lee and Brown,1972).

It is important to appreciate the interdependence of the foundation system and the superstructure, which should be designed as balanced and integrated systems. Since the mathematical analysis is often complicated, powerful computer aided techniques such as the finite element method, finite difference method, fourier analysis, integrated unit analysis and 3-dimensional analysis are employed. The use of these

numerical methods together with the idealizations and assumptions involved, tend to reduce the sensitivity of these techniques (Gazetas and Tassios,1978). Burland (1984) concluded that a design method considering the soil-structure interaction will only place bounds on the likely range of behaviour and will not, in itself, be sufficient to be used as an accurate design method. Thus, the use of these methods are only recommended at this stage, for comparison with standard methods of design and construction.

## 2.6 BASIS OF DESIGN EVALUATION

In parts of the World, where the type of soil, climatic, environmental and ground conditions vary, several design procedures have been reported (Meyerhof,1956 ; Zeitlen and Kornornik,1980 ; Tomlinson,1984 ). Adopting the techniques developed for a particular problem without a full knowledge of the specific conditions arising often leads either to unexpected damage or to expensive inappropriate designs and potentially difficult repairs (Williams and Donaldson,1980). This is particularly true for designs in severe conditions, which are likely penalized for the great uncertainties involved. The design procedure for structures subject to ground movement consists of a series of standard solutions, involving calculations of structural quantities for a given building site. These are introduced to define the type of structural response and details to be provided for each particular structure (Zeitlen and Kornornik,1980).

Although the intention must always be a crack-free building, economic considerations, in the design process, construction and during the lifetime of the building are likely to govern the choice of design. This is noticed particularly in regard to low-rise buildings where it is usually unjustifiable to implement an expensive design or one which will require costly repairs in the event of minor subsidence. To better comprehend the economic considerations involved in the design process, a basis of evaluation is required to study the interaction between the main design objectives. Several reporters (Chen,1975 ; Chan, Toh and Ting,1979) have examined the basis of evaluation of building design by observing associated damage. This is shown schematically in Figure 2.9.

Two main groupings were cited, the first pertains to the various repair operations conducted on the building (Chan et al.,1979). The second is dependent upon the subjective criteria during the building's

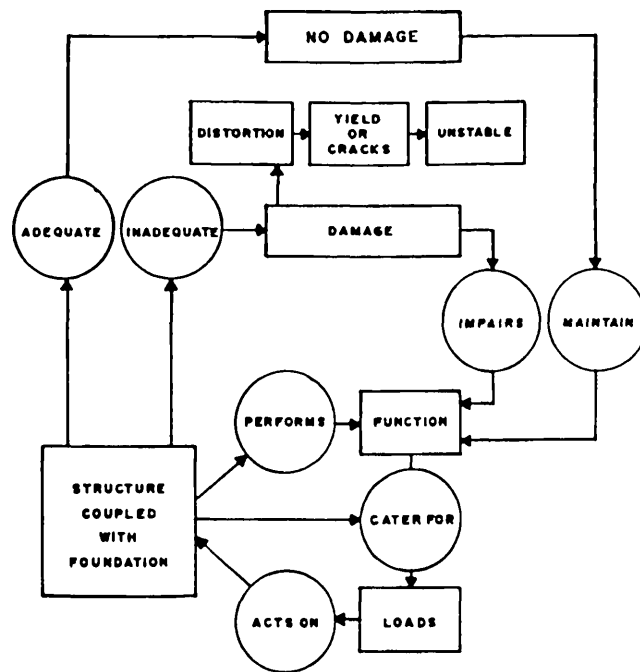


Figure 2.9 Damage evaluation of structures subject to differential movement (adapted after Chan et al.,1979).

lifespan, that is dependent on the client and the user (Zeitlen and Kornornik,1980). Figure 2.9 shows the evaluation cycle for buildings, bridges, silos, etc. affected by either adequate or inadequate foundation-structure systems. Under load, an inadequate foundation results in structural distortions in the way of rigid body movements, displacements and rotations of structural components relative to other members, or in deformations within each structural component.

Excessive distortions may lead to further damage such as the opening up and cracking of the more "brittle" parts, or overstressing and yielding of the more "ductile" portions. Eventually, the structure may become unstable and collapse. Thus, excessive distortions signal the state of distress of a structure. To evaluate the condition of a building, the strains at pertinent parts of a structure are fundamental parameters; but for practical purposes, boundary deformation parameters such as settlement and tilt are more readily measured.

There is a need, also, for a design which is both cost effective in construction and would prove inexpensive to repair. A summary illustrating a comparative study of the costs of the different design techniques is shown in Table(2.1). The Table indicates that there is a considerable increase and cost variation associated with each design.

Table(2.1) Comparison of the cost of preventive designs (adapted from Williams, Pidgeon and Day,1985).

Type of construction	Estimated ground movement (mm)	Maximum deflection ratio	Estimated additional cost *	Reference
Deep strip footings, pads and piers	NR	NR	5-10%	Mitchell and Mackechnie (1972)
Pier and suspended slab foundation compared to stiffened rafts	NR	NR	15%	Williams <u>et al.</u> (1985)
Piles and floor slab compared to shallow foundations	100	NR	30%	Domaschuk <u>et al.</u> (1984)
Normal-continuous brick walls on strip foundations	0-6	1:4000	0%	Williams <u>et al.</u> (1985)
Modified normal reinforced footings and lintels	6-12	1:2000	1-3%	Williams <u>et al.</u> (1985)
Split construction with reinforced brickwork	12-50	1:480	5-10%	Williams <u>et al.</u> (1985)
Piles to limited depth with split construction & reinforced brickwork	50-100	NR	20%	Williams <u>et al.</u> (1985)
Underreamed piles with suspended floors	100+	NR	30%+	Williams <u>et al.</u> (1985)
Stiffened raft foundations	NR	NR	7-15%	Williams <u>et al.</u> (1985)

Notes:

-\* If not mentioned, cost is compared with conventional shallow foundations.

Additional costs do not take into account repairs of the superstructure.

-NR = not recorded.

## **2.7 BASIS OF STRUCTURAL DESIGN**

There is an inherent difficulty present in any attempt to form a basis of design in areas of ground movement, especially since the interaction of several factors is involved. Particularly difficult is the identification of main factors for economical design, as well as the other factors affecting serviceability and damage. Three main groupings are defined as follows.

### **2.7.1 Importance of the structure**

Structures are divided into two categories depending upon the amount of damage that can be tolerated (Gidigas,1980), namely,

- Primary structures are those whose continued operation is vitally important, for example general assembly halls, power houses, industrial factories, hospitals etc.
- Secondary structures are those which can accommodate a higher degree of damage than primary structures, such as multi-storey buildings, schools and colleges, sport centres etc.

### **2.7.2 Economic considerations**

The cost factor includes both the design criteria and the amount of construction expenditure (Donaldson,1975). For light structures, for example low-rise housing, the design must be inexpensive and resort to simple, non-sophisticated procedures and avoid elaborate equipment (Burland,1984).

### **2.7.3 Subjective criteria**

The tolerable degree of building damage depends on the user and the client at the time of construction (Burland and Wroth,1974 ; I.Struct.E.,1978). To account for such a subjective criteria the following factors are taken into consideration:

- 1) The degree of cracking which the structure can safely tolerate without serious structural damage;
- 2) The extent to which cracks and distortion to architectural finishes of the building would be detrimental to its appearance;
- 3) The degree of cracking which the owner of the building would be prepared to accept with respect to the amount of expenditure on design or construction;
- 4) The extent to which the cost of prevention or control of cracks is

justifiable in terms of the cost and type of the proposed structure. This is different between low-rise and multi-storey structures. For the latter case, there are fewer limitations on the type of solution to be employed. This is because the extra cost of providing such measures or complicated designs form only a small part of the total cost of the whole project. In construction, the type of workmanship is high enough to provide sophisticated preventive measures. The same cannot be said, however, of light structures such as dwelling houses, for they would suffer much structural damage. Thus, optimization between the economical factors and the degree of damage is justifiable in this case.

## **2.8 STRUCTURAL DESIGN IN AREAS OF GROUND MOVEMENT**

Two very different design philosophies are possible. The first is to attempt to devise designs which are able to accommodate all possible movement in such a way as to obviate any need for repairs during the anticipated life of the structure. These might include foundations piled down to bedrock or, in some circumstances, heavy raft foundations. These techniques are commonly used for high-rise buildings and other structures where either the cost of repair or replacement is high, or the use demands special structural integrity. However, not only are the costs of such techniques clearly way beyond justification for typical low-rise buildings, but there always remains some slight risk of damage.

The alternative philosophy is to accept that some damage is likely, perhaps inevitable, and to devise a design which allows repairs to be effected before the structure becomes unusable, that is, before a serviceability limit state (such as that of visible cracking, or of excessive deflection) is reached. To be of practical interest especially for low-rise buildings, such a design should be both simple to construct and obviate the need for high-technology parts or equipment, either during construction or subsequent repair. The design should also be of a cost commensurate with that of simple structures, such as low-cost dwellings or secondary structures, refer to Section 2.7.1.

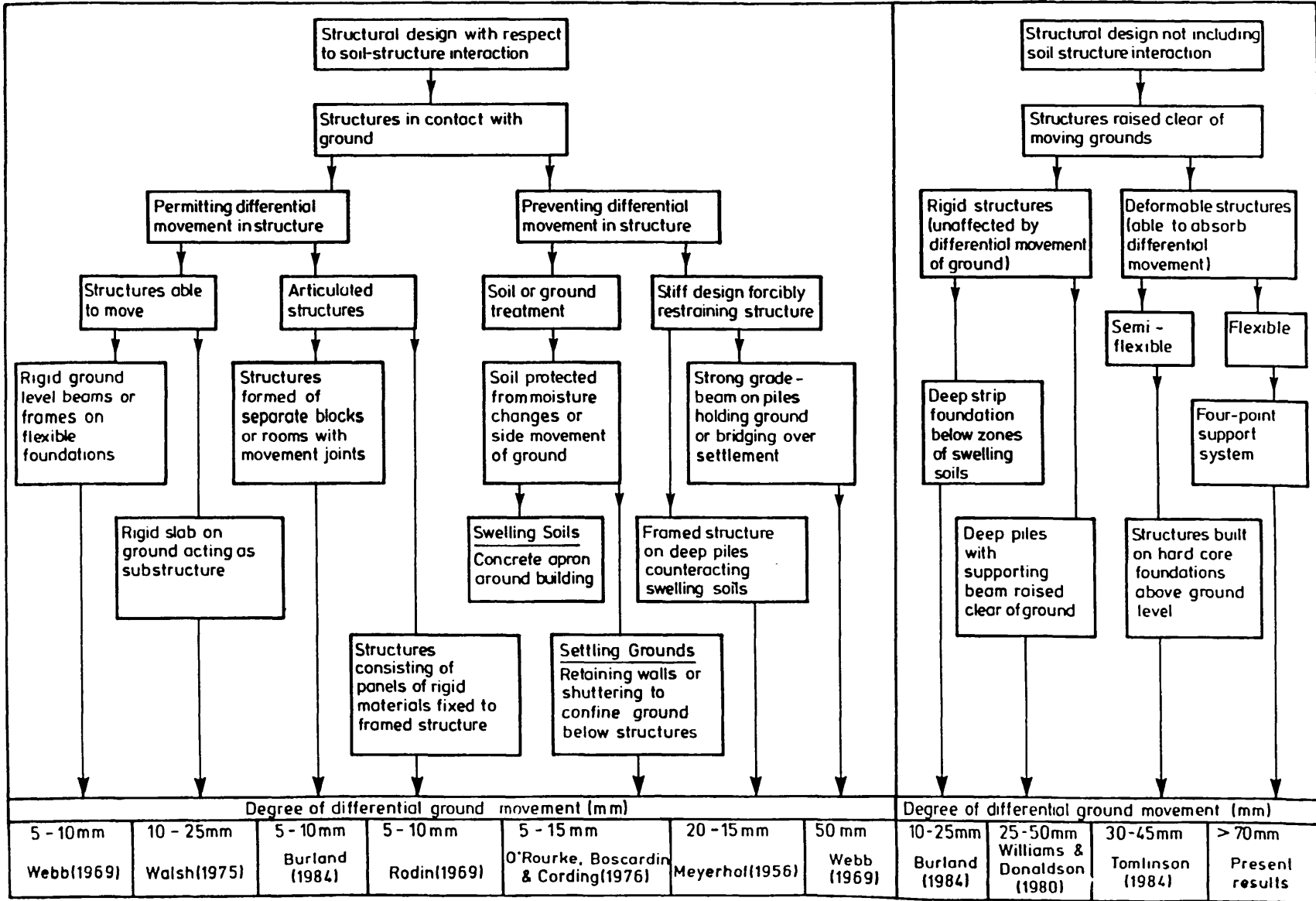
There are many different types and combinations of both structures and of the foundations which support them. In order to define the various types of foundation structural support systems, depending

upon the different methodologies and design concepts, a new classification is mooted. The classification is based on whether or not soil-structure interaction is employed in the design process, and serves to distinguish between the different design philosophies. Also, it will aid the choice of the optimum design method with respect to both cost and amount of predicted movement (Table(2.2)). Soil-structure interaction effects can be virtually eliminated if the structure is raised clear of the ground. However, when the foundation is in full contact with the ground, two alternatives arise. The first is if the ground is unrestrained, in which case the structure attempts to adjust its internal forces into equilibrium by resisting the loss of local support. Secondly, if restrained, the ground exerts large pressures on the restraint, that is, the foundation or some other part of the structure (Table(2.2)). For differential movement to take place between parts of the building, either it must be accommodated within the structure by designing a suitably articulated structure, or else the structure as a whole must be able to move.

If movement is to be prevented, there are two approaches, either to treat the ground, or to design a stiff structure. Insofar as the ground determines the movement, the swelling and shrinking of expansive soils can be prevented by controlling the soil moisture underneath the building. If the movement is caused by new construction, tunnelling or nearby excavations, wall shutterings and sheet piling can sometimes serve to confine the ground underneath the building. This would maintain an adequate bearing pressure under the foundation structure. If a stiff design is chosen to prevent structural distortion, it can be either a stiff foundation structure, forcibly restraining the ground, or a frame structure designed to counteract the differential movement.

Generally, the other design technique, that is, by avoiding soil-structure interaction, leads to a simpler solution. For rigid structures, a rigid foundation, either bypassing the swelling zone or maintaining the structural geometry during subsidence, is essential. If the foundation structure is not strong enough to withstand differential movement, whether due to economic, structural or other reasons, then it is designed to accommodate the deformation.

Current practical design solutions have been categorized as described above, and are tabulated with respect to the amount of movement that each method can incorporate before visual damage emanates (Table(2.2)).



Table(2.2) Summary of traditional methods of design for ground movement.



## 2.9 REVIEW OF PREVIOUS DESIGNS

The various design techniques found in practice have widely differing costs and degrees of effectiveness. In the interests of high quality and low maintenance, high capital costs using reliable methods are justified. However, an expensive installation which still fails and needs heavy maintenance is the worst of all; considerably worse than a cheap solution with tolerable cracks. The most common design methods in practice are described below.

The first four solutions listed (Sections 2.9.1-2.9.4), rely on the acceptance of some movement in the building, where foundations are shallow and cheap. Such a building can be made flexible either by using flexible materials or by hanging rigid panels on a flexible frame. Alternatively, the building can be articulated, that is, divided into units able to move independently. Each unit is small and strong enough to limit internal movement. There is the additional choice between having the independent units almost touching each other (Section 2.9.2), or separating them by usable spaces. The space can be roofed, provided that the roof structure can tolerate the relative movements (Section 2.9.1).

Another technique is to disallow movement. This is achieved by preventing the cause of soil movement, for example, significant differences in soil moisture under the building (Section 2.9.5). Similarly for settling ground, retaining walls or shuttering might prevent ground movement and thus stress relaxation under the building.

The whole building can also be designed as a stiff structure, either as a strong frame box or by constructing a firm foundation (Sections 2.9.6-2.9.7).

### 2.9.1 Separate rooms or blocks

These consist of three or more structurally independent blocks each about 4-5 m square. The space between the blocks is roofed and enclosed, generally by screens and doors, with shallow brickwork foundations supporting bearing walls. Having no structural dimension (stiffness), and relatively flexible construction, this method is favoured as it is likely to limit damage. The low initial construction cost renders continuing maintenance costs acceptable (Snell, 1980).

### 2.9.2 Prefabricated panels on flexible frame

A successful approach to movement in a structure is the concept of a flexible or articulated frame. It is built on a flexible slab designed to conform to ground curvature. Pin jointed frames with flexible cladding were employed in the "CLASP" system (Lacey and Swain,1956 ; Gibson,1957). Precast concrete cladding was also used where the movement was accommodated within the cladding system. Sliding of adjacent panels relieved the movements at both horizontal and vertical joints of the precast panels (Figure 2.10). The most critical engineering features of the building are the diaphragm action of the roof and floor decks, and the stability action of the vertical bracing. These were achieved by providing adequate vertical bracings in each section of the building. Joints were provided so as not to increase the stiffness of the superstructure. Alternatively, Barber (1969) recommended that a central tower carrying all horizontal forces can be used in conjunction with articulation joints, provided that the diaphragm action of the roof is adequate.

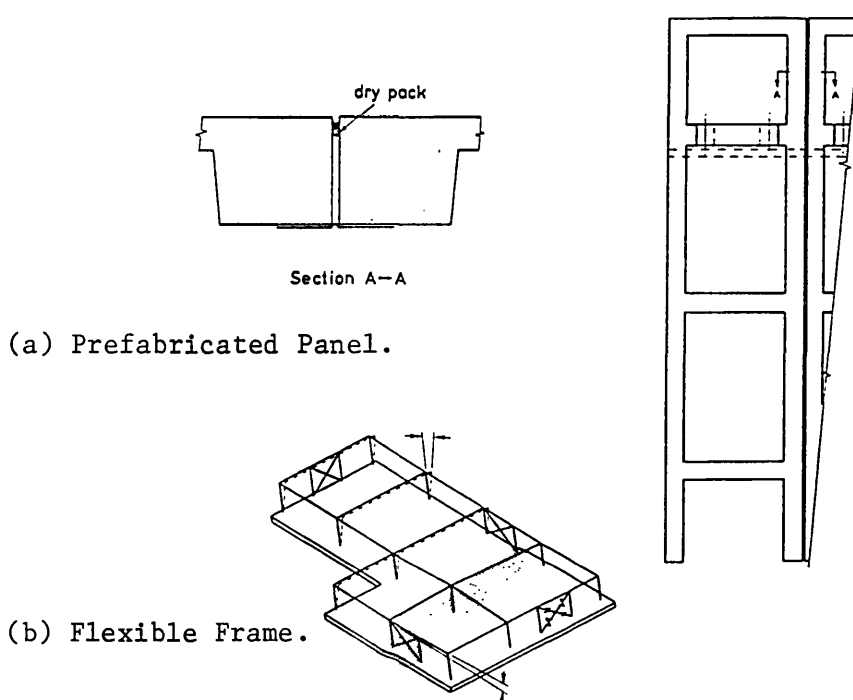


Figure 2.10 Use of flexible panels and frames to accommodate ground movement. Diagram(a) shows the movement joint between adjacent panels. Diagram(b) shows the use of spring bracings to ensure verticality of the frame (adapted after Barber,1969 ; Rodin,1969).

### 2.9.3 Flexible building material

Another technique is to induce flexibility in a building by using mud or soft mortar between bricks or blocks. A considerable amount of movement can be taken up in a well-distributed distortion of the mortar (BRE,1977). The use of lime mortars for brickwork has the effect of lowering the strength of the mortar by decreasing the cement content, and thus decreasing the rigidity of the wall (BRE,1973 ; BRE,1974). The more flexible brickwork would take more differential movement by developing a large number of small cracks rather than a single large one. For low-cost housing, wattle-and-daub walls were found to absorb movement, but require more frequent maintenance than brickwork (Danby,1975).

### 2.9.4 Open joint or split design

The structure is designed to allow distortion to take place without wall cracking. This is achieved by dividing the structure into small stable units by the placement of movement joints to ensure that the separate portions of the superstructure remain stable (Webb,1969). Typical movement joint location is shown in Figure 2.11.

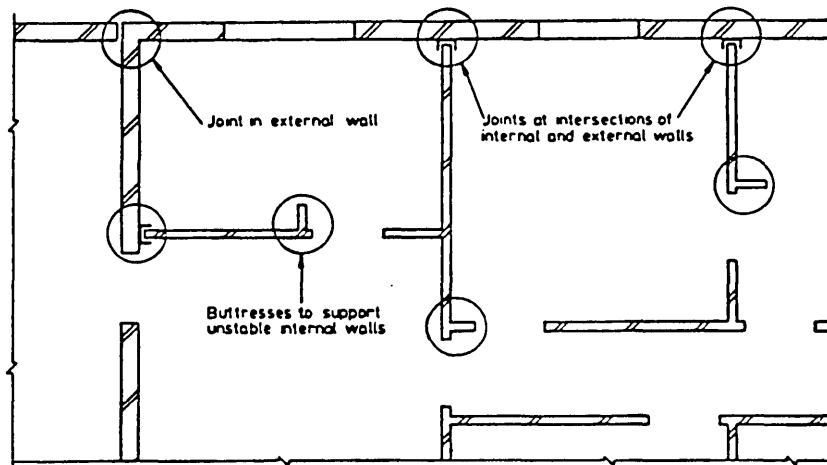


Figure 2.11 Location of joints in split design of masonry buildings (after Webb,1969).

The design steps are (Boardman,1956 ; Rodin,1969 ; Webb,1969):

- (1) To provide vertical joints so that the walls are subdivided into a number of panels which can move relative to each other. These are L- or T-shaped in plan in order to provide stability against overturning;
- (2) To provide joints in walls longer than 4.0 m and at each door and window opening. In the case of double skin walls, steel shoes are

- used to anchor both external and internal walls while permitting 0.5 in. movement in either direction;
- (3) Reinforcement of walls; individual external wall panels between joints are reinforced to resist the bending and shear stresses resulting from foundation distortion, which must be considered by differential settlement or unexpected subsidence. The reinforcement is designed to carry one-half of the bending moments and shearing forces by assuming the following support conditions:
- a) The panel is simply supported at its ends;
  - b) The panel is cantilevering on either side of a mid-span support; and
  - c) Design of openings for windows and doors depends upon the depth of the beam under the opening sill.
- (4) Floors are suspended from the foundation walls independently of the superstructure walls to reduce differential movement and subsequent damage.

#### **2.9.5 Soil contact**

This method can be applied in varying degrees and often in combination with the other techniques. In practice, generally two procedures are used. The first is in the form of a "sealing apron" at the joint between the foundation and superstructure. Bituminous seals are employed to prevent water leakage under the apron, or they are effectively bonded to the wall and laid with folds to accommodate movement near the wall. The purpose of such a membrane is as much to prevent drying out as to prevent local wetting. The apron extends outward from the building walls below ground level if rubber is used, or in the case of plain concrete, a 1.0-1.5 m slab width is used.

The second procedure if the expansive soil layer is shallow (not more than 1.5-2.5 m deep), is to replace it with an inert backfill. Alternatively, part of the soil may be removed, thus ensuring that the upheaval pressure exerted on the superstructure is within acceptable limits. Another solution is to lay a hard core, or a cushion of granular material, on top of the clay soil (Agib,1983 ; Tomlinson,1984). The primal function is to provide an environmental separator between the soil and the superstructure. A depth of 400 mm of well compacted hard gravel or sandstone is sufficient to distribute evenly the soil pressure on a concrete slab 100 mm thick (refer to Figure 2.12) (Tomlinson,1984) .

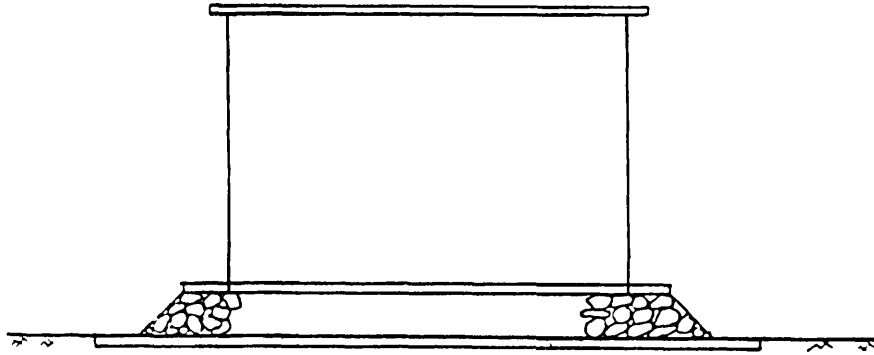


Figure 2.12 Structure separator used to reduce the effects of ground movement by cushioning on a layer of gravel (after Agib,1983).

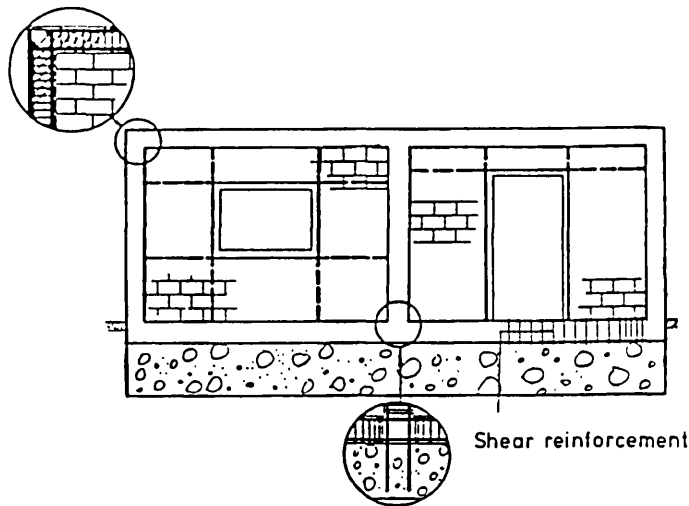
### 2.9.6 Rigid box system

In this method, the foundation, columns and roof are designed as a strong frame which is further stiffened by brick infill panels. The resulting box is strong enough to move monolithically under the influence of significant ground movement. It can sustain the movement if rigidly tied to stiff foundations, however, if shallow foundations are employed, limited cracking is expected (Snell,1980), Figure 2.13. This design is used more often in earthquake resisting structures (Carrillo-Gil,1980), but has been employed to form a rigid structure that cantilevers over subsiding grounds (Mautner,1948). However, the cost is high and is justified only in special circumstances, for example nuclear power stations, restored monumental buildings, etc.

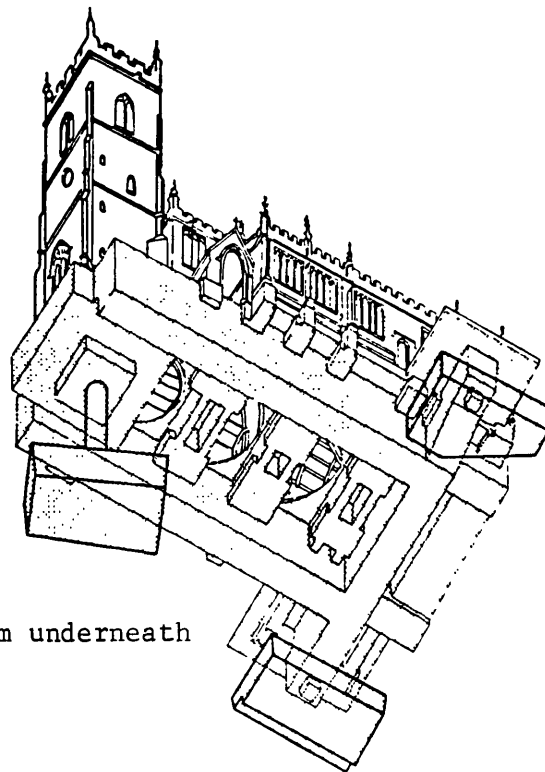
### 2.9.7 Stiff structures

This design is normally used when the cost is justified in terms of the importance of the structure. The structure is designed with regard to the relative stiffnesses of the soil and structure. However, due to the comparatively indeterminate character of the soil-structure interaction, this often leads to a conservative design (Holland,1981 ; Tomlinson,1984).

The design procedure is based on a probable mechanism of deformation of the structure. This is caused by ground movements that produce the maximum value of moments, shears and deflections likely to be expected. It takes into account the soil support condition, predicted loading of the structure, and the relative stiffness of the soil and the structure. A mathematical model of the soil-structure



(a) Rigid Frame.



(b) Rigid foundation beam underneath the whole structure.

Figure 2.13 Stiff design to prevent differential movement of structures (adapted after Carrillo-Gil,1980 ; Agib,1983 ; Jones,1985).

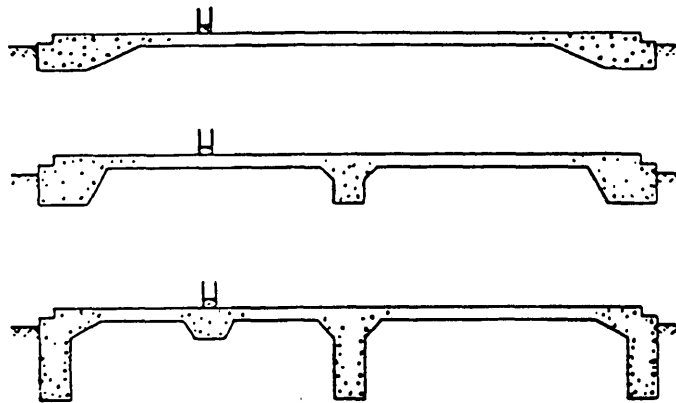
interaction is assumed based on the various deformation patterns of the ground and the structure. The stiffness of the structure includes the effect of the foundation system; the foundation is required to be stiff enough to carry the superstructure without incurring damage. The two types of stiff designs commonly used in practice are:

**(I) Raft slab**

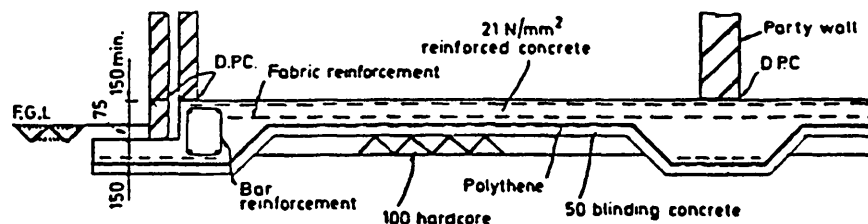
The function of a slab-on-ground is to provide a structural and

environmental separator between the superstructure and the underlying foundation (Walsh,1975; Holland,1981 ; Tomlinson,1984).

a) The structural requirements are to distribute the applied load on poorer foundation conditions and to utilize its strength and stiffness to limit differential movements. Additionally, it keeps distortion of the superstructure within acceptable limits. A grid pattern of stiffening beams, or increase in the slab thickness, or both, are required to provide a higher bending stiffness for the slab (Walsh,1978), Figure 2.14.



(a) Types of raft slabs.



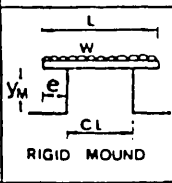
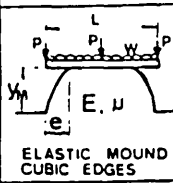
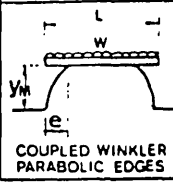
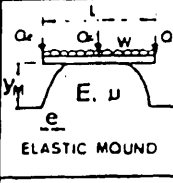
(b) Typical slab detail.

Figure 2.14 Typical design of raft slabs (after Tomlinson, Driscoll and Burland,1978).

b) The environmental requirement provides a concrete barrier from ingress of moisture and unstable ground.

Over the last two decades many design theories for housing slabs on moving clays have been reported (BRAB,1968 ; Fraser and Wardle,1975 ; Walsh,1978 ; PTI,1978). Nevertheless, only a few have an underlying rational basis which permit them to be applied universally, and lead to economical design, whereas others devised empirical formulae were not considered in this text. The general details of the four most commonly used theories are outlined in Table(2.3).

Table(2.3) Summary of general design details of slabs-on-ground (after Holland,1981).

DESIGN METHOD	B.R.A.B. (1968)	P.T.I. (1978)	WALSH (1978)	SWINBURNE
SLAB LOADING AND INITIAL MOUND SHAPE	 RIGID MOUND	 ELASTIC MOUND CUBIC EDGES	 COUPLED WINKLER 'K' PARABOLIC EDGES	 ELASTIC MOUND
ASSUMMED SLAB ACTION	SIMPLIFIED THREE DIMENSIONAL			RIGOROUS THREE DIMENSIONAL
DETERMINATION OF FACTORS CONTROLLING INITIAL MOUND SHAPE	FROM EMPIRICAL RELATIONSHIP WITH CLAY TYPE AND WEATHER $C = 1 - \frac{4e^2}{L^2}$ WITH 'e' ESTIMATED	FROM FOLLOWING - 'e' FROM THORNTWHAITE MOISTURE INDEX - 'y_m' FROM: - CLAY - CLAY MINERAL - SUCTION PROFILE - e - VELOCITY OF MOISTURE	'e' AND 'y_m' HAVE TO BE ESTIMATED	'e' AND 'y_m' ESTIMATED BY PROCEDURES OUTLINED BY HOLLAND AND LAWRENCE
CALCULATION OF "I"	FULLY CRACKED SECTION BEAMS ONLY	UNCRACKED USING ENTIRE CROSS-SECTION	PARTIALLY CRACKED ENTIRE CROSS SECTION	UNCRACKED USING ENTIRE CROSS-SECTION
CONCRETE LONG-TERM "E" VALUE (E_c = 28 DAYS COMP. STRENGTH)	0.5 E_c	0.5 E_c	0.75 E_c	0.5 E_c
SLAB REINFORCEMENT TYPE	REBAR	REBAR AND OR POST-TENSIONED	REBAR	REBAR AND OR POST-TENSIONED

REBAR = BAR AND MESH REINFORCEMENT

Two parameters are considered, shown in Figure 2.15, e and  $y_m$ ,  
 e = edge distance of the mound, and  
 $y_m$  = mound differential heave or settlement.

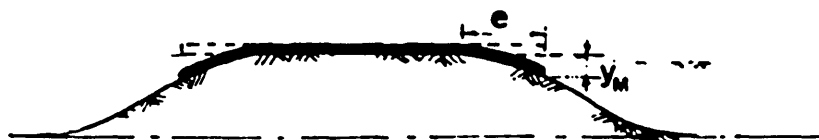


Figure 2.15 Critical design parameters of slab-on-ground (after Holland,1981).

The theoretical background of these techniques is discussed in detail in Chapter 7. The main points to note about these methods are as follows:

(1) It is necessary to accurately define the initial ground mound shape under the slab. With the exception of BRAB (1968), the initial mound shape is defined by the two parameters e and  $y_m$ . BRAB (1968) assumes the initial mound has rigid vertical sides, and defines its shape using a moment multiplier, c, which is called the ratio of the



support. Holland and Lawrance (1980) and Holland and Cimino (1980) have shown that  $c$  can be related to  $e$  by the following expression,

$$e = \frac{L(1-c)}{c}$$

(2) The adoption of either cracked or uncracked section properties was found to have a very significant effect on the moment capacity and the calculated maximum deflection (Holland *et al.*, 1980 ; Holland, 1981). This is due to the fact that for cracked sections, it is difficult to define an allowable value of the concrete tensile stress. Also, the value adopted for the long term Young's modulus of concrete,  $E_c$ , was found to contribute significantly to the calculated slab deflection and the allowable damage thereof. Holland (1981) adopted 50% of the short term  $E_c$ , which allowed in effect, for concrete creep and a lower strength of field cured concrete.

(3) For all the methods except for BRAB (1968), the variation of the soil stiffness (Young's modulus,  $E_s$  or modulus of subgrade reaction,  $k_s$ ) does not influence the slab design. However, BRAB (1968) assumes the mound to be rigid and, thus, no allowance is made for any reduction in  $e$  due to the squashing of the mound, which the other three methods do follow (that is, modifying the ground profile due to application of load).

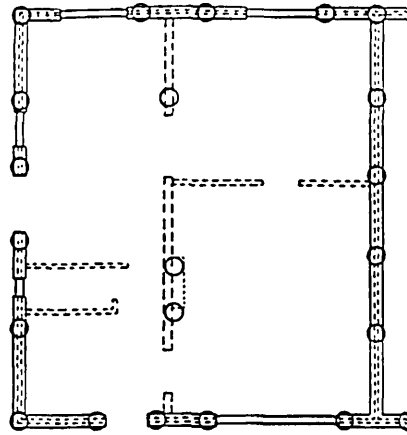
(4) For post-tensioned slabs, Holland and Cimino (1980) concluded that accurate prediction of losses in the cables, concrete and at the slab subgrade interface is difficult. Since the beam depth and cable spacing is dependent on the effective level of prestress introduced, the losses would significantly affect the slab design.

## (II) Piles

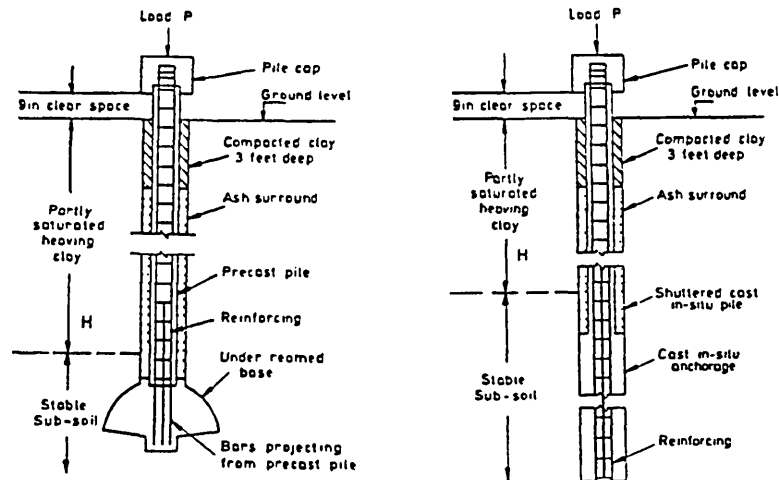
This method is adopted where the use of stiff rafts would result in large differential settlements and intolerable cracking. The bearing of the foundation is carried down to a depth below the change zone, that is, where the soil behaviour is stable (Tomlinson, 1984).

The piles support reinforced concrete grade beams that carry loadbearing walls. They are normally placed at the corners and at appropriate intermediate positions along the walls. In areas of deep water table, piles are founded at not less than twice the depth of seasonal soil movement or on bedrock. They are subject to uplift forces and adhesion which results from the swelling of clays in rainy seasons. Reinforcement is provided to prevent transverse cracking and lifting of

the pile shaft. To economize the shaft length required to resist both bearing and uplift forces, an underreamed bulb end serves to reduce the pull-out forces (refer to Figure 2.16).



(a) Plan showing the position of piles underneath a strip foundation.



(b) Types of piles.

Figure 2.16 Design detail of piles (after Webb,1969 ; BRE,1980).

In mining subsidence areas, buildings on piled foundations are employed because of the overburden conditions on mine roofs. Tomlinson (1984) recommended that piles should be installed at a suitable bearing stratum beneath the workings. In order to reduce the effect of shear caused by horizontal movement of the overburden superstructure, an articulation space between the foundation and the superstructure is provided. The space is filled with a plastic material to prevent it from being filled with accumulated debris. Bitumen resin of 350 mm thickness is used to fill the space and provide a slip surface (Weehuizen,1959 ; Tomlinson,1984).

## CHAPTER 3 ASSESSMENT OF DAMAGE CRITERIA FOR STRUCTURES SUBJECT TO GROUND MOVEMENT

### 3.1 INTRODUCTION

This chapter reviews current criteria of damage, which are necessary for assessment of the structural behaviour of the novel design method described in Chapter 5. Damage in structures has been known since antiquity. The problem was even of concern to Hammurabi who, 4000 years ago, referred to it in his famous code. At present, knowledge of damage in structures has become so general due to heightened awareness on behalf of the general public and client. There are numerous causes of damage, such as settling of foundations, variations in humidity and temperature, excessive deformation of structural members etc., or combinations of these factors. The problem of controlling deformation has become more acute with the introduction of **ultimate** design where structures are becoming more slender and therefore more deformable and susceptible to damage. In comparison with the literature on the design of buildings subjected to ground movement, the question of allowable differential movement has received little attention. Only recently has the influence of ground movement on the performance and serviceability of the structure been included in the design process. Several researchers (Bjerrum,1963 ; Feld,1965 ; Burland and Wroth,1974) had pointed out that there is a need for more observations and experimental investigations on defining the damage limits that a building can withstand. This necessitated the collection of data concerning the limits for tolerance of existing structures of various types and rigidities. Empirical relationships were established for the different types of structures employed to cope with settlement (Meyerhof,1953 ; Skempton and MacDonald,1956 ; Polshin and Tokar,1957). These relationships were dependent upon the following:

- type of structure,
- total settlement, and
- amount and rate of differential settlement (measured as the slope between adjacent supports).

The problem of allowable settlement and the structure-serviceability

relationship was discussed by Burland and Wroth (1974). They introduced the first criterion of damage to include both limiting measures of serviceability and structural interaction with the type of building fabric. One major difficulty in collating data of building damage is the wide variation of symbols and terminologies used for describing the settlement, with respect to both the building and the ground (Burland and Wroth,1974 ; Wahls,1981). Inconsistency within the sets of definitions and terminologies used by different investigators impedes any comparative studies of damage criteria. Since it is not the object of this present research to formulate a code for the different structural deformations, the definitions and terms employed by Burland and Wroth (1974) have been adopted (refer to Appendix 1).

Although when settling, structures exhibit 3-dimensional body deformations and resultant strains and stresses, very little research has been undertaken to define the 3-dimensional behaviour of structures (Bally,1975 ; Hooper,1982). This is attributed to both the difficulty of measuring 3-dimensional deformations compared to those inplane, in addition to the fact that out-of-plane distortion is often thought to be less critical than inplane distortion. A set of symbols defining the behaviour of the superstructure in 3-dimensions is described in Appendix 1. This is intended to provide a method by which basic 3-dimensional settlement terms might be incorporated in a general terminology consistent with an inplane one (that is, of Burland and Wroth,1974), so as to allow inclusion of data collected earlier. As a result, the variables defining the structure and the foundation deformations are (Appendix 1):

- maximum settlement, or heave if the displacement is upwards,
- differential or relative settlement (or heave) between two adjacent supports,
- angular rotation of supports,
- tilt or lateral movement (inplane movement),
- warp or out-of-plane movement, and
- angular twist.

### **3.2 CLASSIFICATION OF DAMAGE DEPENDING UPON THE EXTENT OF BUILDING DEFORMATION**

Buildings experience several stages of deformation when subject to ground movement, however the resulting damage is difficult to

classify as it depends upon a subjective criterion (Burland and Wroth,1974), related to the function of the building and the reaction of the users. Nonetheless, classification of damage is vital in order to assess its extent and appraise the need for remedial repairs and the economic consequences. In providing economical measures for design of foundations subject to heave, Jennings and Kerrich (1962) devised a simple classification relating principally to the ease of repairs. The National Coal Board (NCB) (1975) also developed a classification for damage caused by mining subsidence based upon the general extent of damage and cracking of walls. The Institution of Structural Engineers (1978) adopted both classifications shown in Table(3.1), where reference was made to wall damage, particularly in brickwork masonry. Since the description of damage is dependent upon where cracking occurs in a building, the suggested categorization of damage is difficult to apply. Classification of the degree of damage should include an account of the relation between the underlying causes of differential movement and the consequent damage.

Buildings with relatively large geometry in comparison to the width of the crack, such as multi-storey buildings or warehouses, are normally capable (both from stability and serviceability aspects) of absorbing a higher degree of damage. However, the same damage in smaller buildings (for example, in low-rise houses), would be regarded as unacceptable and requiring repair.

Although the classification in Table(3.1) relates only to visible damage, there is no clear distinction between damage affecting visual appearance, and that affecting serviceability and function. Often, the function of the building or one of its serviceability requirements will tend to influence the classification of damage, that is for primary or secondary structures (refer to Section 2.7), and this was not considered.

### **3.3 CLASSIFICATION OF DAMAGE DEPENDING UPON THE OVERALL STRUCTURAL BEHAVIOUR**

Skempton and MacDonald (1956) first introduced a classification for the degree of severity of damage, based upon a survey of damage to buildings caused by differential ground movement. The deformed structures were classified according to the amount of damage that was visible. By considering its type and severity, damage was grouped into

Table(3.1) Classification of damage (after I.Struct.E.,1978).

Category of damage	Degree <sup>(1)</sup> of damage	Description of typical damage <i>Ease of repair in italic type</i>	Approximate crack width <i>mm</i>
0	Negligible	Hairline cracks of less than about 0.1 mm width are classed as negligible	Up to 0.1 <sup>(2)</sup>
1	Very slight	<i>Fine cracks which can easily be treated during normal decoration. Perhaps isolated slight fracturing in building. Cracks rarely visible in external brickwork.</i>	Up to 1 <sup>(2)</sup>
2	Slight	<i>Cracks easily filled. Re-decoration probably required. Recurrent cracks can be masked by suitable linings. Cracks not necessarily visible externally; some external repointing may be required to ensure weathertightness. Doors and windows may stick slightly.</i>	Up to 5 <sup>(2)</sup>
3	Moderate	<i>The cracks require some opening up and can be patched by a mason. Repointing of external brickwork and possibly a small amount of brickwork to be replaced. Doors and windows sticking. Service pipes may fracture. Weathertightness often impaired.</i>	5 to 15 <sup>(2)</sup> (or a number of cracks up to 3)
4	Severe	<i>Extensive repair work involving breaking-out and replacing sections of walls, especially over doors and windows. Window and door frames distorted, floor sloping noticeably<sup>(3)</sup> Walls leaning<sup>(3)</sup> or bulging noticeably, some loss of bearing in beams. Service pipes disrupted.</i>	15 to 25 <sup>(2)</sup> but also depends on number of cracks
5	Very severe	<i>This requires a major repair job involving partial or complete re-building. Beams lose bearing, walls lean badly and require shoring. Windows broken with distortion. Danger of instability.</i>	usually greater than 25 <sup>(2)</sup> but depends on number of cracks

- Notes: 1 It must be emphasised that in assessing the degree of damage account must be taken of the location in the building or structure where it occurs, and also of the function of the building or structure.
- 2 Crack width is one factor in assessing category of damage and should not be used on its own as direct measure of it.
- 3 Local deviation of slope, from the horizontal or vertical, of more than 1/100 will normally be clearly visible. Overall deviations in excess of 1/150 are undesirable.

three categories by Burland et al. (1977) namely,

- aesthetic or architecture,
- serviceability or function, and
- stability.

The first category is concerned primarily with the appearance of the building, that is, the lining of windows and doors, verticality of walls, etc. Thus, the aesthetic limit varies with respect to the type of structure, for example, the limits of primary structures are more strict than those of secondary ones. The second category would comprise limits of cracking and distortion which impair the weather-tightness or any other function of the structure, such as sound insulation of an infill panel, jamming of windows and doors, or leakage of roof and upheaval of floor slabs. The third category is concerned with part or the whole of the structure where there is some risk of collapse, for example increased tilting of towers, fracture of drainages and pipelines, or severe cracking of gable walls, etc. (I.Struct.E.,1980). Since this classification does not define the degree of damage with any measureable quantity, it is influenced by the judgement of the individual observer. Attractive in its broader form, the method is used by several investigators to distinguish between the different phases in building deformation.

### 3.4 REVIEW OF DAMAGE CRITERIA

A clear, unambiguous damage criterion is essential in order to establish a correlation between the differential movement of the structure or the ground, and the visible damage experienced by the building. Various methods of analysis have been proposed based upon different techniques of assessment of damage or cracking. Perhaps the earliest known study was that of the limiting settlement of structures by Skempton and MacDonald (1956), based upon two classifications, damaged or undamaged structures by use of an angular distortion term. However, this attracted criticism concerning its broad application as a design guideline (Terzaghi,1956 ; I.Struct.E.,1978). There is a tendency, moreover, to follow these guidelines without account being taken of the limitations of that study. To better classify the extent of possible application of each criterion, the different criteria are categorized according to the basis of the formulation of the

serviceability limits with the differential movement encountered, namely,

(a) Empirical methods were developed based on statistical surveys of settlement data for a large number of damaged buildings. This method can not offer a unified basis for damage criteria for the following reasons (Burland and Wroth,1974 ; I.Struct.E.,1978):

1. The criterion is limited to the range of structure surveyed, that is type of structure.
2. The criterion is limited to the type of structural material.
3. The limitations of the criterion are due to the conditions and form of ground movement.
4. A unified criterion should include both structural calculation and examining of details of the building and finishes with the objective of checking serviceability, that is, serviceability-structural interaction (Burland et al.,1977).
5. The relation should correlate between the degree of damage and a measureable parameter.

(b) Theoretical methods involve the choice of a structural model that correlates between visible damage and differential settlement, that is, between the serviceable limit of the building fabric and the structural behaviour subject to ground movement. However, a complete analysis including both the ground movement and the cladding of the structure would be highly complex and contain a number of questionable assumptions. Although theoretical methods are favoured due to the ease of application of their recommended guidelines in design, their predictions should be bounded by the lower limit of observed damage. Since each method is dependent upon a theoretical model, its sensitivity is limited by the choice of the boundary conditions, the prescribed deformation mounds, and the rate of settlement. Furthermore, difficulty lies in defining the serviceability limit and the mode of failure, that is, crack initiation and propagation through the structure (Attewell et al.,1986).

#### **3.4.1 Empirical methods**

Terzaghi (1935) observed that settlement of brick walls caused the most distress in buildings at a maximum cracking stress of 60 lb/in.<sup>2</sup> and a corresponding angular distortion of  $3.5 \times 10^{-3}$  radians, equivalent to  $\delta/L$  of about 1/1000 (L is defined as the distance between



two adjacent reference points). In order to have some margin of safety, a maximum differential settlement  $\delta/L$  of  $1/2000$  and a tensile stress of  $30 \text{ lb/in.}^2$  was recommended for buildings with load bearing brick walls or continuous brick cladding.

Short and Simms (1949), from a survey of tests on post-war houses, expressed the allowable settlement in terms of deflection to span ratio. Each part of the building was examined after being subjected to its allowable deflection, and the percentage recoverability of the stiffness of the individual members was reported based upon the extent of repair required. The allowable deflection of floors, roofs and wall panels was found not to exceed  $1/300$ th of the span; the recoverability of stiffness for reinforced concrete and steel beams varied between 80%-90%, while that of brickwork was in the range of 70%-75%.

Terzaghi and Peck (1948), from a study of settlement records, observed that most ordinary structures, such as office buildings, apartment houses or factories, can withstand a differential settlement of  $3/4$  in. without any cracking. Introducing new parameters in the study of settlement, namely, the rate of settlement and the type of foundation, buildings constructed over uniformly loaded continuous footings with flexible raft foundations were able to deform up to 2 in. This was due to the smoothing out of the effects of non-uniformity of the soil (Tschebotarioff, 1951).

Rigby and DeKema (1952), restrained the cracking of brickwalls by using light reinforcement; they observed visible damage at a central deflection of 0.05-0.08 in., i.e.  $\Delta/L = 1/4500-1/7000$ . Capper (1953) proposed that the maximum differential settlement between two adjacent walls or columns should not exceed a certain fraction of the span between the supports. However, these limits were classified against different types of interior finishes and structural forms.

Meyerhof (1953) employed Capper's method to classify the differential settlement according to the type of structure. A limiting "angular distortion" of  $1/250$  for open frames,  $1/500$  for infill frames, and  $1/1000$  for loadbearing walls or continuous brick cladding was suggested if aesthetic damage was to be prevented.

Rausch (1955) reported a series of experiments in order to study the behaviour of walls made of hollow bricks and concrete, 12-15 m long and 6 m high, under the action of mining subsidence. Walls were erected upon steel beams that were vertically deflected by hydraulic jacks mounted on springed floor-anchorage. Their object was to maintain a constant radius of curvature for the whole of the supporting beam during testing. Radii of curvature in the range of 10000-500 m were applied both at sagging and hogging modes in cycles. To facilitate deflection of the wall without introducing shear at its base, rubber cylinders were used to simulate horizontal flexibility of the ground.

Damage caused by hogging was generally greater than that due to sagging, particularly if a tension beam was present at the wall soffit. Most cracking occurred near openings and in the vicinity of applied loads; in some cases, torsional cracks were observed but were smaller in size. Rausch concluded that most cracks were caused by diagonal shortening of the wall, causing tension at the shortened inside of the opening and the elongated outside of the opening (refer to Figure 3.1).

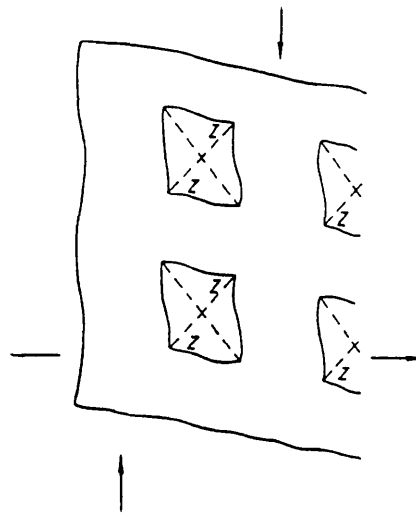


Figure 3.1 Distortion mode of wall with openings under sagging (after Rausch, 1955).

Large crack widths, of 16-20 mm, were recorded for a hogging mode, and 5-15 mm for sagging, with a maximum radius of curvature of 500 m and a maximum differential movement of 20-40 mm. However, a tensile stress of 3-5 N/mm<sup>2</sup> was recorded at the minimum visible crack width, that is, 2-3 mm. Ring anchors provided at half and full wall height reduced cracking for both sagging and hogging, and a tensile stress of 10-15 N/mm<sup>2</sup> was measured at a crack width of not more than 1 mm. A

comparison of the damage patterns of various tests indicated that cracking was delayed when using lime mortar; however, this did not alter the pattern of the cracking, rather, the level of stress in the wall at which cracking was visible decreased.

Skempton and MacDonald (1956) reviewed the settlement of 98 buildings, including both steel and reinforced concrete frame structures, and loadbearing walls. Influence of the foundations on the level of damage was studied, for example, spread footings, mats and piles, while various types of damage in panel walls, interior partitions, floors and structural members were reported. Since most of the damage collated was related to distortional deformations, the criterion for damage used was the ratio of the differential settlement and the distance L between two reference points. Eliminating the tilt parameter for the building deformation, the above criterion was defined as the angular distortion. Figure 3.2 illustrates the definitions of "maximum angular distortion",  $\beta$ , maximum settlement,  $\Delta_{\max}$ , and greatest differential settlement,  $\delta$ , for a building with and without tilt. It was concluded that the limiting angular distortion that is likely to cause cracking in walls and partitions is 1/300 and that values of  $\delta/L$  greater than 1/150 will cause structural damage. Skempton and MacDonald suggested a limiting  $\delta/L$  of 1/500 as a design guideline that would provide some factor of safety against cracking. Assuming that the angular distortion is linearly dependent upon the maximum settlement, they established a correlation expressed by the following equations:

$$\begin{aligned}\beta &= \delta/L - w \\ \rho_{\max} &= k\delta/L \\ \text{or } R &= \frac{\delta/L}{\rho_{\max}} = 1/k\end{aligned}$$

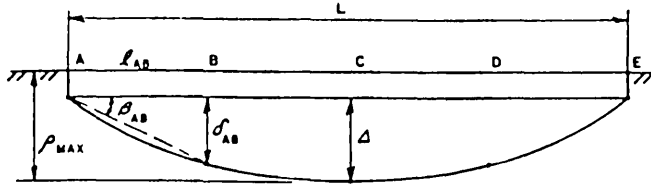
where  $\rho$  = vertical displacement,

$w$  = tilt (rigid body rotation),

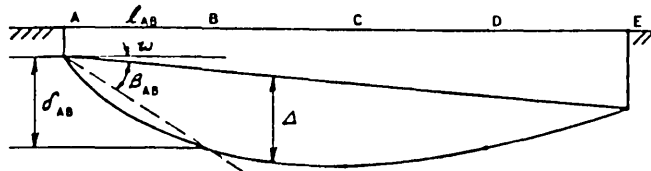
$R$  = ratio of distortion to settlement, and

$k$  = constant depending upon type of foundation and subsoil (refer to Table(3.2)).

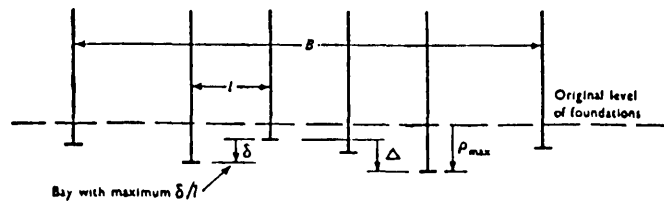
Although the above assumption is influenced by a number of parameters, such as the uniformity of the ground, distribution of loads over the subsoil, width of building and rigidity of the superstructure, the correlation was simple to apply. However, this required both



(a) Settlement without tilt.



(b) Settlement with tilt.



(c) Definition of settlement terminology.

Figure 3.2 Definitions of building settlement with and without tilt (adapted after Skempton and MacDonald, 1956).

experience and judgement to be incorporated in design guidelines.

Also, a correlation between the greatest differential settlement and the angular distortion was established, however this was limited to deformations of structures without any tilt component,

$$\Delta = h\delta/L$$

where

$\Delta$  = greatest differential settlement with no tilt, taken as the difference between the maximum and the minimum settlement of a building;

$h$  = constant depending upon type of subsoil, where  
 for clays,  $h = 550$ ,  $\rho_{\max} < 1.75$  in., and  
 for sands and fillings,  $h = 350$ ,  $\rho_{\max} < 1.25$  in.

Table(3.2) Values of k and corresponding values of  $\rho_{\max}$  for the damage limits, when  $\delta/L = 1/300$  (collated after Skempton and MacDonald,1956).

	Isolated Foundations		Rafts	
	Clays	Sands	Clays	Sands
k	1000	600	1250	750
$\rho_{\max}$ (in.)	3	2	4(3-5)	2.5(2-3)

Polshin and Tokar (1957) presented a survey of observations of settlement of civil and industrial buildings in the USSR and included an allowable settlement criteria from the 1955 USSR Building Code. The structure deformation was expressed by three terms, namely:

- 1) Slope, measured as the difference of settlement of two adjacent supports relative to the distance between them,
- 2) Relative deflection, which defines the ratio of deflection to the length of the deflected member, and
- 3) Average settlement under the building.

Of particular interest is that different types of structures were treated separately in the evaluation of their respective limiting deformation, as the case for frame structures and continuous loadbearing structures. This is attributed to the interaction of the rigidity of the superstructure and the subsoil during settlement (Bab,1954). For rigid types of structures such as concrete or steel framed infilled structures, the slope term was used with a range of 1/200-1/500 for no damage.

Polshin and Tokar's treatment of loadbearing walls introduced several significant concepts. First, instead of "slope", the allowable settlement was defined in terms of relative deflection. Secondly, the maximum allowable deflection ratio was related to the development of a critical level of tensile strain in the wall, which for brick walls was taken as 0.05%. Thirdly, the onset of visible cracking in brick walls was related to the ratio of the length to height, L/H of the walls.

Finally, for multi-storey brick buildings, a larger deflection ratio was recommended for structures supported on plastic clay than for those on sand or hard clay. This is due to the slower rate of settlement of plastic clays that allows time for creep of the structure,

thus accommodating larger differential settlement. For an aspect ratio of  $L/H < 3$ , a maximum relative deflection in the range of  $3-4 \times 10^{-4}$  and for  $L/H > 5$ , a range of  $5-7 \times 10^{-4}$  were recommended. For longer walls, that is  $L/H = 8$  for example one-storey mills, an allowable relative deflection of  $1 \times 10^{-3}$  was suggested.

A relationship between the ultimate relative deflection of walls, "f", and the aspect ratio  $L/H$  ( $L$  = length of wall between settlement joints,  $H$  = height of wall from footing) was derived from observations shown in Figure 3.3.

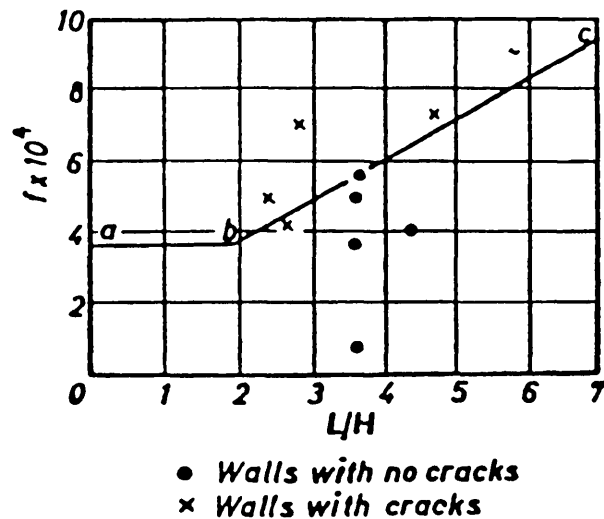


Figure 3.3 Relation between relative deflection of brickwalls and aspect ratio of walls (after Polshin and Tokar,1957).

This illustrated that there was no influence of the wall aspect ratio for  $L/H < 2$  on the variation of limiting strain to cause damage. However, for higher aspect ratios ( $L/H$ ), a decrease of the limiting relative deflection was noted, possibly due to the increase of lateral distortion of walls and shear failure of shallow wall panels. It is of interest to note when comparing the USSR standard for brick buildings on flexible foundations to that for rigid framed buildings, the average settlement allowed was in the same order particularly for brick buildings of lower  $L/H$  values. Although this does not seem realistic, the authors explanation relied upon the acceptability of cracked brick buildings in comparison to rigid concrete structures.

Bjerrum (1963), from observations of damaged structures, described the allowable angular distortions of different types of

structures with respect to their operation, as shown in Table(3.3).

Table(3.3) Limiting damage criteria with respect to the angular distortion as proportion of span (after Bjerrum,1963).

$\frac{1}{100}$	$\frac{1}{200}$	$\frac{1}{300}$	$\frac{1}{400}$	$\frac{1}{500}$	$\frac{1}{600}$	$\frac{1}{700}$	$\frac{1}{800}$	$\frac{1}{900}$	$\frac{1}{1000}$
									\$ Limit where difficulties with machinery sensitive to and settlements to be feared.
									\$ Limit of danger for frames with diagonals.
									\$ Safe limit for buildings where cracking is not permissible.
									\$ Limit where first cracking in panel walls is to be expected.
									\$ Limit where difficulties with overhead cranes are to be expected.
									\$ Limit where tilting of high, rigid buildings might become visible.
									\$ Considerable cracking in panel walls and brick walls.
									\$ Safe limit for flexible brick walls, $H/L < 1/4$ .
									\$ Limit where structural damage of general buildings is to be feared.

An attempt was made to relate the degree of damage to the limiting relative deflection based upon the following factors:

- the time factor, the slower the occurrence of settlement the larger the distortional settlement a building is able to withstand without experiencing much damage,
- sequence and method of construction, and
- other types of cracks occurring in a building due to reasons other than differential settlement, for example, load creep, material shrinkage, or variations of temperature or humidity.

Mayer and Rusch (1967) investigated various types of damage to buildings, particularly to partition walls made of block, and concrete walls caused primarily by excessive deflection of reinforced concrete structural members. Damage was grouped according to the different causes, namely, the support conditions, the shape of walls (especially wall returns, T-section in plan, etc.), and the effect of flexibility of the supports. Although flexibility of structural members depends upon the slenderness ratio, Mayer and Rusch found that it was an inaccurate method to relate that directly to limiting deflection. This is because such a relation would depend upon the structural form and, as a result, empirical factors would be included relating the condition of the walls and the degree of damage encountered. Deformation was defined by five main parameters, that is, maximum deflection, relative deflection, maximum curvature, maximum end rotation and tangent of slope of the deflected part. A limiting degree of sagging,  $f = L/300$ , was observed just before the occurrence of visible damage, defined by jamming of doors, cracking of partition walls or initiation of horizontal cracks separating walls and ceilings or floors. A theoretical formula defining the lower limit of damage in partition walls was proposed, depending upon the allowable deflection of the supporting beam or the slab, as shown below,

$$\frac{f_{sch}}{L} \leq \frac{1}{L_i}$$

where  $L_i = k_i L$ , effective span of supporting beam or slab,

$$k_i = 0.8 \left[ \left( \frac{2X_1}{M_k} + \frac{4M_o}{M_k} + \frac{4X_2}{M_k} \right) \frac{L}{L_k} + 3 \right], \text{ effective span constant,}$$

$f_{sch}$  = limiting value for visible damage, that is, 0.001 for partition walls,

$X_i$  = bending moment at support "i", and

$M_i$  = bending moment at distance "i" from support, while "o" denotes maximum distributed moment.

From observations of 259 cases of damage, Mayer and Rusch also defined the lower limit of damage in partitions caused by construction mistakes, workmanship errors and design faults, (Figure 3.4) as,

$$\frac{L_i}{h} \leq \frac{150}{L_i}$$

where  $h$  = depth of the supporting beam or slab.



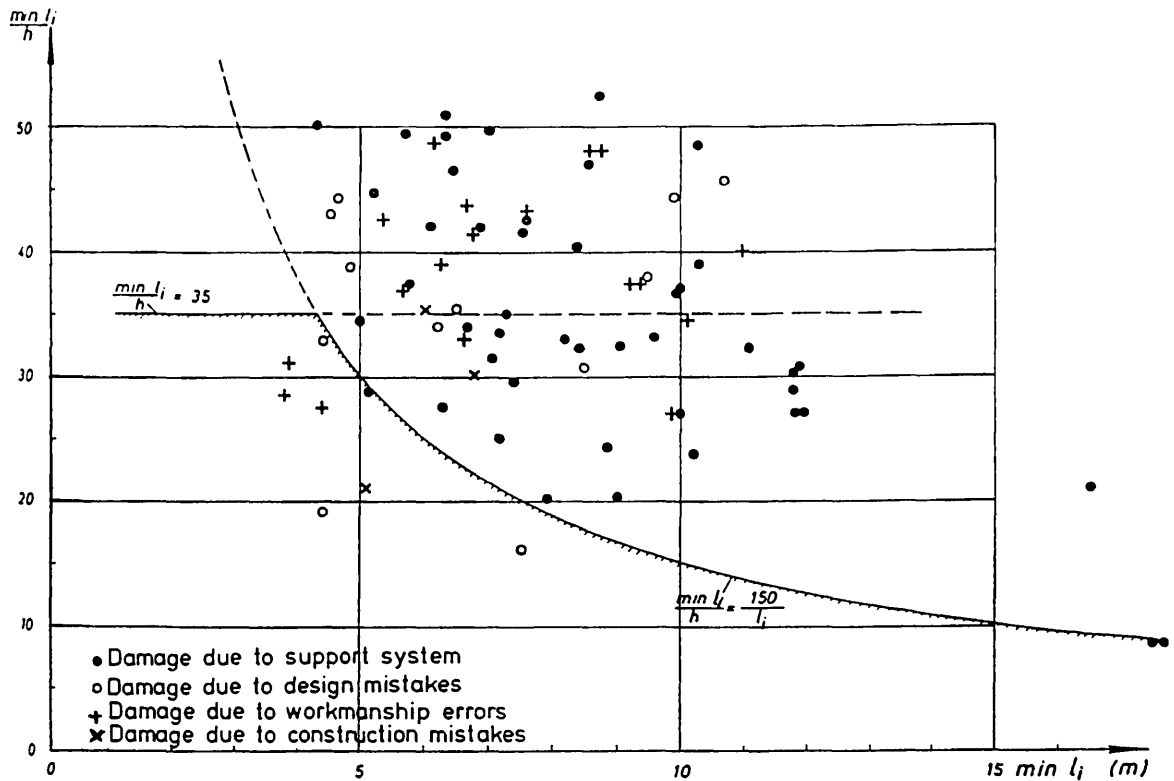

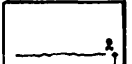

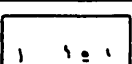
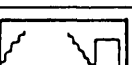
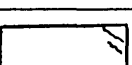
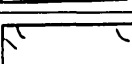
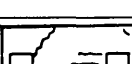
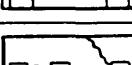
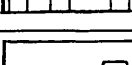
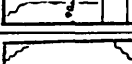
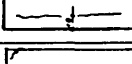
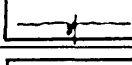

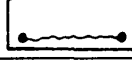




Figure 3.4 Limiting deformation of partition walls (after Mayer and Rusch, 1967).

Centre Scientifique et Technique de la Construction (CSTC) (1967) studied the limiting relative deflection for various brick and concrete masonry walls subject to either differential movement of supports or excessive deflection of slabs. Wall geometry was also included as a parameter influencing the deformation behaviour during settlement; this was defined by the aspect ratio of the wall ( $L/H$ ) and the presence of wall returns. When loaded over a long period, larger relative deflection before cracking was visible in the walls, compared to short term deformations; refer to Table(3.4). Wall openings influenced the pattern of cracking and damage and, in most cases, the openings initiated larger cracks that reduced the allowable deflection limit. Damage of solid walls was in the form of horizontal cracks, occurring at 200 mm from the base of a wall, while for walls with openings, inclined cracking was dominant. Of interest was the influence of cross walls on increasing the limiting deflection ratio for a wall with three openings. In this case, a limiting deflection ratio of  $1/350$  was recorded, while for a wall with one opening with no returns, the limiting deflection was of the same order. However, comparison of walls with openings showed that if the openings were suitably placed so as to avoid crossing the

Table(3.4) Summary of limits of damage (collated after CSTC,1967).

Test No.	Building material (masonry walls)	Aspect ratio L/H	Deflection ratio		Forms of fissures
			short term	long term	
1	Cellular concrete	1.33	1/1050	1/488	
2	Clay bricks	1.51	1/750	1/340	
3	Cellular concrete	2.07	1/2700	1/1080	
4	Cellular concrete	1.83	1/610	1/277	
5	Cellular concrete	1.77	1/480	1/220	
6	Cellular concrete	1.40	1/720	1/327	
7	Clay bricks	1.45	1/1000	1/465	
8	Cellular concrete	3.50	1/590	1/295	
9	Cellular concrete	2.00	1/590	1/295	
10	Cellular concrete	1.40	1/530	1/245	
11	Cellular concrete	2.60	1/223	1/109	
12	Clay bricks	1.98	1/360	1/167	
13	Clay bricks	2.86	1/740	1/342	
14	Clay bricks	2.32	1/1090	1/515	
15	Clay bricks	3.02	1/750	1/348	
16	Clay bricks	2.10	1/150		
17	Clay bricks	1.97	1/360	1/107	

paths of maximum principal stresses in the walls, the allowable deflection ratio was improved by 38%-42% (Table(3.4)).

**Building Research Advisory Board (BRAB) (1968)** categorized damage limits based upon the type of the superstructure with particular reference to flexible structures, such as wooden frames (refer to Table(3.5)). Classification of damage to partition walls was influenced by the type of finishing material which affected the amount of damage that could be tolerated by the user of the building.

Table(3.5) Allowable deflection ratio (after BRAB,1968).

Type of Superstructure	Damage Limit $\Delta/L$
Wood frame and cladding	1/200
Unreinforced loadbearing wall	
-unplastered	1/300
-plastered	1/360

**Pfeffermann (1968)** analysed damage of buildings caused by settlement of foundations and excessive deformation of supports by examining the factors affecting cracking and devising preventive measures and remedies for damage. To study the forms of manifestation of cracks, principle causes of foundation movement were reviewed; damage was caused both by soil movement and structural movement. Lack of joints and excessive anchorage of the structure caused as much damage as settlement of foundations and watering of plastic soils. Generally, cracks formed near openings of doors and windows, where the width of cracks was found to vary seasonally. Damage caused by excessive support movement was categorized separately, since the allowable deflection was dependent upon the rate of settlement, that is, long-term and short-term damage. To prevent crack initiation in partition walls, intermediate supports were provided every 3-4 m. However, for structural deformation due to soil movement, strengthening of walls or compensation of settlement by jacking was used to eliminate visible damage. Damage to walls was found to occur in three forms; the first was horizontal cracking occurring at 250 mm from wall base, and caused by excessive deformation of the supporting beam. The second form was if the beam

deflected more than the wall, then vertical cracks were initiated. Thirdly, in other cases, diagonal cracking propagated from the wall corners defining the failure pattern; this occurred if two adjacent walls settled at their intermediate support. Twenty-seven full scale walls were tested to determine the effects of both wall openings and aspect ratio on the limiting allowable deformation of brick and concrete block walls. Wall loading was applied by dropping intermediate supports, hence the wall was subject to sagging. Allowable relative deflection of 1/400 was measured at a crack width of 2-4 mm when T-shape walls were tested. However, a relative deflection in the range of 1/550-1/1500 was recorded for single leaf walls, with the minimum aspect ratio of the wall experiencing the largest deflection before reaching the serviceability limit, that is, a crack width of 2-5 mm.

**Horn and Lambe (1964)**, in their survey of settlement on the MIT Campus, presented a deflection parameter, namely, settlement distortion ( $\Delta/L$ ), in which L was defined as the distance between two points on the settlement curve and  $\Delta$  the maximum offset between the building profile curve and the chord joining the two points. It was concluded that an average settlement ratio of 1/1600 was sufficient to cause considerable structural cracking in brick or masonry elements. While **Beeby and Miles (1969)** proposed a limiting deflection of  $\Delta/L = 1/350$  for framed reinforced concrete structures, that would restrict both the visual offence of floor unsuitability and damage to finishes, partitions and renderings of walls. By comparison, Horn and Lambe's criteria of local deformation in buildings eliminated any tilt, thus leading to a more conservative allowable movement. However, application of this method depends upon defining the complete profile of the settled ground; in practice this is difficult.

**Comite Europeen du Beton (CEB) (1973)** investigated building damage caused by excessive deformation of reinforced concrete beams and slabs. They concluded that it is difficult to employ rational deformation criteria because of complication of structural deformation due to non-structural parts, that is, partition walls. Classification of damage was based upon monitoring the influence of partition walls on the overall deformation of the structure. This was achieved by defining damage in two groups. The first group comprised rigid partition walls which were locked into the structure; the second consisted of those

which were unlocked between the ceiling and floor, refer to Table(3.6).

Table(3.6) Allowable deformation of rigid partitions (collated after CEB,1973).

Causes of Damage	Partitions locked in structure	Partitions unlocked in structure*
Support misalignments	L/300 - L/750	H/500
Floor deformation	Subject to racking shear	L/200

\* Unlocked, that is, having either vertical joints or not completely fixed to roof, and

H = Height of the partitions.

Grant, Christian and Vanmarcke (1974), in an updated survey of damaged buildings by Skempton and MacDonald (1956), included 95 buildings in addition to the original 98 of Skempton and MacDonald. A close agreement of the 1/300 "slope" limit of Skempton and MacDonald was found and recommended to include functional relations dependent upon the foundation type and the soil condition between the maximum  $\delta/L$  and the maximum settlement. Limiting radius of curvature of the ground of 1/1000 was also recorded for no visible damage. Nonetheless, no added advantage was obtained by employing the curvature parameter. A maximum allowable differential settlement of 30 mm for buildings on sand and 56 mm on clay was recommended as an upper limit for design guidelines.

Walsh (1975,1978) and Holland (1981) tested ground slabs of residential buildings subject to uplift pressures due to expansive soils. Experiments on several slabs in order to determine the effects of articulation of superstructures showed that brick veneer accommodated larger deformation than solid brick walls. Basing their observed deformation on the curvature of the ground profile, full scale tests of residential buildings experiencing visible cracking at the allowable curvature deflection ratio were reported (Table(3.7)).

Starzweski (1974), based upon Polish practice, related the limiting allowable settlements ( $\Delta_{max}$ ) and angular strains with the

Table(3.7) Allowable curvature deflection ratio (collated after Walsh,1975 and Holland,1981).

Type of Superstructure	$\Delta/L$
Stucco timber and articulated brick veneer	1/250
Brick veneer	1/500
Fully articulated solid brick	1/1000
Solid brick	1/2000

Table(3.8) Classification of damage according to the structural form (collated after Starzweski,1974).

Building class	Type of building	Maximum settlement (mm)	Maximum allowable angular distortion
1	Massive structures highly rigid about horizontal axis	50-200	Tilt parameter is more critical, Tilt $< H/100-H/200$
2	Statically determinate structures	100-150	1/100-1/200
3	Statically indeterminate structures with		
	A- Rigid foundation	80-100	1/200-1/300
	B- Isolated footing	60-80	1/300-1/500
4	Prefabricated structures	50-60	1/500-1/700

strength of building or structure. Four groups of structures were classified, mass structures, rigid structures-either statically determinate or indeterminate and prefabricated structures. Notably, the serviceability limit of mass structures was more controlled by tilt rather than by differential movement, refer to Table(3.8). This is not the same for determinate structures, which exhibited larger allowable angular strain compared to indeterminate structures.

Leonards (1975) discussed the tilt parameter in the assessment of

damage to structures and its influential factors, that is, the type of structure and the type of foundation. In the case of framed structures supported by isolated footings, the critical deformation was associated largely with foundation displacement, and also with the rotation of the supports. If the footings were free to rotate during settlement, induced strain in the frame was dependent upon the angular distortion due to the rigid body rotation of the superstructure with no tilt parameter. If rigid foundations were employed, thus restraining relative rotation of supports, the critical parameters were both the angular distortion and the tilt term.

Bally (1975) analysed 3-dimensional differential settlement in buildings using three different parameters, namely, tilt, unit rotation of the supporting beam, and the ratio of minimum to maximum settlement. Since the above parameters were found to vary considerably, statistical data processing of damage to buildings was adopted to study the influence on the maximum allowable settlement. For a 90% probability limit of no damage, Bally concluded that tilt should not exceed 6% nor rotation 0.8% per 10 m bay length. Table(3.9) shows the limiting differential settlement and associated damage for rigid structures resting on compacted soil.

Table(3.9) Limiting tilt, rotation and maximum settlement for rigid buildings (after Bally,1975).

Maximum settlement $S_{max}$ (mm)	Maximum tilt	Maximum torsion	$\frac{S_{min}}{S_{max}}$
0-20	$0.25 S_{max}$	$0.04 S_{max}$	$0.025 S_{max}$
20-50 *	5	0.8	0.5

\* These represent the maximum allowable values and should not be exceeded even if larger settlement was to occur.

O'Rourke, Cording and Boscardin (1976) presented correlations of architectural damage to buildings based upon both vertical settlement and lateral displacement. Lateral displacement caused by nearby excavations or downdrag due to settlement of adjacent buildings was

defined as the differential lateral movement between two points, divided by the distance separating them. Rigid body tilt was also considered, with reference to tall, stiff structures and squat buildings. They concluded that at the threshold of noticeable damage, the limiting tilt was in the range of 1/180-1/200 of the height of the building.

Structural damage to loadbearing brickwalls was categorized according to the direction of the ground movement perpendicular or parallel to the bearing walls. As brick buildings are more sensitive to movements perpendicular to the bearing walls, O'Rourke et al. observed that soil deformation in this direction due to large displacement of the bearing walls caused the loss of floor support. This was due to the roof joints being pulled out of the loadbearing masonry pockets. Ground movements parallel to the bearing walls caused bending, shear and direct tensile distortion of the bearing walls, but the floor supports in this case were affected insofar as the strains induced in the walls. This resulted in local deterioration of the masonry-joint connection. As a result, recommendations for the minimum safe bearing lengths of the roof joists were grouped with respect to the strength of masonry and function of the building. For low strength mortar (lime mortar), the recommended bearing length was 45 mm for domestic buildings and 65 mm for commercial ones; while for high strength mortar, the limiting lengths were 23 mm and 33 mm, for domestic and commercial buildings, respectively.

**Post Tensioning Institute (PTI) (1978) and Wray (1978)** classified damage limits for articulated structures based upon the relative deflection ratio of the walls for visible cracking of the finishes. Post-tensioned slabs were used in areas subject to upheaval pressures so as to provide a precompressed "slab-on-ground", able to accommodate higher tensile strains, and thus reducing the size of cracks in residential slabs. In some cases the slabs were strong enough to induce damage in the superstructure before experiencing any excessive curvature. A classification was thus chosen in order to define the optimum deflection ratio of slabs. However, the classification depended upon some degree of judgement on the choice of type of superstructure, especially for brick buildings (Table(3.10)).

**Alexander and Lawson (1981)** suggested that crack width be included as a subjective serviceability limit for walls, as defined by Burland et al. (1977), while for design an allowable deflection limit of



Table(3.10) Recommended relative deflection ratio for no damage  
(collated after PTI,1978 and Wray,1978).

Type of superstructure	Damage limit ( $\Delta/L$ )
Wood frame and cladding	1/200
Unreinforced loadbearing walls	
-completely articulated	1/500
-partially articulated	1/800
Solid masonry or cavity walls	1/1500 - 1/2000
Brick veneer	
-articulated	1/300
-standard	1/500

reinforced concrete members of 1/200 was proposed. Since differential settlements mostly affected the masonry walls in the case of infill frames or loadbearing walls, structural movements were grouped into two classes:

- large movement sustained by loadbearing walls in sagging or walls confined by a perimeter frame, and
- small movements only sustained by walls in hogging.

For infill panels, they concluded that external restraint on the edges increased shear deformation, causing cracking by diagonal tensioning at an equivalent shear strain of about  $1500 \times 10^{-6}$ . Since, in brickwork the strain capacity is small enough that some degree of inplane cracking would be tolerated, this could be distributed in such a way that local extreme cracks would be avoided. The effect is to include crack width as an upper bound criteria for serviceability.

Yokel, Salomone and Gray (1982) proposed three recommendations for residential housing in areas of mining subsidence. Firstly, to avoid visible damage, the horizontal ground strains induced in the building should not exceed 0.1%. Alternatively, the ground slope is limited to a range of 1/200-1/300 for most types of structures. Thirdly, the total settlement of a building should not exceed 40 mm in sands or 80 mm in clays if structural damage is to be avoided.

Yokel et al. divided structures according to the rigidity of the foundations. Rigid foundations were designed to take an unsupported length of 6 m or 0.67L, whichever was the smaller. Based upon curvature

criteria derived from NCB (1975) (refer to Section 3.4.2(a)) for medium subsidence, the threshold of visible cracking in the superstructure was noticed at a tensile ground strain of 0.001. A tilt of 1/200 was considered not to be disruptive in small buildings. Flexible foundations were designed to resist the moments and shears resulting from the anticipated curvature of the ground profile. A simple relation between the radius of curvature and the induced moment and shear at ground level was established for a critical length of the foundation,  $L_c$ . If flexibility of the design was achieved by articulation, the foundation elements were designed separately. However, if the length of the building was to exceed  $L_c$ , a completely rigid foundation was recommended. Length of the critical location,  $L_c$ , was taken as a function of the shape of the subsidence profile and the bending stiffness of the foundation element. Of interest is that for a case of tensile ground strain (that is, hogging mode), Yokel et al. recommended  $L_{ct}$  to be smaller than the value adopted for compression, in order to limit damage caused by hogging.

In the tension zone,  $L_{ct} = \sqrt{\frac{2EI}{Rw}}$

and in the compression zone,  $L_{cc} = 2\sqrt{\frac{EI}{Rw}}$

where EI = flexural rigidity of foundation element,

R = radius of curvature of the foundation, and

w = gravity load uniformly distributed onto the foundation element.

### 3.4.2 Theoretical methods

The main aim of theoretical methods is to correlate mathematically the relationship between the criteria of damage and the building deformation. Three fundamental concepts of theoretical modelling are reported.

#### (a) Radius of curvature

Rosenhaupt (1964) related the ground settlement to the curvature of the deformed building. Approximating the line of curvature to a parabola, the radius of curvature, R, was represented by,

$$R = L^2/8f$$

where L = total length of building, and

f = maximum deflection.

Although it is difficult to measure the ground curvature, the method was used to correlate damage caused by expansive soils mounds for the following reasons:

- the movement of ground was expressed by the curvature of the deformed building using a simple relationship, that is, linearly proportional to  $1/R$ , and

- the formulae relating the strains and crack width in the wall with the radius of curvature were much simpler than relating these terms with the gradient, that is, the limiting relative settlement.

A series of experiments to test the validity of the proposed method found that the maximum crack width varied linearly with  $1/R$ . A critical value of  $R_c$ , namely the yield point radius of curvature, was defined as  $R_c = 1500$  m (500 ft.) for all types of masonry, where if  $R < R_c$ , the rate at which a crack opened increased beyond serviceability. Different methods were employed to reduce cracking of the walls by stiffening masonry with upper and lower course beams, in addition to columns confining the masonry walls (Rosenhaupt and Mueller, 1963). Another method of confinement was by providing prestressing rods to clamp down the walls between the roof and the floor slabs (Rosenhaupt, Beresford and Blakey, 1967). The latter arrangement caused an increase in the radius of curvature to 2100 m where a maximum crack width of 1-2 mm was reported.

**National Coal Board (NCB) (1975)**, from an extensive study of mining subsidence effect on buildings, the NCB developed a criterion based upon the differential slope or curvature of the ground profile. Buildings were divided into bays and panels, in which each bay was assessed individually. Formulation of the ground strain from curvature was found to be proportional to subsidence and inversely proportional to the depth of the seam. This is represented as follows,

$$\text{Radius of curvature, } = \frac{(\text{Bay Length})^2}{\text{Second differential of subsidence}}$$
$$\text{Average allowable strain, } = \frac{K S_{\max}}{H}$$

where  $S_{\max}$  = maximum possible vertical movement of a point on the surface due to subsidence, and

H = vertical distance between floor of seam being extracted and

any arbitrary datum (usually the ground surface).

This representation was found to be very cumbersome when applied to wide structures, since the ground profile would vary considerably. This meant that the average allowable strain was influenced by the ratio of the width of the panel to the height of the seam  $w/H$ . Approximating the profile to a part of a circle, the strain was deduced from the curvature, however this raised the following points:

1) The smaller the radius of curvature,  $\rho$ , the greater is the strain; thus the strain is proportional to  $1/\rho$ . From Figure 3.5, considering  $\theta$  to be small, then  $L = \rho\theta$ , that is strain is proportional to  $\theta/L$ .

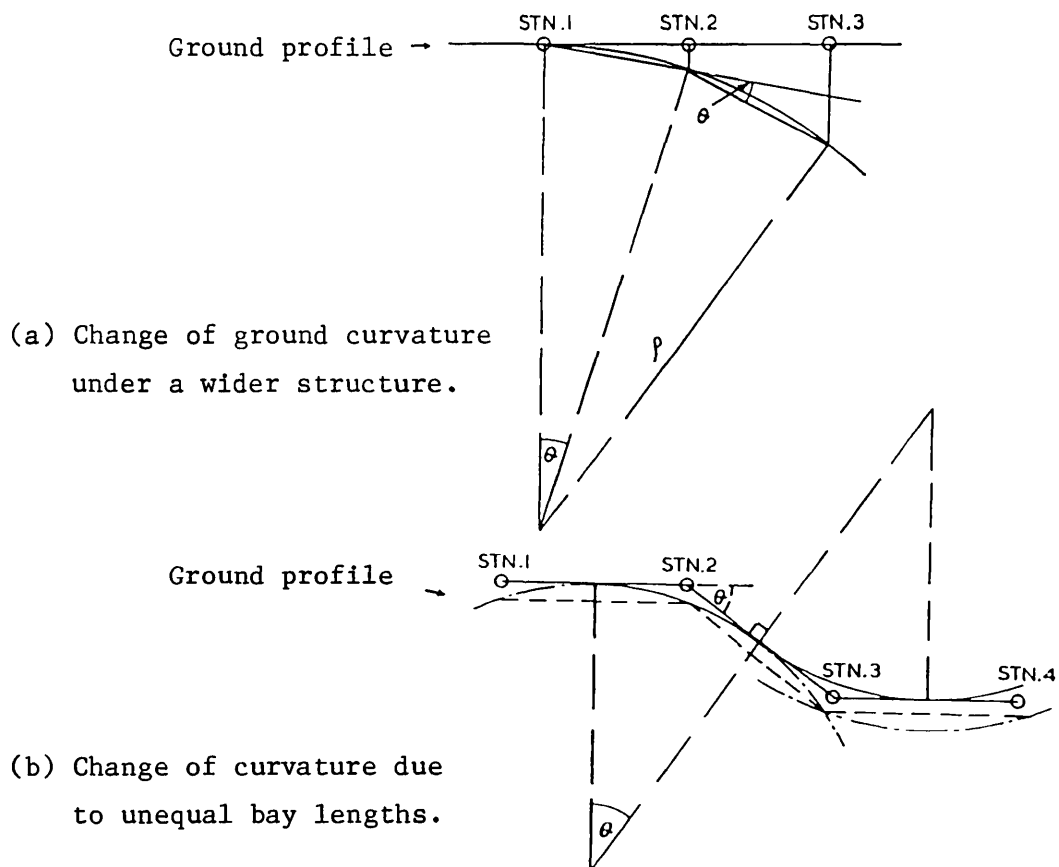


Figure 3.5 Application of radius of curvature of the ground profile to define relative strain in buildings (after NCB,1975).

2) The design depended upon the bay length,  $L$ , and was difficult to apply, as structures may exhibit uneven panel lengths. Also, if the bay length is too long it would form part of two or more curve paths that would be less sensitive to strain deduced from the curvature thereof.

(b) Limiting tensile strain

This model is based upon two concepts, namely,

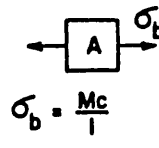
- that damage occurs when an increase in the structure deformation at a critical position exceeds a critical tensile strain of the building material, that is, concrete or brick-masonry. The critical tensile strain is defined as the strain at which local cracking becomes visible.
- that this strain is related to the form of the structure deformation dominant during settlement, that is, bending or shear deformation.

Burland and Wroth (1974) employed the concept of limiting tensile strain by representing a building in a simple rectangular beam model. In this idealization, the deflection ratio  $\Delta/L$ , at which the critical tensile strain,  $\epsilon_{crit}$ , is reached at some point in the beam, is used as the criterion for allowable deflection or settlement. The critical tensile strain may develop either by direct tension in the extreme fibre, A, or by diagonal tension along the neutral axis, B or B', (Figure 3.6(b)). The direct tensile strain,  $\epsilon_b$ , and the diagonal tensile strain,  $\epsilon_d$ , are defined in terms of the bending and shear stresses respectively.

Direct Tension at extreme fibre A

$\epsilon_b$  = direct tensile strain

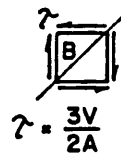
$$\epsilon_b = \frac{\sigma_b}{E} = \frac{Mc}{EI}$$



Diagonal Tension at neutral axis B

$\epsilon_d$  = diagonal tensile strain

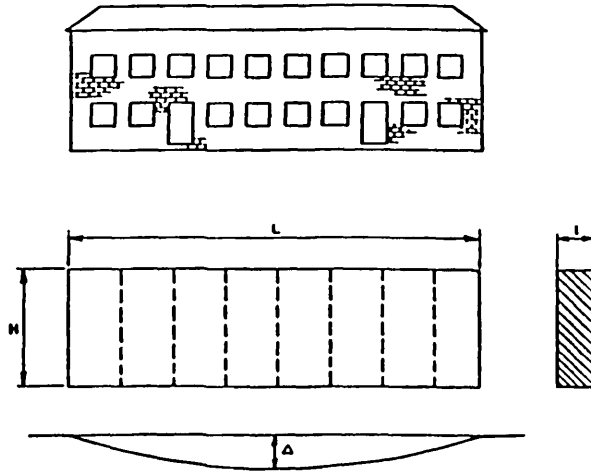
$$\epsilon_d = \frac{\gamma}{2} = \frac{\tau}{2G} = \frac{3V}{4AG}$$



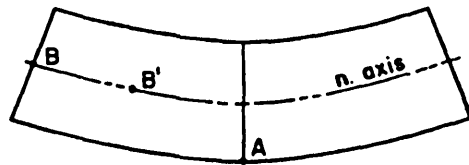
Using the elastic theory for the deflection of beams, the deflection ratio,  $\Delta/L$ , of the deformed beam can be expressed in terms of the elastic properties of the beam and either of the critical tensile strains,  $\epsilon_b$  or  $\epsilon_d$ . Burland and Wroth considered two load conditions:

- a point load P at midspan, and
- a uniformly distributed load, w.

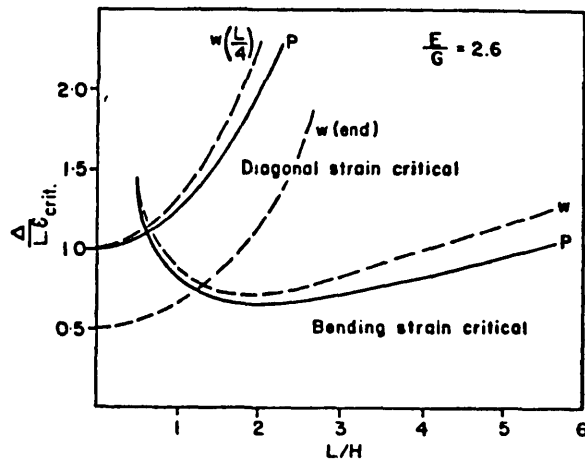
Considering a simple beam of length L, cross-section H x l with the



(a) Deflected shape of soffit of building.



(b) Points of critical tensile strain.



(c) Relation of deflection ratio to aspect ratio of wall.

Figure 3.6 Idealization of a building as a rectangular beam (adapted after Burland and Wroth, 1974).

neutral axis at mid depth,

$$\epsilon_b = \frac{6M}{EH^2} = \text{direct tensile strain at the extreme fibre, and}$$

$$\epsilon_d = \frac{3V}{4GH} = \text{direct tensile strain at the neutral axis.}$$

A relationship between deflection ratio,  $\Delta/L$ , and the angular distortion  $\delta/L = \beta$  was established by assuming that  $\beta$  represented slope of some portion of the beam. Three definitions of  $\beta$  were considered to represent the extreme cases (Wahls,1981):

- $\beta_0$  = slope at the support (maximum slope),
- $\beta_{L/4}$  = slope at  $L/4$ , and
- $\beta_{avg}$  = slope of chord between the support and  $L/4$ .

Burland and Wroth formulated limiting equations based upon  $\epsilon_{crit} = 0.05\%$  for both  $\epsilon_b$  and  $\epsilon_d$  as follows, for point load, the  $\Delta/L$  relation at mid span is given by

$$\frac{\Delta}{L} = \left[ \frac{1}{6} \left( \frac{L}{H} \right) + \frac{1}{4} \left( \frac{H}{L} \right) \left( \frac{E}{G} \right) \right] \epsilon_b$$

or

$$\frac{\Delta}{L} = \left[ \frac{2}{3} \left( \frac{L}{H} \right)^2 \left( \frac{G}{E} \right) + 1 \right] \epsilon_d$$

for a uniform load,

$$\frac{\Delta}{L} = \left[ \frac{5}{24} \left( \frac{L}{H} \right) + \frac{1}{4} \left( \frac{H}{L} \right) \left( \frac{E}{G} \right) \right] \epsilon_b$$

or

$$\frac{\Delta}{L} = \left[ \frac{5}{6} \left( \frac{L}{H} \right)^2 \left( \frac{G}{E} \right) + 1 \right] \epsilon_d$$

Several parameters were included in defining the allowable  $\Delta/L$ , namely,

- a) aspect ratio of wall,  $L/H$ ; where for low values of  $L/H$ , diagonal tensile strain was considered more critical and for large values ( $L/H > 1$ ), direct bending was critical.
- b) variation of shear along the beam was found to represent real beams more practically, if the critical position was taken at quarter point. However, load distribution, that is point or uniform load, was found to have little significance on the allowable differential movement.
- c) ratio of Young's modulus to shear modulus,  $E/G$ , was used for modelling the different types of structures, that is, those which were more flexible in shear and those which were rigid in direct tension. For the former case, flexibility in shear was represented by an  $E/G$  ratio of 12.5, where diagonal strain became more critical. However, for

structures which were very stiff in shear, an  $E/G$  value of 0.5 showed that the limiting tensile strain was dominated by bending.

d) position of the neutral axis was used to model structures with rigid or flexible foundations, that is mat foundations could be modelled by assuming the neutral axis to be at the bottom of the beam. This was also employed to define sagging or hogging modes of deformation.

On the basis of this beam analogy, Burland and Wroth developed the limiting deflection ratio criteria with respect to different types of structures, namely, (Figure 3.6(c))

- that diagonal strain will be critical for framed structures which typically are relatively flexible in shear, and reinforced loadbearing walls, which are relatively stiff in direct tension. This case may be approximated by the behaviour of the rectangular beam with a high equivalent  $E/G$ , and
- that bending strain will be critical for unreinforced masonry walls and structures which have relatively low tensile resistance.

For the sagging mode (settlement curve concave upward), the behaviour may be modelled by the isotropic rectangular beam with the neutral axis at the mid-depth. For the hogging mode (settlement curve concave downward), the behaviour may be approximated by the rectangular beam with low equivalent  $E/G$ , and the neutral axis at the bottom.

### **(c) Limiting stress criteria**

With the advent of powerful numerical techniques for the analysis of structures, a settlement criteria based upon a critical tensile stress being reached in the structure was more easily applied in computer based techniques than curvature or limiting tensile strain. This enabled further settlement parameters to be studied irrespective of their complication, together with a more realistic representation of the settled structures. However, careful interpretation of results from these techniques is necessary, since the broad assumptions on which they are based may lead to unreliable results and conclusions.

**MacLeod and Abu-El-Magd (1980)** introduced new parameters in the settlement analysis that influence the allowable deflection ratio, that is the soil-structure interaction. Two factors were considered, namely, relative stiffnesses of the structure and the subsoil together with the settlement profile condition. Generally, the influence of the



structural stiffness ratio, that is, bending/shear stiffness was of greater significance in the case of sagging settlement. Considering soil-structure interaction, three different soil models were introduced, namely, Winkler, elastic half-space and non-linear models. A parametric study of a four-storey wall with regular pattern of openings was performed using frame analysis. It was concluded that the half-space soil model gave a better prediction of the surface settlement than the Winkler model, showing greater intensity of load transferred at the edges of the building. This is a typical pressure distribution under a raft on a cohesive soil. However, the Winkler model gave a better representation with uniform distribution of pressure that is closer to pressure caused by cohesionless soils, which tends to be maximum at the centre of the raft. The damage criteria was chosen so that initial cracking occurred at a maximum tensile stress in the wall of  $1.5 \text{ N/mm}^2$ .

For walls with bay ratio  $b/h > 0.4$  ( $b/h$  is the ratio of the width to the height of the bay), the position of maximum stress was found to vary with the load pattern. Maximum stresses occurred in the outer bay if the soil was homogeneous but would tend to move towards the centre of the wall if the load intensity increased in the centre. In the latter case, higher stresses were induced, implying an increase in the potential for damage. Of interest is that for flexible structures with increased building length (that is, where the ratio of bending to shear stiffness is low), it would suffer less damage than one with larger openings (meaning an increase in the bending to shear stiffness ratio). Generally, the limiting deformations corresponding to a maximum stress of  $1.5 \text{ N/mm}^2$  in the walls undergoing a sagging mode of settlement was in the range of  $1/1000$ - $1/2400$ , and a range of  $1/4500$ - $1/5800$  for hogging.

Hooper (1982) and Driscoll (1985,1986) analysed settling masonry walls using finite element methods by defining separately wall, foundation and soil elements. Driscoll (1985) based damage criteria upon the stress range corresponding to a critical strain value of  $750 \times 10^{-6}$ , indicating the onset of cracking. Hooper correlated maximum settlement to a tensile stress induced in the walls as a result of a critical vertically applied load. He also illustrated the effect of damping due to the presence of walls causing a reduction in the differential settlement of a footing by a factor of 10, compared to a footing without a wall. In addition, the effect of introducing an open vertical joint in a long facade wall would tend to reduce the effect of differential

movement due to the rigid body rotation of the wall segments. Inclusion of gable walls, that is, wall returns, in the analysis reduced the differential settlement of the footing by 70%, with lower tensile stress induced in the walls.

Driscoll compared the extent of applicability of the Burland and Wroth (1974) deformation criteria (refer to Section 3.4.2(b)) with the numerical representation of a finite element mesh of a single-storey building. Settlement was modelled by causing the structure to deflect in a regular shape, that is either in an arc of a circle or a parabola. By including openings it was found that Burland and Wroth's criteria provided a better fit of the observations of damaged buildings than the more realistic finite element model. However, two points were raised; the first being that the higher stress distribution on inclusion of openings was more noticeable in sagging walls than hogging. This caused a reduction in the allowable deflection ratio of walls with openings to one-half that of solid walls. Secondly, greater reduction in the deflection ratio in hogging by about one-half was achieved by top stiffening of the wall, while in sagging there was no significant difference in reduction of deflection ratio for stiffening, both at eaves level or in the foundation.

### 3.5 COMPARISON OF CRITERIA OF DAMAGE

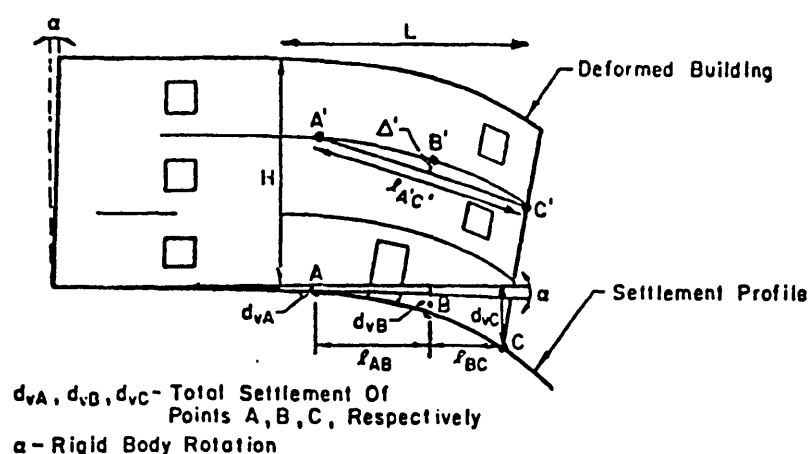
There is inherent difficulty in any attempt to define a criterion of damage, particularly since the interaction of several parameters is involved. Given the complexity of the analysis of all relevant parameters, however, it is important to study both the significance of each and its influence on the damage criteria. Especially difficult is the identification of the critical deformation pattern of the structure, and its relation to the limiting serviceability of the building. This, in turn, tends to affect the choice of the critical settlement parameter, for example, angular distortion or relative deflection, so as to accurately correlate with the degree of damage reached in the building. Various methods have been proposed to correlate visible damage; a summary of the literature is illustrated in Table(3.11). The wide variation is largely attributed to empirical relationships developed for specific types of structures and also, to the different levels of damage assessed. For the latter, a limiting criteria for

visible damage is required so that it may be generally applied in design. To choose a criterion, three main steps are required.

### 3.5.1 Correlation between damage and structure deformation

Two parameters are commonly employed when attempting to correlate between architectural damage and differential settlement, namely, angular distortion and deflection ratio. Angular or lateral distortion,  $\delta_L$ , is described as the differential movement relative to the distance between two points in the structure. This term defines building damage by neglecting rigid body tilt. If tilt is significant, the modified distortion would represent the deformed shape of the structure, but would not relate to its initial state and, therefore to its differential strain. However, the relative deflection ratio,  $\Delta/L$ , is defined as the maximum displacement,  $\Delta$ , relative to a straight line between two points divided by the distance,  $L$ , separating the points. Since this method depends upon the length of the bay, it approximates the deformed shape and is thus unable to give a true representation for local deformation within the bay. Both parameters are illustrated in Figure 3.7 as they apply to the settlement of a building.

Rigid body tilt,  $\alpha$ , is difficult to evaluate since it is dependent upon the deformation capacity of the structure, which is influenced by the type of foundation.



$$\text{Angular Distortion, } \delta_L = \frac{d_{vA} - d_{vB}}{l_{AB}} \text{ Or } \frac{d_{vC} - d_{vB}}{l_{BC}}$$

$$\text{Deflection Ratio, } \Delta/l = \frac{\Delta}{l_{A'C'}}$$

Figure 3.7 Types of building deformation caused by settlement.

Table(3.11) Comparison of criteria of damage for structures subject to ground movement.

Year	Reference	Type of Structure Form	Damage Criteria	Structure Deformation	Limiting damage criteria	Factors affecting maximum values	Comments
1935	Terzaghi	Brickwalls (load bearing or continuous cladding)	Maximum Cracking Stress	-	0.41 N/mm	-	Safe Design factor of 2.0 for no damage
1949	Short and Siems	R.C. and Steel beams	Allowable Deflection relative to span	-	1/300	infill panels and partitions	
1952	Rigby and Dekema	Lightly reinforced brick-walls	Central deflection	Sagging Mode	0.05-0.08 in.		
1948	Terzaghi and Peck	General	Differential sett.; Maximum settlement	Edge Deformation	0.75 in. 2.0 in.	Type of Foundation	Limiting max settlement
1952	Tschebotarioff	General	Total deflection	-	< 2-3 in.		Before visible dam.
1953	Capper	General	Maximum differential sett. w.r.t. span	-	$\Delta = \theta L$ L=Span between adjacent walls	$\theta$ is a function dependent on the type of structure	
1953	Meyerhof	Open frames; Infill frames; Load bearing walls or brick cladding	Angular limiting distortion	-	1/250 1/500 1/1000	Type of structure; form	Safe limit before visible damage
1956	Skempton and MacDonald	Loadbearing walls or partitions, Infill panel walls	Angular distortion term	Tilt term eliminated	1/300 1/150 1/500-1/1000	Dependent on max settlement and type of foundation and subsoil condition	Visible damage Structural damage Factored no crack criteria
1957	Polshin and Tokar	Infill frames (concrete); Loadbearing & brickwalls; One storey-Mills; Buildings with plain brick-walls	Maximum slope; Relative deflection	No correction for tilt	1/500-1/200  $3 \times 10^{-4}$ $4 \times 10^{-4}$ $5 \times 10^{-4}$ $7 \times 10^{-4}$ $\delta = 80 \mu\text{m}$ $\delta = 100 \mu\text{m}$	Dependent on critical level of; tensile strain in; wall and; aspect ratio L/H	No damage of Infill   First crack but servicable

Table(3.11) Continued.

Year	Reference	Type of Structure	Damage Criteria	Structure Deformation	Limiting damage criteria	Factors affecting maximum values	Comments
1963	Bjerrum	Limits provided for various structures	Angular Distortion		$< 1/750$ $< 1/150$	Time factor and method of construction	First crack to Structural damage or instability of frames
1964	Rozenhaut	Buildings & masonry walls	Radius of curvature	Approx. as a parabola	$R=L^2/8f < 1500mm$	Depends on crack width & strain	
1964	Horn and Lambe	Brick, masonry walls	Settlement distortion		1/1600	Maximum offset w.r.t. selected points	
1965	Feld	Loadbearing-walls	Total settlement		0.5-2.0 in.	Increase of rate of sett. causes decrease of total settlement	
1969	Beeby and Miles	R.C. frames	Limiting deflection	Damage to finishes & walls	1/350		
1967	Mayer and Rusch	Partitions in R.C. Frames	Relative deflection	Excessive deflection of slabs and beams. Design faults and workmanship	1/300 1/150	Rotation of adjacent supports and restraint to movement joints	Tilt is not considered
1967	CSTC	Masonry structures	Relative deflection	Lack of fit of supports for b/L	1/10-1/55 1/2700-1/360	Slenderness of supporting beams or slabs, aspect ratio of walls and duration of movement	Presence of wall returns reduce crack width to 1-2 mm
1973	CEB	R.C. structure including partitions	Relative deflection	Excessive deflection of frames	1/300-1/750	Locking of partitions reduce deflection	Locking inc-rease damage limit
1974	Grant, Christian and Vanmarck	Loadbearing-masonry walls	Curvature radius Max allowable differential sett.		1/1000 30-56 mm	Type of subsoil conditions	
1974	Burland and Wroth	Brickwalls	Relative deflection ratio	Sagging mode Hogging mode	$\Delta/LE = 0.5$ $\Delta/LE = 0.22$	Based on L/H ratio of walls and E/G ratio and a limiting tensile strain of 0.075%	
1975	Walsh	Woodframe & cladding Unreinforced	Relative deflection	Edge heave	1/240 1/960	Type of finishing material	

Table(3.11) Continued.

Year	Reference	Type of Structure Form	Damage Criteria	Structure Deformation	Limiting damage criteria	Factors affecting maximum values	Comments
		bearing walls; Brick veneer			1/400		
1974	Starzewski	Mass structure; Rigid or Preabricated structures	Angular Distortion	Tilt Structural distortion	H/100 1/100 1/500	Type of structure and restraints	
1975	NCB	General building	Curvature of ground profile	Horizontal movement	<0.005 for L=10 m	Horizontal strain in	Depends on length of structure
1976	O'Rourke Cording and Boscardin	Brickwalls & loadbearing masonry	Angular distortion;  Lateral distortion		1/1000  1/300 1/150  1/125	Lateral strain	w=3-4 mm  Inconvenienc to occupants w=13-25 mm  Structural damage
1978	Wray	Wood frame & cladding Unreinforced walls Brick veneer	Relative defl.	Centre and edge heave	1/200 1/500 1/800 1/1500-1/2000 1/300-1/500		Type of Articulated structures
1980	MacLeod and Abu-El- Magd	Brick walls	Stress-based criterion	Sagging deformation	Based on limit- ing tensile stress of 0.80- 1.7 N/mm <sup>2</sup>	Soil structure interaction and type of deforma- tion	Shear and Bond failure affect value of stress
1981	Alexander and Lawson	R.C. with bri- ckwork parti- tions Framed structures	Deflection limit		1/200  1500x10 <sup>-6</sup>	Based on Burland and Wroth method	Crack width defined a limit
1982	Yokel, Salomone and Gray	General type of structures	Horizontal strain Slope Total settlement	Hogging or cantilever; mode	< 0.1 % 1/200-1/300 Clay Sand 80 mm 40 mm	Defined as corr- ected length of structure	
1986	Attewel, Yeates and Selby		Stress & crack based criterion			Limiting stress value defined visible crack	Using rigid body deforma- tion to ca- lculate cra- ck width

It is important to consider rigid body tilt in stiff narrow structures or where there is flexible articulation between the foundation and the superstructure. In these cases, the serviceability limit is reached as this affects the stability of the structure. This is evaluated from the inclinations of the front and rear walls, together with lateral distortion of the gable walls. Figure 3.8 shows the effects of rigid body settlement, tilt and angular twist of separate footings on the deformation of a building.

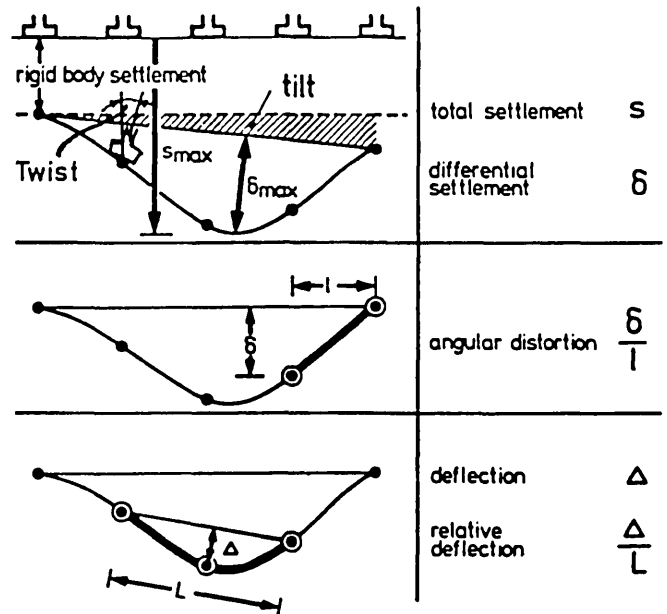


Figure 3.8 Types of deformation of separate footing foundations.

Although buildings are subject to several settlement profiles, there are two basic components of structure deformation, bending and shear distortion. Deflection ratio,  $\Delta/L$ , is closely related to the radius of curvature, hence it gives a good indication of the bending deformation, and also provides a measure of differential settlement without excluding rigid body tilt or angular twist. Otherwise, since angular distortion is able to relate more accurately to local deformation, it is used to define shear deformation. In addition, the distortion term is used to define deformation of bays of loadbearing structures with openings that experience damage due to diagonal shortening or stretching of openings.

Several limiting relationships were established for the allowable deflection of structures. Nevertheless, variations and, in some cases, conflicting correlations were reported for the criteria defining the onset of visible damage. Due to the different parameters considered and the differing degree of damage allowed for, these variations are to be expected. Figure 3.9 summarizes the best known criteria of damage with respect to walls in sagging and hogging. Although there is broad agreement that the limiting deflection ratio decreases upon increasing  $L/H$ , there are a few cases where that effect was either insignificant or where even an increase in deflection ratio was noted (Polshin and Tokar, 1957 ; Burland and Wroth, 1974). Additionally, although the limiting deflection ratio normally increased with a decrease in the aspect ratio  $L/H < 2$ , others reported no change (Polshin and Tokar, 1957

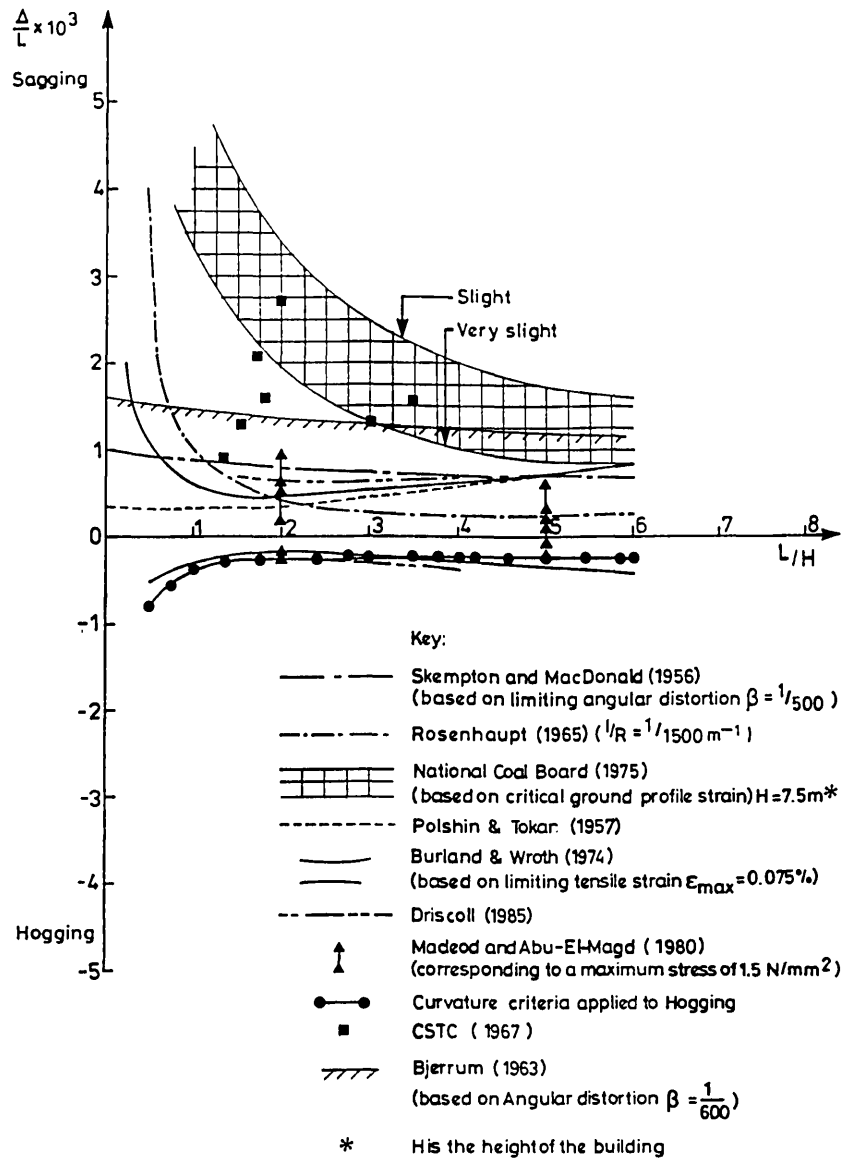


Figure 3.9 Comparison of criteria of damage for inplane deformation of buildings.

; Skempton and MacDonald,1956). This is because a general criteria was chosen for both loadbearing walls and infill frames; in fact, the latter case was also affected by shear deformation (Bjerrum,1963 ; Skempton and MacDonald,1956). Generally, criteria based upon curvature or bending, that is, damage caused by flexure, shows an exponential relationship between the relative deflection ratio and the aspect ratio of the wall (NCB,1975 ; Rosenhaupt,1964). Thus, for high walls with shorter spans, larger deflection ratios can be accommodated in both sagging and hogging. This is attributed to the position of the neutral axis; where the larger lever arm increases the moment capacity, thus reducing the magnitude of strain in the extreme fibres. Considering the combined shear and bending deformation of the walls, Burland and Wroth (1974)



predicted an increase in the deflection ratio for  $L/H > 2$  in both sagging and hogging. However, MacLeod and Abu-El-Magd (1980) and Rosenhaupt (1964) recorded an even greater reduction in the deflection ratio on an increase in the aspect ratio. For walls in hogging, the limiting deflection ratio is seen as dominated by flexural bending of the walls. Thus, for walls subject to both sagging and hogging, Burland and Wroth (1974) criteria predicted closer results in comparison to criteria based upon curvature.

### **3.5.2 Parameters affecting damage criteria**

Existing damage criteria do not include all the relevant parameters that would significantly affect structural deformation, particularly the time dependent behaviour of both the soil and the structure. This is attributed to the choice of a model that represents the building behaviour, together with the broad simplifying assumptions that are carried out to reduce complex interaction between the structure and its supporting soil. It is necessary to point out that it is difficult, and in some cases impossible, to carry out an analysis that will give an accurate prediction of the differential settlement and the resulting stresses (Burland, 1984 ; MacLeod and Abu-El-Magd, 1980). At present, it is only possible to define the main parameters and their effects on the existing criteria for allowable settlement.

#### **(a) Stiffnesses of the structure and the soil**

The structural stiffness influences the distribution of the applied load on the subsoil and, subsequently, its reaction on the structure. Upon settlement, changes in load distribution initiate structural deformation that occur in two forms, either as shear or bending deformations. Burland and Wroth (1974) and later MacLeod and Abu-El-Magd (1980) indicated that the limiting differential settlement is dependent upon the ratio of bending to shear stiffnesses. Thus, two buildings with the same structural stiffness would behave differently under settlement if their stiffness ratios are different. However, the structural stiffness cannot be considered separately from that of the soil, since a given structure may behave as though flexible when supported by very rigid soil, but will behave as though rigid on a very soft soil (MacLeod and Abu-El-Magd, 1980). Polshin and Tokar (1957) observed that structures on softer grounds acquired more settlement; thus the stiffer the soil the greater will be the maximum stresses in

the structure. However, for flexible structures, an increase in the soil stiffness would tend to cause a decrease in the differential settlement and, thus, a decrease of the maximum stresses induced in the structure.

#### (b) Strength of the building Material

Previous research has relied upon observations and empirical rules to define the relationship between the allowable differential movement and the degree of damage, defined in terms of the amount of visible cracking. These were provided without relating the basis of judgement of damage to the actual fabric of the building. Nevertheless, the strength of the building material affects both the amount of cracking that can be tolerated and the nature of failure of the structure. That is, for low strength brickwork, failure is less brittle than in high strength concrete. Polshin and Tokar (1957) and, later, Burland and Wroth (1974) defined the critical tensile strain at the onset of visible cracking as 0.05% for brickwork or, more generally, 0.075% for most building materials. Since measurement of strain is dependent upon the gauge length and the position of the gauge relative to the crack, that is, critical section, large variations in strain records were reported by Beeby and Miles (1969). In order to reduce the range of strain at visible damage, they recommended the use of the local strain in the vicinity of the crack. In addition, Abu-El-Magd and MacLeod (1980) and Longfoot (1984) studied the critical tensile strength of masonry by testing wallets in indirect bending. In order to relate the observed strain to the theoretical models, reference was made to the limiting stress. Longfoot (1984) noted that there are several modes of failure. The strength at the onset of stable visible cracking was found to fluctuate according to the type of test, rate of loading and the stress distribution or pattern of loading of the specimen. However, the variation in the strength of the building material is as high as that of the limiting strain. For bricks tested in direct tension, a mean stress of  $0.68 \text{ N/mm}^2$  was recorded at fracture, corresponding to a tensile strain of 35 microstrain. For walls tested in bending, however, a limiting stress of  $1.52 \text{ N/mm}^2$  was measured, corresponding to a tensile strain of 110 microstrain.

#### (c) Degree of damage

Most limiting criteria are concerned primarily with identifying

the allowable differential movement at which cracking is initiated. Very little indication of the severity and extent of damage on the structure adequacy or stability is included in any criteria. Skempton and MacDonald (1956) were the first to classify damage into architectural and structural, while Burland et al. (1977) defined a third class by including serviceability, or function criteria. ACI (1968) also divided damage into four broad categories. These are sensory acceptability (depending on reaction of the public), serviceability of the structure or its adequacy of use as a building, effect on non-structural elements (that is, cracking in walls and ceilings, jamming of doors), and lastly, structural elements that are related to structural cracking.

#### **(d) Out-of-plane limits**

Owing to the complexity of the 3-dimensional behaviour of structures, none of the earlier investigations have attempted to define limits of out-of-plane deformation at the onset of visible damage. Increased differential settlement was noticed for walls with returns (Pfeffermann,1968 ; CSTC,1967). Further research was conducted into defining relative limiting movements of facade and gable walls (O'Rourke et al.,1976 ; Hooper,1982). A need was recognized to study the influence of out-of-plane structural members in limiting settlement of the whole structure. Also, the understanding of formation of out-of-plane deformations is necessary to assist in formulating an overall limiting criteria (that is, 3-dimensional criteria) for structures subject to differential movement (refer to Section 3.6).

#### **3.5.3 Basis of criteria for the onset of damage**

Past work has aimed at establishing criteria of damage at serviceability by relating observed deformation to damage (Skempton and MacDonald,1956 ; Polshin and Tokar,1957 ; Bjerrum,1963). There is a need to develop a method of design that is based upon the relation of structural response to the cause of damage. Most damage manifests itself as cracking; however, the extent to which a crack becomes noticeable is a function of the surface on which the crack appears. This includes the position of the affected surface, its texture, and the ambient lighting, together with the reaction of the user. In order to clarify both any subjective factor in judging the extent of damage and the non-linear behaviour of the structure due to formation of cracking,

design criteria are based on the onset of visible damage. Visible damage is classified as in categories 1 and 2 of Table(3.1). Two main criteria were introduced in the literature and these are discussed as follows.

**(a) Criterion based on the concept of limiting tensile strain**

Polshin and Tokar (1957) defined the onset of visible cracking in a given material as one that is associated with a limiting or "critical" tensile strain  $\epsilon_{crit}$ . It is important to relate the critical tensile strain with local fracture observed at a limiting crack width. LittleJohn (1974) and Green, MacLeod and Stark (1976) observed visible damage of buildings subject to mining subsidence as 0.10-0.26 mm wide cracks, while O'Rourke et al. (1976) recorded 0.4 mm at the threshold of noticeable distortion. Burland and Wroth (1974) and I.Struct.E. (1978), however, defined visible damage at 1-2 mm. In reinforced concrete members, cracking is more controlled than brickwork; earlier work by Base et al. (1966) defined architectural damage as a relation between crack width  $w$ , and average strain  $\epsilon$ , where  $w/\epsilon = 90$ . BRE (1979), Alexander and Lawson (1981) and Fenton and Suter (1986) noted that the strain at which cracking is visible on wall panels would generally tend to occur at the same order of magnitude as the permissible shrinkage strain (refer to Table(3.12)). Sahlin (1971) noted that if the mortar was weaker than the blocks, the average limiting shrinkage strain of masonry was found to be  $4.2 \times 10^{-4}$ . If the blocks were weaker, the extensibility of masonry was in the range of 0.01%-0.015% at visible cracking.

It is necessary to note that the critical tensile strain likely to cause visible cracking in walls is different from the ultimate strain of the material at failure (Burland and Wroth,1974). This is due to the concept of internal cracking of the material under load. Nevertheless, the limiting strain of the finishing material is the governing parameter, unless this exceeds the allowable distortion of the structure. A summary of the critical strain for masonry is shown in Table(3.13).

O'Rourke et al. (1976) and Attewel et al. (1986) observed that a criteria for the onset of cracking in brickwork buildings should also take into account the age and quality of the brickwork. This is a situation where the concept of limiting tensile strain proves more satisfactory in defining the strain "history" of the building. As a

result, old brickwork is likely to contain more cracks, and the mortar is considered to be softer.

Table(3.12) Permissible shrinkage strain of building materials  
(collated after BRE,1979 ; Alexander and Lawson,1981 ;  
Fenton and Suter,1986).

Material	Shrinkage strain
Mortar and fine concrete	0.02 - 0.06%
1:0:3	0.037%
1:1:6	0.055%
Dense concrete	0.03 - 0.10%
Calcium silicate brickwork	0.01 - 0.05%
Autoclaved brickwork	0.03 - 0.06%

Table(3.13) Summary of limiting tensile strain at visible damage.

Material	Limiting tensile strain at visible cracking	Reference
Brickwork	$500 \times 10^{-6}$	Polshin and Tokar (1957)
Unreinforced- masonry walls	$1500 \times 10^{-6}$ (Shear strain)	Alexander and Lawson (1981)
Masonry walls	$750 \times 10^{-6}$	Burland and Wroth (1974)
Infill panels (Brickwork)	$1150 \times 10^{-6}$ (Shear strain)	Mainstone (1971) and Mainstone and Weeks (1970)
Brickwalls	$380-600 \times 10^{-6}$	Burhouse (1969)

**(b) Stress-based criterion**

Since stresses are linearly proportional to the applied loads and, thus, are a means of relating damage to the relative stiffness of the building, a stress based criterion has been proposed (MacLeod and Abu-El-Magd,1980 ; Attewel et al.,1986). Structure-soil models were used to predict the allowable differential settlement of brickwalls while limiting the tensile stresses reached within the walls.

Based upon a maximum tensile elastic stress that is directly related to a limiting critical strain, an elastic analysis was used in order to model the uncracked structure and the subsoil. The resultant stress

patterns were evaluated with respect to the likelihood of the start of a crack. Several elastic analytical procedures reported in the literature are discussed in Chapter 7. For brickwork, Attewel et al. (1986) suggested that as cracking initiated, in most cases the crack would run through the wall degenerating the structure into two separate components. Estimation of the crack width from rigid body deformation enabled the degree of damage to be assessed by reference to the crack width and  $\Delta/L$ . Recommendations of limiting stresses of brickwork and other materials are shown in Table(3.14).

Table(3.14) Limiting tensile and shear stresses for masonry.

Material	Tensile stress (N/mm <sup>2</sup> )	Shear stress (N/mm <sup>2</sup> )	Reference
Brickwork(1:1:6)	0.35-0.5	0.15-0.30	Attewel <u>et al.</u> (1986)
Brickwork(1:0.25:3)	0.5-1.4	0.35-0.7	Attewel <u>et al.</u> (1986)
Plain concrete	0.1 $f_{cu}$		Attewel <u>et al.</u> (1986)
Brickwalls	0.6-1.7		Abu-El-Magd and MacLeod (1980)
Masonry	2.5		Alexander and Lawson (1980)
Brickwork		0.7	Samarasinghe <u>et al.</u> (1981)

Attewel et al. (1986) suggested that variation of the limiting critical stress is smaller than that of the limiting tensile strain; this is only true after first cracking. However, fluctuation of the critical tensile strain might result due to sudden crack opening, which registers higher strains than the limiting values; this case arises at ultimate. Nevertheless, criterion based upon limiting strain gives an indication of the material failure, while the stress criterion is associated with the mode of structural failure.

In order to effectively relate the building deformation and the stress criterion, the stress-strain relation of the material needs to be established. This is required to relate the computed stress to the actual damage or limiting strain of the material and also, to be able to model the material non-linear behaviour after the elastic limit. This induces non-linearity of behaviour on analysis of post-yield structures due to the deformation of the structure. Although non-linear computer methods are available to cope with such complications, they should be

regarded with great care since doubtful correlations might result (MacLeod and Abu-El-Magd,1980 ; MacLeod,1987).

### 3.6 OUT-OF-PLANE SERVICEABILITY LIMIT

Burland and Wroth (1974) have drawn attention to the fact that there is a need to establish the limiting criteria for out-of-plane behaviour of walls. It is necessary first to determine the out-of-plane critical tensile strain and stress before visible cracking emanates.

Generally, an increase in the deformation of the structure increases the possibility that out-of-plane distortion will influence the limiting serviceability before an inplane one, for example, excessive tilting of narrow buildings. This means that for settlement analysis of structures, representative models of the structure need to include 3-dimensional members that contribute to the stress and strain distribution. A rational method of modelling by Hooper (1982) illustrated the use of 3-dimensional non-linear analysis of gable and facade walls for assessment of allowable differential settlement of brick buildings. Nevertheless, owing to the excessive computer time and cost, this is impractical if it is to be used for every load case. Since brick and blockwork walls are mostly affected on differential settlement, only the out-of-plane behaviour of brickwork and blockwork is discussed here.

There are two planes at which brickwork fail and crack in the out-of-plane sense; one is parallel and the other orthogonal to the bed plane. Extensive research investigating the flexural strength of brickwalls has indicated that there is little variation in the strength of the walls, irrespective of the mortar mix and the percentage absorption of bricks. Table(3.15) shows a summary of collated results for the limiting stresses of masonry in the out-of-plane direction at the onset of visible damage.

Investigating the lateral resistance of brickwork, West, Hodgkinson and Haseltine (1978), Anderson (1976) and Hendry (1973) concluded that the flexural strength of brickwork depends upon three main parameters, namely:

- boundary conditions of walls,
- geometry of walls, and
- limiting serviceability criteria.

Table(3.15) Limiting stresses at the onset of visible cracking  
 (collated after West, Hodgkinson and Haseltine,1978 ;  
 Drysdale and Essawy,1988).

Mortar mix cement:lime: sand	Flexural strength (N/mm <sup>2</sup> )		
	Normal	Parallel	Orthogonal ratio
1:0.25:3	2.10-2.0	0.73	3.13
1:1:6	2.00-1.5	0.71-0.50	3.23
1:2:9	1.86-1.10	0.57-0.40	3.30

### 3.6.1 Boundary conditions of walls

Boundary conditions include the influence of both the type of edge restraint and the presence of wall returns. Restraint at the top of the wall increased the lateral resistance by 25% (Haseltine, West and Tutt,1978), but caused a decrease in the ultimate deflection. If wall returns are present, edge deflections increase, allowing higher deflection at ultimate load, but no significant increase in the ultimate load was recorded (Anderson,1976; West, Hodgkinson, Haseltine and de Vekey,1986).

Short returns experienced early cracking and, in some cases, severe cracking developed in the returns, while longer returns allowed less restricted movement by accommodating inplane movement through arching without inducing cracks (Alexander and Lawson,1981). Failure was observed most often in the main wall as flexure, while shear at the intersection of the returns and the main wall was also noted (Anderson,1986 ; West et al.,1986). As a result, the stress limit at which cracking occurred in the main wall was found to depend on the return ratio, L/R (length of main wall to length of return). Figure 3.10 shows collated results illustrating the relationship between cracking strength and ultimate strength of walls with one and two returns. For walls with two returns, the load at cracking decreased to about 0.2 of the ultimate for L/R = 7, while as L/R decreased to 4, the cracking load increased to about 80% of the ultimate. However, different behaviour characterized walls with one return, where as L/R increased, the first cracking occurred at higher load than that measured at lower return ratios. This suggests that the movement of the free edge of walls with one return contributed largely to increased warping



of the wall upon loading, thus cracking developed at a higher load level. It is interesting to note that for longer lengths of main wall, the load at which cracking initiated did not exceed a ratio of cracking strength to ultimate strength of 0.8. Generally, return walls were found to increase both the magnitude of deformation of the walls subject to lateral loading, and that at which first cracking occurred.

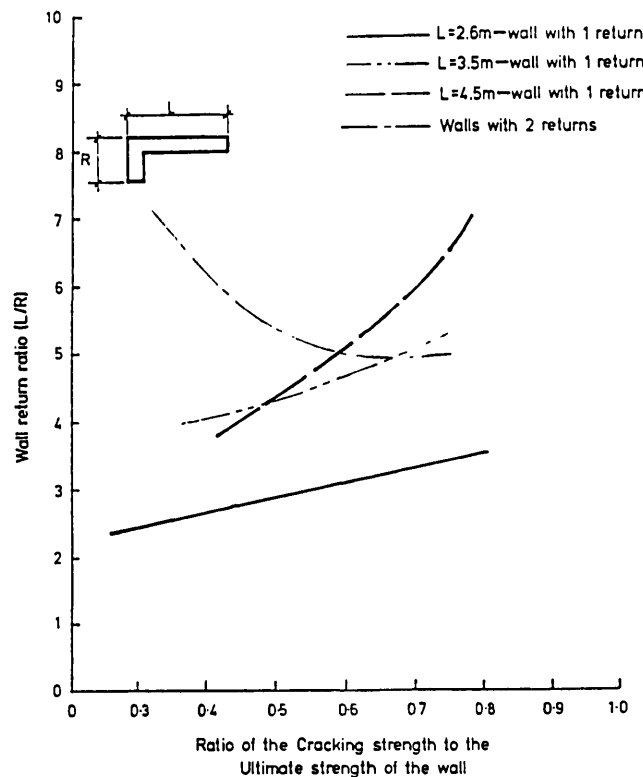


Figure 3.10 Relationship between the ratio of cracking strength to ultimate strength and the wall return ratio (adapted after Anderson, 1985).

### 3.6.2 Geometry of walls

Figure 3.11 shows the relationship of the ultimate lateral load versus the aspect ratio of walls as collated from work by West et al. (1978) and Anderson (1985). For low aspect ratio,  $L/H < 1$ , the wall accommodated the largest pressure, while for  $1 < L/H < 2$ , the failure pressure was the lowest recorded. However, for  $L/H > 2$ , the pressure increased again to its maximum point. This was found to depend upon the type of failure pattern, where for  $1 < L/H < 2$ , diagonal cracking occurred at lower pressure. Meanwhile, vertical cracking developed for  $L/H > 2$  with a more brittle failure pattern.

Also, Haseltine and Tutt (1986) reported that testing of lateral resistance of walls with openings decreased the ultimate load to 40%-45%

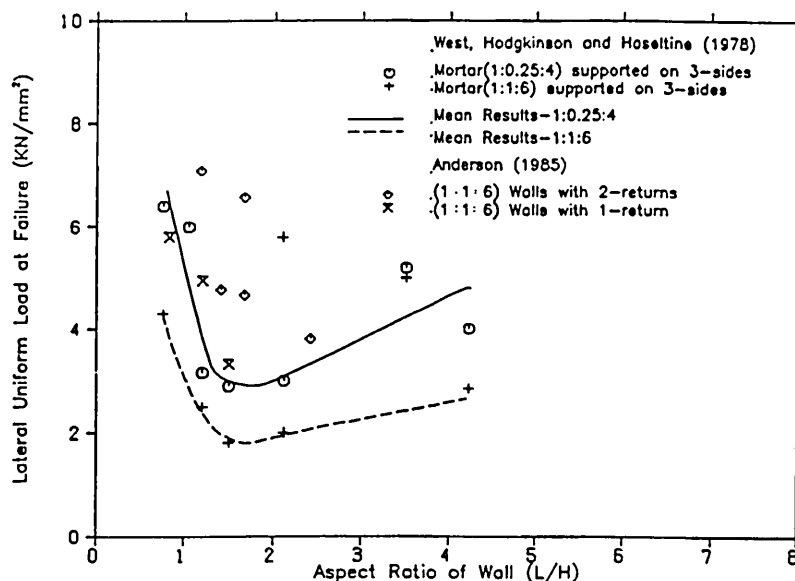


Figure 3.11 Variation of lateral pressure with respect to aspect ratio of masonry walls.

of the ultimate resistance of solid walls.

### 3.6.3 Limiting serviceability criteria

There is a tendency for brickwork to arch laterally when subjected to longitudinal compression, particularly if affected by eccentric loading. Several investigators studied the effect of the limiting curvature and the end rotation of walls in defining serviceability load conditions (Furler and Thurlimann, 1978 ; Baker, 1978). They found that this curvature would give an indication of the allowable curvature limit for out-of-plane behaviour of brickwork. Furler and Thurlimann (1978) observed the limiting curvature at first visible cracking by monitoring the growth of crack width in masonry. As a result, this allowed the establishment of the degree of damage on excessive deformation of masonry walls (refer to Table(3.16)).

Anderson (1986) and Curtin (1986) reported from extensive testing of lateral resistance of walls that the first visible crack occurred when the local strain was of the order of  $350-450 \times 10^{-6}$ , that is, 0.04%-0.05%. Using elastic analysis, the stress level calculated at the occurrence of the first crack was reported to be in the range of 1.0-0.75 N/mm<sup>2</sup>. Also, the maximum lateral deflection at the onset of visible damage for walls fixed on three sides was observed at a strain level of 0.4 mm/m, that is, 0.04% for block and brick masonry. De Vekey (1984), also, studied the allowable out-of-plane deflection of

several types of walls with and without wall-ties, and reported an increase of 40% in the allowable deformation for walls with ties (Figure 3.12).

Table(3.16) Allowable limiting curvature at visible cracking (collated after Furler and Thurlimann,1978 ; Baker,1978).

Crack width (mm)	Allowable curvature limit (out-of-plane deformation)
0.10	$1.2 \times 10^{-5}$
0.30	$3.2 \times 10^{-5}$
0.50	$3.5-5.0 \times 10^{-5}$

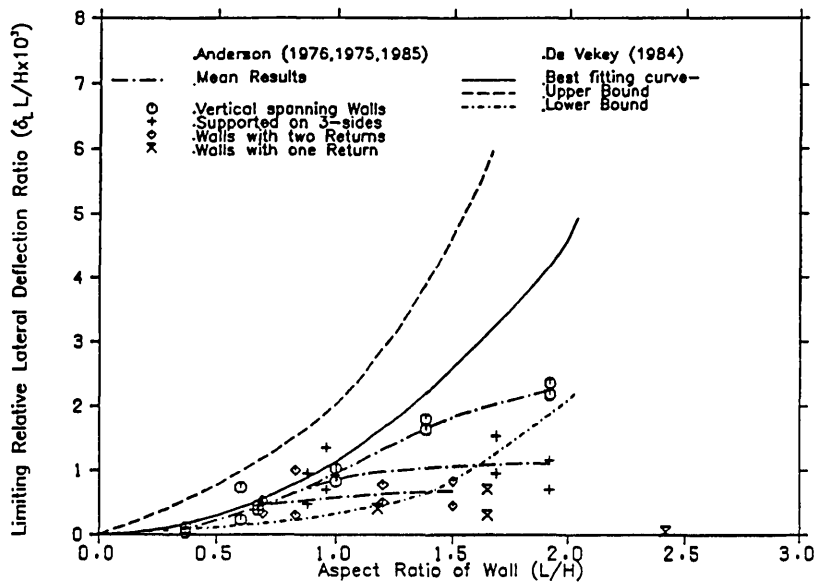


Figure 3.12 Comparison of criteria of damage for lateral deformation of masonry walls.

Figure 3.12 illustrates the relationship of the limiting relative deflection ratio normalized with respect to the height of the wall. Results by Anderson (1976,1985) and De Vekey (1984) were plotted to study the general trend of limiting deflection with respect to the aspect ratio of the walls. Generally, for larger L/H ratios, the allowable relative deflections undergo a considerable increase.

## CHAPTER 4 REVIEW OF DESIGNS FOR ACCOMMODATING GROUND MOVEMENT AND METHODS OF REPAIR

### 4.1 INTRODUCTION

The problem of the design of structures subjected to ground movement has long been a central concern of geotechnical engineering. Since it involves a wide range of considerations, namely, combining many of the elements of soil mechanics and structural engineering, its solution is best approached by defining the various aspects of the problem. As early as the 13th century, it was recognized that differential settlement caused damage to the superstructure. The method of dealing with this in design was to make the foundations as stiff as possible (Terzaghi, 1935). The contribution of the superstructure was totally neglected, as the foundation-structure interaction was considered to be of little significance in reducing the degree of damage that might occur in the event of ground movement. Other approaches were only propounded in the 1940's-1950's (Mautner, 1948 ; Boardman, 1958), namely, partial protection or articulation, that is, the use of flexible building materials and design methods (Gibson, 1957 ; Rodin, 1969). In active ground movement regions (meaning expansive soils), it is often not economically possible to ensure that the majority of buildings resist the effects of differential movement without incurring permanent damage. This suggests either the inclusion of maintenance costs early in the design process by allowing for repairs or the complete protection of the superstructure.

Based on the capacity of the structure to absorb part or all of the differential ground movement without incurring much distress, the various design techniques are classified in three categories:

- (1) Design by complete protection: Preserving the superstructure from any induced secondary stresses due to differential movement of the ground. These methods are described in Sections 2.9.6-2.9.7. Alternatively, the structure may be supported by rigid foundations that would allow complete movement of the structure but no differential displacements of its members, for example, three-point-supported structures.
- (2) Design by partial protection: Subdivision of the structure in

plan into rigid sections bridged with flexible joints so that each section resists independently the ground movement.

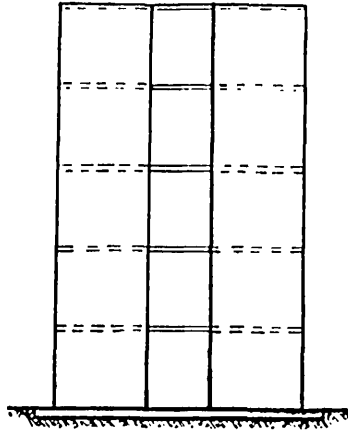
- (3) Design by permitting movement: Permit the independent movement of structural members by including construction joints.

#### 4.2 DESIGN BY PARTIAL PROTECTION

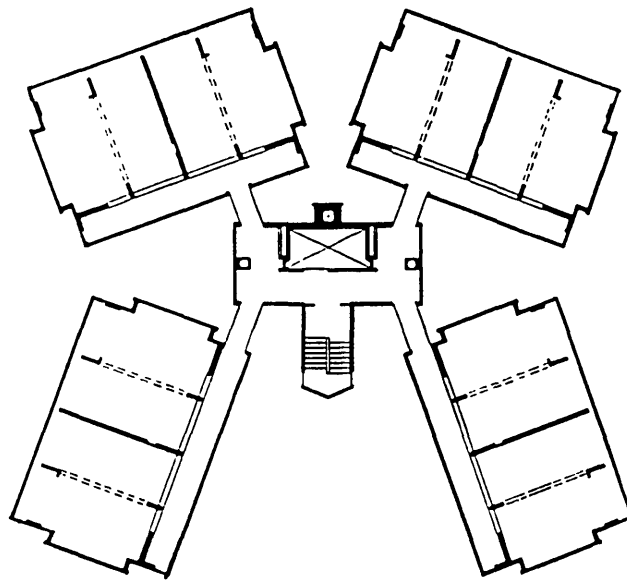
In cases where the structure is already geometrically rigid in one plane, such as framed structures, or where complete protection of spacious buildings, such as churches, halls, workshops etc. is not economically feasible, partial protection design techniques are employed. Two main methods are available:

- (1) Methods relying on the provision of joints to allow dissipation of part of the differential movement so as to minimize the induced damage. This technique is used in mining areas for protection mainly against the horizontal movement that causes most damage where slight protection is provided in the vertical plane. For small houses, a strip foundation with tensile reinforcement was found to reduce the stretching of buildings due to horizontal movement. In lieu of deep foundations, a basement with partition walls will act as a rigid box and be able to resist the forces in the vertical and horizontal planes. Spacious buildings where the interior panels and partition walls have no stiffening would suffer more from horizontal movements than vertical displacements (Mautner,1948 ; Jones,1985). Prestressing the structure in a plane parallel to the horizontal, either by the use of steel rods at roof level or the use of underpinned grade beams at ground level, reduced the ground effects on stretching the structure.

- (2) Methods subdividing the building into separate stiff units, rigid enough to counter the differential movement. Freely supported structural hangers bridging the gap between the units enable the whole structure to move relatively as two or more independent bodies, without causing distress due to interaction of adjacent walls (Rodin,1969 ; Lenczner,1981). Figure 4.1 illustrates two rigid structures joined by articulated supports to facilitate differential movement between the rigid parts, where the joining structure can be used as a staircase, service room etc. The success of this technique clearly relies upon the choice of the length of the independent structures, that is critical on the stiffness of each part in the vertical plane, so that to eliminate the probability of damage.



(a) Simply supported floors bridging between rigid framed structures (after Priestly,1986).



(b) Several rigid blocks joined by a central block to facilitate independent movement of each structure (after Beckman and Dunican,1966).

Figure 4.1 Design of structures by partial protection against ground movement.

#### 4.3 DESIGN BY PERMITTING MOVEMENT

The need to develop an economic design which compromised the cost of complete protection of the structure on the one hand and having permanent deformation on the other hand was first realized in the 1950's (Gibson,1957 ; Lacey and Swain,1957). This method allows some differential ground movement in the superstructure and defines ways of

reducing the secondary effects of that movement. The latter are excessive cracking of walls, stability of the deformed structure and degradation of its strength. In order for the structure to be able to move with minimum distress, articulation can be introduced in the following ways (Lacey and Swain,1957 ; Simms and Briddle,1966):

- (a) reducing restraint between the foundation and the superstructure, thus minimizing structural response due to horizontal movement of the foundation and ground,
- (b) minimizing redundancies of the superstructure so that part or the whole of it may move as independent rigid body movements rather than deforming, and
- (c) the more the building is wedded in the ground (that is, foundation), the more likely it is to suffer from ground movement.

The first method allows the ground to move and stretch while the building slides on it. The use of a damp proof membrane or any slippage material such as sand may be employed generally in areas of mining subsidence (Chen,1975 ; Gibson,1957). This is applied mainly to reduce the effects of horizontal movement of the ground by allowing relative sliding of whole or part of the structure over the foundation. The second method is applied mainly in bridge design, where the structure is articulated in such a manner that the stress distribution within the structure is unaffected by 3-dimensional movements, that is, by making the structure 3-dimensionally statically determinate (Simms and Briddle,1966). This is advantageous as rigid body movement does not induce any stresses due to settlement, for example as in suspended decks. Since the foundation of any building would be subject to high stresses, design by permitting movement using orthodox foundations was found to increase the danger of damage (Gibson,1957 ; Walsh,1975 ; PTI,1978). Finally, the third method is concerned with providing the minimum depth of foundation required for stability and structural safety. This is particularly necessary for high slender structures, or structures subject to landslides and high wind loads, etc., that exhibit large overturning moments (Wu and Scheessele,1986). The CLASP system of construction (Heathcote,1965) employed this technique to reduce the ground restraint on independent articulation of the structure, which in turn, called for a lighter superstructure.

Two main approaches emerged from the above points and are

currently in practice, governing design methods for permitting differential movement. The first approach is to devise structures in such a way that they accommodate the movement while ensuring that the superstructure remains intact and safe. This is accomplished by damping the movement within the structure using a specially built-in device. This technique safeguards the structure against deformation and cracking, since all of the movement is taken by the device. To attract more deformation and structural distress, devices are fitted at critical locations of stress concentrations such as the joints between the foundation and the superstructure. In general, these techniques are applied in seismic designs of structures that are required to dissipate the energy of dynamic structural response into the device. Since the structural integrity depends on the performance of the devices and their location in the structure, the method is clearly expensive. Nevertheless, there still remains some risk of damage since partition walls are vulnerable to differential movement, and these in turn, would crack due to the skew of the building on deforming.

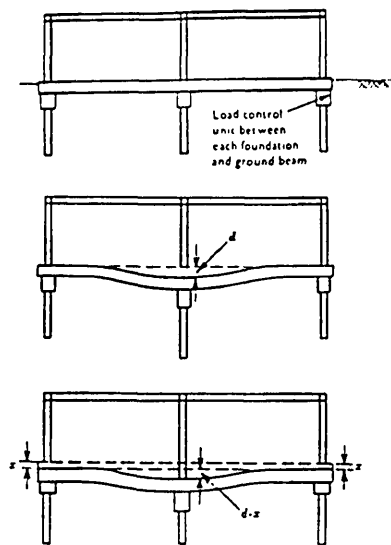
The alternative approach, often found in active regions of seasonal ground movement, is to allow cracking of the superstructure without causing significant permanent deformation. Occurrence of permanent deformation of the superstructure is accompanied by energy dissipation; the energy being created by the response of the structure to the ground motion as a result of loss of support. However, the structural deterioration should not affect the safety of the structure, only evincing itself as cracking and deformation of non-structural elements, such as partitions and walls. Examples of these two approaches are given below.

#### **4.3.1 Design based on energy absorption devices**

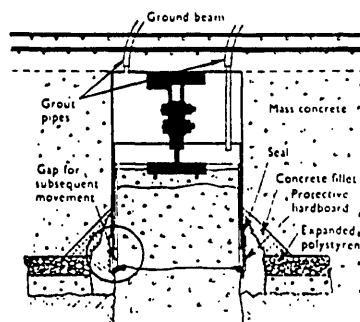
Devices are normally based upon rotational friction, slips or rigid deformation that allow differential movement to occur without affecting the safety of the structure. Slip or rotation at the device imposes a limit on the load that may be transmitted, thus giving protection against progressive deterioration of strength and stiffness of the structure. This would occur in the event of excessive deformation of supports, or in case of partition walls, deflection of the supporting beams and slabs. Its main advantage is to limit support reactions and maximum stresses to predetermined magnitudes, restricting the stresses not to reach their serviceable or ultimate state. It would thus confer



at working load, some of the properties of load redistribution and excessive deformation which in normal instances are achieved only by cracking in reinforced concrete structures or by the formation of plastic hinges in steel structures. Clark, Bassett and Bradshaw (1973) introduced a load control device, namely, a plate friction mechanism installed on top of a foundation cap. The object being, as the foundation deflected away from the structure, the load transferred to the fixed supports increased until reaching a preset value in the bolted plate device (shown in Figure 4.2). Slip occurred, reducing the shear stresses and deflection of the ground beams, thus restoring the stress distribution in the deflected beam and supports.



(a) Slip of load control devices fitted above ground supports.

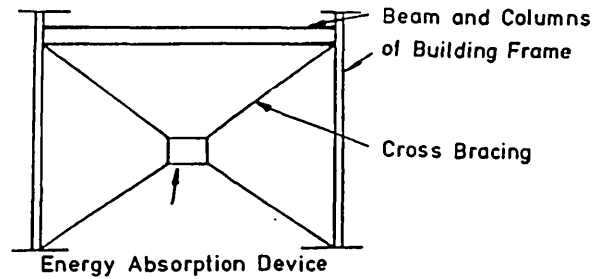


(b) Provision of load device under ground beam.

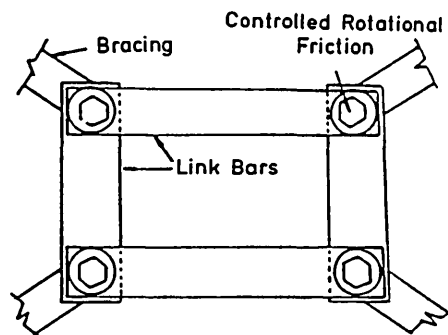
Figure 4.2 Limiting differential settlement by load control devices (after Clark et al., 1973).

Other research in this field has examined the provision of ductile bracing elements in steel buildings, in order to incorporate any sway and tilting of the building subject to high wind or seismic movement

(Roeder and Popov,1977 ; Ikeda and Mahin,1986). Figure 4.3 illustrates a device fitted in the wind bracings to provide articulation so as to ensure verticality of the building after damage.



(a) Energy absorption device fitted in wind bracing of steel frames.



(b) Detail of Energy absorption device.

Figure 4.3 Energy absorption device to allow sway of building frames  
(after Anagnostides, Hagreaves and Wyatt,1988).

Lacey and Swain (1957) and Heathcote (1965) reported the introduction of the CLASP system as an articulated pinjointed steel frame for buildings in areas of mining subsidence. Bracings were introduced to safeguard against wind loading, etc., thereby providing stability. Buildings were designed to "lozenge" if stresses exceeded a certain retained value in the compression struts, which were fitted in the bracings that restricted any distortion. To free the structure to deflect with the ground at working load and keeping load control on the bracings, the bracings were fitted with embodied springs. These were provided in order to "give" at a certain stress value, that is, related to the amount of differential vertical settlement of the building. Since the springs were in a preset compression value less than the factored buckling strength of the bracing, the frame would, therefore, be restored to its original position. Thus, there was no need to change the bracings of the deformed structure, since the springs would automatically retain their initial stress equilibrium (Figure 4.4).

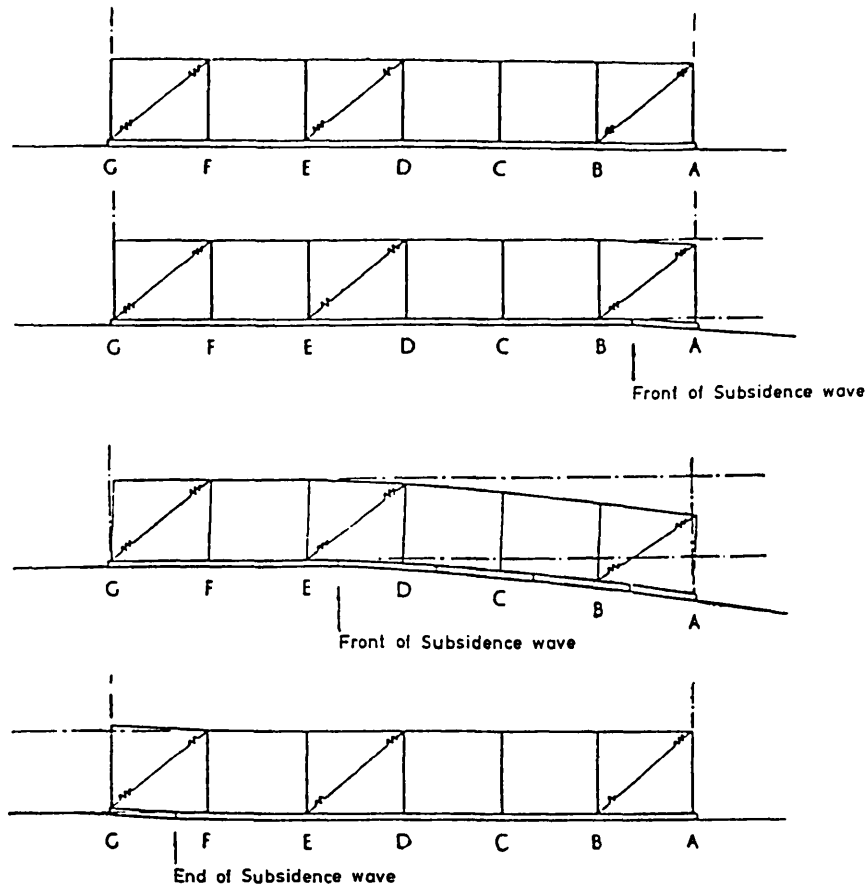
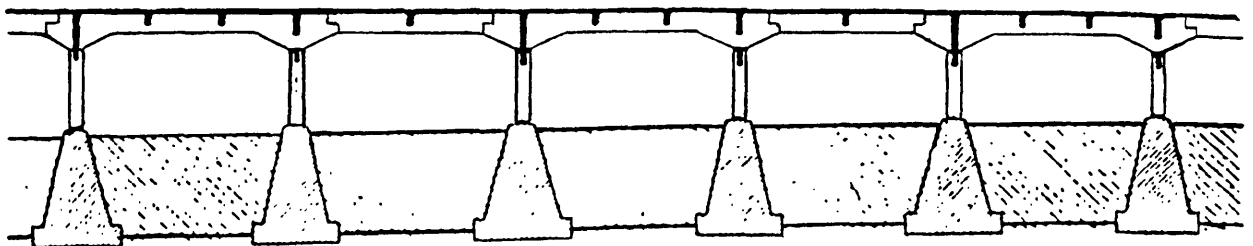


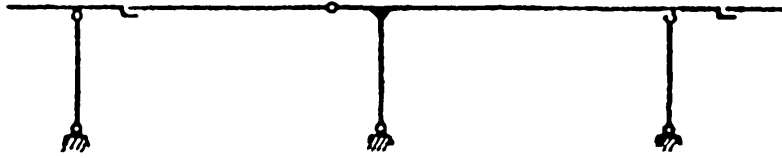
Figure 4.4 Effect of embedded springs on the bracings of building frames subject to a subsidence wave (after Lacey and Swain,1957 ; Heathcote,1965).

#### 4.3.2 Design based on occurrence of permanent deformation

This design is influenced by the type of superstructure and its degrees of freedom, whether determinate or indeterminate. If determinate, the structure is able to deform with no secondary stresses due to differential movement, such as simply supported bridges or pinned support frames (Meyerhof,1953 ; Simms and Bridle,1966), refer to Figure 4.5.



(a) Suspended span bridge allowing differential movement of piers (after Mautner,1948).



(b) Determinate frames allowing deformation with no secondary stresses  
(after Meyerhof,1953).

Figure 4.5 Design by permitting movement with no induced secondary stresses.

If the structure is indeterminate, the structural form would restrict any relative movement of the supports. The safe utilization of this design philosophy is to maximize dissipation of the stress concentrations due to differential movement, thereby enhancing the ductility of the structure. This ductility occurring after the elastic stage will provide the excessive deformation which allows relative movement of the supports. Simms and Briddle (1966) suggested that the walling system in the structure may be utilized to absorb some deformation, as for example T- or L-shaped walls could be subject to combined torsion and bending. As a result, such a wall is able to take more deformation than a wall subject only to inplane bending. If the wall system has low torsional stiffness, for example open roof box-structure, large twist can be accommodated without inducing large bending moments, causing an increase in the relative movement of the walls. Additionally, Barber (1969) pointed out that the use of more ductile material, such as rubber cladding, would enhance the behaviour rather than high strength materials, as larger deflections and deformations prior to the ultimate state are achieved.

#### 4.4 METHODS OF REPAIR FOR STRUCTURES IN AREAS OF GROUND MOVEMENT

Various corrective measures and repair techniques are reported for reinstatement of structures affected by serviceability and structural distress (Feld,1965 ; Tomlinson,1984). The uncertainties of the effectiveness of the repairs prompted either an expensive foundation design or a costly repairable scheme throughout the lifetime of the structure. Feld (1965) concluded that repairing flexible structures is more cost effective than repairing a deformed rigidly designed one. In

addition, the cost of correcting a repairable structure is far less than any repair procedures that have to be devised for structures at a later date (Moncarz, Osteraas and Wolf,1986). This is because repair procedures were not integrated initially within the structure of the building, thus interaction between structural members may restrict effectiveness of repairs and initiate further damage. Also, where design and repair have to be treated as two independent operations, the cost and demand for special skills increase as, in some circumstances, major repairs have to be conducted, such as constructing of complete foundation systems or clamping of roof structures (Mautner,1948 ; Jones,1985).

In any assessment of the design and economics of structures designed to permit relative movement, especially low-rise buildings, the need to reach an optimum solution satisfying both the design limit states (ultimate and serviceability) as well as the cost of the building must be appreciated (Burland,1984 ; Donaldson,1975). For the above type of buildings, since by design the structure is inevitably bound to deform and crack, the serviceability limit states (deflection, cracking, vibration and durability) should not be exceeded. With an appropriate degree of safety in reserve, the structure may be allowed to reach its serviceability limit if it will perform satisfactorily during its intended life. Thus, there is a necessary requirement to limit the behaviour that exposes flexible structures to more deflection and thus excessive deformation. This is proposed to be taken into account by the repairability of the structural system. Although repair techniques are methods of construction, their early involvement in the design process is a necessary condition. This is because they should be considered, so that the structure will not unduly deteriorate under the action of its primal design objective (that is, allowing movement) over its anticipated life; this suggests that repair is the most critical limit state. As a result, a new serviceability limit state is mooted, which is concerned with the structure's behaviour before and after differential movement, namely, the repairability. However, this limit would only apply to structures designed to allow relative movement to occur during their working lives, analogous to durability measures for structures exposed to severe atmospheric and weather conditions. The limits will be either the amount of relative deflection that the structure is able to cope with (as well as the user of the building), or the level above which repairability is hindered owing to further

structural distress, such as jamming of cracks by debris, excessive window or door distortion, etc., whichever being the least.

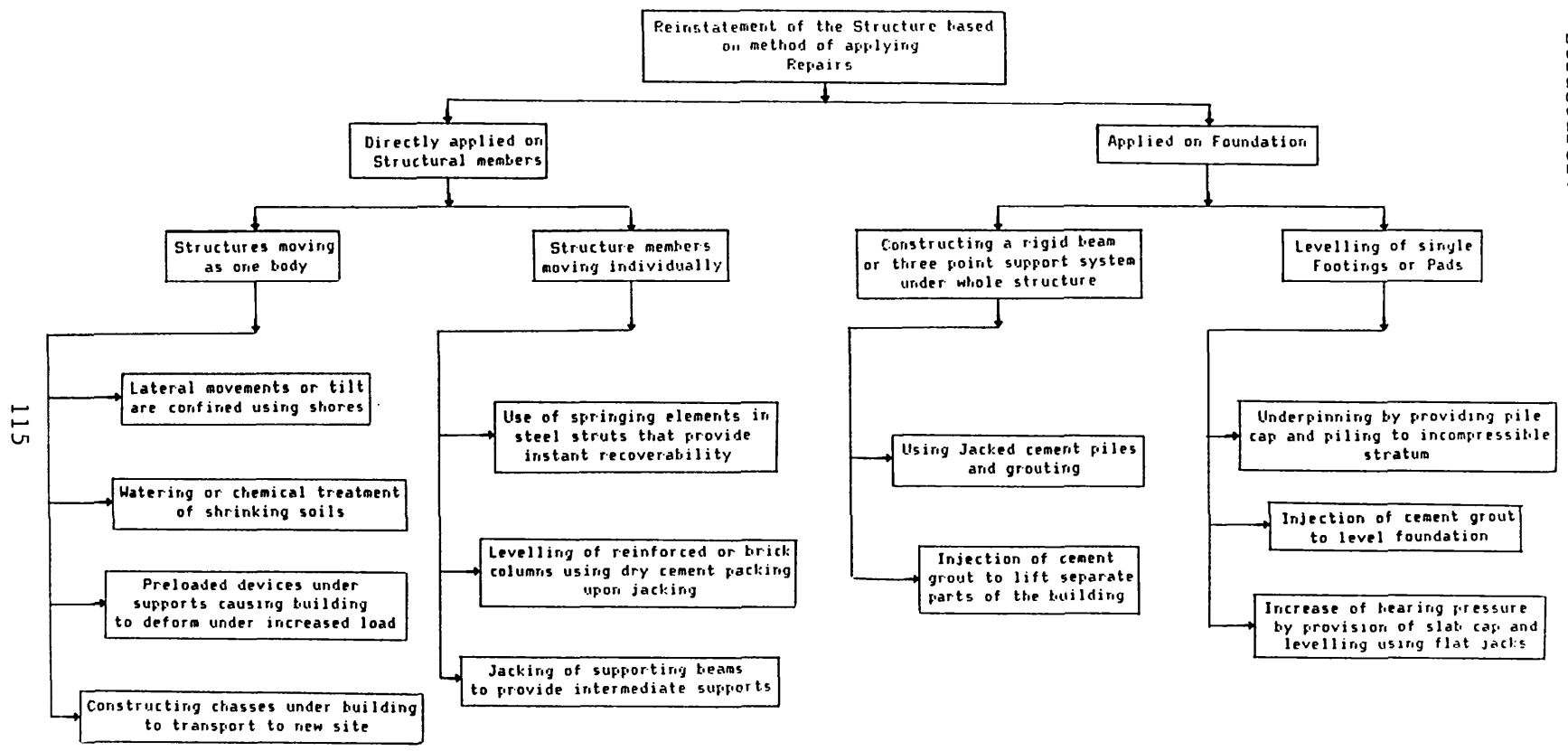
#### 4.5 TECHNIQUES FOR REINSTATEMENT OF STRUCTURES

Economy is vital at two stages, firstly during the initial design, and secondly, at the repair stage where the structure is to be put back into working use. The requirement at the second stage is difficult to forecast when design is made sufficiently strong. Alternatively, if distortions become evident, an early change in structural design with sufficient articulation to prevent large carryover of loading on the members that would result in excessive damage, might avoid the additional costs of repair. Also, if the structure distorts or if deflections exceed Code limits, structural reinstatement is inevitable. Since structural reinstatement involves recovering of part or whole of the load shed after deformation, its application after construction is generally more cumbersome and expensive than surface repairs (Warrier,1977). It is thus recommended that for such cases where movement of the ground is expected, structural repairs are to be considered in the design process.

Several techniques are commonly used for the reinstatement of structures. They differ in cost, application of each method and the approach to apply in different forms of structures. Based on the method of applying repairs, the techniques are classified in Table(4.1), according to whether the force of repair is transmitted directly or indirectly to the superstructure members. The force of repair is taken as part or whole of the lost load due to differential movement of the supports. Indirect application through the foundation distributes the repair force to structural members in the same proportion as the structure load is transmitted to the foundation. Thus reinstatement of the whole building is safer, and it is less likely to induce further secondary stresses in the event of body tilt and twist. However, this method is more expensive and, in some cases, impossible to apply practically (Tomlinson,1984). Alternatively, levelling of parts of the building directly is more difficult to apply and should proceed with great care. This is because it is dependent on two main factors, which are the structure form and the type of restraint during relevening of different parts of the structure, such as window and door openings, roof-joists and partition walls. In Table(4.1), current practical

methods are also categorized, with an indication of whether the repair technique is applied locally or over the whole structure.

Table(4.1) Summary of traditional methods for reinstatement of structures.



#### 4.5.1 Method of injection of cement grout

Buildings can be raised in order to compensate for settlement by the injection of cement grout into the bearing joint between the structure and the foundation. For this technique to be efficient and cost effective, the foundations are isolated and cement grout is pumped at high pressure into a pocket provided under the bearing end of the column of the superstructure or the foundation pad (Pleithner and Bernatzik, 1953 ; Falkner, 1980) (Figure 4.6).

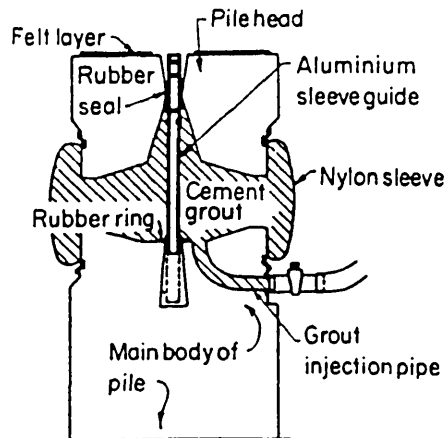


Figure 4.6 Grouting of foundations to compensate settlement of structures (after Tomlinson, 1984).

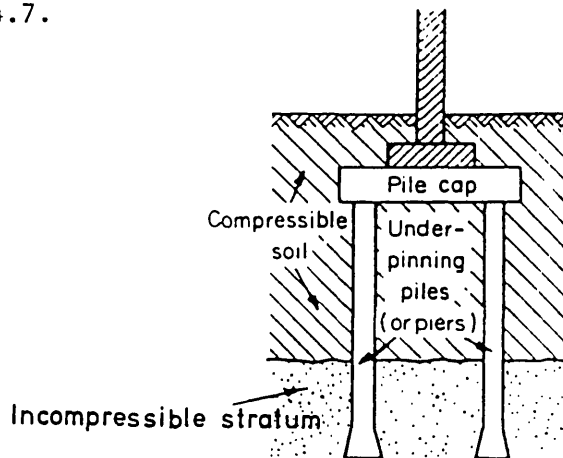
Since raising the structure by grout pumping, proceed by reacting firstly on the bearing soil, large jacking loads of buildings can be applied only by isolating that region and reducing the permeability of the soil using cement based mixes. Large jacking forces of 100 MN can be applied and 20 mm lift distance has been achieved (Kupfer, 1986). Firstly, the structure is cleared from any hindrance between the foundation and the structure so as to bear safely (structurally) on specific points, referred to as bearing points. Secondly, injection of the grout at localized points serves to set the level of the building before all the supports or bearing points are brought simultaneously to the required level. As the required level is reached, the pumping is cut off by means of a safety release valve, maintaining the volume of the grout until it sets. This method was also used to fill cavities formed due to old mine workings underneath building sites. Boreholes are drilled around the building site to provide strong grout pillars, on which raft slabs span across. The main filling material is normally sand-cement grout, injected by pneumatic placer or pumps, having an aggregate cement ratio of 3.5:1. A topping finer grout of cement ratio



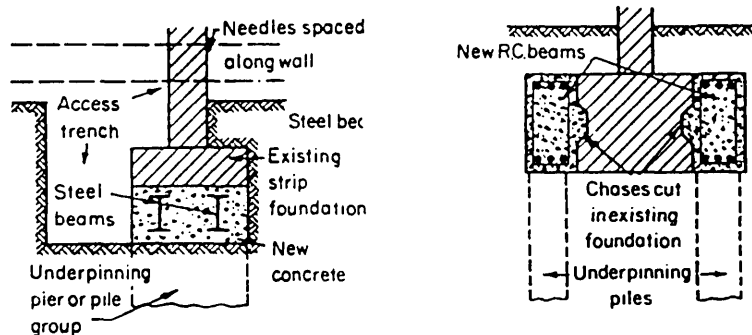
of 2:1, using finer mix (that is, pulverised fuel-ash cement), was also recommended to serve as a filler for smaller voids (Proctor,1948 ; Tomlinson,1984).

#### 4.5.2 Underpinning

The underpinning of structures is a more highly skilled operation than grouting, and is performed in several ways. One way is to level the supports of the structure against subsidence or tilting by underpinning between the structure and the foundation. In addition, it is used to increase the bearing strength of the foundation by underpinning under the foundation level. Underpinning methods are numerous, depending on the cause for its undertaking, for example jacked piles, pretest method, etc. (Tomlinson,1984 ; Degerlund,1986), refer to Figure 4.7.



(a) Underpinning of single footing using pile caps.



(b) Underpinning wall foundations using beam spanning between piers.

Figure 4.7 Levelling of structures by underpinning techniques (after Tomlinson,1984).

If the aim is to arrest settlement, foundation levels are extended down to stable grounds by piers or piles; however, a stable supporting beam

constructed over the pile is required to distribute the load to the existing foundation. Alternatively, if it is intended to level the structure, a pier cap is constructed and the structure is safely jacked to level position using a cap ring beam. Difficulties can be experienced either in supporting the foundations prior to construction of the piles or in filling the gap between the foundation and the underpinned bearing supports (Prentis and White,1950 ; Tomlinson,1984).

#### 4.5.3 Jacking method

Patent jacking systems have been used extensively where movement of the structure exceeds 10-15 mm or where the movement is of an irregular pattern, as for example, during restoration of the Yankee Stadium and the Munich Olympics Stadium (Feld,1965). Advantages of jacking are that jacking points can be incorporated locally in the structure, such as construction pockets in walls or at top of columns, in the event of relevening of structural members being required. Additionally, it is used to restore the supports while the gap between the foundation and the new position of columns is filled with dry pack or pumped grout (Hoole, Stephenson and Bingham-Hall,1984). After the structure is raised to its required position, the gap between the needle beams and the R.S. channels can be packed before the wedges are removed and the jacks released (Figure 4.8).

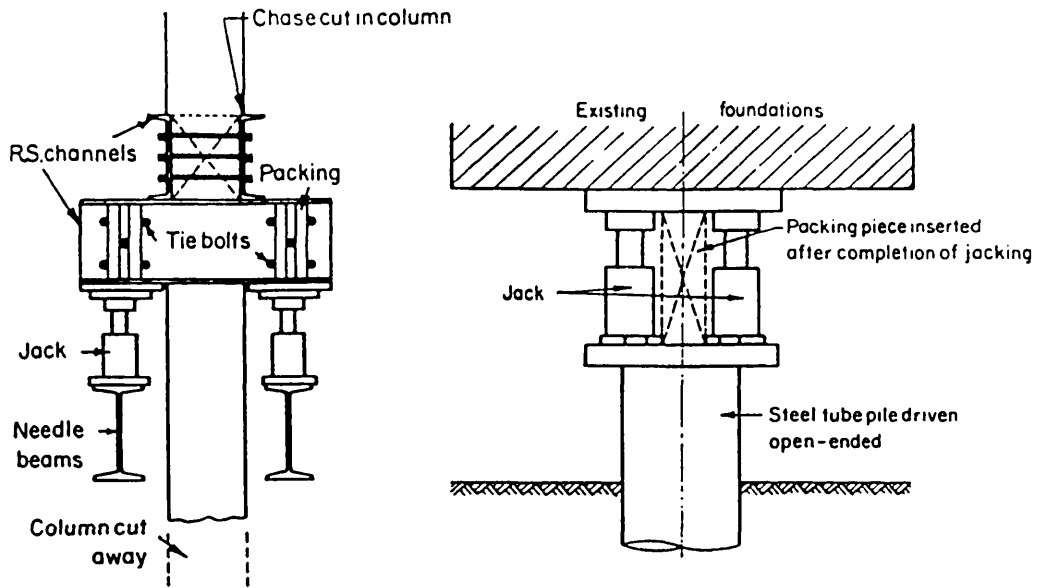
Low-rise buildings supported on foundation slabs directly in contact with the ground subject to differential movement can also be repaired by mechanical jacking of the slabs, thereby reducing cracking of walls and relevening the structure (Brown,1987). In the slab-jacking operation, grout was pumped beneath the slab to increase the bearing load of the supporting ground under the restored building.

A rigid chassis can also be employed under the building to facilitate jacking up the structure in a levelled state upon it, so that complete structures can be transported (Olsen,1958 ; Pryke,1967 ; Warriar,1977). For building restoration, jacking is preferred to winching for two main reasons, one is that jacking controls the level of the building locally, that is, relative deflection of the supports, and the safe jack load at specific points in the structure can be monitored.

The second reason is that it avoids the stretching of cables and jerking motion, which occurs in the case of winching.

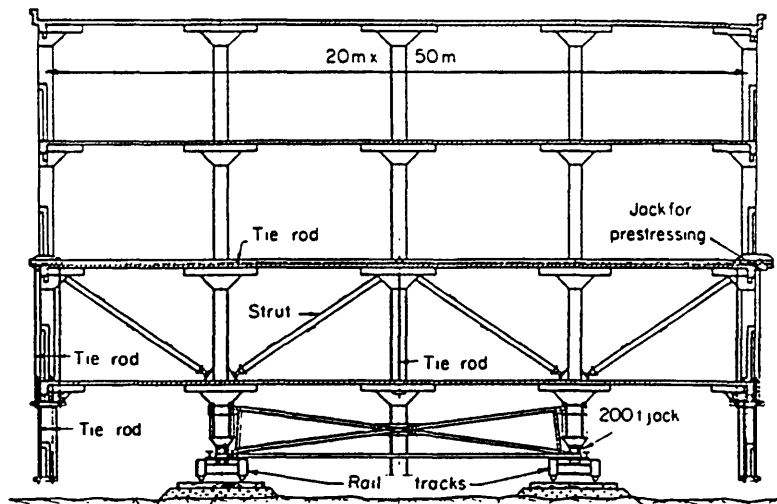
Safe employment of jacks is achieved by fitting them under rigid chasses which are firmly bolted to the columns of steel frames or

reinforced concrete buildings. Sockets in the sides of column bases can also accommodate the jacks (refer to Figure 4.8). However, it is recommended that jacks are placed between needle beams and cleats supported on an independent temporary structure for stability against overturning during eccentric operation (Tomlinson,1984).



(a) Jacking of reinforced concrete and brick columns.

(b) Jacking method used in underpinning foundations.



(c) Transportation of a five-storey warehouse to a new locaton using jacking techniques (after Olsen,1958).

Figure 4.8 Levelling of structures using jacking techniques (after Tomlinson,1984).

#### 4.5.4 Heave recovery by watering

The severe distortion and distress of buildings caused by seasonal heave can be eliminated using the "spray irrigation" technique (Williams,1980). By this technique expansive soils can be watered, either to compensate for the loss of moisture (that is, shrinkage of ground), or levelling the ground profile by watering at various points to reach a condition of even heave.

For slabs on uneven ground, Holland (1981) reported another method of compensation of moisture, by which boreholes are drilled under the slab, and are then filled with water in the low areas of the slab. Both techniques rely on the recovery of heave by the soil on supply of moisture required to fill its pores. Although these methods are simple and inexpensive, careful supervision is required to minimize the risk of further distress.

## CHAPTER 5 DESCRIPTION OF A NOVEL DESIGN METHOD -- THE FOUR-POINT-SUPPORT-SYSTEM

### 5.1 INTRODUCTION

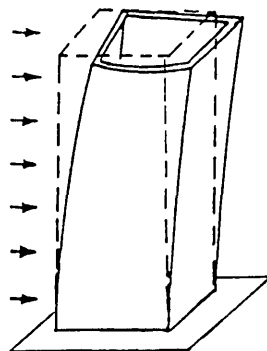
A method for designing low-rise structures to cope with the problems of ground movement is required, as discussed in Chapter 2, which is relatively inexpensive and easily implemented. A novel system is mooted here, based on the philosophy of allowing ground movement to take place and absorbing part of the differential movement within the structure through permanent deformation. An increase in the ductility of the structural form, particularly the walls, is introduced to enhance the overall structural deformation. However, the condition of weather-tightness and serviceability in residential housing puts an extra restriction on the deformability of the building. Following Section 4.4, repairability is being introduced early in the design process so as to limit hindrance for stress-free movement of the structure during reinstatement of the building.

### 5.2 FLEXIBLE STRUCTURAL SYSTEMS

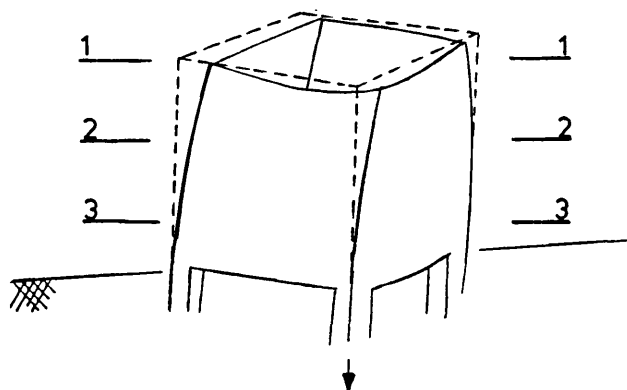
The obvious choice of structural form is a flexible system which is capable of resisting the applied external loads with some deformation, but without the development of kinematic or dynamic mechanisms. Its capacity to deform will depend principally on the structural form and the ultimate curvature capacity of the structural members. There are basically two broad classes of structural form: those resisting the applied loads by virtue of their geometry, that is, framed structures, trusses etc., and those resisting the loads owing to their stress state, prestressed structures, mass structures etc. To deform elastically, the structure is required to be geometrically unrestrained, thus allowing stress-free deflection (that is, by reducing the number of indeterminacies). However, post-elastic ductile deformation is also desirable before visual damage becomes apparent (that is, increase in deformation, formation of hinges, etc.). To allow the retention of structural integrity during and after differential movement without considerably altering the geometry (which would occur if large cracking

was allowed), large cracking can be arrested by maintaining the stress distribution using a confining stress path within the structure. This confinement may be provided by a bounding frame preventing dilation of cracks, or prestressed forces due to pre-compression of part of the structure, etc. An example is in the design of structures subject to wind and seismic loading, the most common structural form is the cantilever, which allows considerable horizontal deflection before exceeding its elastic state, whereas it is stressed down by its own weight.

The four-point-support-system (FPSS) evolved from the realization that when an open box supported at its four corners is subjected to any lateral or longitudinal load, the walls deform in both inplane and out-of-plane bending (Figure 5.1). These, in turn, induce



(a) Open box core subject to lateral forces.



(b) Open box core subject to longitudinal differential movement.

Figure 5.1 Deformation of an open box structure subject to lateral or longitudinal load and displacement.

less stress concentration on the walls per unit deformation of the structure than if only bending stress was applied on the wall. Two loading conditions are possible; one is if the walls are loaded parallel

to the plane of their supports, then they will induce a high bending resistance as a box section. The other is if loaded normal to the plane of the supports (as the case for differential settlement), the walls will deform "non-uniformly", as plane sections do not remain plane. This is as a consequence of its thin-walled cross-sectional area relative to its plan area, which would lead to warping deformation, flexure and corresponding longitudinal stresses (that is, stresses along its height), refer to Figure 5.2.

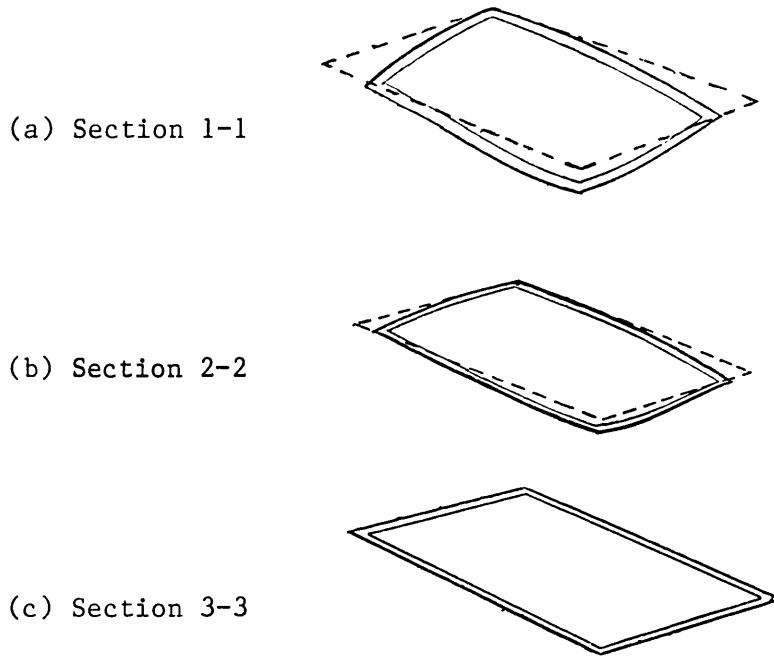


Figure 5.2 Deformation of FPSS walls at the three horizontal sections shown in Figure 5.1(b) (Deflection is exaggerated for clarity).

As the FPSS experiences differential movement of the supports, the effect of wall continuity over the corners will induce a twisting action in the walls with little bending. This type of structure is inherently flexible. Moreover, jacking of the supports can be employed to remove the wall distortions and, hence, any cracking that may have resulted. By employing a small depth of the beams spanning between the support points, an increase in the deflection of the beam-wall structure will induce a compressive stress path owing to arch action of the walls; this will restrict the opening of cracks. Since the FPSS is intrinsically flexible, it is not necessary to found the support points at great depths in a stable stratum. Much shallower depths can be considered, and this offers the opportunity to develop more economic foundation

solutions (Burland,1984). The detailed structural behaviour of this system will now be considered.

### 5.3 STRUCTURAL FORM OF THE FPSS

The simplest rigid structural/foundation system is the three-point-support. It has the important property, that it will always form a flat plane when supported on foundations at three corners (Figure 5.3).

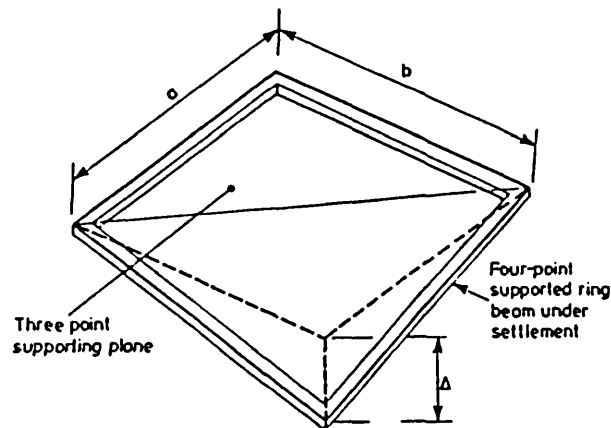
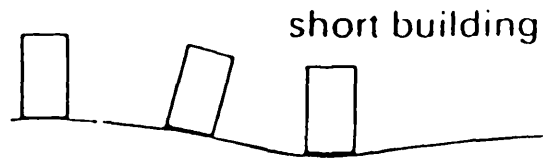


Figure 5.3 Three- and four-point-support-systems.

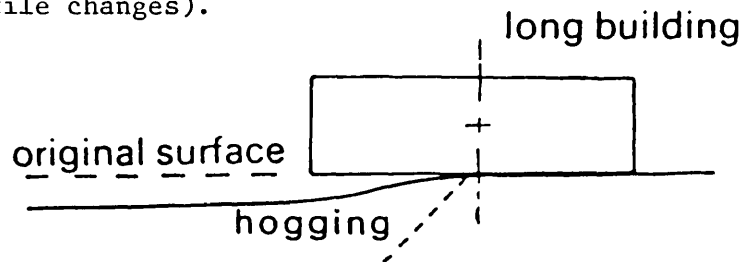
No distortion can occur if differential settlement takes place, and the system will always maintain the integrity of a structure founded upon it. As a result, no secondary stresses are induced by the differential movement of the supports, except on excessive tilting of the foundation plane, which might cause stability problems due to gravity (Figure 5.4).

However, three-point-support-systems are expensive (Jones,1985), since they require stiff structural elements some of which experience a hogging mode of deformation which is damaging to masonry walls (Burland and Wroth,1974). If a fourth support is present, it will provide the flexibility of the system outside the rigid plane, that is, it can move outside the plane defined by the other three support points if the structure is flexible (Figure 5.3). Thus, at every position of the building arising from differential movement, there always exists a rigid three point system supporting the fourth point outside their plane as a cantilever. In addition, on settlement of the fourth support, the system will distribute a large proportion of the differential movement into the structure including that part which is supported by the plane of the other three supports. This is achieved by deformation of the wall panels and the floor system.





(a) Stability problems of short slender buildings (dependent upon the length of the building with respect to the position at which the ground profile changes).



(b) Less problems of stability of long buildings, where they experience more hogging or sagging deformations.

Figure 5.4 Problems arising from excessive tilting of buildings (after Attewel et al.,1986).

In flexible systems, the most critical engineering features are the diaphragm action of both the roof and the floor slabs, together with the stabilizing action of the vertical bracing. This is provided either by the framing system or the infill panels of the structure. For the FPSS, the diaphragm action of the roof and the floor will restrain the tendency for the fourth support to deform differentially by increasing the torsional stiffness, thus reducing the inplane and out-of-plane stresses contained within the core of the four walls. An open or non-restricted roof will permit larger deformation of the walls and, therefore, to the fourth support, but will increase the warping of the walls. It follows that the roof structure should be flexible to inplane shear in order to be able to deform compatibly, for example, slide on top of the walls. This detail is discussed in Section 5.3.4.

### 5.3.1 Slab or articulated ring beam

The basic system was first described as the "Four-Point-Support Jacked Slab" by Burland (1984). It comprised a slab, having edge beams at its four sides, supporting masonry walls. However, the deformed shape of the slab was found to be highly complex (Mansour,1985 ; Mansour, Burland and Perry,1987 ; Burland, Mansour and Perry,1988) when

studied in conjunction with the distorted four walls (Figure 5.5). The slab would tend to induce out-of-plane twisting and the resultant stresses along the slab would vary considerably. To utilize fully the flexibility of the FPSS, and to incorporate simpler behaviour, a ring beam has been adopted in place of the slab.

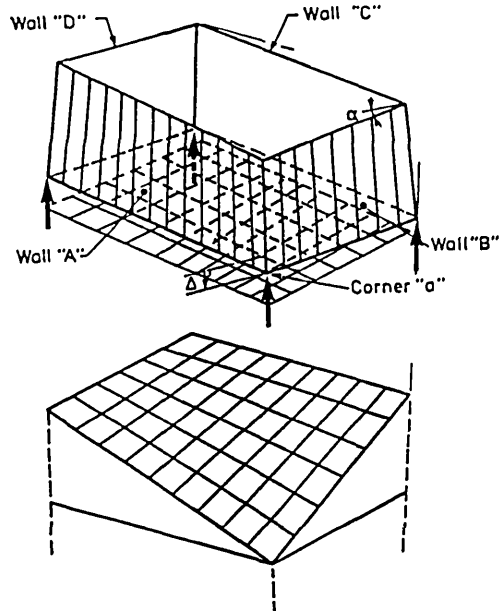
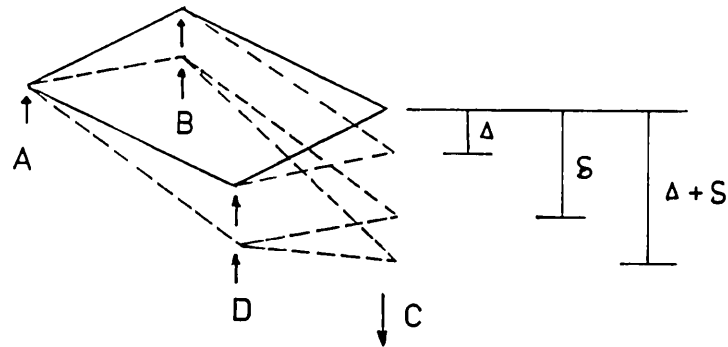


Figure 5.5 Deformed shape of walls and suspended slab of the four-point-support-system (FPSS).

On movement of any corner "a" (Figure 5.5), the principal stresses in the beam-wall panels, "A" and "B", result from inplane bending, that is, rotating as cantilevers, while the behaviour of panels "C" and "D" is then pure out-of-plane twist, rather than combined inplane flexure and twist which would have resulted from slab-wall interaction.

A concrete ring beam is provided at soffit level of the masonry walls to act as a supporting grade beam for the superstructure. This is provided by point support foundations at the four corners of the beam. Raising the ring beam clear of the ground will minimize the effect of soil-structure interaction on the suspended superstructure, and will limit the soil reaction to the supports only. Thus, the beams will deflect free from the ground, inducing arch action in the walls and, in addition, tying the beam-wall together. This will allow cantilevering of unreinforced masonry walls without the risk of sudden collapse. To articulate the ring beam in such a way as to permit differential movement of any fourth support, it is designed with short columns at its four supports so that relative movement is accommodated by the use of concrete hinges at the beam-short column joint. Point supports are also

provided to allow rigid body rotation of the ring beam after hinge formation, thus allowing tilt of supports on settlement (Figure 5.6).



$\delta$  = tilt of three-point-support-system ABD.

$\Delta$  = differential settlement of support C from plane ABD.

Figure 5.6 Effect of tilt of the supports on the total settlement of the FPSS.

### 5.3.2 Walls

In practice, buildings are designed on the assumption that the frame would take the secondary stresses generated by unequal settlement. Infill panels are disregarded, or the walls are assumed to exhibit no

- $\phi_i$  = Rigid body rotation of Wall i
- $\theta_i$  = Maximum warp of Wall i (out of plane deformation)
- $\alpha_i$  = In-plane deformation of Wall i

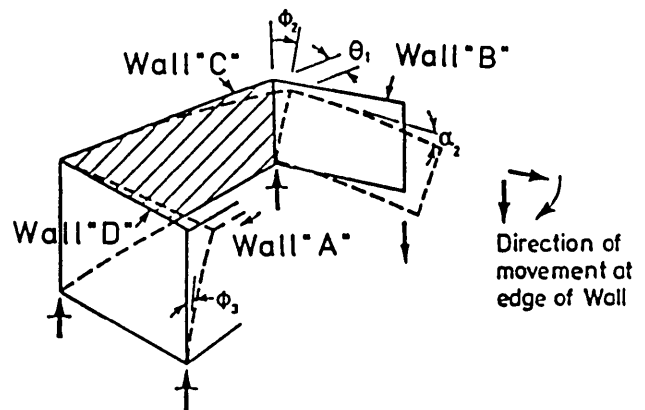


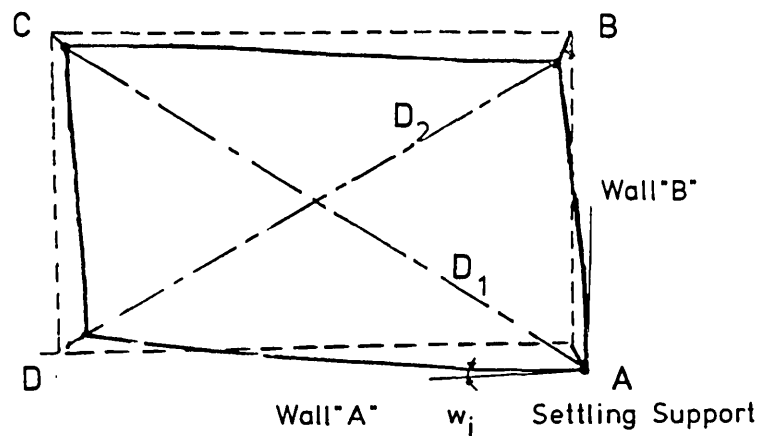
Figure 5.7 Effect of cross walls in increasing deformability of the FPSS.

flexural and torsional strength. Figure 5.7 shows the wall deformation of the FPSS during settlement of one of its supports, where the following structural properties are observed:

- deformation of main walls "A" and "B" consist of inplane bending due to cantilevering and out-of-plane warping due to shortening of the length of the main walls, since the top corners of the box deform non-uniformly as plane sections do not remain plane,

- twisting of adjacent walls "C" and "D" provides flexibility for the cantilevering of main walls "A" and "B". This allows additional deflection and, in turn, causes torsional damage in walls "C" and "D", which is less noticeable than inplane bending. In addition, stability of the main walls is still maintained since the torsional resistance of the adjacent walls is approximately one-half of its ultimate strength even after cracking, if flexure was present (Park and Paulay,1975),

- box action of the FPSS producing a twist (out-of-plane bending) in walls "A" and "B", dissipates part of the differential movement energy; the energy being the structural response on settlement of support "a". This can be clearly seen as the diagonal  $D_1$  at the top of the wall elongates, while the opposite diagonal  $D_2$ , shortens (Figure 5.8). Due



$D_1$  = diagonal CA,

$D_2$  = diagonal BD, and

$w_i$  = out-of-plane warping of wall "i".

Figure 5.8 Warping of walls of the FPSS (in plan view) due to shortening and lengthening of diagonals  $D_2$  and  $D_1$ , respectively.

to the settlement at corner "B" and the fact that the two L-shaped walls at the settling end B-B' are continuous, the diagonals of walls A and B become shortened, that is,  $D_A$  and  $D_B$  (Figure 5.9). This, in turn, induces compression along these diagonals, and

- additional confinement, helping to arrest cracking in the wall, is introduced by the arch action of the wall. To ensure an arch action with a larger compressive force, the relative stiffness of the beam to the wall,  $K$ , is kept in the range of  $10 < K < 15$ . The reduction in the relative stiffness is limited by the induced wall stresses and the serviceable deflection of the beam before settlement.

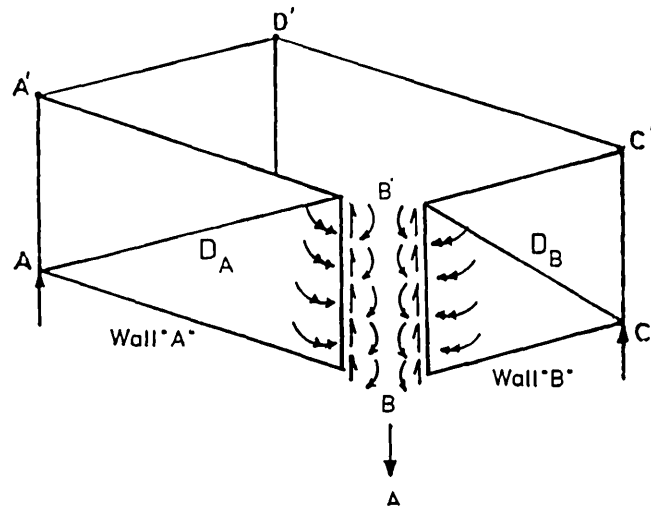


Figure 5.9 Equilibrium of end forces at the settling wall corner B-B'.

### 5.3.3 Repairability measures

An important and frequently neglected criterion in the design of low-rise buildings is the ease with which they may be repaired. The incorporation of an inexpensive method of repair consequent upon large ground movement is clearly a desirable objective. For the FPSS, jacking is proposed as a repair procedure at the corners of the ring beam. This permits re-positioning of the beam and reinstatement of the structure should this be required. In this way the building need never reach a condition exceeding any of the serviceability limit states.

Since there is interaction between structural members during and after repairs, measures must be taken to minimize complication of design detailing and application of the repair method, as follows:

- the structure should be designed to maintain its integrity, both during differential settlement and after repairs. The FPSS satisfies this requirement due to the stability of the four walls as a box. If the FPSS is to be used for buildings of large plan area containing a number of rooms, it is necessary to construct it in separate modules, with articulation between each module;

- jacking pads are incorporated in the structure at positions such that no further distress can occur. This fail-safe method is intended to ensure that jacking gaps are only effected at safe positions in the structure during construction, and not in positions chosen by the repair engineer. For the FPSS, there is no other place where jacks could be placed except at the corners of its supports;

- jacking is accommodated in the structure so as to annul the effect of settlement directly, that is, settlement is occurring at the same position where reinstatement of the structure is resumed. Thus,

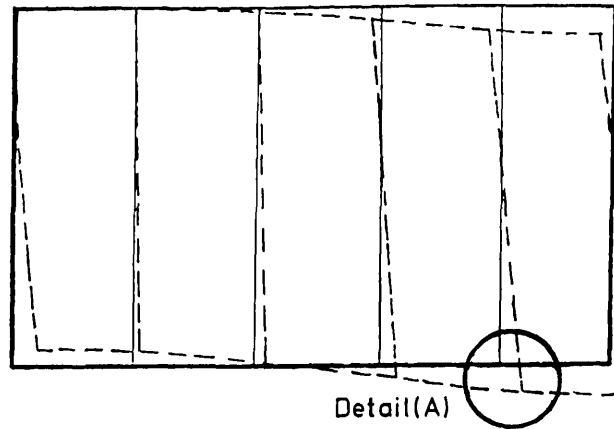
reinstatement of the structure is not a repair treatment for the effects of settlement, but directly involves minimizing the causes of settlement, that is, the differential movement of the supports;

- repairs by application of a jacking load in order to recover initial stiffness of the structure should commence at a location of minimum compressive stress concentration (Warrier,1977). This is to reduce concentration of stresses in local regions that would initiate further distress. This is true of the FPSS, since jacking would commence at the position of minimal compressive stress; and

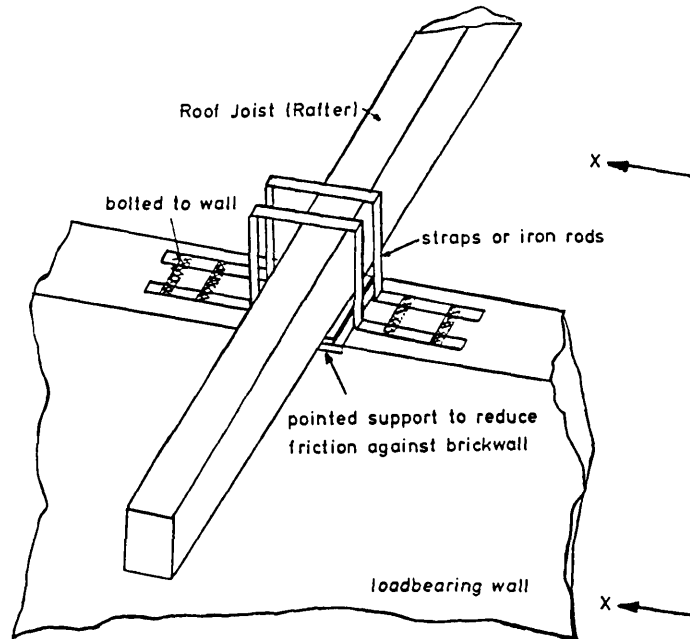
- repairs are employed before a level of deflection is reached beyond which re-jacking would initiate more damage. The latter can be due to possible closure of cracks by debris or jamming of doors and window openings. Additionally, repairs are applied where other serviceability limits, such as weather-tightness of walls, visible cracking, etc., can be avoided.

#### **5.3.4 Roof structure**

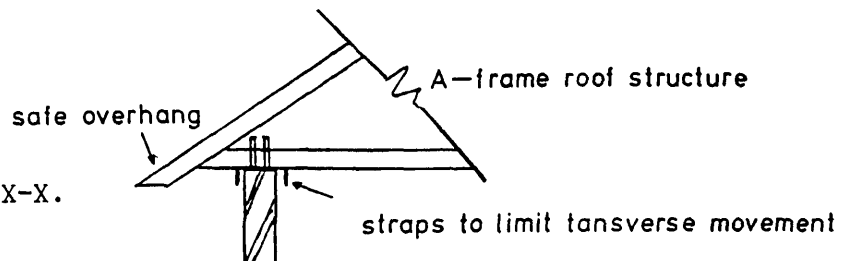
The success of this system is dependent upon the choice of roof structure so as to allow differential movement of the walls without any restriction in both horizontal and vertical directions. It follows that the roof should be flexible to inplane shear (along the plane of the roof), and should not require sophisticated methods of articulation hindering their construction or requiring excessively good workmanship and special skills. The roof structure is designed to allow relative horizontal movement by incorporating long overhangs of rafters or joists, while vertical differential movement is permitted by simply supporting the rafters on two positions on opposite walls, as shown in Figure 5.10. Figure 5.10(a) illustrates a plan view of distorted FPSS at roof level, where the roof joists are distorted horizontally in two directions. Slippage of the roof joists on top of the wall is designed to permit horizontal, vertical and rotational movement of the rafters, irrespective of the loadbearing walls. Thus, the roof is devised as an integrated structure while it is simply bearing on the walls. Provisions to hold the roof against suction due to wind or accidental collapse owing to excessive slippage are required, and should be applied in such a way as to safeguard the weather-tightness of the roof-wall connection. Figure 5.10(b) shows a typical roof-wall connection, where vertical and horizontal guides are introduced to limit movement of the roof. Additionally, it is point supported in order to reduce friction.



(a) Plan view showing relative movement of roof joists.



(b) Detail(A).



(c) Section X-X.

Figure 5.10 Detail of sliding roof to accommodate vertical and transverse movement.

#### 5.4 MODELLING OF THE FPSS

To study the practicability of the FPSS, experimental testing is required. Thus, it is important to define the main factors influencing the structural behaviour before and after damage, so that they may be included in a parametric study. In this investigation, the following

factors were considered:

- the effect of the wall geometry, defined by the aspect ratio (L/H) on the capacity of the wall to deform (in flexure and twist). In addition, its effects in modifying the dominant stress distribution within the wall (that is, whether bending or shear) and, thus, in altering the pattern of cracking for large excessive deflections; and
  
- the supporting ring beam influences the articulation of the FPSS in three ways; firstly, the ability of the system to deform without restraint. Secondly, the use of point supports increases the rotation of the beam about the supports prior to cracking. Thirdly, after cracking, introduction of hinges in the concrete beam near the support further increases deformation of the walls and the cantilevering beams.



## CHAPTER 6 DESCRIPTION OF TEST RIG, FABRICATION AND TESTING OF MODELS

### 6.1 INTRODUCTION

The experimental part reviews the feasibility of applying the four-point-support-system (FPSS) as a design technique for low-rise buildings in areas of ground movement. The model system described here is intended to simulate a real structure supported on its four corners, with no provisions made for openings such as doors and windows. The return walls and the ring beam of the FPSS, described in Section 5.2, are vital for modelling the overall behaviour of the support system, and necessitated the use of a 3-dimensional structural model. Since the flexibility of the method was under investigation, restraints were minimized to allow the model to deflect more easily. This was achieved by releasing, as far as possible, the walls from boundaries such as the roof and the floor slab (refer to Section 5.3).

### 6.2 EXPERIMENTAL PROGRAMME

The tests were aimed at examining in more detail the load-deflection relationships of the FPSS, in the pre- and post-cracking phases. With regard to the reinforced concrete ring beam, studies were to be made of the redistribution of the load on settlement of supports and of the rotational capacity. Its effect in reducing the support restraint on the warping of walls was also investigated. Of immediate concern was the serviceability state of the FPSS after settlement, and the repairability of the damage caused by warping of walls. Since the walls not only increased the flexibility of the support system but, also, were likely to cause brittle torsional failure, design measures were taken to reduce brittle failure. The investigation can be grouped into two parts. The first was to determine and apprehend the deformation of the FPSS before the first serviceable limit state in the beam-wall structure was reached. The second was to define the repairable capacity of the FPSS by re-levelling the ring beam using jacks under the supports. Thus, the tests were planned with the following objectives:

- a) To determine the maximum differential movement that the FPSS is able

to cope with before visible damage emanates, to examine the different failure modes, and the influence of repairability in improving the lifetime performance.

- b) To examine the structural factors affecting the behaviour of the FPSS, in particular, the aspect ratio of the walls, reinforcement ratio and provision of weak joints. This includes rotational capacity of the supports and the warping of walls.

Five brick boxes, each incorporating the FPSS were tested. Appropriate notations were designated for each test as shown in Table(6.1).

Table(6.1) Symbols designating tests.

Structure face <sup>o</sup>	Test No.	Description of test	Wall notations ( $L_1 > L_2$ )		
			Specimen No.*	beam $L_1$ **	beam $L_2$ **
1A	1	Lateral movement of low walls with fixed supports.	W1A	W1AA	W1AB
1B	2		W1B	W1BA	W1BB
2A	3	Vertical movement of low walls with fixed supports.	W2A	W2AA	W2AB
2B	4		W2B	W2BA	W2BB
3A	5	Vertical movement of low walls with point supports.	W3A	W3AA	W3AB
3B	6		W3B	W3BA	W3BB
4A	7	Vertical movement of high walls with point supports.	W4A	W4AA	W4AB
4B	8		W4B	W4BA	W4BB
5A	9	Reinforced top courses of high walls with point supports.	W5A	W5AA	W5AB
5B	10		W5B	W5BA	W5BB

Notes:

- <sup>o</sup> Each FPSS structure is tested twice, on two opposite corners A and B.
- \* Example of structure notation, W1A comprises a pair of beam-wall W1AA for span  $L_1$  and W1AB for span  $L_2$ .
- \*\* Tests W4BA and W4BB represent test specimens of FPSS model No. 4, test B, for both spans A (designating span  $L_1$ ), and B (designating span  $L_2$ ).

The casting and testing programme was as follows. The reinforced concrete ring beam was cast, demoulded after 10 days and set in position. Each beam of the ring beam was propped at its third span points to minimize any residual stresses induced during bricklaying. This allowed as much bricklaying as necessary without risk of

overloading the beam. For each box, building the brick walls took 5 days; the method of quality control is described in Section 6.5.2. Preparation for testing started 10 days after bricklaying, to allow sufficient time for curing. Setting up of gauges and the loading system took 5 days and the duration of loading (Test A) took approximately a further 5 days. For the other corner of the box, that is Test B, 14 days were required to set up and test.

In cases where severe damage occurred during Test A, remedial repairs were necessary in order to minimize the influence on the other corner during Test B. The repair technique is illustrated in Section 6.7.

### **6.3 TEST MODELS**

#### **6.3.1 Choice of model**

The test specimen is a model of the four-point-support-system (FPSS) envisaged to represent in general terms, an actual building that might be subject to ground movement. The choice of the laboratory model must be representative, both of the geometrical scaling and of the properties of the materials employed. This is vital for any relationships that are established to be representative of the actual prototype structure. The direct method for modelling is to satisfy the laws of similitude by linearly scaling down the size of all materials, including aggregates, bricks and mortar, by the scale factor. However, scaled down materials would suggest an increased surface area per unit weight compared to normal size bricks and mortar. Therefore, a larger quantity containing finer materials and specially manufactured model bricks would be required; these are not readily available. Thus the approach of scaling down linearly the size of materials was not considered practicable. This would also induce an increase in the strength of the mortar by 15%-20% (Hendry and Murthy, 1965 ; Sinha 1976). Since, the serviceability limits were also under consideration, scaling was minimized to reduce any extraneous results. Within the available laboratory space and limitation of cost of the test rig, a half-scale model was opted for, thus avoiding the more difficult problems of scaling.

An attempt to model masonry structures by Vogt (1956) using 1/4-scale bricks and, later, 1/10-scale bricks was found successful to predict the elastic behaviour. The engineering feasibility of model brickwork in structures was established (Hendry and Murthy, 1965 ;

Murthy and Hendry,1966 ; Sinha and Hendry,1976) by direct comparison of prototype brickwork and that of models. Hendry and Murthy (1965) undertook work on 1/3- and 1/6-scale models, by employing 1/3- and 1/6-scaled bricks. The tests were concerned with the relationship between mortar strength and the strength of brickwork with reference made to scaled bricks. It was concluded that the strength of full-size brickwork can be reproduced with reasonable accuracy by means of model tests. However, for the control specimens of the mortar, the strength of 1 in. cubes was considered instead of 2.78 in. cubes used for full-size bricks. Extension of the basic modelling techniques developed by Hendry and his co-workers at the University of Edinburgh was made in studies of deflections and stresses in multistorey brick structures under lateral loads (Sinha, Marcenbrecher and Hendry,1970 ; Kalita and Hendry,1970).

Previous research on masonry structures by Holmes (1961) and Stafford-Smith and Riddington (1977) considered the composite behaviour of infill frames. Models of 1/3- and 1/4-scale were successfully employed. Full-size bricks and blocks were also used on scaled models. Dawe and McBride (1984) tested large-scale masonry walls incorporating full-size blocks and using normal mortar mix. Reference was made to serviceability limit state by monitoring cracks in model walls without incurring erroneous results.

Benjamin and Williams (1958) conducted one of the earlier series of tests on model masonry in studies dealing with the shear resistance of infill frames. Similar behaviour of 1/3-scale models compared to full-size specimens was achieved. It was concluded that errors due to model scaling were not as significant when compared to variations resulting from workmanship and construction materials. Yorulmaz and Sozen (1968) concluded that replicas of prototype tests were producible in models. Models were found successful in providing considerable insight into the interaction of masonry with the bonding frame, compared with the prototype.

West et al. (1986), reviewing the resistance of masonry to lateral loading, tested model walllets. Full-scale bricks were employed with nominal 10 mm mortar thickness of Type I, II and III according to BS 5628. They concluded that smaller specimens were more sensitive than full-size walls.

Longfoot (1984), simulating inplane bending in walls, tested models (12 courses high for 1/3- and 1/2-scale models) to determine the limiting strain required to initiate failure on settlement of supports.

Full-size bricks were used, and a mortar mix 1:1:4 was adopted with no material scaling. Longfoot concluded that the serviceability limit of the walls was related to the choice of the material of construction.

Sabnis, Harris, White and Mirza (1983) tested model masonry under different stress patterns, compressive, flexural bond and shear. Correlation of results between the model and the prototype ranged from good to excellent. In compression, masonry models have shown that similar behaviour to the prototype can be achieved if scaled bricks of the same compressive strength are employed. For flexural bond and shear, they recommended that consideration be given to the tensile strength of joint mortar. This included the effect of reducing the ratio of the size of the mortar joint with respect to the brick width. Good correlation between the elastic moduli of the model and that of the prototype was obtained.

Since not only the elastic behaviour is important but also, post-cracking behaviour, the requirements of modelling are further complicated. Becica and Harris (1977) adopted techniques in modelling of masonry structures that parallel those used in reinforced and prestressed concrete structures. However, additional difficulties could arise since masonry model specimens (walls, prisms etc.) are not cast but, rather are fabricated. Harris and Becica (1978) and Sabnis et al. (1983) observed that cracking of masonry model specimens occurred at a slightly higher load level than in the prototype.

Experimental research concerning model analysis, particularly in the field of concrete (Long,1980 ; Waldron and Perry,1980) investigated problems associated with scaled materials in models. To ensure that models would behave in a manner similar to the prototype, primary parameters affecting the behaviour of the model were satisfied. These were the ratio of tensile to compressive strength for modelling using microconcrete, or the use of artificial wires to reduce cracking in smaller reinforced concrete models. Using the same analogy, an important parameter in investigating the FPSS behaviour is its serviceability limit state. The critical serviceability limit state here is the extent of cracking of the walls, that is, material deterioration. In order to satisfy the modelling requirements for serviceability, together with the laboratory limitations, full-scale bricks and materials were adopted for the 1/2-scale model for the present tests.

Although full-size materials were used, it was necessary to match the experimental conditions in order to duplicate the serviceability of

the structure during testing. This was recognized in the fabrication of the walls and by applying laws of similitude to cracking.

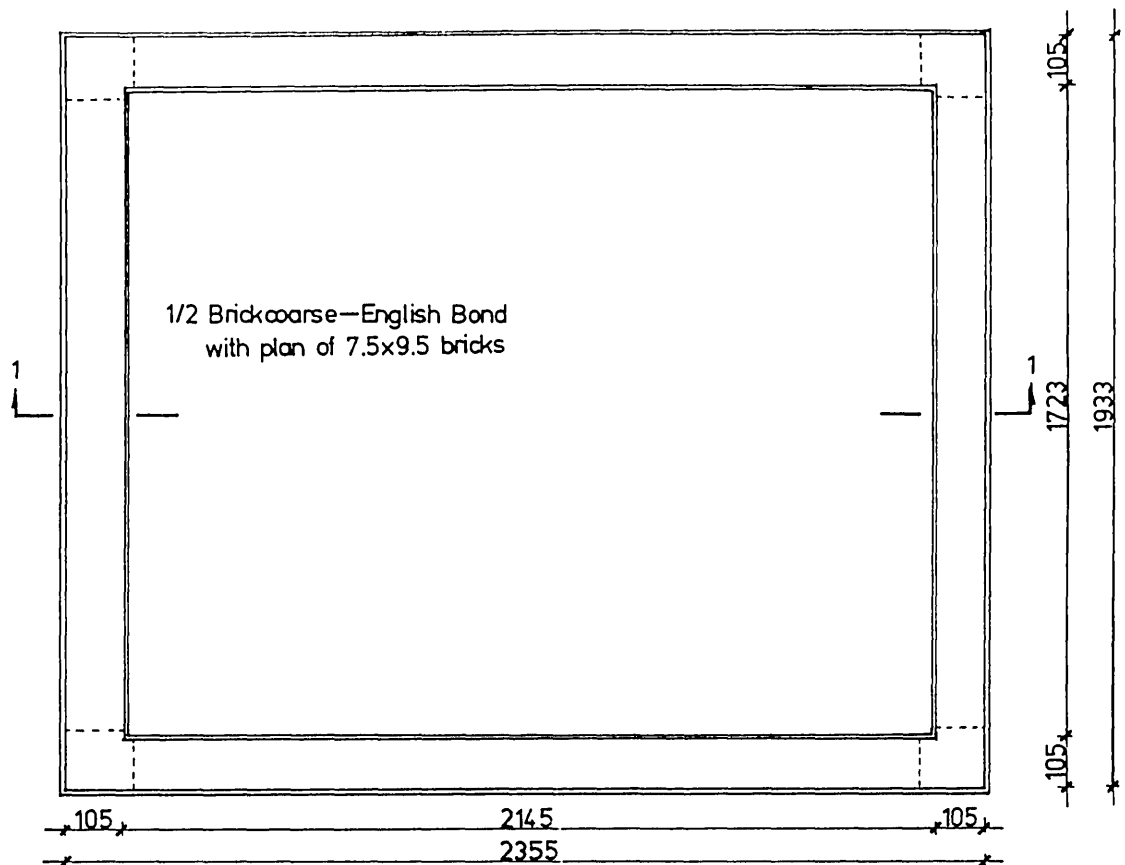
Cracking similitude in masonry is dependent on two factors: the initiation of cracking and the crack spacing and width. Initiation of cracking is a function of the tensile strength of masonry. This is either the tensile strength of mortar if the mortar is weaker than the bricks, or tensile strength of bricks if the bricks are weaker. Since, in this case, weaker brickwork was chosen (Section 6.4.3), most of the cracking propagated along the brick-mortar interface. Crack spacing and width are both dependent on the bond between the two materials, that is, bricks and mortar. Thus, the tensile strength of mortar is vital to the modelling of the FPSS. Sabnis et al. (1983) suggested for scaling of the inelastic structural behaviour that the ratios of elastic moduli, masonry unit stress, and Poisson's ratio, of the prototype to the model should approach unity. This technique was adopted in modelling the material properties. Similarly, for the concrete ring-beam and steel reinforcement, the ratios of their stress and strain to that of the prototype did not exceed unity.

For the reinforced concrete ring beam, modelling of reinforcement necessitated the use of mild steel bars in order to achieve a practical size of bars. Also, to prevent any shear failure due to the scaled spacing, smaller bars for shear reinforcement  $\Phi 4$  mm, were adopted with minimum spacing conforming to BS 8110:1985. A normal concrete mix was used with maximum aggregate size of 10 mm in order to provide the nominal cover and to simulate better cracking of the 1/2-scale beams.

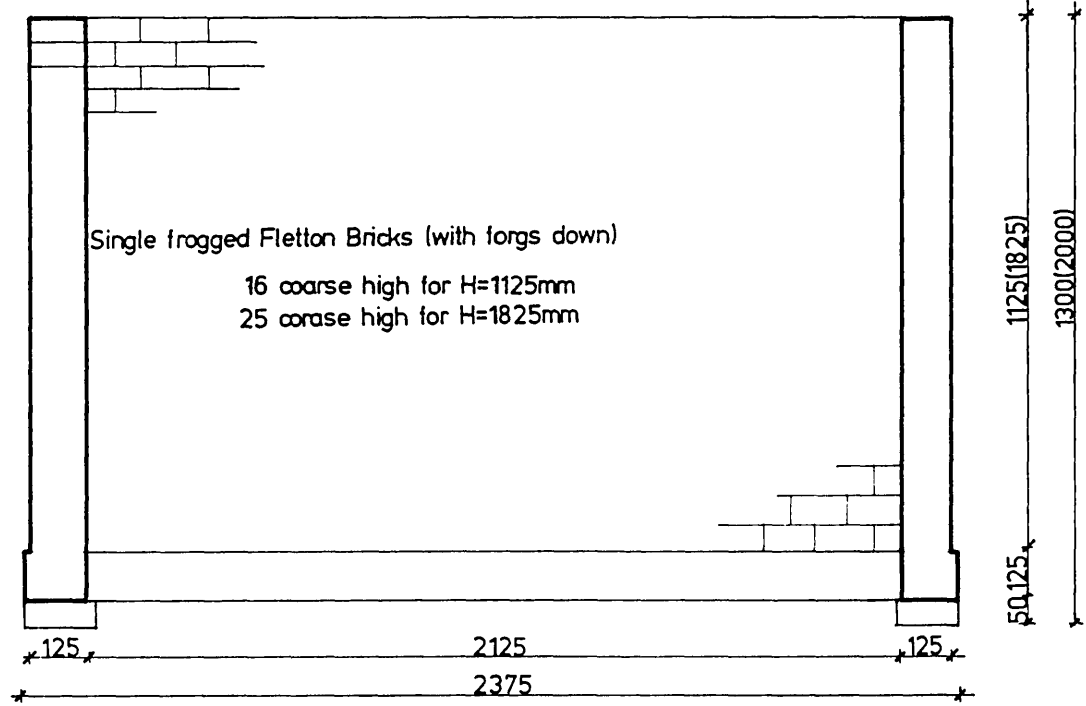
### 6.3.2 Geometry

The dimensions of the FPSS model were derived from prototypes of typical low-rise buildings. Aspect ratios of walls (L/H) in the range of 2.0-1.625 and 1.25-1.0 represent typical residential structures, warehouses and factories, respectively. The dimensions of the model representing a box-core wall were 2250x1828 mm. The walls were 1125 mm high for the shorter model or 1828 mm for the higher model. Brickwork masonry was used with English type bonding and single leaf width (1/2-brick). Mortar beds of 10 mm thickness were pointed "flush" with the bricks, to facilitate detection of cracks during the test. Figure 6.1 shows the dimensions and wall details of the models.

The ring beams supporting the brickwork consisted of a square reinforced concrete beams with short columns at the four corners of the



PLAN



SECTION 1-1

All Dimensions are in mm.

Figure 6.1 General arrangement of FPSS walls.





box structure. Dimensions were deduced from scaling of the prototype proposed by Burland (1984), neglecting floor thickness. The model ring beam, with plan dimensions of 2300x1900 mm, had a beam depth and width of 125x125 mm. It was supported on rigid steel column bases simulating the foundation of the prototype. Main reinforcements consisted of 2R $\phi$ 8 mm at both the top and bottom of the beam for area  $A_{s2}$ , and for area  $A_{s1}$ , 2R $\phi$ 10 mm for bottom bars (Figure 6.2). Typical area of steel was calculated as that necessary for a prototype beam of 250x250 mm cross-section to sustain both arch action and compressive load from the wall, together with the overhead weight, refer to Appendix 2. The shear reinforcement consisted of R $\phi$ 4 mm with a minimum spacing of 100 mm. The spacing was necessary to provide sensible shear resistance for the model beams. For practical reasons, at every corner a steel plate, 1.2 mm thick, was welded to the end of reinforcement bars. This was used as the base of the short column and to facilitate clamping of the ring beam to the supports. The short columns were designed to provide the space required for dowelling of the beam reinforcement, and to facilitate measurement of the rotation of the support. The dimensions of the short columns were 175x125x125 mm. The four plates at each corner of the ring beam served as a datum mark to control the relative deflection of the FPSS.

## **6.4 MATERIALS**

### **6.4.1 Reinforcement steel**

Mild steel was chosen for both main and shear reinforcement. Due to the high ductility of mild steel, it was introduced to increase the deformation capacity of the beam hinges. Since the reinforcement was not expected to yield elsewhere, the measurement of post-yield response was not required. Yield and ultimate strength were determined by testing the bars in tension for each type of reinforcement, that is, R $\phi$ 8 mm and R $\phi$ 4 mm and R $\phi$ 10 mm. Tensile strength was measured using a 50 ton (500 KN) Amsler Machine which was able to control the length of the specimen through an implicit gradation on the reaction frame. The elongation of bars was also measured by an X-Y plotter built into the machine. Figure 6.3 shows a typical stress-strain curve for the reinforcement bars. Mean values of three tests are listed in Table(6.2).

### **6.4.2 Concrete**

Since it is envisaged that the FPSS will be used in developing

countries, and also the design philosophy is based on the flexibility of its members, Grade 30 concrete was used for the beam. Properties of the concrete mix (by weight) are given in Table(6.3), as proportion by weight.

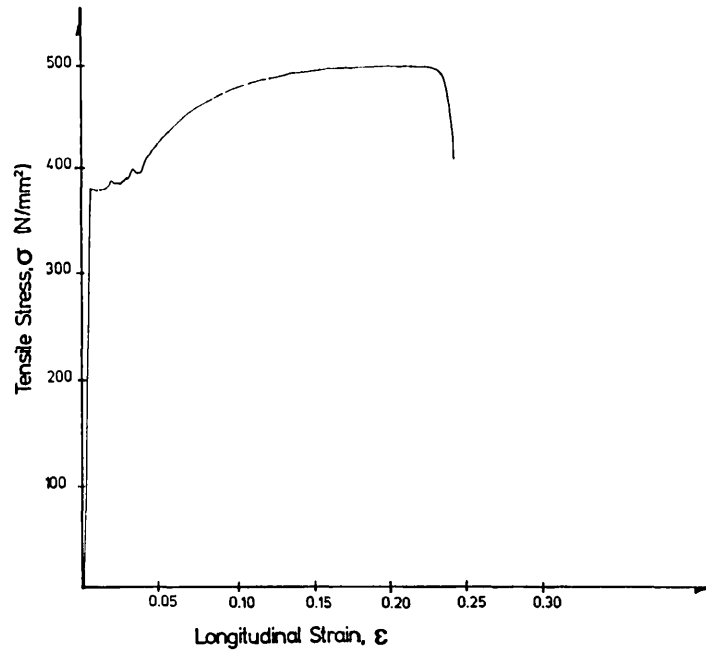


Figure 6.3 Typical stress-strain relationship for reinforcement bars.

Table(6.2) Properties of reinforcement bars.

Type of reinforcement *	Yield strength (N/mm <sup>2</sup> )				Ultimate strength (N/mm <sup>2</sup> )				Elongation at failure (%)
	f <sub>sy1</sub>	f <sub>sy2</sub>	f <sub>sy3</sub>	Average	f <sub>su1</sub>	f <sub>su2</sub>	f <sub>su3</sub>	Average	
RΦ4mm	397	413	380	396	454	477	517	482	32
RΦ8mm	361	356	372	363	499	489	510	499	25
RΦ10mm	378	374	375	375	498	504	501	501	21

\* R = denotes mild steel bars.

#### 6.4.3 Bricks

For the reasons discussed in Section 6.4.2, single frogged common bricks with nominal crushing strength of 25 N/mm<sup>2</sup> were used. Bricks were tested in accordance with BS 3921:1985 and their properties are given in Table(6.4).

Table(6.3) Properties of concrete.

10 mm Aggregate*	2.191
Coarse sand**	1.721
Fine sand <sup>o</sup>	0.752
Total water	0.627
Cement(OPC)	1.0
Average cube strength at 28 days	35 N/mm <sup>2</sup>
Slump test	45 mm

Notes:

- \* Coarse aggregate passing sieves 3/8-3/16 in.
- \*\* Coarse sand passing sieves 3/16 in., No. 10 and No. 25.
- <sup>o</sup> Fine sand passing sieves No. 25 and No. 100. Fine aggregate (coarse and fine sand) conforms to grading zone M, according to BS 882:1983.

Table(6.4) Properties of bricks.

	Compressive stress (N/mm <sup>2</sup> )*	Suction rate (kg/m <sup>2</sup> /min) <sup>o</sup>	Absorption rate (%)**
Average	28.10	2.825	19.5
Standard Deviation	1.44	0.725	2.14
Coefficient of variation	5.14%	25.7%	11%

Notes:

- \* A representative sample of 20 bricks was chosen.
- <sup>o</sup> Suction rate performed for 1 minute with a sample of 10 bricks.
- \*\* Absorption rate measured by the 24 hr immersion test.

#### 6.4.4 Mortar

The mortar mix used was Type III complying with Table 1 in BS 5628:1985, Part 1. This strength was required for two reasons. Firstly, in order to promote cracking of the brickwork through the mortar around the bricks. Secondly, to acquire a less stiff mortar by

using lime. Properties of the mortar mix shown in Table(6.5) are in accordance with BS 1200:1984 and BS 4551:1980 (ASTM C207-82).

Table(6.5) Properties of mortar.

	By volume	By weight
Soft sand*	6	4.88
Total water	2.45	1.02
Lime**	1	0.46
Cement	1	1
Initial rate of flow	110%	
Crushing cube strength at 28 days	6+2 N/mm <sup>2</sup>	
Rate of retention <sup>o</sup>	80%-90%	

Notes:

\* Building sand conformed to grading type S of BS 1200:1984.

\*\* Hydrated building lime conformed to BS 890:1972 (ASTM-C207:1980).

<sup>o</sup> Rate of retention was determined according to BS 4551:1980 (ASTM-C91:1982).

## 6.5 MATERIAL QUALITY CONTROL

### 6.5.1 Concrete

The ring beam was cast in two batches with a standard pan mixer having a capacity of 120 kg. Timber mould was placed to lie uniformly on level ground, and evenly oiled prior to casting. Figure 6.4 shows the ring beam formwork with the reinforcement cages of the four beams in position. For every test specimen manufactured, 6x100 mm control cubes and 4 cylinders (150 mm dia.x300 mm) were also cast. Ring beams were demoulded 3 days after casting, covered with wet hessian and polythene, cured for 6 days, and kept in laboratory conditions (20°C and 65% relative humidity). Controls were demoulded 24 hours after casting and kept in the same conditions as the ring beams, until tested at the same age as the model box structure.

The crushing strength of the cubes and cylinders, together with the age at testing, are given in Table(6.6).

Table(6.6) Results of control tests for concrete ring beam.

Test No.	Cube strength $f_{cu}(N/mm^2)$				Cylinder strength $f'_c(N/mm^2)$				Age at testing (days)
	$f_{cu1,2}$	$f_{cu3,4}$	$f_{cu5,6}$	Average	$f'_{c1,2}$	$f'_{c3}$	$f'_{c4}$	Average	
W1A									141
W1B	54.0	50.5	49.4	51.3	44.0	40.1	39.0	41.0	
W2A									110
W2B	55.8	54.8	55.4	55.3	40.8	42.2	39.7	40.9	
W3A									68
W3B	36.1	38.2	33.4	35.9	29.8	26.7	27.1	27.9	
W4A									45
W4B	35.9	35.0	34.6	35.1	28.7	28.0	29.6	28.7	
W5A									32
W5B	43.4	43.5	44.8	43.9	29.8	29.7	29.3	29.6	

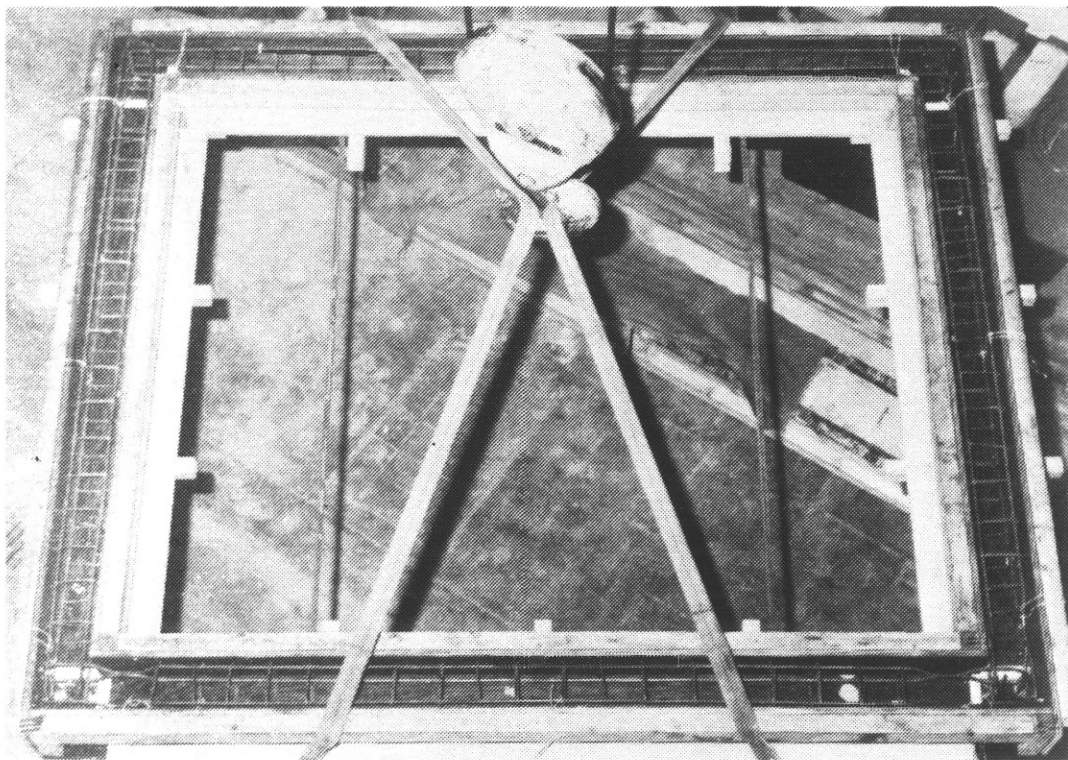


Figure 6.4 Formwork of FPSS ring beam.

### **6.5.2 Brickwork**

The mortar was mixed using a blade mixer with total capacity of 80 kg. Each mortar batch weighed about 65-75 kg, by mixing one bag of soft sand with the appropriate weight of cement and water. Mixing duration was about 5 minutes, monitored in order to control the mortar mix throughout bricklaying. After mixing, the pan was covered with polythene to delay the mix drying out during bricklaying and the mortar was only used within a defined time of 30 minutes. Two control cubes (100x100 mm) were cast for each mix, and the workability of the mix was determined by the flow test.

Bricks were inspected before use and submerged for approximately 10 seconds just before the mortar mix was ready. Brickwork control prisms were built during bricklaying, with dimensions 375x200x100 mm and 4 courses high. Control brickwalls consisted of three courses with dimensions 950x270x105 mm, were constructed to monitor the modulus of rupture. Bricks were laid frogs-down in order to reduce the shear effect of the frogs. The effect was to achieve a weaker brickwork, both to simulate weak mortar brickwork in developing countries, and to achieve more flexibility in the brickwork during differential movement.

The results of the prism crushing tests for brickwork and the modulus of rupture of the walls are given in Table(6.7).

### **6.5.3 Assessment of moduli of elasticity and rupture for brickwork**

The modulus of elasticity of the brickwork was measured according to ASTM E447-84. Three brickwork prisms, 375x200x100 mm, were tested one day after the testing of the structural model. The prisms were gauged with two LVDTs at the wider sides, measuring longitudinal strain over the middle-third. The LVDTs were fixed to brackets glued on the brickwork, as shown in Figure 6.5.

A hydraulically operated Amsler Testing machine (300 ton), combined with an RDP servo-controlled closed-loop loading system, was used with displacement control. Further details are referred to by Kotsovos (1983). The load and the strain measured over the gauged length of the brickwork were recorded using an HP 85 data logger system (refer to Section 6.6). Readings were taken every 5 seconds and, near failure every 2.5 seconds, with a strain rate of loading of  $6 \times 10^{-6}$  strain/second.

The crushing strength results are listed in Table(6.7); a value

of 3-4 KN/mm<sup>2</sup> was obtained (average of three prisms) for Young's modulus, shown in Figure 6.6.

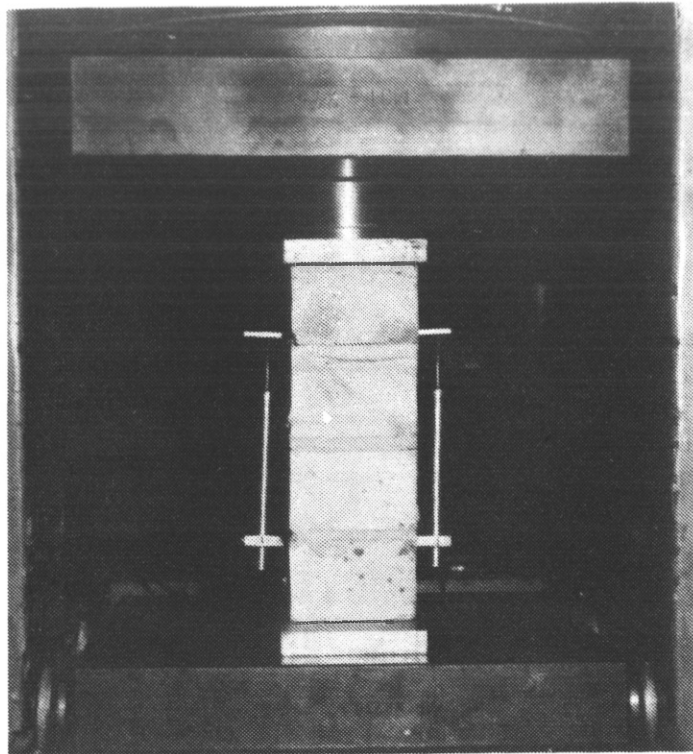


Figure 6.5 Typical compressive test for brickwork prisms.

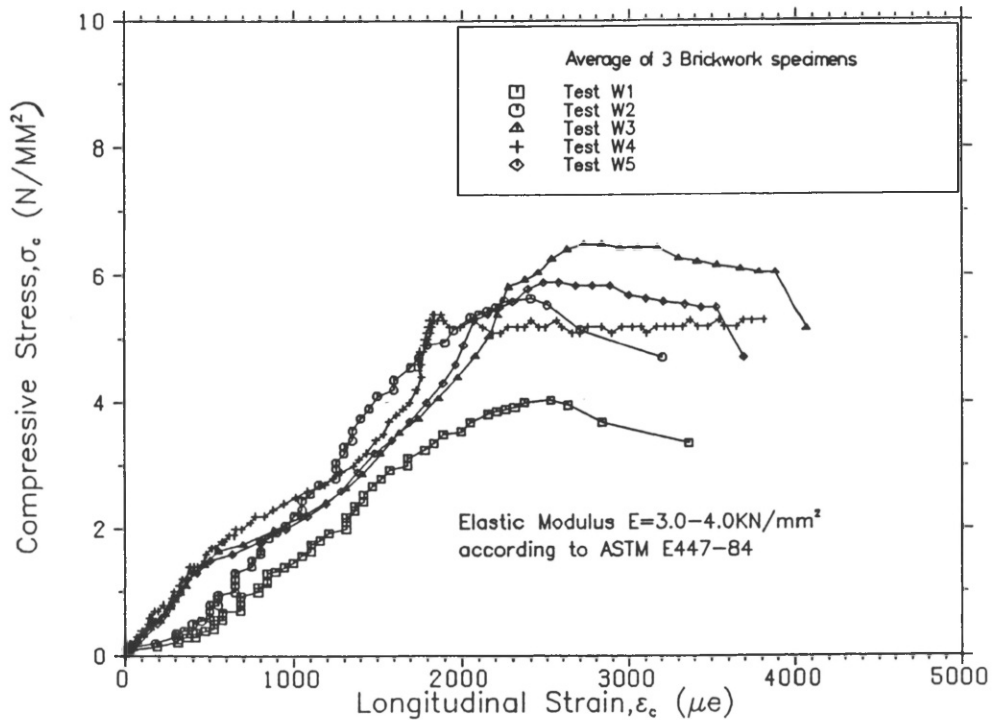


Figure 6.6 Stress-strain relationship of brickwork prisms for each model.

The modulus of rupture for inplane bending was obtained using an indirect tensile test, that is the four point bending test. Three wallets were tested one day after testing of the structural model, with dimensions of 950x270x105 mm according to ASTM E518-80. Figure 6.7 shows the general view of the test rig, and the results are shown in Table(6.7).

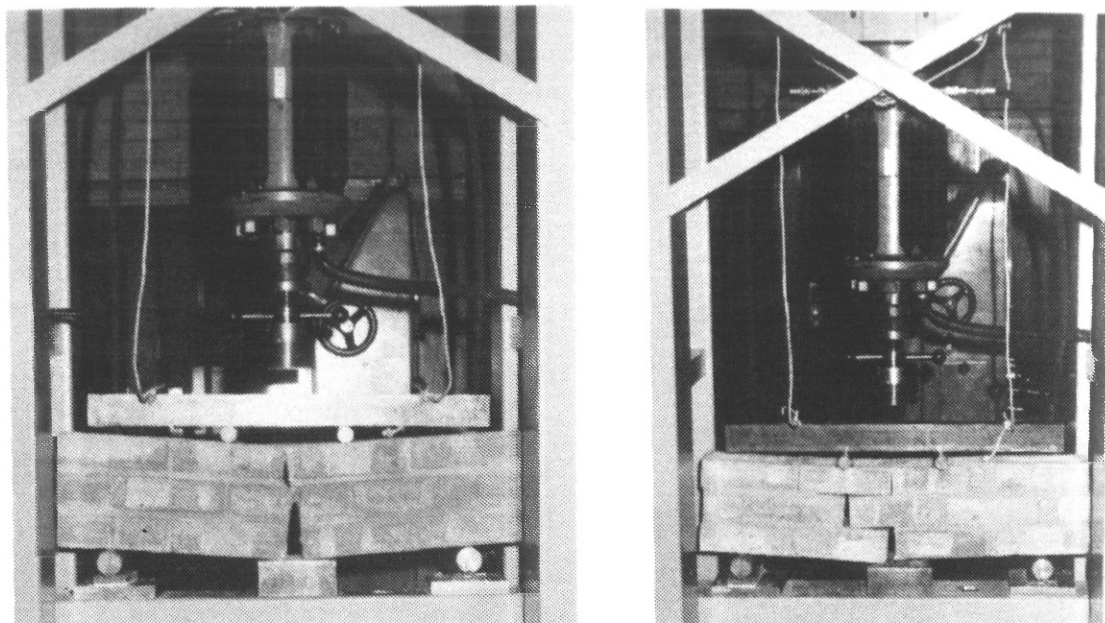


Figure 6.7 Typical testing of brickwork wallets in indirect tension.

Table(6.7) Results of control tests for brickwork prisms and mortar cubes.

Test No.	Mortar cube strength (N/mm <sup>2</sup> )					Brickwork prism strength (N/mm <sup>2</sup> )					Modulus of rupture (N/mm <sup>2</sup> )	Age at testing (days)	
	f <sub>m1</sub>	f <sub>m2</sub>	f <sub>m3</sub>	f <sub>m4</sub>	Average	f <sub>b1</sub>	f <sub>b2</sub>	f <sub>b3</sub>	f <sub>b4</sub>	Average			
W1A	7.9	8.6	6.5	-	7.7								
W1B	8.8	8.0	7.7	9.4	8.4	5.2	3.3	3.8	2.3	3.8	1.03	141	
W2A	12.6	10.5	11.4	9.1	10.9								
W2B	9.0	8.5	12.3	9.8	9.9	3.4	5.7	4.0	4.9	4.5	1.52	110	
W3A	9.4	13.6	10.2	-	11.1								
W3B	11.8	10.0	9.8	9.3	10.2	4.8	7.5	6.9	-	6.4	0.54	68	
W4A	7.4	9.0	9.9	8.8	8.7								
W4B	10.7	7.5	8.9	10.6	9.4	4.8	6.7	6.5	4.9	5.7	0.40	45	
W5A	12.3	14.7	12.0	-	13.0								
W5B	13.0	14.3	12.2	-	13.1	6.2	5.9	7.8	6.8	6.7	0.81	32	



## 6.6 EXPERIMENTAL EQUIPMENT AND SET-UP

### 6.6.1 Test rig

The arrangement of the test rig is as shown in Figure 6.8. It comprised a reaction rig, loading system, supporting rig, jack and load cell and scaffolding platform. The reaction rig consisted of two standard portal testing frames stressed down to the laboratory floor. Each portal frame column was made of two channels 250x50x1.5 mm and 2.5 m long. The columns were connected at the top by a rigid box section 800x300x38 mm, 2.0 m long acting as a main girder. The two frames were joined by two box sections 200x100x15 mm, 4.0 m long acting as secondary girders supporting the loading system. Each frame was secured to the floor by 4x31 mm studs, each stressed to 25 ton. When testing the high wall, concrete blocks 800x400x600 mm were used to increase the overhead space by lifting the reaction rig, refer to Figure 6.8.

A permanent scaffolding platform was constructed on the reaction rig in order to provide easy access to the raised brickwork box. The platform was used during bricklaying by the builders, and as an elevated stage for laying the dead load on top of the wall. During testing, it was also used to detect cracking of the wall and as a safety barrier in order to prevent swinging of the weights outside the rig zone if the wall collapsed. Figure 6.12 shows the test rig with the permanent scaffolding.

### 6.6.2 Load arrangement

The loading system simulating superimposed load of the roof and higher storeys consisted of heavy steel blocks, each weighing 400 lb (approximately 180 kg). They were laid on top of the wall at 300 mm centres, shown in Figure 6.9, using flexible safety chains. The blocks were fixed to a steel channel base using 15 mm diameter studs. Through the middle of the block, each stud was firmly bolted to the channel, as shown in Figure 6.10. The channel was introduced to position the blocks centrally on the wall, with dimensions of 200x50x15 mm. The loading system was placed on 12 mm timber sleepers to accommodate the curvature and roughness of the brickwork. This was introduced to reduce any local distress before testing. A 25 mm gap was left between the blocks to accommodate any tilting of the blocks during excessive deflection on testing.

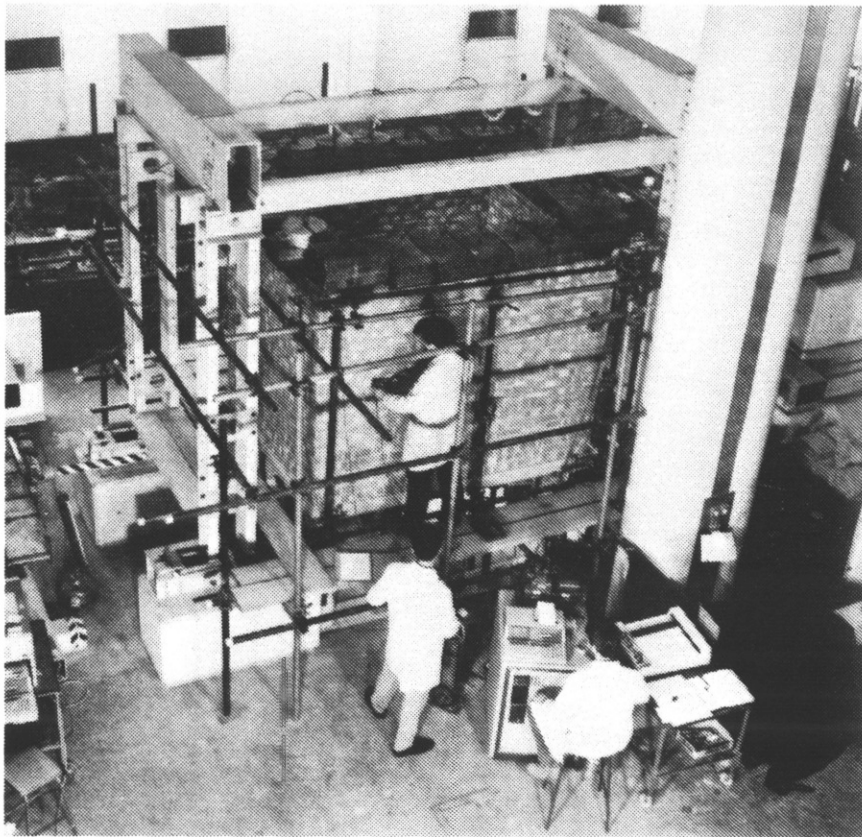
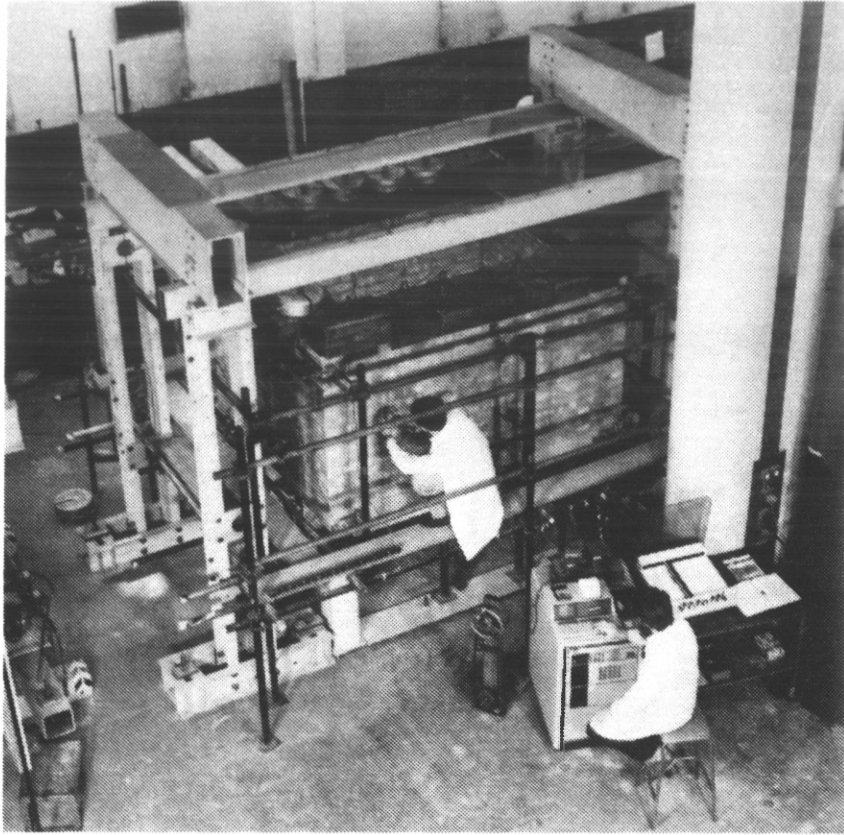
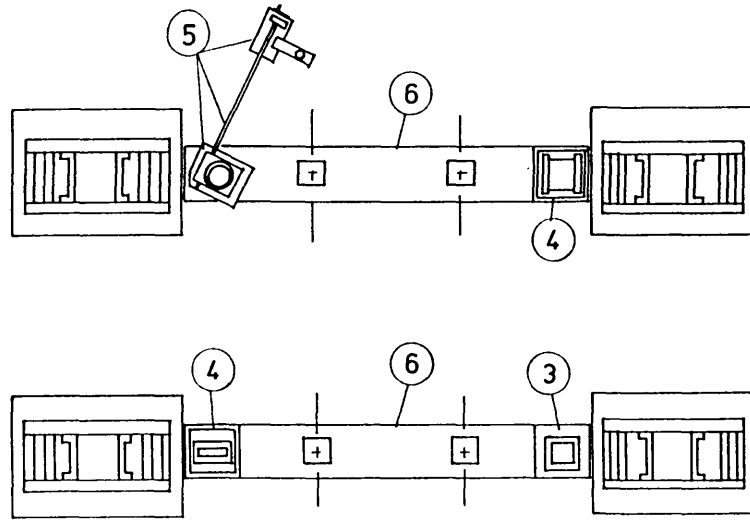
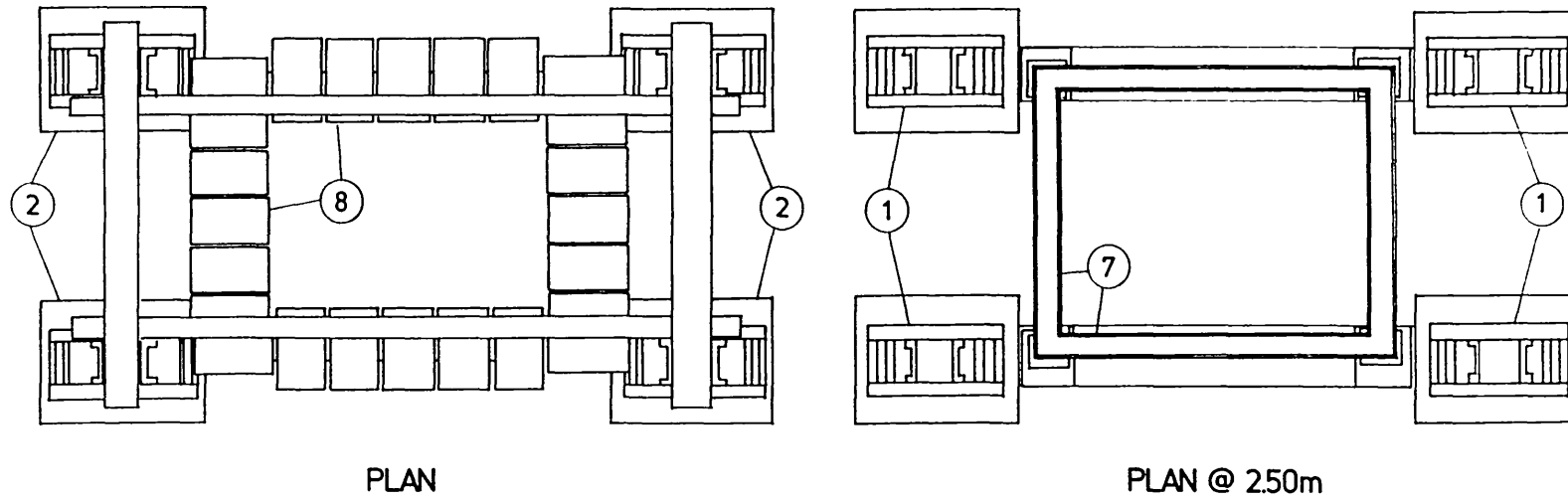


Figure 6.8 Test rig arrangement for the short and high walls.





- ① Portal frame
- ② Concrete block bases
- ③ Fixed support
- ④ Point support
- ⑤ Jacking system
- ⑥ Base plate bolted to Laboratory Floor
- ⑦ Brickwork core walls
- ⑧ Steel weight blocks

PLAN @ 100m

Figure 6.9(b) Plan of test rig at various levels.

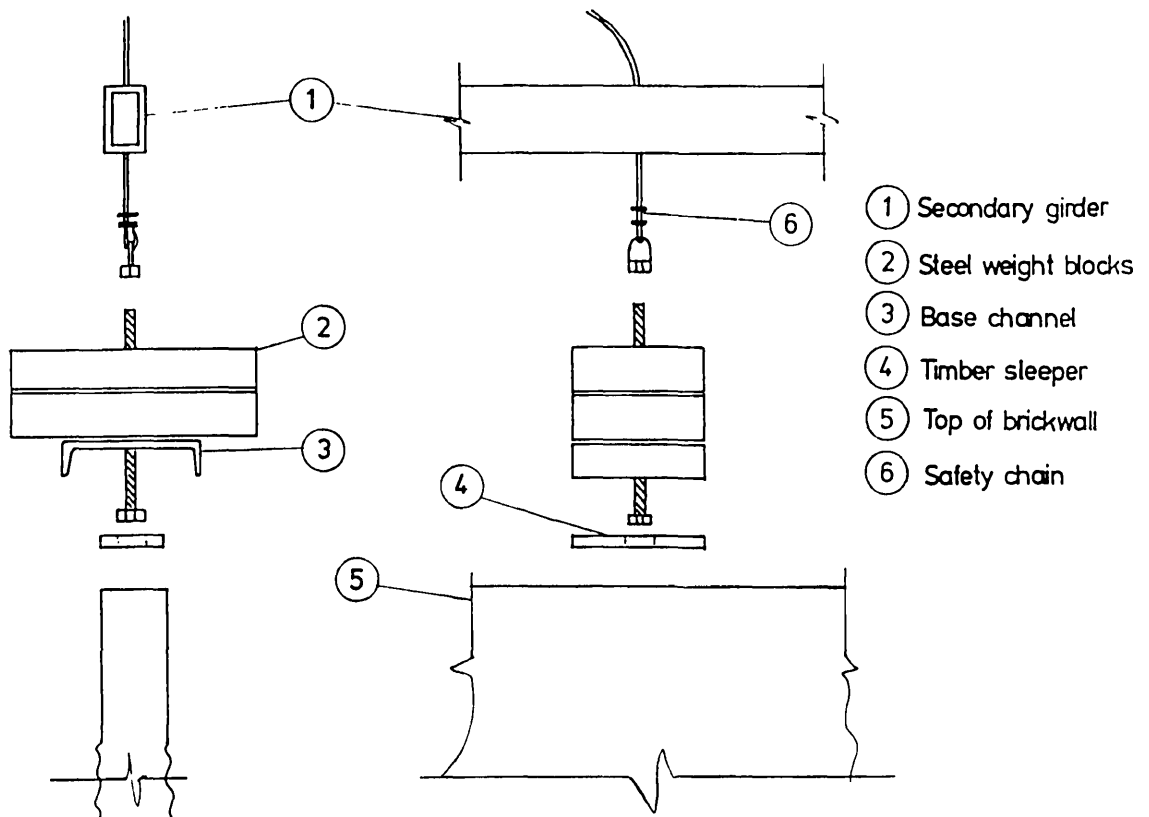


Figure 6.10 Superimposed loading on top of the walls.

### 6.6.3 Support system

The support system of the ring beam was designed to simulate the substructure (foundation). It consisted of either point or clamped supports fixed to rigid steel columns, refer to Section 5.3. These columns were used to support three corners, while the fourth support comprised the screw-jack and the load cell system. The rigid columns resembling the stem of the pad foundation were made of steel box section 250x250x25 mm and 650 mm high. This height was required to meet the minimum jack length available. Steel plates 300x300x12.5 mm were welded at the top of the column, providing a flat levelled support. The four supports were fixed to two rigid steel plates in two pairs. Each plate with dimensions of 2000x400x25 mm was used to simulate the foundation pad, refer to Figure 6.11. These plates were stressed to the laboratory floor securing the supports rigidly to the ground.

To provide point supports, 30 mm diameter rollers were glued on top of the rigid columns using seraltite. However, the beam columns were fixed firmly in tests W1 and W2 to the steel supports. This was achieved by clamping the supporting column and the steel plate, which was welded at the bottom of the FPSS short columns (Section 6.3.2), as shown in Figure 6.11.

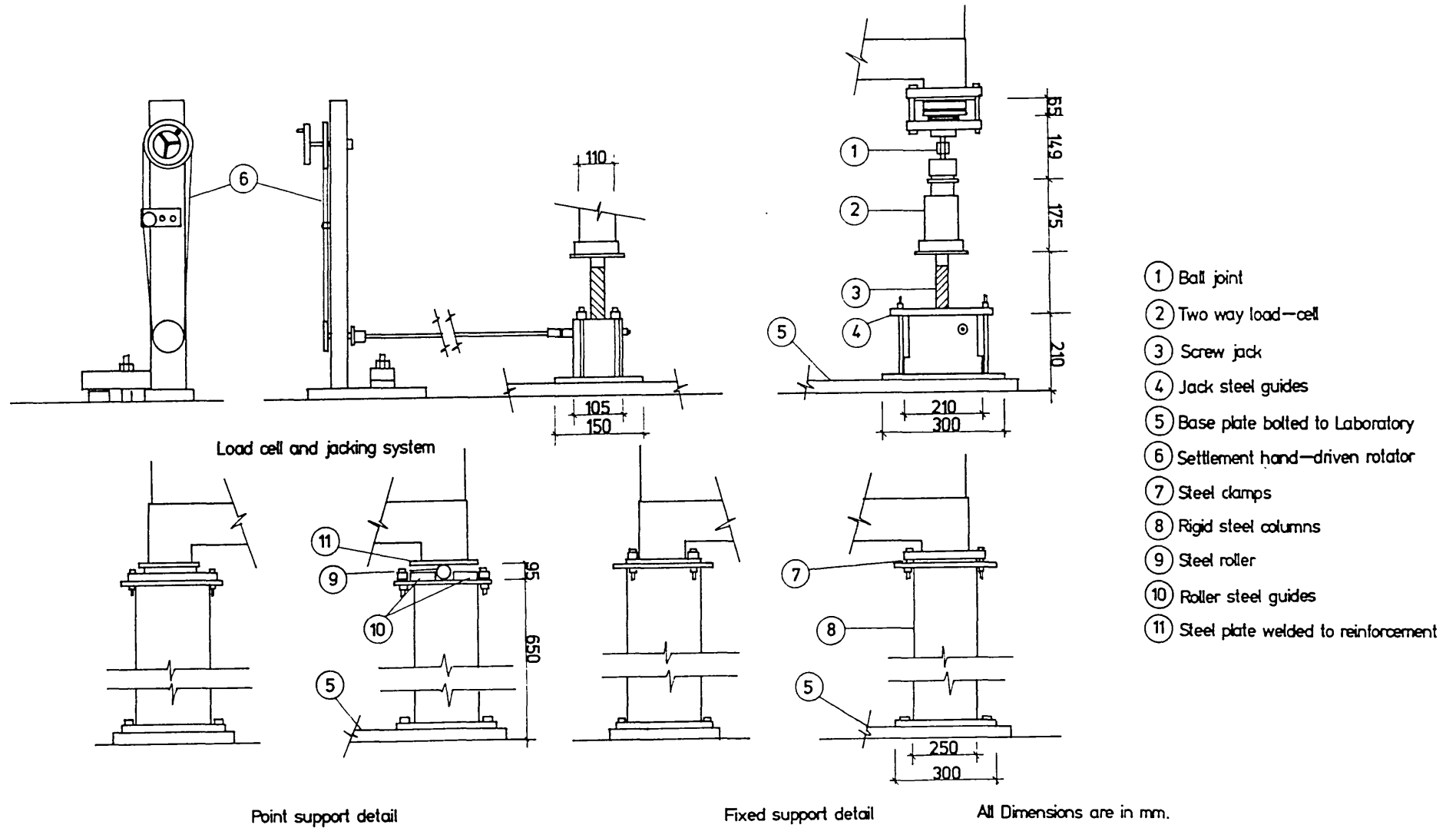


Figure 6.11 General arrangement of support system.

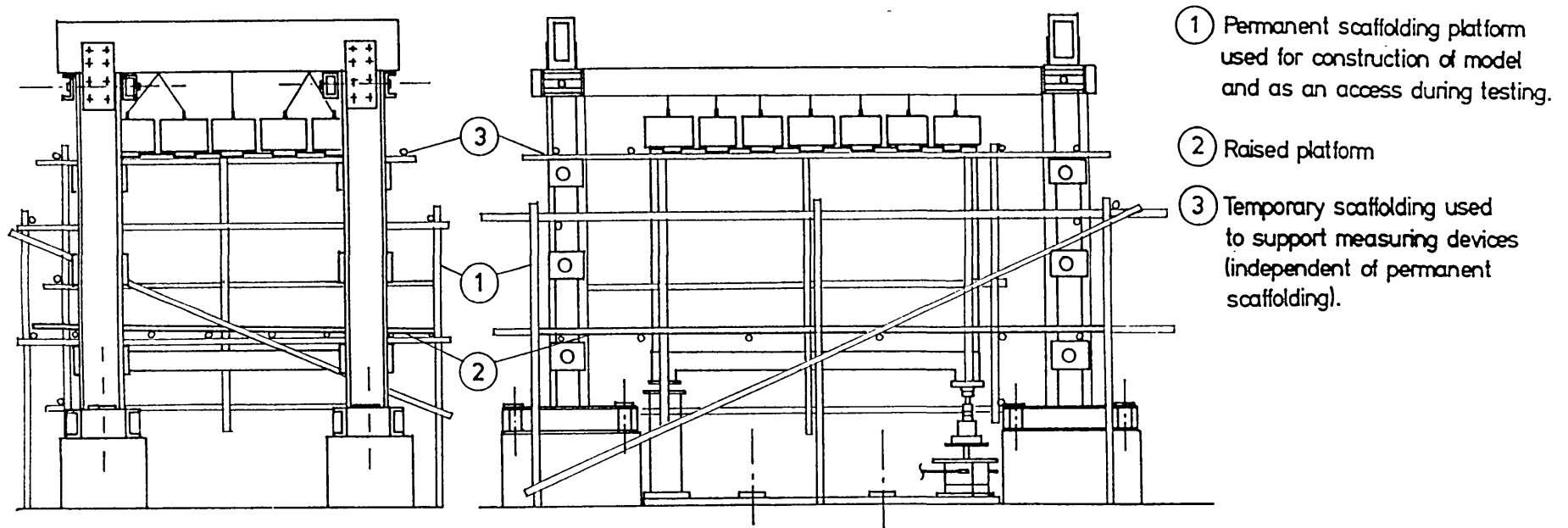


Figure 6.12 General arrangement of scaffolding platforms.

#### 6.6.4 Jacking and load cell system

Since the FPSS was tested over a long period of time, it was decided to use a screw jack without resorting to hydraulically operated machines, since creep of such equipment occurs over a long testing period. This system was capable of operating both in load control mode, and deflection control mode where a screw jack was incorporated. The screw jack had a total head movement of  $\pm 100$  mm. Support load was measured using a load cell fixed on top of the jack. Figure 6.13 shows the jack and the load cell arrangement.

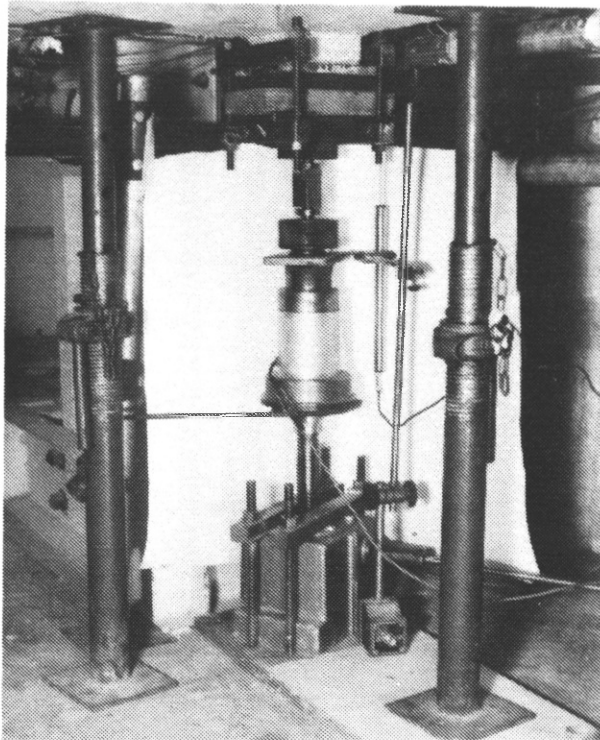


Figure 6.13 Jack and load cell arrangement.

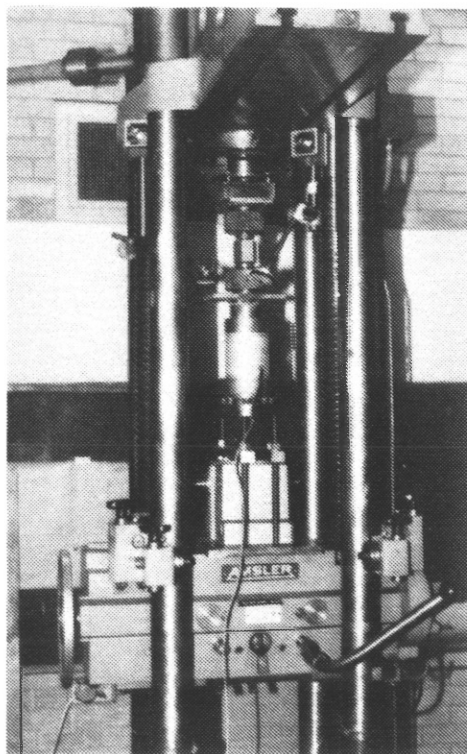
To facilitate 3-dimensional rotation of the settling support during testing, a ball joint system was provided under the beam support. This consisted of two ball joints held together by 40 mm long stud in the axis of movement. Each ball with a rotational capacity of  $7-8^\circ$  (0.135 radians), was encased to provide both a flat surface at either end of the ball joint system, and to accommodate tension as well as compression, refer to Figure 6.11(a). Prior to testing, the ball joint system was released by locking one ball in two dimensions to prevent stability problems, while the other ball was released completely. Figure 6.11(b) shows the clamping arrangement of the jacking system with



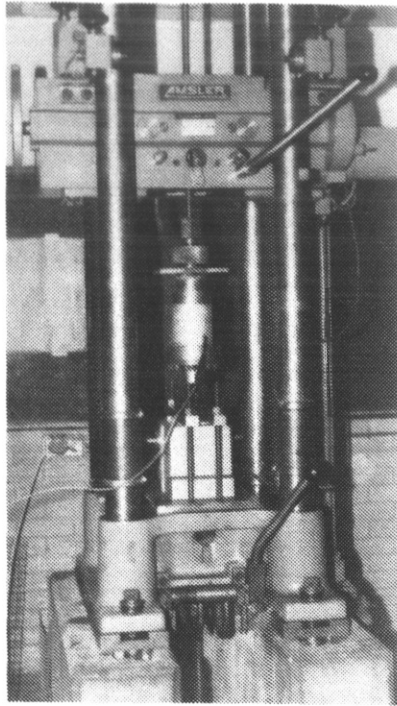
the structure model (FPSS).

The load cell was made from aluminium HEW15P alloy. After gauging, it was tempered to 100°C for 4 hours to minimize relative movement of the gauges and the cell walls. The load cell was calibrated to  $\pm 10$  ton to record both tensile and compressive forces. Cycle loading of the cell was performed approximately 20 times, up to 10 ton and back to zero, in order to eliminate residual stresses in the gauges.

To minimize errors from the jacking system, it was calibrated as a whole system. A 50 ton Amsler Machine was employed capable of applying both tension and compression (refer to Figure 6.14). Prior to calibration, the jacking system was cycled 20 times up to a load of 10 tons, and then back to zero, both in tension and compression. Readings were then taken at 0.5 ton increments up to a load of 10.0 ton in compression. Similarly for tension, incremental measurements were taken up to 6.5 ton and then back to zero load. This procedure was repeated three times, until no drift of readings was recorded. A straight line was adopted for the best fit of the readings, shown in Figure 6.15. A calibration factor of 245.098 ton/volt was obtained with a 98% confidence interval.



(a) Calibration in compression.



(b) Calibration in tension.

Figure 6.14 Calibration of jacking system.

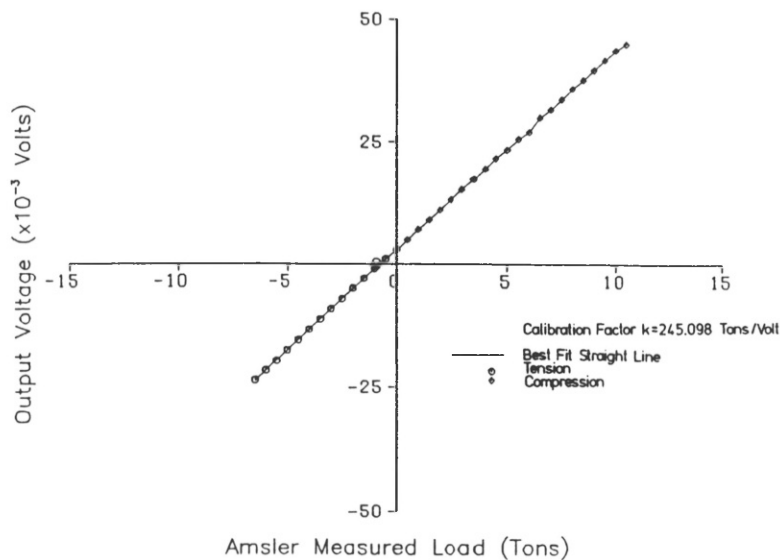


Figure 6.15 Calibration of load cell.

### 6.6.5 Concrete and steel strain measurements

Strain of the reinforcement bar was measured with standard electrical resistance strain gauges which had the properties described in Table(6.8).

Table(6.8) Properties of strain gauges.

Definition	Steel reinforcement	Concrete cylinders
Type of gauge	PLS-10-11	PL-60-11
Gauge length	10 mm	60 mm
Gauge resistance	$120 \pm 0.3 \Omega$	$120 \pm 0.3 \Omega$
Gauge factor	2.08	2.09

Pre-yield strain gauges were employed at three locations on each beam to study the load distribution on the beam. The gauges were placed on both the top and bottom bars of the main reinforcement, refer to Figure 6.2. All beams were similarly gauged, that is, at the middle of the beam and at the hinge locations near the supports. Thus, strain gauges were placed so as to measure the expected maximum strain in bars.

Prior to gauging, the reinforcement bars were specially prepared. First, they were rubbed with emery cloth at the different positions to form a smooth surface with no visible dents. Then they were cleaned with Jenkline liquid to remove all metal traces, followed by an M-PREP Conditioner (a water based acid surface cleaner). To prepare the surface for gauging, it was further cleaned with an M-PREP Neutraliser (a water based alkaline surface cleaner). The gauge was fixed on the surface using an epoxy adhesive, A-12. It was then firmly attached to the reinforcement bar by sellotape, so that the complete gauge surface was in contact with the bar for at least 24 hours at room temperature. After wiring the gauges, they were coated with waterproofing agent M-Coat A12. This was required to protect the gauges against formation of a "wet" joint during casting.

For assessment of the elastic modulus of concrete, two gauges were fixed on opposite sides on the middle-third of the control concrete cylinders. Ends of control specimens were ground to provide parallel surfaces. This was essential to minimize the end effects of the load platens on testing. Gauges placed longitudinally along the cylinder were glued using PS-2 epoxy adhesive.

#### 6.6.6 Brickwork-wall strain measurement

Monitoring the strain pattern in the wall was difficult for two

reasons. First was due to the large area of the walls, thus requiring either large numbers of electrical strain potentiometers (gauge length 50 mm) or LVDTs with longer gauge lengths. Secondly, on the initiation of cracks, local measurement of wall strain using the smaller electrical potentiometers would be misleading. A primary concern was that if electrical LVDTs were adopted, the number of gauges would be too large to record with the data logger. Thus, as an alternative, Demec gauges with a 200 mm gauge length, were opted for, as the most economical and practical solution. Since this solution involved manual work in taking strain measurement, it was necessary to develop an in-house electronic Demec gauge. This was achieved by combining the Demec gauge with a sensitive electrical resistance LVDT. Thus, automatic readings were recorded using the data logging system without cumbersome manual handling of data. To synchronize movement of the LVDT and the Demec mechanical gauge, a steel rostrum fitted with an LVDT-bracket was fixed on the invar bar. The LVDT was mounted on the bracket in such a way that the LVDT-spindle was fastened to the Demec dial. Comparison of the LVDT and the Demec dial was necessary to calibrate the working limits of the electronic Demec gauge. Their characteristic properties are shown in Table(6.9). Figure 6.16 shows the electronic Demec gauge fitted with the electrical LVDT.

Table(6.9) Properties of electronic Demec gauge.

Definition	Demec dial gauge	Electrical LVDT	Electronic Demec
Type	D627-D-200	DG13.0	D627-D-200
Gauge length	200 mm	92 mm	200 mm
Length of travel	6.35 mm	5.0 mm	5.0 mm
Gauge factor	$1.01 \times 10^{-3}$ strain/division	1.7069 mm/volt	$5.9803 \times 10^{-3}$ strain/volt
Accuracy (measurement repeatability)	$\pm 1$ scale division ( $\pm 8$ microstrain)	0.15 micron	$\pm 12$ microstrain
Voltage supply	-	10 volt	10 volt

The electrical gauge was calibrated by fixing the Demec gauge on

regulated movable demec points fixed on a micrometer. LVDT readings were taken at increments of 0.0125 in. on the Demec dial up to a total movement of 5 mm and then back to zero. Plotting the results and taking the best fit for a straight line, a value of  $5.9803 \times 10^{-3}$  strain/volt was acquired as a calibration factor, refer to Figure 6.17.

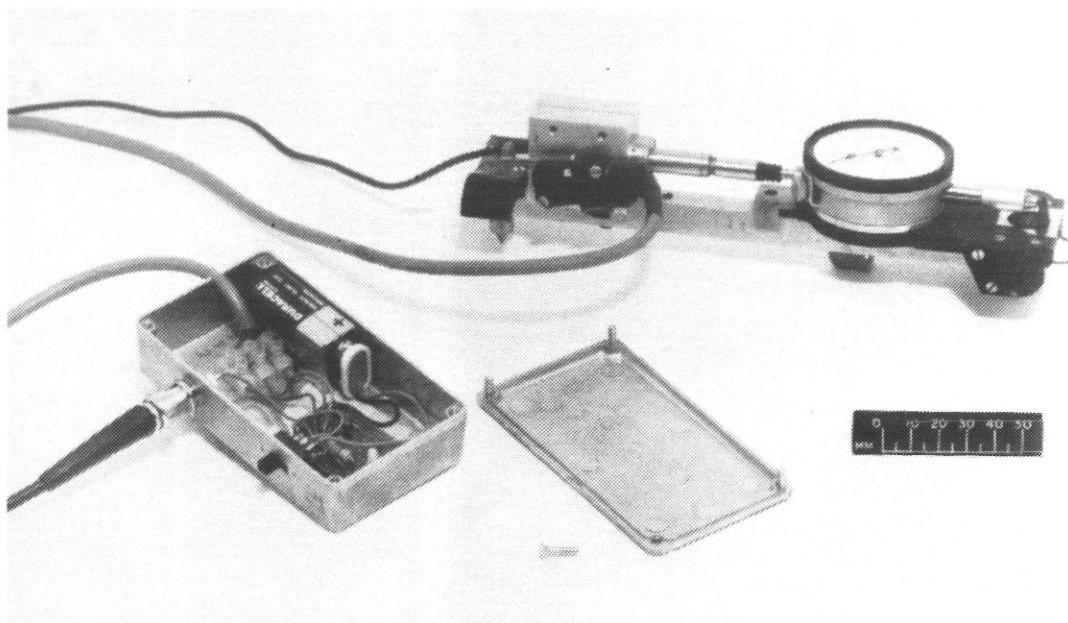


Figure 6.16 Electronic Demec gauge.

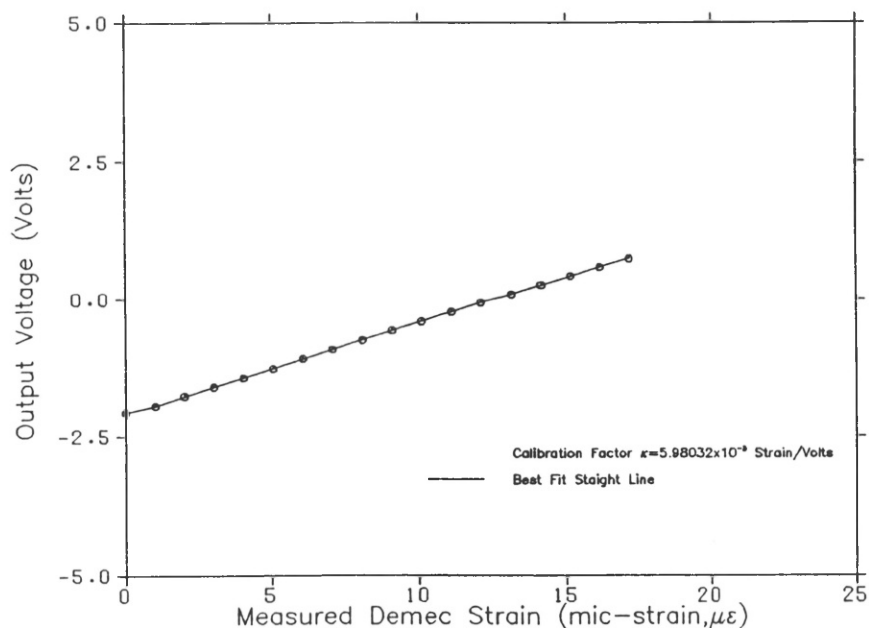


Figure 6.17 Calibration of electronic Demec gauge.

To increase the efficiency of the gauge, a remote-control circuit was developed. This was required to reduce the measurement time and the amount of manual work involved. The logic circuit is shown in Figure 6.18.

1. HP 85 Computer
2. HP 85 Data logger
3. HP 85 Acquisition system
4. HP 85 Bus
5. Input voltage supply 10 volt
6. High sensitive LVDT (developed)
7. Remote control button and circuit (developed)
8. Demec electronic gauge (developed)

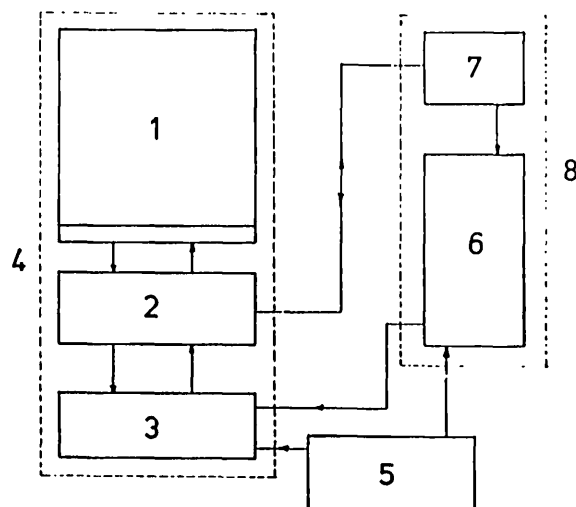
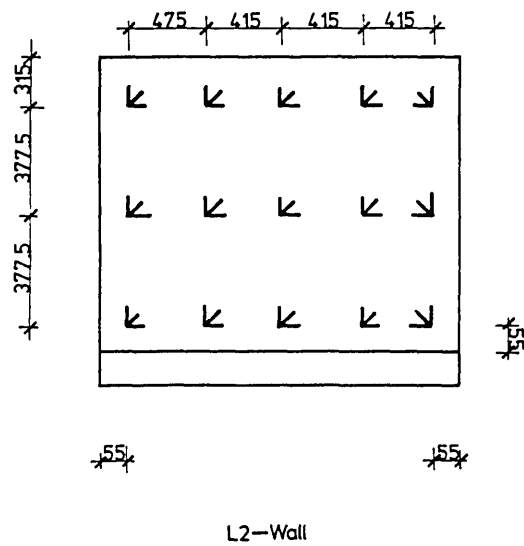
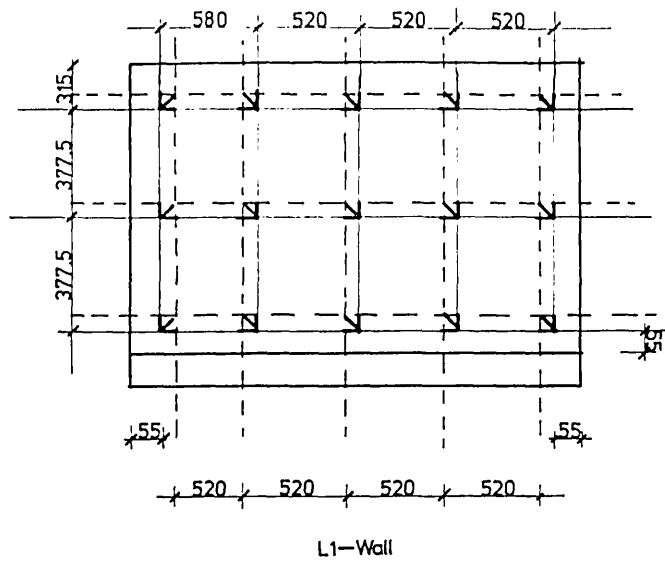


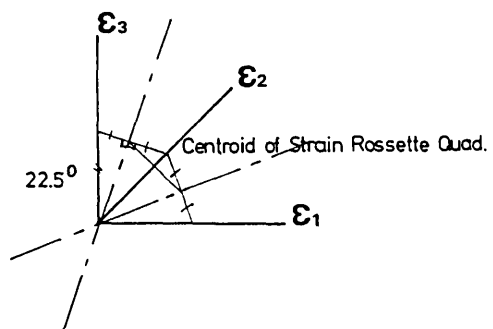
Figure 6.18 Logic circuit of electronic Demec gauge.

Initially, the HP 85 bus was controlled by the HP 85 computer. Before measurement of wall strain, the computer transferred control of the HP bus (refer to Section 6.7) to the data logger as an option in the developed software. Initiating the remote control button closed the circuit, and sent an excitation pulse, which triggered the HP 85 data logger internally. Internal triggering of the data logger sent an open command to the data acquisition system. This was necessary to open the prescribed channel, in order to record the reading of the LVDT. Reading of the LVDT was repeated 5 times and the mean was sent to the HP 85 computer. The whole process was repeated until the program loop attenuated. Appendix 3 describes the circuit and the initiation of the excitation pulse, with reference to the HP 85 data logger.

A uniform grid for strain measurement was used to define the strain pattern in the wall. Subdividing the wall to three horizontal regions by five vertical local zones, strains in 15 local areas were measured. Strain rosettes of  $45^\circ$  were located in each region, shown in Figure 6.19(a), to define the magnitude and direction of principal strains. This type of rosette was chosen for two reasons. Firstly, the horizontal and vertical strains were measured directly, and not calculated from other readings. Secondly, in a  $45^\circ$  rosette, if one Demec point become detached due to crack propagation, strain would still be measured from the other two readings. This would not be the case for a  $60^\circ$  rosette, where the whole rosette would fail. However, the strain centroid of the  $45^\circ$  rosette would lie outside the regular grid, as shown



(a) Measurements of strain in wall.



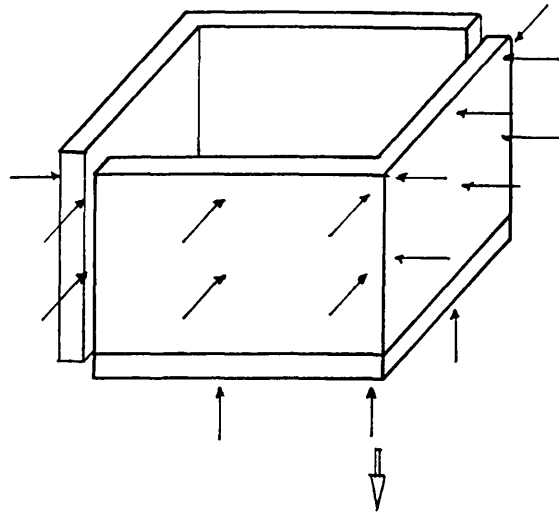
(b) 45° rosette.

Figure 6.19 Position of strain rosettes in the wall.

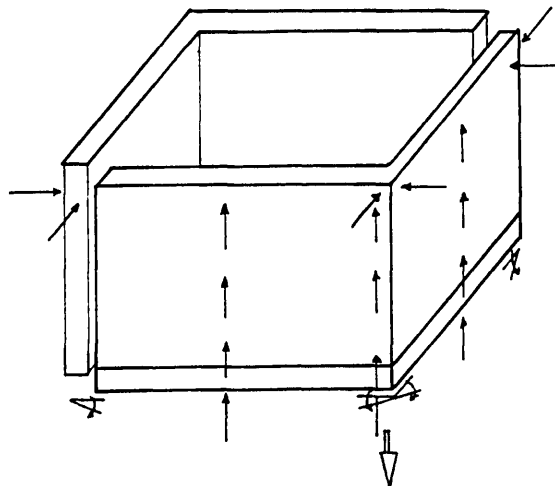
in Figure 6.19(b). This was allowed for in the analysis of data by offsetting the grid pattern of the wall strain.

#### 6.6.7 Deflection measurements during settlement

Vertical and horizontal movements of the wall and the ring beam were measured, using LVDTs. Two types of DC-LVDT were used. Type LVDT-100, with a gauge length of  $\pm 100$  mm, was used for measuring the maximum settlement of the support. Type LVDT-50, having a gauge length  $\pm 50$  mm, was used elsewhere. LVDTs were placed as shown in Figure 6.20 to measure vertical and horizontal movements and tilt of the walls and the beams.



(a) Arrangement of LVDTs in test W1A.



(b) Arrangement of LVDTs in tests W1B-W5B.

Figure 6.20 Vertical and horizontal measurements of wall deflections of two L-shaped wall tests.



Change of curvature of the wall was also monitored by measuring horizontal or vertical deflections at three positions recorded along each of the three horizontal zones, top, middle and soffit of the wall. However, only three LVDTs were used, due to the limited capacity of the data logger. Brackets were fixed horizontally on the wall surface, using plastic padding 2Y-219, to facilitate vertical measurement. LVDTs were placed 40 mm away from the wall, in order to be well clear of the wall during settlement.

To hold the wall LVDTs in position, a temporary scaffolding was constructed. It was built independent of the raised platform in order to reduce risk of the LVDTs moving during testing, as shown in Figure 6.8.

The beam rotation was measured using linear clinometers, type CL-10, with gauge length of 100 mm and capable of reading up to 0.140 radians ( $8^\circ$ ). They had an accuracy of  $\pm 2 \times 10^{-4}$  radians ( $\pm 0.011^\circ$ ), and were positioned as shown in Figure 6.20. Brackets of 200 mm length, were fixed on the short column (to allow the beam to rotate independently), using plastic padding CY-219. Prior to testing, clinometers were levelled and the initial readings were recorded.

#### **6.6.8 Data logging and data retrieval systems**

All test measurements were recorded using a Hewlett Packard HP 3054A automatic data acquisition control system. The system consisted of a high speed scanner and a high resolution digital voltmeter (Model HP 3456A). These were interfaced with an HP 85 desktop computer. Automatic readings were recorded through the use of specially written software, which enabled the control of the data acquisition system from the HP 85 computer. A total of 70 readings were taken at each load step, together with 450 wall strain readings. As a result of load creep during testing, the rate at which measurements were taken was increased by automatic recording of data in order to reduce drifting of readings during measurement cycles.

A maximum reading rate of 330 readings/second is claimed by the manufacturer; however, a correct balance between speed and accuracy of readings needed to be met. This was achieved by modifying the computer software. To determine the required accuracy of measurement the logger was calibrated for the LVDTs and strain gauges, and was found to have sensitivities of  $\pm 0.002$  mm and  $\pm 2$  microstrain respectively. Thus, the HP 3456A digital voltmeter was programmed to record at a speed of 10

readings/second when the reading precision was kept to 5 decimal points. At each load step, the LVDTs and the strain gauges were scanned twice and the average was determined.

Initially, a drop of supply voltage due to instability of the current, and the heavy load during testing, caused a decline in the voltage readings. This caused a considerable reduction in voltage measurement. The problem was solved by modifying the measurements by a factor of  $V_{o1}/V_{o2}$ , where

$V_{o2}$  = output voltage at time of taking the required measurement, and

$V_{o1}$  = output voltage at time of taking the zero reading.

Serious consideration was given to the speed and method of taking readings for the wall strain. This was necessary to ensure that the readings were accurately transferred to the computer and, more importantly, to allow incorporation of a remote control device (refer to Section 6.6.6). After comparison of different methods of taking readings by employing various techniques involving modifying the computer software, two problems arose. Firstly, significant delays occurred between the individual voltage readings when they were transferred directly from the voltmeter to the computer memory. Secondly, fluctuation of the Demec gauge readings necessitated taking the mean of several readings.

The use of the voltmeter's internal memory gave a solution to the second problem; its use caused a marginal drop in voltmeter sensitivity (down by 10 microvolt on the 10 volt range). However, this enabled 5 voltage readings to be taken, stored and the mean then transferred in 1.90 seconds. Since there was no need to transfer more than one recording, this caused only 2 seconds delay. One further improvement was adopted by signaling the end of the operation audibly, enabling only one person to operate the electronic Demec gauge.

For data retrieval, the HP 85 computer fitted with a terminal interface RS 232, was employed to transfer data files to the mainframe cyber for post-processing of data. The datafiles transformed into ASCII form were transferred using a terminal emulator package (Transdata 87). The baud rate of the HP 85 set initially at 300 caused long delays in transfer (refer to Section 6.8).

## 6.7 TESTING PROCEDURE

Each structural model comprised two independent tests, as shown

in Figure 6.20. Initially, an L-shaped wall structure was thought to be sufficient for testing the FPSS. However, inplane and out-of-plane interaction between adjacent walls of the box structure deemed to necessitate testing of the whole 3-dimensional structure. This was also necessary to allow monitoring of the limiting out-of-plane behaviour of the FPSS structure. To economize on both the number of 3-dimensional tests and the cost involved, the test results of each model was maximized by designing the rectangular ring beam consisting of two different beam lengths,  $L_1$  and  $L_2$ , where  $L_1/L_2 = 1.23$  (refer to Table(6.10)).

Table(6.10) Test schedule of FPSS models.

FPSS structure No.	Wall test No.	Age at testing (days)	Aspect ratio of wall (L/H)			
			2.0	1.62	1.23	1.0
1	W1AA	122	x			
	W1AB			x		
	W1BA	139	x			
	W1BB			x		
2	W2AA	78	x			
	W2AB			x		
	W2BA	103	x			
	W2BB			x		
3	W3AA	50	x			
	W3AB			x		
	W3BA	64	x			
	W3BB			x		
4	W4AA	28			x	
	W4AB					x
	W4BA	41			x	
	W4BB					x
5	W5AA	29			x	
	W5AB					x
	W5BA	32			x	
	W5BB					x

The FPSS models were tested by inducing settlement by means of the jacking system. Each step comprised 50 rotations of the steering handle (Figure 6.11), which was equivalent to approximately 0.45 mm deflection. Cycles of settlement was performed in multiples of 5 mm and then back to zero, before reaching the serviceability limit state. This was required to monitor the load deflection relation before cracking occurred. Cracking of the wall structure was defined by the occurrence of the descending portion of the load deflection relation. However, the serviceability limit state was only defined at several cycles as the cracks widened beyond 3-4 mm. This was required to study the cyclic behaviour of the FPSS, both before and during crack propagation. To assist in controlling the different stages of loading and to give a representation of the load deflection relation simultaneously, an X-Y plotter was used. Due to lack of the jacking system travel, the test was only performed for settlement of the support, that is hogging mode, but heave was not considered. However, structural design is more sensitive to hogging than sagging, since a hogging mode generally causes more distress and would thus determine the lower limit of serviceability.

The testing of one corner of the FPSS model caused cracking of the two adjacent walls. Repairing of the walls was necessary to reduce any effects that would alter the behaviour of the other half during its testing. This was performed by filling the cracks using an epoxy resin. Sikadur 53 LV was suitable to use for the minimum size of cracks greater than 0.5 mm. Prior to repairing, conical nozzles were glued on the crack surface at 300 mm intervals at both sides of the wall. These were introduced to offer the only entry to and exit from the crack. The cracks were then sealed with an epoxy sealant Colebrand CXL 78T. Using a bulk sealant gun, epoxy resin was injected through the nozzles into the wall starting at the bottom of the wall proceeding upwards. Injection was stopped when the resin emerged from the nozzle at the top brick course. Curing for 3 days was sufficient for the resin to reach a crushing strength of  $20 \text{ N/mm}^2$ , which would give the best results for bond as claimed by the manufacturer. Thus, testing of the other FPSS corner proceeded without delay after one week. An initial test was conducted to check the effectiveness of repair, by performing an indirect bending test of repaired brick specimens. Failure was observed to occur at a new location away from the repaired crack. Introducing reinforcement at the top courses of test W5 limited cracking which enabled testing of the other corner without resorting to any repairs.

To consider effectively the different parameters affecting the behaviour of the FPSS, four prime variables have been opted for in the experimental investigation. These are the aspect ratio of the wall (L/H) reinforcement ratio ( $A_s/bd$ ), support condition and introduction of weak joints in the ring beam. Tables(6.11) and (6.12) show the experimental test schedule.

## 6.8 PROBLEMS ENCOUNTERED DURING TESTING

Some problems experienced during testing, in particular with the electronic equipment or the testing procedure, were as follows:

- Initial zero readings of the wall-strain were recorded before positioning of the weight system and prior to the removal of the props supporting the ring beam. This was necessary to record the original strain pattern of the wall before settlement. However, if cracking were to occur at the adjacent walls, that is the other corner, the recorded strain would represent the whole history of loading of that corner. If strain of the wall due to settlement was only required, another zero reading was recorded just before testing.
- Data retrieval from the HP 85 computer and transfer to the mainframe cyber for further computation using the RS 232, was initially set at a baud rate of 300. A 30-40 minute period was required to transfer a single file containing 11200 (1400X8 bits) bits of data. The research machine of the mainframe cyber had to be used, if a time-out command on the terminal was to be avoided. Changing the baud rate to 9600 was necessary to speed up the operation, which then only took 3 minutes for the same length of file without incurring a time-out error.
- Some of the readings of the electronic Demec gauge displayed unstable behaviour. Large variations of the bridge voltage from the control circuit were observed. The problem was found to be due to formation of "dry joints" for some of the connections. Mending this, without disconnecting the supply voltage battery in the circuit, caused discharging of the battery. This reduced the upright excitation pulse that initiated the data logger; refer to Section 6.6.6. In such a case, no further readings were taken until the battery was recharged.

Table(6.11) Test programme for different types of supports.

FPSS structure No.	FPSS test No.	Reinforcement ratio $A_s/bd(\%)$		Condition of support	
		0.64%	1.0%	Fixed	Point
1	W1A		x	x	
	W1B		x	x	
2	W2A	x		x	
	W2B	x		x	
3	W3A	x			x
	W3B	x			x
4	W4A	x			x
	W4B	x			x
5	W5A	x			x
	W5B	x			x

Table(6.12) Test programme for beam and column joints.

FPSS structure No.	FPSS Test No.	Type of column joint		Aspect ratio of wall	
		Type2 (Weak)	Type1 (Full)	$L_1/H=2$	$L_1/H=1.23$
1	W1A		x	x	
	W1B	x		x	
2	W2A		x	x	
	W2B	x		x	
3	W3A		x	x	
	W3B	x		x	
4	W4A		x		x
	W4B	x			x
5	W5A		x		x
	W5B	x			x

- A noise effect was observed on the X-Y plotter, recording the load-deflection relation during testing. The frequency of the "noise" on such a long term testing program caused unexplainable large patches on the load-deflection relation. It was noticed that if the scale of the LVDT was reduced, the noise was kept minimal. However, the accuracy of the graph would not be acceptable if the scale of the X-Y plotter was reduced. Instead, a larger LVDT was used in order that scaling down the X-Y plotter still gave acceptable accuracy while keeping the noise level to a minimum.
  
- Cyclic settlement of the FPSS walls caused, in some cases, unstable LVDT readings. This was found to be due to jamming of the spindle of some LVDTs. A check was required at each load or deflection step to release the detachment of the spindles.

## CHAPTER 7 THEORETICAL BACKGROUND AND MATHEMATICAL MODELLING

### 7.1 INTRODUCTION

When a structure is situated over a zone of moving ground, it will be likely to deform; the presence of the structure, however, will modify the deformation of the ground. Earlier work defined the ground-structure interaction by considering compatibility of deformation of both the ground and the structure (Hetenyi,1946). Solutions to soil-structure interaction are now described for three simple methods of analysis, namely, beams on elastic foundations, slabs on elastic ground and frame analysis, together with a more advanced method of design, that is, the finite element method. Based on these methods, three models of the FPSS have been developed simulating the structural behaviour during settlement.

### 7.2 BEAMS ON ELASTIC FOUNDATIONS

Taking into account the different types of ground deformation, namely edge and centre deformation, the structure was approximated into beam elements subject to point or uniformly distributed loading. To include the effect of the foundations, the subgrade stiffness was also considered to act as a set of point forces under the beam elements, the object being to relate the deformation of the structure to the induced bending moments and shear forces.

#### 7.2.1 Winkler model using matrices

This is the simplest form of analysis, in which the soil is modelled as a series of discrete linear elastic vertical springs under a beam element. The structure is assumed to act as a simple beam in bending, which limits the application of this analysis to plane walls and rafts (Just, Starzewski and Ronan,1971). Figure 7.1 illustrates the response of both the ground and the structure based on a Winkler ground model.

Consider the Winkler ground model to provide vertical spring stiffness,  $S_i$ , at each of the several discrete points "i". The displacements of the ground at these points,  $d_g$ , under a vector,  $P_g$ , of



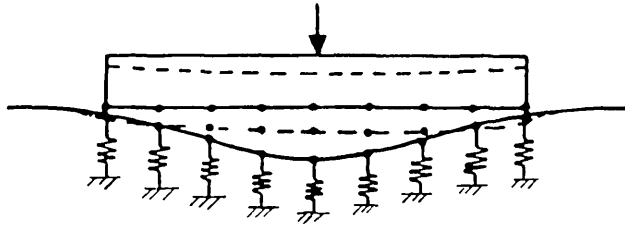


Figure 7.1 Interactive response of ground and structure based on a Winkler ground model.

upward loads, are defined by the matrix equation:

$$P_g = K_{gd} \cdot d_g \quad (7.1)$$

where  $K_{gd} = \begin{bmatrix} S_1 & 0 & 0 & 0 \\ 0 & S_2 & 0 & 0 \\ 0 & 0 & S_3 & 0 \\ 0 & 0 & 0 & S_4 \\ 0 & 0 & 0 & \text{etc.} \end{bmatrix}$

Also, if a matrix equation is written to define displacements,  $d_s$ , in the beam structure at the same interface nodes, then

$$P_s = K_s d_s$$

where  $P_s$  = vector of downward forces on the structure, and

$K_s$  = stiffness matrix for the beam, with respect to interface degrees of freedom only.

Now for equilibrium,  $P_s = P_g$ ,

and for compatibility,  $d_s + d_g = w$

where  $w$  = vector of resultant ground displacement.

$$\text{Thus } (K_s + K_{gd}) d_s = K_{gd} w \quad (7.2)$$

$$\text{and } P_e = K_{gd} w$$

where  $P_e$  = equivalent load on the structure considering the soil-structure system.

By substituting the critical ground profile,  $w$ , in equation(7.2),  $d_s$  can be computed as

$$d_s = (K_s + K_{gd})^{-1} K_{gd} w \quad (7.3)$$

For multi-bay structures, the influence of differential movements of footings for frameless buildings (that is, walls) was analysed by Klepikov, Borodatcheva and Matveev (1980). They considered both vertical and horizontal displacements of 3-dimensional grid foundations

supported on springs (Figure 7.2). To determine the stiffness coefficient of the springs, the walls were designed as separate panels so that the axial forces, moments and shear forces at the junction of the panels and at the nodes were known.

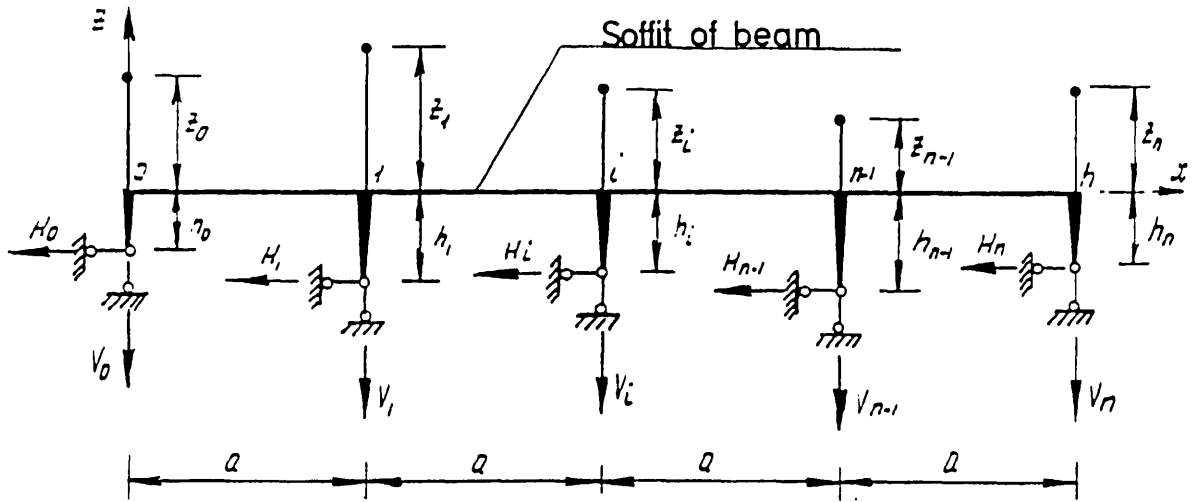


Figure 7.2 Simulation of ground deformation in frameless buildings using vertical and horizontal springs (after Klepikov et al., 1980).

These resultant stresses were in equilibrium with the normal and the transverse forces induced in the beam due to differential movement of its supports. Resolving the differential movement into two directions (Figure 7.2), and considering that these movements are due to horizontal and vertical springs at the beam ends, the equilibrium of forces are represented by,

$$\begin{aligned} N_i^w &= N_i^b, \\ Q_i^w &= Q_i^b, \text{ and} \\ M_i^w &= M_i^b \end{aligned}$$

where

$N_i^w, N_i^b$  = axial forces at node  $i$  of the wall panel and the beam element respectively,

$Q_i^w, Q_i^b$  = shear forces at node  $i$  of the wall panel and the beam element respectively, and

$M_i^w, M_i^b$  = bending moments at nodes of the wall pad and the beam element respectively, given by the following equation

$$\begin{aligned} &= H_0(h_0 + z_1) + H_1(h_1 + z_1) + \dots \\ &- V_0(i+1) a - V_1(i) a - \dots \end{aligned}$$

As a result,  $\sum_{i=1}^n h_i$  was calculated and, similarly, the stiffness of the beam was found by defining the M/Z (moment/section modulus) diagram over the whole length of the building. Thus, the whole building was replaced by a system of cross-beams that has the stiffness of the superstructure. This allowed easier computation of settlement by the use of 3-dimensional grids and, consequently curvature at the soffit of the building (Figure 7.3). However, calculation of the limiting stress at any other level of the building is not possible; this limits the application of this method to low-rise storey buildings.

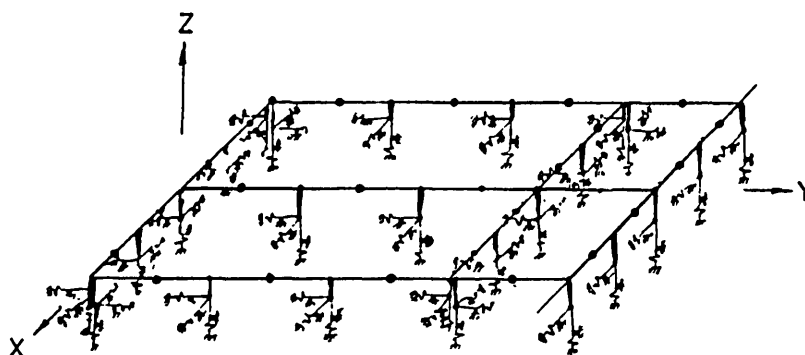


Figure 7.3 Simulation of ground deformation in 3-dimensions using vertical and lateral springs (after Klepivov et al.,1980).

### 7.2.2 Winkler model using numerical methods

Approximating the structure as an infinite beam supported on elastic foundations carrying a central point load and considering the subgrade reaction, the expression for the displacement of the beam is given by Hetenyi (1946) as follows:

$$d_s = \frac{P\lambda}{2K} e^{-\lambda y} (\cos\lambda y + \sin\lambda y) \quad (7.4)$$

where  $d_s$  = structure deformation at any distance  $y$  from edge of beam,

$P$  = applied point load,

$K$  = modulus of subgrade reaction, and

$$\lambda = \frac{K}{4EI}$$

By differentiating equation(7.4), the moments,  $M$ , and the shear forces,  $Q$ , at any distance,  $y$ , from the edge is given by:

$$\text{Moment, } M = \frac{P}{4\lambda} e^{-\lambda y} (\cos\lambda y - \sin\lambda y), \text{ and}$$

$$\text{Shear force, } Q = -\frac{P}{2} e^{-\lambda y} \cos\lambda y$$

### 7.3 FRAME ANALYSIS OF STRUCTURES

To improve structural modelling, a matrix stiffness formulation for a framed structure was used by combining it with a foundation stiffness model (Meyerhof,1947 ; Attewel et al.,1986).

#### 7.3.1 Conventional techniques

These techniques were developed for foundation beams and slabs which are flexible in only one direction. Based on the elastic theory, the foundation is analysed by including the response of flexure of a framed structure (Meyerhof,1947 ; Lee and Harrison,1970 ; Sommer,1979). Thus, the curvatures and deformations of the beam element are part of an overall frame, describing the behaviour of the entire structure. Meyerhof (1947) and Lee and Harrison (1970) adopted conventional methods, that is, moment distribution and slope deflection methods. By backward substitution of deformation, they were able to determine the inducing moments and shear force effects on the superstructure. This was achieved by providing a fixing moment on the simply supported beam that was due to the flexible foundation, approximated as a Winkler medium. Treating the foundation as part of a frame (Figure 7.4) with

$$M_{AB} = 2EK (2\theta_A + \theta_B - 3\phi) + M_{FAB}$$

where  $M_{FAB}$  = function of the contact pressure distribution of the subgrade soil medium.

To satisfy equilibrium, the rotations and relative deflections of the superstructure are calculated and are equated to that of the foundation, that is the raft, at the column raft joint. This is given by:

$$\begin{aligned} (\theta_A + \theta_B) &= (\theta_{AR} + \theta_{BR}) - 2\phi_R \\ (\theta_B - \theta_A) &= (\theta_{BR} - \theta_{AR}) \end{aligned}$$

Thus, for a central point load, the moment produced by differential movement of panel AB can be obtained as:

$$M_{AB} = \frac{PL}{8} \left( \frac{4(2m+3)(\sinh\lambda l - \sin\lambda l) - n\lambda^2 l^2 (\sinh\lambda l - \sin\lambda l)}{n\lambda^2 l^2 (\sinh\lambda l + \sin\lambda l)(m+2) + 2\lambda l(2m+3)(\cosh\lambda l - \cos\lambda l)} \right) \quad (7.5)$$

where  $P$  = applied load,  
 $l$  = span of raft,  
 $m$  = parameter defining beam stiffness,  
 $n$  = factor describing raft stiffness, and  
 $\lambda$  = relative flexibility of the raft.

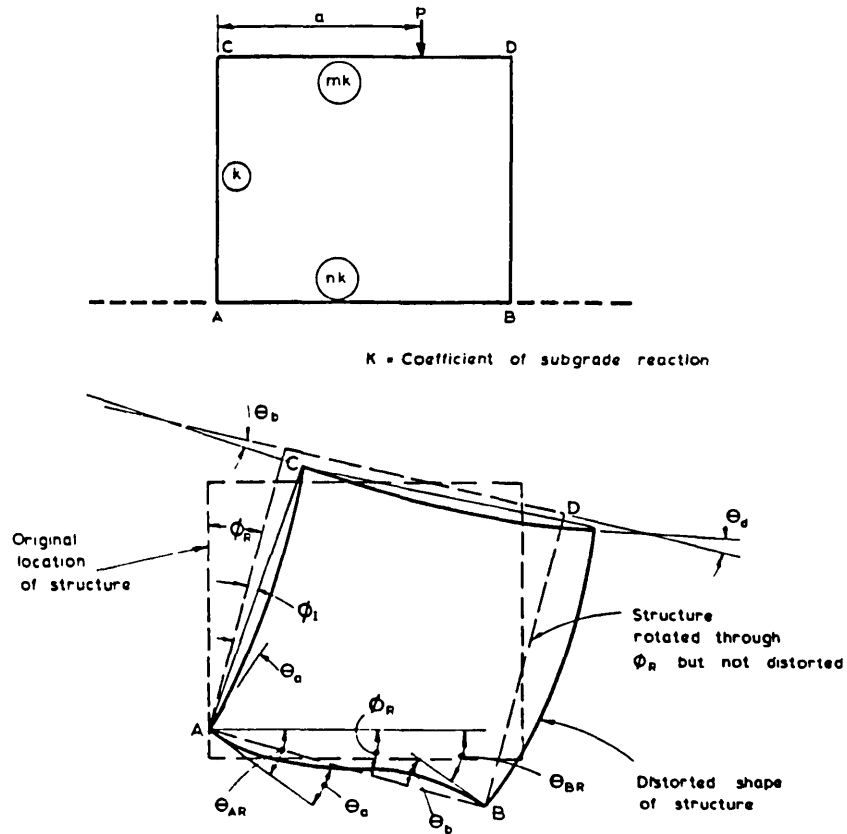


Figure 7.4 Deformation of a frame structure on flexible subgrade (after Lee and Harrison, 1970).

Meyerhof (1947) considered the application of semi-rigid frames as an approximation of an elastic foundation. Using the Cross method, and applying a settlement at support  $i$ ,  $\Delta_i$ , the relative rotation at support  $i$ ,  $\Theta_i$ , was assumed to be linearly proportional to the differential movement. If this rotation was transmitted through the joint of the subgrade and the column (Figure 7.5), then

$$\Theta = \gamma M$$

where  $\Theta$  = relative rotation of column axis measured from the vertical,  
and

$\gamma$  = relative rotation per unit moment,  $M$ .

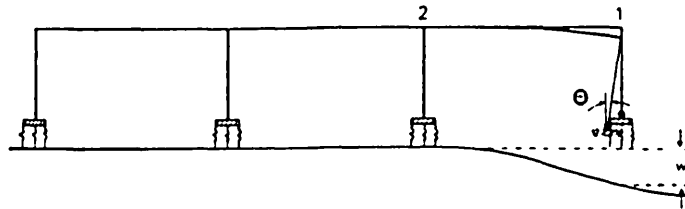


Figure 7.5 Rotation of semi-rigid frames due to settlement beneath a single footing.

The induced moment is given as:

$$M_{AB} = - 2EK \left( \frac{\alpha M_{AB}}{EK} + \frac{\beta M_{BA}}{2EK} + 3R \right)$$

where  $R = \Delta/L$

$$K = \frac{(3\alpha + 2)K'}{2(3\alpha\beta + 2\alpha + 2\beta + 1)}$$

$K' = I/L$

$\alpha = 2EK\gamma_L$

$\beta = 2EK\gamma_R$

$\gamma_L, \gamma_R$  = relative rotation at the left and the right supports, respectively.

### 7.3.2 Stiffness matrix technique

A multi-bay structure with single footings can be considered where the foundation stiffness is modelled as a Winkler foundation, as shown in Figure 7.6. If an individual footing has a differential settlement,  $d_s$ , with a free ground displacement,  $w$ , then the subgrade stress is obtained from the compatibility condition,

$$P_g = K(w - d_s)$$

where  $K$  = coefficient of subgrade reaction.

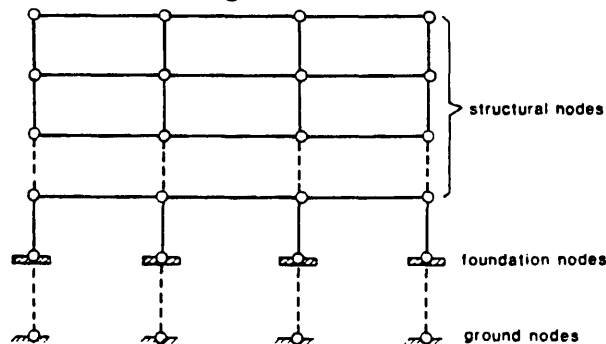


Figure 7.6 Settlement of a multi-bay multi-storey structure with single footing foundation (after Attewell et al., 1986).

As mentioned in section 7.2.1.,

$$P_s = K_s d_s$$

where  $K_s = \frac{12EI}{L^3}$  for bay 1-2

EI = flexural stiffness of bay 1-2, and

L = span of bay 1-2.

From equilibrium of forces,

$$(K_s + K)d_s = K a_i w_i$$

where  $a_i$  = area of footing i,

$w_i$  = ground settlement at footing i, and

$K a_i w_i$  = equivalent force to be applied to footing i for a displacement,  $d_s$ .

Applying generally the above to the analysis of multi-bay multi-storey framed structures (where subscripts, s, denotes structure, g, ground nodes; and, f, foundation), the equation is of the following form (Figure 7.6):

$$K d = P$$

where K = general stiffness matrix of the superstructure and the substructure.

This may also be written as:

$$\begin{bmatrix} K_{ss} & K_{sf} & 0 \\ K_{fs} & K_{ff} + N_{ff} & N_{fg} \\ 0 & N_{gf} & N_{ag} \end{bmatrix} \begin{bmatrix} d_s \\ d_f \\ d_g \end{bmatrix} = \begin{bmatrix} P_s \\ P_f \\ P_g \end{bmatrix} \quad (7.6)$$

where the submatrices, K, are the structural stiffnesses of the structural components, and the submatrices, N, are the stiffnesses of the ground elements,

For vertical displacement,

$$N_{ii} = K a_{ii}$$

For moment/rotation,

$$N_{ii} = \int K y^2 da$$

For  $i = J$ ,

$$N_{ij} = 0$$

One of the difficulties in this approach, however, is the choice of the effective area of the soil associated with each footing; that is, the area to be employed in evaluating the foundation-ground stiffness matrix. Numerical difficulties are also experienced while introducing the ground deformation vector,  $d_g$ , upon solving the matrix equation(7.6). Additional shortcomings are noticed in the application

of this method to framed structures only. Other continuous structural forms, such as walls, are difficult to incorporate into this analysis. Also, transverse displacements that would cause a significant effect upon the induced strains and stresses in the deformed structure cannot be incorporated into this technique (Attewel et al.,1986 ; MacLeod,1987).

#### 7.4 FINITE ELEMENT ANALYSIS METHOD

To improve the analysis of the soil-structure system, the soil and the structure can be modelled so that the displacement of each system interactively affects the other. This is achieved by using the effective stiffness matrices of both the soil and the structure, that is, the respective stiffnesses of the soil and the structure that are required to cause a unit resultant deformation. Additionally, the transverse movement of the soil nodes is included to simulate larger movements in the soil without inducing erroneous results. Thus, equation(7.2) is modified to:

$$(K_s + K_g) d_s = K_g w \quad (7.7)$$

where  $K_s$ ,  $K_g$  = global matrices of the structure and the soil substructure respectively, where the soil is a fully populated matrix including both vertical and transverse displacements. These are defined with respect only to the interface nodal degrees of freedom.

In order to define the stiffness matrices of the soil and the structure, separate finite element models of the ground and the structure are constructed, in such a way that unit displacement is prescribed at one interface node, while the remaining interface nodes are fully restrained. The calculated reactions at each of the interface nodes give a column of the soil submatrix,  $K_g$ , or the structure submatrix,  $K_s$  (Zienkiewicz and Cheung,1967 ; Attewel et al.,1986). Inducing a representative soil movement, the displacements and stresses due to the deformed structure are then calculated.

#### 7.5 SLABS ON ELASTIC GROUND METHOD

"Slabs on elastic foundation" is a design method used in many structures such as floating platforms, foundations resting on soft soil,



airfield concrete pavements, etc. The common approach has been the application of the theory of elasticity for a plate that rests either on a Winkler-type foundation (Hetenyi,1946 ; Timoshenko and Woinowsky-Krieger,1959), or on an elastic isotropic and homogeneous half space medium (Vlasov and Leontev,1966). However, no consideration is taken of the response of the superstructure. Limitations of the structural damage rely upon the critical deformation of the slab, and this in turn, is dependent on the type of the superstructure. Also, several researchers (Richard and Zia,1962 ; Gazetas and Tassios,1978) recommended design formulae based on the ultimate theory of concrete slabs by considering yield line theory and elasto-plastic response after cracking. Lytton (1970), Walsh (1975,1978), Wray (1978) and PTI (1978) developed a technique for the design of slabs on swelling grounds by introducing the concept of mounds representing ground deformation.

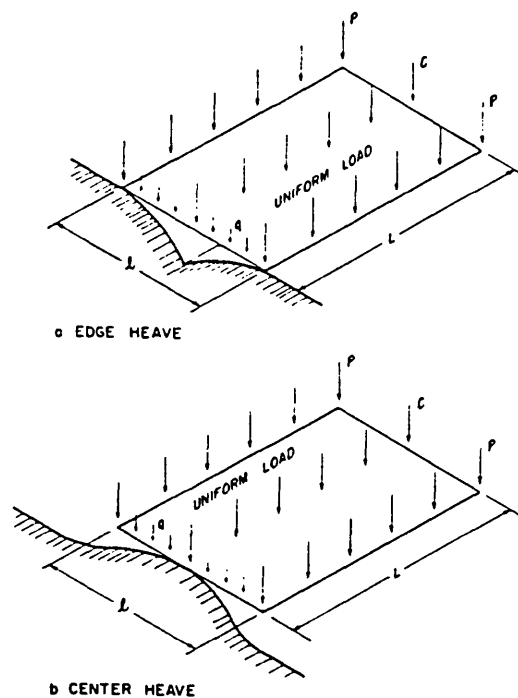


Figure 7.7 General ground mounds (after Lytton and Woodburn,1973).

These are divided into two general patterns, edge and centre heave (Figure 7.7). The structural interaction of the slab with a mounded soil is expressed as an isotropic plate on a coupled spring mound, where the effective deformation of the slab is represented by

$$w_0 = w - y$$

where  $y$  = elevation of the mounded soil relative to its high point, and defined by Lytton and Woodburn (1973) as  $y = cx^m$ ,  
 $x$  = distance from the high point of the ground mound,  
 $m$  = soil mound exponent dependent upon the moisture content, and depth of expansive soil,  
 $w$  = deformed shape of the slab, and  
 $w_0$  = initial shape of the slab.

Thus the differential equation becomes

$$D\nabla^4 w - G_h \nabla^2(w-y) - k(w-y) = P$$

where  $G_h$  = shear stiffness of the soil subgrade,

$P$  = pressure acting on the slab,

$D$  = flexural rigidity of the slab, i.e.  $Et^3/(12(1-\nu^2))$ ,

$t$  = thickness of the slab, and

$k$  = effective modulus of the subgrade.

If the slab is subdivided into small strips,

$$\nabla^4 w - \frac{2t}{D} \nabla^2 w + \frac{k}{D} w = \frac{q}{D} \quad (7.8)$$

where

$$t = \frac{E_0}{4(1 + \nu_0)} \int_0^H Q^2 dz,$$

$$k = \frac{E_0}{(1 - \nu_0^2)} \int_0^H Q^2 dz, \text{ and}$$

$q$  = line load applied at one strip of the slab.

Considering the settlement of the subgrade as proportional to the pressure induced between the slab and the subgrade, the intensity of the reaction,  $P$ , of the subgrade soil is given as:

$$P = kw$$

where  $k$  = modulus of the foundation.

Thus the differential equation becomes (in rectangular coordinates) (refer to Figure 7.8)

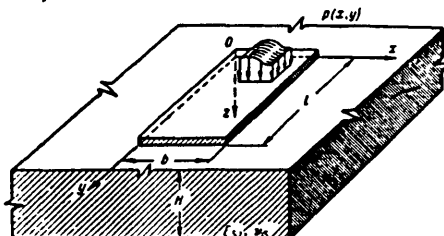


Figure 7.8 Loading condition of a slab on a subgrade of deformable soil.

$$\nabla^4 w = \frac{q}{D} - \frac{k}{D} w \quad (7.9)$$

This has a solution of the following form,

$$w = \sum_{m=1,3,5,\dots} \frac{\sin \frac{m\pi x}{a}}{a} \left[ \frac{4q}{D} \frac{1}{m(\frac{4\pi^4}{a^4} + \frac{k}{D})} + A_m \cosh(B_m y) \cos(G_m y) + B_m \sinh(B_m y) \sin(G_m y) \right] \quad (7.10)$$

where  $A_m$  and  $B_m$  are constants, solved by satisfying the boundary conditions of the slab. The solution to this equation is obtained by numerical integration, and is used in locating the points at which the slab lifts free of the mounded soil surface. Similarly, Walsh (1978) analysed the soil interaction in beams based on a coupled Winkler foundation model expressed in the following differential equation:

$$EI \frac{d^4 y}{dx^4} + A^H \frac{d^2(y-y_o^H)}{dx^2} + B^H(y-y_o^H) + A^S \frac{d^2(y-y_o^S)}{dx^2} + B^S(y-y_o^S) = q \quad (7.11)$$

where  $A^H, A^S = WK_s b^2$  for hard and soft mounds respectively, and zero if the beam is not in contact with the relevant mound,

$B^H, B^S = Wk_s$  for hard and soft mounds respectively, or zero if the beam is not in contact with the mound,

$b =$  cooperating width which determines the extent of the coupling effect,

$W =$  width of the foundation affected by the Winkler beam model,

$EI =$  flexural stiffness of Winkler beam model,

$q =$  loading on the beam,

$y =$  deflection of the beam, and

$y_o^H, y_o^S =$  initial mound shape for the hard and soft mounds, respectively.

The solution is obtained by a trial and error technique, with the aid of computer methods which define the general structure mound profile. Using finite difference methods, moments and shear forces were determined and, consequently, a general equation with best fit results was established (Walsh, 1978). This is given by,

$$\text{Moment, } M = W(1-C)B \frac{L^2}{8}, \text{ and} \quad (7.12)$$

$$\text{Shear force, } V = \frac{4M}{L}$$

where M, V = maximum moment and shear force capacity of the slab,

L = length of slab section,

B = width of slab section,

W = applied load, and

C = constant defining soil-structure interaction based on Winkler beam model.

Lytton and Woodburn (1973) defined a similar equation relating the maximum moment capacity of the slab with a corrective moment which accounts for the compressibility of the soil. Thus, the moment at any point is,

$$M = M_{\max} - \Delta M \quad (7.13)$$

$$\Delta M = C \frac{TL}{8}$$

where T = total load on the slab,

L = length of slab in the direction under consideration, and

C = support index tabulated with reference to the subgrade modulus, maximum differential heave and shape of mounded area, that is, m exponent.

## 7.6 MODELLING OF THE FPSS - ELASTIC MODEL

Having established in Section 5.3 that the primary mode of deformation of the four-point support-system is out-of-plane warping of walls "C" and "D" and inplane deformation of walls "A" and "B", it is necessary to define the interaction response between the two modes of behaviour. This is required to determine the deformation capacity of the two walls (that is, A and C or B and D) in order to limit the amount of differential movement allowed before the limiting tensile strain is reached in either of the two walls. For the box shape of the FPSS, the amount of warping requires a knowledge of the shear centre of the section, and determination of this would be rather complicated for a hand method (refer to Section 7.8). However, to consider a hand method, warping of wall C or A is expressed in terms of the out-of-plane deflection, w, of a plate laterally loaded, while wall A or B is represented as a deep beam supported at its ends by wall C or D, respectively.

Let us first consider wall C or D as a thin plate of thickness,  $h$  (Figure 7.9), subject to a simplified system of edge reactions resulting from the adjacent walls.

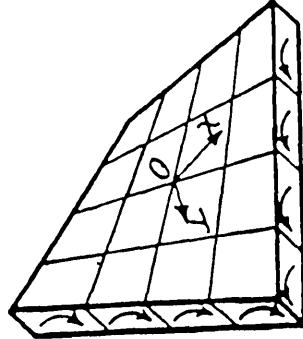


Figure 7.9 Wall C or D subject to system of edge moments.

The deformed shape of the plate would be in the form of an anticlastic surface where the principal curvatures have opposite signs (Mansour, 1985 ; Mills, 1985). The values of the principal curvatures are given by Timoshenko and Woinowsky-Krieger (1959) as

$$\begin{aligned} \frac{1}{r_x} &= -\frac{1}{r_y} = \frac{d^2 w}{dx^2} \\ &= \frac{M}{D(1-\nu^2)} \end{aligned} \quad (7.14)$$

where  $w$  = deflection of the surface of the plate with coordinates  $(x, y)$  in the positive  $z$  direction,

$r_x$  = curvature of the plate in the  $x$ -direction,

$r_y$  = curvature of the plate in the  $y$ -direction,

$M$  = moment applied at the edge of the slab element,

$\nu$  = Poisson's ratio, and

$D$  = flexural rigidity of the slab for an element of thickness,  $h$ .

Thus the deflection is obtained by integrating equation(7.14)

$$w = -\frac{M}{2D(1-\nu^2)} (x^2 - y^2) \quad (7.15)$$

where  $D = \frac{Eh^3}{12(1-\nu^2)}$

Since the plate is in pure bending, acted upon by twisting moments uniformly distributed along its edges (Figure 7.9), this could be represented by a rectangle subject to a system of concentrated forces

of  $2M_1$  at each corner forming a pair of couples along the edges (Figure 7.10).

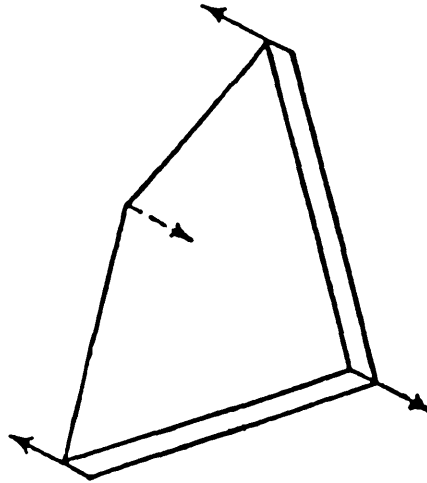


Figure 7.10 Representation of edge reactions on wall C or D by an equivalent system of forces applied at the corners.

The stress state of the plate can be derived, knowing the out-of-plane deformation at a point  $(x,y)$  acted upon by a moment  $M_1$  per unit length at the edge of the plate, and given by

$$\sigma_x = \frac{Ez}{(1-\nu^2)} \left( \frac{1}{r_x} + \frac{\nu}{r_y} \right) \quad (7.16)$$

$$\sigma_y = \frac{Ez}{(1-\nu^2)} \left( \frac{1}{r_y} + \frac{\nu}{r_x} \right) \quad (7.17)$$

and the moments along the X-axis and Y-axis are given as,

$$M_x = D \left( \frac{1}{r_x} + \frac{\nu}{r_y} \right) \quad (7.18)$$

$$M_y = D \left( \frac{1}{r_y} + \frac{\nu}{r_x} \right) \quad (7.19)$$

where the maximum normal stresses are acting at the extreme fibres of the plate at  $z = h/2$ . Thus, the maximum stresses are given by,

$$\begin{aligned} \sigma_x &= \frac{6M_x}{h^2} & ; & \quad \sigma_y = \frac{6M_y}{h^2} \\ &= \frac{6M_1}{h^2} & ; & \quad = \frac{6M_1}{h^2} \end{aligned}$$

Using Hooke's law, the direct strains are given by

$$\epsilon_x = \frac{1}{E} (\sigma_x - \nu\sigma_y)$$

$$\epsilon_y = \frac{1}{E} (\sigma_y - \nu\sigma_x)$$

Thus, the maximum strain in the slab is obtained as,

$$\epsilon_{\max} = \left( \frac{1}{E} \right) \left( \frac{12}{h^2} \right) \left( \frac{2D(1-\nu^2)w}{(x^2 - y^2)} \right)$$

Secondly, let us consider wall A or B as a beam element of thickness  $h$  (Figure 7.11) subject to the following simplified assumptions:

- rigid body rotation of walls by assuming that corners and edges of the walls remain straight after rotation,
- the wall deforms as a cantilever supported by a fixed moment at the fixed support corner equivalent to the adjacent wall,
- superposition of deformations of rigid body rotation and the cantilevering effect along wall A or B.

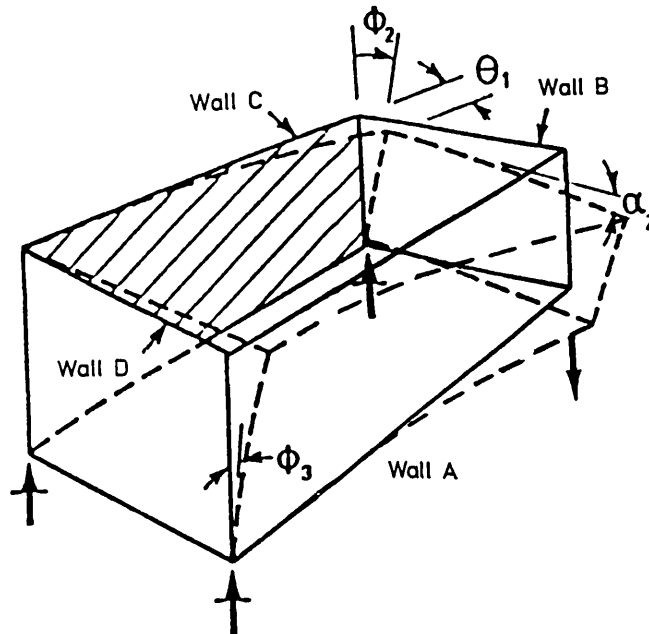


Figure 7.11 Deformation pattern of main walls A or B on settlement of the FPSS.

The rigid deformation of walls A and B is illustrated in Figure 7.11 as a result of distortion of walls C and D,

$$\text{Therefore, } \Delta_1 = \frac{\delta_1 B}{H} \quad , \quad \Delta_2 = \frac{\delta_2 L}{H}$$

Considering wall A or B subject to loss of support and acted upon by a restraining moment at the fixed end (Figure 7.12).

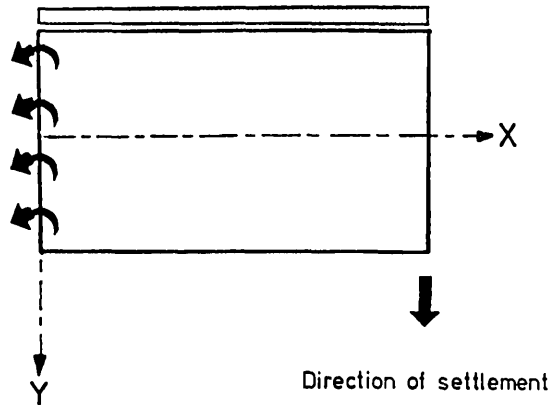


Figure 7.12 Representation of an equivalent system of edge moments applied on wall A or B.

From the theory of elasticity, the stress function of a cantilever can be chosen as (Timoshenko and Goodier, 1959),

$$\Phi = \frac{C_1 xy^3}{6} + y(C_2 x^3 + C_3 x^2 + C_4 x + C_5) + C_6 x^3 + C_7 x^2 + C_8 x + C_9$$

where  $C_1 - C_9$  = constants of integration derived by satisfying the boundary conditions.

Thus, the deflection at any point is obtained as,

$$v = \frac{\nu P xy^2}{2EI} + \frac{P x^3}{6EI} - \frac{PL^2 x}{2EI} + \frac{PL^3}{3EI} \quad (7.20)$$

$$u = -\frac{P x^2 y}{2EI} - \frac{\nu P y^3}{6EI} + \frac{P y^3}{6GI} + \frac{PL^2}{2EI} - \frac{Pd^2 y}{8GI} \quad (7.21)$$

Also, the stresses at any point of the wall are given by Hooke's law as,

$$\epsilon_x = -\frac{Pxy}{EI} + \text{secondary terms}$$

$$\epsilon_y = \frac{\nu Pxy}{EI} + \text{secondary terms}$$

$$\epsilon_{xy} = \frac{2(1+\nu)}{E} - \frac{P}{2E} \left( \frac{d^2 - y^2}{4} \right) + \text{secondary terms}$$

where

$P$  = load applied at the cantilever end equivalent to gravity load of



wall,

EI = flexural stiffness of wall A or B,

L = length of wall,

d = height of wall, and

GI = shear stiffness of wall A or B.

Superimposing  $\Delta_1$ , derived as a function of x and y in equations(7.20,7.21), the total deflections of wall A or B in the X and Y directions are given by

$$\Sigma v = \frac{vP}{2EI} xy^2 + \frac{P}{6EI} x^3 - \frac{P}{2EI} L^2x + \frac{PL^3}{3EI} + \delta_2 \frac{x}{H} \quad (7.22)$$

$$\Sigma u = -\frac{P}{2EI} x^2y - \frac{vP}{6EI} y^3 + \frac{P}{6GI} y^3 + \frac{PL^2}{2EI} - \frac{Pd^2}{8GI} y + \delta_2 \frac{y}{H} \quad (7.23)$$

## 7.7 MODELLING OF THE FPSS - FINITE ELEMENT MODEL

Various micro-modelling techniques that use finite element methods for the numerical simulation of the mechanical behaviour of non-linear types of masonry structures have been set up during the past few decades (Page,1980 ; Sabnis et al.,1983 ; Attewell et al.,1986 ; MacLeod,1987). These have produced results permitting useful comparison between parallel experimental studies. Nevertheless, the modelling of structures in terms of acceptable computational effort can be achieved only if one accepts the drastic simplification by which the structure itself is considered as an assemblage of linear material panels, with each panel acting as a planar continuum medium subject to membrane forces. Thus, successful modelling is strictly linked to the options available for discretization, material constitutive relationships and failure criteria.

To investigate the 3-dimensional structural response of the FPSS so as to include interaction of all four walls with the ring beam during settlement, finite element modelling was employed. Two separate computer programs were used to analyse the behaviour of the FPSS upon settlement. The first program was employed to study the three dimensional problem; due to cost limitations only linear finite element method was used. In the second program, cracking was introduced to study the post-yield response of the structure by using a non-linear 2-dimensional finite element analysis. Both programs consider the masonry as a non-laminated medium with characteristic properties of that

of the brickwork, not of the bricks and mortar separately. To reduce computer store and time requirements for the second program, only the main walls were analysed. Additionally, however, the interactive forces due to adjacent walls on the main ones were considered.

The problems of non-linear numerical modelling, through finite element analysis using the smeared approach for the plane masonry panels, is discussed here (refer to Section 7.7.3) with reference to material constitutive relationships. It is noted that the finite element method is considered to give close predictions only for an upper limit of the state of stresses, in order to help to understand the mechanism of failure of the FPSS, and to study the governing parameters.

### **7.7.1 Three dimensional linear analysis of FPSS**

Finite element analysis was undertaken to investigate the maximum stress and strain state of the FPSS upon settlement, with reference made to the out-of-plane warping and inplane deformation of walls, in addition to the flexure and twist of the ring beam. A finite element package was employed which modelled the basic structure as that of a core wall supported by a ring beam with the beam being supported vertically at the corners (Figure 7.13). The ratio of the height to the length of two adjacent walls is 1:1.25.

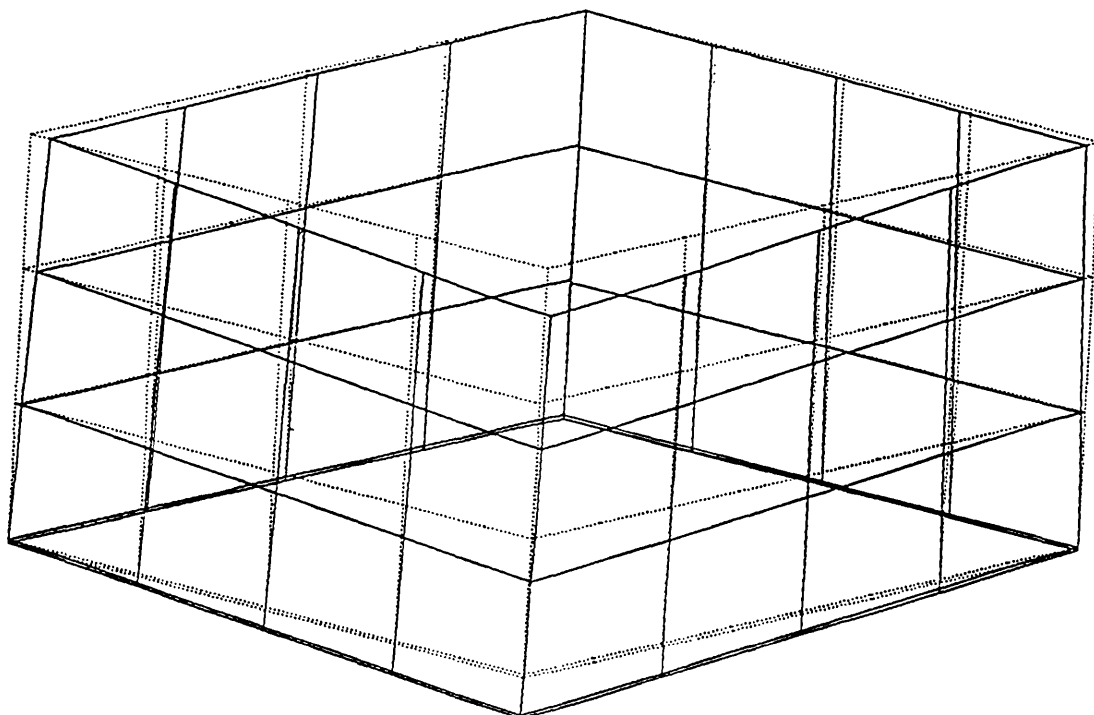


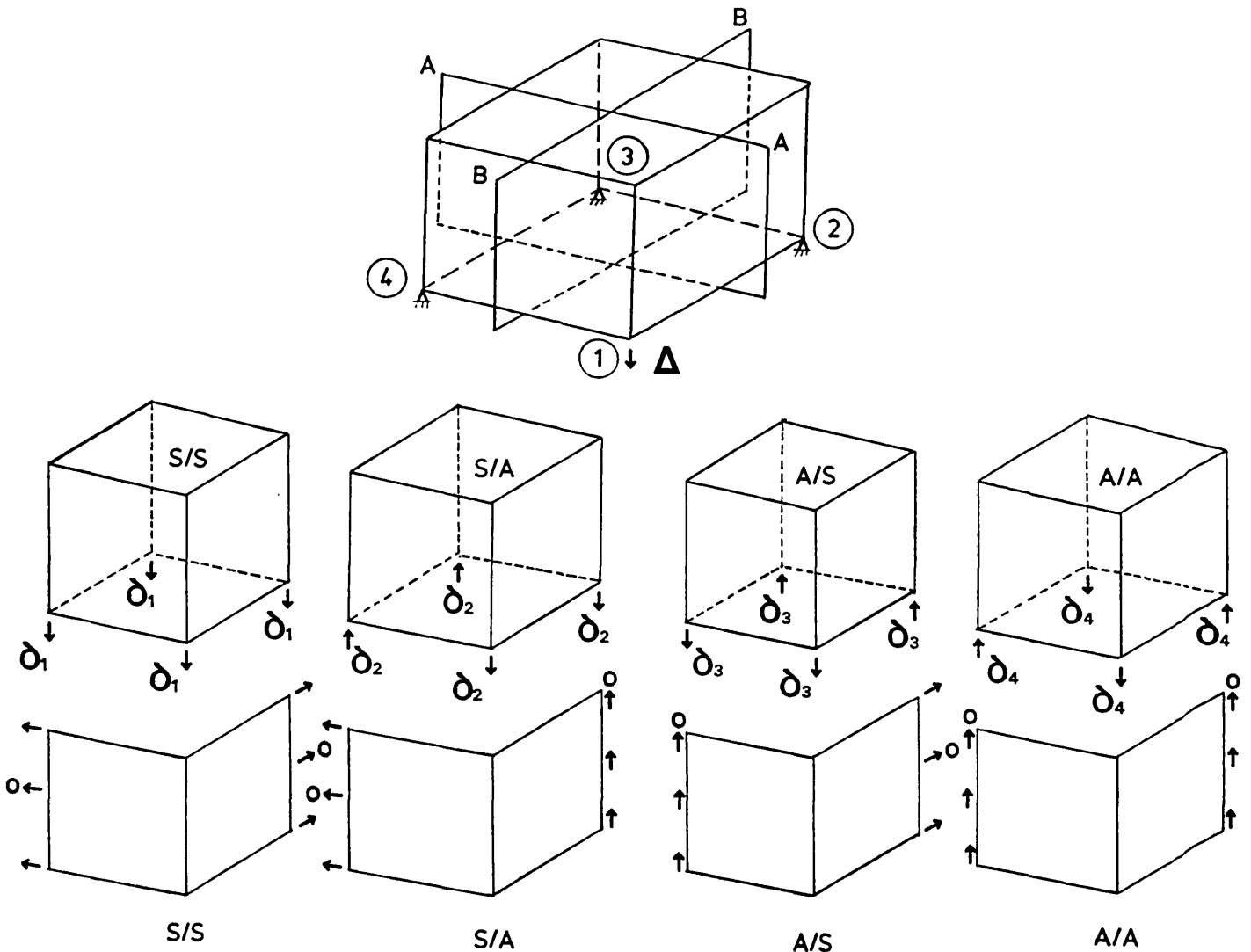
Figure 7.13 Finite element mesh of the FPSS.

Loading of the walls was applied as gravity load, and uniformly distributed loading at the top of the four walls, while vertical settlement was induced at one of the supports. The uniformly distributed vertical load at the top of the wall was arranged as point loads on the nodes of the structure mesh divided using Simpson's Rule. The vertical movement of the support was to simulate part of the building subject to ground movement; the worst being hogging mode due to settlement of the corner. Although this representation may seem complex, the 3-dimensional modelling was necessary in order to study the lateral deformation of walls and warping of cross-walls and its influence on the general deformation of the FPSS. In order to reduce computing time and expenses, only one-quarter of the FPSS is analysed, as shown in Figure 7.14. By using symmetric and anti-symmetric loading cases the structure can be analysed in four steps, (refer to Figure 7.14). To obtain the final stress state, all four cases were superimposed. This has an advantage of using only 1/8th of the computer memory (same as 2-dimensional analysis), and 1/16th of the computation time.

The computer program FINEL was used to perform the linear stress analysis (Hitchings,1981). Two distinct elements were incorporated, namely, the 8-node iso-parametric element and the 2-node beam element. The masonry element employed is a plate 8-noded iso-parametric element having six degrees of freedom at each node in two planes. It is a well tested element that exhibits parabolic distortions along its edges, rather than simpler elements that can only distort linearly necessitating the use of a large number of elements to obtain a comparable level of accuracy. It is recommended that such an element be used with the restriction that the ratio of the longer side length to the shorter side length must not exceed 3, if numerical errors are to be kept to an acceptable minimum.

The 2-node beam element for the ring beam was selected because it deforms in the same pattern as the 8-node iso-parametric, thus ensuring compatibility of deformations between the masonry wall and the supporting beam. The concrete beam element is taken as a 3-dimensional element, carrying torsion and rigidly fixed at the corner. This study is also required to determine the edge forces that define boundary conditions in the 2-dimensional non-linear analysis simulating the influence of adjacent walls and corners (refer to Section 7.7.6). Additionally, the analysis is concerned with defining the deformation

pattern, namely, due to inplane bending of the main walls, or warping of adjacent walls, and to establish a correlation between both the out-of-plane and inplane deformation, and the maximum settlement of the FPSS.



For compatibility at the following corners:

- (1)  $\delta_1 + \delta_2 + \delta_3 + \delta_4 = \Delta$
- (2)  $\delta_1 + \delta_2 - \delta_3 - \delta_4 = 0$
- (3)  $\delta_1 - \delta_2 - \delta_3 + \delta_4 = 0$
- (4)  $\delta_1 - \delta_2 + \delta_3 - \delta_4 = 0$

A : Anti-symmetric deformation.

S : Symmetric deformation.

Figure 7.14 Representation of FPSS as 4-quarter finite element meshes.

### 7.7.2 Linear stress distribution of the FPSS

In the elastic state, the computed maximum stresses and strains of the FPSS are recorded in Table(7.1), for a differential movement of 3.5 mm. For a limiting tensile strain at the onset of visible cracking in the range of 0.075%-0.1% (Burland and Wroth,1974), the deflection ratio of the FPSS could be linearly interpolated from Table(7.1), and was found to be in the range of 1/510-1/414.

Table(7.1) Maximum stresses and strains induced in the FPSS F.E. model.

Differential movement (mm)	Main wall L (mm)	Adjacent wall B (mm)	Tensile stresses $\sigma_t$ (N/mm <sup>2</sup> )		Tensile strain (%)	
			L=2250	L=1828	L=2250	L=1828
3.5	2250	1828	1.03	0.107	0.034	0.054
			1.62	-0.11	0.034	0.054
3.5	1828	2250	L=1828	L=2250	L=1828	L=2250
			1.05	0.116	0.47	2.60

On reaching the post-cracking state, more deformation was expected, but this could not be predicted by the linear finite element analysis. Nevertheless, larger deflections were anticipated due to increased deformations and crack opening.

Figures 7.15-7.22 show the stress distribution of the main and adjacent walls when subject to 25 mm of settlement, where positive magnitudes of stresses denote compression. The vertical and the horizontal stress distribution along horizontal sections of the wall are illustrated in Figures 7.15-7.17, where A, B and C resemble the horizontal,  $\sigma_{xx}$ , the vertical,  $\sigma_{yy}$ , and the out-of-plane stresses,  $\sigma_{zz}$ . At the settling end of the main wall, high tensile vertical stresses are developed with maximum magnitudes at the bottom of the wall (Figure 7.17), while compressive stresses are induced at the top of the wall. Figures 7.18-7.19 and Figure 7.20 show the stress distribution along the vertical edges of the main and adjacent walls respectively. Figure 7.20 shows a gradation of vertical stresses along the vertical edge at the settling end of the wall, where maximum compressive stresses are induced at the top of the wall. Tensile stresses also develop at the top of the wall (at the fixed support), which indicate that there is

a band width along the diagonal in the middle of the wall of compressive stresses. This causes tensile stresses to develop along a diagonal orthogonal to the previous one. Although at the fixed support (Figure 7.19), the vertical stresses at the bottom of the wall are generally in compression, induced tensile stresses at the extreme soffit of the wall are also present. This is considered to be due to warping of the adjacent wall at that corner, which causes rotation of the main wall. Thus the vertical stresses are shed by both applying a component of horizontal forces at the adjacent wall, and shifting of the maximum vertical stresses to some distance away from the fixed support.

Figures 7.21-7.22 illustrate the stress distribution along horizontal sections of the adjacent wall, namely, at the top and at half height of the wall, respectively. Since the adjacent walls deform laterally, the most critical stresses are the horizontal stresses. Figures 7.21-7.22 show that the horizontal stress distribution at the top of the wall varies, with tension being induced at the return of the settling wall, and compression at the other fixed corner. However, the stress distribution at the middle of the wall consists of compressive stresses developed at the two ends of the wall returns with tension at the mid span of the wall.

Clearly, for the adjacent walls, tensile stresses are concentrated at the warping end of the wall (Figure 7.19); these in turn induce high tensile stresses at the top of the main wall (Figure 7.15). These stresses are equivalent to cantilever moments required to hold the main wall from deforming due to settling at one end. As a result, higher compressive stresses develop at the fixed end of the main wall. However, as the wall settles, the diagonal opposite to the settling support shortens due to confinement by the other settling main wall, that is, acts as a strut in compression. This is explained by the high horizontal compressive stress distribution at the top of the wall (at the settling corner, refer to Figure 7.15), and is seen clearly in Figure 7.18, where there is compressive horizontal stress distribution along the edge of the wall at the settling end. Since no fixity is provided at the fixed end of the main wall except by the adjacent wall, the main wall rotates as much as the adjacent wall would be able to deform laterally. This can be caused by the value of the wall element, since also, no translational rotation is allowed.

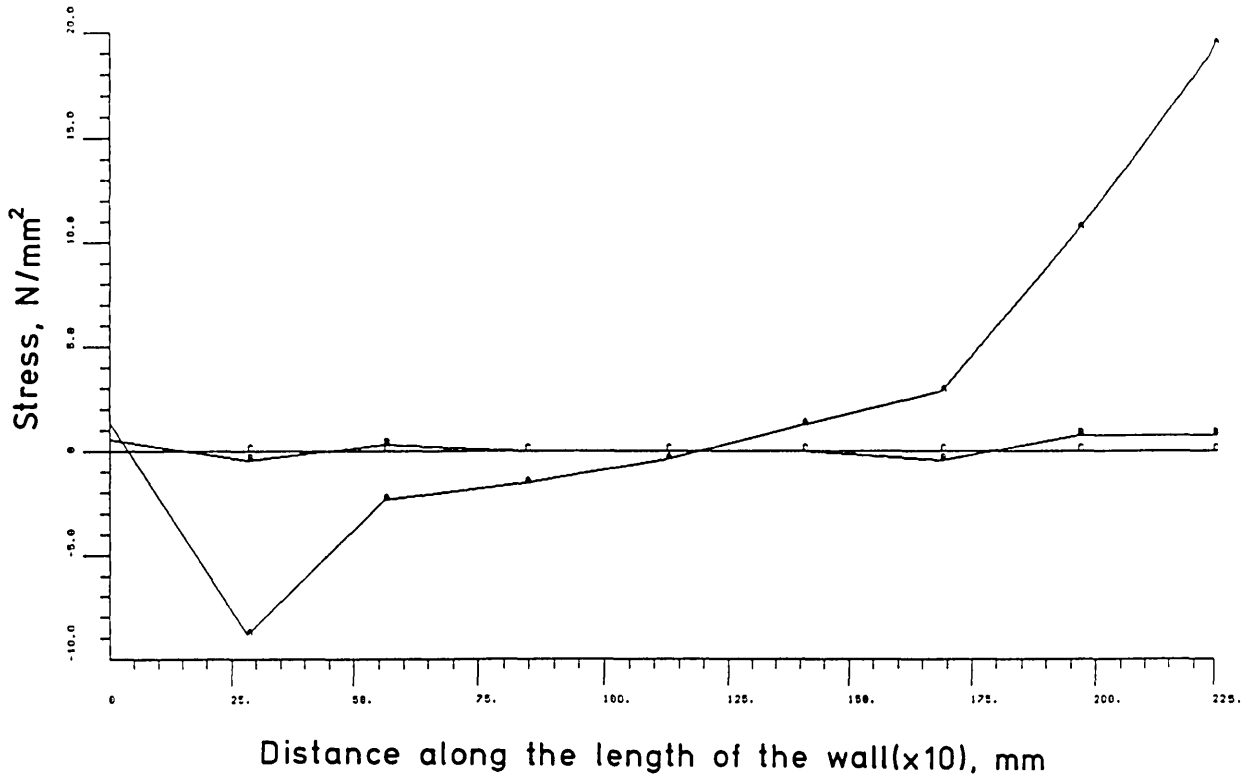


Figure 7.15 Stress distribution along the top horizontal section of main walls.

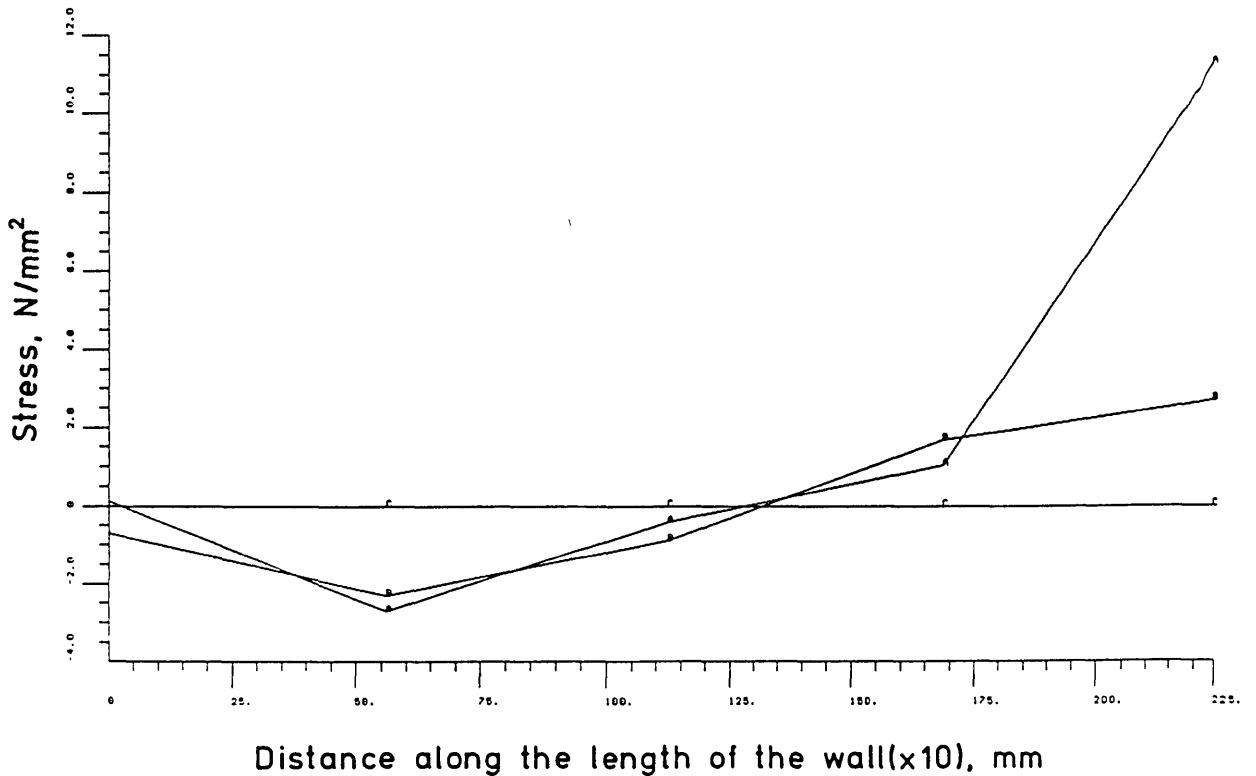


Figure 7.16 Stress distribution along middle height of the horizontal section of main walls.

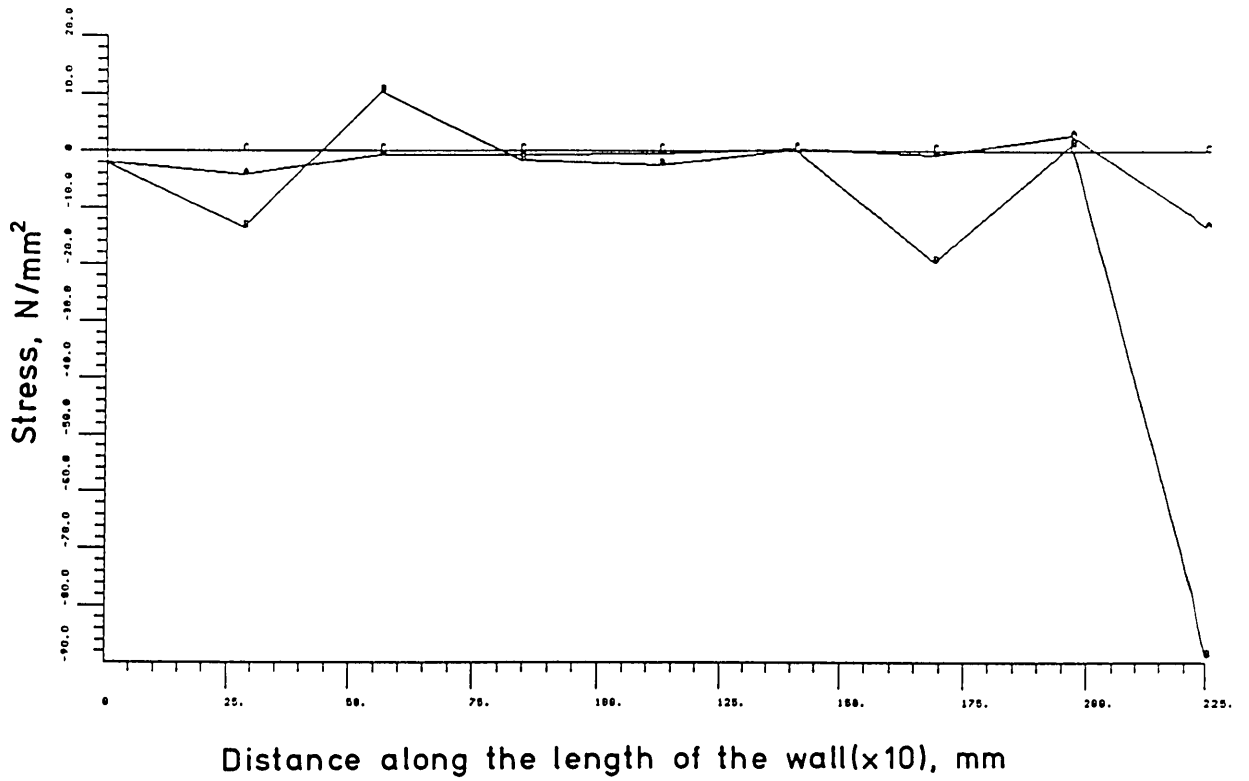


Figure 7.17 Stress distribution along the soffit horizontal section of main walls.

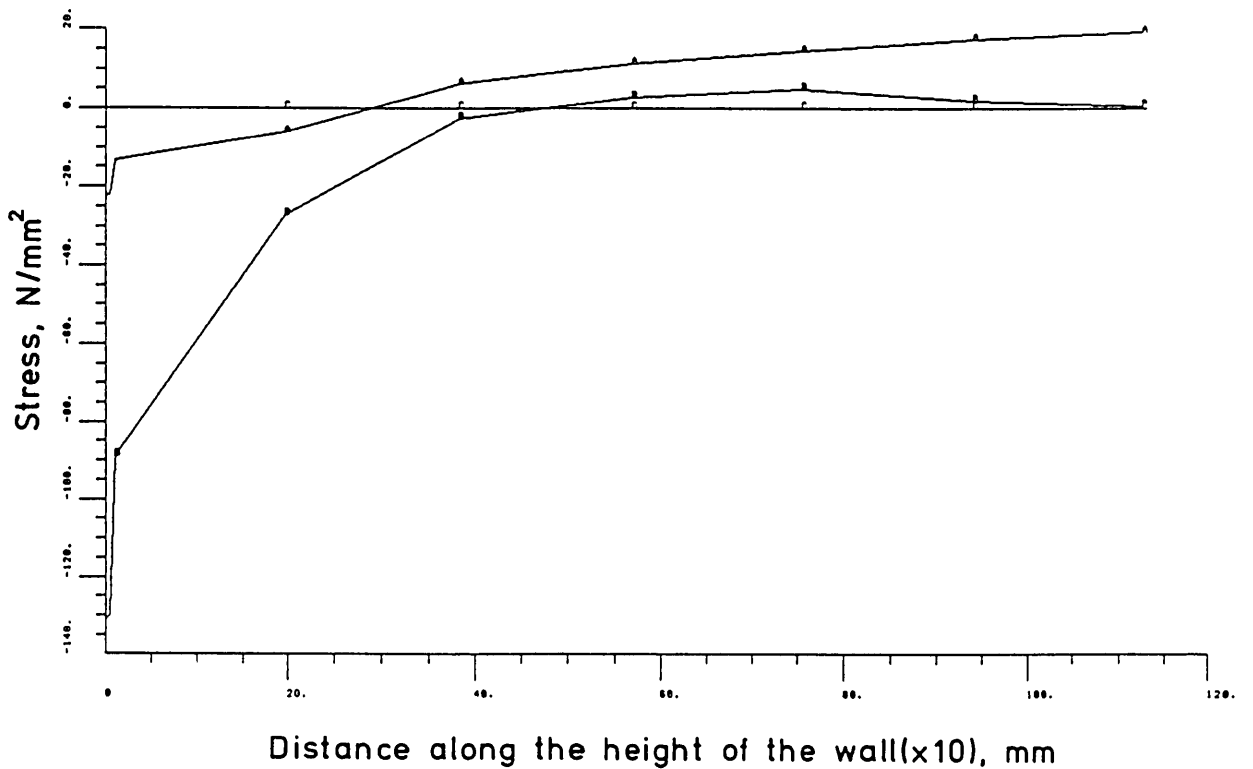


Figure 7.18 Stress distribution at vertical section of main walls at the settling corner.



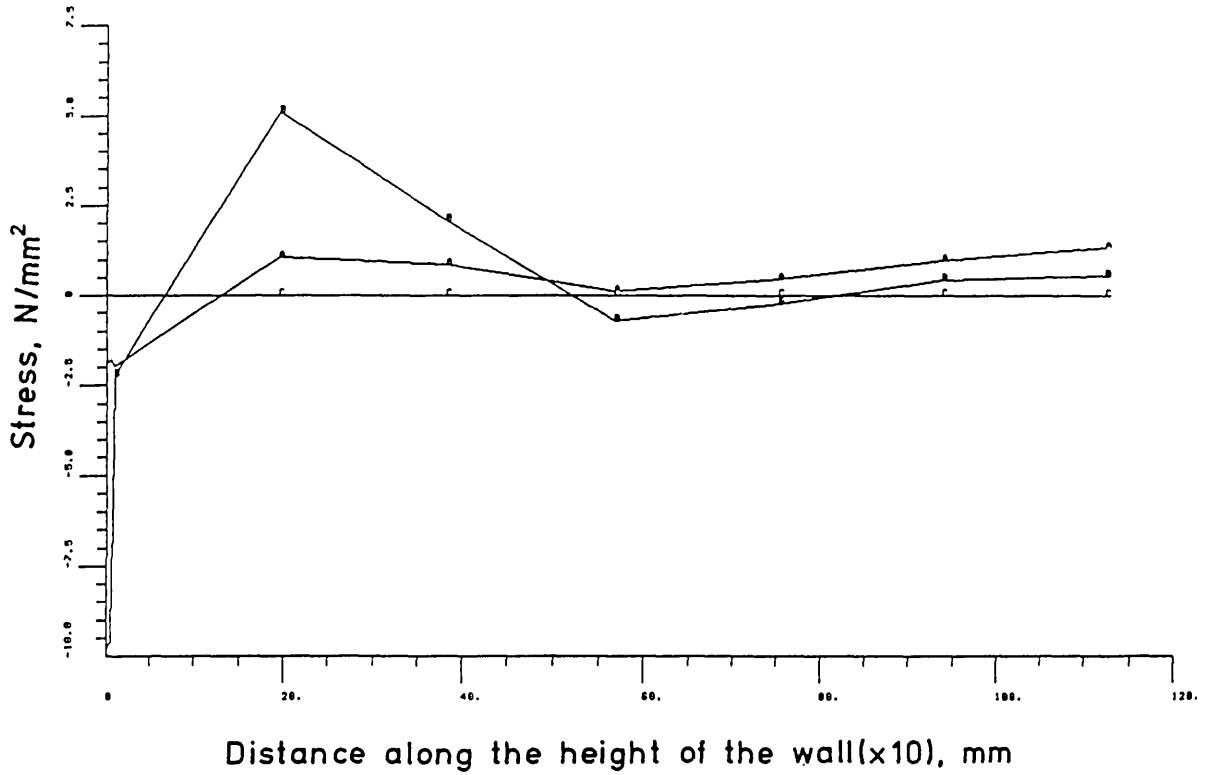


Figure 7.19 Stress distribution at vertical section of main walls at the fixed corner.

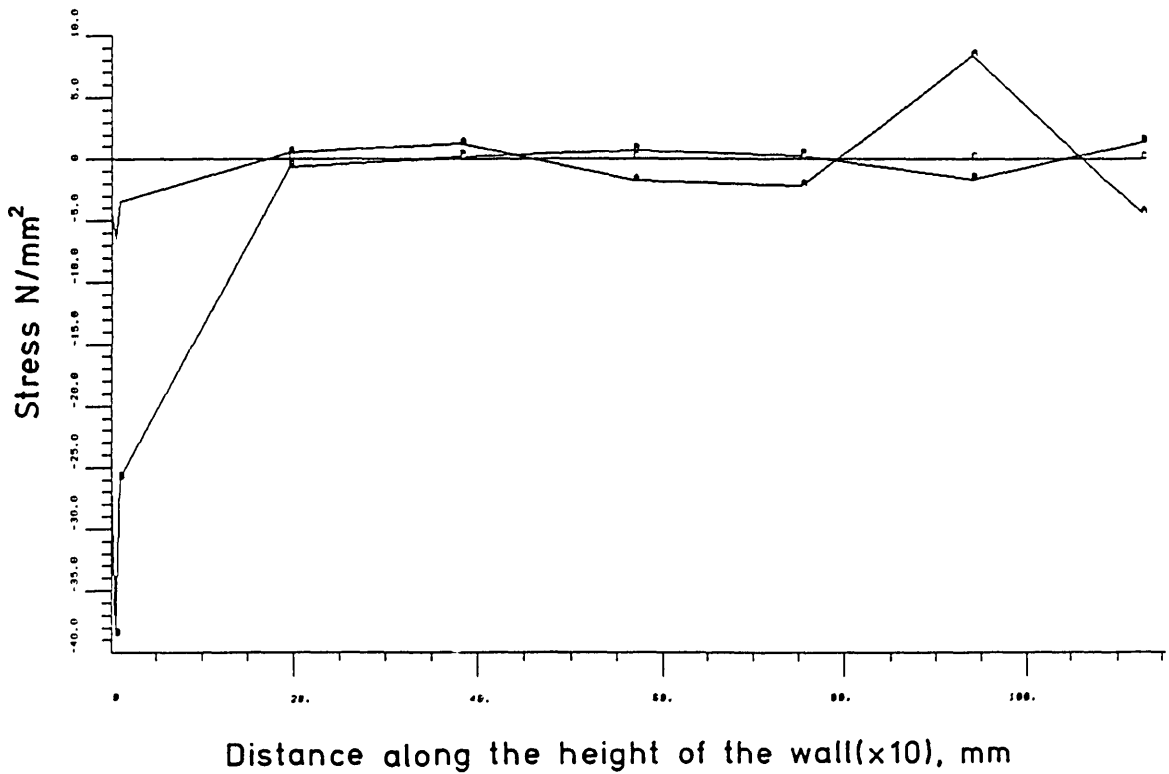


Figure 7.20 Stress distribution at vertical section of adjacent walls at an opposite corner to the settling one.

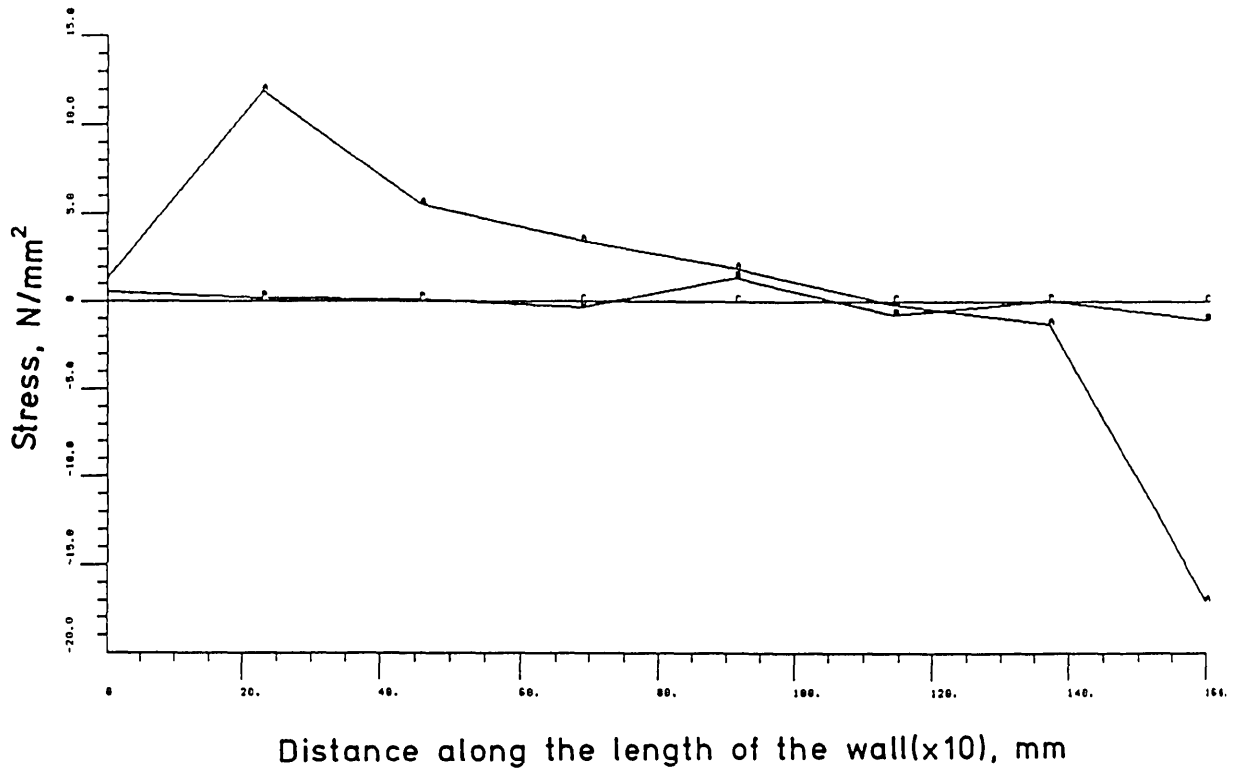


Figure 7.21 Stress distribution along the top horizontal section of adjacent walls.

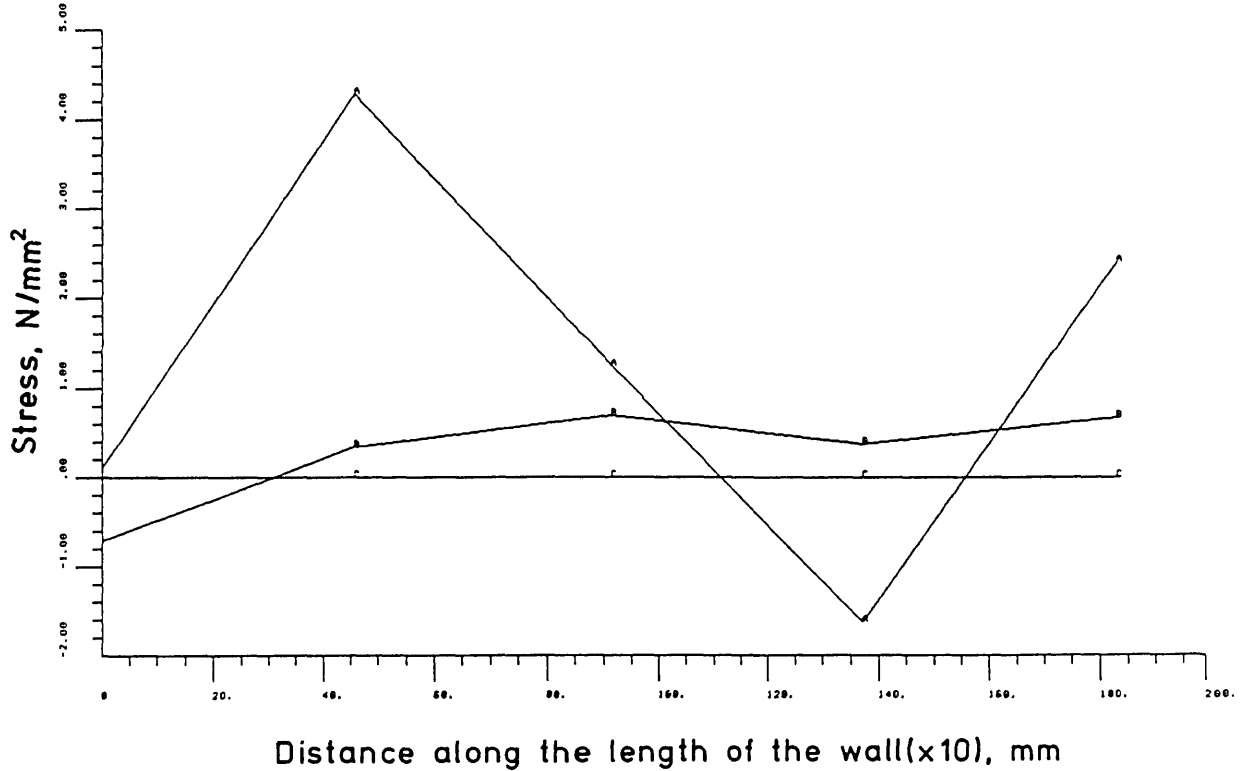


Figure 7.22 Stress distribution along middle height of the horizontal section of adjacent walls.

### 7.7.3 Review of the biaxial failure envelop of brickwork masonry

Brickwork masonry is a material which exhibits directional properties due to the influence of the mortar joints acting as planes of weakness. Several investigators have defined failure in terms of the two principal stresses at any point, together with the influence of a third variable, namely, the bed joint orientation relative to the principal stresses (Johnson and Thompson, 1969 ; Drysdale, Hamid and Heidebrecht, 1979 ; Yokel and Fattal, 1976 ; Stafford-Smith, Carter and Choudhury, 1970 ; Hendry, 1978). As a result, Page, Samarasinghe and Hendry (1982) and Samarasinghe and Hendry (1982) have defined a 3-dimensional failure surface in terms of the principal stresses  $\sigma_1$ ,  $\sigma_2$  and their respective orientations to the bed joint,  $(\theta)$  and  $(90^\circ + \theta)$ . They found that as the bed joint orientation in relation to the tensile stress,  $\sigma_t$ , is reduced, the failure strength of brickwork in biaxial stress state increased. Hegemier, Nunn and Arya (1978) in their summary of numerical methods, were concerned about the applicability of this concept to masonry modelling, since the bed joint angle is of little influence on the resulting failure mechanism.

Samarasinghe and Hendry (1982) obtained a failure surface for brick masonry in the tension-compression principal stress range, and incorporated all possible failure modes, namely, joint failure, combined brick joint failure, and brickwork compression failure. Page (1980) derived a failure envelop in the tension-tension range, while Dhanasekar, Page and Kleeman (1985) reported experimental investigation of the compression-compression principal stress range.

Several criteria for the inplane failure of masonry are used for the numerical modelling of walls. Failure envelopes are defined in terms of two principal stresses ( $\sigma_1, \sigma_2$ ), and the orientation of  $\theta$  of  $\sigma_1$  to the plane of bed joints. Another method employed is in terms of a stress state related to the bed joint, consisting of a normal stress  $\sigma_n$ , a stress parallel to the bed joint  $\sigma_p$  and a shear stress,  $\tau_s$  (Page, 1978 ; Dhanasekar et al., 1985 ; Samarasinghe, Page and Hendry, 1981). Other methods were reported that depend upon the failure pattern and the cracking criteria, such as the limiting shear, tensile bond, shear bond and compressive strength of masonry. These were used in defining empirical coefficients of theoretical relations of the behaviour of masonry walls (Yuan, Shuo, Bin and Bin, 1985 ; Motta and D'Amore, 1985 ; Hegemier et al., 1978). With the advent of finite element techniques, the former method is better suited to be incorporated into general types

of structural analysis. However, difficulty in modelling finite elements of masonry presented problems to researchers concerning the choice of representative elements (Page,1978 ; Saw,1974). Two methods were used, either elements representing individual bricks and mortar layers (Page,1978), or using the smeared approach (Hegemier et al.,1978). Page (1978) used an iterative finite element analysis to model bricks and joints separately, so as to simulate a collapse mechanism after the progressive failure of a number of elements. It is clear that the computer time and storage facilities of such a program are very high and expensive to run. Ali and Page (1987) employed a failure surface developed initially for concrete irrespective of the bed angle, and incorporated a finite element mesh for both bricks and mortar that was found to produce comparative results with laboratory experiments.

#### **7.7.4 Two dimensional finite element non-linear analysis of masonry walls of FPSS**

This analysis is required to predict the stress distribution of the main walls of FPSS, and to determine the strain distribution at the onset of visible damage. The effects of warping of the cross walls increases the deformation of the FPSS but, in fact, it is the deformation of the main walls that limits the differential movement capacity of the FPSS before severe cracking occurs. In order to avoid unnecessary duplication of work, a non-linear finite element program for concrete, developed in the Concrete Structures Section at Imperial College, was adopted. To use the non-linear computer-based methods in the analysis of masonry walls on reinforced concrete ring beams, it is essential that the strength and the deformational properties of both concrete and brickwork are expressed in a suitable form to be incorporated compatibly in the program. The normalized stresses in biaxial compression-compression, tension-compression and tension-tension were employed for both concrete and brickwork (bedding planes perpendicular to the vertical). To include the brickwork constitutive relationships in the same non-linear model developed for concrete, it was necessary to run a comparison between the constitutive relationships of concrete and brickwork under generalized states of stress. This was required in order to establish whether the concrete model already existing in the program could be used to model the FPSS structure.

For concrete, the mathematical formulation of the constitutive

relationships proposed by the CMRG (Concrete & Material Research Group at Imperial College) concerned with uniaxial, and biaxial stress states was adopted (Kotsovos,1979 ; Bedard,1983), while for brickwork masonry the work of Page (1978) and Page et al. (1982) was employed in the comparison. The non-linear response of concrete is based upon the internal stress concept, which takes the form of extension and crack propagation in localized regions in order to relieve high tensile stress concentrations which develop near the crack tip under increasing applied compressive stress (Kupfer, Hilsdorf and Rush,1969). The mathematical expressions describing the non-linear deformational response of concrete are given in Kotsovos (1979), while the non-linear finite element program works on a 2x2 integration rule (Gaussian quadrature rule), where the properties of the element stiffness matrix are calculated, and relief of tensile stresses occur. As the tensile stress is exceeded at a particular Gaussian point, no further shed of stresses is allowed at that point.

The deformation behaviour of brickwork is similar to concrete, especially when the size of brick in relation to that of the structural element is small (Hendry,1978). Interaction between bricks and mortar provide most of the non-linearity of the system where, if the mortar strength is weaker than that of bricks, the non-linearity of the behaviour is initiated by cracking of the mortar or at the brick-mortar interface. Stafford-Smith et al. (1970), Turnsek and Cacovic (1971) and Shrive and Jessop (1982) discussed the initiation and propagation of cracks in masonry under different states of stress. They suggested that the flaw propagation concept of portland cement concrete applies equally to masonry in uniaxial compression and tension. Additionally, they showed that a continuum element can successfully represent masonry without individually defining characteristic properties of both mortar and bricks. Furthermore, owing to the accuracy achieved generally in numerical modelling, a similar technique to that of concrete, based on the limiting tensile stress to define cracking, is sufficient in that case.

#### **7.7.5 Comparison of the biaxial failure envelopes of brickwork and concrete**

The existing program incorporates the non-linearity of the material constitutive relationship (concrete or brickwork), behaving as an isotropic material within the limits of stress defined by the failure

envelope Since for brickwork the failure envelope is influenced by the variation of the orientation of the bedding plane to the principal stresses (Page et al., 1982), in order to establish if any modification of the existing relationships contained within the program, it is important to compare the concrete and the brickwork stress envelopes so as to determine the variation between the two materials.

Figures 7.23-7.25 show the deviation of brickwork and concrete envelope derived from the results of Page et al. (1982), Dhanasekar et al. (1985), Kotsovos (1979) and Kotsovos and Newman (1981) respectively. For compression-compression, tests conducted by Dhanasekar et al. (1985) showed that brickwork masonry behaves independently of the bed joint angle if the ratio  $\sigma_1/\sigma_2$  is small (Figure 7.23). In the case of compression-tension (Figure 7.24), the two envelopes overlap at the top range of the brickwork; the difference between the envelope mean is in the order of  $0.03-0.04 f_c$ . In addition, variation in the tension-tension stress envelope (Figure 7.25), is within the range  $0.01-0.02 f_c$ ; however, the cracking formation criterion and stress envelope in the program would be unable to realize such sensitivity. Generally, the upper range of the brickwork envelope which coincides with the concrete range has a bed orientation,  $\theta = 90^\circ$ , while as  $\theta$  decreases, the brickwork stress ratio,  $\sigma/f_c$  becomes smaller, causing an increase in the deviation of the brickwork envelope from that of the concrete. For low strength brickwork masonry,  $f_c$  is smaller, thus the two envelopes (that is, concrete and brickwork), coincide over a wide range; this is true in comparison to the strength of materials used in the FPSS models (Section 6.5.4). Since the results of brickwork are scattered, it is reasonable to consider the concrete envelope as representative with respect to the accuracy achieved in the program.

Sawko (1982) considered different strengths of bricks and mortar and observed that for Fletton bricks of an average compressive strength of  $25.5 \text{ N/mm}^2$ , the stress-strain relationship coincides with that of concrete. Other similar investigations were reported by Taylor and Mallinder (1987), Edgell (1982) and Powell and Hodgkinson (1976). In addition, the ascending portion of the relationship can be considered as parabolic, similar to the concrete code BS 8110 (1985).

Although close comparison of behaviour is clearly evident, it is necessary to assess the sensitivity of the non-linear program when the bed orientation angle,  $\theta$ , is not included in the failure criteria, especially in the analysis of wall structures.

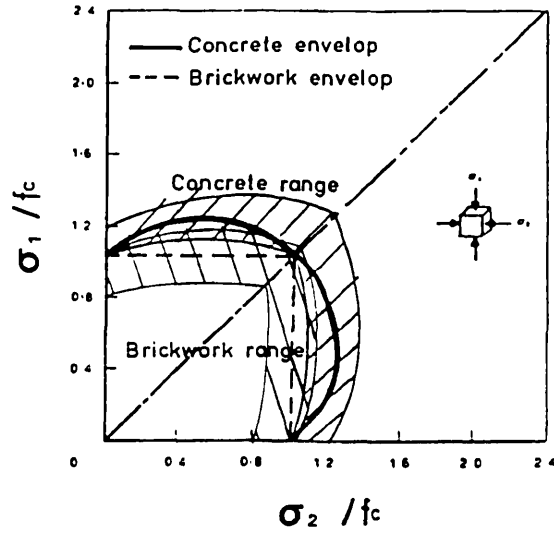


Figure 7.23 Biaxial envelope for concrete and brickwork under compression-compression stresses (adapted after Kotsovos, 1979).

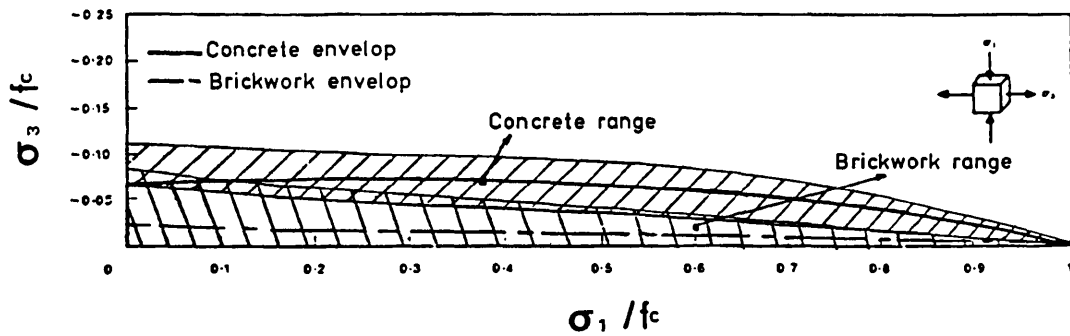


Figure 7.24 Biaxial envelope for concrete and brickwork under compression-tension stresses (adapted after Kotsovos, 1979).

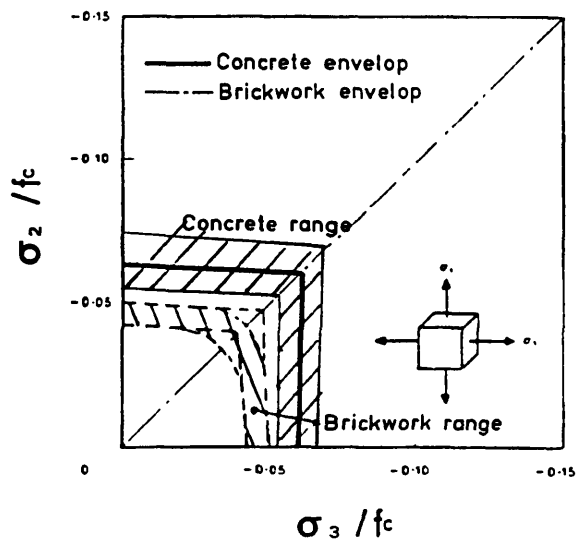


Figure 7.25 Biaxial envelope for concrete and brickwork under tension-tension stresses (adapted after Kotsovos, 1979).

This was achieved by comparing the results of a program run of a brickwall on beam subject to point loading at mid-span, with finite element analysis according to Page (1978). The comparison also studied the effects of not considering individual finite elements of bricks and mortar, but using the smeared approach for brickwork as employed in concrete. The results have shown that there is close comparison of the pattern and magnitude of the maximum stresses induced in the wall, where about 81%-87% of the ultimate load was obtained. As a result, the non-linear finite element analysis was employed to study the post-cracking behaviour of the main walls of the FPSS.

#### **7.7.6 Representation of boundary conditions of FPSS**

In order to use the 2-dimensional non-linear program successfully, correct boundary conditions are needed to obtain the true representation of FPSS in 2-dimensions. The object is to estimate the maximum differential movement that the system can withstand before the serviceability limit is reached. Since the FPSS is a three dimensional structure, the boundary conditions should be able to provide the inplane restraint of out-of-plane members. The main concern is the inplane behaviour, assuming failure to occur in main walls before out-of-plane instability (that is, forces and edge conditions of perpendicular walls).

The basic structure is a wall-on-beam, simply supported at either end. Point loading at each node at the top of the wall simulates dead and live loadings, while edge load at the two vertical sides represents boundary interaction with adjacent walls. The 8-node iso-parametric element is chosen for the wall, so that the structure mesh in 2-dimensions is compatible with that of 3-dimensions. The reinforced concrete beam is modelled using an 8-node iso-parametric element, while the steel reinforcement is represented by a 3-node bar element, so that the beam deforms compatibly with the wall. The steel element in the program is formulated in such a way that it can exhibit only longitudinal stiffness in plane stress applications (that is, no lateral or bending stiffnesses). Incremental loading of the beam-wall structure is achieved by progressive settlement of 0.10 mm, while measuring the strain distribution with the structure so as not to exceed the limiting tensile strength. The process is repeated in load steps until progressive cracking of the structure and failure, beyond which no further deformation can be accommodated due to instability of the



structure. However, in order to be able to simulate the interaction of adjacent walls at each load step, increments of cross wall stresses were applied. These were equivalent stresses caused by differential settlement of 0.10 mm of the FPSS calculated in 3-dimensional analysis (Section 7.7.1). In this way, the interactive stresses due to wall returns are included in determining the flexural deformation of the main walls.

The edge conditions are deduced from the 3-dimensional linear finite element analysis (refer to Section 7.7.1), in terms of end forces. The following assumptions are made:

- Out-of-plane stresses and lateral deformation of main walls do not influence the inplane state of stress and, thus, no change in the limiting serviceability due to differential movement of the FPSS. This is due to the fact that the resistance of the box action of the FPSS is stronger than the inplane resistance of main walls.

- Lateral stresses of adjacent walls cause warping deformation that does not exceed the serviceability limit. Additionally, the interaction between the adjacent walls and the main walls would remain constant. This is acceptable since lateral deformation of adjacent walls that contribute the largest portion of differential movement of the wall would have occurred before that of inplane deformation of the main walls.

- Inplane deformation of main walls occurs after lateral deformation of cross walls, and superposition of deflection of both stress states are applicable. This is a conservative assumption since torsional deformation can occur between adjacent walls at a later stage of inplane deformation, and this may cause increased deflection.

#### **7.7.7 Non-linear stress distribution of the FPSS**

This analysis focuses primarily on the study of the capacity of the main walls to bend, subject to differential movement of their supports, when bounded by the edge conditions of wall returns. This is required in order to simulate the 3-dimensional response of the adjacent walls on the main walls. Also, the analysis attempts to determine the limit of inplane deformation that the wall would reach before exceeding the limiting tensile strain, that is, before visible cracking appears. Three load cases that are likely to cause the possible failure patterns of the FPSS have been considered in assessing the strain distribution within the wall (Figure 7.26). Figures 7.27-7.29 show the post-cracking

behaviour of the main walls when subject to the different loading cases. In addition, the crack propagation is illustrated in various stages of loading. Increments of settlement were applied at 0.10 mm stages of displacement until failure. Notations of the crack formation are as given below:

II : First crack forming at this load step.

I : First crack formed before this load step.

II : Second crack forming at this load step.

I : Second crack formed before this load step.

Three distinct modes of failure were developed. The first mode is diagonal cracks that extend from the top of the wall at the settling corner to the bottom of the wall at the fixed support, or at some distance away from the support. The second mode of failure occurs with a number of vertical cracks initiating at the top of the wall at the supporting end of the beam propagating towards the bottom of the wall at the same end. Thirdly, the concrete beam experienced some form of cracking in two positions, either at the settling end or at some distance away from the fixed support. In most of the cases, extensive cracking propagated at the top half of the wall along a diagonal opposite to the settling support, which caused instability of the mesh that defined ultimate failure. Instability in most of the cases was caused due to loss of point loading at the edges because of excessive deflection of the mesh; clearly this is a case which would not occur in practice. However, for a limiting principal tensile strain of about 0.035%-0.05% computed during the loading stages, a relative deflection ratio in the range of 1/900-1/850 was recorded. It is clear that the amount of differential movement is not sensitive to the type of loading, but the failure pattern is influenced by the different loading conditions and applied boundary conditions.

Figures 7.30-7.32 illustrate a summary of the non-linear analysis defining the relationships between the relative deflection ratio with the stiffness of the FPSS, in addition to the maximum tensile stress and strain reached at the various load stages of each load case. The relative stiffness of the FPSS is defined as the ratio of the equivalent applied load to cause a deformation of  $\delta$  divided by the total deformation,  $\Delta_T$ . It is also clear from the pattern of the relationships that they are not sensitive to the type of loading, nevertheless, the loading cases influenced the maximum tensile stresses and strains induced in the walls.

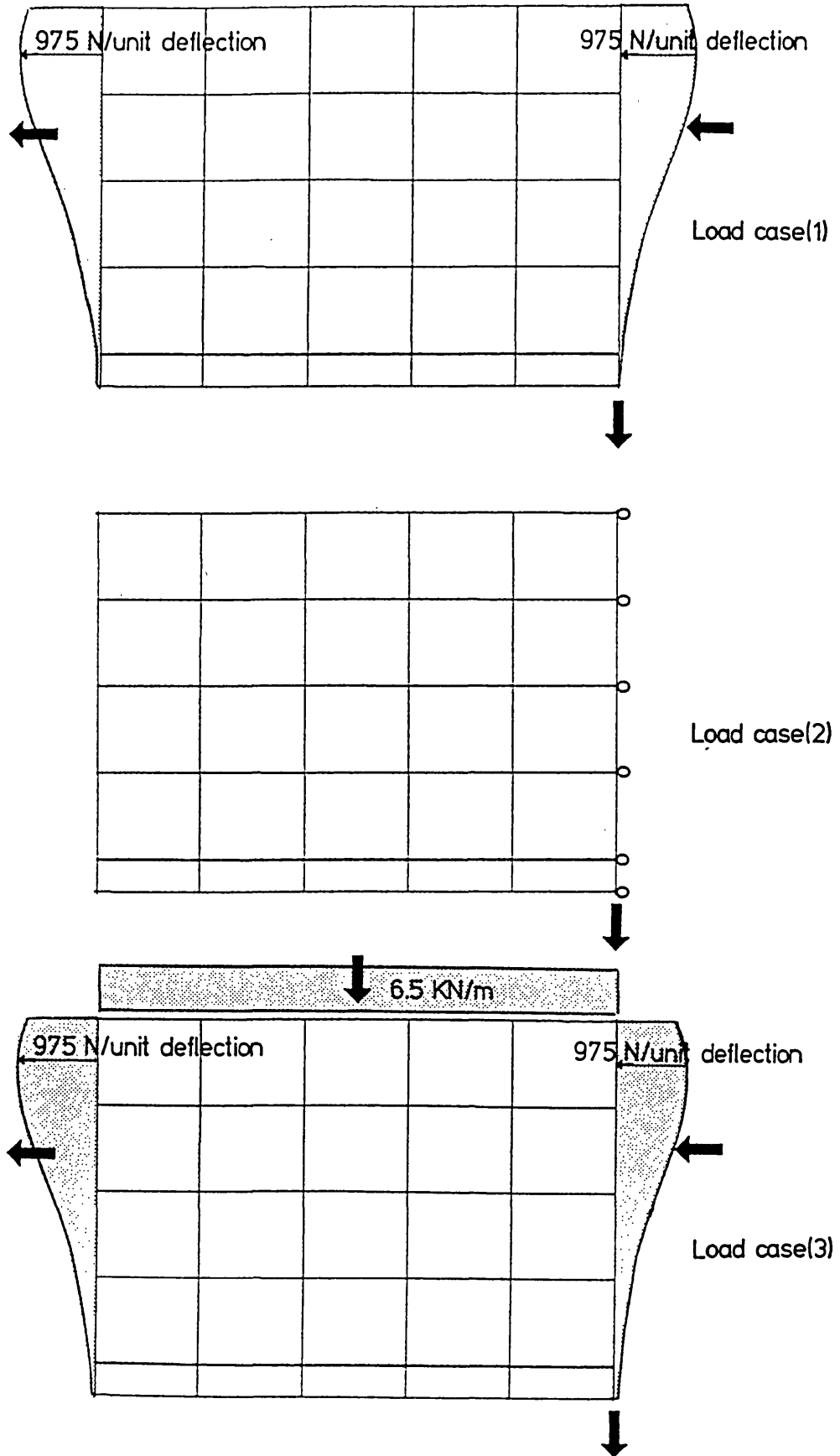
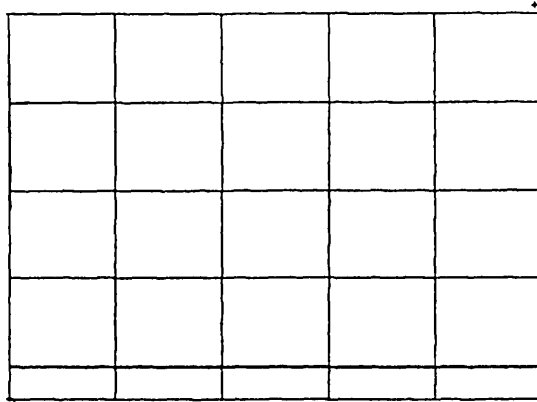
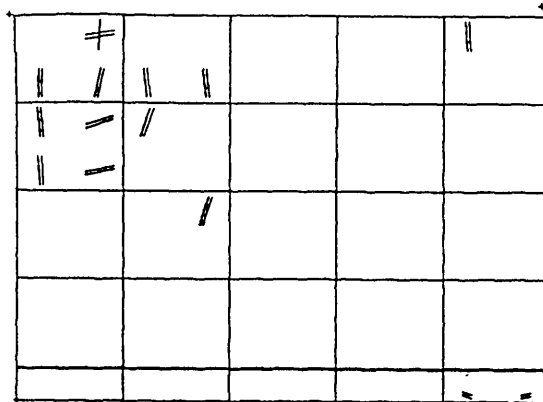


Figure 7.26 Cases of loading of main walls of FPSS subject to settlement.

LOAD = 83664.000 (LOAD STEP 31)



LOAD = 116050.000 (LOAD STEP 43)



LOAD = 116276.000 (LOAD STEP 44)

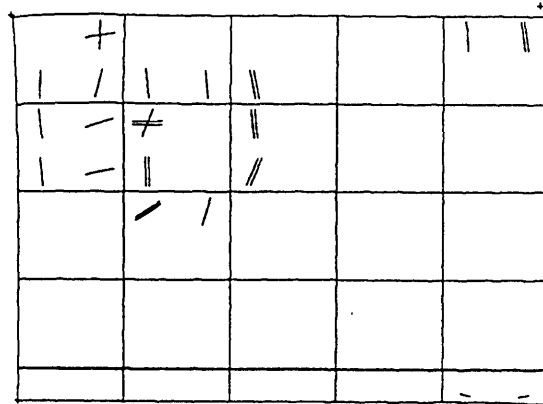
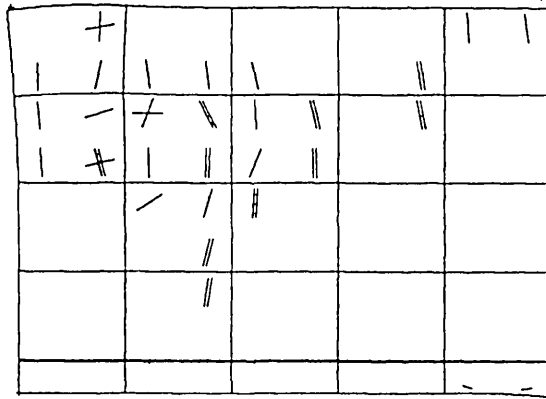


Figure 7.27 Stages of loading of main walls of FPSS subject to load case(1).

LOAD = 116440 K00 (LOAD STEP 45)



LOAD = 116572 K00 (LOAD STEP 46)

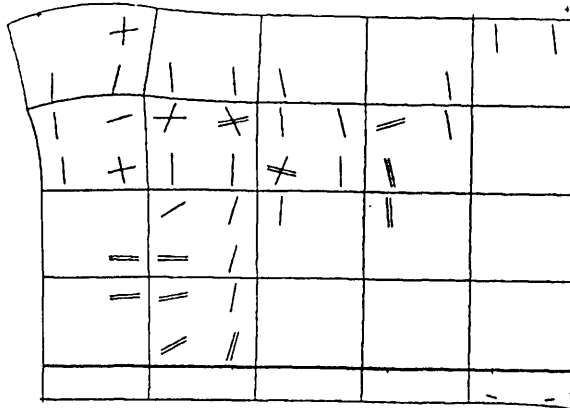


Figure 7.27 Continued.

LOAD = 2398.00KN (LOAD STEP 5)

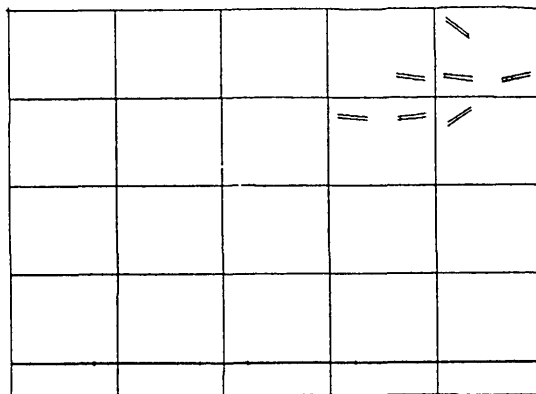
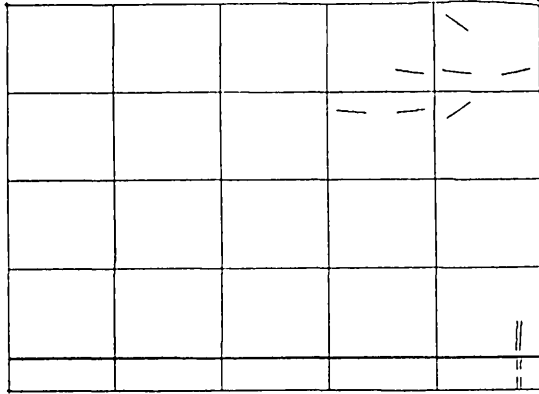
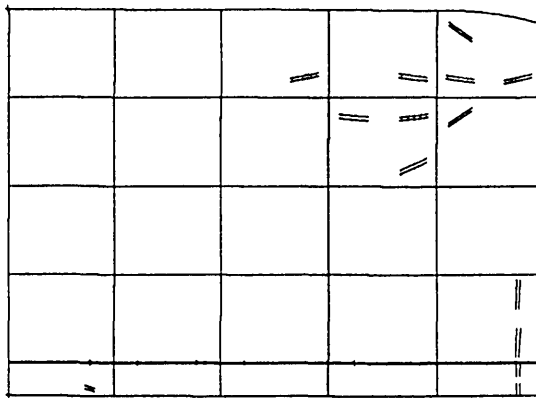


Figure 7.28 Stages of loading of main walls of FPSS subject to load case(2).

LOAD = 2869.60KN (LOAD STEP 9)



LOAD = 4784.40KN (LOAD STEP 36)



LOAD = 5693.40KN (LOAD STEP 65)

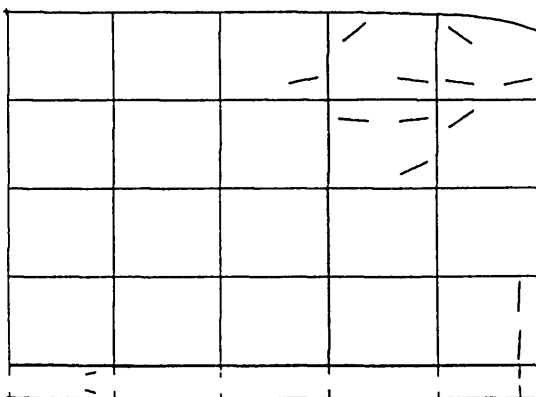


Figure 7.28 Continued.

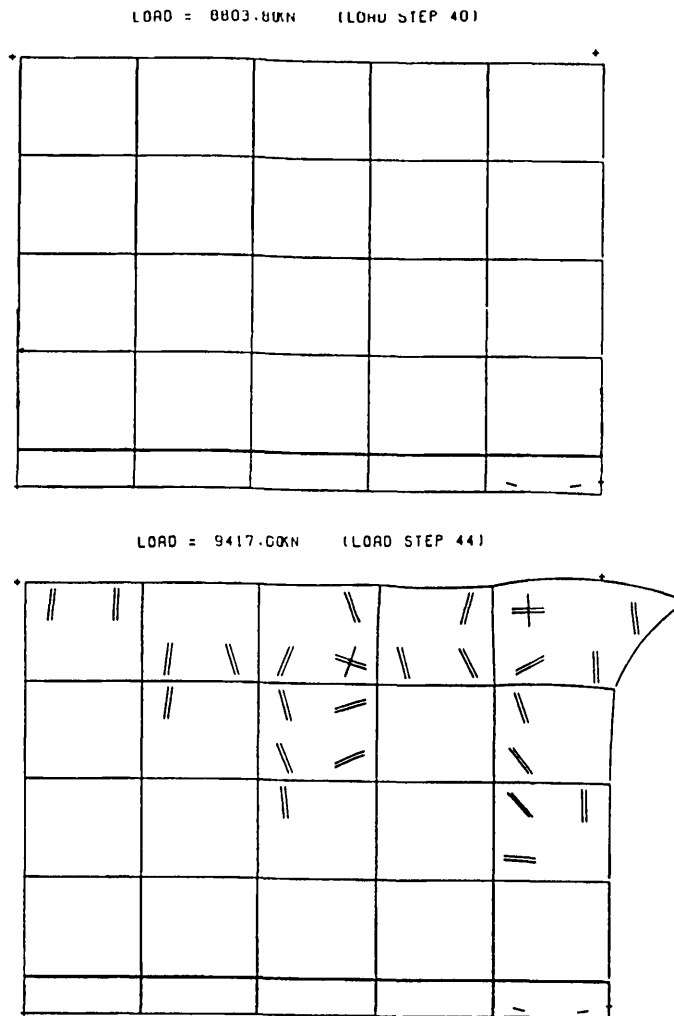


Figure 7.29 Stages of loading of main walls of FPSS subject to load case(3).

A relative deflection ratio in the range of 1/900-1/725 (refer to Figure 7.32), was computed for the three cases with maximum tensile stress of 12 N/mm<sup>2</sup> for load case(2), while for load cases(1) and (3), maximum tensile stress in the range of 1.5-2.5 N/mm<sup>2</sup> developed (Figure 7.31). Figure 7.32 illustrates the relationship of the maximum tensile strain reached at each load case with the relative stiffness of the FPSS. As the FPSS stiffness degraded, there was a marked increase in tensile strain in load cases(2) and (3). For load case(1), it reached an approximately constant strain of 0.01%, whereas for load cases(2) and (3), maximum tensile strains of 0.25% and 0.11%, respectively were computed.

It is apparent that the deformation of walls with returns subject to differential movement is much higher than inplane sagging or

hogging. MacLeod and Abu-El-Magd (1980) computed a maximum deflection ratio of 1/4000-1/6000 (for hogging mode of deformation), while the FPSS wall could withstand an average deflection ratio of 1/1100-1/1000 for a limiting tensile strain of 0.01%. Additionally, the stiffness of the FPSS wall degraded to about 25%-30% of its original stiffness before reaching a relative deflection ratio of 1/2500-1/3000 for the three load cases. Thus, for inplane deformation of walls, only small differential movement is taken by bending and flexing, where more movement is due to crack opening. However for the FPSS walls, more differential movement is allowed resulting from the body rotation of the main walls that is due to the presence of adjacent walls, and reduction of the edge forces and moments that hold the walls during settlement, thus permitting the walls to deform more freely.

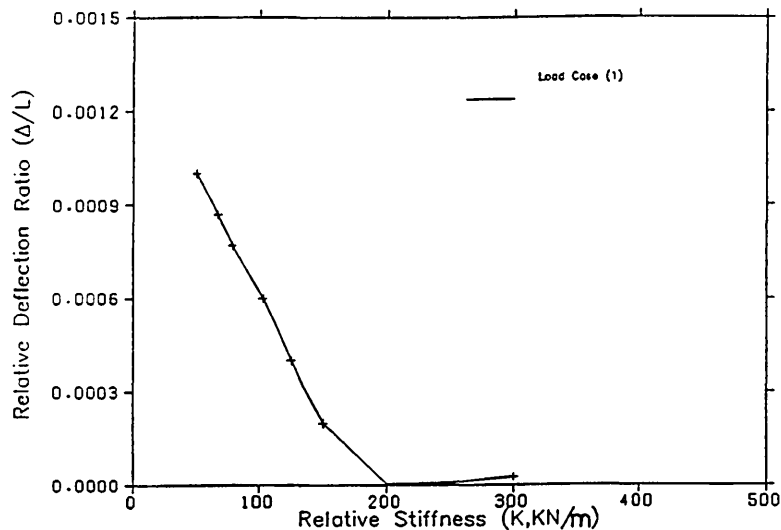


Figure 7.30(a) Variation of deflection ratio with relative stiffness of the FPSS - Load case(1).

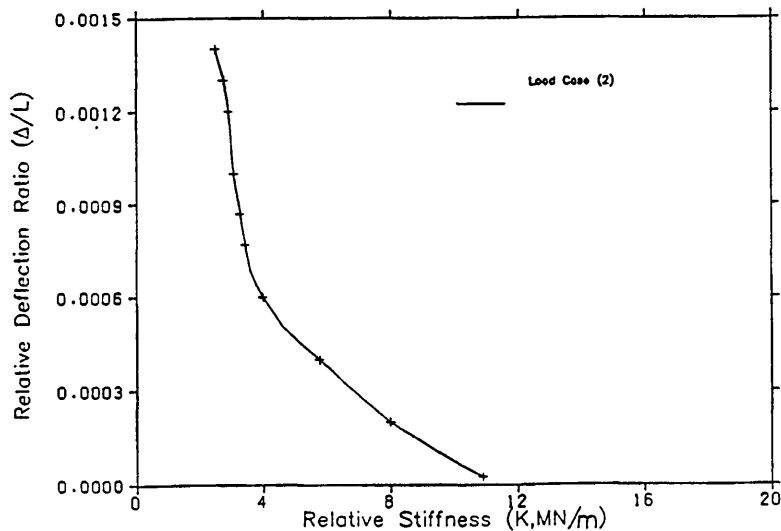


Figure 7.30(b) Variation of deflection ratio with relative stiffness of the FPSS - Load case(2).



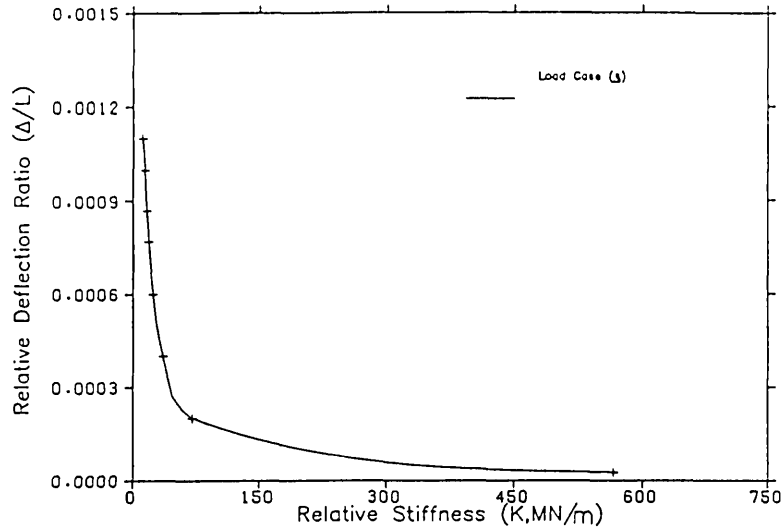


Figure 7.30(c) Variation of deflection ratio with relative stiffness of the FPSS - Load case(3).

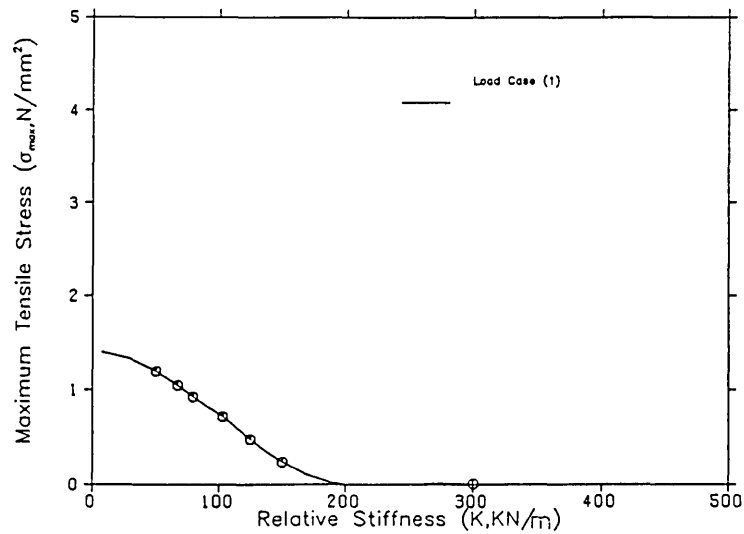


Figure 7.31(a) Variation of maximum induced stress with relative stiffness of the FPSS - Load case(1).

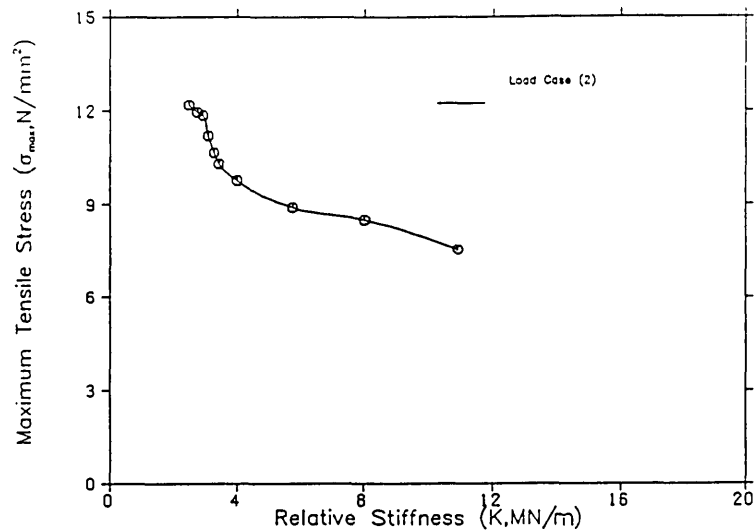


Figure 7.31(b) Variation of maximum induced stress with relative stiffness of the FPSS - Load case(2).

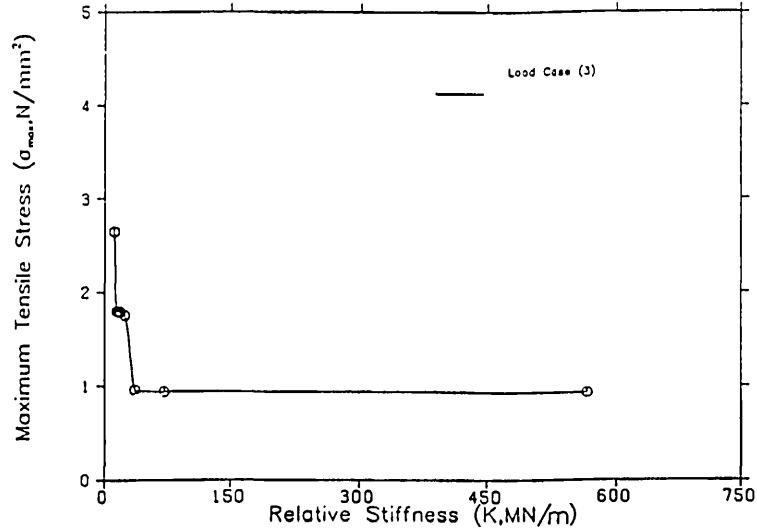


Figure 7.31(c) Variation of maximum induced stress with relative stiffness of the FPSS - Load case(3).

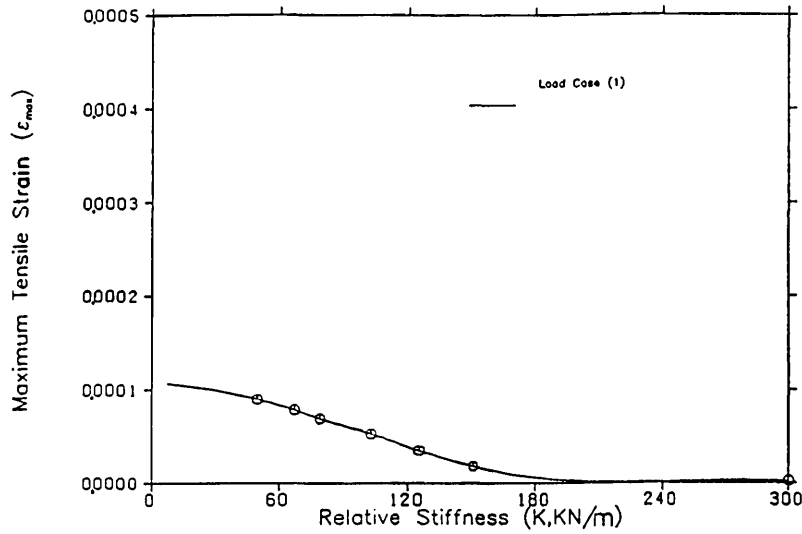


Figure 7.32(a) Variation of maximum induced strain with relative stiffness of the FPSS - Load case(1).

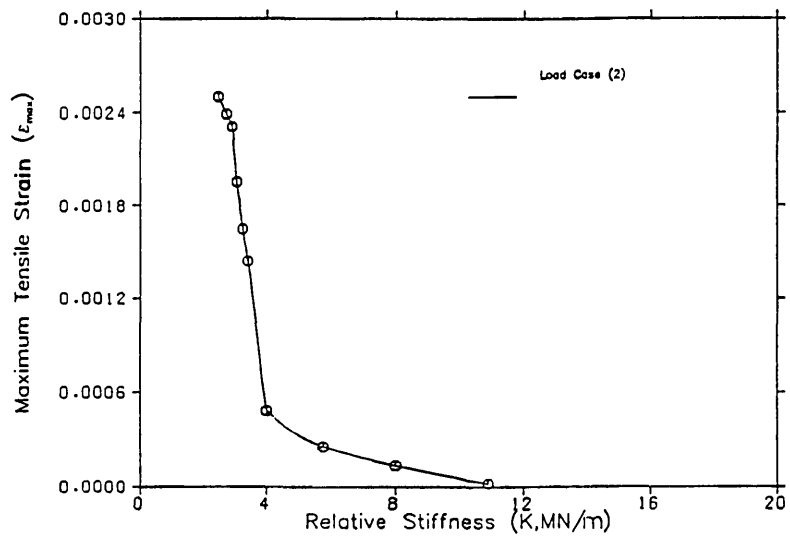


Figure 7.32(b) Variation of maximum induced strain with relative stiffness of the FPSS - Load case(2).

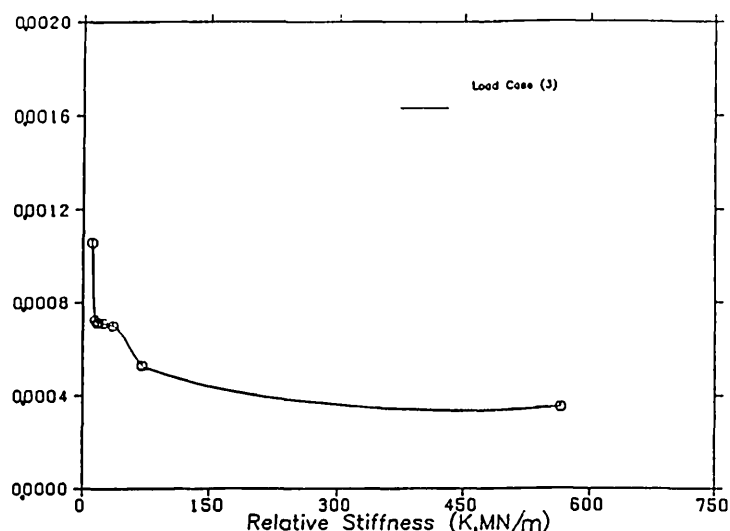


Figure 7.32(c) Variation of maximum induced strain with relative stiffness of the FPSS - Load case(3).

## 7.8 THEORETICAL MODELLING OF THE FPSS

### 7.8.1 Introduction

The idealized behaviour of the FPSS walls is similar to that of a core wall structure subject to torsional moments. Difficulty arose in simulating the behaviour of settlement, due to the interaction of the ring beam with the walls. Since the basic deformation of the FPSS can be clearly seen as a combination of torsional deformation and distortional warping, the behaviour of the structure is similar to that of a closed core wall subject to torsion and bending. A considerable amount of research has been published on the analysis and design of core wall structures subject to bending. Most of this work has incorporated a continuous medium approach to replace each connecting beam or slab by an equivalent medium over the whole storey height, while others employed a discrete element approach for the idealized beam element of the core and similarly for the connecting beam or slab. Since the restrained behaviour of the core walls, owing to the presence of slabs or edge beams, caused significant reduction in the warping and twist of the walls, the above analytical approach was not realistic for that of the FPSS.

The thin walled elements which are assembled to form a core wall structure are more feasible to simulate the behaviour of the FPSS. This is because the plates are flexible in the out-of-plane direction and, as stiff in their own plane as the FPSS walls, that is, the core wall structure is relatively weak in torsion due to the bimoment effect. The fundamental principle of torsion of thin walled structures is given by Vlasov (1961) and Kollbrunner and Basler (1969). The Vlasov theory of

thin walled sections has already been applied to core walls subject to torsion (Stafford-Smith and Taranath,1972 ; Mallick and Dungar,1977).

The assumptions necessary to apply the theory of thin plates subject to torsion are as follows (Vlasov,1961):

- The contour of a cross-section maintains its shape, that is, after deformation, the projection of the cross-section is simply translated and rotated as rigid body into the original shape.
- Individual points of the cross-section are allowed to warp, thus they can be displaced in the direction of the longitudinal axis, Z, refer to Figure 7.33.
- The length (s) of the middle line of the core wall section does not change due to deformation.

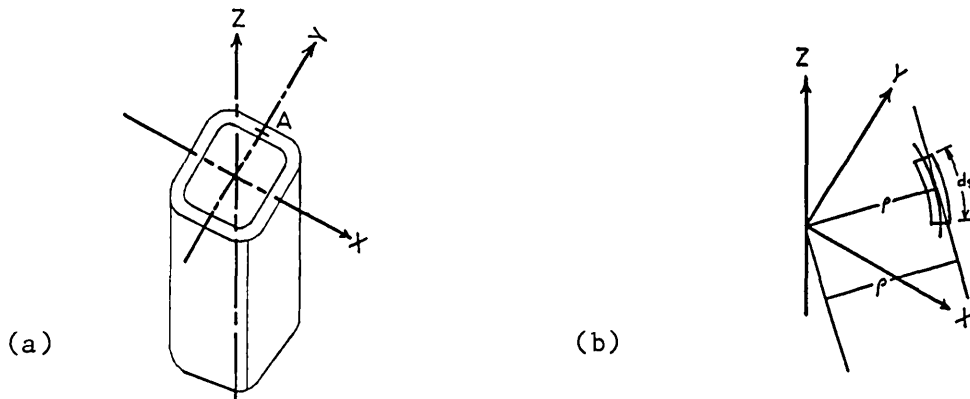


Figure 7.33 A closed section box (a), with an elemental section (b).

### 7.8.2 Non-uniform torsion and warping

To derive expressions for a closed section core wall, first it is necessary to include both the rigid body rotation twist, that is, with no distortion, and the warping displacement (Figure 7.33),

$$u_s = \lambda(z) w(s) \quad (7.24)$$

where

$\lambda(z)$  = a warping function that is dependent upon variation of the twist per unit length, i.e.  $\theta = \frac{d\Phi}{dz}$ , and

$w(s)$  = a twisting function of a section of the core walls perpendicular to their longitudinal axis, where for simple torsion,

$$u_s^* = \frac{M_z}{G \Omega^2} \int_0^s \frac{ds}{\delta} - w\Phi \quad (7.25)$$

where,  $M_z$  = external torque at the section under consideration and is

equal to  $\int q \rho ds$   
 $q$  = shear flow per unit length, and  
 $ds$  = indicates the integration along the closed middle line of the section of the core.

According to the standard theory of elasticity, Timoshenko (1956) showed that the tangential stress derived for warping and twist is related to the shearing stress (Figure 7.34),

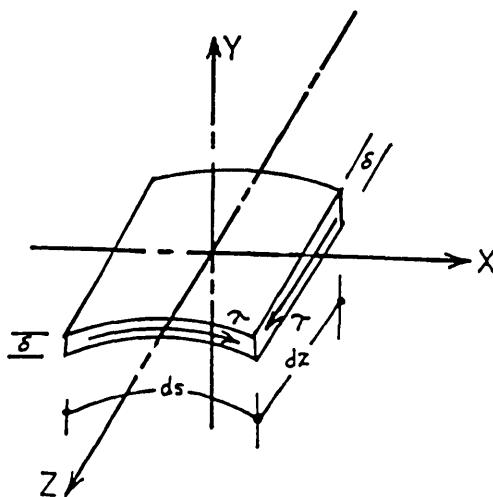


Figure 7.34 A differential element represented as a thin plate (after Mallick and Dungan, 1977).

$$\tau = G \left( \frac{\partial u}{\partial s} + \frac{\partial W}{\partial z} \right) \quad (7.26)$$

where,

$\tau$  = tangential shear stress,

$u(s)$  = displacement component of any point on the middle line of the cross section in the direction of the longitudinal axis of the structure,

$W$  = displacement component in the direction of the tangent to the middle line ( $W = \rho\theta$ ),

$\rho$  = perpendicular distance from the shear centre to the tangent at the section,

$\phi$  = angular displacement of the section,

$G$  = modulus of shear rigidity,

$\delta$  = wall thickness of the cross section,

$\Omega$  = double area enclosed by the middle line of the section,  $\int \rho ds$

$\theta$  = angle of rotation of the core wall per unit length along its longitudinal axis, that is,  $\theta = \frac{d\phi}{ds}$ .

$ds$

From basic elasticity (Timoshenko,1956),  $\Theta$  can be written as,

$$\Theta = \frac{M_z}{G \Omega^2} \int \frac{ds}{\delta} \quad (7.27)$$

Differentiating equation(7.24) and substituting in equation(7.26),

$$\tau = G \left( \rho \Theta - \lambda \left( \rho - \frac{\Omega}{\delta \oint \frac{ds}{\delta}} \right) \right) \quad (7.28)$$

This produces a torque moment (Vlasov,1961) of,

$$\begin{aligned} M_z &= \oint \tau \delta ds \\ &= G \left( \Theta \oint \rho^2 dA + \lambda \left( \oint \rho^2 dA - \frac{\Omega^2}{\oint \frac{ds}{\delta}} \right) \right) \end{aligned}$$

or

$$M_z = I_p G (\Theta + \lambda \mu_w) \quad (7.29)$$

where,  $I_p$  = tangential second moment of area,  $\oint \rho^2 dA$ ,

$I_s$  = St. Venant torsional stiffness factor,  $\frac{\Omega^2}{\oint \frac{ds}{\delta}}$ , and

$\mu_w = 1 - \frac{I_s}{I_p}$ , that is, coefficient of warping.

To derive the normal stresses induced due to warping, one considers the equilibrium of shear and normal forces at any section of the wall,

$$\frac{\partial(\delta \sigma_z)}{\partial z} + \frac{\partial q}{\partial s} = 0 \quad (7.30)$$

Using equation(7.30), Mallick and Dugar (1977) formulated the differential equation for a closed section,

$$\frac{d^4 \phi}{dz^4} - a^2 \frac{d^4 \phi}{dz^4} = \frac{m_z}{E_1 I_w} - \frac{m_z}{G I_s} \quad (7.31)$$

where,  $a = \sqrt{\frac{\mu_w G I_s}{E_1 I_w}}$

$$E_1 = \frac{E}{(1-\nu^2)}$$

$I_w$  = principle sectorial moment of inertia of the cross section, that is,  $\oint w^2 dA$ , and

$$m_z = \frac{-dM_z}{dz}$$

For an open section,  $\mu_w = 1$  (Timoshenko, 1956) whereas for a closed section the value of  $\mu_w$  is less than 1. For loads applied at the end points only (Figure 7.35), equation (7.31) can be written as,

$$\frac{d^4\phi}{dz^4} - a^2 \frac{d^2\phi}{dz^2} = 0 \quad (7.32)$$

Additionally, the longitudinal direct stresses in the section of the core combined with the warping or twist of thin walled members gives rise to a generalized bimoment  $B_z$ , where

$$B_z = - \frac{E}{(1-\nu^2)} \frac{I_w}{\mu_w} \frac{d^2\phi}{dz^2}$$

and the longitudinal direct stress associated with the warping or twist of the member is given by:

$$\sigma(z, s) = \frac{B_z \bar{w}(s)}{I_w}$$

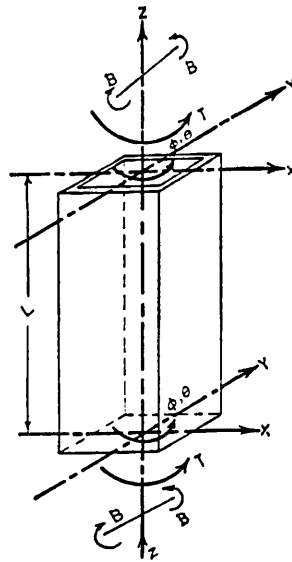


Figure 7.35 A closed section beam element subjected to two degrees of freedom at each node (after Mallick and Dungan, 1977).

### 7.8.3 Stiffness matrix of a thin walled beam element subjected to non-uniform torsion

The solution of the differential equation (7.32) was assumed to be of the form where the thin walled closed section element is subjected

to two degrees of freedom at its two ends (Mallick and Dungar,1977), refer to Figure 7.35,

$$\phi = C_1 + C_2z + C_3\sinh(az) + C_4\cosh(az) \quad (7.33)$$

where  $C_1 - C_4 =$  constants of integration determined by the boundary conditions at the two end nodes of the core element.

The boundary conditions are considered at each node and are given as,

$$\begin{aligned} \text{At } z = 0, \quad \phi_z &= \phi_1 \quad \Theta_z = \Theta_1 \\ B_z &= B_1 \quad M_z = M_1 = T_1 \\ \text{At } z = L, \quad \phi_z &= \phi_2 \quad \Theta_z = \Theta_2 \\ B_z &= B_2 \quad M_z = M_2 = T_2 \end{aligned}$$

where  $T_1, T_2$  are applied torque at end nodes 1 and 2 of a core element, and  $B_1, B_2$  are the applied bimoments.

The resultant stiffness matrix for thin walled closed section beam element is of the following form,

$$Q = \frac{G I_s}{(2 - 2\cosh aL + aL\sinh aL)}$$

$$\begin{bmatrix} T_1 \\ B_1 \\ T_2 \\ B_2 \end{bmatrix} = Q \begin{bmatrix} \text{asinh}aL & & & \text{Symmetric} \\ (1-\cosh aL) & L\cosh aL - \frac{\sinh aL}{a} & & \\ & & a & \\ -\text{asinh}aL & -(1-\cosh aL) & \text{asinh}aL & \\ (1-\cosh aL) & \frac{\sinh aL}{a} - L & -(1-\cosh aL) & L\cosh aL - \frac{\sinh aL}{a} \end{bmatrix} \begin{bmatrix} \phi_1 \\ \Theta_1 \\ \phi_2 \\ \Theta_2 \end{bmatrix} \quad (7.34)$$

and the stress and vertical displacement at any point  $(s,z)$  is given as

$$\sigma(s,z) = \frac{B_z}{I_w} \bar{w}(s) \quad (7.35)$$

$$u(s,z) = \bar{w}(s) \left( \frac{-\Theta(z)}{\mu_w} + \frac{M_z}{\mu_w G I_p} \right) \quad (7.36)$$

#### 7.8.4 Theoretical investigation of the deformation response of the FPSS

Considering the FPSS model as used in the test programme (refer to Chapter 6), the section and characteristic properties are given in Appendix 4. The applied loading can be represented as illustrated in Figure 7.36. Using the principle of superposition, the applied load is subdivided into three load cases. A symmetric case(1), that can be



resolved into a bimoment applied at the bottom of the box structure (Figure 7.36(b)), and a skew symmetric case(2) that can be resolved further into two cases. These are a diagonal bimoment and a diagonal torsion applied along a diagonal passing through the settling support, refer to Figures 7.36(c), 7.36(d). The settlement at one corner causes primary bending along the middle of the box structure, Figure 7.36(b).

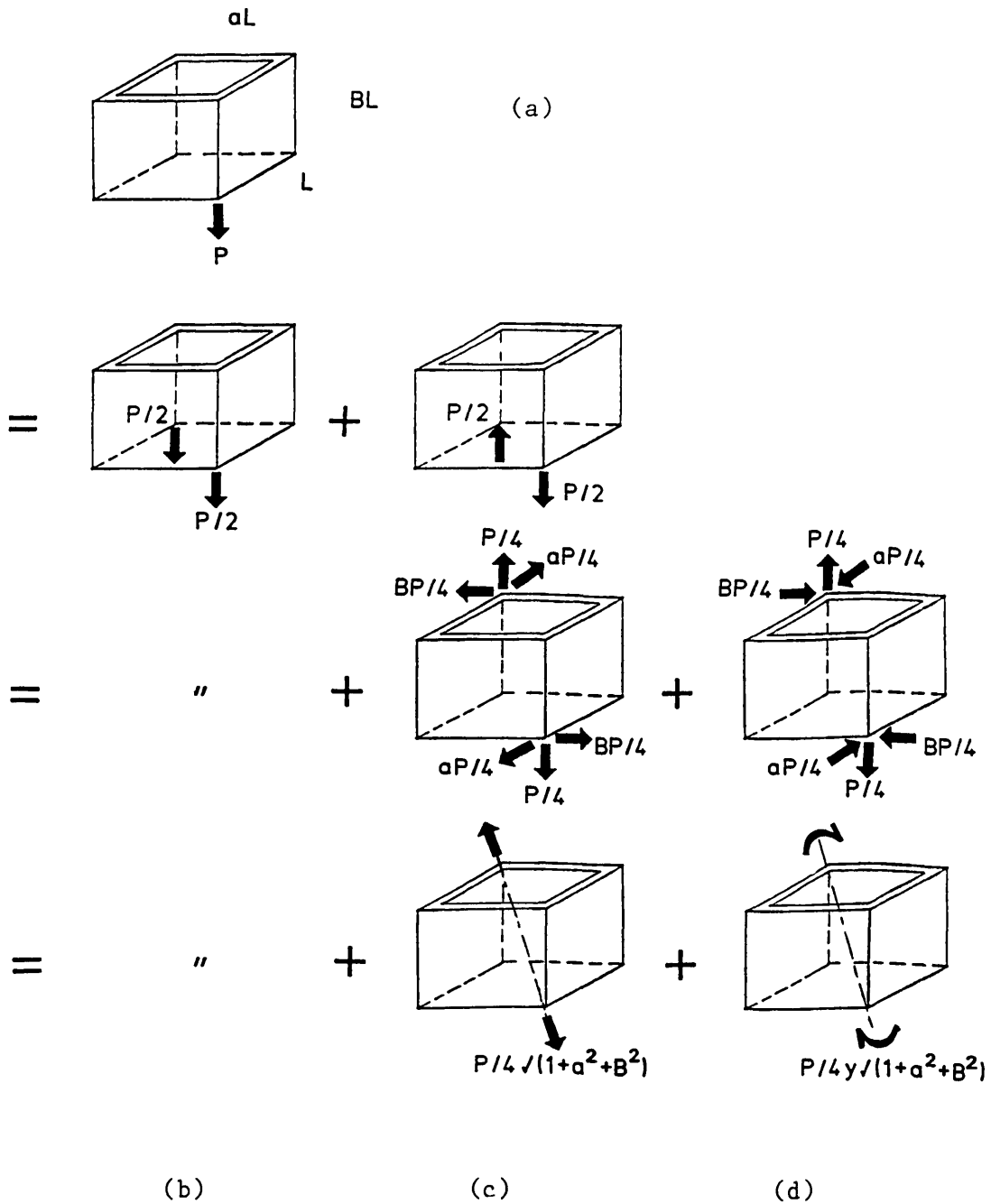


Figure 7.36 Representation of a system of body forces simulating settlement of the FPSS.

Pure distortional warping of the box acting through two opposite corners of the FPSS, that is the settling support and the top corner of the wall is illustrated in Figure 7.36(c), and also torsional rotation is acting along the same diagonal in Figure 7.36(d). The resultant forces and moments due to the three cases of loading are shown in Table(7.2).

Table(7.2) Resultant forces and moments for loading cases(1,2,3).

Design parameters	Case(1)	Case(2)	Case(3)
At z=0, Bimoment, $B_z = B_1$	$\frac{P\sqrt{L^2 + B^2}}{4}$	$\frac{P\sqrt{1 + a^2 + b^2}}{4} x$	0
Torsion, $T_z = T_1$	0	0	$-\frac{P\sqrt{1 + a^2 + b^2}}{4} y$
At z=H, Bimoment, $B_z = B_2$	0	$-\frac{P\sqrt{1 + a^2 + b^2}}{4} x$	0
Torsion, $T_z = T_2$	0	0	$-\frac{P\sqrt{1 + a^2 + b^2}}{4} y$

where,  $a = B/L$ , ratio of short to longer spans of the box structure,  
 $b = H/L$ , ratio of the height of the box to the longer span,  
 $x =$  perpendicular distance between the line of action of the distortional warping resultant and the opposite corner of the FPSS (refer to Figure 7.36(c)),

i.e.  $x = H \sin(\tan^{-1} \frac{L^2 + B^2}{H})$

$y =$  perpendicular distance between the lines of action of the resultant torsional forces (refer to Figure 7.36(d)),

$$= \frac{\sqrt{L^2 + B^2 + H^2}}{2}$$

i.e.  $y = L\sqrt{1 + a^2 + b^2}$

Substituting the design parameters in equations(7.34,7.35), and solving for  $\phi$ ,  $\theta$ , the translational rotation and stresses at any point (s,z) can be calculated. Appendix 4 describes the method of calculation adopted in the theoretical model for reinforced and unreinforced masonry walls.

Despite the advances in computer aided analysis of structures subject to settlement based upon the finite element methods, the analysis used here failed to give a full understanding of the 3-dimensional behaviour of the structure. As a result, approximation of the structure to a 2-dimensional problem is necessary. This would incorporate more simplifying assumptions and as a consequence, the results would be less accurate. Simple numerical techniques, referred to in Sections 7.6 and 7.8, are easy to apply and seem to be more satisfactory in approaching the solution of the problem of design of the FPSS subject to differential movement of its supports. Comparison of these techniques are discussed more widely in Chapter 9.

## CHAPTER 8 EXPERIMENTAL OBSERVATIONS AND TEST RESULTS

### 8.1 INTRODUCTION

The experiments were designed to examine whether the FPSS exhibits flexibility on settlement, resulting in less visible damage for a given displacement. A thorough inspection of all the test models, before, during and after testing was undertaken to monitor the regular change of internal strains and forces within the wall, in order to define the deformation mode. In this chapter, support load during settlement, steel strains in the ring beam, relative deflection, tilt and strain of the walls are looked at separately for each model. Different deformation patterns in the wall-beam structure are described with reference to the degree of settlement encountered. The tests are also described with respect to their support condition and aspect ratio of the walls (L/H), namely, tests W1, W2 and W3 for the former case, and tests W4 and W5 for the case with lower aspect ratio. A method designed especially to protect walls with low aspect ratio against brittle vertical cracking was employed. This consisted of light reinforcement bedded in the mortar below the top five courses of brickwork. The cracking was reduced considerably, thus increasing the capacity of the structure to accommodate more settlement (refer to test W5). In this chapter, only a part of the results are presented. The rest of the results are given in Appendix 6, which will be referred to from time to time.

### 8.2 DISTRIBUTION OF STRAIN IN THE RING BEAM STEEL

The strain distribution in the longitudinal steel of the ring beam, shown in Figures 8.1-8.10, clearly indicates that the critical section is that nearest to the fixed support (location 1 or 7). Comparison of strain at various positions along the beam, shown in Table 8.1, illustrates the effects of support condition and type of short column-beam joint on the magnitude of strain induced in the steel during settlement. As expected, the reinforcement experienced lower strains for all FPSS models with point supports than those having fixed supports. The maximum strain of all tests recorded for the

reinforcement was 2343 microstrain in tension for test W2AB with fixed support, (Figure 8.3). However, for point supports, the maximum strain was 641 microstrain at the supporting end (Figure 8.5). Since hogging was the prime mode of deformation, the general distribution of strain along the beam was that of tension, increasing more at the supporting end, then slightly less at the middle and least at the settling end (refer to Table 8.1).

Cyclic settlement of the FPSS had little influence on the magnitude of the residual steel strains recorded. Residual strains in the range of 1355 microstrain were measured in test W1AA after reinstatement of the structure, however, this value was found to depend upon the type of support and the aspect ratio of the wall (L/H) (tests W4 and W5). For lower aspect ratios, 200-250 microstrain were still present on re-jacking the support (Table 8.1). Point supports induced less residual strains than fixed supports, that is, due to the increased rotational capacity of the beam which caused a decrease in local deformation of the reinforcement. Cracks propagated through the concrete beam forming a hinge as rotation were being restrained by the fixed support, thus inducing a permanent strain in the steel reinforcement.

Table 8.1 Summary of steel reinforcement strains.

Test No.	Column joint *	Support condition	Maximum relative deflection ratio ( $\Delta/L$ )	Max. steel strain ** in tension at positions		
				A	B	C
W1AA	Type 1	FIXED	1/63	1857	128	161
W1AB	Type 1		1/51	253	64	631
W1BA	Type 2	FIXED	1/52	726	406	47
W1BB	Type 2		1/42	273	103	32
W2AA	Type 1	FIXED	1/78	1338	214	123
W2AB	Type 1		1/63	2343	102	122
W2BA	Type 2	FIXED	1/76	734	78	62
W2BB	Type 2		1/61	998	374	171

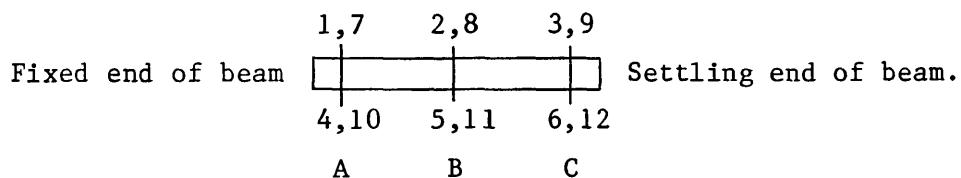
Table(8.1) Continued.

Test No.	Column joint*	Support condition	Maximum relative deflection ratio ( $\Delta/L$ )	Max. steel strain** in tension at positions		
				A	B	C
W3AA	Type 1	POINT	1/74	181	328	78
W3AB	Type 1		1/60	641	47	78
W3BA	Type 2	POINT	1/80	282	227	281
W3BB	Type 2		1/65	78	203	609
W4AA	Type 1	POINT	1/216	141	19	25
W4AB	Type 1		1/175	478	26	15
W4BA	Type 2	POINT	1/113	118	175	106
W4BB	Type 2		1/91	193	37	34
W5AA	Type 1	POINT	1/102	126	181	206
W5AB	Type 1		1/83	118	76	312
W5BA	Type 2	POINT	1/70	92	187	343
W5BB	Type 2		1/60	2126 <sup>o</sup>	125	2340 <sup>o</sup>

Notes:

- \* - Type 1 is a typical, commonly used joint; refer to Table(6.12).
- Type 2 is a concrete hinge, designed to carry half the moment capacity of Type 1.

\*\* - Locations of steel strains with respect to beam is as shown,



<sup>o</sup> - Strain gauges are considered broken, giving erratic readings.

Table 8.1 compares measured strains at different locations in the beam with respect to the type of support, that is, point or fixed, and the beam column joint (that is, Type 1 or Type 2 defined in the footnote of Table(8.1)). For FPSS models with point supports and Type 2

joints, an average value of 252 microstrain was recorded at the critical section, while for Type 1 joints, 641 microstrain was measured at a similar magnitude of settlement.

The effect of the weak joint is to attract cracking that facilitates increased rotation without inducing further strain on the steel in the concrete beam. In addition, rotation of the point supports caused less induced strain in the reinforcement on settlement (Figure 8.6). This is due to dissipation of part of the deformation on the angular rotation of the FPSS. As a result, it was observed that this minimized the cracks in the beam, and also reduced fatigue or crack opening upon cyclic re-jacking of the structure. This caused some gauge wires to break during testing due to excessive deformation and crack propagation in the beam (Figures 8.7 & 8.10).

Strains recorded in the bottom bars were, in general, lower than those of the top bars, except for tests W3, W4 and W5, where maximum strain registered in the bottom bars was 641 microstrain and for top bars was 265 microstrain. As cracks propagated towards the bottom of the beam at the supporting end, the strain in the bottom bar increased considerably. However, strain recorded in the top bar in test W5BB reached a value of 2340 microstrain and high residual strain was present, even after reinstatement. In some cases, the load dropped but no decrease of strain was noticed (Figure 8.10).

Strains at mid-span of the beam appeared to be approximately independent of the range of L/H values investigated, where maximum strain of 406 microstrain was recorded in test W1BA. There was a tendency for strains at mid-span to increase if strains at locations 1 and 4 or 7 and 10 (that is, at the fixed support) increased and, likewise, to decrease if the strains at these critical positions were low.

Although lower strains were measured upon the introduction of point supports (Table 8.1), there was not enough evidence to deduce quantitatively the influence of support condition and types of beam-column joints on the variation of strain in the steel reinforcement.

## **8.3 DEFLECTIONS**

### **8.3.1 Wall-beam structure**

The relationships of the load versus the deflection of FPSS models undergoing settlement are illustrated in Figures 8.11-8.20.

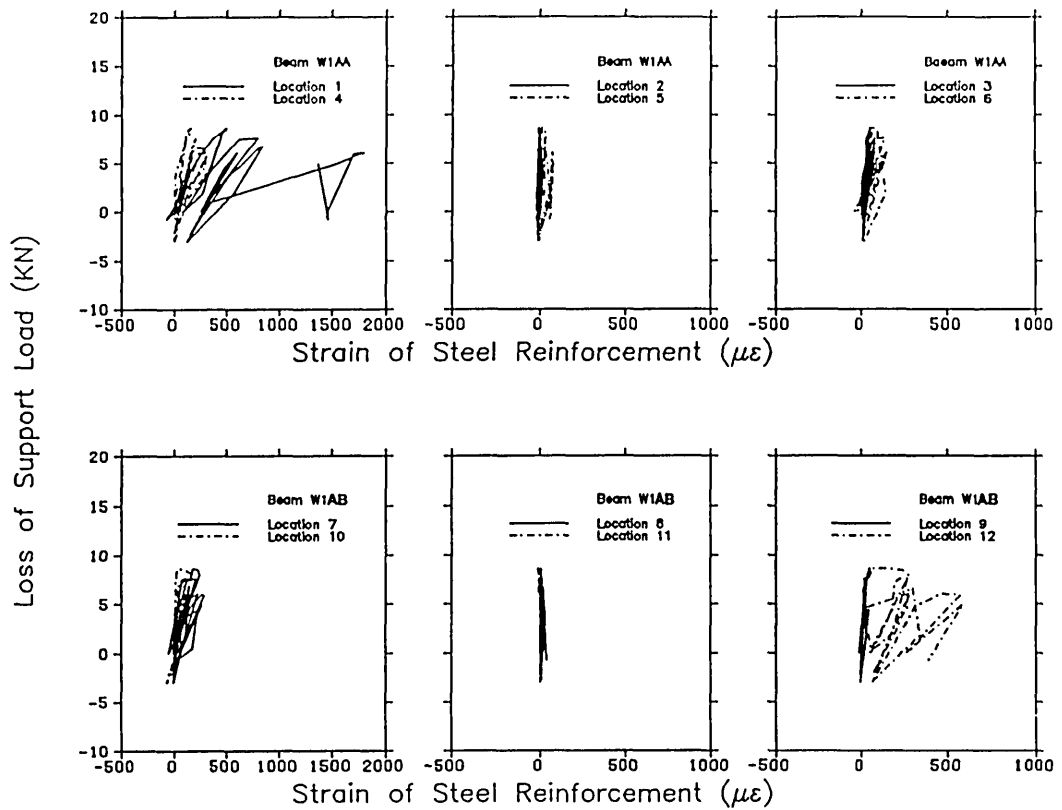


Figure 8.1 Effect of cyclic settlement on steel strain of ring beam (Test W1A).

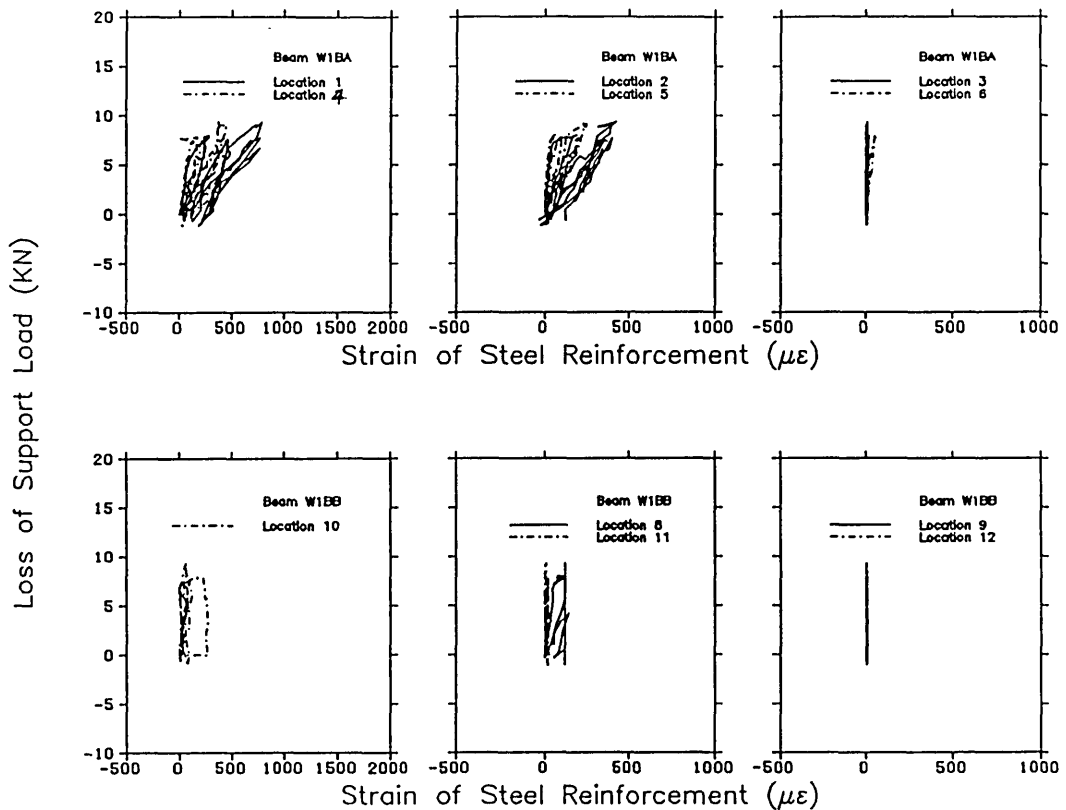


Figure 8.2 Effect of cyclic settlement on steel strain of ring beam (Test W1B).



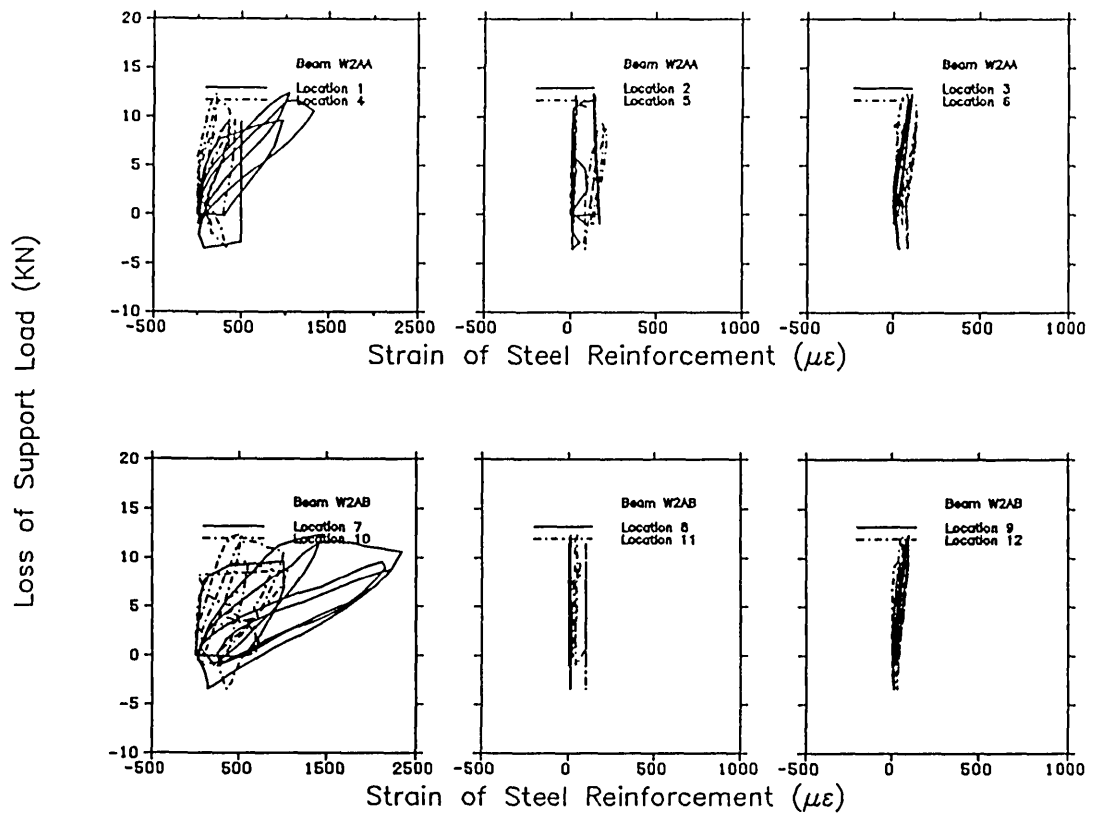


Figure 8.3 Effect of cyclic settlement on steel strain of ring beam (Test W2A).

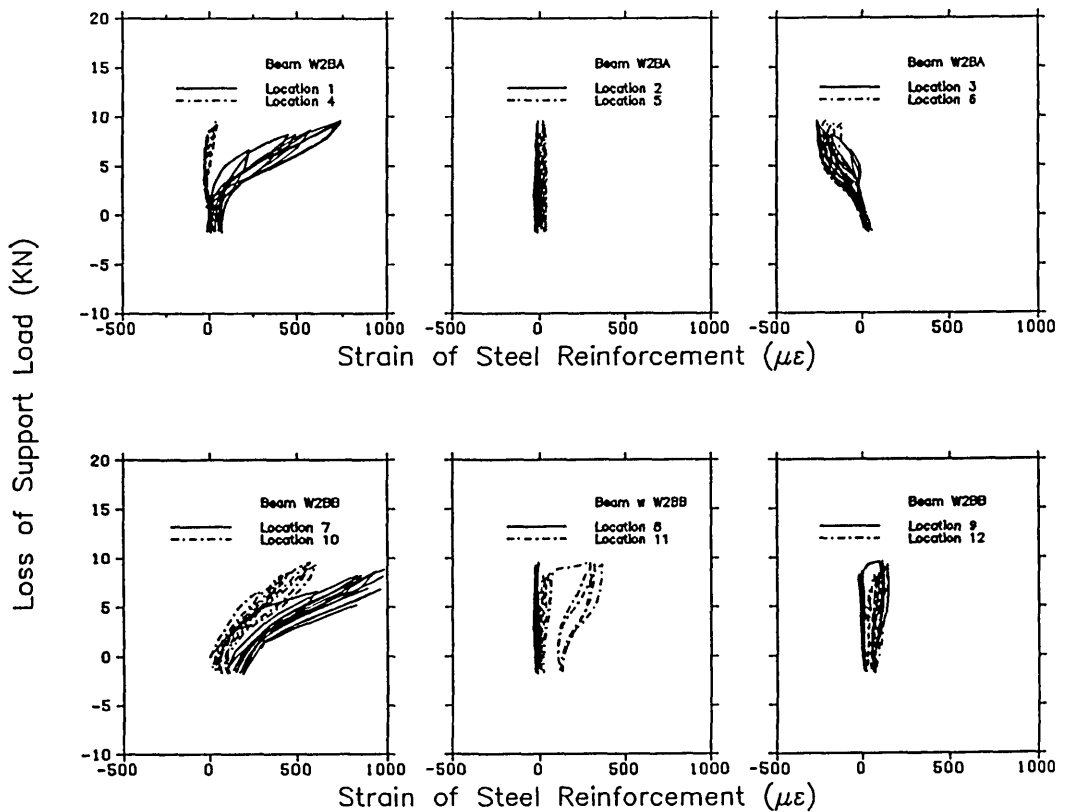


Figure 8.4 Effect of cyclic settlement on steel strain of ring beam (Test W2B).

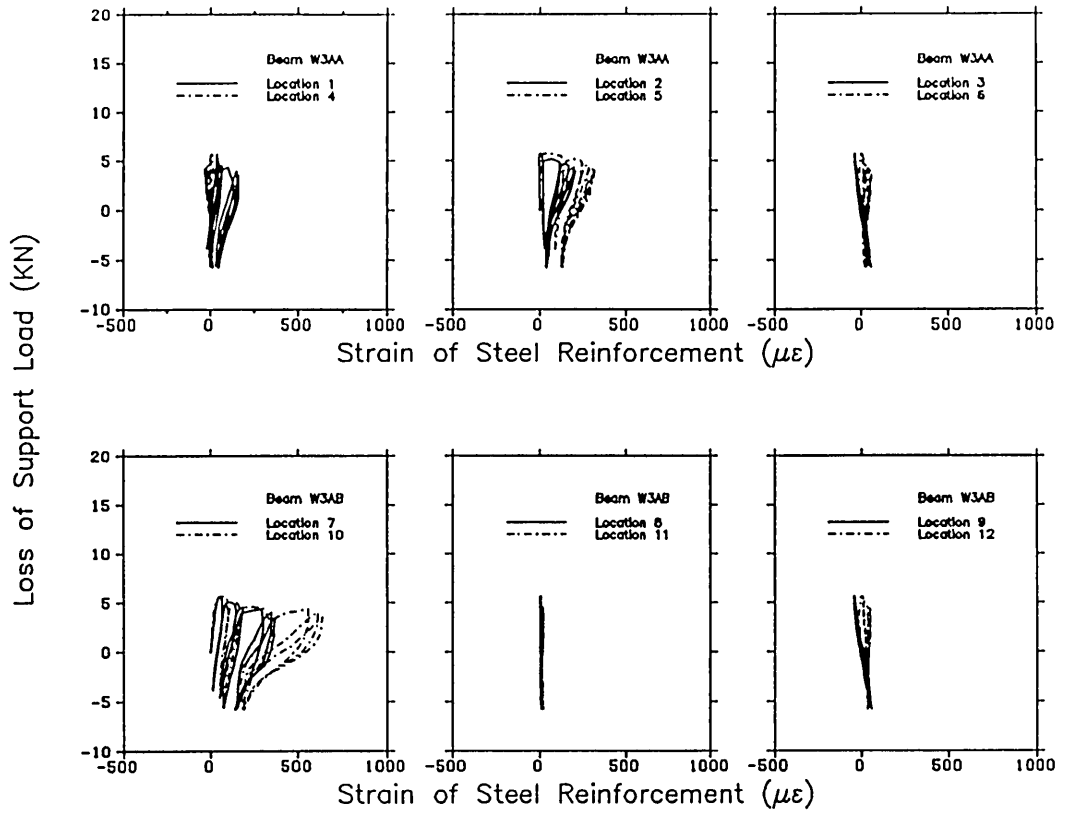


Figure 8.5 Effect of cyclic settlement on steel strain of ring beam (Test W3A).

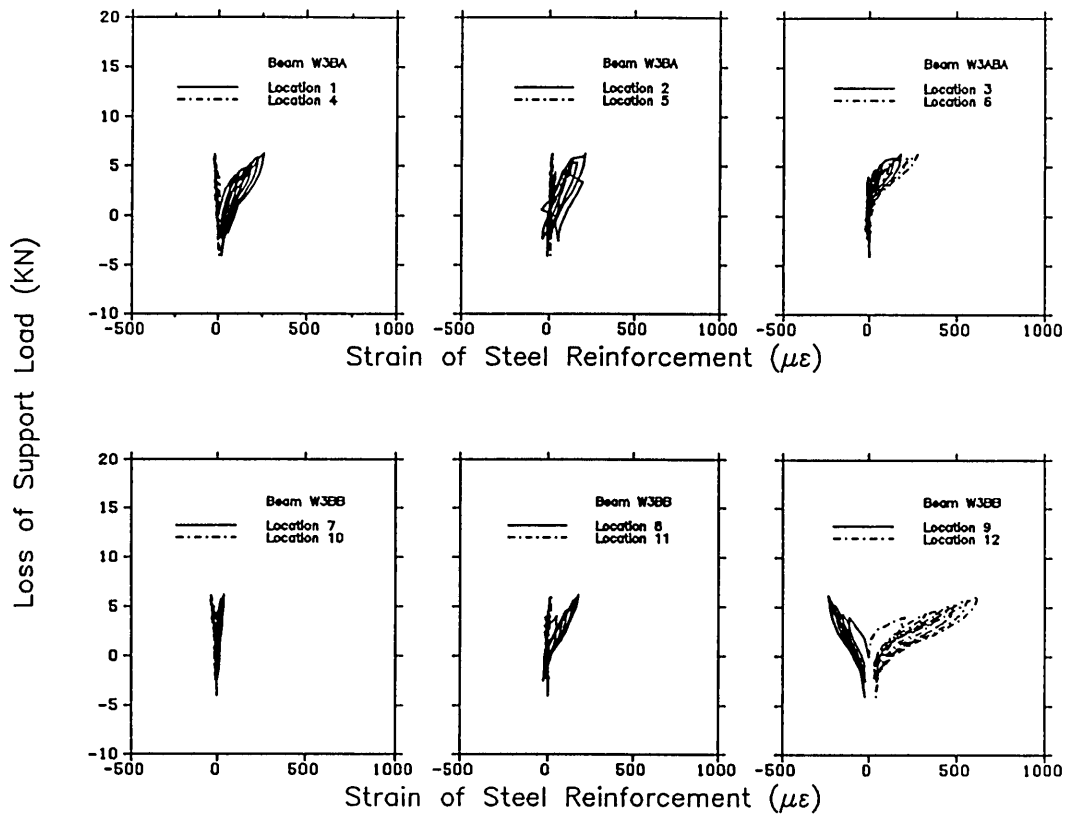


Figure 8.6 Effect of cyclic settlement on steel strain of ring beam (Test W3B).

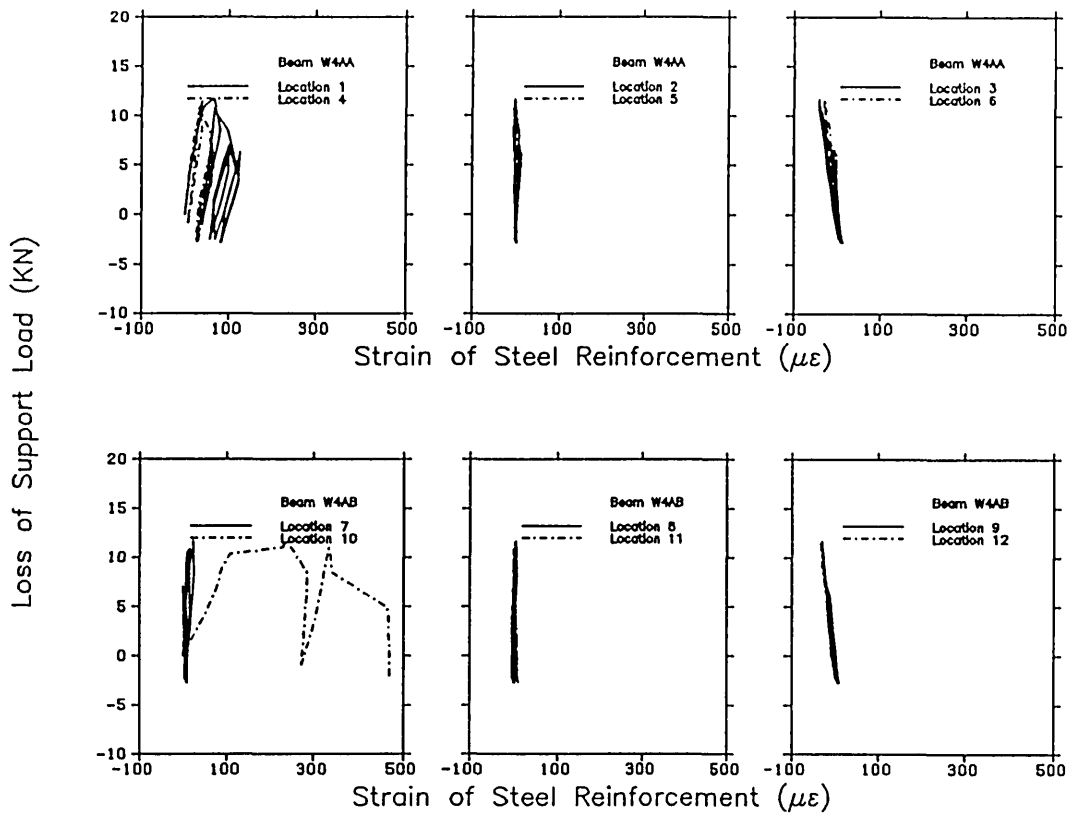


Figure 8.7 Effect of cyclic settlement on steel strain of ring beam (Test W4A).

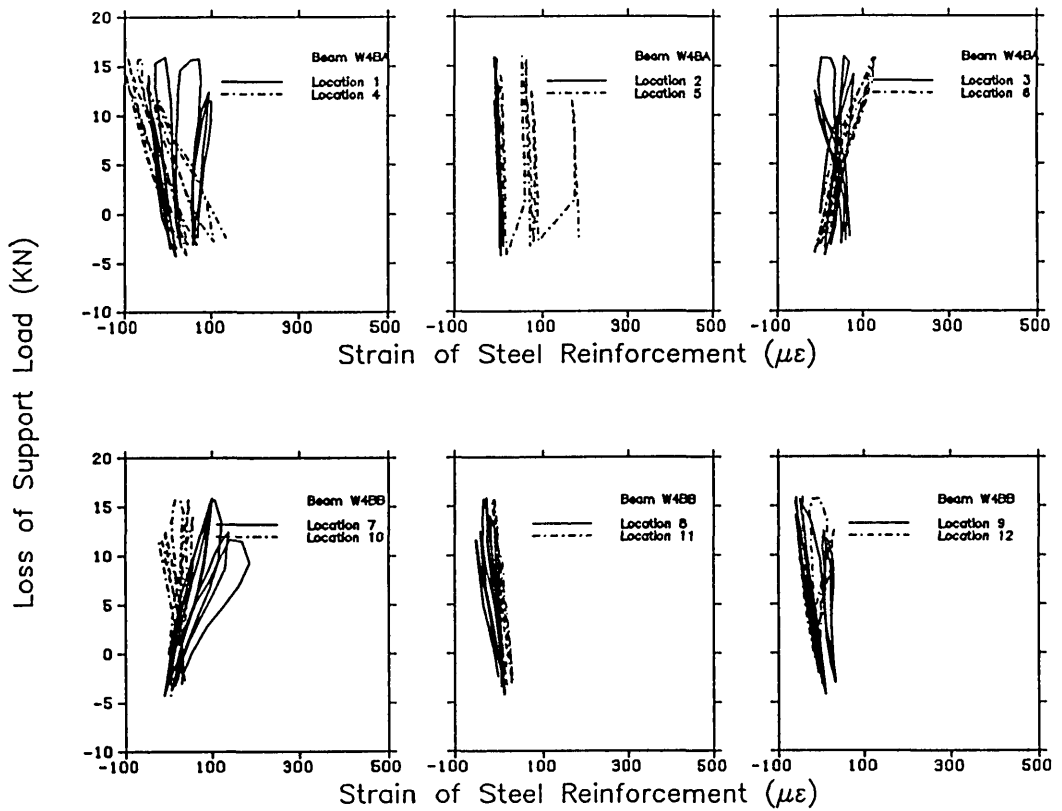


Figure 8.8 Effect of cyclic settlement on steel strain of ring beam (Test W4B).

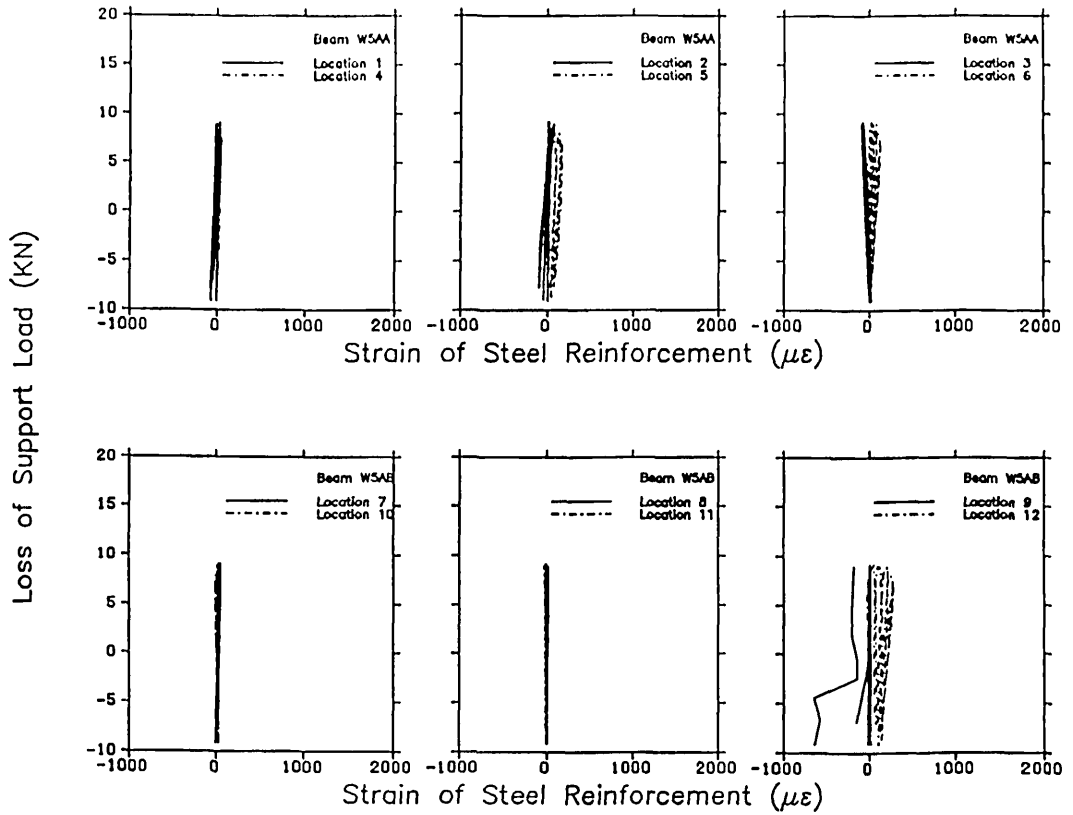


Figure 8.9 Effect of cyclic settlement on steel strain of ring beam (Test W5A).

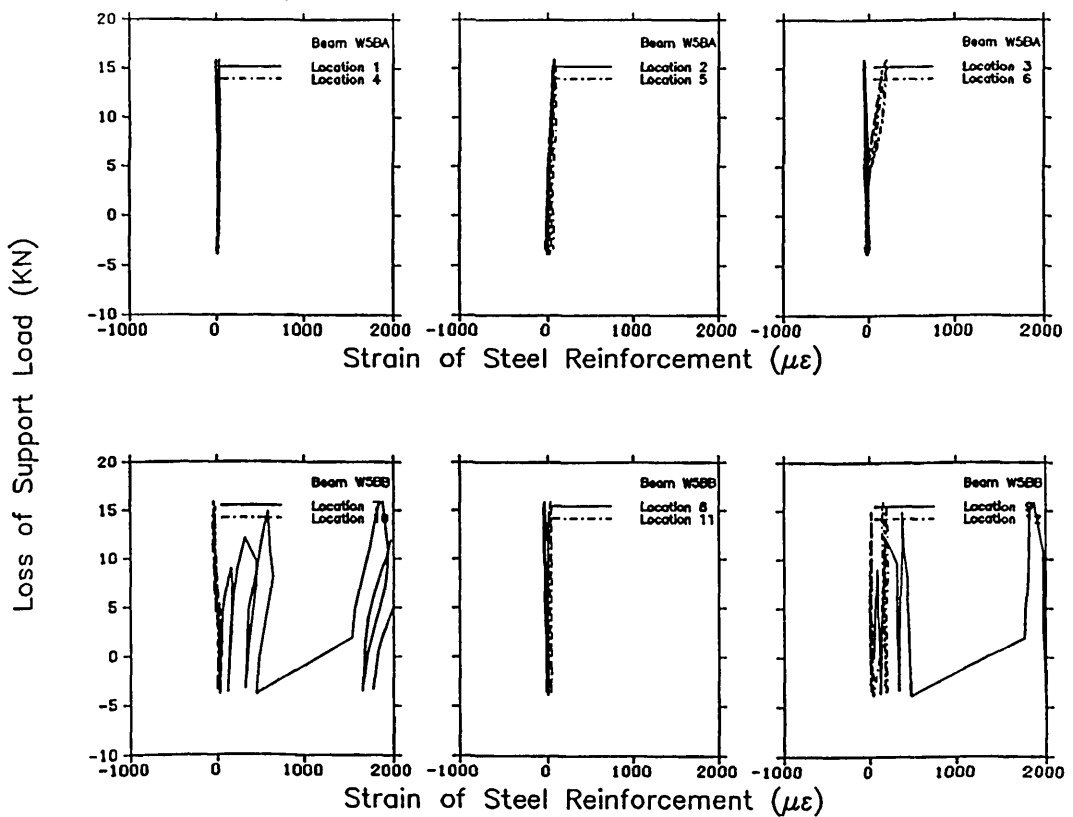


Figure 8.10 Effect of cyclic settlement on steel strain of ring beam (Test W5B).

These are given for three main locations at the settling corners of the FPSS, namely, top, middle and soffit of the brickwork wall. Maximum relative deflection,  $\Delta/L$ , in the range of  $1/42$ - $1/52$  was recorded before the FPSS experienced visible damage. In comparing the load-deflection relationships, higher deflection is noted at the top of the brickwork wall than at the soffit. An increase of deflection is due to the out-of-plane tilting of the walls during settlement; this results in larger values at the top of the wall, diminishing to zero at the bottom. However, these variations of deflection between the three locations only occurred at the maximum differential settlement, while all of them coincided on approaching zero differential settlement.

Cyclic settlement and re-jacking of the FPSS was performed at an increasing magnitude of deflection until visible cracks emanated. In addition, the recoverability of the FPSS system after reinstatement of the structure, by re-jacking to its original position, was shown to reach the position of zero differential settlement without structural hindrance or jamming. This was accompanied by significant structural stiffness degradation at each cycle, that is, an increase of deflection per unit support load. On cycling of the settled support, it is clear that the magnitude of reduction of support load does not exceed a certain limiting value, that is, dependent upon the capacity of the structural stiffness of the FPSS to sustain such reduction of support load without further deformation.

A maximum relative deflection of  $1/42$  was recorded for walls of aspect ratio,  $L/H = 2.0$  in test W1B, but reduced to  $1/91$  with a decrease in the aspect ratio to  $1.0$  in test W4B. For walls of aspect ratio  $1.0$  and  $1.25$ , maximum relative deflection in the range of  $1/91$ - $1/113$  was reached before the test was stopped due to propagation of large visible cracks (refer to test W4A and W4B). However, reinforcement placed below the top five courses increased the allowable deflection ratio to  $1/60$ - $1/90$  before a crack width of  $2$ - $2.5$  mm developed.

Different behaviour of FPSS models during testing was observed between the point supported walls and the fixed supported ones, (Figures 8.11-8.20). Walls exhibited less restraint when point supported, and demonstrated an increase in the relative deflection ratio within the limits of visible damage, that is,  $w = 2$ - $3$  mm. Fixed supported walls possessed a stiffer response. Thus, for test W2, a large drop of supporting load of  $12.5$  KN was required before a maximum settlement of  $20$ - $25$  mm was attained. However, for point supported

walls, 30 mm settlement was recorded, which corresponded to a 5.0 KN drop of support load. Additionally, the damage and crack width of point supported walls were lower in comparison to fixed supports (refer to Figures 8.11-8.20). For test W3, an average deflection ratio of 1/74 corresponded to a crack width of 2-3 mm, while for the same order of deflection, a crack width of 8-10 mm was noted for test W2.

A typical load-deflection relationship for fixed supports consisted initially of a small linear elastic portion followed by a larger curvilinear relation as cracks initiated (refer to Figures 8.11-8.13). Introducing a point support increased the length of the initial linear portion, with a definite point at which the curvilinear portion of the relation was initiated (Figures 8.15-8.18). This could be explained by the increased initial deflection of the FPSS during the early stages of settlement, owing to the rotation of the point supports. Also, introduction of weak column joints caused further reduction in the stiffness of the wall-beam structure, even at the initial stage, thus the curvilinear path is seen to dominate the relationship (Figures 8.14 & 8.16).

Although measurement during cycling was closely monitored, some LVDTs did not record consistently, either due to the rough surface of the wall which may have caused jamming, or due to placing some of the LVDTs horizontally that led to the recording of unstable readings. Due to the small number of gauges per model, lateral deflections were monitored in tests W1AA-W1BB instead of inplane deflections, which were measured for tests W2AA-W5BB. This enabled some study of both lateral and inplane deflections of the FPSS models.

### 8.3.2 Core wall deflection

To monitor the change of wall profile due to relative settlement of the corner, vertical deflections measured at three horizontal sections, namely, top, middle and bottom of wall for tests W1B-W5B, are shown in Figures 8.21-8.25 & A6.1-A6.3. At each cycle of settlement and re-jacking of the structure, the deflection recorded at every horizontal line was taken at three positions; namely, the two edges and mid-span of the wall. It is clear that the pattern of the wall profile at the top of the wall is more convex than the profile at the soffit, where it is more concave (Figure 8.21). Additionally, the part of the wall profile with greater hogging is seen to occur at the settling corner. Although for walls W1A-W3B, the maximum deflection occurred at the top of the

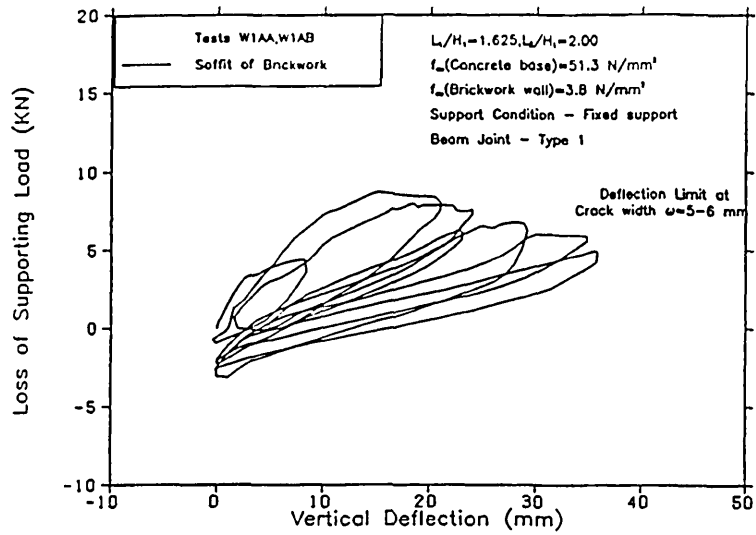


Figure 8.11 Relation between reduction in support load and corner deflection (Test W1A).

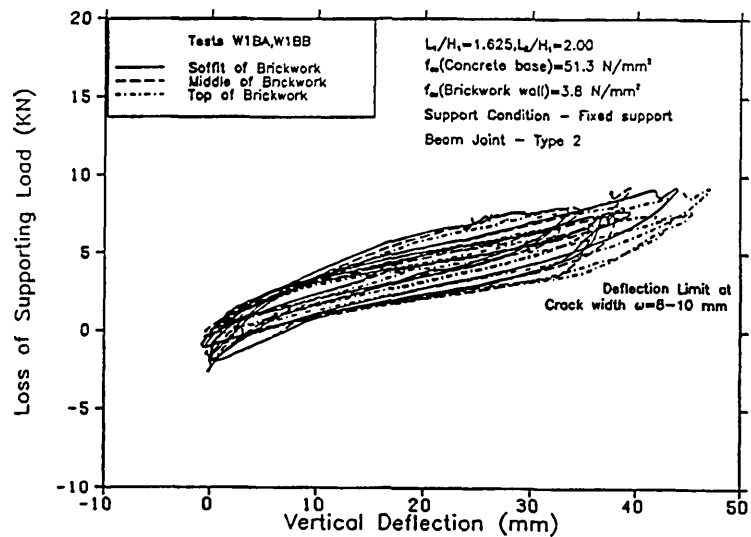


Figure 8.12 Relation between reduction in support load and corner deflection (Test W1B).

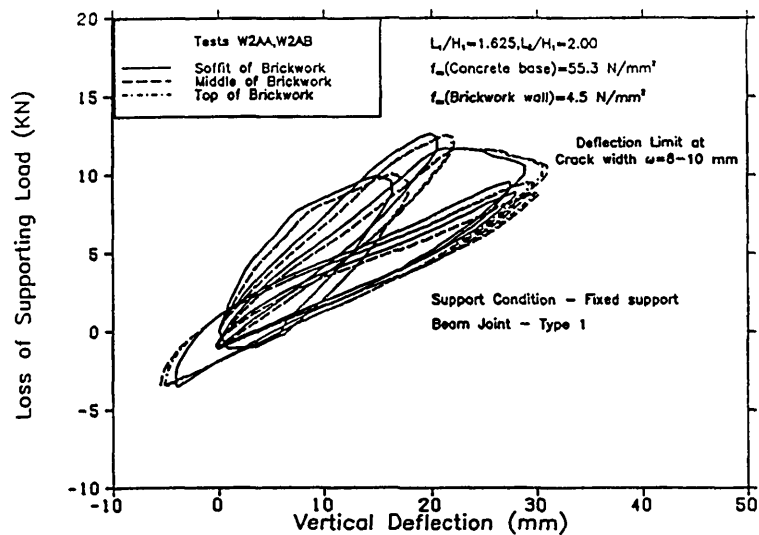


Figure 8.13 Relation between reduction in support load and corner deflection (Test W2A).

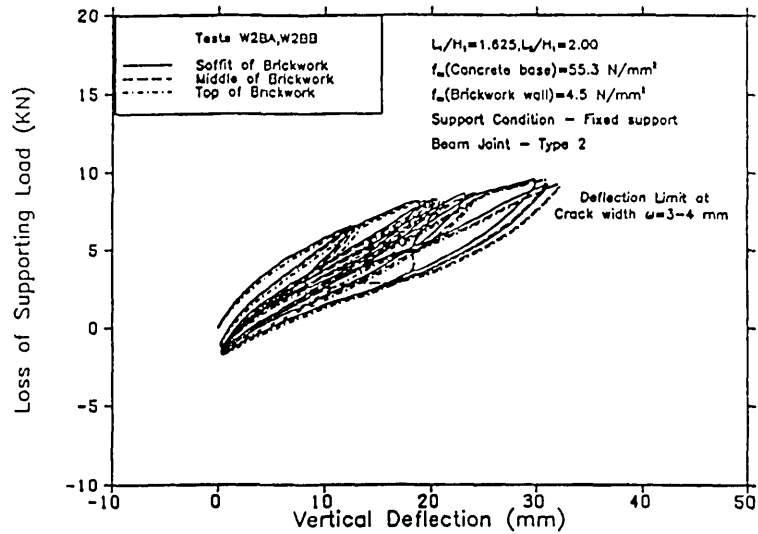


Figure 8.14 Relation between reduction in support load and corner deflection (Test W2B).

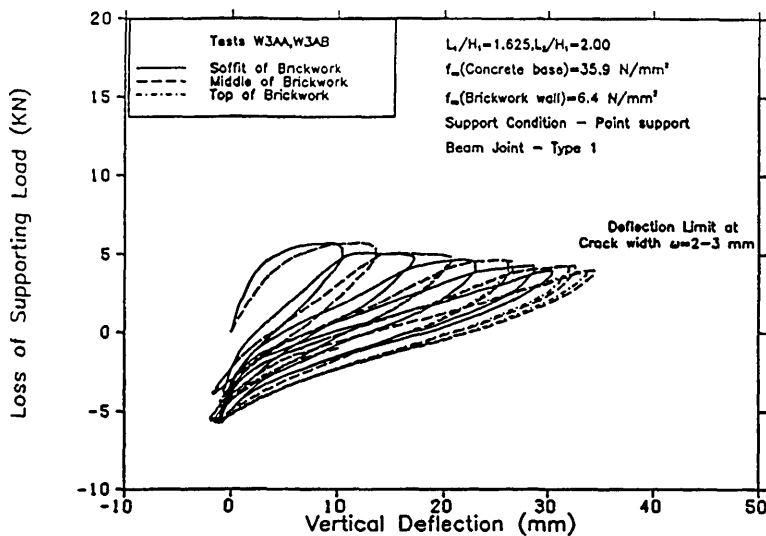


Figure 8.15 Relation between reduction in support load and corner deflection (Test W3A).

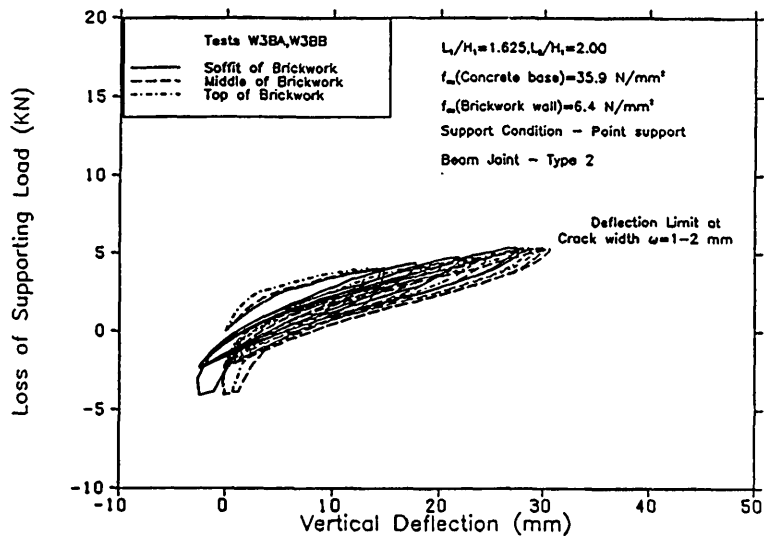


Figure 8.16 Relation between reduction in support load and corner deflection (Test W3B).



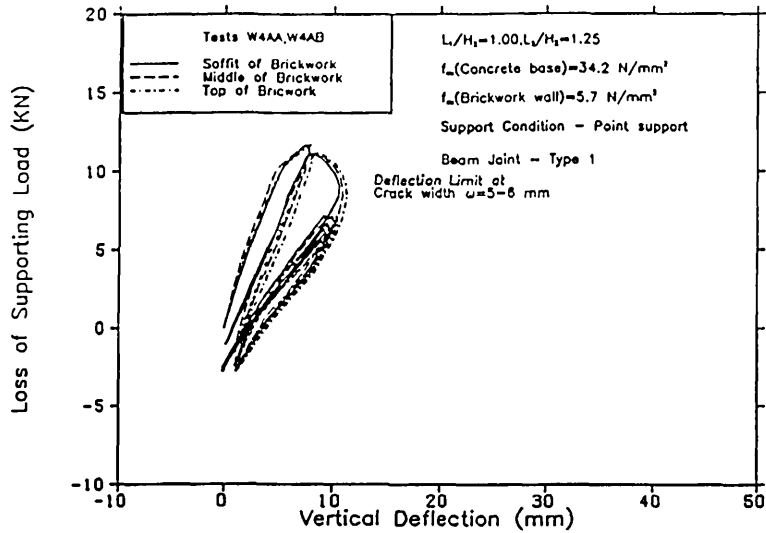


Figure 8.17 Relation between reduction in support load and corner deflection (Test W4A).

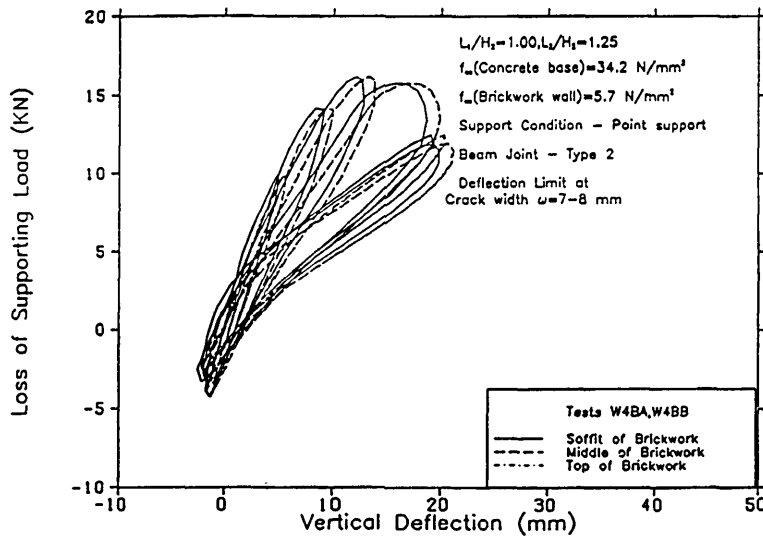


Figure 8.18 Relation between reduction in support load and corner deflection (Test W4B).

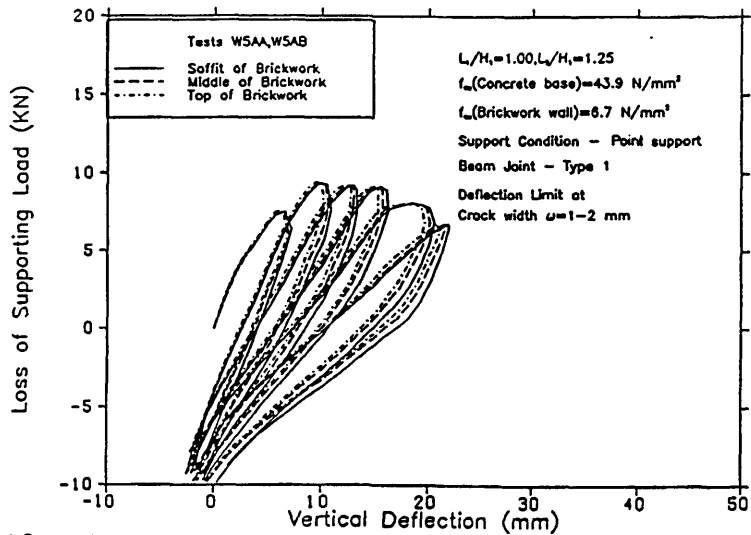


Figure 8.19 Relation between reduction in support load and corner deflection (Test W5A).

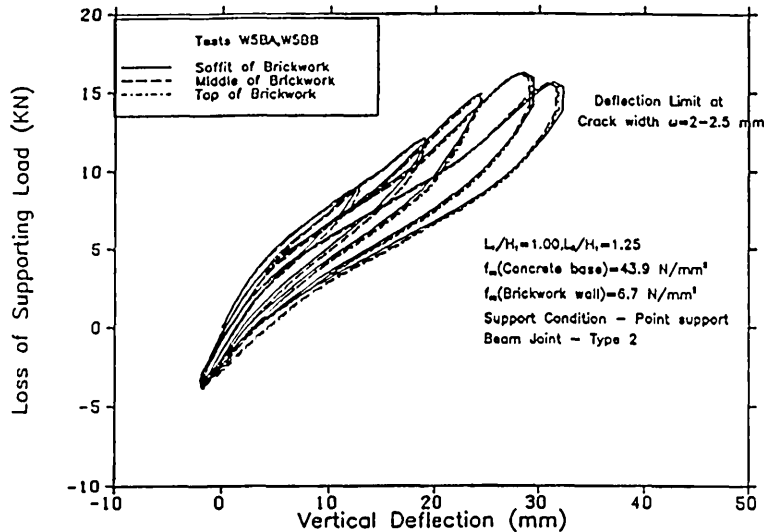


Figure 8.20 Relation between reduction in support load and corner deflection (Test W5B).

wall, nevertheless, at one-half of the wall nearer to the fixed supports, maximum deflection occurred at the soffit of the wall. This could be explained by assuming that at the settling corner, tilting of the wall lead to an increase in its vertical deflection, while at the middle of the wall this effect is smaller. It is evident upon comparison between fixed-supported walls (Figure 8.21) and point-supported walls (Figures 8.22-8.23), that walls with point supports exhibit less hogging. At low wall aspect ratios, that is, tests W4 and W5, less variation of deflection occurred between the top, bottom, and soffit of the wall (Figures 8.24-8.25), while the maximum variation occurred in test W2 (Figures 8.21 & A6.1). This shows that high walls behaved more stiffly following deformation upon settlement; that is, shorter walls tilt more easily.

When using point supports, during the first part of each cycle of settlement, there was a tendency for the middle of the wall to deform as much as the settling corner (Figures 8.22-8.23). This is clearly due to the rotation of the beam, which reduced the difference of deflection between the fixed and the settling ends of the wall at the early stages of settlement. However, for fixed supports, variations in the deflection of the wall could be seen in the initial increments of settlement of the FPSS structure (Figures 8.21 & A6.1). As a result, less curvature was experienced for walls with point supports, resulting in the accommodation of more settlement for the same limits of visible damage.

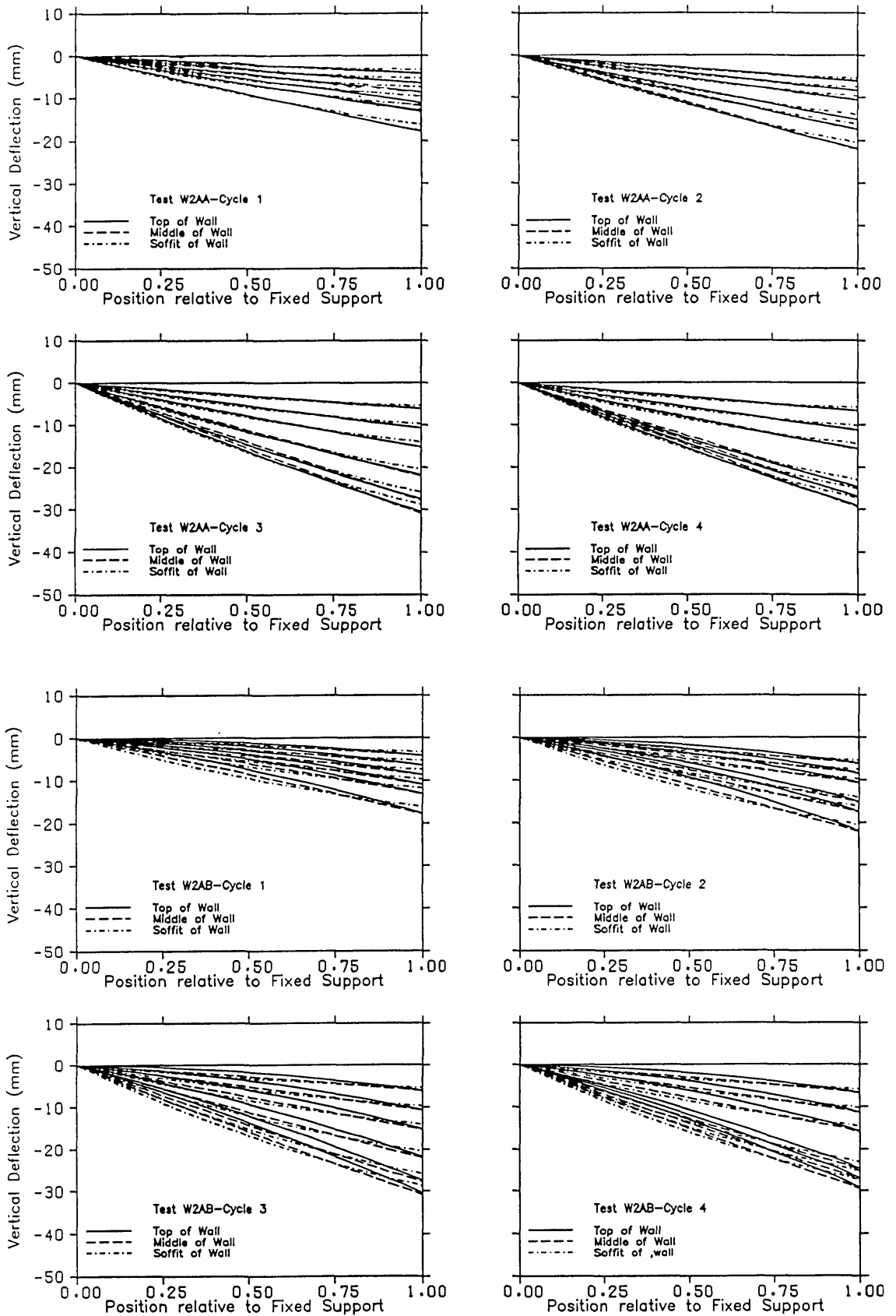


Figure 8.21 Effect of cyclic settlement on the vertical deformation of the wall (Test W2A).

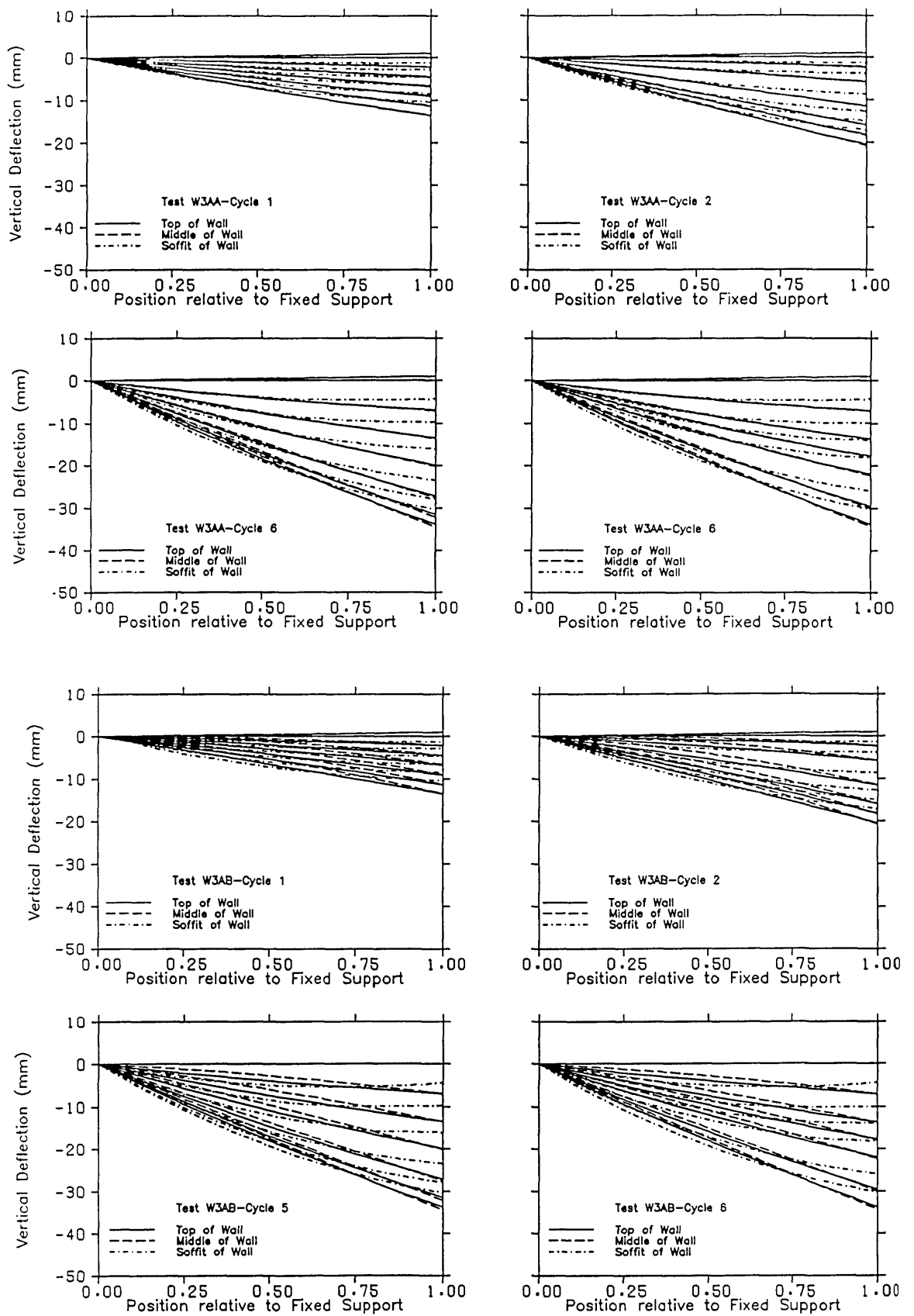


Figure 8.22 Effect of cyclic settlement on the vertical deformation of the wall (Test W3A).

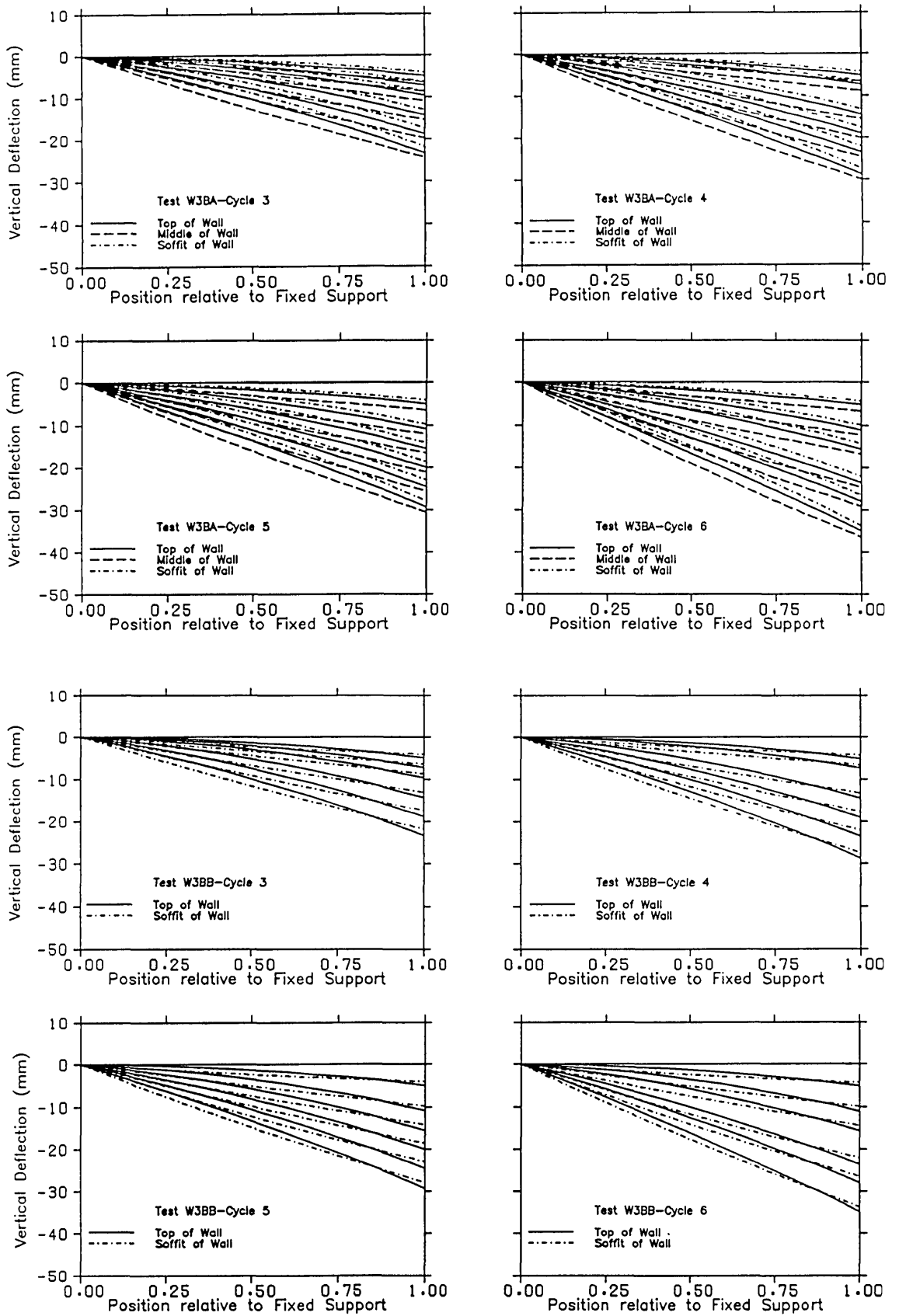


Figure 8.23 Effect of cyclic settlement on the vertical deformation of the wall (Test W3B).

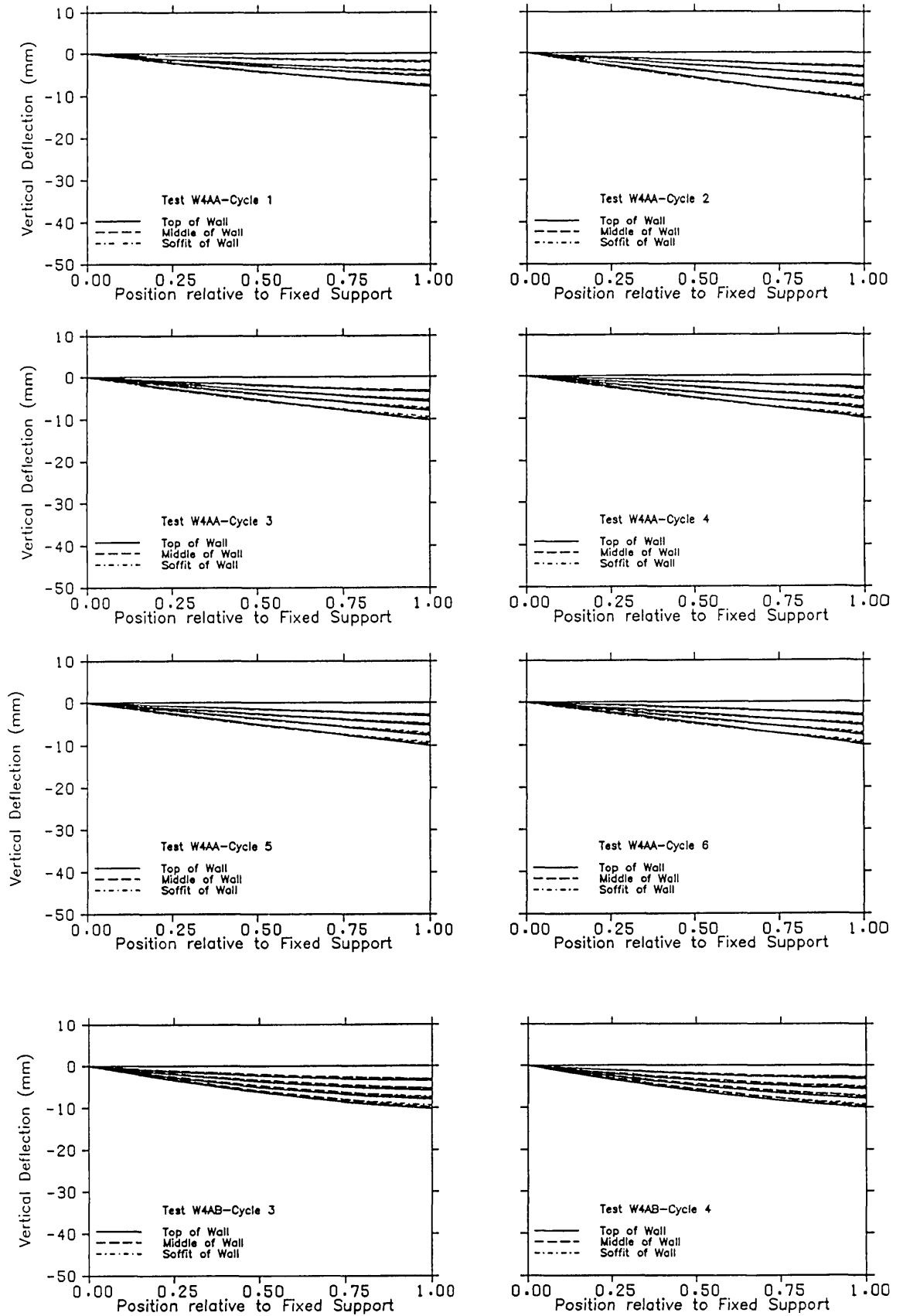


Figure 8.24 Effect of cyclic settlement on the vertical deformation of the wall (Test W4A).

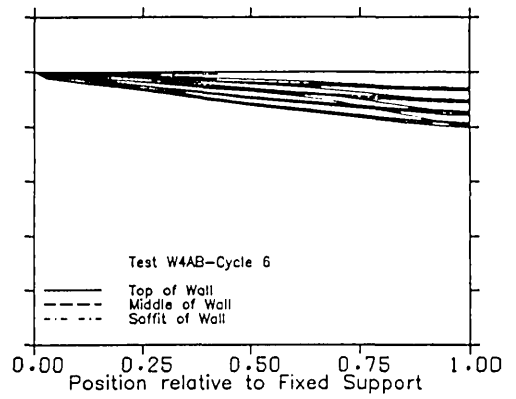
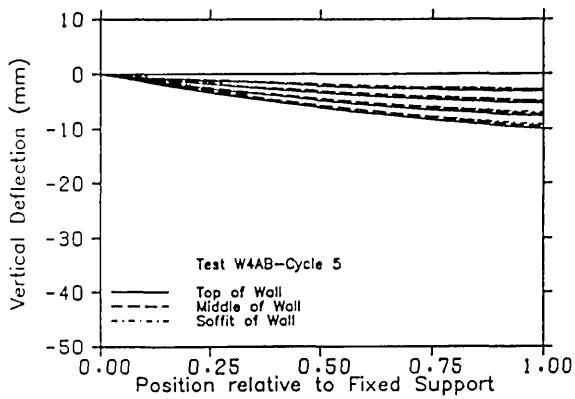


Figure 8.24 Continued.

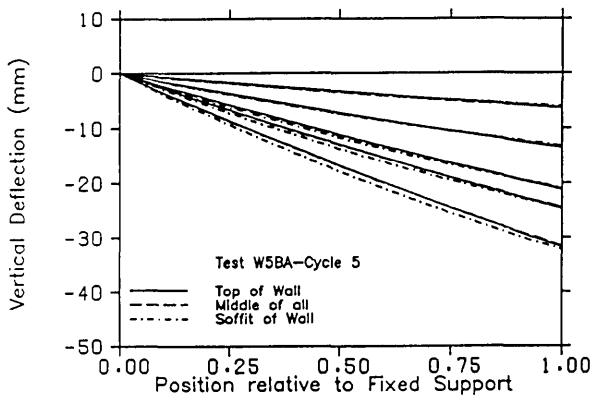
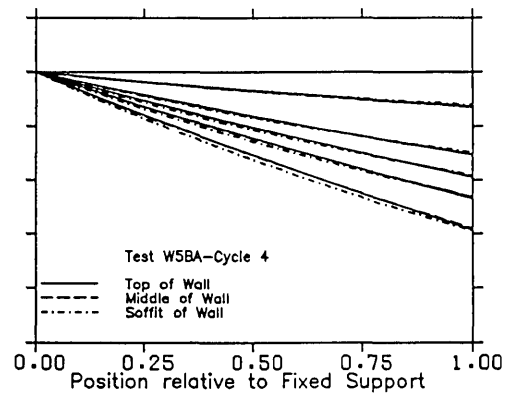
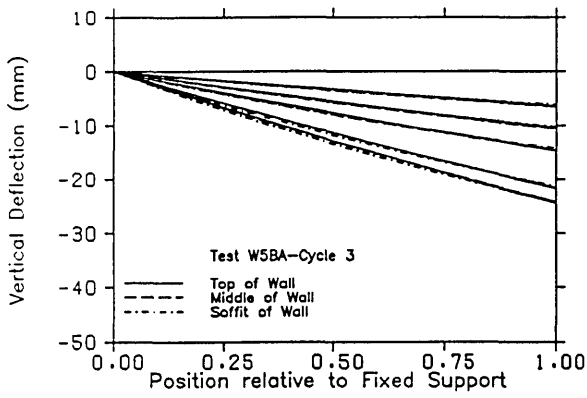
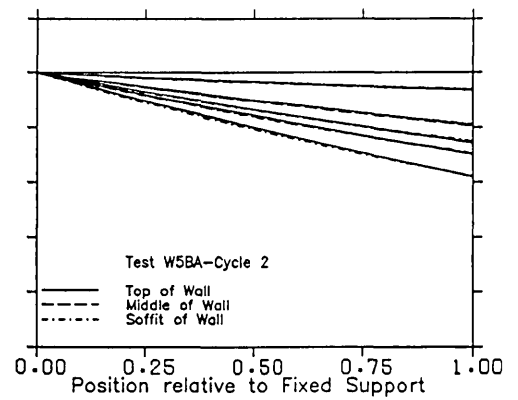
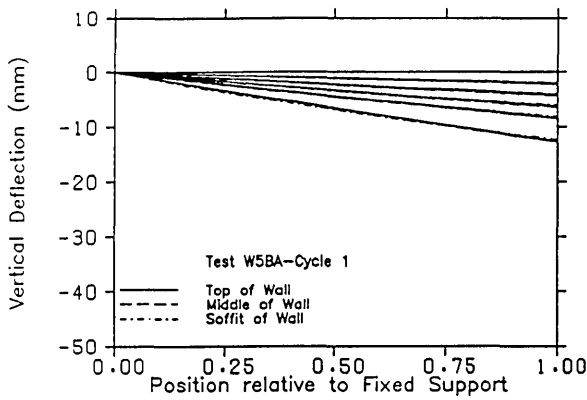


Figure 8.25 Effect of cyclic settlement on the vertical deformation of the wall (Test W5B).

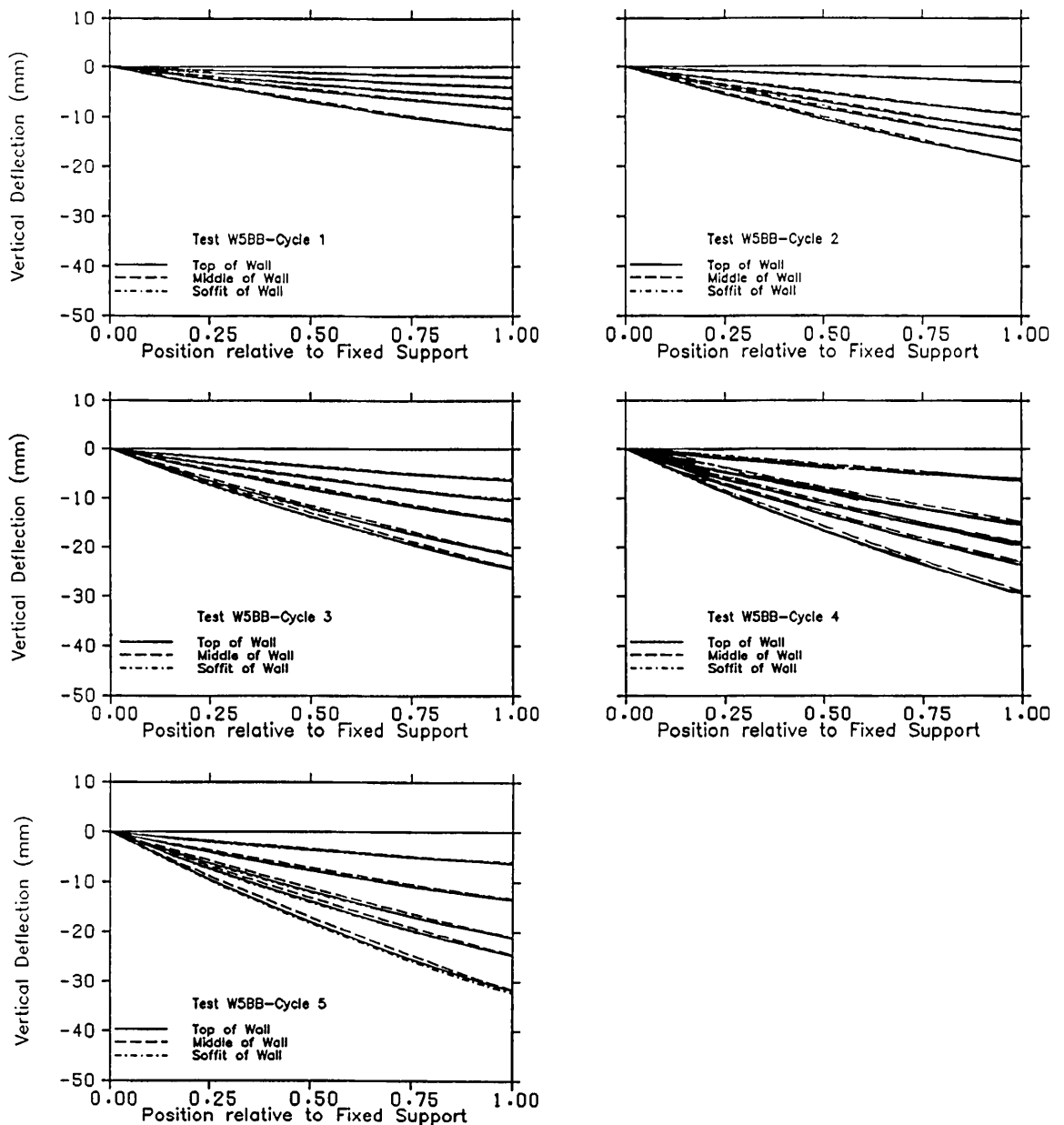


Figure 8.25 Continued.

### 8.3.3 Out-of-plane warping and lateral distortion of walls

Figures 8.26-8.30 show the relationship between lateral distortion and loss of support load. The magnitude of the out-of-plane warping and lateral distortion is fairly large in comparison with the maximum vertical deflection of the FPSS. Maximum lateral distortion of 26 mm was recorded in test W1 (Figure 8.26), and 36 mm in test W5 (Figure 8.30). On cyclic settlement of the FPSS wall (settlement and



rejacking), lateral movement of the wall increased with respect to the same loss of support load. However, it is clear that upon rejacking of the structure, most of the lateral distortion decreased to zero, except for tests W4 and W5 where 2 mm permanent deformation was recorded. Although reinstatement of the structure was achievable in most cases, a larger jacking force was required to restore the structure to its initial state than the load due to loss of support. In tests W1 and W2 (Figures 8.26-8.27), no extra load was required, while for tests W3 and W4, 5 KN extra load was needed to restore the structure to the position of zero lateral distortion. Furthermore, for tests W5AA and W5AB, 10 KN extra load was measured after six cycles of settlement (Figure 8.30). Noticeable cracking of the wall occurred at the plateau of the load-deflection relationship, that is, in the range of 5-10 KN. On further reduction of the supporting load, the wall continued to distort. This indicated either rigid body rotation of the wall or further crack opening. Measurements of lateral movement at the top of the wall showed an offset between the settling and the fixed ends, which was due both to the magnitude of tilt and opening of cracks (Figures 8.28-8.30).

Figures 8.31-8.35 show the relationship between the maximum out-of-plane warping of walls and loss of support load. Test W1BB recorded 30 mm at the onset of visible damage, while 34 mm warp was measured for test W5BA. Warping was recorded at the top of the wall as the difference between lateral deflection of the wall at the fixed and settling edges of the wall. This gives an indication, in plan, of the amount of diagonal lengthening at the settling end, that is, 3-dimensional distortion of the FPSS. For fixed supports, the greater the span of the wall, the more the warping deformation (Figures 8.31-8.32). For point supports, however, large warp was experienced by the shorter span walls (Figure 8.33). Nevertheless, increasing the strength of the walls by introducing bed joint reinforcement at the top of the wall in test W5 (Figure 8.35), caused larger warp to be induced in the longer span, that is, tests W5AA and W5BA.

#### **8.3.4 Angular rotation and tilt of ring beam**

Angular rotation of the point supported walls, tests W3AA-W5BB, was measured at every load step at the short column beam joint of the ring beam. Figures 8.36-8.38 show the relationship between reduction of support load and angular rotation. In some cases, cracks propagated

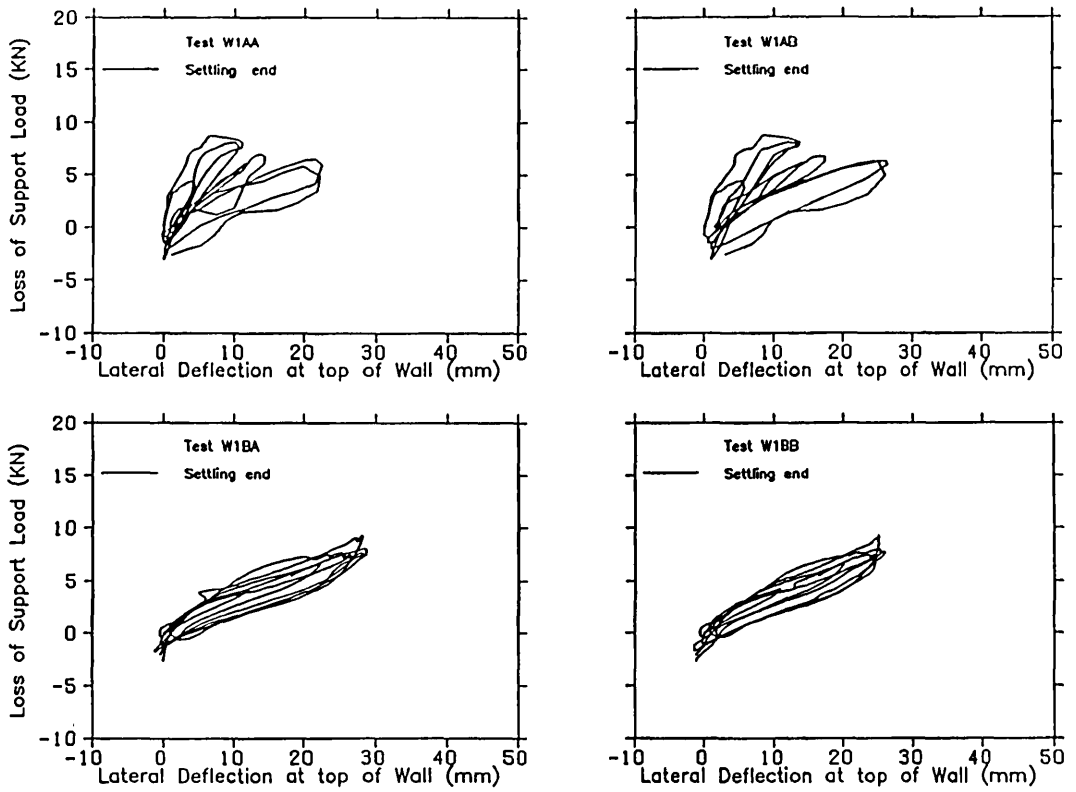


Figure 8.26 Effect of cyclic settlement on the lateral distortion of the wall (Test W1).

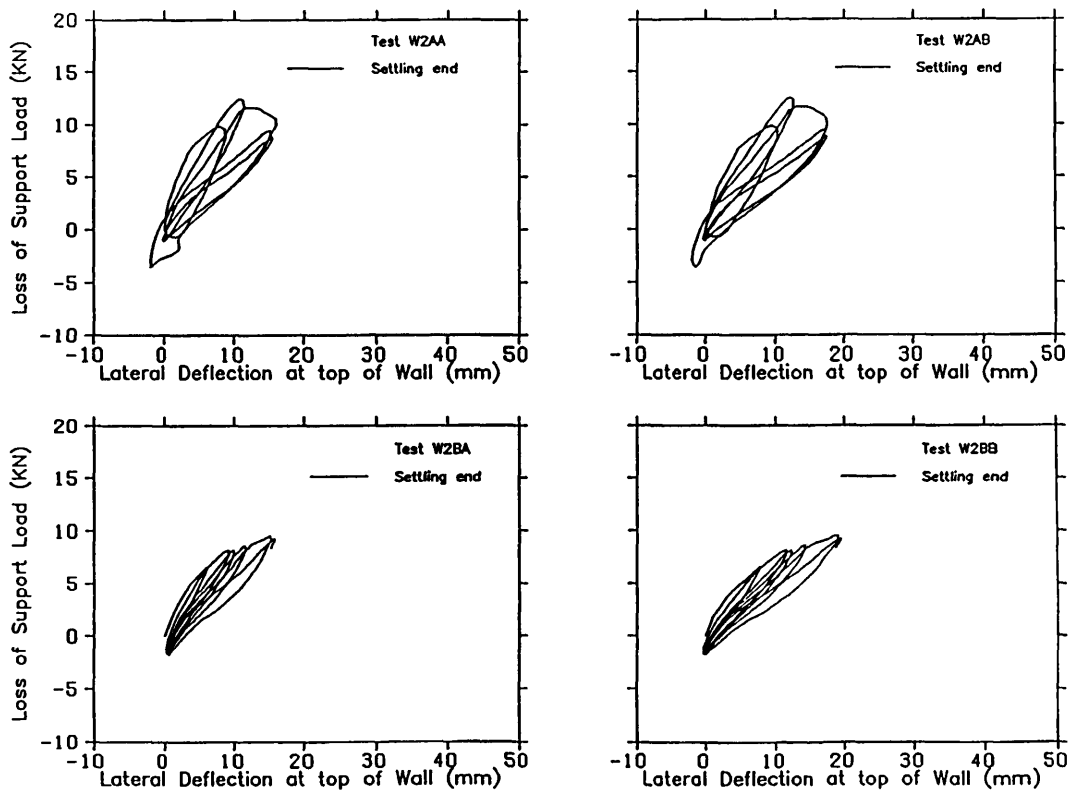


Figure 8.27 Effect of cyclic settlement on the lateral distortion of the wall (Test W2).

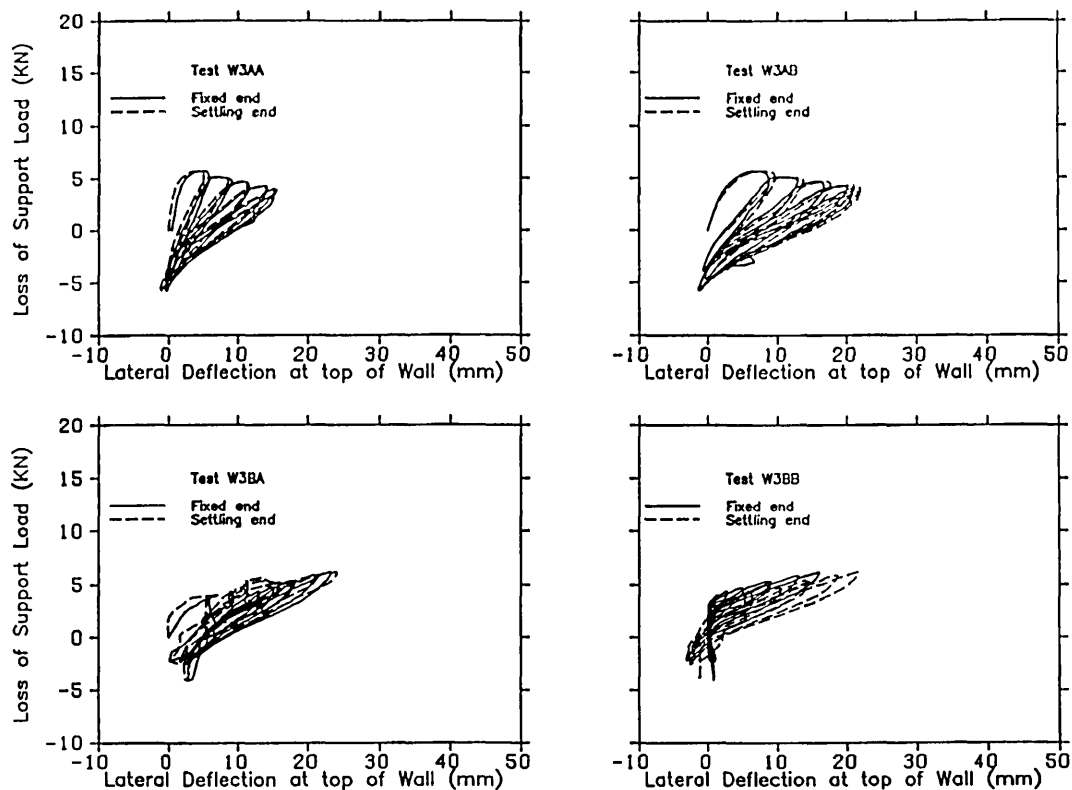


Figure 8.28 Effect of cyclic settlement on the lateral distortion of the wall (Test W3).

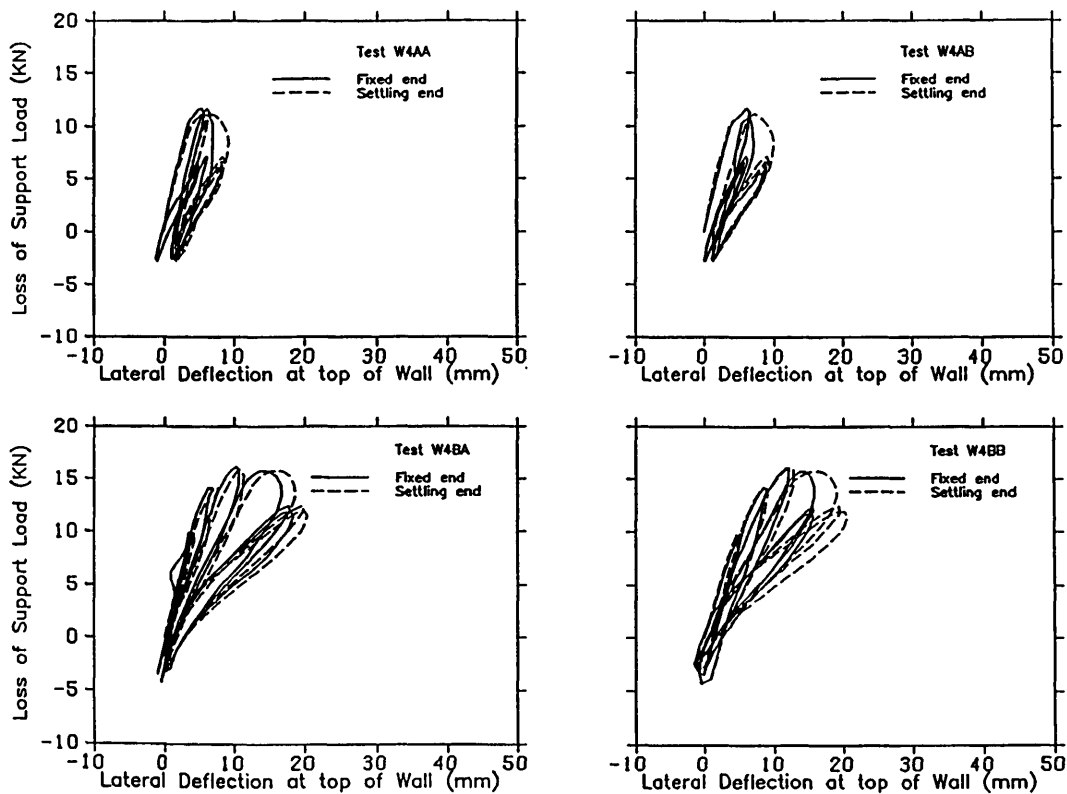


Figure 8.29 Effect of cyclic settlement on the lateral distortion of the wall (Test W4).

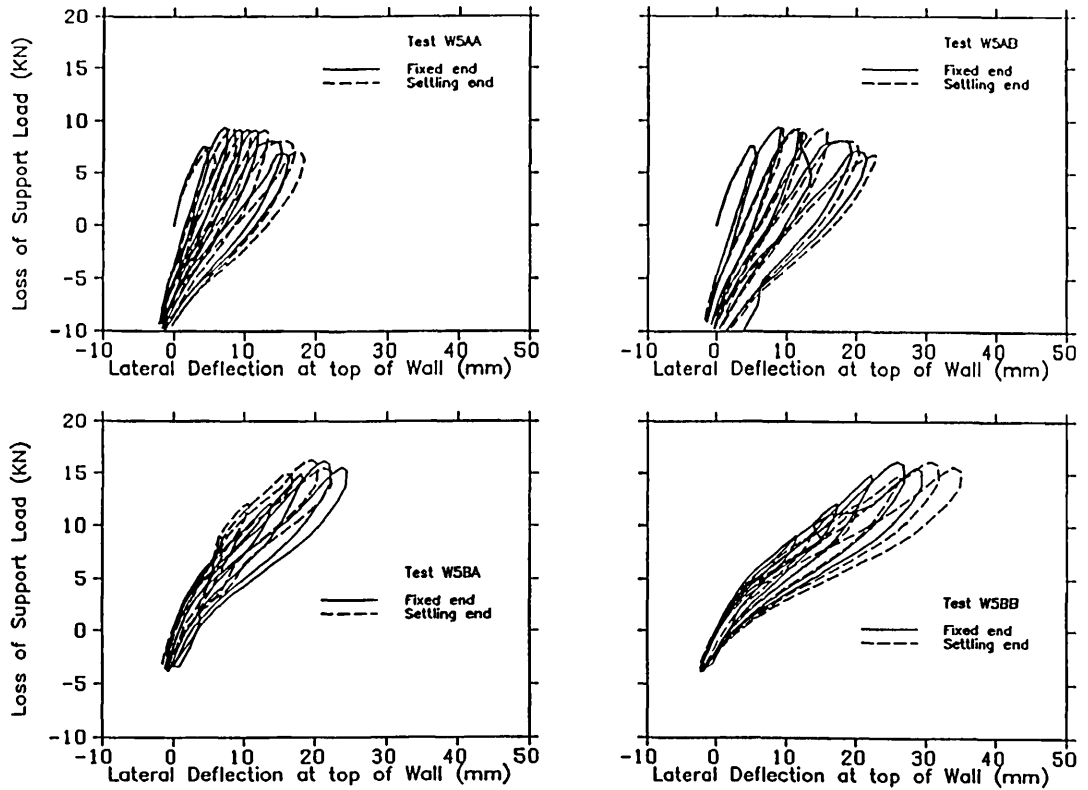


Figure 8.30 Effect of cyclic settlement on the lateral distortion of the wall (Test W5).

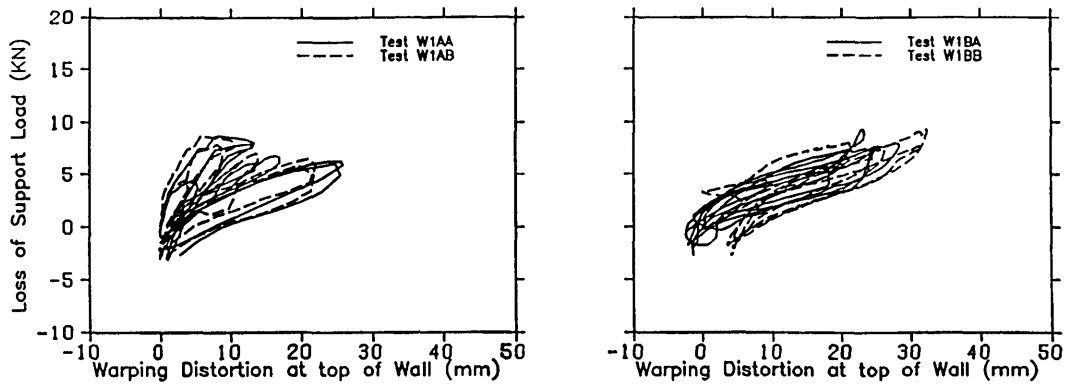


Figure 8.31 Effect of cyclic settlement on the out-of-plane warping of the wall (Test W1).

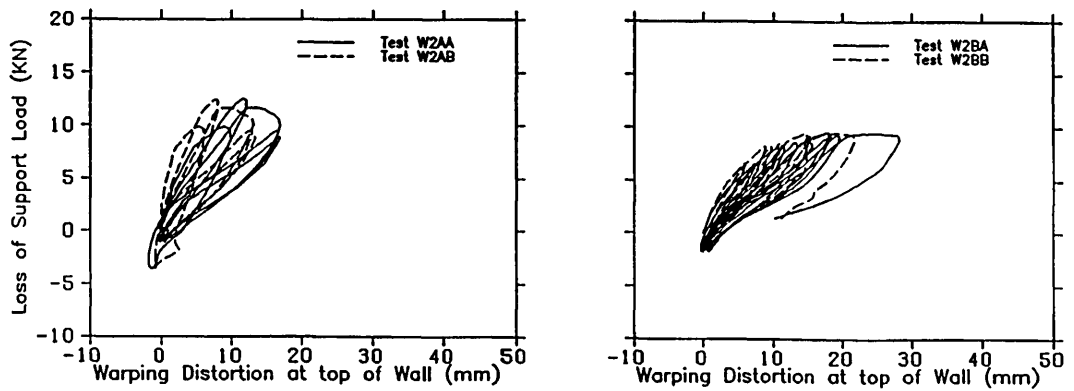


Figure 8.32 Effect of cyclic settlement on the out-of-plane warping of the wall (Test W2).

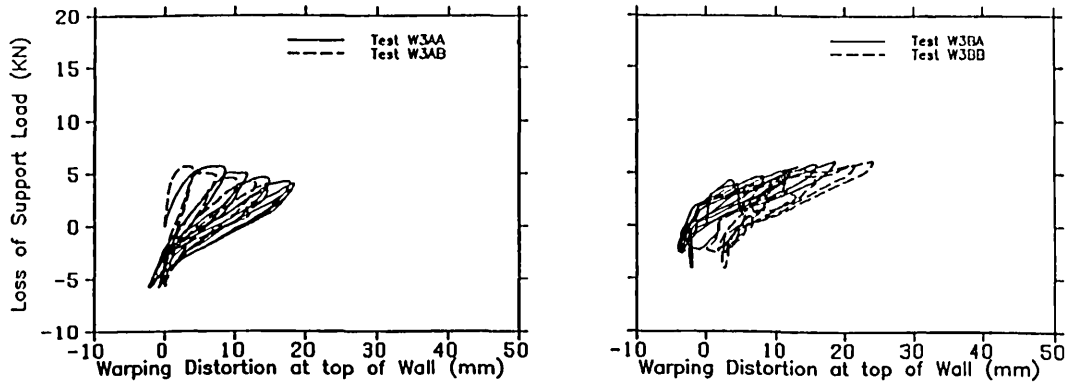


Figure 8.33 Effect of cyclic settlement on the out-of-plane warping of the wall (Test W3).

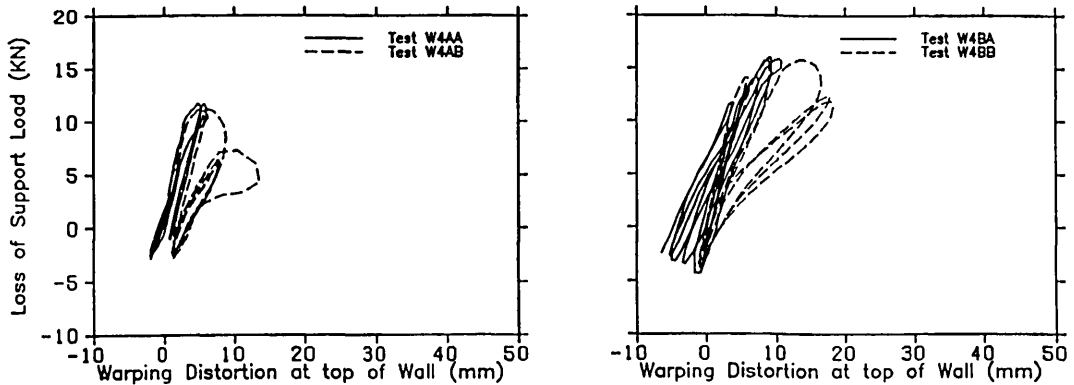


Figure 8.34 Effect of cyclic settlement on the out-of-plane warping of the wall (Test W4).

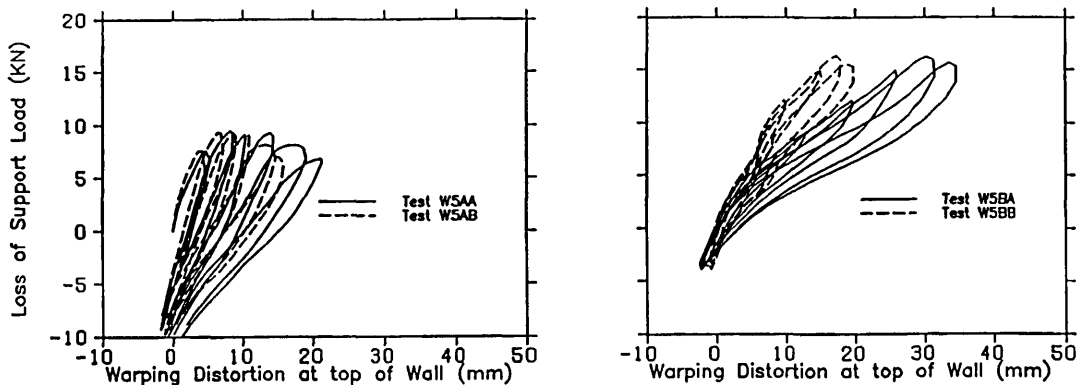


Figure 8.35 Effect of cyclic settlement on the out-of-plane warping of the wall (Test W5).

through the bracket which supported the clinometer gauge, causing disruption of readings. To avoid such circumstances, the gauge was fixed separately on either the beam or the short column. A maximum rotation of 0.24 radians was recorded at test W3BB, at the onset of visible damage in the wall, while maximum rotation of 0.11 radians was recorded for test W4BB and 0.14 radians for test W5BB. As expected, the maximum rotation was measured in the shorter span beams with the larger aspect ratio ( $L/H$ ) (Figure 8.36). Walls with lower aspect ratio ( $L/H$ ),

that is, tests W4AA-W5BB recorded a lower angular rotation of 0.24 radians (Figures 8.37-8.38). The pattern of the load-angular rotation relationship consisted of an ascending curvilinear relation with a descending part at the end of the curved path; the latter due to the stiffness degradation of the FPSS. However, for walls with lower aspect ratios, a stiffer form of relation was observed with a short curved part denoting a less ductile behaviour (Figures 8.37-8.38). The above effect is reduced upon the introduction of weak joints at the beam-short column joint, which caused an increase of rotation (refer to tests W4BA, W5BA and W5BB). As a result, a bi-linear curve was formed that illustrated two forms of rotations occurring in the beam. The first is due to rotation of the ring beam owing to the point supports, and the second is due to formation of the concrete hinge at the weak joint (Type 2). Increased rotation was measured in the range of 0.048 radians for test W4 and 0.02 radians for test W5. Additionally, angular rotation of the same order was recorded at the settling end of the beam, which was due to the ball seated jack under the settling support. This clearly demonstrates the amount of rotation and tilt that the settling supports can accommodate.

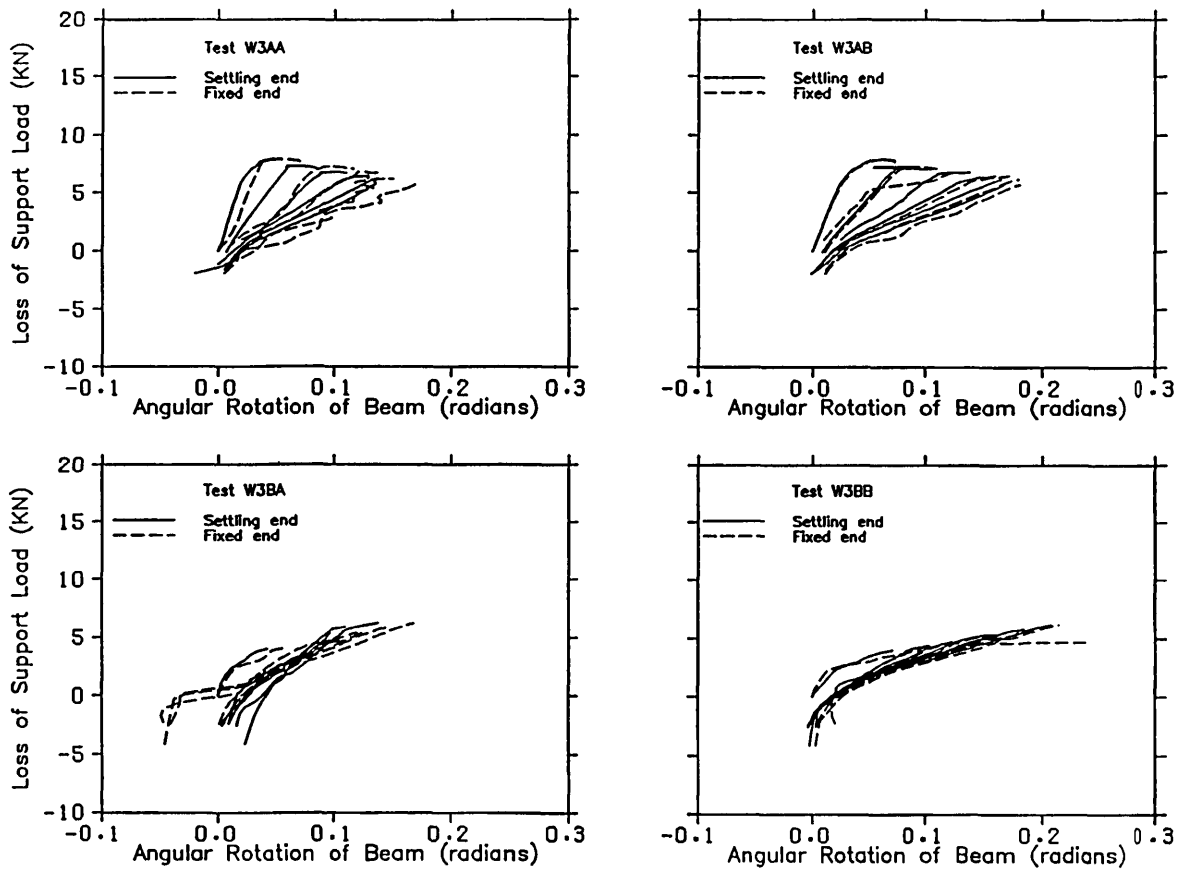


Figure 8.36 Effect of cyclic settlement on angular rotation of ring beam (Test W3).

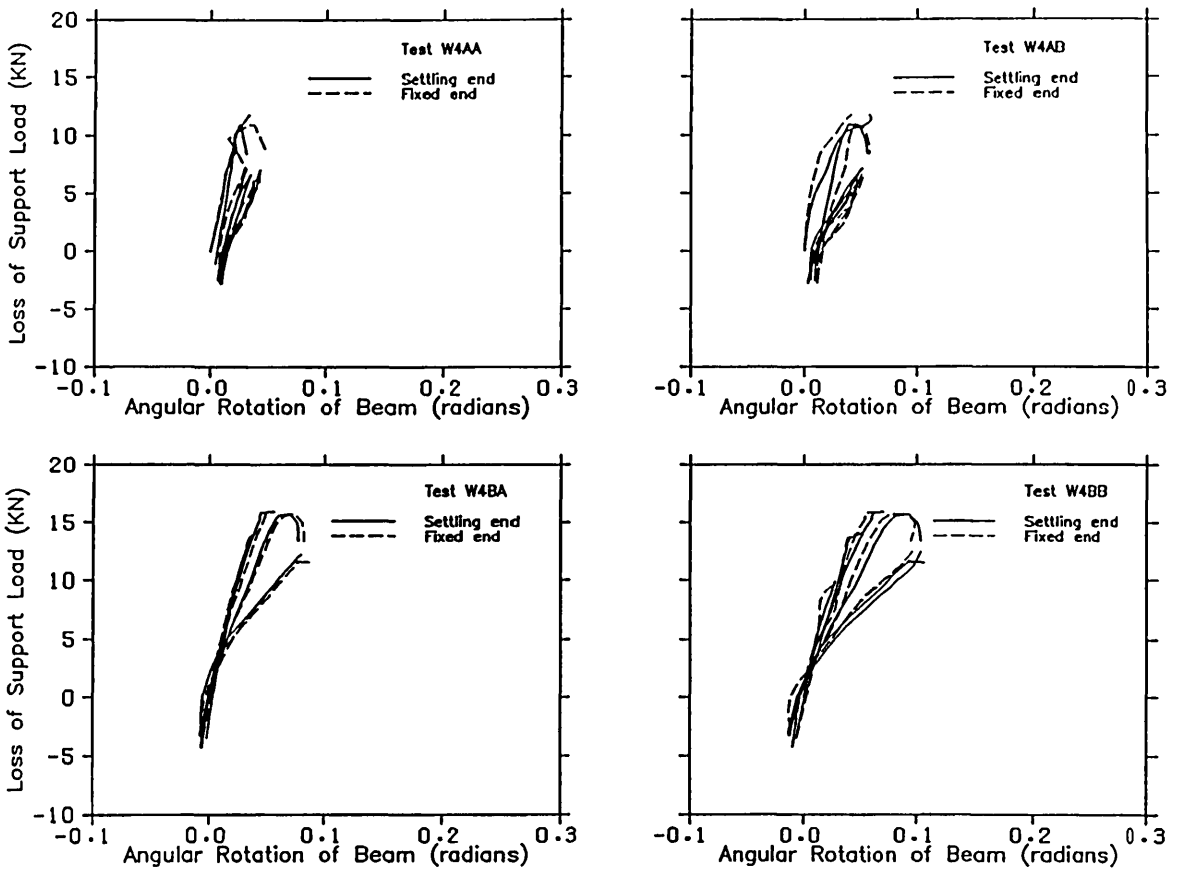


Figure 8.37 Effect of cyclic settlement on angular rotation of ring beam (Test W4).

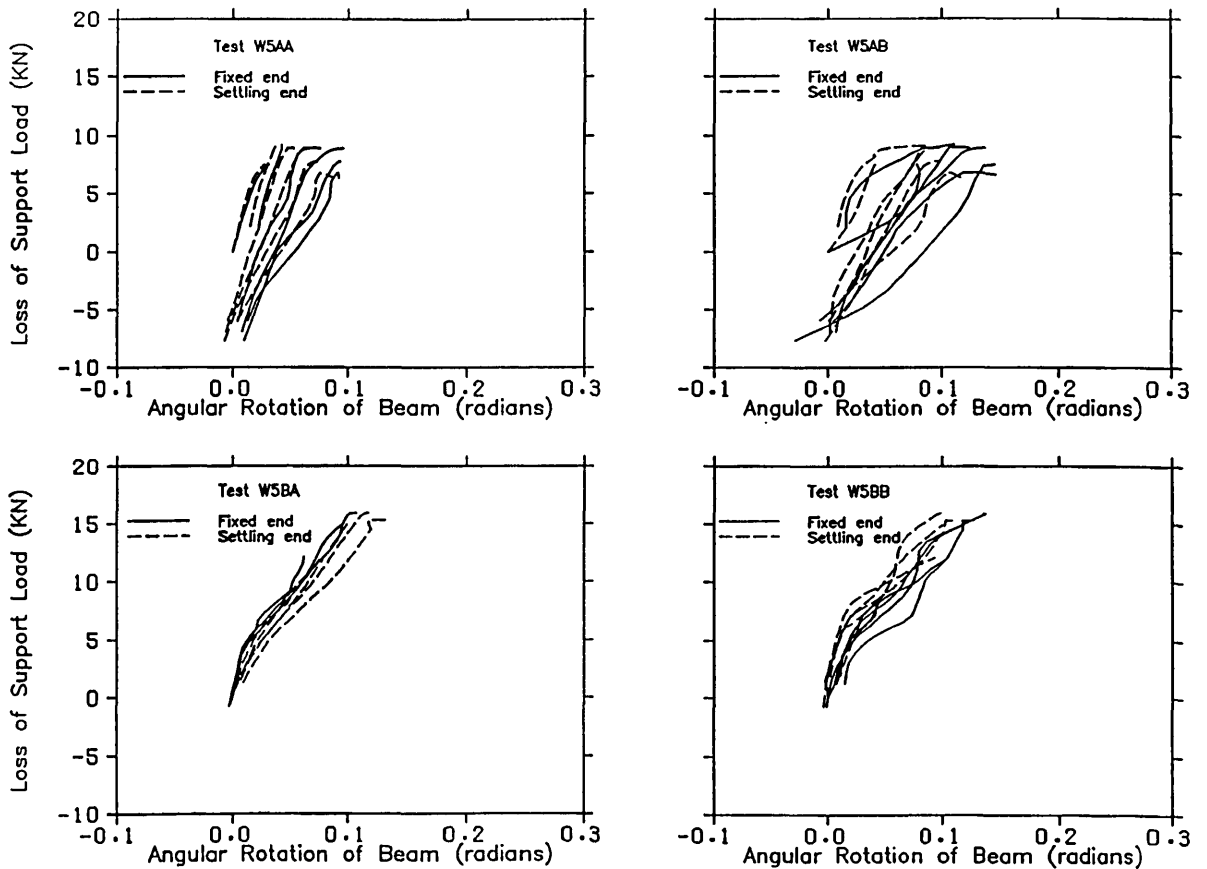


Figure 8.38 Effect of cyclic settlement on angular rotation of ring beam (Test W5).

## 8.4 WALL STRAIN

### 8.4.1 Vertical strain distribution

Vertical strain in the wall was measured at three horizontal levels; top, middle and bottom, as shown in Figures A6.4-A6.8. Zero strain was taken to be in the condition immediately prior to settlement.

In some cases, during wall strain measurement and due to the crack propagation through the wall, the Demec gauge length was too small to measure cracks wider than 2-3 mm. As a result, the maximum strain was used as a default, that is, 6500 microstrain. During cyclic settlement and re-jacking of the FPSS, the strain distribution was measured at the peak of each cycle. This was necessary to monitor the progress of cracks and the regular distribution of strain along the wall at maximum deflections. In most cases, Figures A6.4-A6.6 show the progressive build-up of vertical compressive strain along a diagonal stretching from one corner of the wall to the other, opposite the settling support. However, the strut contained a highly compressive region only at the corners; at the middle of the wall the compressive region or strut band dilated with less magnitude of strain. This concentration of strain reached a maximum value of 4305 microstrain in compression at both corners, while on cracking the default strain of 6500 microstrain was recorded (Figure A6.4). At mid-height of the wall, the higher compressive zone either occurred at the central region of the wall or shifted more towards the edges of the wall (refer to Figures A6.4-A6.6). However, the magnitude of compressive strain was lower than that recorded at the corners.

As expected, tensile strain developed nearer to the settling support, at some distance away from the compressive diagonal strut, where a maximum strain of 1100 microstrain in tension was recorded for tests W1BB, W2BA and W3AA (Figures A6.4-A6.5). For test W2B, compressive strain was recorded at mid-span of the wall at the beam wall interface (Figure A6.5), where a large part of the strain was present at the centre span of the beam. However, for tests W1, W2 and W3, much of the load distributed along the beam before settlement was transferred to the supporting end after settlement, by way of the compressive strut. This was distributed along one-third of the span nearer to the supporting end, as shown in Figures A6.4-A6.6.

Measured wall strains of the FPSS wall with low aspect ratio (L/H), that is tests W4 and W5, were smaller per unit settlement than those of test W3, refer to Figures A6.7-A6.8. Maximum strain of



1890 microstrain in compression was recorded in test W4BB, while in tests W5BA and W5BB, a maximum strain of 561 microstrain was measured (Figure A6.8). Similar behaviour could be seen clearly in walls W1, W2 and W3, with the compressive strain band along the diagonal opposite to the settling support. However, in test W5 at the beam-wall interface, the compressive strain was distributed along the whole span with maximum magnitude of strain occurring either nearer to the fixed support or at mid span (Figure A6.8). No clear distinction of strain distribution in the wall was observed for different types of joints or support systems.

#### **8.4.2 Horizontal strain distribution**

Figures A6.9-A6.13 illustrate the horizontal strain distribution in the wall along five vertical regions, namely, the two edges, quarter, mid and three-quarter span from the fixed support. Similarly to the vertical strain, two main distributions occurred. The first was a compressive strain distribution that developed along the fixed supports and at the top of the wall at the settling edge, with maximum strain of 4105 microstrain (Test W5BB). The second was tensile strain distribution which developed along a diagonal extending from the settling support to the opposite wall corner, with maximum strain of 3630 microstrain recorded at the settling end in test W3AA. Also, as for vertical strain distribution, for low aspect ratios of wall (tests W4 and W5), lower magnitudes of horizontal strain were recorded than those of tests W3. A maximum strain of 2100 microstrain in compression in test W5 was measured (Figure A6.13), while 1560 microstrain in compression was recorded in test W4 (Figure A6.12). It is also clear that larger compressive strain was accommodated in test W5 than in test W4. These strains were measured at the fixed support and at the top of the wall at the settling end.

Before settlement, it is known that the neutral axis of the beam-wall structure has a parabolic shape (Saw,1974 ; Stafford-Smith and Riddington,1977), which is lower at the mid-span of the wall and higher at the supports. After settlement, the neutral axis lowers at the settling end, while rising to quarter-height at the mid-span of the wall and maintaining its height or rising even higher at the fixed support (refer to Figure 8.39).

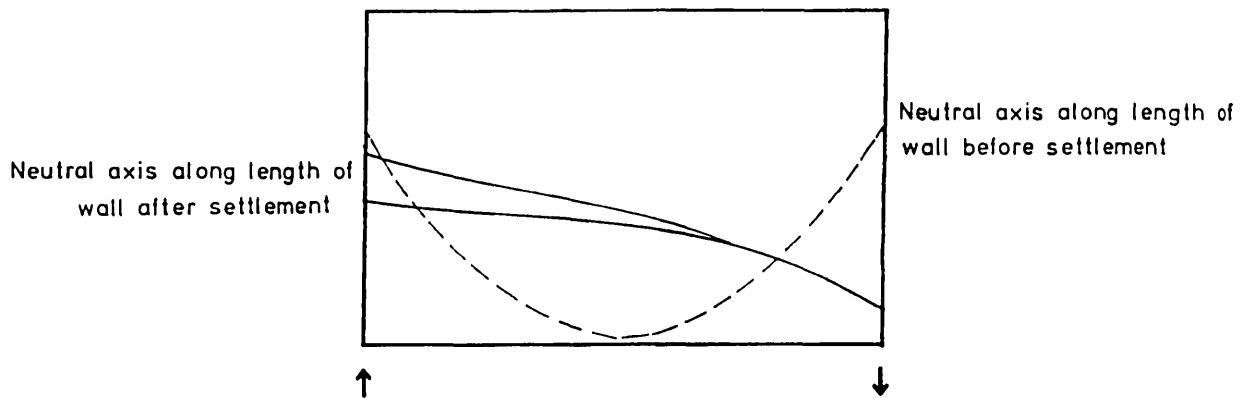


Figure 8.39 Position of neutral axis before and after settlement.

### 8.4.3 Principal strain distribution

To study the regular change of strain distribution along the wall, principal strains measured along the external surface of the core walls are plotted in contour form to clarify both the degree and pattern of the strain during settlement. Figures 8.40-8.44 show the progressive build-up of the maximum principal strains along the wall during cycles of settlement of both wall A and B. The contour plot is the result of 15 experimental strain rosette measurements at the intersections of the dotted grid (refer to Section 6.7). A fortran program GENCON was developed to plot the contours as no available package could be utilized using such scarce points. The program consists of two parts, the first serving to generate a finer mesh by inserting intermediate grid points. This is achieved by fitting a spline curve through the original points along the X-axis and the Y-axis separately, that is, along each dotted and sub-dotted lines, and then interpolating intermediate points. Choice of the spline is very important if extraneous errors are to be avoided in the interpolation of actual data (refer to Appendix 5).

Optimizing the fineness of the grid is necessary so as not to generate false troughs and crests which would interfere with the interpretation of the results and the contour plots. The second part of the program consists of a package (Burgoyne, 1986) that traces points of equal stresses or strains. This was utilized and developed to adjust its own strain steps and contour levels (refer to Appendix 5). Using an existing plotting package GIPS, the plots were then processed via a laser printer.

Figures 8.40-8.41 show the initial strain distribution in walls W1AA and W1AB before settlement where maximum compressive strain was concentrated at the ends of the wall, that is, at the supports. It is

noted that strain in the wall was measured at the maximum deflection in each settlement cycle. Settlement at the right bottom corner of the wall caused high compressive strain to develop at the supporting left bottom corner and at the right top corner of the wall. It will be shown later that these high compressive strains were associated with tensile strains in the orthogonal direction (refer to Figure 8.45). Maximum tensile strains were measured at the left top corner of the wall that extended towards the mid-height of the wall at the supporting end (Figure 8.40-Cycle 5). Similar behaviour was recorded for walls W1BA and W1BB with higher concentrations of compressive strain in the beam at some distance away from the supporting left end (Figures A6.14-A6.15). Maximum principal compressive strains of 2460 microstrain were recorded in cycle 2 at the top of the wall at the settling corner, while compressive strain of 2128 microstrain was measured in cycle 6 at the beam-wall interface. In cycle 4, it is shown that the compressive strut shifted from the left bottom corner to some distance away from the left support (Figure A6.14).

For tests W2AA-W2BB, high tensile strain of 7511 microstrain was developed at the settling edge of the wall, with compressive strain of 4688 microstrain recorded at some distance away from the supporting end.

Due to the formation of a vertical crack at the top left corner of the wall in test W2BA, a high tensile strain of 958 microstrain was recorded in cycle 10 (Figure A6.16).

Figures 8.42 & A6.17 show the strain distribution in walls W3AA-W3BB, where a maximum compressive strain of 3202 microstrain was measured. It should be noted that lower compressive strains of 2106 microstrain were recorded in tests W3BA and W3BB (Figures A6.18). Figures 8.42 & A6.17 show the progressive change of strain pattern of the diagonal compressive strut to one extending from the top right corner of the wall to middle span of the beam. However, tests W3BA and W3BB show that the highly compressed region is at the top right corner of the wall, while tensile strain developed at the middle of the wall and near the beam-wall interface (Figure A6.18).

For the 1828 mm high walls, strain distribution in walls W4AA, W4AB, W4BA and W4BB are shown in Figures 8.43 & A6.19. High compressive zones were recorded at both the top right corner and the bottom left end of the beam, where a maximum strain of 516 microstrain was measured. There is little evidence to indicate that there was a diagonal compressive strut as in the previous tests (tests W1, W2 and W3). Also,

high compressive strain was measured at some distance away from the support in test W4BB where a strain of 2114 microstrain was measured (Figure 8.43). The largest tensile strain was recorded in walls W4AB and W4BB, that is in the walls with lowest aspect ratio,  $L/H = 1.00$ . Generally, at later stages of settlement, the walls were subject to compressive strain along the beam-wall interface, while the top of the wall was subject to tensile strain.

To reduce crack opening in test W4, test W5 was reinforced below the top five courses and the strain distributions were as shown in Figures 8.44 & A6.20-A6.21. It is clear that there was a high compressive zone at the top right corner and the top left corner of the wall, where in some cases these extended along the edge of the wall to the beam-wall interface. However, lower strains were recorded at the right edge of the wall at middle height where in some cases tensile strain was present. Additionally, at later stages of settlement, the highest compressive strains were recorded at some distance below the top of the wall (Figure 8.44). Furthermore, in tests W5AB, W5BA and W5BB, tensile strain was recorded at the right edge of the wall extending towards the middle span of the beam (Figure A6.20). This caused most of the wall loading to be transferred to the beam-wall interface through the stiffened wall edges (Figure A6.21).

Figures 8.45-8.51 show the direction and magnitude of maximum and minimum principal strains in the wall at selected cycles. The notations used in the figures are as follows:

101~~X~~-69

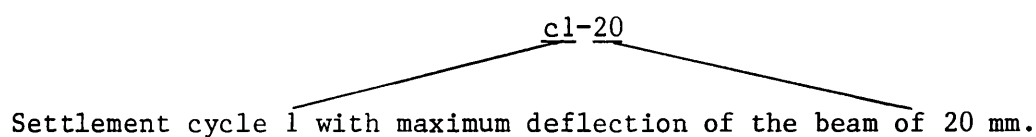
Maximum principal strain of and a minimum principal strain of  
101 microstrain in compression                      69 microstrain in tension

Before settlement, the maximum principal strain distribution shows that the wall is in compression along a path extending from the two supports towards the centre of the wall. On settlement, the direction of the maximum principal strain is in compression along the diagonal opposite to the settling corner, while along the same diagonal the minimum principal strain recorded is in tension (Figures 8.45-8.46). After settlement and due to crack propagation in wall W3, minimum principal strain in the range of 1078-1897 microstrain in tension was also

recorded at the fixed support (Figures 8.47-8.48). This could be explained due to the rotation of the ring beam that caused the wall to lift at the supporting end. In test W4, the maximum principal strain was in compression only at later stages of settlement, while after the first cycle, the wall exhibited compressive strain at both edges (Figures 8.49-8.50). Introducing reinforcement below the top five courses of the wall (test W5), induced an increase in the capacity of the wall to accommodate larger tensile strain, where the minimum principal strain recorded was in the range of 5393-6500 microstrain in tension. As in test W4, the distribution of strain in wall W5 consisted of a path of compressive strain along the length of the wall at mid-height (Figures 8.50-8.51). At the top, the wall was subject more to tensile strain or smaller magnitude of compressive strain.

### 8.5 DAMAGE CAUSED DURING TESTING

A thorough inspection of all walls was made both before and after testing. During testing, the progressive propagation of cracks and failure patterns were monitored at every load step, as shown in Figures 8.52-8.56. Comparison of the damage encountered in all tests is given in Table(8.2). Recordings of maximum deflection, wall tilt and beam rotation are also listed with reference to the damage observed. The following notation is used in the illustrative figures:



Most of the damage experienced in the reinforced concrete ring beam was in the joint between the short column and the beam, with cracking starting at the top fibre and extending towards the bottom. Damage occurred on both faces of the beam at the fixed support, but no cracking was visible at the settling end (Figure 8.52-8.54). Also, in tests W1AA and W5BA, shear cracking developed at some distance from the fixed supports (Figures 8.52 & 8.56). On average, crack widths of 1-1.5 mm were measured in tests W3AA-W3BB, while in tests W1 and W2, 2-2.5 mm were recorded at maximum settlement of 35.2 mm. Upon rejackng the supports, examination of the front concrete face in tests W3AA-W3BB showed little evidence, if any, of cracking, while in test W1AA, a crack width of 0.5 mm was observed. It is clearly seen that cracking

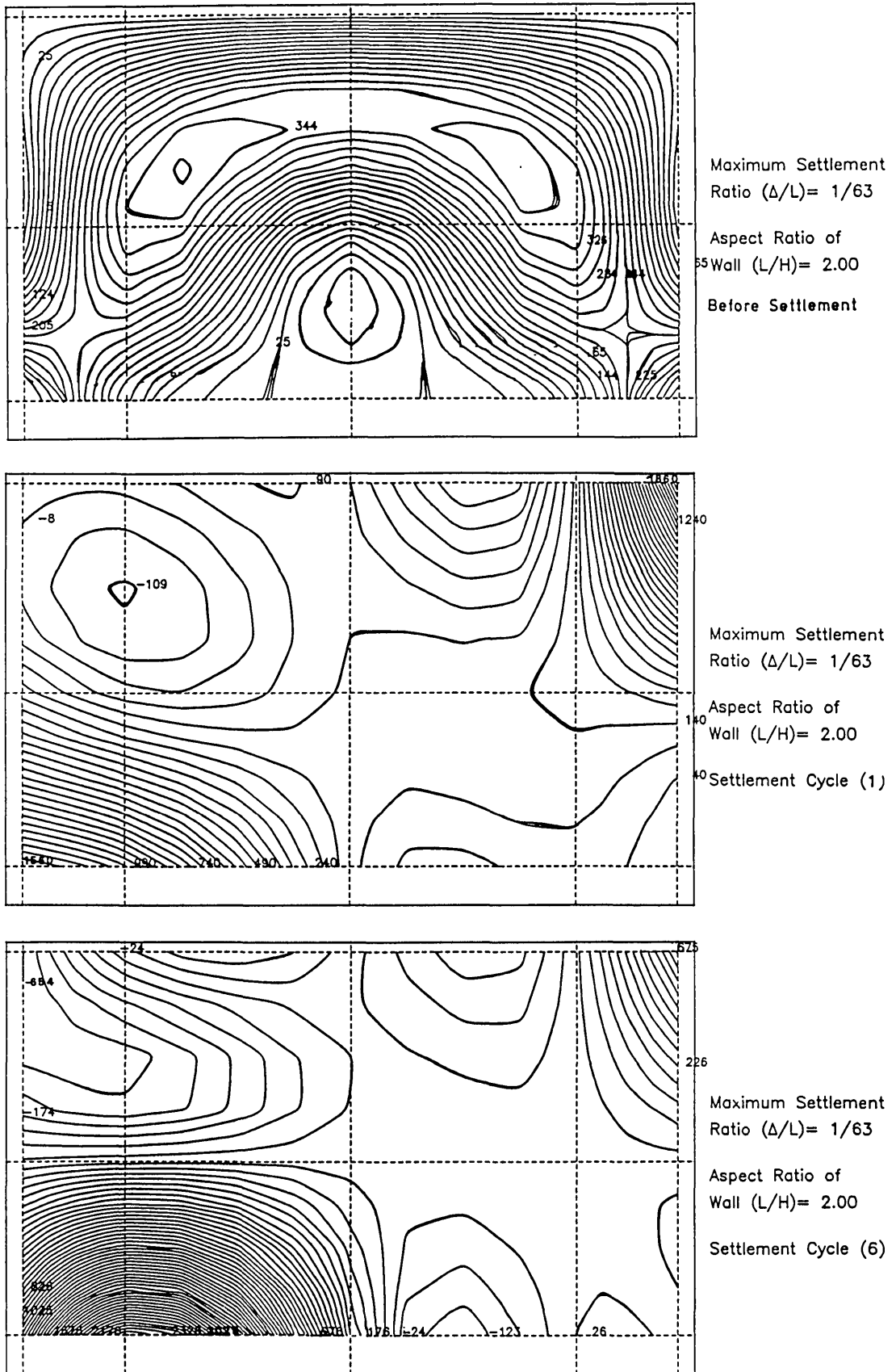


Figure 8.40 Maximum principal strain distribution of wall (Test W1AA).

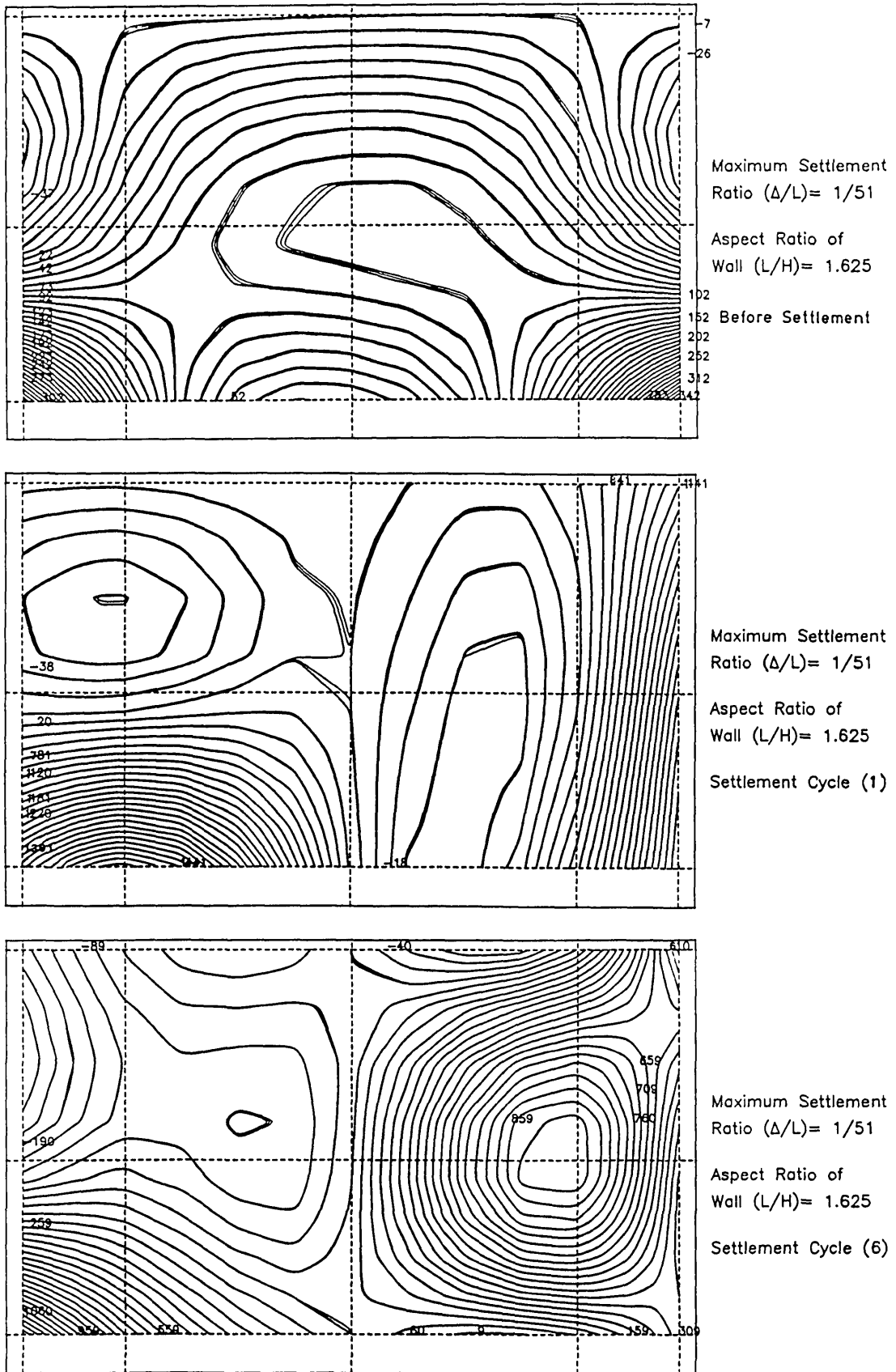


Figure 8.41 Maximum principal strain distribution of wall (Test WLAB).

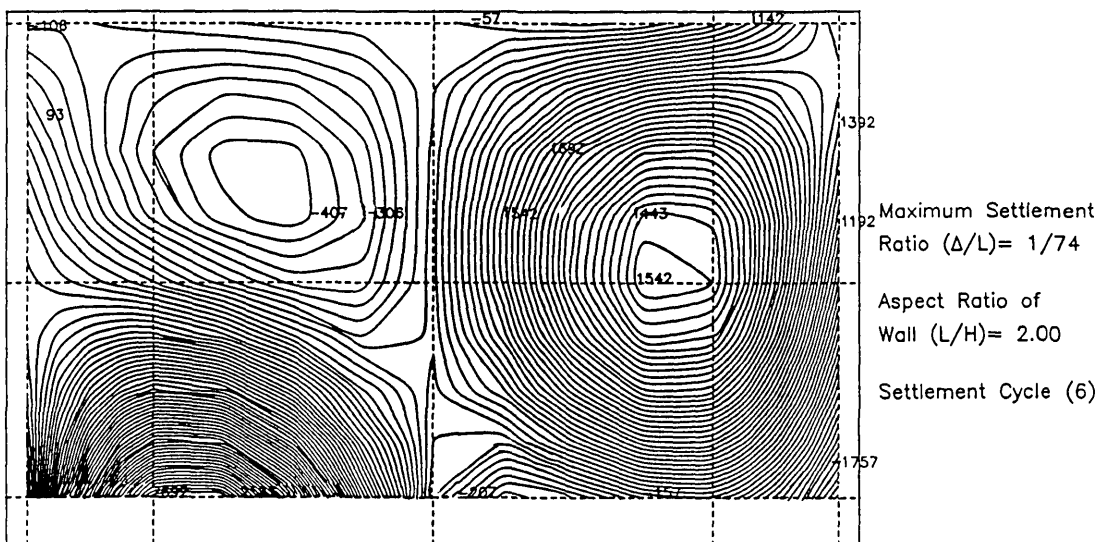
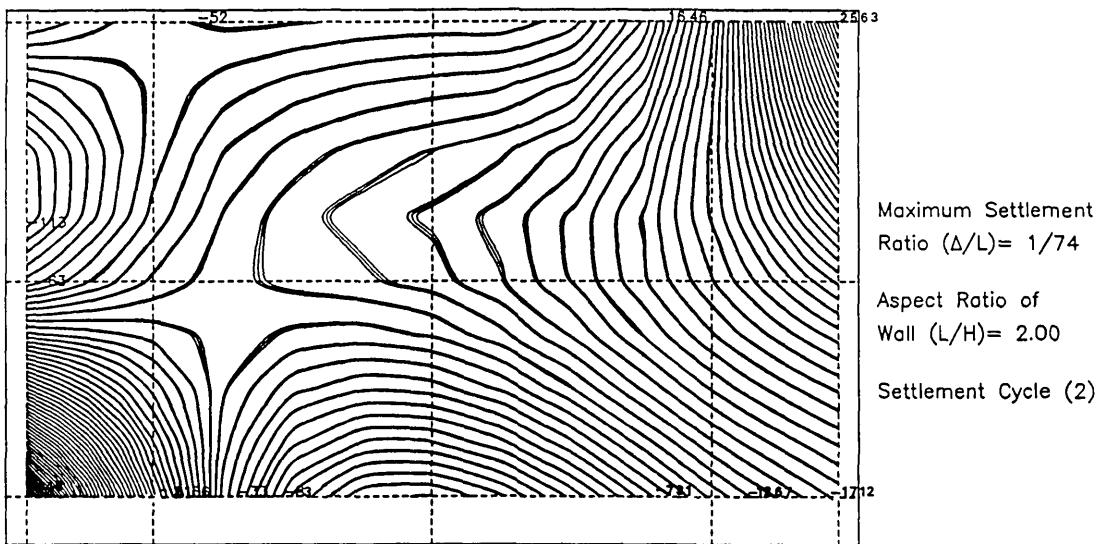
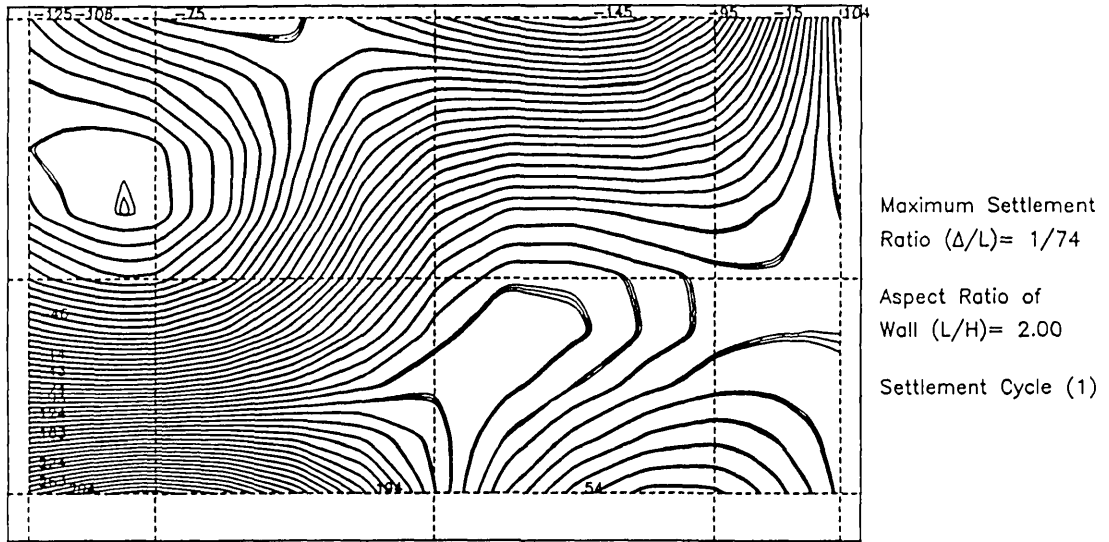


Figure 8.42 Maximum principal strain distribution of wall (Test W3AA).



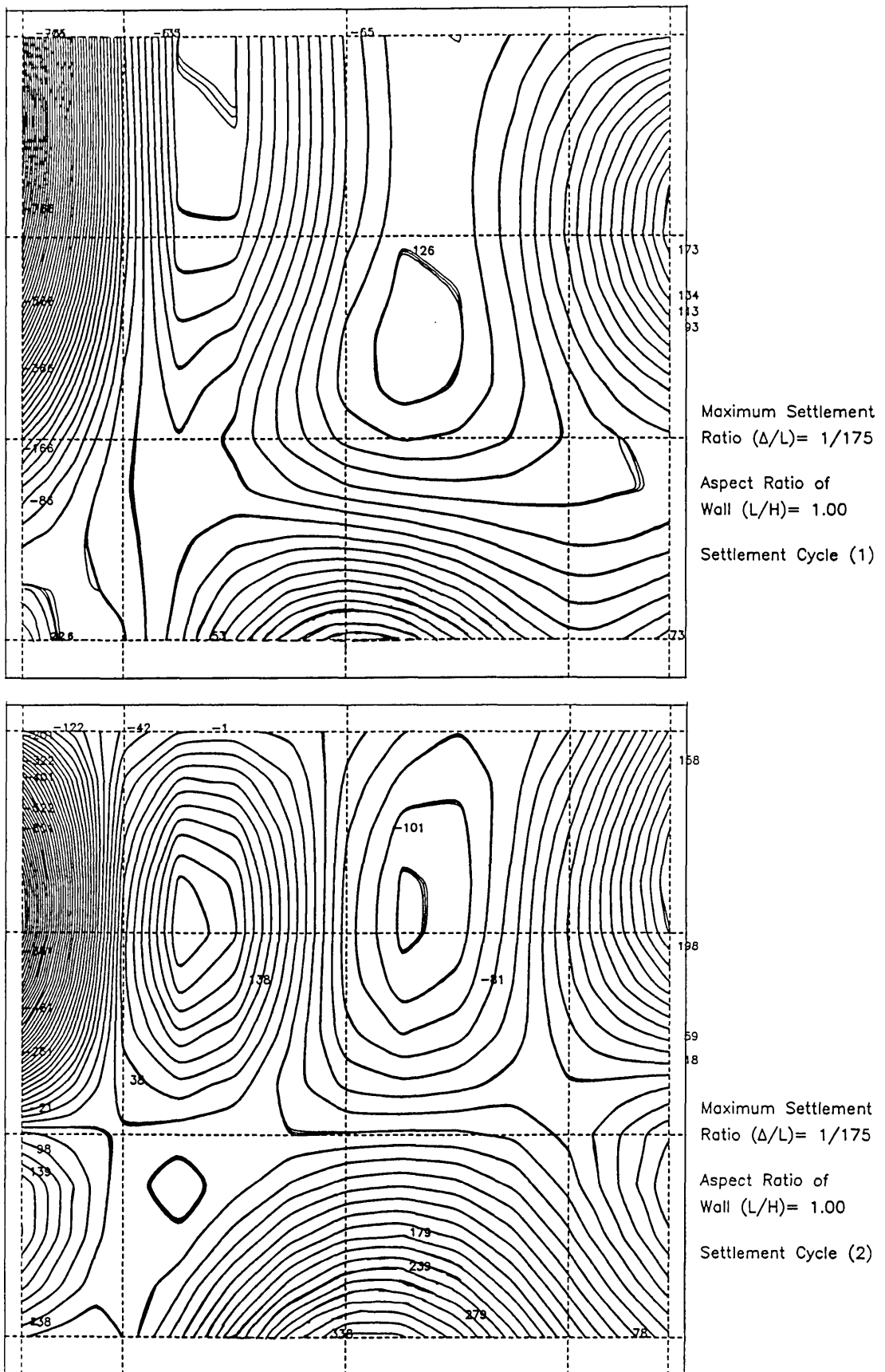


Figure 8.43 Maximum principal strain distribution of wall (Test W4AB).



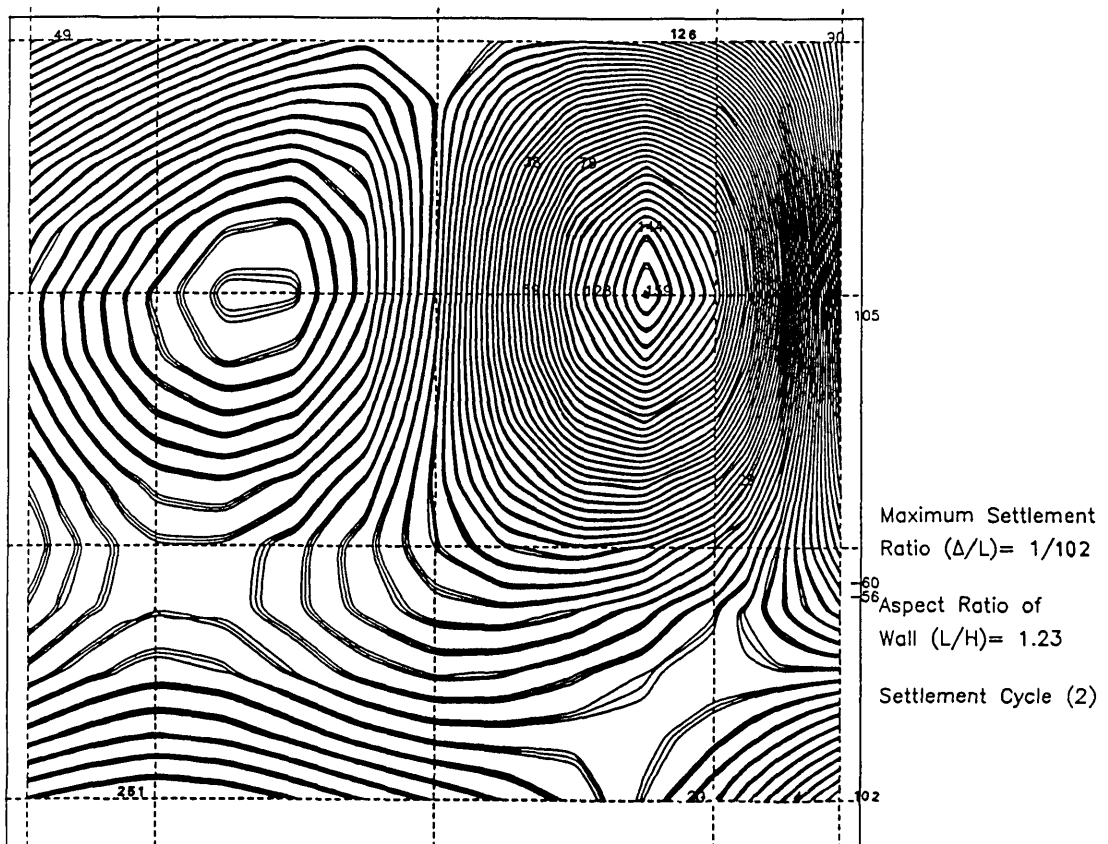
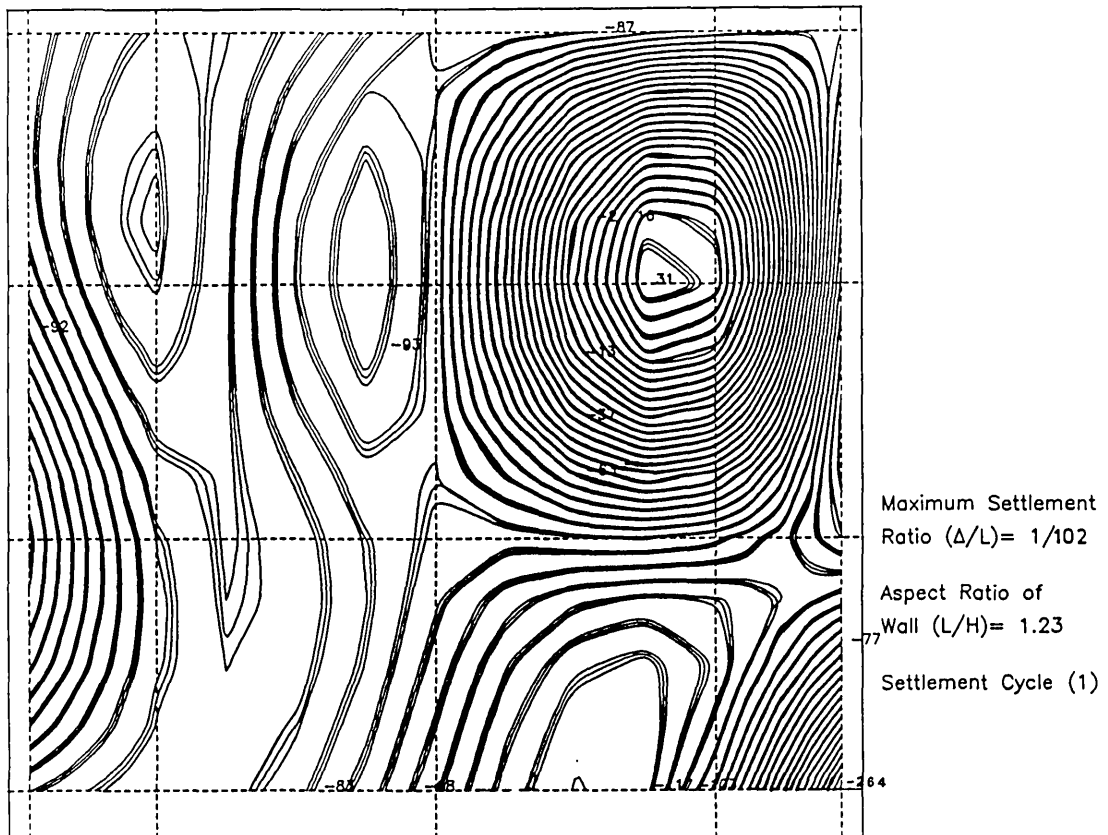


Figure 8.44 Maximum principal strain distribution of wall (Test W5AA).

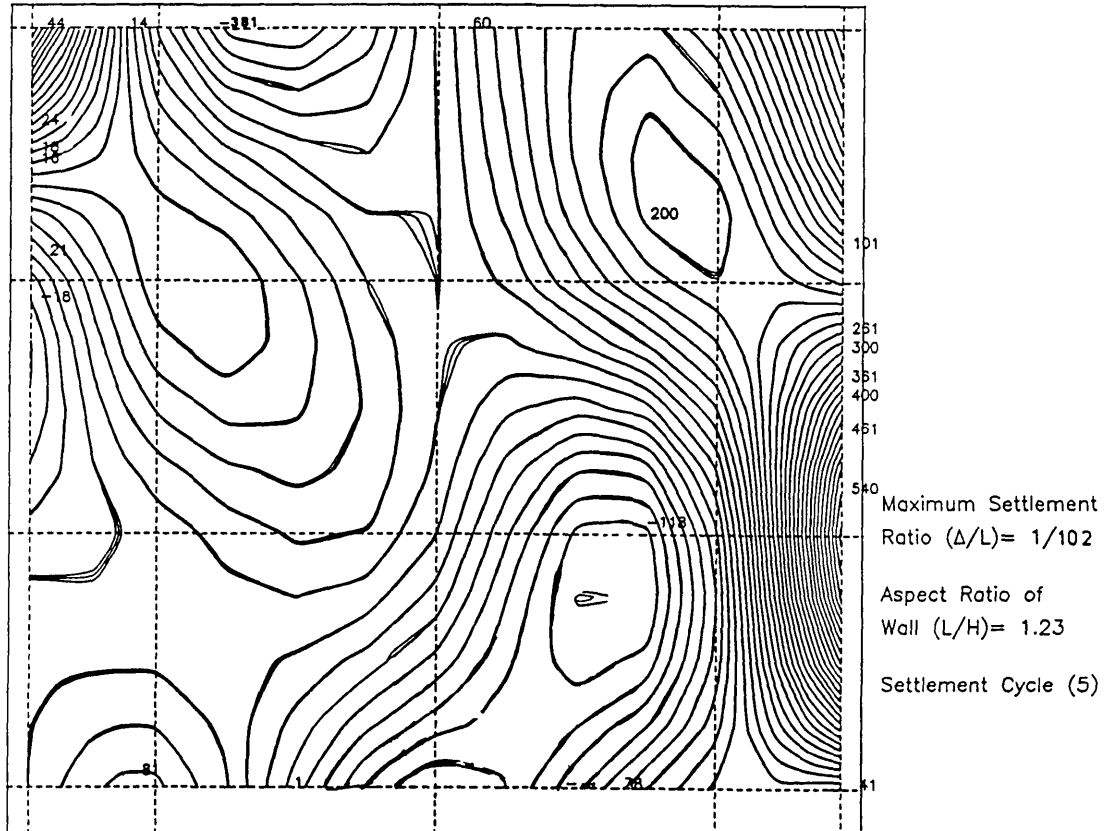
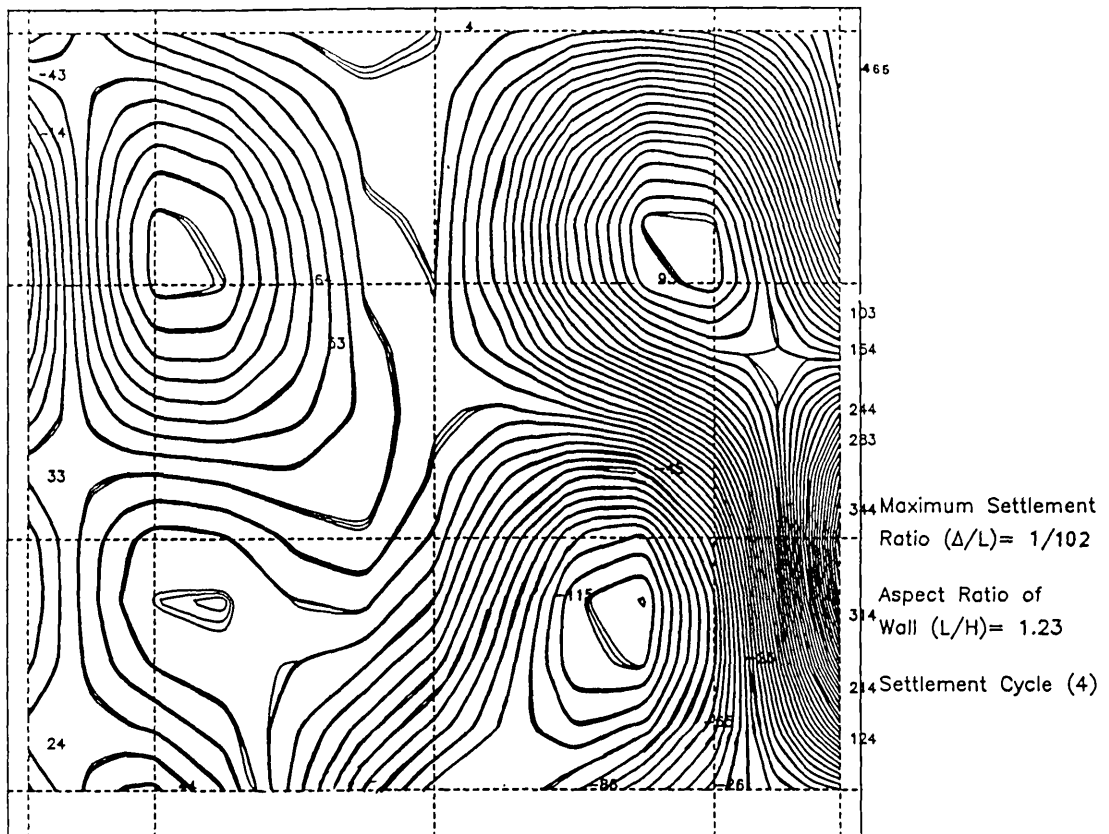


Figure 8.44 Continued.

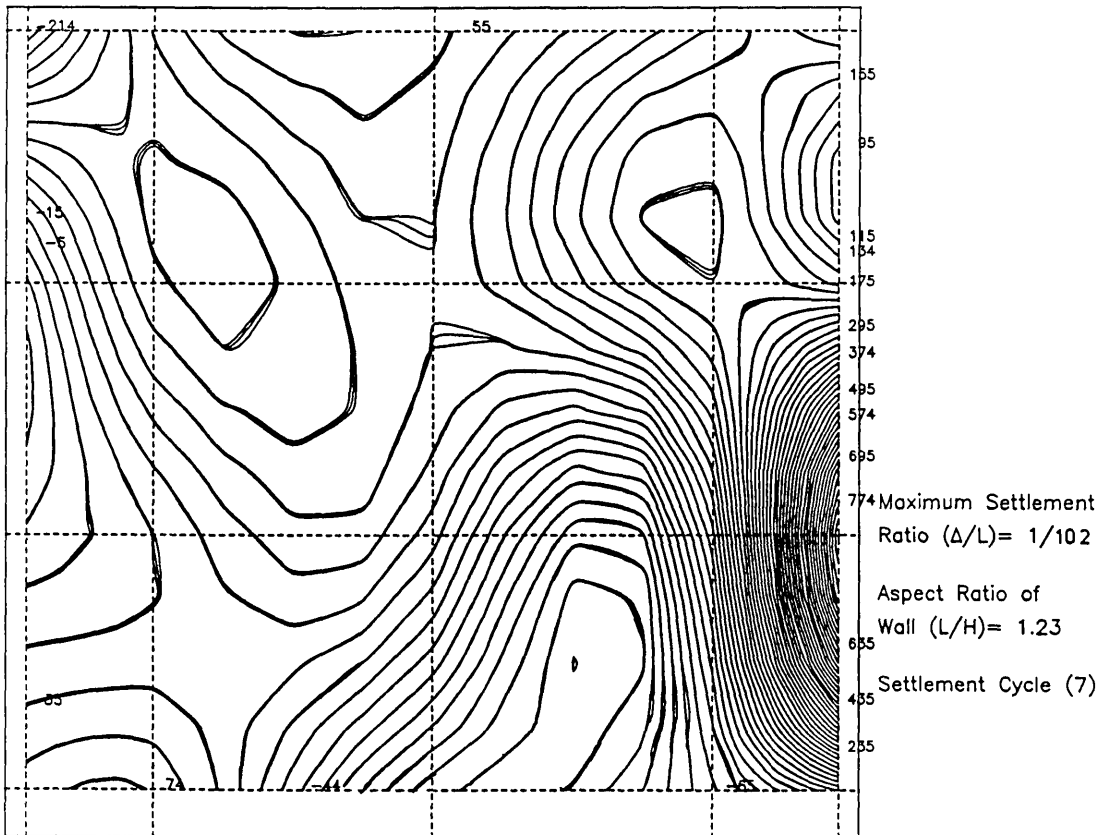
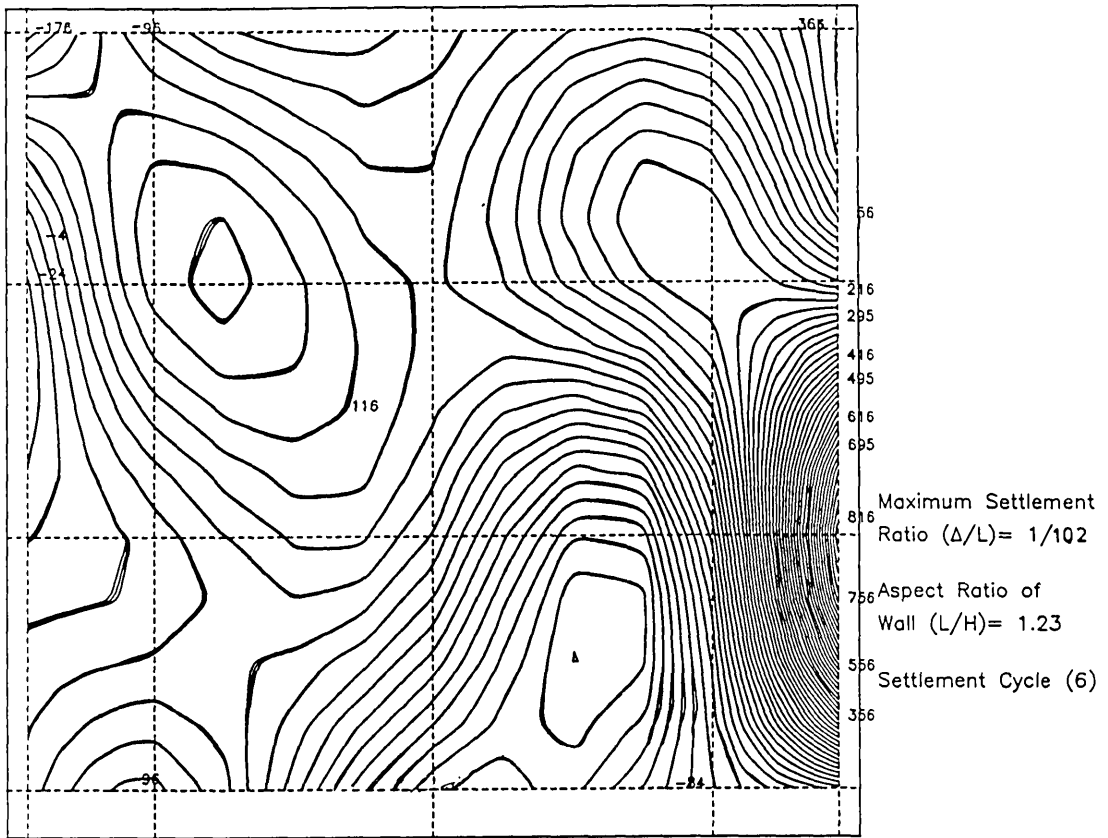


Figure 8.44 Continued.

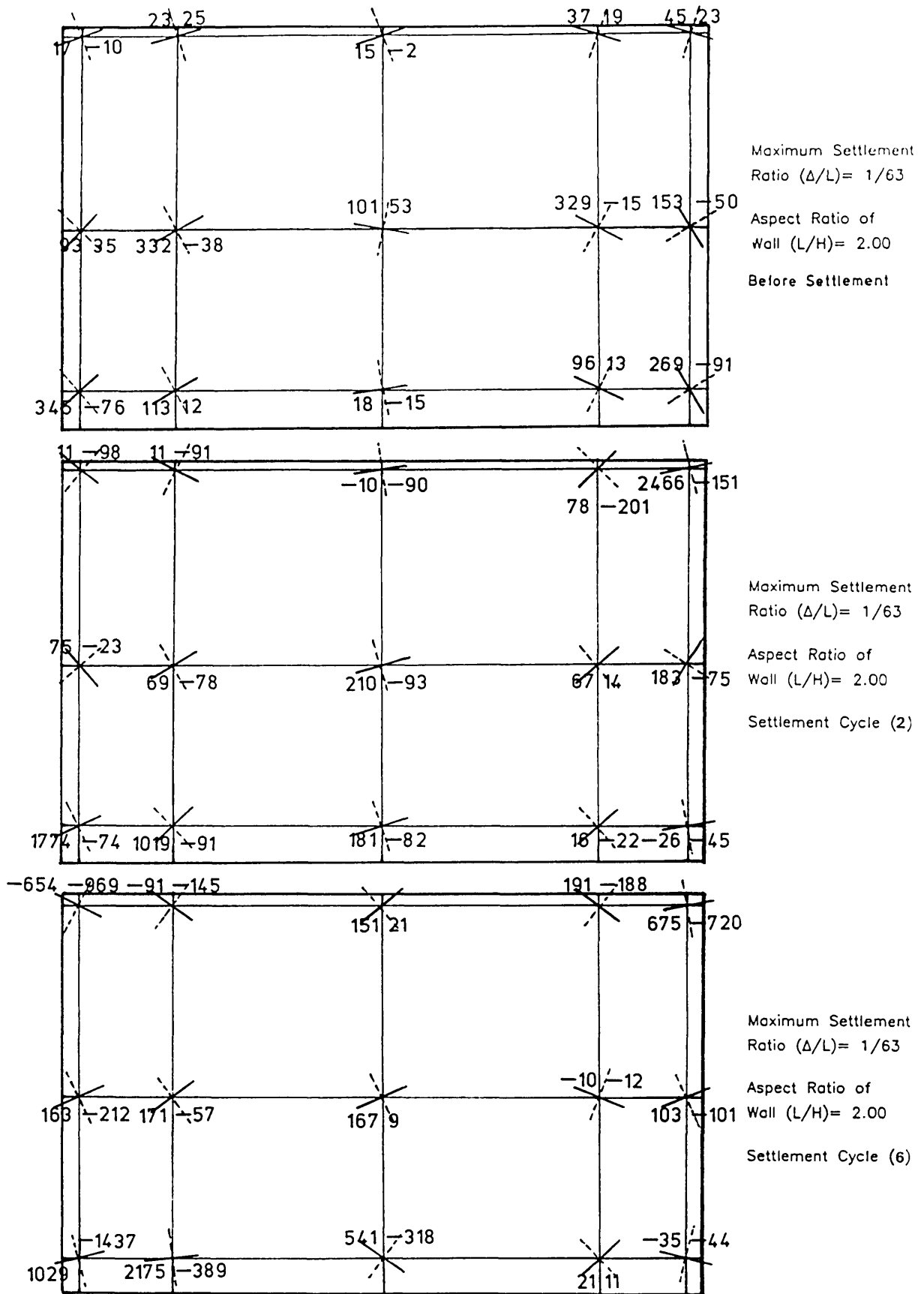
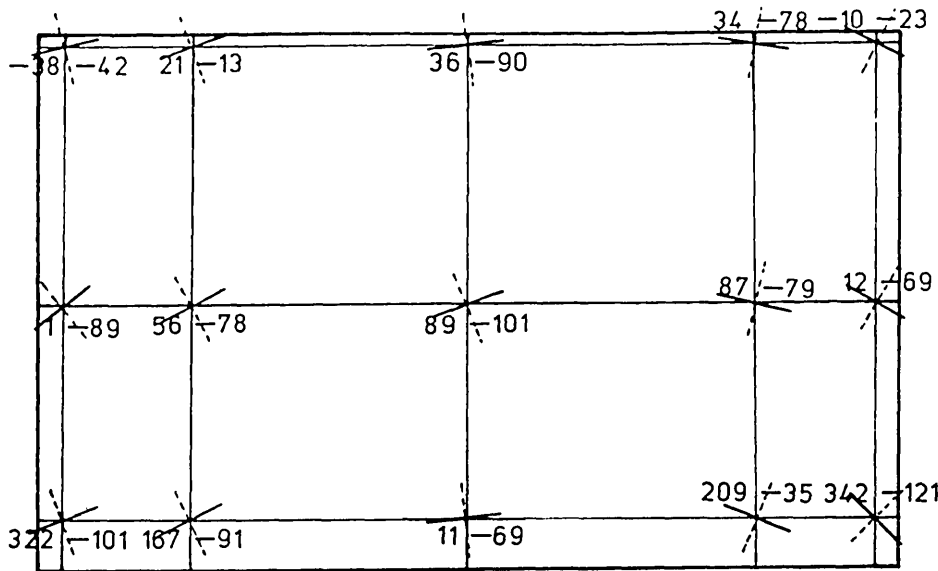
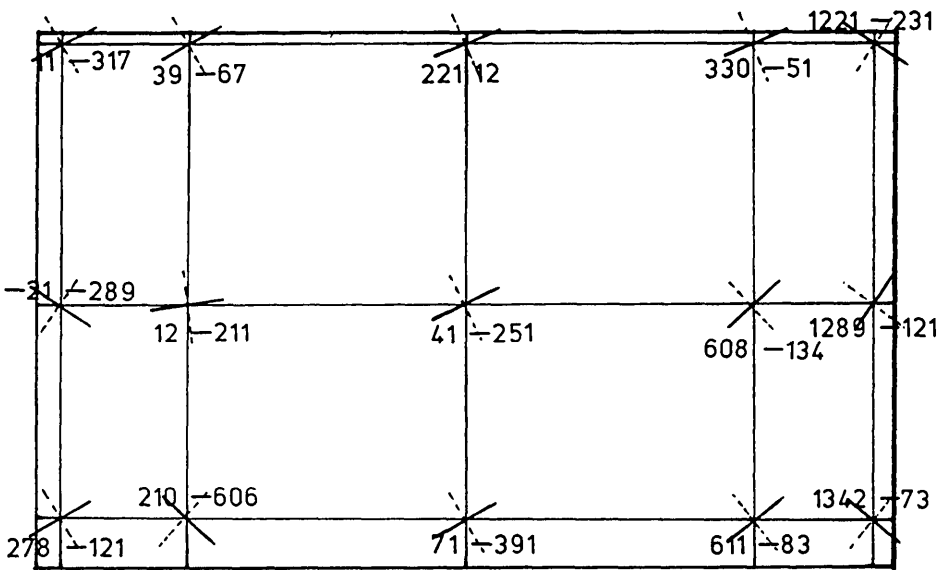


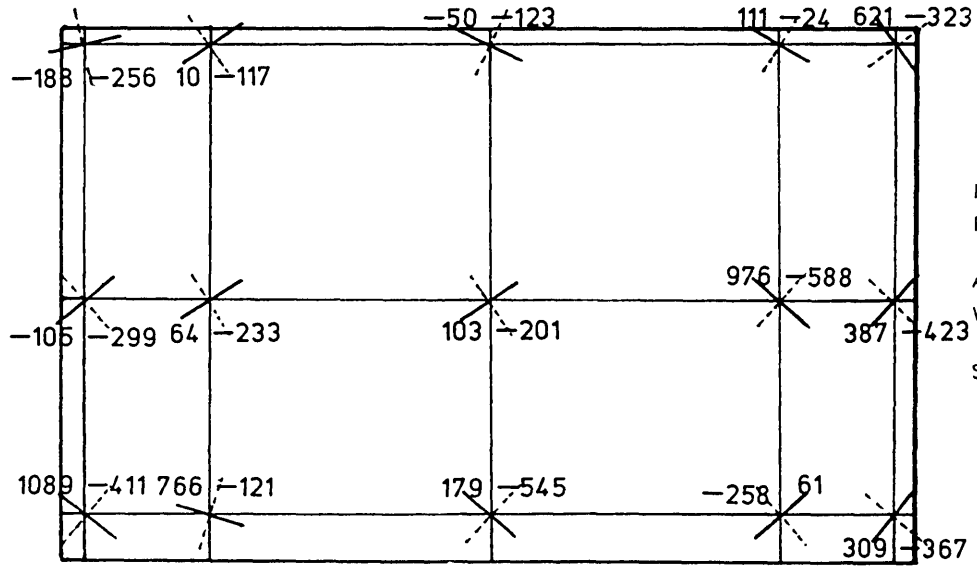
Figure 8.45 Distribution of maximum and minimum principal strain (Test W1AA).



Maximum Settlement Ratio  $(\Delta/L) = 1/51$   
 Aspect Ratio of Wall  $(L/H) = 1.625$   
 Before Settlement



Maximum Settlement Ratio  $(\Delta/L) = 1/51$   
 Aspect Ratio of Wall  $(L/H) = 1.625$   
 Settlement Cycle (4)



Maximum Settlement Ratio  $(\Delta/L) = 1/51$   
 Aspect Ratio of Wall  $(L/H) = 1.625$   
 Settlement Cycle (6)

Figure 8.46 Distribution of maximum and minimum principal strain (Test WLAB).

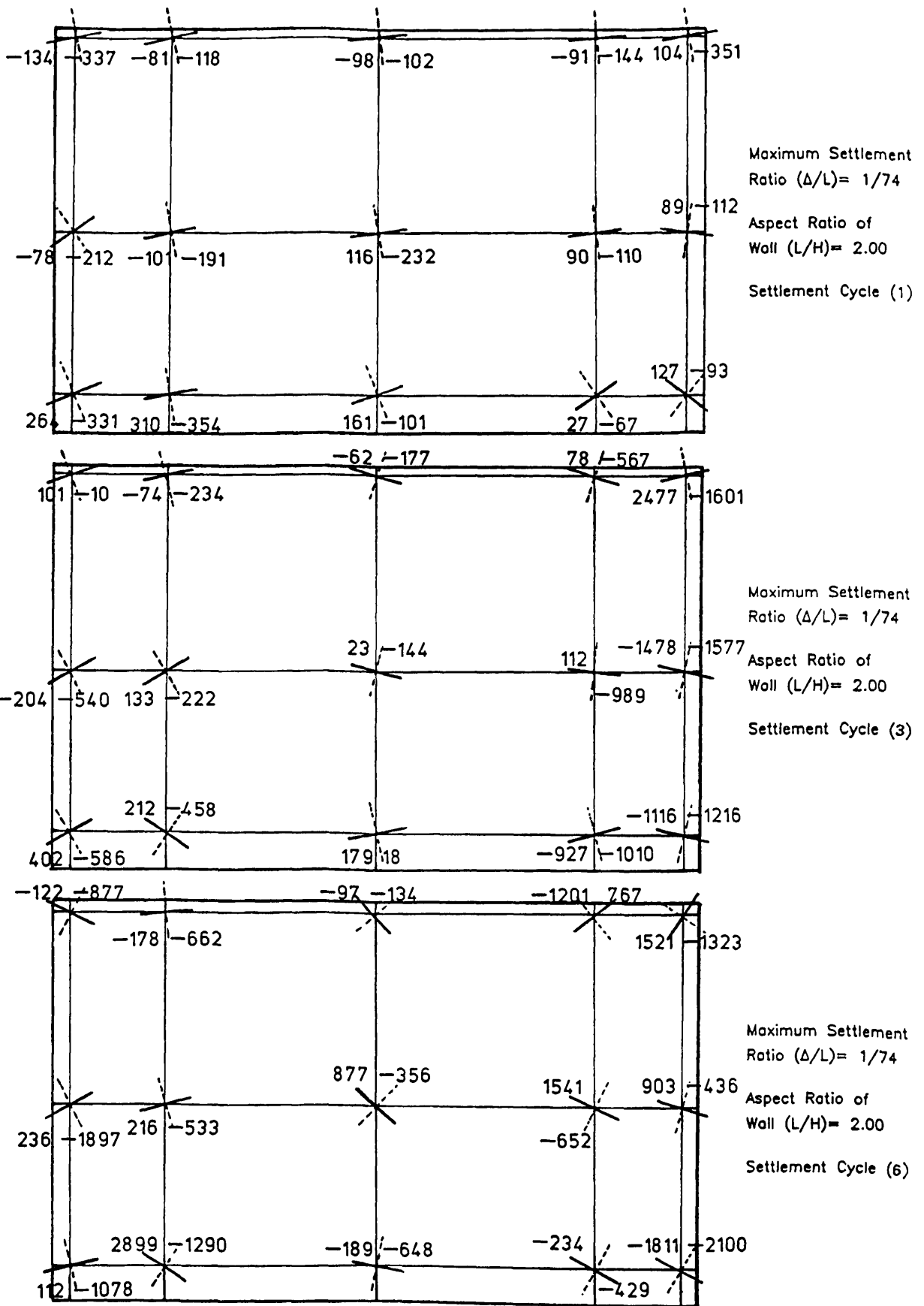


Figure 8.47 Distribution of maximum and minimum principal strain (Test W3AA).



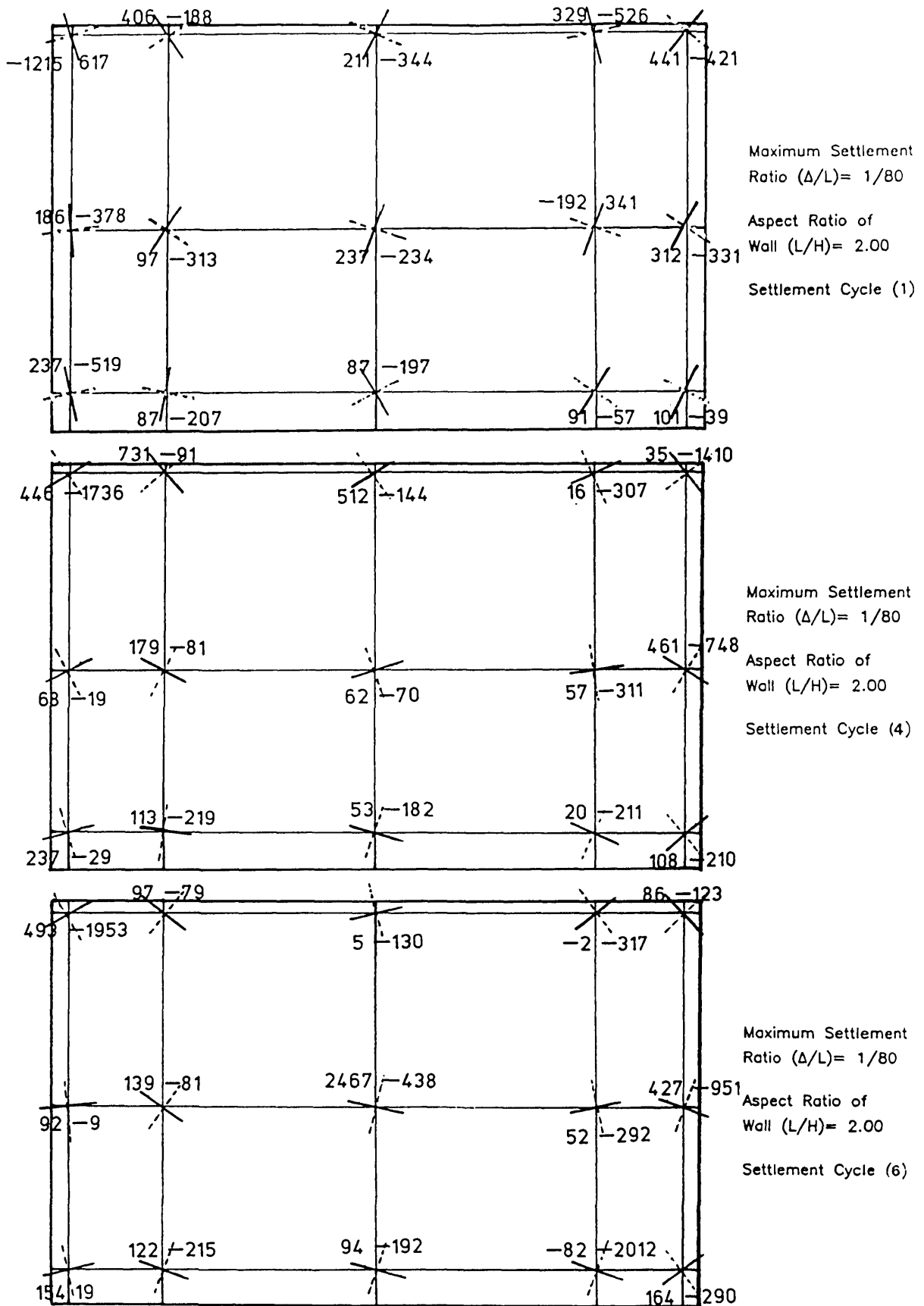


Figure 8.48 Distribution of maximum and minimum principal strain (Test W3BA).

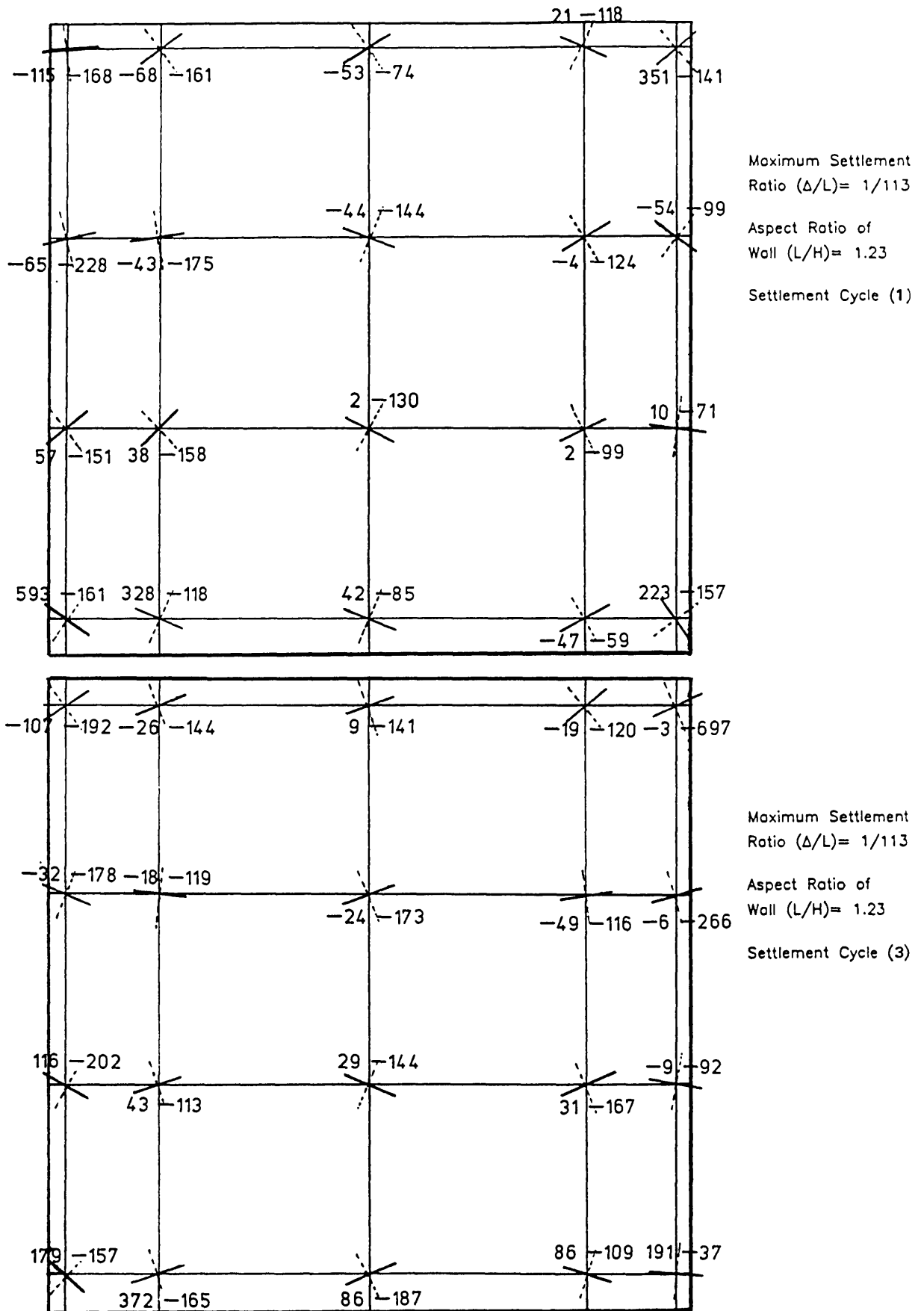
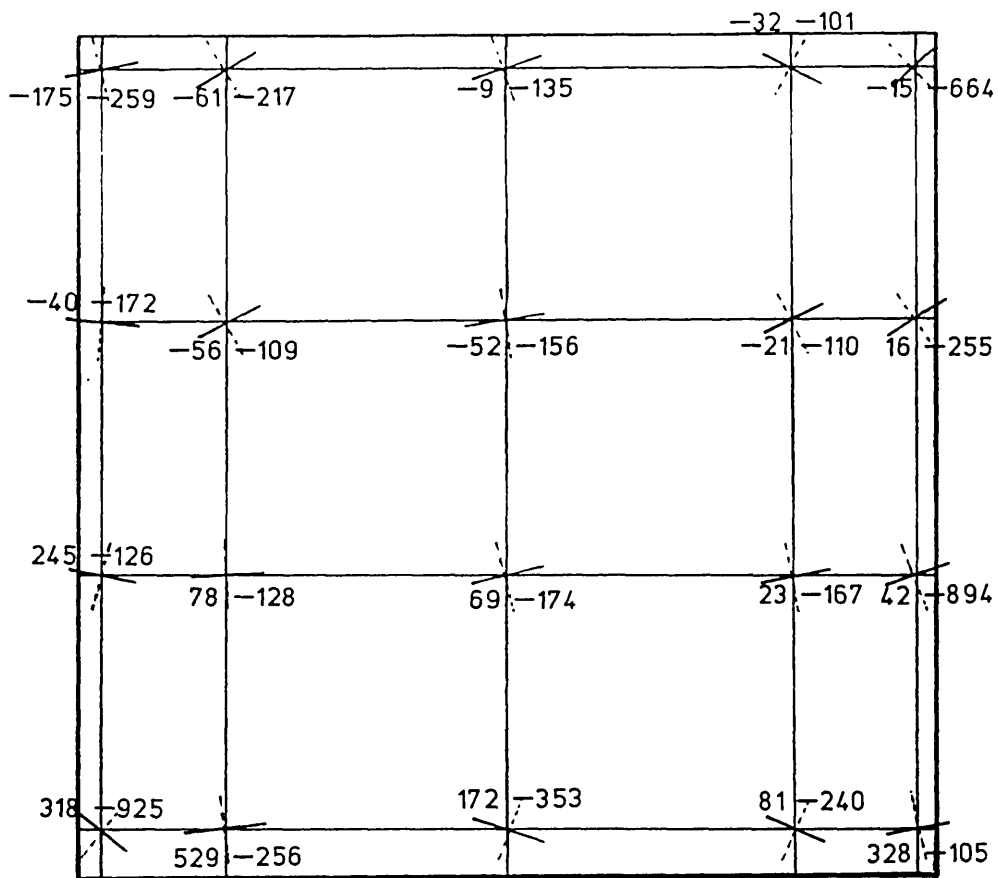
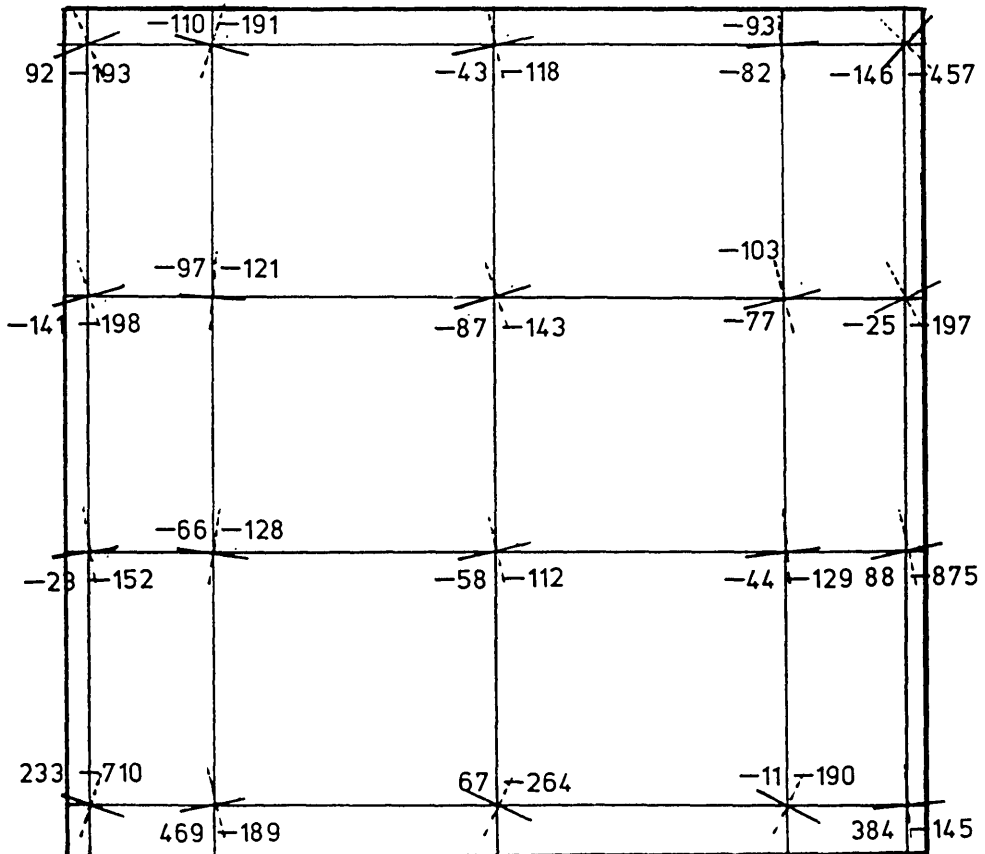


Figure 8.49 Distribution of maximum and minimum principal strain (Test W4BA).



Maximum Settlement Ratio ( $\Delta/L$ )= 1/113  
 Aspect Ratio of Wall (L/H)= 1.23  
 Settlement Cycle (5)



Maximum Settlement Ratio ( $\Delta/L$ )= 1/113  
 Aspect Ratio of Wall (L/H)= 1.23  
 Settlement Cycle (6)

Figure 8.49 Continued.

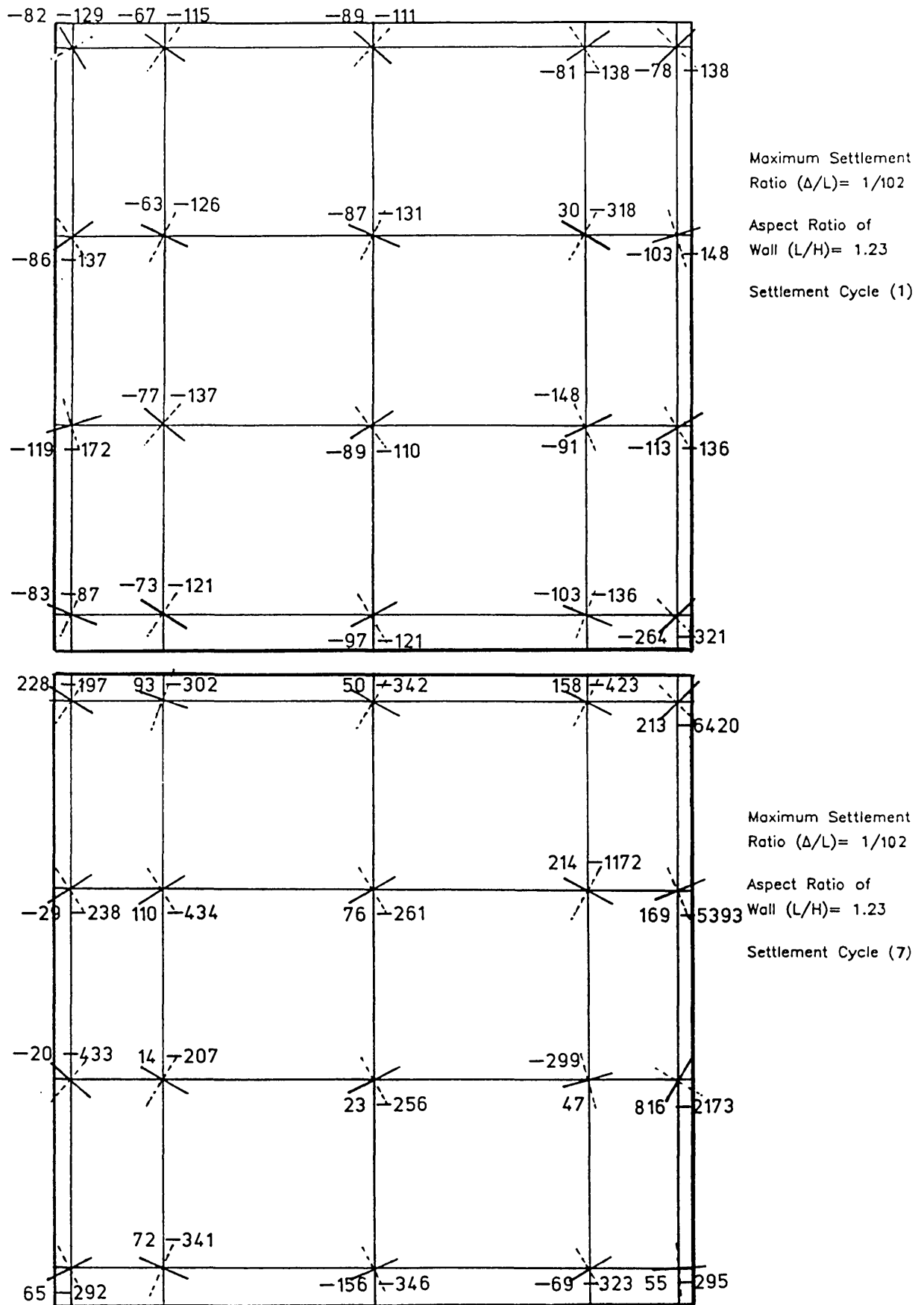


Figure 8.50 Distribution of maximum and minimum principal strain (Test W5AA).

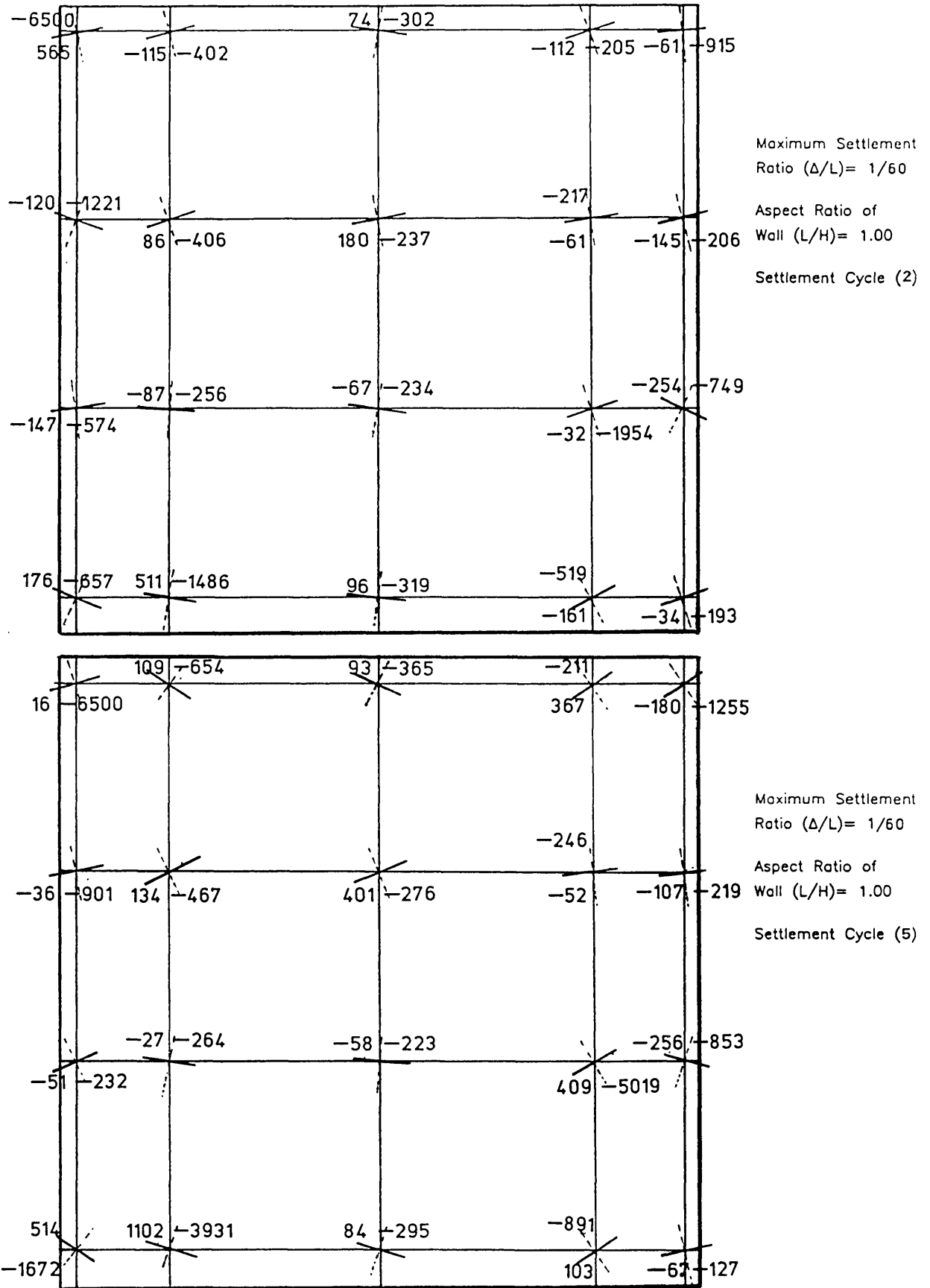


Figure 8.51 Distribution of maximum and minimum principal strain (Test W5BB).

propagated at lower load lost in the shorter beam than in the longer one (that is, with high aspect ratio), but the same crack width was measured at equal deflection ratios of the two beams. All beams cracked when using fixed supports, while for the beams supported on rollers (point supports), little cracking was detected (tests W3 and W5). In tests W1 and W2, early cracking occurred at a maximum support movement of 11 mm, while in test W3, the hinge crack occurred much later, at 21 mm settlement. Increased crack width was also measured on excessive deformation in tests W1 and W2, that was due to the rotation of the beam, while in test W3, increased rotation due to the point support caused reduction in the crack width.

Two distinct failure patterns occurred in the walls. The first was caused by diagonal cracking across the wall, and the other was due to a vertical splitting crack at the fixed support edge of the wall. Diagonal cracks propagated opposite to the settling support, starting at the top of the wall, as shown in Figure 8.52. Simultaneously, cracks were initiated at the bottom of the wall near the fixed supports, but no sign of cracking was observed at the middle of the wall except in later stages of settlement (test W3). However in tests W1 and W2, cracking in the walls propagated from the top corner at the settling support to the bottom opposite corner. Crack width of 7-8 mm was recorded for tests W1 and W2, with maximum crack width at the top of wall and minimum at the bottom. Cracks along the diagonal were observed first in the short wall, except upon the occurrence of a vertical crack where damage was recorded in the two longer walls at the same differential settlement (Figures 8.52-8.53). For tests W3BA and W3BB, the diagonal crack shifted closer to the settling support with higher deflection ratio and smaller crack width of 1-2 mm (Figure 8.54).

The occurrence of a vertical crack was brittle and sudden, stretching three to four courses of brickwork at one time. Even if diagonal cracking preceded the vertical crack, the later one dominated the failure pattern in the latter stages of settlement. As a result, crack width increased only along the vertical crack and no change was recorded in the initial diagonal crack. Thus the maximum crack width was measured at the top of the wall upon occurrence of vertical crack, that is, 8-10 mm in test W2AA (Figure 8.53). Diagonal cracks propagated through the mortar only around the bricks, while vertical cracking split straight through both the mortar and the bricks (refer to Figures 8.53-8.55).

Table(8.2) Description of damage of FPSS models.

Test No.	Maximum deflection of ring beam (mm)	Maximum warping (mm)	Maximum lost load at settling support $\frac{P_t - P_i}{P_t}$ (%)	Maximum beam rotation $\Theta$ (radians)	Description of damage	
					Ring beam	Brickwork wall*
W1AA	35.2	26.4	45	-	Shear crack near the fixed support end, at 500mm from support. Hinge cracking at the fixed support.	Diagonal cracking from top of wall to bottom opposite to settling support.
W1AB		21.4		-		Diagonal cracking from top of wall (2 courses down) to bottom brick course, w = 5-6mm.
W1BA	43.7	27.8	50	-	Hinge crack at the fixed support.	Diagonal cracking from 3 courses down the top of wall to the bottom of wall, with slight vertical crack, w = 14 mm.
W1BB		31.4		-	Hinge crack at the support with $w_{max} = 0.5mm$ .	Diagonal cracking from 4 courses down the top of wall. Cracking at the beam wall interface, w = 8-10mm.
W2AA	28.8	17.1	45	-	Two hinge cracks at the fixed support. Hinge crack at the fixed support.	Diagonal cracking from top to 4th-5th brick course.
W2AB		13.6		-		Diagonal cracking starting at the bottom and top of wall, followed by vertical splitting crack, w = 8-10mm.
W2BA	29.8	28.2	52	-	Hinge crack.	Diagonal cracking followed by vertical crack w = 2 mm. Diagonal cracking extending from top of wall to the beam-wall interface at the fixed support, w = 3-4mm.
W2BB		21.5		-	Hinge crack.	
W3AA	30.5	18.2	65	0.15	No damage.	Vertical cracking at edge of settling walls followed by diagonal cracking. Diagonal cracking opposite to settling support, w = 2-3mm.
W3AB		14.6		0.18	Hinge crack occurring at cycle 4.	
W3BA	28.9	18.6	63	0.21	No damage.	Diagonal cracking extending from top of wall to 4-5 courses high at bottom. Two diagonal cracking; one from top of wall to 10th brick course and the other starting at 10th course from the wall edge to the wall-beam interface, w = 1-2mm.
W3BB		23.5		0.23	Hinge crack occurring at cycle 6 with $w_{max} = 0.2mm$ .	
W4AA	10.4	7.8	31	0.10	No damage.	No cracks apparent at tested walls but experienced cracking at adjacent walls - mainly as vertical splitting crack, w = 5-6mm.
W4AB		13.2		0.13	No damage.	
W4BA	20.1	10.7	37	0.09	No damage.	Vertical edge crack propagating from top of wall to 8th course. Vertical splitting cracking at fixed support end stopping at the 5th course (bottom of wall) while vertical cracking at settling end at 9th brick course, w = 7-8mm.
W4BB		18.2		0.10	No damage.	
W5AA	21.7	21.6	32	0.10	No damage.	Vertical crack at edges of wall, as the diagonal cracking occurring at cycles 5-6 at maximum deflection, w = 1-2mm.
W5AB		16.38		0.12	No damage.	
W5BA	32.1	35.1	40	0.11	Shear crack at mid span. Hinge crack at the support in cycle 5.	Vertical crack occurring at settling edge followed by diagonal crack extending from middle of the wall to mid span at the beam wall interface, w = 2-2.5mm.
W5BB		20.8		0.13		

\* All diagonal cracks propagated opposite to the settling support.

w - width of crack.

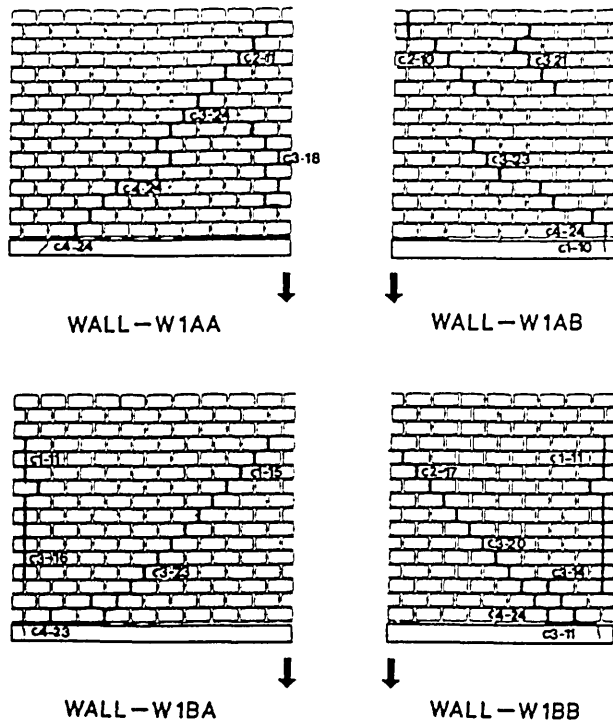


Figure 8.52 Crack propagation during settlement (Test W1).

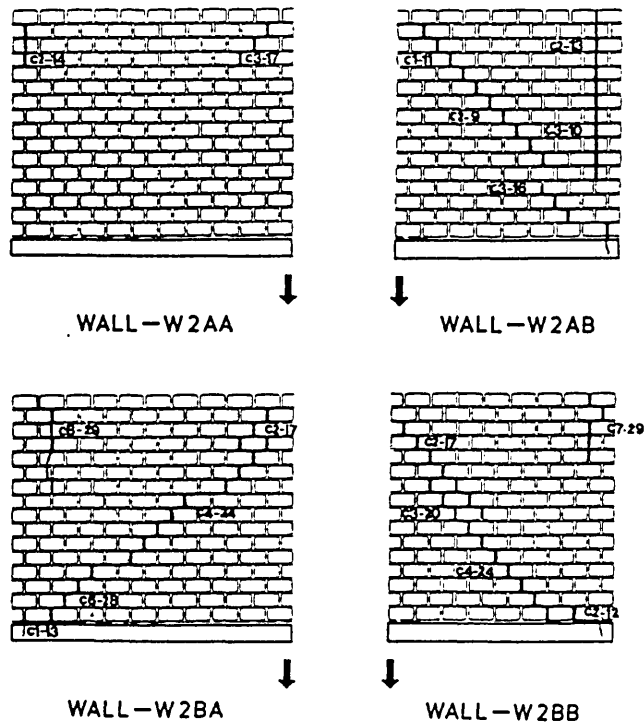


Figure 8.53 Crack propagation during settlement (Test W2).



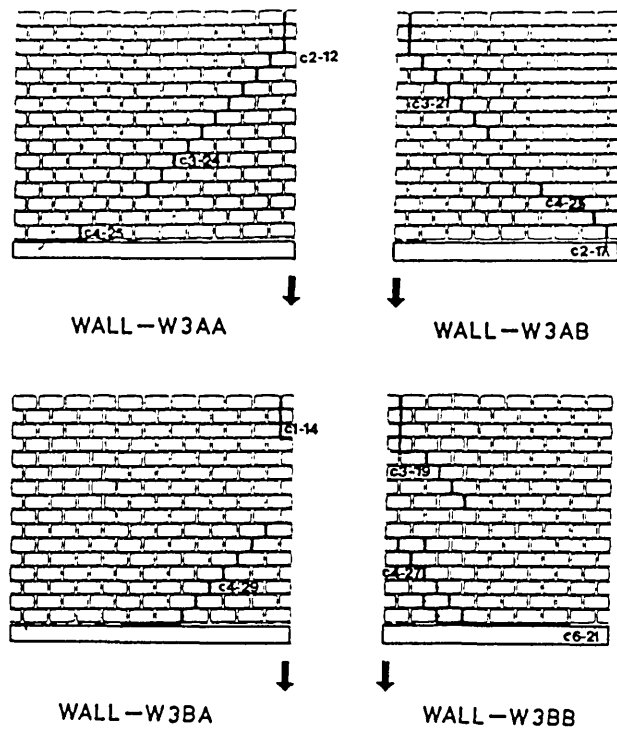


Figure 8.54 Crack propagation during settlement (Test W3).

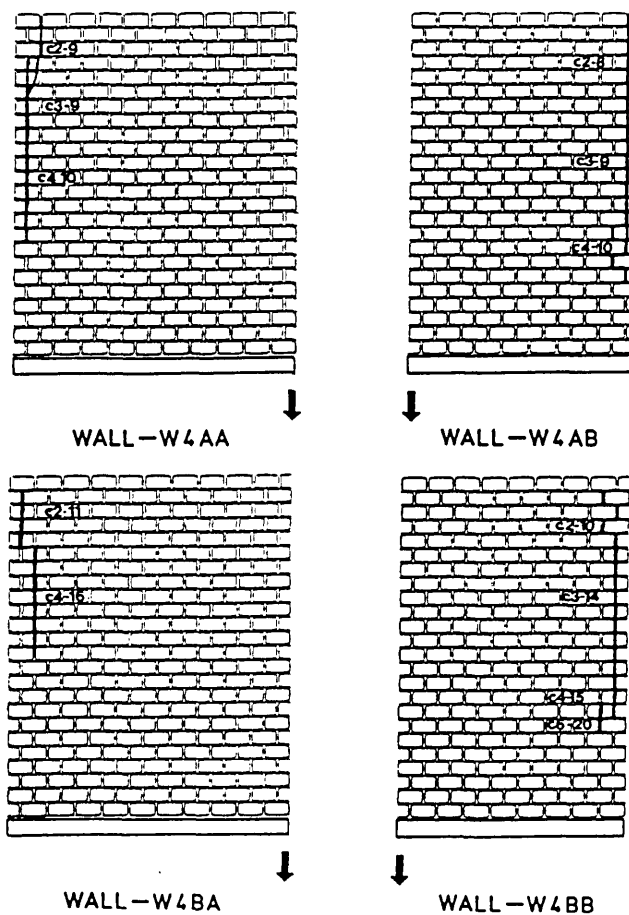


Figure 8.55 Crack propagation during settlement (Test W4).

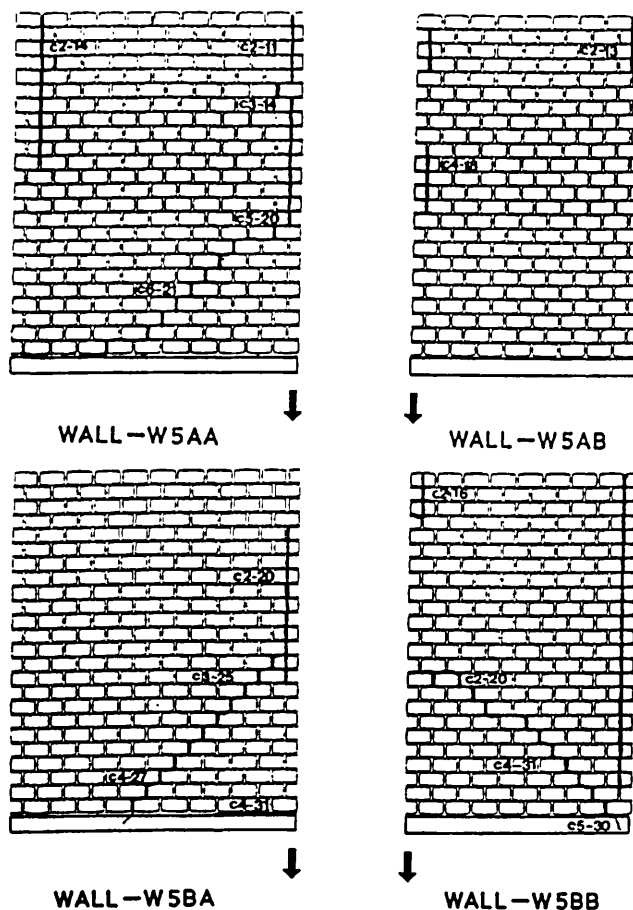


Figure 8.56 Crack propagation during settlement (Test W5).

Reinstatement of the structure by the rejack of the supports closed most of the diagonal cracks, where a maximum crack width of 0.5 mm was present only in test W3, reduced from an initial 1.5–2.5 mm crack. In test W2, however, a crack of width of 2–3 mm remained after five cycles of settlement and restoring the support to its initial position. Cyclic settlement of test W2AB (Figure 8.53) increased the vertical crack width to 8–10 mm where the test was abandoned since 4–5 mm crack was still remaining at zero settlement. This was possibly due to debris and loose mortar particles obstructing crack closure. No clogging was observed in the diagonal cracks, even when the support was taken to 30 mm of settlement.

For tests W4 and W5 with walls of low aspect ratios, vertical cracks dominated the pattern of the wall failure (Figures 8.55–8.56). In both tests W4A and W4B, large cracks of 7–8 mm developed; upon rejack, a residual 2–3 mm crack was present. The effect of reinforcement of the top courses of the brick wall (test W5), is that vertical cracking was delayed, occurring at later stages of settlement, thus initiating a diagonal crack (Figure 8.56). Cracking was limited to 1–2 mm, while settlement of the supports was taken to a maximum of

32.1 mm. This is in comparison to test W5A, where only 21.7 mm was recorded. Increased deformation of the structure also caused cracking to occur in the ring beam at point supports at later stages of settlement (test W5BB). In test W5BA, however, cracking in the beam developed at mid-span after propagating through the wall.

#### **8.6 PHOTOGRAPHS OF WALLS**

Figures 8.57-8.64 show the damage caused in tests W1-W5.

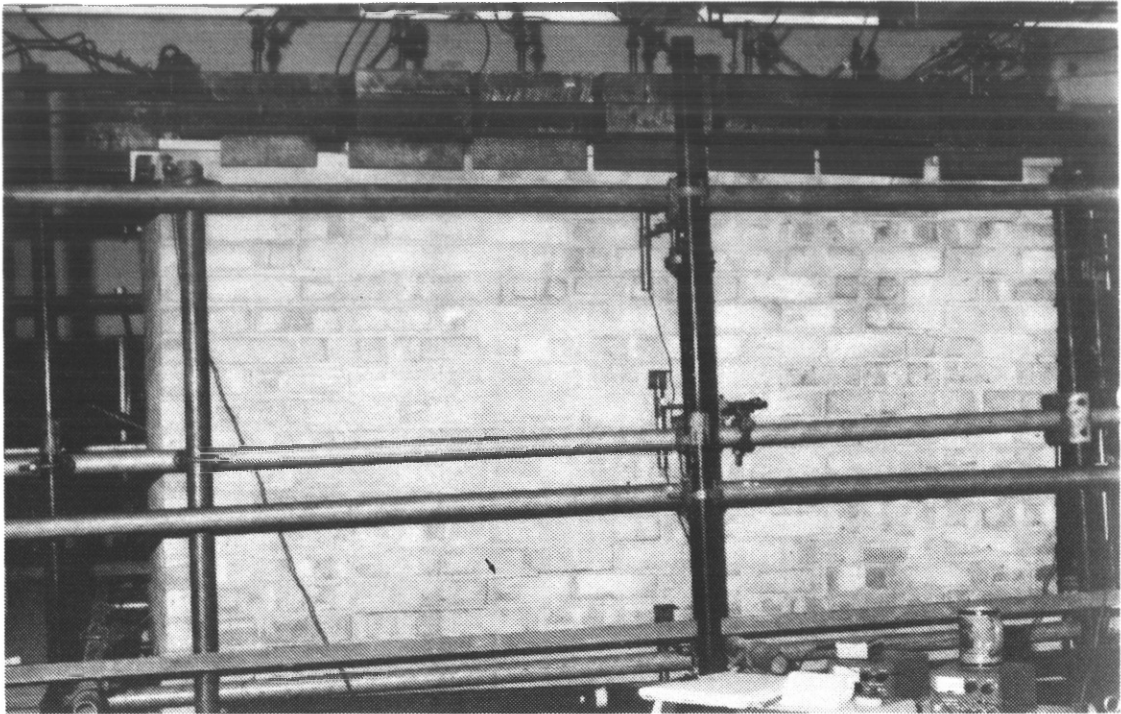


Figure 8.57 Diagonal cracking of FPSS wall after settlement (Test W1).

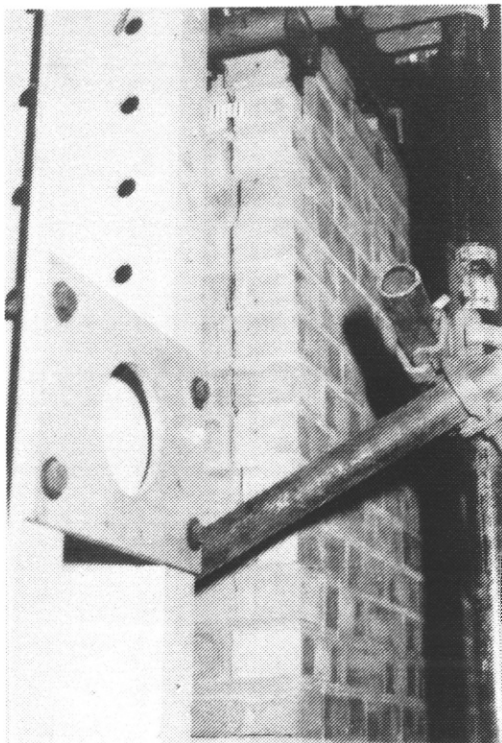


Figure 8.58 Vertical cracking along edge of wall (Test W2).

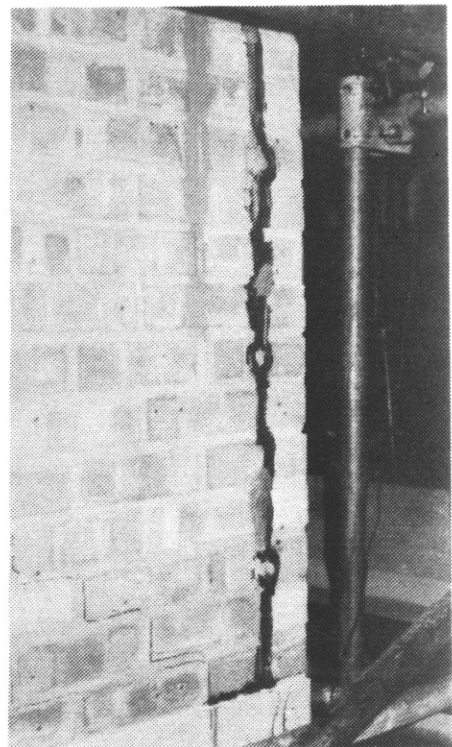


Figure 8.59 Repairs of vertical crack (Test W2).

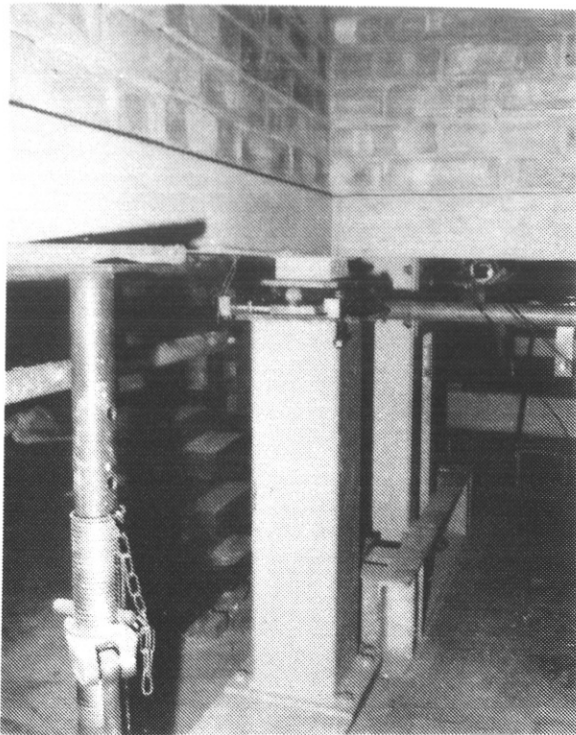


Figure 8.60 Rotation of point support on settlement (Test W3).

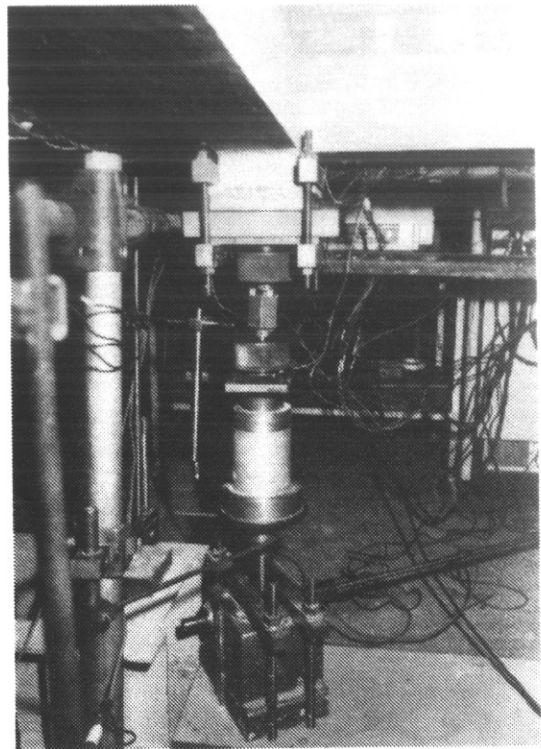


Figure 8.61 Tilting of settling support due to rotation of ball joint (Test W3).

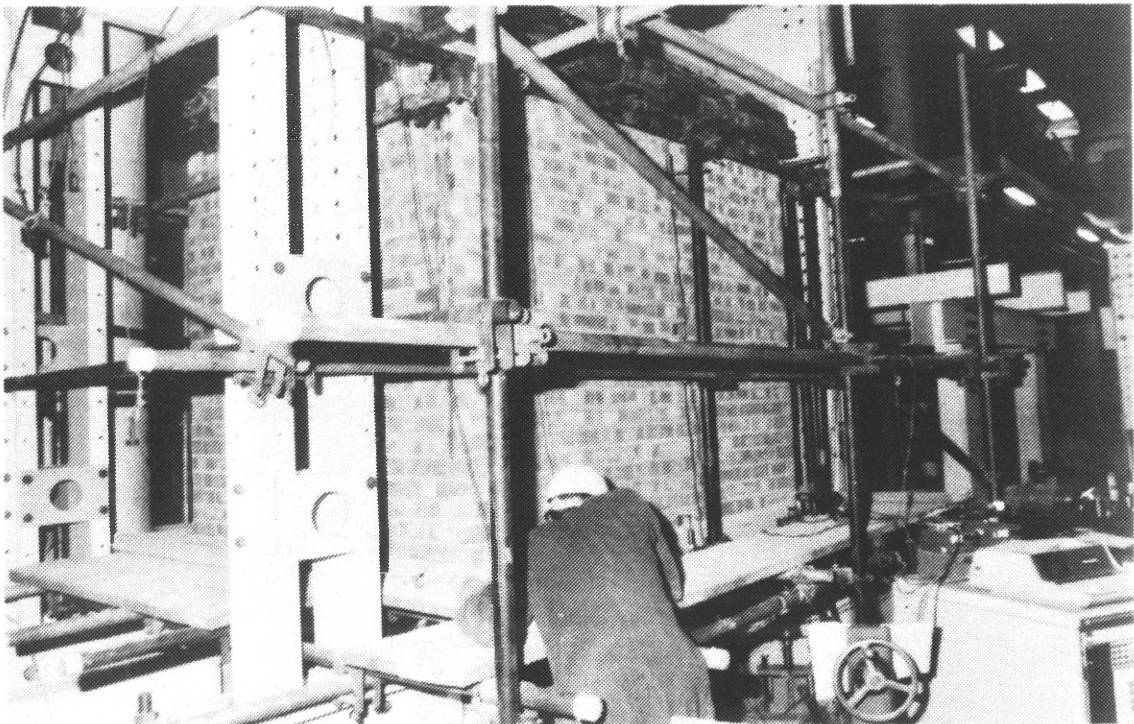


Figure 8.62 Vertical splitting crack along edge of adjacent wall (Test W4).

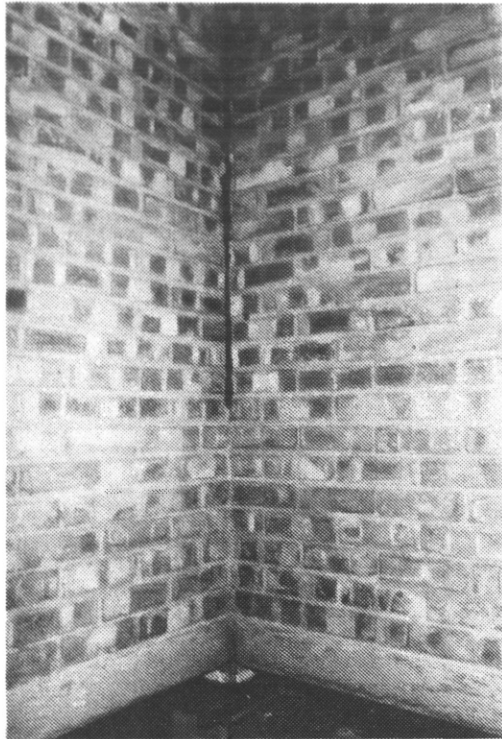


Figure 8.63 Vertical edge crack at the intersection of main and adjacent walls (Test W4).



Figure 8.64 Diagonal cracking at lower courses of wall during settlement (Test W5).



## CHAPTER 9 GENERAL DISCUSSION AND ASSESSMENT OF THE FOUR-POINT-SUPPORT-SYSTEM

### 9.1 INTRODUCTION

This chapter discusses the experimental results reported in Chapter 8, and presents comparisons of theoretical models and experimental results. Assessment is made of the four-point-support-system as a design solution for enhancing the behaviour of structures subjected to differential settlement. In some cases, a comparison of experimental results is made with results obtained from the literature. The feasibility of theoretical models for predicting differential settlement with respect to the limiting criteria of damage is described.

### 9.2 STRUCTURAL BEHAVIOUR OF FPSS

#### 9.2.1 Differential movement of supports

The experimental results have shown that the FPSS allows a considerable increase of differential movement and rotation of the supports with minimal damage in the walls in comparison with traditional masonry buildings (refer to Table(8.2)). A study of the amount of deformation has shown that point supporting of the ring beam allowed rotation, that increased the capacity of the structure to deform without increasing the degree of damage. The low moment capacity of the ring beam resulted in an increase of deformation that initiated cracking of the walls at later stages of settlement. The effect is that only about 45%-52% of the supporting load was allowed to dissipate at maximum deflection. Thus, reduction of the cantilevering effect of the structure over its settled supports, decreased the tendency of brittle failure of the walls. Introducing point supports increased the loss of supporting load at the settling end to approximately 63%-65% for the same amount of settlement (refer to Table(8.2)). Thus, the structure was able to deform more easily, with a larger loss of support load; where settlement was accommodated within the walls of the structure rather than in the ring beam. This had the effect of reducing the degree of cracking in the wall.

Since the maximum deflection of the FPSS model is influenced by the degree of damage and the observed width of crack, the experiments

undertaken showed that the maximum limiting deflection is dependent on the aspect ratio of the walls and the strength of the ring beam.

A study of the degree of damage observed, Figure 8.52 through to 8.56, together with the maximum deflection recorded, shows that the walls with lower aspect ratio (L/H) experienced more cracking at low magnitudes of differential settlement than walls with high aspect ratios. The wall aspect ratio also affected the pattern of cracking, where diagonal cracks occurred at higher aspect ratios, whilst the higher walls (that is, low aspect ratio) developed vertical cracks at lower magnitude of settlement. Settlement of the FPSS box was accommodated partly by the ring beam and partly by deformation of the box walls. For the walls with a longer span (that is, high aspect ratio), more deformation could take place before serious cracking was observed. Thus, first cracking was induced in the ring beam as well as the walls. However, for shorter spans, the walls were not able to take large deformation without inducing serious cracking in the walls, while the ring beam suffered little or no damage (Table(8.2)). The magnitude of limiting deflections that the walls were able to accommodate is dependent upon the mode of deformation and the effect of the aspect ratio in modifying this mode. The use of a ring beam with low stiffness compared to that of the wall changes the behaviour of the beam-wall structure during settlement from a cantilever structure, as the case may be for a stiffer beam, to a flexible base where the walls are better able to rotate. The magnitude of this increase in rotation and, therefore of the increase in maximum deflection, is directly dependent upon the type of support, that is, point or fixed support, and on the strength of the ring beam. Likewise, introducing a weak short column joint in the ring beam near the supports is also shown to increase the rotation of the beam (refer to Figures 8.54-8.56).

### **9.2.2 Deformation of walls**

Examining the lateral deformation of the walls compared to the magnitude of maximum vertical deflection, the flexible deformation of the walls with minimum cracking is apparent. Although both FPSS models W2 and W3 (Figures 8.27 & 8.28) have been subject to approximately the same differential settlement, larger lateral deformation in W3 was measured. The increase in deformation, and the reduction of the degree of damage observed (Table(8.2)) confirms that point supported walls are able to move more easily and with minimal damage. The high walls (W4



and W5) were able to deform more laterally with respect to the maximum deflection of the beam than short walls (W3), but with wider cracks. The effect of reinforcing below the five top courses of the wall (test W5), was found to reduce the crack width considerably and, thus, the wall was able to deform more laterally than in test W3 (Figure 8.30).

A study of the out-of-plane warping of walls, Figures 8.31 through 8.35, has shown that wall W4 (low wall aspect ratio), subjected to less settlement, exhibited the same degree of warping as that of a wall with high aspect ratio (test W3) and having a larger magnitude of settlement (refer to Table(8.2)). Thus, the high walls (low aspect ratio) accommodate the large lateral deformation through larger distortional warping. Also, if the supports were fixed and were not able to rotate freely (test W1 & W2, with high aspect ratio), short walls would tend to accommodate large warping deformation. Figures 8.26 & 8.27 show that the lateral deformation of the wall did not change at the last cycles of settlement. For further settlement, it was observed that increases in crack width occurred rather than wall deformation. This effect was even greater in test W4, Figure 8.29. The evidence from the limited number of tests suggests that, to enable the walls to deform with less damage, they should be able to rotate freely (test W3), thus dissipating the differential movement through twisting of the adjacent walls. Lightly reinforcing the top courses increased the wall capacity to deform laterally and warp, rather than stiffening the top of the wall (W5). As a result, this caused a greater differential deflection to be accommodated with less damage, hence the ductility of the walls was enhanced.

### **9.3 CYCLIC BEHAVIOUR OF FPSS**

Hysteresis curves relating load lost at the settling support to maximum vertical deflection show the stiffness deterioration due to cyclic settlement of the support. A large percentage of the stiffness degradation in each model occurred in the first two cycles. Although the stiffness of the model decreased, together with an increase of deflection amounting to over 200%, the loss of support load was observed to drop only slightly for squat walls (Figures 8.11 through 8.16). For high walls, test W4, a large drop of load was observed, whilst the hysteresis cycles show a brittle failure pattern characterized by sudden increase in support load with slight increase in deflection. Examining

the effect of reinforcement on reducing the stiffness deterioration, wall W5 was able to accommodate larger deflection while maintaining no sudden drop of load. The result was also to reduce tilting of the top of the wall, with maximum vertical deflection at the soffit rather than at the top (Figure 8.19-8.20).

For most models, the tendency of the wall on unloading or on reinstating the structure to its initial position is to follow a pattern parallel to the loading relationship. This observation confirms that the structure is able to sustain the loss of support without failure, and is also stable on re-jacking of the support to the position of zero movement. The evidence is that the support is able to move differentially once more without a sudden large drop in the load or a jump in the magnitude of settlement observed. Additionally, the structure in all tests was able to reach its initial position without a large increase in the jacking force, whilst for tests W5AA and W5AB, the wall required the same magnitude of load lost at settlement to be reinstated. From the limited number of tests, it is observed that there is a requirement for larger magnitudes of jacking load to reinstate the structure in models having full beam-column joints rather than weaker joints. Thus, the weaker joint allows easier re-jacking of the structure, limiting the force required to close up the cracks.

Figure 9.1 shows the relationship between the energy ratio due to settlement and the magnitude of the vertical settlement measured at the peak of each cycle. The energy ratio  $E_D/E_T$  is defined as the ratio of the area enclosed in each hysteresis loop,  $E_D$ , to the total stored energy per cycle,  $E_T$ , defined as the total area under the ascending curve. The energy ratio per cycle generally was highest at the first cycle, and decreased for all the walls in the second and third cycles, where sudden drop of the graph denote cracking of the walls.

It seems evident that the energy ratio in test W3 (point supported walls) is generally higher than that lost by wall W2. The additional energy is dissipated by the increased articulation of the walls, in this case the increased rotation of the ring beam allowed more deformation before the initiation of visible damage. In both tests of model W2, for deflections exceeding 20 mm, there was a substantial decrease in the energy ratio, which explains the sudden increase in the degree of damage. For wall W4 (with low aspect ratio), there was a sudden decrease in the energy ratio at settlement that denoted a substantial decrease in the stiffness of the wall. However, the high

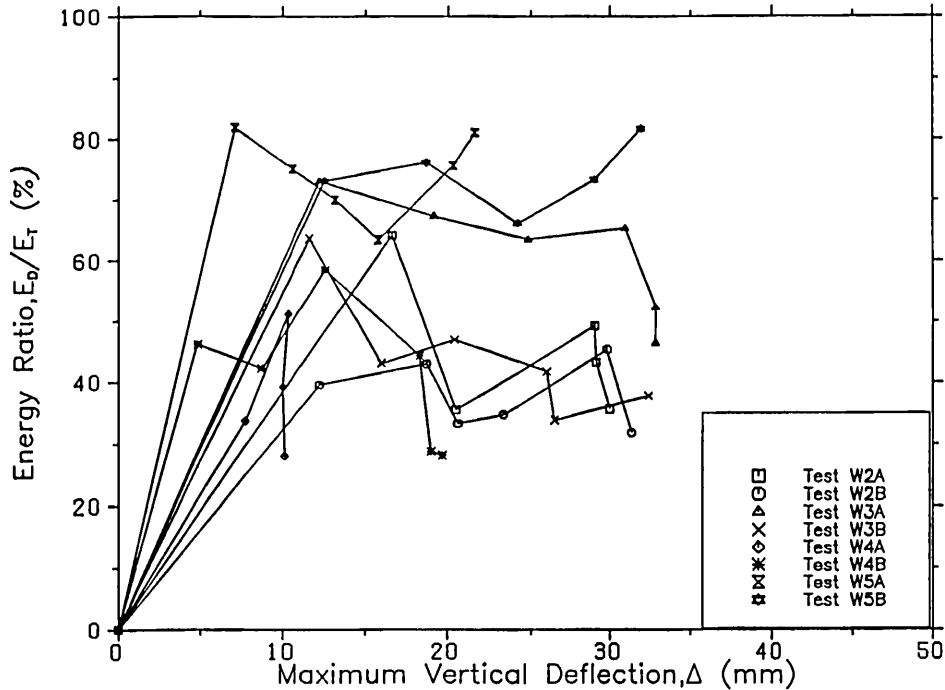


Figure 9.1 Variation of the energy ratio with the maximum vertical deflection of the FPSS model.

wall in test W5 showed an additional strength resulting from the external reinforcement; the effect being to retain on average a constant energy ratio on an increase of deflection (Figure 9.1). Although there was a decrease in the energy ratio, the reinforcement came into action by sustaining that loss of energy; at later cycles of settlement, an increase in the energy ratio was measured after cracking.

During cyclic settlement, the effect of a drop of the hysteresis loop due to crack propagation can be seen in Figure 9.2. Figure 9.2 shows the variation of the damping ratio,  $\xi$ , at each cycle of settlement, defined as the ratio of the area enclosed by each loop,  $E_D$ , that is, the damping-energy loss per cycle, to the strain energy stored at maximum displacement (Clough and Penzien, 1975),

$$\xi = \frac{E_D}{2\pi A}$$

where A = area of triangle enclosed by the maximum deflection.

This shows the damping effect caused at each cycle of settlement due to cracking of the walls. It is clearly demonstrated that walls with fixed supports (W2), and walls with low aspect ratio (high walls, W4), registered the lowest damping ratios; they also experienced the most serious damage. Point supports, in effect, increased the damping

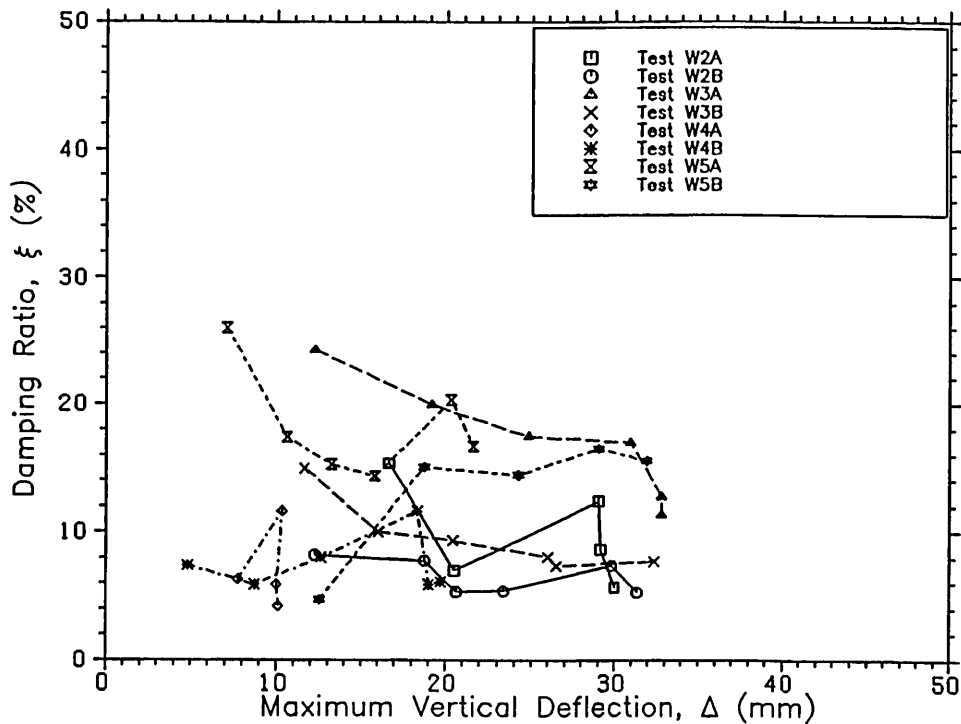


Figure 9.2 Variation of the damping ratio with the maximum vertical deflection of the FPSS model.

ratio, and thus the walls experienced less damage (W3). This was also the case for test W5, where the walls at maximum deflection recorded a large damping ratio that showed a greater tendency to absorb settlement, allowing the wall to be subjected to a larger magnitude of differential movement.

#### 9.4 STRUCTURE DETERIORATION AND STIFFNESS DEGRADATION

Examining the magnitude of strain at which visible damage occurred, as well as the appearance of the models after settlement, the limiting relative deflection of the FPSS was determined at the onset of visible damage. The limiting deformation referred to is the wall damage in the range of 1-2 mm crack width. The wall strain recorded at the limiting deformation varied between 301-986 microstrain. Since, in most cases, cracking propagated remote from the wall strain rosettes, the strain recorded in Table(9.1) was not necessarily measured at the crack.

The corresponding relative deflection ratio at the limiting strain was in the range of 1/222-1/81 for walls of aspect ratio 2.0-1.625 whereas, for walls of aspect ratio in the range of 1.23-1.0, a relative deflection ratio of 1/465-1/138 was measured. It is interesting to note

that there is variation in the angle of deflection between the deflection of the beam and that of the edge of the wall, that is, the difference between the relative deflection ratio and the tilt ratio, where the difference increases for walls with low wall aspect ratio (W4 and W5).

Table(9.1) Summary of limiting deformation of experimental testing of models.

Test No.	Max. deflection $\Delta_{max}$ (mm)	Relative deflection ratio ( $\Delta/L$ )	Relative tilt ratio ( $\delta/H$ )	Max. principal tensile strain $\epsilon_{max}$ ( $\mu\epsilon$ )	Max. crack width $w$ (mm)	Limiting curvature ( $m^{-1}$ )	
						Soffit	Top
W1AA-W1AB	20.65	1/109-1/88	1/96 -1/79	301	1 - 1.5	-	-
	23.54	1/95 -1/77	1/93 -1/78	726	1.4- 1.9	-	-
	28.71	1/78 -1/63	1/80 -1/67	1293	2.0- 3.0	-	-
	35.16	1/64 -1/52	1/53 -1/44	1837	5.0- 6.0	-	-
W1BA-W1BB	16.13	1/139-1/113	1/96 -1/108	621	2.5- 3.0	1/3125 - 1/4761	
	33.23	1/67 -1/55	1/45 -1/47	2167	5.0- 5.5	1/1819 - 1/2801	
	43.20	1/52 -1/42	1/41 -1/45	4023	8.0-10.0	1/952 - 1/1651	
W2AA-W2AB	15.81	1/142-1/115	1/134-1/117	654	1.0- 2.0	1/2137 - 1/407	
	20.00	1/112-1/91	1/104-1/93	1216	4.0- 5.5	1/538 - 1/1320	
	28.06	1/80 -1/65	1/72 -1/67	2304	8.0-10.0	1/463 - 1/3610	
W2BA-W2BB	11.93	1/188-1/153	1/201-1/156	967	1.5- 2.0	1/1294 - 1/1831	
	18.39	1/122-1/99	1/128-1/97	986	1.5- 2.5	1/1272 - 1/1174	
	22.90	1/98 -1/80	1/100-1/82	1803	3.0- 3.5	1/279 - 1/1057	
	29.35	1/76 -1/62	1/76 -1/61	2069	3.0- 4.0	1/288 - 1/711	
W3AA-W3AB	10.10	1/222-1/181	1/216-1/133	354	0.7- 1.0	1/2562 - 1/1085	
	22.26	1/101-1/82	1/104-1/69	1601	1.5- 2.0	1/1087 - 1/1332	
	30.01	1/75 -1/61	1/76 -1/55	2100	2.0- 3.0	1/668 - 1/694	
W3BA-W3BB	14.51	1/155-1/126	1/187-1/468	1215	0.5- 0.7	1/522 - 1/346	
	20.96	1/107-1/87	1/78 -1/122	1736	0.8- 1.0	1/1657 - 1/345	
	27.10	1/83 -1/67	1/51 -1/72	1953	1.0- 2.0	1/1067 - 1/351	
W4AA-W4AB	7.42	1/303-1/246	1/396-1/303	806	1.5- 2.0	1/11718- 1/8437	
	10.32	1/218-1/177	1/268-1/269	1251	2.0- 4.0	1/46875- 1/5551	
	10.01	1/224-1/182	1/217-1/214	1832	5.0- 6.0	1/1753 - 1/9238	
W4BA-W4BB	4.85	1/465-1/377	1/507-1/414	697	2.0- 3.0	1/681 - 1/1869	
	12.58	1/178-1/145	1/176-1/152	925	4.0- 6.0	1/996 - 1/994	
	19.03	1/118-1/96	1/104-1/117	1101	7.0- 8.0	1/2739 - 1/570	
W5AA-W5AB	6.77	1/332-1/269	1/415-1/352	321	0.5- 0.8	1/2572 - 1/1380	
	13.23	1/170-1/138	1/315-1/157	782	1.0- 1.5	1/2381 - 1/2787	
	21.29	1/105-1/85	1/117-1/87	6420	1.0- 2.0	1/52734- 1/494	
W5BA-W5BB	11.94	1/188-1/153	1/304-1/169	586	0.7- 1.0	1/870 - 1/1906	
	23.87	1/94 -1/77	1/103-1/83	1749	1.5- 2.0	1/644 - 1/913	
	31.94	1/70 -1/57	1/77 -1/63	6500	2.0- 2.5	1/412 - 1/831	

An increase in the height of the walls restricted lateral movement due to the increased distortional stiffness owing to the geometry of the structure. Thus, shorter walls were able to move laterally more easily,

however, fixed supported walls (W1 and W2) showed a difference between the deflection ratio and the tilt ratio, at the early cycles. As the beam cracked, the walls were able to tilt correspondingly to beam rotation.

A study of the curvature of the wall profiles shows that walls were subject to larger curvature on the top than at the soffit, Table(9.1). However, for walls with fixed supports, tensile curvature denoting hogging was recorded that resulted in severe cracking of the walls. Additionally, for walls W4 and W5, the mode of deformation was also hogging curvature, that is convex upwards at the top of the wall and sagging at the soffit. In test W3, point supports allowed rotation of the walls, thus maintaining the sagging curvature of walls at the top, reducing the effect of cracking due to hogging.

Stiffness degradation of the FPSS models during settlement gives an indication of the capacity of the structure to deform without inducing restraint or, incurring more damage to its members. A study of the variation of stiffness measured, defined as the ratio of support load to the maximum vertical deflection measured at the settling support (Figures 9.3 & 9.4), shows that the maximum degradation of stiffness occurred in the range of 4-5 mm vertical deflection of the support; that is at a relative deflection of 1/500. As the stiffness of the structure decreased suddenly, it was able to deform more easily without reaching zero stiffness, that is ultimate failure. An examination of the reduction of support load at the settling corner with respect to the magnitude of differential movements shows little variation between the first and the final cycles of settlement. This implies that the FPSS did not undergo major stiffness degradation while remaining structurally coherent even after several cycles of settlement. This form of behaviour is attributed to the hinges in the ring beam, and the ability of the walls to deform without excess restraint.

For walls with fixed supports (W2A and W2B) and those with low aspect ratio (W4A and W4B), there is a sharp reduction in the stiffness upon settlement. However, point supports are shown to lead to more ductile behaviour of the walls with larger deformation, than for fully fixed supports (W3A and W3B). For high walls, the effect of point supports is negligible and the wall deformed in a brittle manner, whilst a more ductile behaviour with less damage was obtained by reinforcing the top quarter-height of the wall.

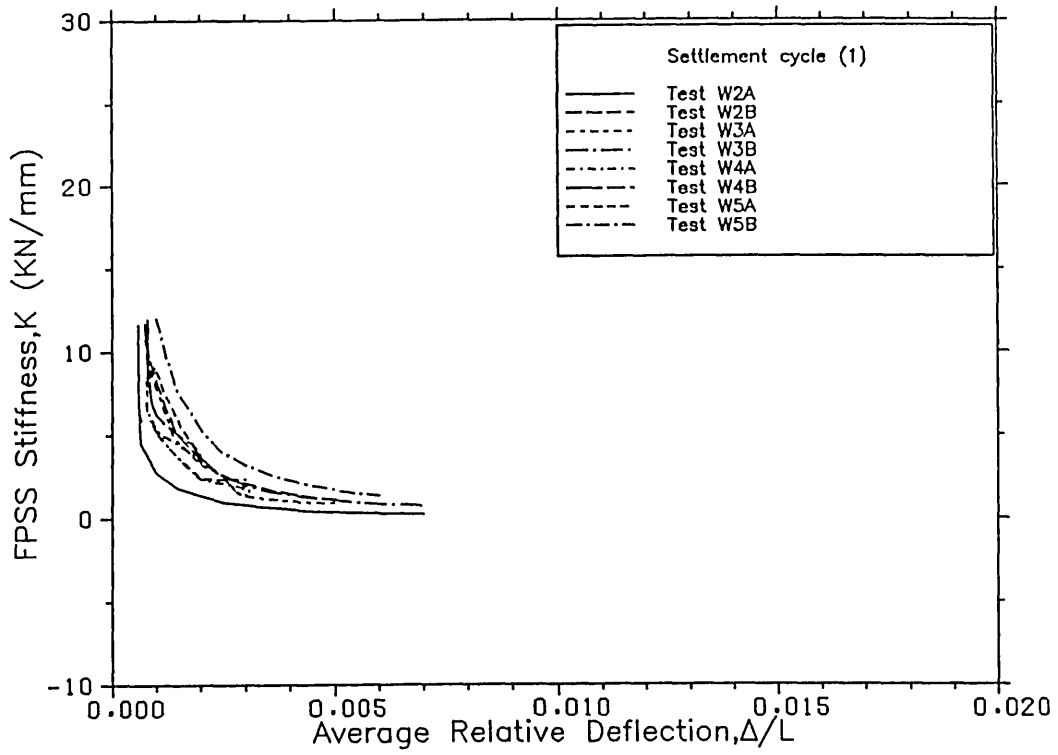


Figure 9.3 Stiffness degradation at first cycle of settlement.

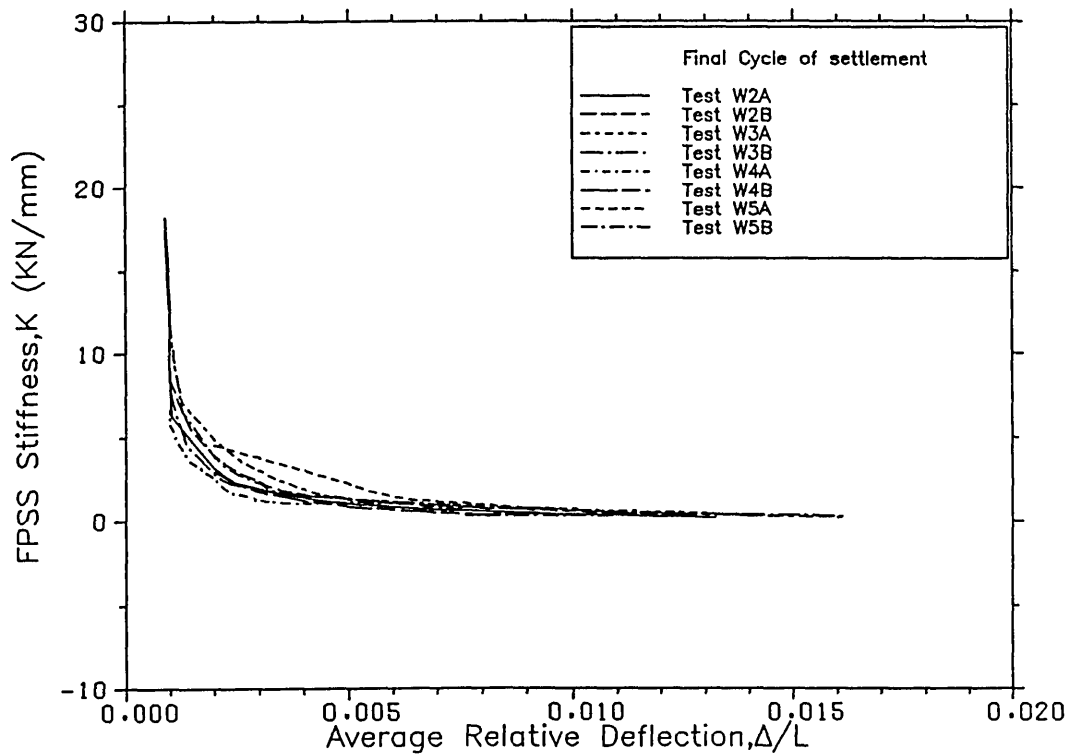


Figure 9.4 Stiffness degradation at last cycle of settlement.

## 9.5 REINSTATEMENT OF THE STRUCTURE

Apart from the requirement of the structure to aesthetic repairs, there are numerous cases where structural reinstatement of part or whole of the structure is needed. The existing evidence shows that differential settlement can often cause major damage that would require immediate repairs (Feld,1965 ; Mayer and Rausch,1967 ; Thomas and Fisher,1974). Since the FPSS structure is intended to deform allowing uneven levelling of its structural body, reinstatement of the structure becomes of increasing concern to the success of the design.

The experiments undertaken have proved that the jacking up of a subsided structure at the settled support until re-alignment with the other three supports has been achieved, closing most of the visible cracks, and allowing the structure to retain its integrity. A study of the percentage recoverability, Table(9.2), defined as the ratio of slope of the load-deflection relationship at one cycle of settlement to the slope of the previous cycle, shows the effect of jacking to reinstate the structure to its original position. The percentage recoverability is dependent upon both the maximum vertical deflection (that is, relating to the maximum degree of damage of the structure), and the strength of the wall. For walls with fixed supports (tests W1 and W2), and for high walls exhibiting larger restraint (test W4), it is evident that the structure is less liable to recover most of its initial state than W3. For test W3, a high recoverability of the strength of the walls was achieved with re-jacking because of fewer restraints on rotation of the walls (Table(9.2)). For the high walled model, test W4, 55.1% of the structural stiffness was retained at a maximum deflection of 10 mm, whilst for the top reinforced walls (W5), the structure was able to retain more than 66% of its stiffness (tests W5AA-W5AB), or more than 80% (tests W5BA-W5BB).

For the walls having the largest recoverability rate (W3 and W5), a greater increase of jacking load was required to restore the structure to its initial position. Introducing a weak joint at the beam-short column position (tests W1B, W2B, W3B, W4B and W5B), had the effect of reducing the restoring jacking load. It should be noted that it is also feasible that this reduction is caused by the stiffness degradation of the whole of FPSS model, which has experienced damage at the first set of tests (that is, tests W1A, W2A, W3A, W4A and W5A).



Table(9.2) Summary of stiffness degradation and restoring force of experimental tests.

Test No.	Maximum deflection at peak of cycle $\Delta$ (mm)	Percentage** recoverability on re-jacking $\left(\frac{\delta P}{\delta \Delta}\right)_i / \left(\frac{\delta P}{\delta \Delta}\right)_{i-1}$ (%)	Stiffness* degradation $\left(\frac{\delta P}{\delta \Delta}\right)_i / \left(\frac{\delta P}{\delta \Delta}\right)_o$ (%)	Percentage increase in jacking load $\frac{P_i - P_o}{P_o}$
W1AA-W1AB	8.67	-	-	-
	20.65	91.2	91.2	13.3
	24.35	86.1	77.5	14.0
	23.4	51.2	39.6	14.3
	28.71	63.1	25	21.2
	35.16	64.0	16	17.1
	36.7	99.6	15.7	16.3
W1BA-W1BB	16.13	-	-	3.5
	33.23	71.5	71.5	6.5
	38.71	55.6	39.7	8.3
	43.20	80.1	31.8	9.5
W2AA-W2AB	15.81	-	-	7.6
	20.0	69.2	69.2	7.7
	28.06	61.1	42.3	16.8
	27.10	58.2	24.62	8.1
	26.7	91.2	22.45	7.5
W2BA-W2BB	11.93	-	-	6.3
	18.39	79.9	79.9	7.5
	22.90	66.7	53.3	8.1
	29.35	96.7	51.5	10.4
W3AA-W3AB	10.17	-	-	22.4
	16.45	68.78	68.78	25.6
	22.26	81.8	56.26	34.9
	27.74	66.63	37.48	34.3
	30.01	83.4	31.29	34.2
W3BA-W3BB	14.51	-	-	9.8
	19.1	50.1	56.1	9.9
	20.96	97.8	48.9	21.3
	27.10	93.2	45.69	11.5
W4AA-W4AB	7.42	-	-	7.6
	10.32	84.9	84.9	15.3
	10.01	82.2	69.8	16.1
	10.00	78.7	55.1	16.0
W4BA-W4BB	4.85	-	-	6.7
	8.71	79.1	79.1	8.8
	12.58	95.54	75.65	9.2
	17.74	82.4	62.3	6.3
	19.03	93.4	58.2	6.2
	20.01	86.6	50.4	6.0
W5AA-W5AB	6.77	-	-	11.2
	10.32	97.1	97.1	26.1
	13.23	96.9	94.1	35.2
	15.81	96.3	90.6	37.4
	19.67	81.4	73.7	42.1
	21.29	90.0	66.4	43.9
W5BA-W5BB	11.94	-	-	2.3
	18.10	99.8	99.8	5.9
	23.87	93.2	93.1	9.8
	28.71	99.1	92.3	10.2
	31.94	89.9	82.9	10.5

\* Stiffness degradation measured as the percentage change of gradient of the load-deflection relationship at any cycle "i", with respect to the initial slope denoted by "o".

\*\* Percentage recoverability of the strength of the structure is measured as the change of gradient of the load-deflection relationship with respect to the previous cycle of settlement.

## 9.6 COMPARISON OF EXPERIMENTAL RESULTS WITH PREDICTIONS OF THEORETICAL MODELS

Initially, three theoretical models, as described in Chapter 7, were used to calculate the maximum vertical deflection of the FPSS models corresponding to a given limiting tensile strain induced in the walls. Although the mathematical models developed have a limited range of validity, it is necessary to compare their predictions with the experimental results, so as to clarify the limitations of their application. Thus, predictions of different theoretical methods developed for calculating the maximum vertical displacement,  $\Delta$ , and wall tilt,  $\delta_{\text{tilt}}$  are shown in Tables(9.4) and (9.5). These are compared with the experimental results shown in Table(9.3) with reference made to the magnitude of tensile strain reached in the walls. The locations at which the maximum principal strain was calculated was taken to be at the top corner of the wall as deduced by the theoretical models described in Sections 7.6, 7.7 & 7.8.

Table(9.3) Experimental results for the maximum vertical deflection and lateral displacement of the FPSS models.

Test No.	Principal tensile strain (microstrain)*	Vertical deflection, $\Delta$ (mm)		Lateral displacement, $\delta$ (mm)	
		Maximum deflection	First cracking	Maximum displacement	First cracking
W1AA-W1AB	301 1837	36.70	9.3	26.67	5.03
W1BA-W1BB	621 4023	43.20	12.32	26.8	8.3
W2AA-W2AB	587 2304	28.06	9.8	16.81	4.17
W2BA-W2BB	967 2069	29.35	11.9	19.58	5.60
W3AA-W3AB	354 2100	30.01	12.1	22.50	5.86
W3BA-W3BB	476 1953	27.10	15.05	23.76	7.51
W4AA-W4AB	806 1832	10.32	7.31	8.33	4.92
W4BA-W4BB	697 2101	20.01	8.06	19.20	4.17
W5AA-W5AB	821 6020	21.29	9.10	22.08	6.25
W5BA-W5BB	986 6500	31.94	13.06	29.12	8.61

\* Strain measured at the top edge of the wall.

Table(9.4) Theoretical predictions of maximum vertical deflection of the FPSS supports.

Test No.	Equivalent limiting stress (N/mm <sup>2</sup> )	Maximum vertical deflection, $\Delta$ (mm)			
		3-D elastic model *	2-D elastic model	3-D F.E. model	Modified 3-D F.E. model
W1AA-W1AB	1.02	9.73	12.78	3.5	4.61
	4.90	43.69	59.53	21.36	22.89
W1BA-W1BB	1.66	14.80	19.77	6.91	8.18
	4.80	41.80	56.69	46.78	49.93
W2AA-W2AB	1.75	16.23	21.01	6.92	8.31
	4.70	38.91	55.52	27.30	30.63
W2BA-W2BB	2.21	19.11	13.36	11.57	13.24
	4.43	37.63	51.96	24.75	26.78
W3AA-W3AB	1.35	12.89	16.29	4.18	5.40
	4.51	37.67	52.79	24.84	28.07
W3BA-W3BB	1.59	15.67	19.10	5.62	6.78
	4.72	38.93	54.49	23.68	25.59
W4AA-W4AB	2.13	4.15	15.60	5.93	6.89
	4.62	8.91	33.57	13.68	15.29
W4BA-W4BB	1.85	3.86	13.80	5.13	6.89
	4.70	9.76	34.32	15.13	18.36
W5AA-W5AB	12.31	8.02	-	6.03	7.02
	24.02	21.29	-	21.61	24.76
W5BA-W5BB	14.70	11.9	-	7.06	8.77
	24.1	31.94	-	22.93	26.08

\* Using the theory of thin plates.

Table(9.5) Theoretical predictions of lateral displacement of the FPSS models.

Test No.	Equivalent limiting stress (N/mm <sup>2</sup> )	Maximum lateral movement, $\delta$ (mm)		
		2-D elastic model	3-D F.E. model	Modified 3-D F.E. model
W1AA-W1AB	1.02	6.14	1.96	3.02
	4.90	29.52	11.96	13.13
W1BA-W1BB	1.66	9.64	4.10	4.76
	4.80	28.93	26.19	27.96
W2AA-W2AB	1.75	10.24	3.87	4.86
	4.70	28.32	15.39	17.96
W2BA-W2BB	2.21	13.25	6.47	7.41
	4.43	26.69	13.87	15.21
W3AA-W3AB	1.35	8.14	2.35	3.62
	4.51	27.18	13.91	15.79
W3BA-W3BB	1.59	9.58	3.16	4.12
	4.72	28.32	13.26	14.46
W4AA-W4AB	2.13	5.73	4.82	5.61
	4.62	12.57	11.12	12.47
W4BA-W4BB	1.85	5.05	4.16	5.62
	4.70	12.83	12.39	14.92
W5AA-W5AB	12.31	6.73	4.89	5.70
	24.02	13.11	17.56	20.16
W5BA-W5BB	14.70	8.03	5.74	7.25
	24.10	14.76	18.63	21.23

The maximum vertical deflection calculated using the various theoretical models gives a close prediction for the walls at first cracking. The 3-dimensional elastic model gives the least deviation from the measured results. After first cracking, larger deviation of the predicted results was observed, as shown in Figures 9.5 and 9.6. The deviations can be attributed principally to the assumption that the stress distribution within the idealized structures are <sup>not</sup> uninfluenced by both material and structural non-linearity.

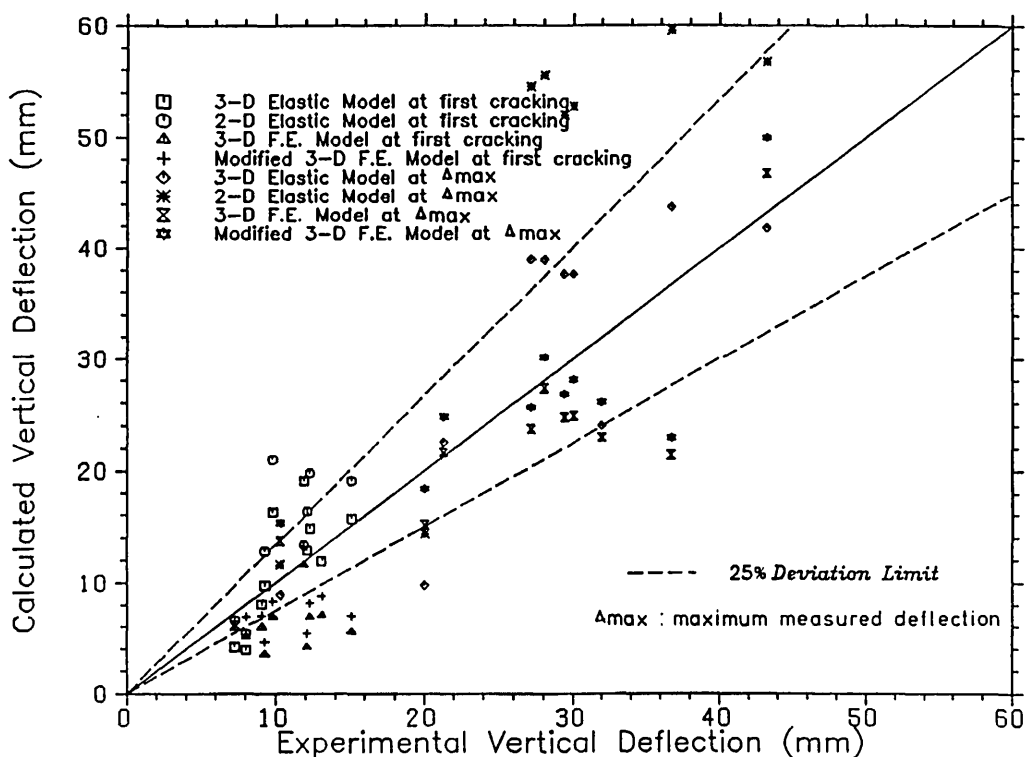


Figure 9.5 Comparison of experimental results with theoretical predictions of the vertical deflection of the FPSS supports.

Predicted results obtained by the 2-dimensional elastic model give an overestimate of the experimental results, on average by approximately 40%. This model, however, does not consider the interaction of adjacent walls, which would partly restrain the vertical movement. Most of the vertical movement of the supports is attributed to the out-of-plane deformation of adjacent walls (that is, rotation of the main walls), while the inplane deformation of the wall is approximately in the range of 5%-10% of the total vertical movement (that is, calculating the vertical movement of a cantilevered structure). Since material non-linearity is important, the limiting tensile strain measured at first cracking and at maximum deflection, together with the stress-

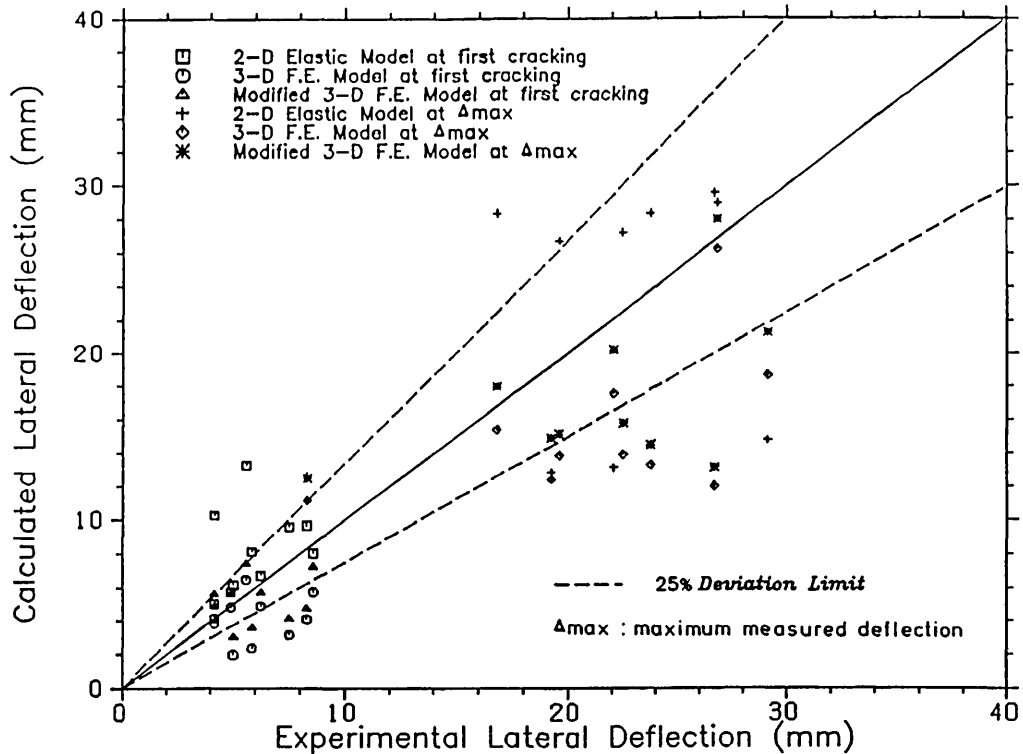


Figure 9.6 Comparison of experimental results with theoretical predictions of lateral displacement of the FPSS walls.

strain relationship of the brickwork, are used to determine the equivalent limiting stresses. These are used in calculating the maximum vertical and lateral movements of the walls. Although the 2-dimensional elastic formula used for assessing the lateral, vertical and strain magnitudes gives higher values, this perhaps could represent an upper bound of the experimental results. For walls W5, with increased stiffness in the top courses due to the bed reinforcement, the model is clearly unsuitable and a finite element model is likely to be better suited.

Both the 3-dimensional finite element model and the modified 3-dimensional finite element model show large discrepancies from the experimental results. The reasons for such a conservative underestimate are that these methods consider only inplane deformation of the walls and do not accommodate torsional warping. This is due to the fact that the finite elements used are plate elements that are stiff in their plane but have no torsional stiffness. The modified 3-dimensional finite element model considers the non-linear behaviour of the material and the geometry after first cracking of the main walls only. However, the interaction with the adjacent walls is substituted by inplane forces acting at the edges of the wall. From these models, it was found that

the out-of-plane deformation of adjacent walls contributes largely to the vertical displacement of the main walls. However, for walls W4 and W5, the increased stiffness of the walls was better represented by the 3-dimensional finite element model, where the increased height of the walls restricted out-of-plane movement of the adjacent walls.

The formula for predicting the vertical displacement of the FPSS box structure by including the distortional twist of the walls (refer to Section 7.8.2), gives estimates closest to the actual observed experimental values. At first cracking, the 3-dimensional elastic model shows close agreement with the experimental results, while at maximum deflection, coupled with the fact that the equivalent limiting stress varies largely with crack width, fairly reasonable agreement with maximum vertical displacement is obtained. With high walls W4 and W5, closer prediction was obtained at maximum deflection. At first cracking, the model underpredicts the magnitude of differential movement of wall W4, while for wall W5, a close estimate is achieved. This is thought to be due to the sudden crack that opened in wall W4, where the limiting strain at first cracking increased suddenly. In test W5, the effect of reinforcement was to stabilize this increase and thus a closer prediction of the model is obtained.

Methods based on elastic plate theory give closer predictions than the finite element method of analysis taking no account of out-of-plane deformation, and are therefore better suited to design due to the simplicity of the approach. These methods are able to consider both the inplane and the out-of-plane deformation of the box-structure and, thus, it is possible to check that each wall does not reach a limiting strain condition in either inplane or out-of-plane deformation.

For a similar check, 3-dimensional finite element method should include 3-dimensional elements, that is, shell elements, and this would cause further complication and increase the cost of computation, particularly when including non-linearity of the material. However, techniques based on plate theory are able to give a better understanding of the deformation of the FPSS box structure. They do not rely upon the use of sophisticated packages or large computers, but are readily available for hand method calculations. It seems that an additional major deficiency of the latter methods remain the absence of a suitable constitutive relation for masonry. This is solved in this text by resolving to the stress-strain relationship of masonry.

## 9.7 LIMITING DEFORMATION OF THE FPSS

As previously mentioned, the response of the FPSS to differential movement can be assessed by comparing the structural deformation to limiting deformation of structures subject to settlement from previous research. The limiting deformation of the FPSS walls can be divided into inplane and out-of-plane displacements, where limiting deformation refers to deformations at the onset of visible damage, that is crack width,  $w = 1-2$  mm. Figures 9.7 and 9.8 show a comparison of the observed deformation of the FPSS models, that is maximum vertical displacement,  $\Delta$ , and wall tilt,  $\delta_{\text{tilt}}$ , with various criteria of limiting deformation of walls in both sagging and hogging. It is evident that the FPSS walls accommodate larger relative deflection ratios when subject to settlement with minimum visible damage for both the inplane

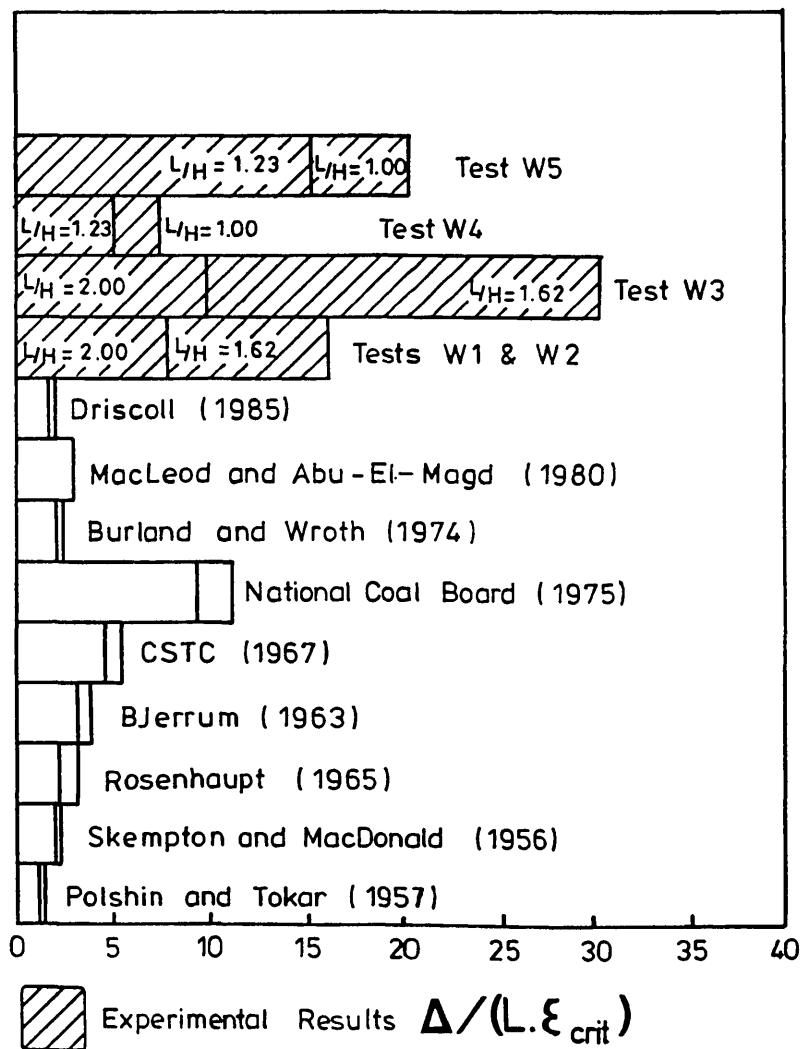


Figure 9.7 Allowable deflection ratio of structures relative to the limiting tensile strain.

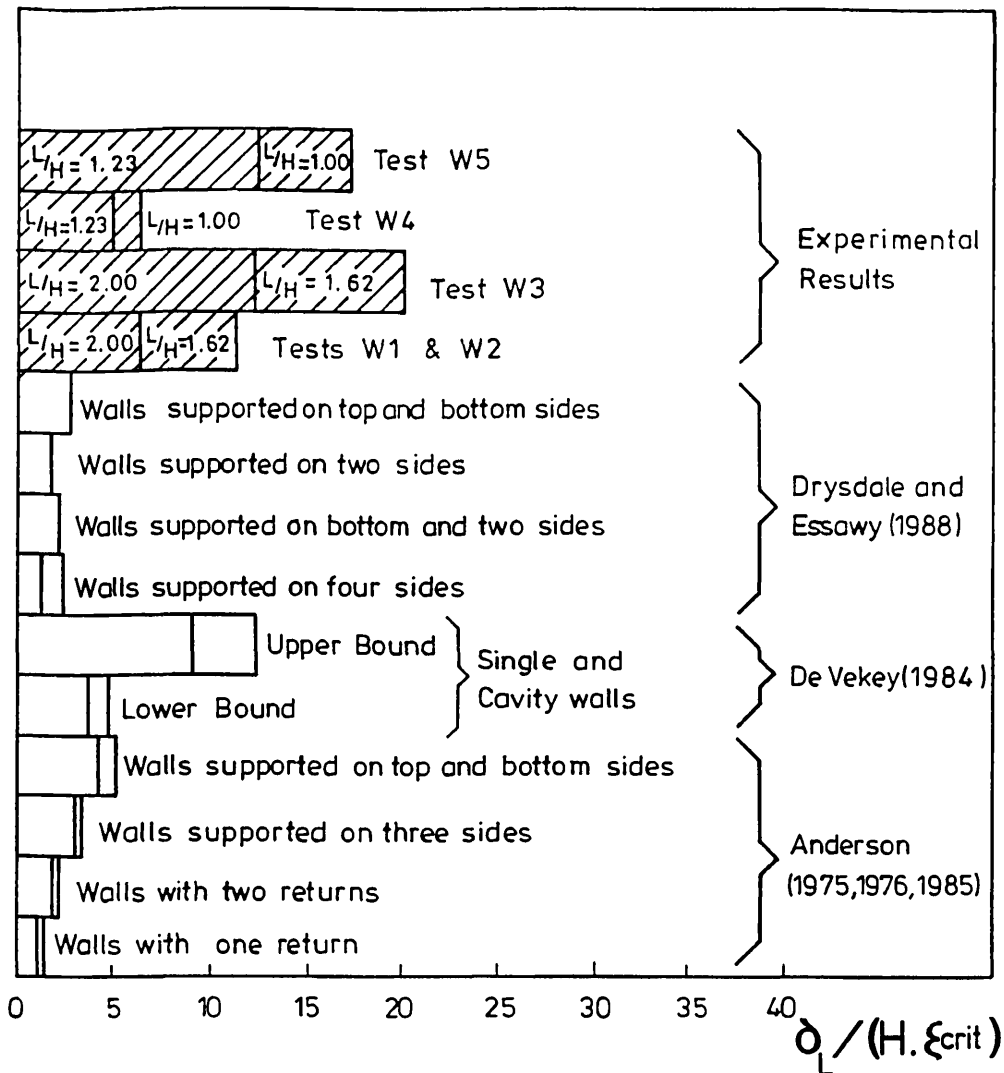


Figure 9.8 Allowable tilt ratio of structures relative to the limiting tensile strain.

and out-of-plane response of the walls. Of interest is that in test W3, larger deformation with respect to the limiting tensile strain was recorded compared to tests W1 and W2. This is attributed to the support conditions, that is, point supports in test W3, which allowed larger deformations of the walls before visible damage appeared. This is also dependent upon the aspect ratio of the wall, where for lower aspect ratio, the effect of point supports becomes increasingly important in accommodating a large deflection ratio. Thus, for an aspect ratio of  $L/H = 2.00$ , point supports caused an increase in the allowable deflection ratio of approximately 27%, where for an aspect ratio of  $L/H = 1.62$ , an increase of about 76% was observed. Similarly, an increase in the allowable tilt ratio,  $\delta_{\text{tilt}}$ , was observed in test W3 (that is, point supported walls), whereas for an aspect ratio of  $L/H = 1.62$ , an increase of about 89% was observed to 85% for an aspect ratio



of  $L/H = 2.00$ . It is clear that the allowable tilt ratio is not sensitive to the aspect ratio, however this is due to the interaction of tilting of one wall with the warping of an adjacent wall. As a result, adjacent walls resisting warping would cause a reduction in the magnitude of tilting of the main walls.

Another important parameter for the increase in the allowable deflection and tilt ratios is the geometry of the box. Thus, for the shallow boxes examined in the present project, greater deformation was observed in tests W1, W2, W3. For the deep box, that is test W4, lower deflection and tilt ratios were observed. These observations are best represented by the aspect ratio of the box diagonal to the height of the wall, i.e.  $D/H = \sqrt{L^2 + B^2 + H^2} / H$ , whereas for tests W1, W2 and W3,  $D/H = 2.764$  and for tests W4 and W5,  $D/H = 1.875$ . Thus, for a low box diagonal ratio, a decrease in the deformation is observed. This is due to the fact that shallow box structures accommodate differential settlement by the twisting of adjacent walls and flexure of their main walls, while for deep box structures, distortional warping becomes the primary mode of deformation that causes an increase in the warping of adjacent walls (refer to Section 8.3.3). As a result, the capacity of the walls to accommodate movement is decreased, since differential settlement of the main walls would cause large tilting of the side walls due to rigid body rotation. The large tilting would result in an earlier state of cracking. However, placing bed reinforcement in the top five courses of the walls (as done in test W5), increased the limiting deflection and wall tilt by over 100% of that recorded in test W4. The reinforcement increased the warping distortion of the walls, and thus more tilt was accommodated and larger deformation was allowed. Additionally, it caused restraining of the typical vertical cracking pattern of the deep box structure (as seen in test W4), leading the lower part of the unreinforced wall to deform as a shallow box, where diagonal cracking similar to those in tests W1, W2 and W3 developed.

## **9.8 INTERIM GUIDANCE FOR DESIGN OF THE FPSS**

### **9.8.1 Allowable deflection ratio**

Comparing the values of maximum vertical settlement for the FPSS models tested, it can be observed that the magnitudes are nearly in linear proportion with the percentage of loss of support load,  $P_i/P_t$  and the rotation of the point supports. However, these values are noted to be nearly independent of the self-weight and superimposed load on the

walls. For these tests, the maximum differential movement was also dependent upon the strain level in the wall, aspect ratio of the wall, and the box aspect ratio. Thus, the allowable relative deflection ratio can be expressed as a function of

$$\left(\frac{\Delta}{L}\right)_{\text{all.}} = F \left( \frac{P_i}{P_t}, \frac{L}{H}, \epsilon_{\text{lim}}, \frac{D}{H}, \Theta \right) \quad (9.1)$$

where  $\left(\frac{\Delta}{L}\right)_{\text{all.}}$  = the allowable relative deflection ratio,

$L/H$  = aspect ratio of the walls,

$\epsilon_{\text{lim}}$  = limiting tensile strain of the wall (microstrain),

$D/H$  = box ratio of the structure,

$\Theta$  = rotation of the supports (radians), and

$\frac{P_i}{P_t}$  = percentage of loss of support load,  $P_i$  to total load,  $P_t$ .

Based on the method of least squares, and using a standard package "MINITAB", the above equation was solved by multiple regression of the five variables. Table(9.6) shows a comparison between the calculated allowable relative deflection ratios and the experimental results.

Table(9.6) Comparison of calculated allowable deflection ratio of empirical formula with experimental results.

Test No.	Allowable deflection ratio ( $\delta/L$ )		Ratio of loss of support load ( $P_i/P_t$ )	Aspect ratio of wall ( $L/H$ )	Box ratio of FPSS $\frac{\sqrt{L^2+B^2+H^2}}{H}$	Ring beam rotation $\Theta$ (radians)	Limiting tensile strain at onset of visible cracking, $\epsilon_{\text{crit}}$ (microstrain)
	Calculated	Experimental					
W1AA	1/107	1/95	0.364	2.0	2.764	-	726
W1AB	1/93	1/77	0.364	1.624	2.764	-	800
W1BA	1/120	1/108	0.356	2.0	2.764	-	621
W1BB	1/95	1/96	0.356	1.624	2.764	-	786
W2AA	1/117	1/118	0.538	2.0	2.764	-	684
W2AB	1/98	1/105	0.538	1.624	2.764	-	801
W2BA	1/95	1/112	0.434	2.0	2.764	-	867
W2BB	1/81	1/99	0.434	1.624	2.764	-	986
W3AA	1/83	1/96	0.281	2.0	2.764	0.151	845
W3AB	1/84	1/82	0.281	1.624	2.764	0.162	761
W3BA	1/86	1/83	0.247	2.0	2.764	0.124	787
W3BB	1/73	1/67	0.247	1.624	2.764	0.176	899
W4AA	1/345	1/303	0.575	1.231	1.875	0.039	806
W4AB	1/294	1/246	0.575	1.0	1.875	0.041	897
W4BA	1/370	1/373	0.474	1.231	1.875	0.035	697
W4BB	1/333	1/465	0.474	1.0	1.875	0.076	731
W5AA	1/89	1/105	0.351	1.231	1.875	0.086	4231
W5AB	1/84	1/85	0.351	1.0	1.875	0.131	4042
W5BA	1/86	1/80	0.521	1.231	1.875	0.105	4683
W5BB	1/76	1/71	0.521	1.0	1.875	0.128	5033

The best fit for the experimental results is found to be:

$$\left(\frac{\Delta}{L}\right) = 2.384 \times 10^{-6} \left(\frac{P_i}{P_t}\right)^{-0.103} \left(\frac{L}{H}\right)^{-0.289} \left(\frac{D}{H}\right)^{3.345} \Theta^{0.006} \epsilon_{lim}^{0.773} \quad (9.2)$$

This equation gives a regression equation fit of 94.2%, with 100% indicating a perfect fit, and Durbin-Watson statistic factor of 0.79. The Durbin-Watson statistic factor is used to test for autocorrelation in the data, with a smaller value illustrating a positive correlation. It is clear that for lower values of the load ratio,  $(P_i/P_t)$ , better correlation of the formula is found. Of interest is to note that the equation is able to predict the effect of increase of deflection on provision of bed reinforcement for the top courses in test W5 without inducing large erroneous results. Some discrepancies exist, which perhaps, could be attributed to the variation of magnitude of tensile strain, together with the rotation of the beam. Although the proposed formula is based on a limited range of tests, it seems that reasonable predictions of the allowable deflection ratio can be obtained. More experimental data are needed, however, in order to justify the validity of such a formula.

If the empirical formula is based on experimental results of tests W1, W2, W3 and W4 (that is, excluding W5), a better correlation is achieved with the following relationship:

$$\left(\frac{\Delta}{L}\right) = 5.129 \times 10^{-6} \left(\frac{P_i}{P_t}\right)^{-0.273} \left(\frac{L}{H}\right)^{-0.261} \left(\frac{D}{H}\right)^{3.415} \Theta^{0.002} \epsilon_{lim}^{0.610} \quad (9.3)$$

Equation(9.3) gives a regression equation fit of 96.1%, with a Durbin-Watson statistic factor of 0.85. Clearly, a better fit is obtained for the experimental results for unreinforced masonry structures; a separate correlation should be found for reinforced masonry structures. However, due to the limited data on reinforced masonry structures, no separate formula could be developed here. Figure 9.9 compares both the experimental results with the empirical formula developed for the allowable relative deflection. Equations(9.2) and (9.3) define the limit of allowable deflection ratio for wall aspect ratios of  $L/H = 2.0$  and  $1.0$  respectively. It is clear that if wall reinforcement is excluded, that is equation(9.3), an increase of allowable deflection ratio is predicted that complies with the

experimental results. It is shown that the aspect ratio of the wall and the box aspect ratio influence the allowable deflection ratio, together with the limiting tensile strain at the onset of visible damage. However, the influence of the beam rotation is shown more to affect walls with high aspect ratios than high walls with low aspect ratios.

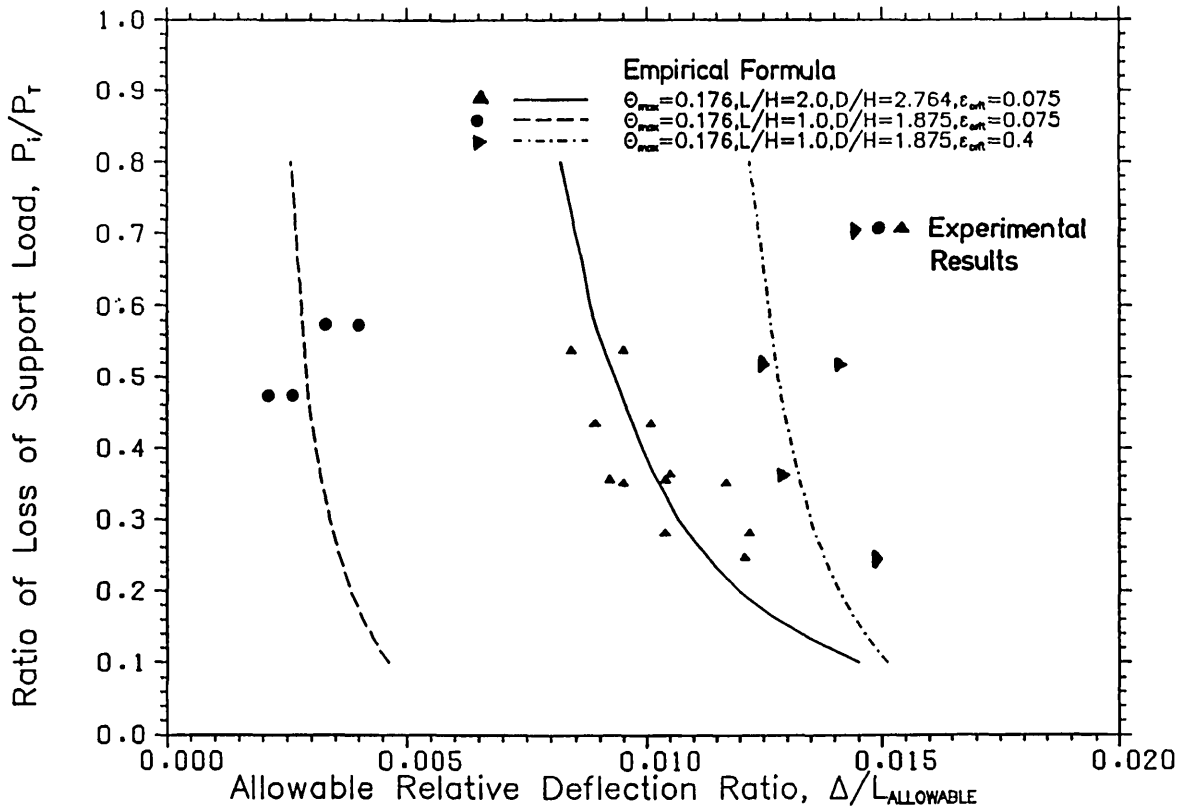


Figure 9.9 Comparison of experimental results with predictions of equations(9.2 & 9.3).

### 9.8.2 Reinstatement of the structure

Comparing the observed damage with the percentage of stiffness recoverability where the structure is jacked back to its initial position, it is clear that when larger settlement occurs, recoverability reduces. Therefore, the percentage recoverability of the structure can be expressed in terms of the relative deflection ratio,  $\Delta/L$ , percentage increase of jacking load due to reinstatement,  $(P_i - P_o)/P_o$ , aspect ratio of the wall  $L/H$  and the degree of damage that the wall experienced before re-jacking, that is, percentage recoverability,

$$\frac{\left(\frac{\delta P}{\delta \Delta}\right)_i}{\left(\frac{\delta P}{\delta \Delta}\right)_o} = F \left( \frac{\Delta}{L}, \frac{P_i - P_o}{P_o}, \frac{L}{H}, \text{Damage} \right) \quad (9.4)$$

where  $\frac{\Delta}{L}$  = allowable relative deflection ratio,

$L/H$  = aspect ratio of the walls,

$\left(\frac{\delta P}{\delta \Delta}\right)_i$  = slope of the load-deflection relationship at cycle "i",

$\left(\frac{\delta P}{\delta \Delta}\right)_o$  = initial slope of the load deflection relationship,

$\frac{P_i - P_o}{P_o}$  = percentage increase in support load,

and damage of the wall was represented by a measure of the maximum tensile strain induced in the walls,  $\epsilon_{max}$ .

The results of all cycles of settlement in each structural model, that is, models W1, W2, W3 and W4 were taken into consideration, and the correlation is as follows,

$$\frac{\left(\frac{\delta P}{\delta \Delta}\right)}{\left(\frac{\delta P}{\delta \Delta}\right)_o} (\%) = 309.028 \left(\frac{\Delta}{L}\right)^{-0.261} \left(\frac{P_i - P_o}{P_o}\right)^{-0.184} \left(\frac{L}{H}\right)^{-0.112} \epsilon_{max}^{-0.335} \quad (9.5)$$

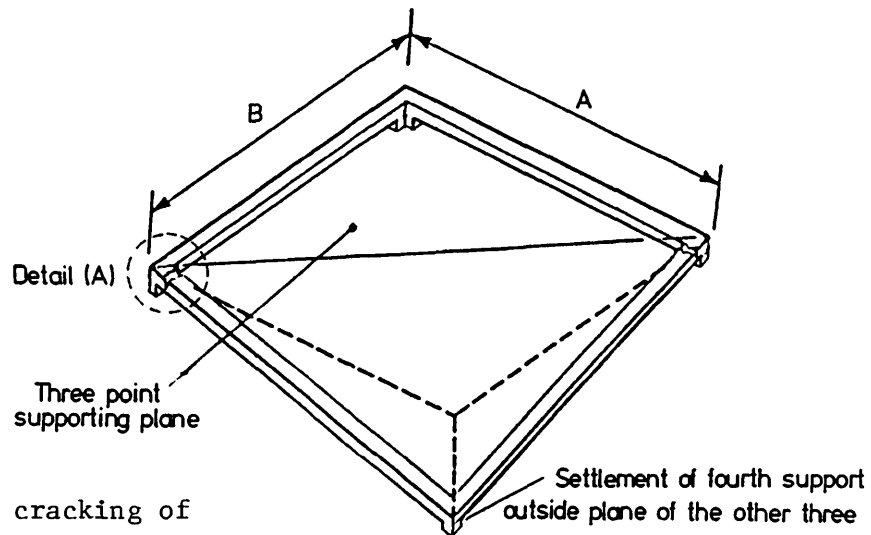
The equation has a regression equation fit of 74.2% with a Durbin-Watson factor of 1.27. Clearly, a better correlation was not obtainable and this is due to the large variation in recording of maximum tensile strain and also that the mode of failure was not considered. However, this equation is thought to be helpful in providing the designer with a correlation between the maximum deflection that the FPSS can withstand before reinstatement and the expected stiffness recoverability of the structure. A measure of the life expectancy and serviceability could also be determined. As a result, for safe reinstatement of the structure and increasing the probability of high recoverability of stiffness, the deflection and the maximum strain in the wall should not reach a certain critical value before damage in the structure can be restored. Therefore, the limits deduced from the experiments indicate a range of 1/95-1/83 for deflection ratio and a limiting tensile strain in the range of 1500-2200 microstrain.

### 9.8.3 Ring beam

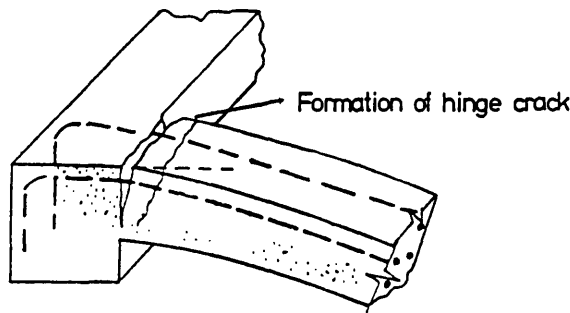
In the form of the strains in the steel reinforcement recorded at three points along the top and bottom bars, for each beam, the results indicate the contribution of the ring beam during settlement. It is

clear that the maximum strains experienced by the reinforcement were measured at the supporting ends of the beam at later stages of settlement (Figures 8.1-8.10). This is also illustrated by frequent cracking of the beam at the supporting end, resulting in an increase of the tensile strain in the reinforcement (Figures 8.52-8.56).

The general mode of failure exhibited throughout the tests was a flexure crack forming a hinge at the supporting end. This occurred at each test, that is, tests W1A through W5B, with half of the ring beam being hinged (Figure 9.10(a)), and the top reinforcements resisting most of the cantilevering load. If cracking propagated to the bottom of the beam, the steel reinforcement then came into action and the cantilevering load was then shared by both top and bottom reinforcement bars. If a larger magnitude of rotation was required, a decrease in the depth of the top reinforcement from the bottom of the beam, that is, the formation of a concrete hinge, would have allowed much greater unrestricted rotation before the steel was activated. However, once the concrete hinge was formed and the top steel reinforcement was in action, any further rotation was dependent upon the magnitude of elongation of the steel bars.



(a) Typical cracking of FPSS ring beam.



(b) Detail(A).

Figure 9.10 Typical deformation of the ring beam during settlement.

The top bars, remaining at least partially anchored in the surrounding concrete column at the supporting end, would mean that the hinge would extend to the bottom of the beam, allowing the bottom reinforcement bars to resist part of the cantilevering load. Therefore, when considering the influence of the ring beam as the supporting base of the walls during settlement, the tests indicated that the beam would act as a stabilizing support on settlement and as a jacking spreader beam on reinstatement of the structure. As walls exhibited hogging mode of failure on settlement, that is, cracks being initiated at the top propagating to the bottom of the wall, the beam acted as a tie, reducing the brittleness of failure. The evidence suggests that the reinforcement bar elongation contributes to the increase of hinging of the beam by holding the beam in a serviceable state, without reaching the ultimate failure (Figure 9.10). Upon reinstatement, the beam acts to distribute the jacking load uniformly onto the walls, thus reducing the effect of local failures due to concentration of forces. The beam, remaining partially anchored by the reinforcement at the hinge (Figure 9.10(b)), would allow non-restrictive movement of the beam and, as a result, all the input energy of re-jacking would be employed effectively to reinstate the structure.

## 10.1 CONCLUSIONS

### 10.1.1 Review of literature of design of structures

A literature survey of the damage criteria at the onset of visible damage revealed that the limiting damage for structures subject to differential movement is dependent upon the use of the structure, the form of the structure and, importantly, the reaction of the user. To eliminate subjective parameters, so as to include the criteria as a design state, the limiting deformation of the building material is employed in order to place bounds on the extent of allowable deformation. Comparison of various categorizations of the limiting damage, with reference to the allowable movement of the structure, is reported. This, in turn, revealed a wide spread of results that is dependent upon the allowable extent of damage, the critical tensile strength of the structure material or finishes and the plane of deformation (that is, inplane or out-of-plane deformations). For the present research, an investigation into load bearing walls found that the limiting deformation of masonry walls varies additionally with the aspect ratio of the wall ( $L/H$ ), return wall ratio, ( $R/L$ ), form of deformation (that is, sagging or hogging mode) and the pattern of wall cracking.

A study of the critical tensile strength of the building material recognized that the limiting tensile strain influences the allowable deformation of the structure adopted for the damage criteria, more so than characteristic values of stress. As a result, a relationship between the limiting tensile strain and the extent of damage is readily expressed, and on this basis an expression for estimating the allowable differential movement of the structure was determined for this present research. An alternative (and probably optimistic) method of employing the limiting stress based on elastic and non-linear mathematical models gave wider variation of predictions (Chapters 3 and 7).

A review of the practical methods of the design of structures subject to differential movement was conducted (Chapter 2), with the objective of establishing a basis upon which the allowable predicted deformation of those structures could be made and, hence, of classifying structural design with respect to the limiting movement that each



structure can accommodate. A thorough investigation of the two design concepts, that is, flexible and rigid, was carried out with reference to the economical requirement for low-rise buildings. This has favoured flexible designs that allow larger differential movements to be incorporated with less resulting damage. Since this implies that greater deformation is expected to occur during the anticipated lifetime of the structure, a necessary requirement is to study either the feasibility of using the deformed structure or necessary repair measures. A literature review of the methods of structural reinstatement for structures revealed two concepts of structural reinstatement, that is passive or active. These two concepts are dependent upon whether structural recoverability occurs simultaneously with reaching an allowable deformation, that is active reinstatement, or remains to be corrected at a later stage. Thus, it was recognized that the reparability of flexible structures should be considered at an early stage of design in order to allow for this effect without causing structural distress or difficulties in operation during structural reinstatement.

#### 10.1.2 Present investigation

An investigation into a flexible form of structure in relation to differential settlement, the four-point-support-system, was undertaken. The experimental and theoretical work has been concerned with the performance of masonry walls which were subject to both settlement at one corner and reinstatement of the structure by jacking its supports to the initial position. The following conclusions have been reached:

1. The four-point-support-system is much more tolerant of differential movements than other structures reported in the literature. This increased tolerance has been achieved without impairing the stability of the structure. Additionally, this conclusion holds even after a number of cycles of differential movement.
2. The jack and load cell system devised to control settlement, either by load controlling or settlement control, proved to be successful. The ascending portion of the load-deflection relationship, together with the unloading portion, were monitored successfully. As a result, this enabled determination

of the descending portion of the relationship.

3. Cyclic testing of the FPSS increased the allowable vertical deformation, with no increase in the magnitude of cracking in tests W1, W2, W3. In test W4 (with low aspect ratio), increased initial cracking was observed with more brittle propagation of the crack, that caused sudden increase in deformation at a decrease in the amount of lost load at the settling support. Thus, with higher loss of load carrying capacity at the settling support (that is, with less restriction in movements), less damage was experienced in the walls and a more ductile form of deformation was observed.
4. The ring beam acts in concert with the load bearing walls, providing additional confinement to the walls on hogging, and reducing the depth of crack through the walls. This results in increasing the stability of the structure during settlement and, thus, more deformation may be allowed for than the movement capacity of the walls. Hence, it provides a safety factor against overestimating the settlement capacity of the FPSS. The additional articulation of the ring beam by providing concrete hinges at its corners, increased the deformational capacity and rotation of the walls with reduced magnitude of cracking.
5. The open nature of the roof structure of the FPSS model has contributed largely to the enhanced deformation of the structure, with little damage. This is clearly observed due to the large warping deformation of the walls, shortening of the diagonal opposite the settling support and lengthening of the diagonal passing through the settling support. Thus the increase in deformation is critical to the non-restrictive movement of the walls at eave (roof) level.
6. It is apparent that the amount of lateral deformation experienced by the FPSS develops as a consequence of vertical settlement of the support, and reduces the magnitude of maximum tensile strain reached in the walls. This can be seen when comparing fixed supported walls to point supported walls, where the latter experiences larger vertical deformation with less

strain induced in the walls. Additionally, lateral deformation can directly influence the maximum vertical deflection if rigid body rotation of the wall is allowed. This effect is smaller in high walls but increases as  $L/H$  increases. The cross walls, unlike continuous walls, would allow more lateral movement of the adjacent walls to occur by increasing the warping deformation.

7. Point-supported walls were able to acquire more deformation with minimum damage than fixed supports, due to the larger rotation capacity of the ring beam. Additionally, the residual deformation at the end of an unloading cycle decreased when compared to fixed supported walls. At low aspect ratio of the wall (high wall, test W4), the wall residual deformation increased compared to that of the immediately preceding cycle. Thus point supports were able to maintain a high probability of recoverability of the initial structural state during unloading.
8. High walls (test W4), were severely damaged during settlement, but were nevertheless, able to attain a higher deformation capacity in comparison to structures reviewed from the literature. Provision of bed reinforcement at the top five courses of the walls was able to control cracking to a minimum, but this did not introduce restriction against vertical deformation. As a result, more than twice the maximum vertical deformation in comparison to the unreinforced structure was acquired.
9. The failure patterns of the short and the high walls were different, with the shorter wall having a dominant diagonal crack, where for the high walls, vertical edge cracks were observed. The evidence suggests that the forms of deformation differ due to the dominance of either torsional (twist) deformation or warping deformation in the walls. For walls with large  $L/H$  values, the vertical differential movement causes larger twisting of the walls than for walls with a low  $L/H$  value. The deformation of low  $L/H$  walls is characterized by larger distortional warping, resulting in cracking with the two cracked portions in different planes (refer to Section 8.6).

10. The structural repair of the FPSS was achieved by direct jacking of the movable support back to its initial position. This has proved successful in reinstating the structure. The strength retained by the structure after reinstatement was found to depend upon the magnitude of the maximum deformation, to which the structure was subjected in the immediately preceding loading cycle. No significant increase in jacking force above the initial support load was required to restore the structure except for the high walls (test W4), or short walls exhibiting vertical cracking, where the restored jacking force increased by about 15% on average. In test W5, the increase in jacking force was the highest recorded due most probably to the effect of steel reinforcement in the upper mortar. When cracks are of category I on the I.Struct.E.(1978) scale (crack width,  $w = 1-2.5$  mm), jacking caused them to disappear. However, for cracks in excess of category I ( $w = 3.5-5$  mm), residual cracks of 0.5-1.0 mm remained after jacking. In the case of the unreinforced high wall (test W4), cracks could not be restored and a residual crack of 2-2.5 mm was noted. In spite of reduction of stiffness usually resulting from cyclic settlement of FPSS, the general behaviour was not affected. However, in case of the high wall, test W4, a large difference in behaviour was found, possibly due to the effect of sudden or brittle cracking of the walls. After first cracking, the FPSS structure was found to exhibit a high percentage of recoverability upon jacking, in the range of 80%-95% (Table(9.2)).
11. Three theoretical methods of predicting the allowable deformation of the FPSS were investigated. The first, based upon 2-dimensional elastic theory, was found to give close predictions until first cracking, with 15% deviation from the experimental observations. The finite element method used to model 3-dimensional behaviour, was able to predict the overall behaviour even after cracking, but with a 25% deviation. This is due to the ill-conditioned type of finite plate elements that were not able to express torsional deformation. Alternatively, shell elements were not used due to the high cost and time of computation. The third method, based on 3-dimensional elastic theory, and incorporating warping and a torsional function by

using the Vlasov theory of thin walls, yielded the closest predictions to the experimental observations with a maximum deviation of 10% for both the pre- and post-cracking stages. An empirical equation, relating the allowable deformation and the magnitude of loss of support load of the FPSS, was developed for use as an interim guidance for design. Good correlation between experimental observation and the empirical relationship was obtained, with a regression factor of 94.2%. A correlation defining the percentage recoverability of the FPSS with the maximum deflection and extent of damage reached in the wall, was obtained with a regression factor of 74.6%. This expressed the limits of deformation allowed for the structure, before repairs could be applied to reinstate it to 80%-95% of its initial state.

## 10.2 RECOMMENDATIONS FOR FUTURE RESEARCH

Although study of the structural response of the FPSS under settlement is attempted within the presented work, difficulty in assessing the serviceability limit state was encountered. The research programme also attempted to cast more light upon the understanding of masonry structures subject to settlement, with the aim of being able to design structures sufficiently flexible to accommodate movement, which would both suffer less damage and not require sophisticated design measures and elaborate construction equipments. Our knowledge of the structural behaviour during settlement and reinstatement would benefit from more experimental and theoretical studies. Future work related to the study of the FPSS is required specifically in the following areas:

1. To study the behaviour of the FPSS subject to the effect of heave, that is, upwards differential vertical displacement.
2. To determine how the beam-wall stiffness affect the deformation characteristics of the FPSS. More specifically, to study the effect on the confinement of cracking along the walls offered by arch action.
3. To determine the structural response on the FPSS of walls with

openings, and to study the amount of cracking occurring and methods of reducing the extent of damage encountered. This is essential in order to warrant the use of FPSS as a practical design method.

4. It would be profitable to extend the present work and include a study of minimum bed reinforcement necessary at eaves level in order to reduce the effect of crack propagation during settlement, and of the general effect of increased ductility on the structure after cracking.
5. To investigate the effect of increase of applied superimposed load on the walls, simulating higher stories, and to study the limits of application of the four-point-support-system to higher-storey structures.
6. Extending the analytical method to enable predictions of maximum settlement of walls with openings, and to be able to incorporate the method as a simple package for micro-computers in order to facilitate its use in design offices.
7. Since the design of FPSS is critically dependent upon the roof-structure, tests with various forms of roof-supports to roof-structures are needed to identify the cost effective and practical solutions.

## REFERENCES

- ABU-EL-MAGD, S.A. ; MACLEOD, I.A. (1980) "Experimental Tests on Brick Beams under inplane Bending Conditions", The Structural Engineer, Volume 58B, Number 3, September, pp.62-66.
- AGIB, A.R.A. (1983) "Foundations on Expansive Soils", Proceedings, Seminar on Expansive Clay Soil Problems in the Sudan, Wad Medani, Sudan, pp.33-50.
- ALEXANDER, S.J. ; LAWSON, R.M. (1981) "Design for movement in Buildings", Construction Industry Research and Information Association (CIRIA), Technical Note 107, London, 54pp.
- ALI, S. ; PAGE, A.W. (1987) "Non-linear finite element analysis of masonry subjected to concentrated load", Proceedings, Institution of Civil Engineers, Part 2, Volume 83, December, pp.815-832.
- AMERICAN CONCRETE INSTITUTE (1968) "Allowable Deflections", Proceedings, American Concrete Institute, Report by Subcommittee 1, ACI Committee 435, Volume 65, Number 6, pp.433-444.
- AMERICAN SOCIETY FOR TESTING AND MATERIALS (1980). Flexural Bond Strength of Masonry. Philadelphia: ASTM, E518.
- AMERICAN SOCIETY FOR TESTING AND MATERIALS (1982). Mortar for Unit Masonry. Philadelphia: ASTM, C270.
- AMERICAN SOCIETY FOR TESTING AND MATERIALS (1984). Sampling and Testing Brick. Philadelphia: ASTM, C67.
- AMERICAN SOCIETY FOR TESTING AND MATERIALS (1984). Compressive Strength of Masonry Prisms. Philadelphia: ASTM, E447.
- ANAGNOSTIDES, G. ; HAGREAVES, A.C. ; WYATT, T.A. (1988) "An energy absorption device for steel braced frames", Engineering Seismology and Earthquake Engineering, Research Report, Imperial College, Number 88/1, February, London.
- ANDERSON, C. (1976) "Lateral loading tests on Concrete Block Walls", The Structural Engineer, Volume 54, Number 7, pp.239-246.
- ANDERSON, C. (1985) "Tests on transverse laterally loaded masonry walls", Technical Report S/053/85, Polytechnic of the South Bank, London.
- ANDERSON, C. (1986) Personal communication.
- ATTEWEL, P.B. ; YEATES, J. ; SELBY, A.R. (1986) "Soil Movements Induced by Tunneling and their Effects on Pipelines and Structures", Blackie Publishers, London.
- BAB, H. (1954) "Forschungen und Untersuchungen im Grundbau", Bautechnik, Volume 31, pp.309-335.
- BAKER, L.R. (1978) "The lateral strength of brickwork - An Overview", Proceedings, British Ceramic Society, Number 27, December, pp.169-188.

BALLY, R.J. (1975) Discussion on paper by Grant, R., Christian, J.T., Vanmarcke, E.H. (1974) "Differential Settlement of Buildings", Journal, American Society of Civil Engineers, Geotechnical Division, Volume 101, Number 9, September, pp.981-983.

BARBER, H. (1969) "The effects of Mining Subsidence on the external cladding of Buildings", Proceedings, Symposium of Design for Movement in Buildings, The Concrete Society, London, October, pp.3/1-3/13.

BECICA, I.J. ; HARRIS, H.G. (1977) "Evaluation of Techniques in the Direct Modelling of Concrete Masonry Structures", Structural Model Laboratory Report No. M77-1, Department of Civil Engineering, Drexel University, Philadelphia, June.

BECKMANN, P. ; DUNICAN, P. (1966) "The Use of Shear Walls in High Buildings", Proceedings, Symposium on Tall Buildings with particular reference to Shear Wall Structures, University of Southampton, edited by Coull, A. and Stafford-Smith, B., Pergamon Press, April, pp.101-118.

BEDARD, C. (1983) "Non-Linear Finite Element Analysis of Concrete Structures", Ph.D. Thesis, Concrete Structures Section, Department of Civil Engineering, Imperial College, London.

BEEBY, A.W. ; MILES, J.R. (1969) "Proposals for the control of deflection in the new unified Code", Concrete Magazine, Volume 3, Number 3, pp.101-110.

BENJAMIN, J.R. ; WILLIAMS, H.A. (1958) "The behaviour of one-storey brick shear walls", Journal, American Society of Civil Engineers, Structural Engineering Division, Volume 84, Number 4, July, pp.1723/1-30.

BJERRUM, L. (1963) Discussion, Proceedings, European Conference on Soil Mechanics and Foundation Engineering, Wiesbaden, Volume III, pp.135-136.

BOARDMAN, V.R. (1956) "Reinforcement of Brickwalls to reduce cracking on Heaving Foundations", South African National Building Research Institute, Bulletin Number 14, pp.47-81.

BOARDMAN, V.R. (1958) "Three point support system of Brick Buildings to prevent cracking caused by Foundation Movement", National Building Research Institute (South Africa), Bulletin Number 16, pp.20-46.

BRITISH STANDARDS INSTITUTION (1970). Methods of Testing Mortar and Specification for Mortar Testing Sand. London: BSI, BS 4551.

BRITISH STANDARDS INSTITUTION (1972). Building Limes. London: BSI, BS 890.

BRITISH STANDARDS INSTITUTION (1980). Sands for Mortar for Plain and Reinforced Brickwork, Brickwalling and Masonry. London: BSI, BS 1200.

BRITISH STANDARDS INSTITUTION (1985a). Specifications for Clay Bricks. London: BSI, BS 3921.

BRITISH STANDARDS INSTITUTION (1985b). Design Loading for Buildings: Dead and Imposed Loads. London: BSI, BS 6399:Part 1.



BRITISH STANDARDS INSTITUTION (1985c). Structural Use of Unreinforced Masonry. London: BSI, BS 5628:Part 1.

BRITISH STANDARDS INSTITUTION (1985d). Structural Use of Concrete. London: BSI, BS 8110:Part 1.

BROWN, R.W. (1987) "Repairing slab foundations damaged by expansive soils", Concrete Construction, December, pp.1037-1041.

BUILDING RESEARCH ADVISORY BOARD (1968) "Criteria for Selection and Design of Residential Slabs-on-Ground", Building Research Advisory Board, National Academy of Sciences - National Research Council, Publication Number 1571, Washington D.C.

BUILDING RESEARCH ESTABLISHMENT (1973) "Mortars for Bricklaying", Building Research Establishment Digest, Number 160, Garston, Watford, December.

BUILDING RESEARCH ESTABLISHMENT (1974) "Clay Brickwork:1", Building Research Establishment Digest, Number 164, Garston, Watford, April.

BUILDING RESEARCH ESTABLISHMENT (1977) "Repairing Brickwork", Building Research Establishment Digest, Number 200, Garston, Watford, April.

BUILDING RESEARCH ESTABLISHMENT (1979) "Wall cladding : designing to minimize defects due to inaccuracies and movements", Digest No. 223, Building Research Station, Garston, Watford, March.

BUILDING RESEARCH ESTABLISHMENT (1981) "Assessment of damage in low-rise buildings, with particular reference to progressive foundation movement", Digest No. 251, Building Research Station, Garston, Watford, June.

BURGOYNE, C.J. (1986) Personal communication.

BURHOUSE, P. (1969) "Composite action between brick panel walls and their supporting beams", Proceedings, Institution of Civil Engineers, Volume 43, Part 1, June, pp.175-194.

BURLAND, J.B. (1984) "Buildings on Expansive Soils", Theme Lectures, Proceedings, First National Conference on Science and Technology of Buildings with special reference to Buildings in Hot Climates, Khartoum, Sudan, pp.59-84.

BURLAND, J.B. ; BROMS, B. ; DE MELLO, V.B.F. (1977) "Behaviour of Foundations and Structures", State of the Art Report, Proceedings, Ninth International Conference on Soil Mechanics and Foundation Engineering, Tokyo, Volume 2, pp.495-546.

BURLAND, J.B. ; MANSOUR, S.R.N. ; PERRY, S.H. (1988) "An Articulated Foundation for Masonry Structures liable to Subsidence", Proceedings, Eighth International Brick Masonry Conference, (to be published).

BURLAND, J.B. ; WROTH, C.P. (1974) "Settlement of Buildings and Associated Damage", Building Research Establishment, Current Paper CP 33/74, Garston, Watford, April.

- CAPPER, P.L. (1953) "Soil mechanics in relation to structural engineering", The Structural Engineer, Volume 31, Number 47, p.324.
- CARRILLO-GIL, A. (1980) "Construction and design of Light Structures in Peru", Proceedings, Fourth International Conference on Expansive Soils, Colorado, Volume 1, June, pp.469-476.
- CASSIE, W.F. (1969) Discussion on paper by Barber, H. "The effects of Mining Subsidence on the external cladding of Buildings", Proceedings, Symposium of Design for movement in Buildings, The Concrete Society, London, October, pp.A/11-13.
- CENTRE SCIENTIFIQUE ET TECHNIQUE DE LA CONSTRUCTION (1967) "Fissuration des Maçonneries", Technical Information Note No. 65, Brussels, 74pp.
- CHAN, S.F. ; TOH, C.T. ; TING, W.H. (1979) "Observed building deformations and associated damage", Proceedings, Tenth International Conference on Soil Mechanics and Foundation Engineering, Stockholm, Volume 2, June, pp.75-78.
- CHEN, F.H. (1975) "Foundation on Expansive Soils", Amsterdam, Elsevier Publishers.
- CLARK, P.J. ; BASSETT, R.H. ; BRADSHAW, J.B. (1973) "Plate friction load control devices - Their application and Potential", Proceedings, Institution of Civil Engineers, Volume 55, Part 2, June, pp.335-352.
- CLOUGH, R.W. ; PENZIEN, J. (1975) "Dynamics of structures", McGraw-Hill Co., New York.
- COMITE EUROPEEN DU BETON (1973) "Limitations des fleches", Manuel de Calcul "Fleches", Bulletin D'Information Number 91, Second Partie, Final draft, May, 85pp.
- CURTIN, W.G. (1986) "An investigation of the structural behaviour of post-tensioned brick diaphragm walls", The Structural Engineer, Volume 64B, Number 4, December, pp.77-84.
- DANBY, M. (1975) "Buildings and the Environment", Building Research Station, Overseas Building Note Number 165, Garston, Watford, December.
- DAWE, J.L. ; MACBRIDE, R.T. (1984) "Experimental Investigation of the Shear Resistance of Masonry Panels in Steel Frames", Proceedings, Seventh International Conference on Masonry, Melbourne, Australia, pp.791-801.
- DEGERLUND, C. (1986) "Solving the Problem", Civil Engineer (London), March, pp.38-39.
- DE VEKEY, R.C. (1984) "Performance specifications for wall ties", Building Research Establishment, Building Report No. 45, Department of the Environment.
- DHANASEHAR, M. ; PAGE, A.W. ; KLEEMAN, P.W. (1985) "The failure of brick masonry under biaxial stresses", Proceedings, Institution of Civil Engineers, Part 2, Volume 79, June, pp.295-313.
- DOMASCHUK, L. ; FLATT, D.G. ; KOTANSKI, J. ; KWOK, K. (1984)

"Performance of House Foundations on Expansive Soils", Proceedings, Fifth International Conference on Expansive Soils, Adelaide, pp.207-211.

DONALDSON, G.W. (1975) "Contribution to Discussion on Speciality Session on Current Theory and Practice on Expansive Clays", Proceedings, Sixth African Regional Conference on Soil Mechanics and Foundation Engineering, Durban, Volume 2, pp.174-175.

DRISCOLL, R. (1985) Discussion on paper by Thorburn, S. "The real behaviour of structures - soil-structure interaction", The Structural Engineer, Volume 63A, Number 8, August, pp.241-243.

DRISCOLL, R. (1986) Personal communication.

DRYSDALE, R.G., ESSAWY, A.S. (1988) "Out-of-plane bending of Concrete Block Walls", Journal, American Society of Civil Engineers, Structural Engineering Division, Volume 114, Number 1, January, pp.121-133.

DRYSDALE, R.G. ; HAMID, A.A. ; HEIDEBRECHT, A.C. (1979) "Tensile Strength of Concrete Masonry", Journal, American Society of Civil Engineers, Structural Division, Volume 105, Number 7, July, pp.1261-1276.

EDGEELL, G.J. (1982) "Stress-strain relationships for Brickwork", Proceedings, British Ceramic Society, Number 30, Load-bearing Brickwork(7), September, pp.197-212.

FALKNER, H. (1980) "Local unexpected settlements on the multi-storey structure SAB in Berlin", Proceedings, Eleventh Congress of International Association of Bridge and Structural Engineers, Vienna, Volume 2, August, pp.1075-1080.

FELD, J. (1965) "Tolerance of Structures to Settlement", Journal, American Society of Civil Engineers, Soil Mechanics Division, Volume 91, Number 3, May, pp.63-77.

FENTON, G.A. ; SUTER, G.T. (1986) "Differential movements and stresses in high-rise masonry veneers - Case study", Proceedings, Canadian Journal of Civil Engineering, Volume 13, Number 6, December, pp.713-721.

FRASER, R.A. ; WARDLE, L.J. (1975) "The Analysis of Stiffened Raft Foundations on Expansive Soils", Proceedings, Symposium on Recent Developments in the Analysis of Soil Behaviour and Their Application to Geotechnical Structures, University of New-South Wales, Sydney, Australia, pp.89-98.

FURLER, R. ; THURLIMANN, B. (1978) "Strength of brick walls under enforced end rotations", Proceedings, British Ceramic Society, Number 27, December, pp.189-203.

GAZETAS, G. ; TASSIOS, T.P. (1978) "Elastic-Plastic Slabs on Elastic Foundation", Journal, American Society of Civil Engineers, Structural Division, Volume 104, Number 4, April, pp.621-636.

GIBSON, D. (1957) "Buildings without Foundations", A Lecture on the Problems of Buildings on Moving Ground, Journal, Royal Institution of British Architects (RIBA), Volume 65, Number 2, December, pp.47-53.

GIDIGASU, M.D. (1980) "General Report on Foundations in Problem Soils", Proceedings, Seventh African Regional Conference on Soil Mechanics and Foundation Engineering, Durban, Volume 2, pp.689-703.

GLICK, G.W. (1936) "Foundations of the New Telephone Building in Albany", Proceedings, First International Conference on Soil Mechanics and Foundation Engineering, Harvard University, Cambridge, Massachussetts, Volume I, pp.278-286.

GRANT, R. ; CHRISTIAN, J.T. ; VANMARCKE, E.H. (1974) "Differential Settlement of Buildings", Journal, American Society of Civil Engineers, Geotechnical Division, Volume 100, Number 9, September, pp.973-991.

GREEN, D.R. ; MACLEOD, I.A. ; STARK, W.G. (1976) "Observations and Analysis of Brick Structures on Soft Clay", Proceedings, International Conference on the Performance of Building Structures, Glasgow, Pentech press, March, pp.321-336.

HARRIS, H.G. ; BECICA, I.J. (1978) "The Behaviour of Concrete Masonry Structures and Joint Details Using Small Scale Direct Models", Proceedings, North American Masonry Conference, University of Colorado, Boulder, August, pp.2/14-16.

HASELTINE, B.A. ; FISHER, K. (1973) "The Testing of Model and Full-Size Composite Brick and Concrete Cantilever Wall Beams", Proceedings, British Ceramic Society, Load Bearing Brickwork (4), Number 21, April, pp.243-260.

HASELTINE, B.A. ; TUTT, J.N. (1986) "The resistance of masonry to lateral loading-Implications of research on design recommendations", The Structural Engineer, Volume 64A, Number 11, November, pp.341-350.

HASELTINE, B.A. ; WEST, H.W.H. ; TUTT, J.N. (1978) "The design of laterally loaded brickwork panels with inplane restraints", Proceedings, British Ceramic Society, Number 27, December, pp.147-167.

HEATHCOTE, F.W.L. (1965) "Movement of Articulated Buildings on Subsidence Sites", Proceedings, Institution of Civil Engineers, Volume 30, Part 1, pp.347-368.

HEGEMIER, G.A. ; NUNN, R.O. ; ARYA, S.K. (1978) "Behaviour of Concrete Masonry under Biaxial Stresses", Proceedings, North American Masonry Conference, University of Colorado, Boulder, pp.1/1-28.

HENDRY, A.W. (1973) "The lateral strength of unreinforced brickwork", The Structural Engineer, Volume 51, Number 2, pp.43-50.

HENDRY, A.W. (1978) "A note on the strength of brickwork in combined racking shear and compression", Proceedings, British Ceramic Society, Number 27, Load-bearing Brickwork(6), December, pp.47-52.

HENDRY, A.W. ; MURTHY, C.K. (1965) "Comparative Tests on 1/3 and 1/6 Scale Model Brickwork Piers and Walls", Proceedings, British Ceramic Society, Load Bearing Brickwork, Volume 4, July, pp.45-66.

HETENYI, M. (1946) "Beams on Elastic Foundations", University of Michigan Press, Michigan.

HITCHINGS, D. (1981) "Finel User's Manual", Department of Aeronautics, Imperial college, London ,July.

HOLLAND, J.E. (1981) "The Design, Performance and Repair of Housing Foundation", Swinburne Institute of Technology Publishing Press, Victoria, Australia.

HOLLAND, J.E. ; CIMINO, D.J. (1980) "Behaviour and Design of Post-Tensioned Residential Slabs on Expansive Clays", Proceedings, Third Australian-New Zealand Conference on Geomechanics, Wellington, New Zealand, Volume 1, May, pp.19-24.

HOLLAND, J.E. ; LAWRENCE, C.E. (1980) "Seasonal Heave of Australian Clay Soils", Proceedings, Fourth International Conference on Expansive Soils, Denver, Volume 1, pp.302-324.

HOLLAND, J.E. ; PITT, W.G. ; LAWRENCE, C.E. ; CIMINO, D.J. (1980) "The Behaviour and Design of Housing Slabs on Expansive Soils", Proceedings, Fourth International Conference on Expansive Soils, Denver, Volume 1, pp.448-468.

HOLMES, M. (1961) "Steel Frames with Brickwork and Concrete Infilling", Proceedings, Institution of Civil Engineers, Volume 19, August, pp.473-478.

HOLTZ, W.G. (1983) "The influence of vegetation on the swelling and shrinking of clays in the United States of America", Geotechnique, Volume 33, Number 2, pp.159-163.

HOOLE, P. ; STEPHENSON, J.W. ; BINGHAM-HALL, A.W. (1984) "Lebanon 1982 - Clearance and Reinstatement of the devastated refugee camps", Proceedings, Institution of Civil Engineers, Volume 76, Part 1, November, pp.871-882.

HOOPER, J.A. (1982) Discussion of paper by MacLeod, I.A. and Abu-El-Magd, S.A. "The behaviour of brickwalls under conditions of settlement", The Structural Engineer, Volume 60A, Number 5, May, pp.166-175.

HORN, H.M. ; LAMBE, T.W. (1964) "Settlement of buildings on the MIT Campus", Journal, American Society of Civil Engineers, Soil Mechanics Division, Volume 90, Number 5, September, pp.181-195.

IKEDA, K. ; MAHIN, A. (1986) "Cyclic response of steel braces", Journal, American Society of Civil Engineers, Structural Division, Volume 112, Number 2, February, pp.342-361.

INSTITUTION OF STRUCTURAL ENGINEERS (1978) "Structure-Soil Interaction", A State of the Art Report, Institution of Structural Engineers, London, April.

INSTITUTION OF STRUCTURAL ENGINEERS (1980) Symposium on Structural failures in buildings, London, April, 80pp.

JENNINGS, J.E. ; KERRICH, J.E. (1962) "The heaving of buildings and the associated economic consequences, with particular reference to the Orange Free State Goldfields", The Civil Engineer in South Africa, Volume 4, Number 11, pp.221-248.

JOHNSON, F.B. ; THOMPSON, T.M. (1969) "Development of diametral testing procedures to provide a measure of strength characteristics of masonry assemblages", Designing, Engineering and Constructing with Masonry Products, edited by Johnson, F.B., Gulf Publishing Co., Houston, Texas, pp.51-57.

JONES, P.H.C. (1985) "Support for St Wilfrid's", Journal, Concrete Society, Volume 19, Number 10, October, pp.7-10.

JUST, D.J. ; STARZEWSKI, K. ; RONAN, P.B. (1971) "Finite Element Method of Analysis of Structures resting on elastic Foundations", Proceedings, Symposium on the Interaction of Structure and Foundation, Birmingham, July, pp.108-117.

KALITA, U.C. ; HENDRY, A.W. (1970) "An Experimental and Theoretical Investigation of the Stresses and Deflections in Model-Cross Wall Structures", Proceedings, Second International Brick Masonry Conference, Stoke-on-Trent, April, pp.187-201.

KLEPIKOV, S.N. ; BORODATCHEVA, F.N. ; MATVEEV, I.V. (1980) "Non-linear foundation behaviour in the analysis of frameless buildings under the action of foundation displacements", Proceedings, Second International Conference on Ground Movements and Structures, Cardiff, edited by Geddes, J.G., Pentech-Press, April, pp.275-287.

KOLBRUNNER, C.F. ; BASLER, K. (1969) "Torsion in Structures and Engineering Approaches", Springer-Verlag, Berlin.

KOTSOVOS, M.D. (1979) "A mathematical description of the strength properties of concrete under generalized stress", Magazine of Concrete Research, Volume 31, Number 108, September, pp.151-158.

KOTSOVOS, M.D. (1983) "Effect of testing techniques on the post-ultimate behaviour of concrete in compression", Materials and Structures, RILEM, Volume 16, Number 91, January-February, pp.1-12.

KOTSOVOS, M.D. ; NEWMAN, J.B. (1978) "Generalised stress-strain relations for concrete", Journal, American Society of Civil Engineers, Engineering Mechanics Division, Volume 104, August, pp.845-856.

KOTSOVOS, M.D. ; NEWMAN, J.B. (1981) "Fracture Mechanics and Concrete Behaviour", Magazine of Concrete Research, Volume 33, Number 115, June, pp.103-112.

KRYNINE, D. (1947) "Soil Mechanics", McGraw Hill Publishing Co., Inc., New York.

KUPFER, J. ; HILSDORF, H.K. ; RUSCH, H. (1969) "Behaviour of Concrete under Biaxial stresses", Proceedings, American Concrete Institute, Structural Division, Volume 66, Number 8, August, pp.656-666.

KUPFER, H. (1986) "Rekonstruktion Des Kirchturmes Diessen", D.Bauingenieur, Volume 61, Number 5, May, pp.205-208.

LACEY, W.D. ; SWAIN, H.T. (1957) "Design for Mining Subsidence", Architects Journal (London), Volume 126, pp.557-570.

- LEE, I.K. ; BROWN, P.T. (1972) "Structure-Foundation Interaction Analysis", Journal, American Society of Civil Engineers, Structural Division, Volume 98, Number 11, November, pp.2413-2431.
- LEE, I.K. ; HARRISON, H.B. (1970) "Structure and Foundation Interaction Theory", Journal, American Society of Civil Engineers, Structural Division, Volume 96, Number 2, February, pp.177-197.
- LENCZNER, D. (1981) "Movements in Buildings", Second Edition, Pergamon Press, Oxford, England.
- LEONARDS, G.A. (1975) Discussion on paper by Grant, R., Christian, J.T., Vanmarcke, E.H. (1974) "Differential Settlement of Buildings", Journal, American Society of Civil Engineers, Geotechnical Division, Volume 101, Number 7, July, pp.700-702.
- LITTLEJOHN, G.S. (1974) "Observation of brick walls subjected to mining subsidence", Proceedings, Conference on settlement of Structures, Cambridge, Pentech press, London, pp.384-393.
- LONG, A. (1980). "A Review of Recent Developments in Concrete Modelling", Reinforced and Prestressed Microconcrete Models, edited by Garas, F.K. and Armer, G.S.T., The Construction Press, London, pp.1-16.
- LONGFOOT, B.R. (1984) "In-plane bending of clay brick walls" Proceedings, Seventh International Brick masonry Conference, Volume 2, Melbourne, Australia, pp.847-855.
- LYTTON, R.L. (1970) "Design Criteria for Residential Slabs and Grillage Rafts on Reactive Clay ", Division of Applied Geomechanics, Commonwealth Scientific and Industrial Research Organisation (CSIRO), Melbourne, Australia, Parts I and II, November, 82pp.
- LYTTON, R.L. ; WOODBURN, J.A. (1973) "Design and Performance of Mat Foundations on Expansive soils", Proceedings, Third International Conference on Expansive soils, Haifa, Volume 1, July, pp.301-307.
- MACLEOD, I.A. (1987) "Use of bed-joint reinforcement in brick buildings to resist settlement", The Structural Engineer, Volume 65A, Number 10, October, pp.369-376.
- MACLEOD, I.A. ; ABU-EL-MAGD, S.A. (1980) "The Behaviour of Brickwalls under conditions of settlement", The Structural Engineer, Volume 58A, Number 9, September, pp.279-286.
- MAINSTONE, I.A. (1971) "On the stiffnesses of infilled frames", Building Research Establishment, Current Paper No. 2/72.
- MAINSTONE, R.J. ; WEEKS, G.A. (1970) "The influence of a bounding frame on the racking stiffnesses and strengths of brick walls", Building Research Establishment, Current Paper No. 3/70.
- MALLICK, D.V. ; DUNGAR, R. (1977) "Dynamic characteristics of core wall structures subjected to torsion and bending", The Structural Engineer, Volume 55, Number 6, June, pp.251-261.
- MANSOUR, S.R.N. (1985) "Design of Structures to withstand upheaval ground pressures", M.Sc. Thesis, Concrete Structures Section, Imperial

College, London, June.

MANSOUR, S.R.N. ; BURLAND, J.B. ; PERRY, S.H. (1987) "A Novel Design for Low-rise Masonry Structures on slowly moving ground", Proceedings First International Conference on Structural and Engineering Analysis and Modelling, Kumasi, Ghana, July, pp.127-144.

MAUTNER, K.W. (1948) "Structures in Areas Subjected to Mining Subsidence", The Structural Engineer, Volume 26, pp.35-69.

MAYER, H. ; RUSCH, H.R. (1967) "Bauschaden als Folge der Durchbiegung von Stahlbeton-Bauteilen", Deutscher Ausschuss fur Stahlbeton, Heft 193, 90pp.

MAYES, R.L. ; CLOUGH, R.W. (1975) "A Literature Survey - Compressive, Tensile, Bond and Shear Strength of Masonry", University of California, Report EERC 75-15, Berkeley.

MEYER, K.T. ; LYTTON, R.L. (1966) "Foundation Design in Swelling Soils", Meeting, American Society of Civil Engineers, Texas Section, Austin, pp.1-35.

MEYERHOF, G.G. (1947) "The settlement analysis of Building Frames", The Structural Engineer, Volume 25, pp.369-409.

MEYERHOF, G.G. (1953) "Some recent foundation research and its applications to design", The Structural Engineer, Volume 31, pp.151-167.

MEYERHOF, G.G. (1956) Discussion on paper by Skempton, A.W. and MacDonald, D.H. "The allowable settlement of Buildings", Proceedings, Institution of Civil Engineers, Volume 5, pp.774-775.

MILLS, M.R. (1985) "Founding on expansive soils : present practice and a novel foundation system", M.Sc. report, Soil Mechanics and Engineering Seismology Section, Imperial College, London, October.

MITCHELL, R.L. ; MACKECHNIE, W.P. (1972) "Construction on Volumetrically Active Soils", Rhodesian Engineers, Volume 10, Number 5, pp.43-50.

MONCARZ, P.D. ; OSTERAAS, J.D. ; WOLF, J. (1986) "Design for Maintainability", Civil Engineer (New York), Volume 56, Number 6, June, pp.62-64.

MOTTA, F. ; D'AMORE, E. (1985) "Numerical Modelling of the Structural Behaviour of Masonry Buildings", Proceedings, Seventh International Brick Masonry Conference, Melbourne, Australia, Volume 1, pp.509-518.

MURTHY, C.K. ; HENDRY, A.W. (1966) "Model Experiments in Load Bearing Brickwork", Building Science, Volume 1, Pergamon Press, London, pp.289-298.

NATIONAL COAL BOARD (1975) "Subsidence Engineer's Handbook", National Coal Board, Department of Mining Engineering, London.

OLSEN, K.A. (1958) "The re-siting of structures", Proceedings, Institution of Structural Engineers 50th Anniversary Conference, London, pp.364-371.



O'ROURKE, T.D. ; CORDING, E.J. ; BOSCARDIN, M. (1976) "Ground Movements related to Braced excavations and their influence on Adjacent Buildings", Final Report, US Department of Transportation, Report DOT-TST 76T-23, University of Illinois, Department of Civil Engineering (UILLU-ENG-76-2023), Urbana-Champaign.

OSMAN, M.A. ; CHARLIE, W.A. (1984) "Engineering properties of expansive soils in Sudan", Proceedings, Fifth International Conference on Expansive Soils, Adelaide, pp.311-315.

PAGE, A.W. (1978) "Finite Element Model for Masonry", Journal, American Society of Civil Engineers, Structural Division, Volume 104, Number 8, August, pp.1267-1285.

PAGE, A.W. (1980) "A Biaxial Failure criterion for Brick Masonry in the Tension-Tension range", International Journal of Masonry Constructions, Volume 1, Number 1, pp.26-29.

PAGE, A.W. ; BROOKS, D.S. (1985) "Load Bearing Masonry-A Review", Proceedings, Seventh International Brick Masonry Conference, Volume 1, Melbourne, Australia, pp.81-99.

PAGE, A.W. ; Samarasinghe, W. ; HENDRY, A.W. (1982) "The Inplane failure of Masonry-A Review", Proceedings, British Ceramic Society, Number 30, September, pp.90-100.

PARK, R. ; PAULAY, T. (1975) "Reinforced Concrete Structures", John Wiley & Sons Publishers, New York.

PFEFFERMANN, O. (1968) "Cracking of Brickwork partitions due to excessive deformation of the support - Experimental Study", Annales de l'Institut technique du batiment et des travaux publics, Number 250, pp.1453-1482.

PLEITHNER, M. ; BERNATZIK, W. (1953) "A new method of compensating settlement of Buildings by Injections of Cement Grout", Proceedings, Third International Conference on Soil Mechanics and Foundation Engineering, Switzerland, Volume 1, pp.450-453.

POLSHIN, D.E. ; TOKAR, R.A. (1957) "Maximum Allowable non-uniform settlement of Structures", Proceedings, Fourth International Conference on Soil Mechanics and Foundation Engineering, Volume 1, pp.402-405.

POST TENSIONING INSTITUTE (1978) "Design and Construction of Post-Tensioned Slab-on-Ground", Post-Tensioning Institute, First Edition, Arizona.

POWELL, B. ; HODGKINSON, H.R. (1976) "Determination of Stress/Strain Relationship of Brickwork", Technical Note, Number 249, British Ceramic Society, Stoke-on-Trent.

PRENTIS, E.A. ; WHITE, L. (1950) "Undermining", Second Edition, Columbia University Press, New York.

PRIESTLY, M.J.N. (1986) "Seismic Design of Concrete Masonry Shear Walls", Proceedings, American Concrete Institute, Volume 83, Number 8, January-February, pp.58-68.

- PROCTOR, C.S. (1948) "Cap Grouting to stabilize foundation on Cavernous Limestone", Proceedings, Second International Conference on Soil Mechanics and Foundation Engineering, Rotterdam, Volume 4, pp.302-303.
- PRYKE, J.F.S. (1967) "Moving Structures", The Consulting Engineer, Volume 31, Number 9, pp.85-89.
- RAUSCH, E. (1955) "Behaviour of Walls under the action of Mining Subsidence", Fortschritte und Forschungen im Baowesen, Heft 22, 34pp.
- RICHARD, F.E. ; ZIA, P. (1962) "Effect of Load Loss of Support on Foundation design", Journal, American Society of Civil Engineers, Soil Mechanics Division, Volume 88, Number 1, February, pp.1-27.
- RIGBY, C.A. ; DEKEMA (1952) "Crack resistant housing", Public Works of South Africa, Volume 2, Number 95.
- ROEDER, C.W. ; POPOV, E.P. (1977) "Inelastic Behaviour of eccentrically braced steel frames under cyclic loading", Report No EERC-77/18, University of California, Berkeley.
- RODIN, J. (1969) "The Implications of movement on Structural Design", Proceedings, Symposium of Design for movement in Buildings, The Concrete Society, London, October, pp.4/1-4/25.
- ROSENHAUPT, S. (1964) "Stresses in Point supported composite Walls", Proceedings, American Concrete Institute, Volume 61, Number 7, July, pp.795-810.
- ROSENHAUPT, S. ; BERESFORD, F.D. ; BLAKEY, F.A. (1967) "Test of a Post-tensioned Concrete Masonry Wall", Proceedings, American Concrete Institute, Volume 64, Number 12, December, pp.829-837.
- ROSENHAUPT, S. ; MUELLER, G. (1963) "Openings in masonry walls on settling supports", Journal, American Society of Civil Engineers, Structural Division, Volume 89, Number 3, June, pp.107-132.
- SABNIS, G.M. ; HARRIS, H.G. ; WHITE, R.N. ; MIRZA, M.S. (1983) "Structural Modelling and Experimental Techniques", Englewood Cliffs, London, Prentice Hall.
- SAHLIN, S. (1971) "Structural Masonry", Prentice-Hall Inc., Englewood Cliffs, New Jersey.
- SAMARASINGHE, W. ; HENDRY, A.W. (1982) "The Strength of Brickwork under Biaxial Tensile and Compressive stress", Proceedings, British Ceramic Society, Load-bearing Brickwork(7), Number 30, pp.129-139.
- SAMARASINGHE, W. ; PAGE, A.W. ; HENDRY, A.W. (1981) "A finite element model for the inplane behaviour of brickwork", Proceedings, Institution of Civil Engineers, Volume 71, Part 2, March, pp.171-178.
- SAW, C.B. (1974) "Linear Elastic Finite Element Analysis of Masonry Walls on Beams", Building Science, Volume 9, pp.299-307.
- SAWKO, F. (1982) "Numerical Analysis of Brickwalls under compressive loading", Proceedings, British Ceramic Society, Load-bearing Brickwork(7), Number 30, September, pp.213-222.

SHORT, A. ; SIMMS, L.G. (1949) "Survey of Loading Tests on some Post-War house prototypes", Proceedings, Institution of Civil Engineers, Volume 27, February, Part 1, pp.67-97.

SHRIVE, N.G. ; JESSOP, E.L. (1982) "An examination of the Failure mechanism of Masonry Piers, Prisms and Walls subjected to compression", Proceedings, British Ceramic Society, Loadbearing Brickwork(7), Number 30, September, pp.110-117.

SIMMS, F.A. ; BRIDDLE, R.J. (1966) "Bridge Design in Areas of Mining Subsidence", Institution of Highway Engineers, Journal, November, pp.19-34.

SINHA, B.P. (1976) "Strength of Mortar for Brickwork", Proceedings, Institution of Civil Engineers, Part 1, Volume 60, November, pp.655-662.

SINHA, B.P. ; HENDRY, A.W. (1976) "Structural testing of brickwork in a disused quarry", Proceedings, Institution of Civil Engineers, Part 1, Volume 60, February, pp.153-162.

SINHA, B.P. ; MARCRENBRECHER, A.H.P. ; HENDRY, A.W. (1970) "Model and Fullscale Tests on Five-storey Cross-wall Structure Under Lateral Loading", Proceedings, Second International Brick Masonry Conference, Stoke-on-Trent, April, pp.201-208.

SKEMPTON, A.W. ; MACDONALD, D.H. (1956) "The allowable settlement of Buildings", Proceedings, Institution of Civil Engineers, Volume 5, Part 3, May, pp.727-784.

SNELL, M.J. (1980) "Note on Small Buildings on Swelling Soils", Technical Report, Sir MacDonal and Partners, Cambridge, England, September.

SOMMER, H. (1979) "Recent findings concerning allowable differential settlement of structures-criteria of damage", Proceedings, Seventh International Conference on Soil Mechanics and Foundation Engineering, Brighton, Volume 3, pp.275-280.

STAFFORD-SMITH, B. ; CARTER, C. ; CHOUDHURY, J.R. (1970) "The Diagonal Tensile Strength of Brickwork", The Structural Engineer, Volume 48, Number 6, June, pp.219-225.

STAFFORD-SMITH, B. ; RIDDINGTON, J.R. (1977) "The Composite Behaviour of Elastic Wall-beam System", Proceedings, Institution of Civil Engineers, Part 2, Volume 63, June, pp.377-391.

STAFFORD-SMITH, B. ; TARANATH, B.S. (1972) "Analysis of tall core supported structures subjected to torsion", Proceedings, Institution of Civil Engineers, Part 2, Volume 53, September, pp.173-188.

STARZEWSKI, K. (1974) Discussion, Proceedings, Conference on Settlement of Structures, Cambridge, Pentech Press, London, April, pp.808-810.

TAYLOR, N. ; MALLINDER, P.A. (1987) "On the limit state properties of masonry", Proceedings, Institution of Civil Engineers, Part 2, Volume 83, December, pp.33-41.

TERZAGHI, K. (1935) "The actual factor of safety in Foundations", The Structural Engineer, Volume 13, pp.126-142.

TERZAGHI, K. (1956) Discussion on paper by Skempton, A.W. and MacDonald, D.H. (1956) "The allowable settlement of Buildings", Proceedings, Institution of Civil Engineers, Volume 5, Part 3, May, pp.775-776.

TERZAGHI, K. ; PECK, R.B. (1948) "Soil Mechanics in Engineering Practice", John Wiley, New York.

THOMAS, J.B. ; FISHER, A.W. (1974) "St Paul's Cathedral-measurments of settlement and movements of the structure", Proceedings, Conference on Settlement of Structures, Cambridge University, Pentech-Press, April, pp.221-233.

TIMOSHENKO, S.P. (1956) "Strength of Materials, Part 2", Van Nostrand, New York, Third Edition.

TIMOSHENKO, S.P. ; WOINOWSKY-KREIGER, S. (1959) "Theory of Plates and Shells", McGraw-Hill, New York, Second Edition.

TIMOSHENKO, S.P. ; GOODIER, J.N. (1959) "Theory of Elasticity", McGraw-Hill, New York, Second Edition.

TOMLINSON, M.J. (1984) "Foundation Design and Construction", Pitman Publishers, London, Fourth Edition.

TOMLINSON, M.J. ; DRISCOLL, R. ; BURLAND, J.B. (1978) "Foundation for low-rise Buildings", The Structural Engineer, Volume 56A, Number 6, pp.161-173.

TSCHEBOTARIOFF, G.P. (1951) "Soil Mechanics, Foundation and Earth Structures", McGraw-Hill Publishing Co., New York.

TUGAENKO, Y.F. ; MATUS, Y.V. ; STOYANOVA, T.I. (1984) "Chimney Tilt Correction", Soil Mechanics and Foundation Engineering, Volume 21, Number 1, January-February, pp.11-13.

TURNSEK, V. ; CACOVIC, F. (1971) "Some experimental results on the strength of Brick Masonry Walls", Proceedings, Second International Brick Masonry Conference, edited by West, H.W.H. and Speed, K.H., Stoke-on-Trent, England, April, pp.149-155.

VLASOV, V.Z. (1961) "Thin walled elastic beams", Translated from Russian, Israel Program for Scientific Translation, Jerusalem, Second Edition.

VLASOV, V.Z. ; LEONTEV, U.N. (1966) "Beams, Plates and Shells on elastic foundations", Translated from Russian, Israel Program for Scientific Translation, Jerusalem, Second Edition.

VOGT, H. (1956). "Considerations and Investigations on the Basic Principle of Model Tests in Brickwork and Masonry Structures", Library Communication No. 932, Building Research Station, Garston, England.

WAHLS, H.E. (1981) "Tolerable Settlement of Buildings", Journal, American Society of Civil Engineers, Geotechnical Division, Volume 107, Number 11, November, pp.1489-1504.

WALDRON, D. ; PERRY, S.H. (1980) "Small Scale Microconcrete Control Specimens", Reinforced and Prestressed Microconcrete Models, edited by Garas, F.K. and Armer, G.S.T., The Construction Press, London, pp.261-276.

WALSH, P.F. (1975) "The Design of Residential Slabs-on-Ground", Division of Building Research Technical Paper (Second Series) Number 5, Commonwealth Scientific and Industrial Research Organization (CSIRO), Victoria, Australia.

WALSH, P.F. (1978) "The Analysis of Stiffened Rafts on Expansive Soils", Division of Building Research Technical Paper (Second Series) Number 23, Commonwealth Scientific and Industrial Research Organization(CSIRO), Victoria, Australia.

WARRIER, G.P. (1977) "Restoration of Hardinge Bridge in Bangaladesh", Proceedings, Institution of Civil Engineers, Part 1, Volume 62, August, pp.399-418.

WEBB, D.L. (1969) "Foundations and Structural Treatment of Buildings on Expansive Soils in South Africa", Proceedings, Second International Research and Engineering Conference on Expansive Clay Soils, South Africa, pp.126-147.

WEEHUIZEN, J.M. (1959) "New Shafts of the Dutch State mines", Proceedings, Symposium on Shaft Sinking and Tunnelling, Institute of Mining Engineers, London, pp.28-60.

WEST, H.W.H. ; HODGKINSON, H.R. ; HASELTINE, B.A. (1978) "The lateral load resistance of brickwalls without precompression", Proceedings, British Ceramic Society, Number 27, December, pp.107-128.

WEST, H.W.H. ; HODGKINSON, H.R. ; HASELTINE, B.A. ; DEVEKEY, R.C. (1986) "Research results on brickwork and aggregate blockwork since 1977", The Structural Engineer, Volume 64A, Number 11, November, pp.320-331.

WILLIAMS, A.A.B. (1980) "Severe Heaving of block of flats near Kimberley", Proceedings, Seventh Regional Conference for Africa on Soil Mechanics and Foundation Engineering, Volume 1, pp.301-310.

WILLIAMS, A.A.B. ; DONALDSON, G.W. (1980) "Building on Expansive Soils in South Africa", Proceedings, Fourth International Conference on Expansive Soils, Denver, Volume 1, pp.834-844.

WILLIAMS, A.A.B. ; PIDGEON, J.T. ; DAY, P. (1985) "Expansive Soils", Transaction, Institute of Civil Engineers (South Africa), Volume 27, Number 7, pp.367-377 & 407.

WILSON, J.G. ; GARWOOD, T.G. ; SARSBY, R.W. (1984) "The settlement of low-rise buildings constructed over Peat", Proceedings, Third International Conference on Ground Movements and Structures, Cardiff, Pentech Press, July, pp.526-538.

WRAY, W.K. (1978) "Analysis of Stiffened slabs-on-ground over expansive soils", Proceedings, Fourth International Conference on Expansive Soils, Volume 1, Denver, Colorado, June, pp.558-581.

WU, A.H. ; SCHEESSELE, D.J. (1986) "A cost effective shallow foundation accommodates three feet of settlement", Civil Engineer (New York), Volume 53, Number 3, March, pp.65-67.

YOKEL, F.Y. ; FATTAL, S.G. (1976) "Failure Hypothesis for Masonry Shear Walls", Journal, American Society of Civil Engineers, Structural Division, Volume 102, Number 3, pp.515-532.

YOKEL, F.Y. ; SALOMONE, L.A. ; GRAY, R.E. (1982) "Housing Construction in areas of Mine Subsidence", Journal, American Society of Civil Engineers, Geotechnical Division, Volume 108, Number 9, September, pp.1133-1149.

YORULMAZ, M. ; SOZEN, M.A. (1968) "Behaviour of Single-Storey Reinforced Concrete Frames With Filler Walls", University of Illinois, Civil Engineering Studies, Structural Research Series No. 337, Urbana, May.

YUAN, L.N. ; SHUO, F.M. ; BIN, S.G. ; BIN, M.T. (1985) "The behaviour and strength of brick and reinforced concrete composite wall beams", Proceedings, Seventh International Brick Masonry Conference, Melbourne, Australia, Volume 2, pp.1101-1112.

ZEITLEN, J.G. ; KORNORNIK, A. (1980) "A Foundation Code for Expansive Soil Conditions", Proceedings, Fourth International Conference on Expansive Soils, Denver, Volume 1, pp.609-615.

ZIENKIEWICZ, O.G. ; CHEUNG, Y.K. (1967) "The finite element method in Structural and Continuum mechanics", McGraw-Hill, London.

APPENDIX 1 TERMINOLOGY FOR THE DEFORMATION OF STRUCTURES UNDER SETTLEMENT

A1.1 The definitions and symbols suggested by Burland and Wroth (1974) are adopted and these are described below for convenience. Figure A1.1 illustrates the various inplane deformation terms.

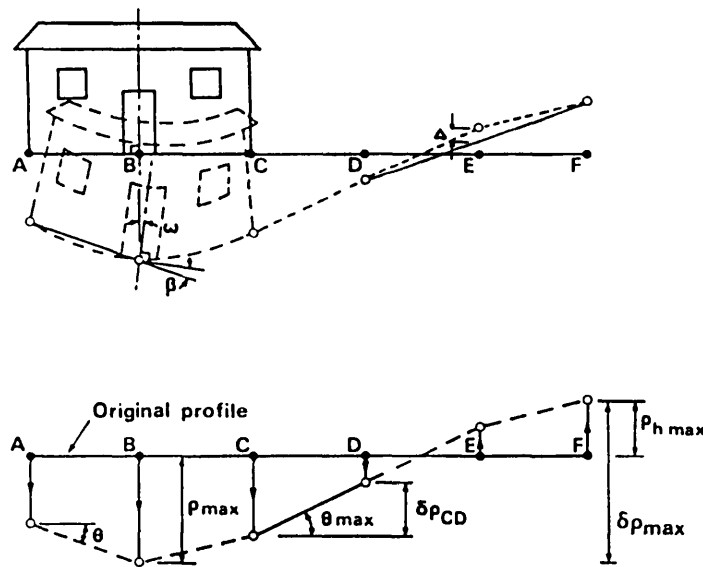


Figure A1.1 Definitions of settlement terms (after Burland and Wroth, 1974).

where

- $\delta_{\rho}$  = Differential or relative settlement of one reference point to the other,
- $\theta$  = Rotation of the straight line joining two reference points at the foundation level,
- $w$  = Tilt or rigid body rotation of the whole superstructure or of a well defined part of it, and
- $\frac{\Delta}{L}$  = Relative deflection ratio defined as the ratio of the maximum displacement of the structure relative to the straight line connecting two reference points to the length of the straight line.

A1.2 Three-dimensional deformation of structures involves defining both inplane and out-of-plane structural movement. Bally (1975) and Wilson, Garwood and Sarsby (1984) suggested the representation of 3-dimensional movement of the foundation similar to a rectangular block, as shown in Figure A1.2. This relates only to the differential settlement and rotation of each corner of the block to the adjacent one. However, to assess the crack condition of the walls, a terminology that relates the out-of-plane deformation of the walls is devised below.

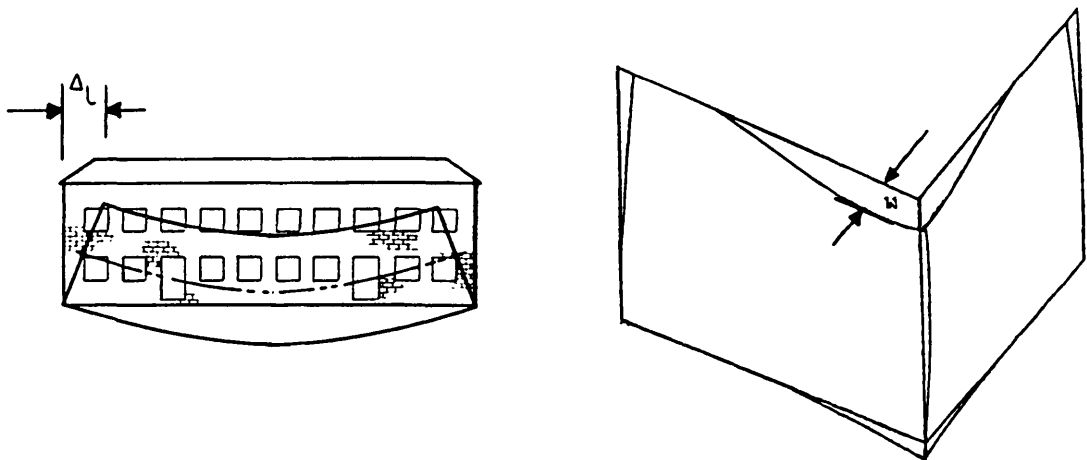


Figure A1.2 Definitions of tilt and out-of-plane warping.

where

$\Delta_L$  = Lateral deflection measured as the horizontal inplane movement of the wall perpendicular to its vertical plane,

$\Delta_L/H$  = Lateral deflection ratio defined as the ratio of lateral deflection between two reference points to the height of the walls between the reference points, and

$w$  = Warping displacement is defined as the horizontal out-of-plane movement of the wall measured perpendicular to its vertical plane.



## APPENDIX 2 DESIGN OF FPSS MODELS

Considering a full-scale FPSS structure, for low-rise building with the following characteristics:

Design load according to Walsh (1975) and BS 6399:Part 1, for a two-storey building,

For domestic structures, live load =  $1.0 \text{ KN/m}^2$

Dead load of walls and roof =  $3.0 \text{ KN/m}^2$

Dead load of slab =  $3.5 \text{ KN/m}^2$

Thus, Design load for two-storeys

$$= 1.0 \times 2 \times 1.6 + 6.5 \times 2 \times 1.4 = 20 \text{ KN/m}^2$$

For a 4 x 4 m module, total design load

$$= 20 \times 4 = 80 \text{ KN/m}$$

Beam dimensions = 4500 x 250 x 250

Concrete strength,  $f_{cu} = 35 \text{ N/mm}^2$

Yield strength of reinforcement,  $f_y = 400 \text{ N/mm}^2$

Brickwork strength,  $f_k = 5 \text{ N/mm}^2$

Elastic modular ratio,  $E_c/E_w = 4$

Wall thickness = 210 mm (one brick course)

### A2.1 Brickwall

Characteristic parameter of deep beam,  $K$ , for a wall on beam (Stafford-Smith and Riddington, 1977), where  $E$ ,  $I$  and  $L$  are the modulus of elasticity, second moment of area and span of the beam and  $E_w$  and  $t$  are the modulus of elasticity and thickness of the wall, respectively.

$$\begin{aligned} K &= \sqrt[4]{(E_w t L^3)/EI} \\ &= (0.21 \times 4.5^3 \times 12) / (4 \times 0.25^4)^{0.25} \\ &= 11.01 \end{aligned}$$

Maximum Moment in deep beam,  $M_{max}$  for an applied load of  $W_w$  is given by (Stafford-Smith and Riddington, 1977),

$$M_{max} = \frac{W_w L}{4(E_w t L^3/EI)^{1/3}}$$

$$= \frac{80 \times 4.5}{4 \left( \frac{0.21 \times 4.5^3 \times 12}{0.25^4 \times 4} \right)^{1/3}} = 3.67 \text{ KN/m per metre run}$$

Maximum stress in wall is given by (Stafford-Smith and Riddington, 1977),

$$= 1.63 \left( \frac{W_w}{L_t} \right) \left( \frac{E_w t L^3}{EI} \right)^{0.28}$$

$$= 1.63 \left( \frac{80}{4.5 \times 0.21} \right) \left( \frac{0.21 \times 4.5^3 \times 12}{0.25^4 \times 4} \right)^{0.28}$$

$$= 2.026 \text{ N/mm}^2$$

A half-scale model of this FPSS structure has the following properties,

Design load,  $W_{wm} = 0.25 \times W_w = 0.25 \times 80 = 20 \text{ KN}$

Base dimensions, 2250 x 125 x 125 mm

Brickwall dimensions, 105 mm thickness - half brick course (to maintain the stress level).

Characteristic parameter

$$K_m = \left( \frac{0.105 \times 2.25^3 \times 12}{4 \times 0.125^4} \right) = 11.01$$

Maximum moment in model beam

$$M_m = \frac{20 \times 2.25}{4 \left( \frac{0.105 \times 2.25^3 \times 12}{0.125^4 \times 4} \right)^{1/3}} = 0.45 \text{ KN/m per metre run}$$

To keep the same stress level,  $W_{wm} = 0.25 \times W_w$

Maximum stress level in model

$$= 1.63 \left( \frac{20}{2.25 \times 0.105} \right) \left( \frac{0.105 \times 2.25^3 \times 12}{0.25^4 \times 4} \right)^{0.28}$$

$$= 2.0 \text{ N/mm}^2 \text{ (same as full-scale structure)}$$

## A2.2 Ring Beam

$$\text{Area of reinforcement, } A_s = \frac{\pi}{4} \times (18)^2 \times 2 = 100.53 \text{ mm}^2$$

$$\text{Percentage of reinforcement, } \frac{A_s'}{bd} = 0.643\%, \quad \frac{A_s}{bd} = 1.0\%$$

$$\text{Using BS 8110 Design charts, Part 3, } \frac{M_u}{bd^2} = 2.5$$

$$\begin{aligned} \text{Thus, } M_u &= 2.5 \times 125 \times 115 \\ &= 4.140 \text{ KNm} \end{aligned}$$

$$\begin{aligned} \text{Extra load added to wall} &= W_{wm} - W_{wall} \\ &= 20 - 5.15 = 14.85 \text{ KN} \end{aligned}$$

Therefore, the surplus weight required per 0.28 m (width of dead-weight bearings on wall)

$$= \frac{14.85 \times 100 \times 0.28}{2.15} = 185 \text{ Kg (about 420 lb).}$$

### APPENDIX 3 IN-HOUSE DEVELOPMENT OF ELECTRONIC DEMEC GAUGE

The HP 85-Data logger model 3456A has four trigger modes to initiate a measurement cycle by the Data Acquisition System. In order to record a measurement at a specific time by the Demec gauge, an externally applied trigger pulse was set up by the control circuit to initiate the instrument externally. The pulse was applied to the External Trigger Input connector located on the rear panel of the HP Model 3456A with a pulse width not less than  $500 \times 10^{-9}$  sec. The External Trigger Input is TTL compatible, with the actual triggering of the instrument occurring on the falling (negative) edge. By application of the pulse, the HP 3456A was then triggered, thus initiating a measurement cycle. After this cycle had been completed, the instrument was in "ready mode", ready to be triggered again for a new cycle. Also, if any triggering was attempted during the measurement cycle, the trigger signal was ignored until the cycle was completed, thus reducing errors caused by accidental mistakes. However, to start a new measurement, the HP 3456A had to be triggered again. This was applied automatically through specially developed software which was run on the HP-85 desktop computer.

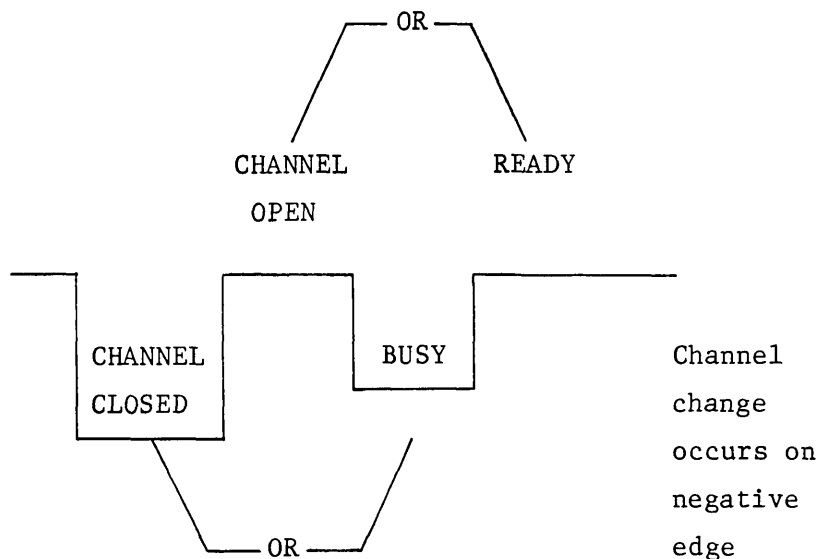


Figure A3.1 External signal requirements.

The negative going edge of a TTL pulse was able to increment the channels in the closing sequence for analog switches. A TTL "low" indicated that a channel was closed, and a TTL "high" indicated that a channel was open. If a signal was sent during the a measurement cycle, the signal levels would be busy (refer to Figure A3.1).

A control circuit was developed that generated an excitation signal, and was able to initiate the measurement cycle. The output signal measured on a Digital Storage Oscilloscope was taken at 4 volt/cm, 5  $\mu$ sec; shown in Figure A3.2. The first upright signal was sufficient to initiate the signal. Noise caused by the switch button as shown in Figure A3.2 did not alter the signal. This was because the rest of the signal was generated after the start of the measurement cycle.

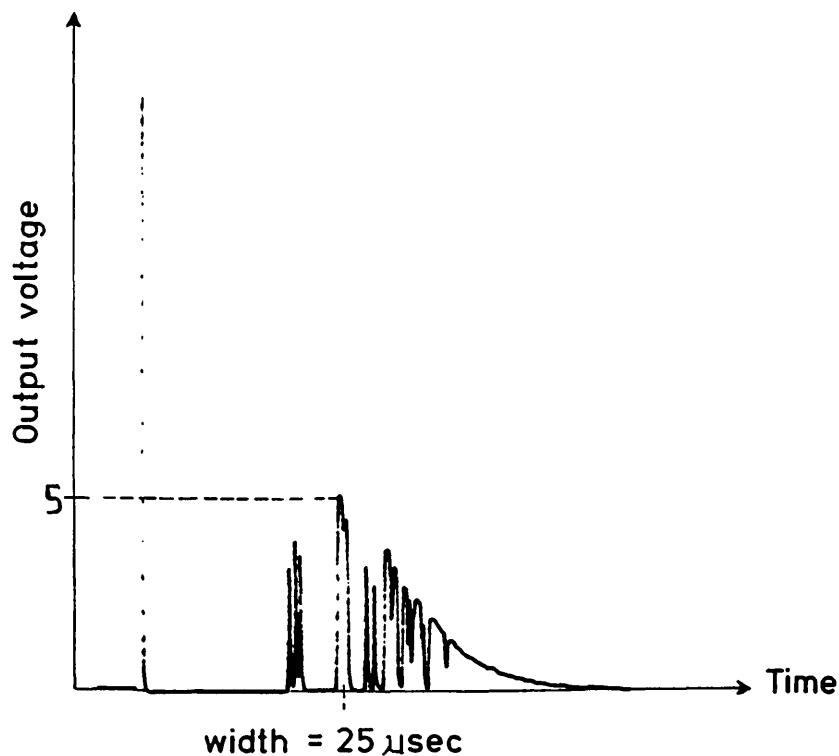


Figure A3.2 Upright signal of Demec gauge.

APPENDIX 4 THEORETICAL INVESTIGATION OF THE MAXIMUM VERTICAL DEFLECTION OF THE FPSS

A4.1 Definitions of the section properties of the FPSS structure.

$$\begin{aligned}
 H &= 1125 \text{ mm}(1828 \text{ mm}) & B &= 2250 \text{ mm} \\
 D &= 1828 \text{ mm} & \delta &= 105 \text{ mm} \\
 E &= 4 \text{ KN/mm}^2 & \nu &= 0.17 \\
 E_1 &= \frac{E}{(1-\nu^2)} = 3.089 \text{ KN/mm}^2 & G &= \frac{E}{2(1+\nu)} = 1.289 \text{ KN/mm}^2
 \end{aligned}$$

$$\begin{aligned}
 I_w &= \frac{\delta B^2 D^2 (D-B)^2}{24(B+D)} = 3.232 \times 10^{15} \text{ mm}^6 & I_p &= \frac{\delta B D (D+B)}{2} = 8.806 \times 10^{11} \text{ mm}^4 \\
 I_s &= \frac{2\delta B^2 D^2}{(B+D)} = 8.711 \times 10^{11} \text{ mm}^4 & \mu_w &= 1 - \frac{I_s}{I_p} = 0.0108
 \end{aligned}$$

Principal sectorial area,  $w(s) = BD = 1.028 \times 10^6 \text{ mm}^2$

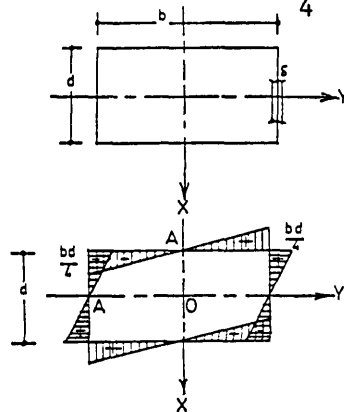


Figure A4.1 Principal sectorial area of a closed rectangular section.

$$\begin{aligned}
 I_{XX} &= 5.905 \times 10^{11} \text{ mm}^4 \\
 I_{YY} &= 4.252 \times 10^{11} \text{ mm}^4 \\
 I_J &= 10.157 \times 10^{11} \text{ mm}^4 \\
 a &= \sqrt{\frac{\mu_w G I_s}{E_1 I_w}} = 1.204 \times 10^{-3} \\
 aL &= 1.354 \\
 Q &= \frac{G I_s}{2 - 2\cosh aL + a \sinh aL} = 8.8967 \times 10^{12} \text{ KNmm}^2
 \end{aligned}$$

A4.2 Design procedure for unreinforced walls (Test W1, W2 and W3).

$\epsilon_{\max} = 301$  microstrain, corresponding to a stress of

$$\sigma_{\max} = 1.02 \text{ N/mm}^2$$

$$B_2 = \frac{\sigma I_w}{\bar{w}(s)\delta} = \frac{1.02 \times 1.232 \times 10^{15}}{1028250 \times 105} = 30533.99 \text{ KNmm}$$

but, from equation(7.34)  $B_2 = -1.716B_1 + 1.395T_1$

$$= -1.716 \left( \frac{T_1}{2} \cdot \frac{4H}{L^2} \cdot \frac{D}{4} \right) + 1.395T_1$$

$$= -0.263T_1$$

i.e.  $T_1 = -116003.29 \text{ KNmm}$

Substituting in equation(7.36), the maximum vertical deflection is given as,

$$u(s,z) = \bar{w}(s) \left( \frac{-\theta(z)}{\mu_w} + \frac{M_z}{\mu_w G I_p} \right)$$

$$= \frac{1028250}{0.0108 \times 1.289 \times 8.806 \times 10^{11}} \cdot \frac{-116003.29}{1}$$

$$= 9.731 \text{ mm}$$

#### A4.3 Design procedure for partially reinforced walls (Test W5).

The analysis is subdivided into two portions, one has the characteristic properties of reinforced masonry and the other is treated as unreinforced masonry. This is provided by dividing the walls into two portions, the latter one has a height of  $H_1 = 1447 \text{ mm}$  and the former has a wall height of  $H_2 = 381 \text{ mm}$ .

The properties of the reinforced portion is given as follows,

$$E = 15 \text{ KN/mm}^2 \quad \nu = 0.17$$

$$E_1 = \frac{E}{(1-\nu^2)} = 15.45 \text{ KN/mm}^2 \quad G = \frac{E}{2(1+\nu)} = 6.410 \text{ KN/mm}^2$$

$$a = \sqrt{\frac{\mu_w G I_s}{E_1 I_w}} = 5.384 \times 10^{-4} \quad aL = 0.2051$$

$$Q = \frac{G I_s}{2 - 2\cosh aL + aL \sinh aL}$$

$$= \frac{6.410 \times 8.711 \times 10^{11}}{2 - 2\cosh 0.205 + 0.205 \sinh 0.205} = 3.77 \times 10^{16} \text{ KNmm}^2$$

From equation(7.34), and for  $L = 1447 \text{ mm}$ ,

$$\begin{bmatrix} \phi_2 \\ \theta_2 \\ \frac{B_2}{GI_s} \\ \frac{T_2}{GI_s} \end{bmatrix} = \begin{bmatrix} 1 & 2298.45 & -1.942 & -851.15 \\ 0 & 2.942 & -3.331 \times 10^{-3} & -1.942 \\ 0 & -2297.9 & -2.942 & 2.767 \\ 0 & 0 & 0 & 1 \end{bmatrix} \begin{bmatrix} 0 \\ 0 \\ 1.201 \times 10^{-7} \\ 9.662 \times 10^{-8} \end{bmatrix}$$

$\phi_2 = -8.247 \times 10^{-5}$   
 $\theta_2 = -1.880 \times 10^{-7}$   
 $B_2 = -96549.94 \text{ KNmm}$

and for  $L = 381 \text{ mm}$ ,

$$\begin{bmatrix} \phi_3 \\ \theta_3 \\ \frac{B_3}{GI_s} \\ \frac{T_3}{GI_s} \end{bmatrix} = \begin{bmatrix} 1 & -0.038 & -0.021 & -2.677 \\ 0 & 1.021 & -1.112 \times 10^{-4} & -0.021 \\ 0 & -383.65 & 1.021 & 0.207 \\ 0 & 0 & 0 & 1 \end{bmatrix} \begin{bmatrix} -8.247 \times 10^{-5} \\ -1.880 \times 10^{-7} \\ -8.598 \times 10^{-8} \\ 9.662 \times 10^{-8} \end{bmatrix}$$

For  $\epsilon_{\max} = 821 \text{ microstrain}$ , corresponding to a stress of  
 $\sigma_{\max} = 12.31 \text{ N/mm}^2$   
 Therefore,  $B_3 = \frac{\sigma I_w}{\bar{w}(s)\delta}$

From the above equations for  $L = 381 \text{ mm}$ ,

$$\begin{aligned} B_3 &= 1.880 \times 10^{-7} \times 383.64 \times GI_s - 1.021 B_2 + 0.207 T_2 \\ &= 0.541 T_2 \end{aligned}$$

Thus,  $T_2 = -63254.96 \text{ KNmm}$

Also from the above equation for  $L = 1447 \text{ mm}$ ,

$$\begin{aligned} B_2 &= \left( \frac{-T_2}{2} \right) \left( \frac{4H}{L^2} \right) \left( \frac{D}{4} \right)^3 \\ &= 78620.28 \text{ KNmm} \end{aligned}$$

$$\begin{aligned} \text{but } B_2 &= -2.942 B_1 + 2.767 T_1 \\ &= -0.822 T_1 \end{aligned}$$

Therefore,  $T_1 = -95646.09 \text{ KNmm}$

The maximum allowable deflection is given by equation(7.36) as,

$$\begin{aligned} u(s, z) &= \bar{w}(s) \left( \frac{-\theta(z)}{\mu_w} + \frac{M_z}{\mu_w GI_p} \right) \\ &= 1028250 \frac{-95646.09}{0.0108 \times 1.289 \times 8.806 \times 10^{11}} = -8.02 \text{ mm} \end{aligned}$$



## APPENDIX 5 WALL STRAIN CONTOURS

Subroutine GENCON consists of two separate programs, namely,

(a) Program NAGCON1, and

(b) Program CONTOUT.

Program NAGCON1 generates a fine mesh of  $17 \times 13$  points by interpolation using a Nag routine file E01ACF. This routine is capable of interpolating at a given point (A,B) from a table of function values defined on a rectangular grid in the X-Y plane, by fitting bi-cubic spline functions. The entire grid is used for interpolation instead of simply the adjacent points, thus two separate spline curves were fitted along the X and Y axes through each point. The surface of the spline is specified by the rectangular grid of points lying in the X-Y plane and by the values of  $F(x,y)$  at each point on the grid. The co-ordinates of the points are defined by  $N1$  equidistant points along the X-axis and  $M1$  points along the Y-axis. However, non-equidistant points could also be accommodated by defining an imaginary rectangular grid superimposed over the original data.

For each  $Y_j$  grid level, a cubic spline is fitted to the input values  $F(x_i, y_i)$  for  $i=1,2,\dots,N1$  and  $F(a, Y_j)$  is determined. Also, a cubic spline is fitted to these calculated values  $F(a, Y_j)$  for  $j=1,2,\dots,M1$  and the interpolated values are obtained first by fixing the X-coordinates. The process is then repeated in the reverse order, that is, for each  $X_i$  a cubic spline is fitted to  $F(x_i, Y_j)$  for  $j=1,2,\dots,M1$  and  $F(x_i, b)$  is determined and then a cubic spline is fitted to  $F(x_i, b)$  for  $i=1,2,\dots,N1$  and the interpolated value is calculated.

Program CONTOUT traces points of equal magnitude and generates a data file for a plotting package GIPS. An existing program CONTOUR (Burgoyne, 1986) was modified to define the different levels of contours required according to the range of the maximum and minimum strains available in the wall. This was necessary to enable contouring at different levels since wide spread of strains was present. The scale of plotting was defined at each cycle of settlement to accommodate all strain levels, however this was different for each load cycle. In order to reduce the effect of the program interpolation of equal strains, a subroutine was added to check that no troughs or crests were generated at points away from the rectangular grid of data points.

## APPENDIX 6 EXPERIMENTAL RESULTS AND DATA

In this appendix, plots of test results are included for each structural model , namely:

- (1) Vertical deflection of the wall at three horizontal sections, namely, top, middle height and soffit of wall.
- (2) Vertical and horizontal wall strain at each settlement stage.
- (3) Selected wall strain contours before settlement and at each settlement stage.

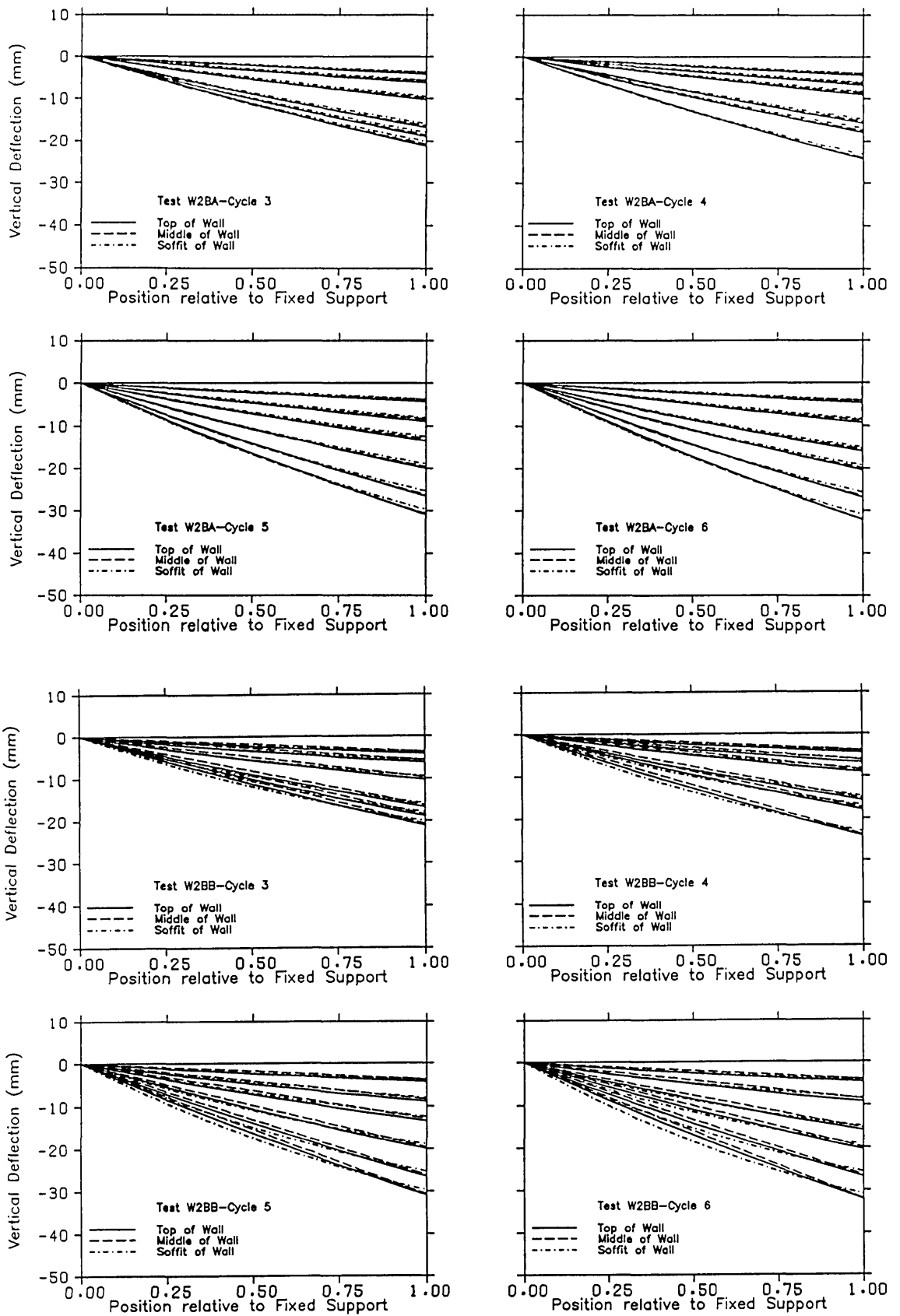


Figure A6.1 Effect of cyclic settlement on the vertical deformation of the wall (Test W2B).

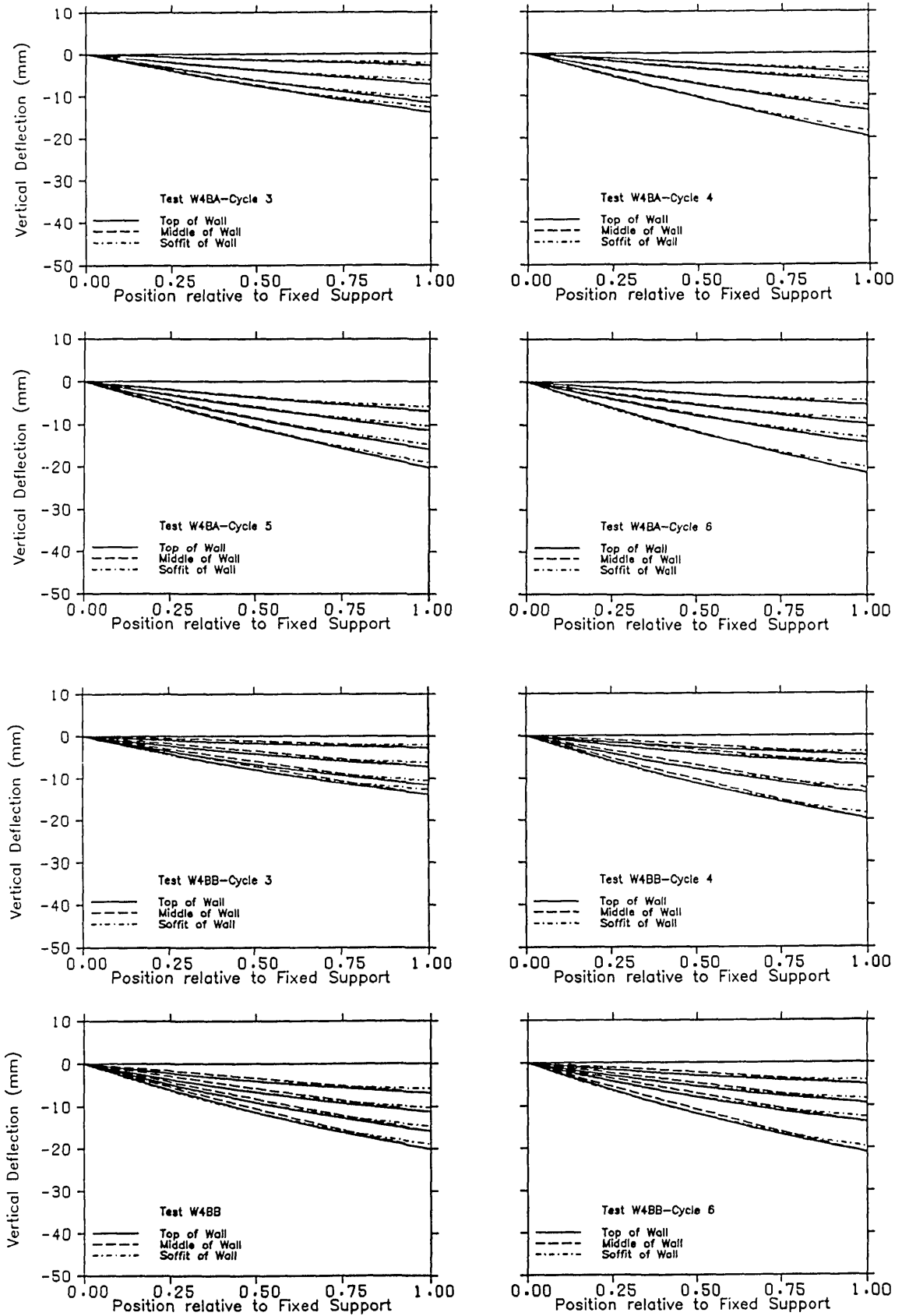


Figure A6.2 Effect of cyclic settlement on the vertical deformation of the wall (Test W4B).

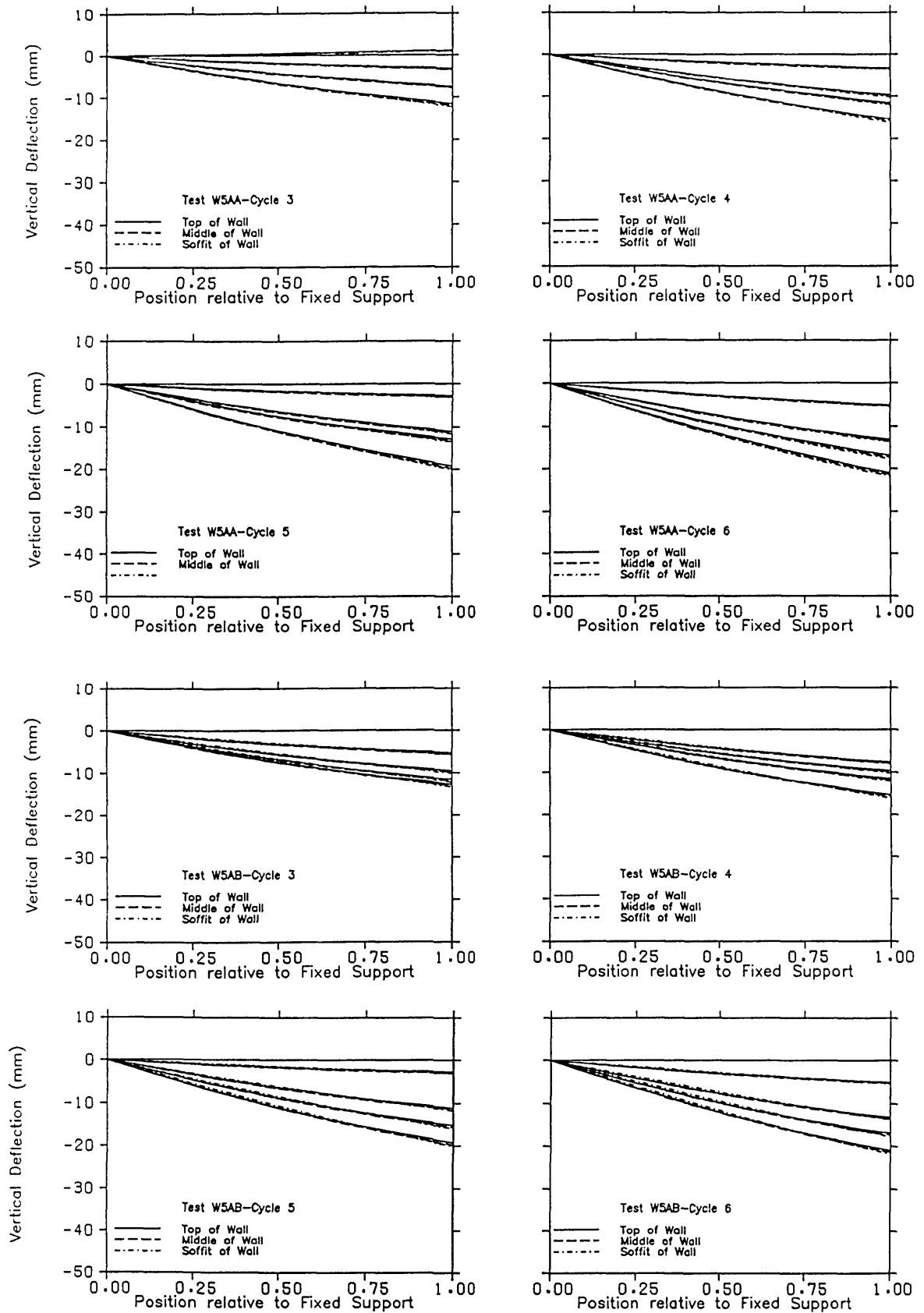


Figure A6.3 Effect of cyclic settlement on the vertical deformation of the wall (Test W5A).

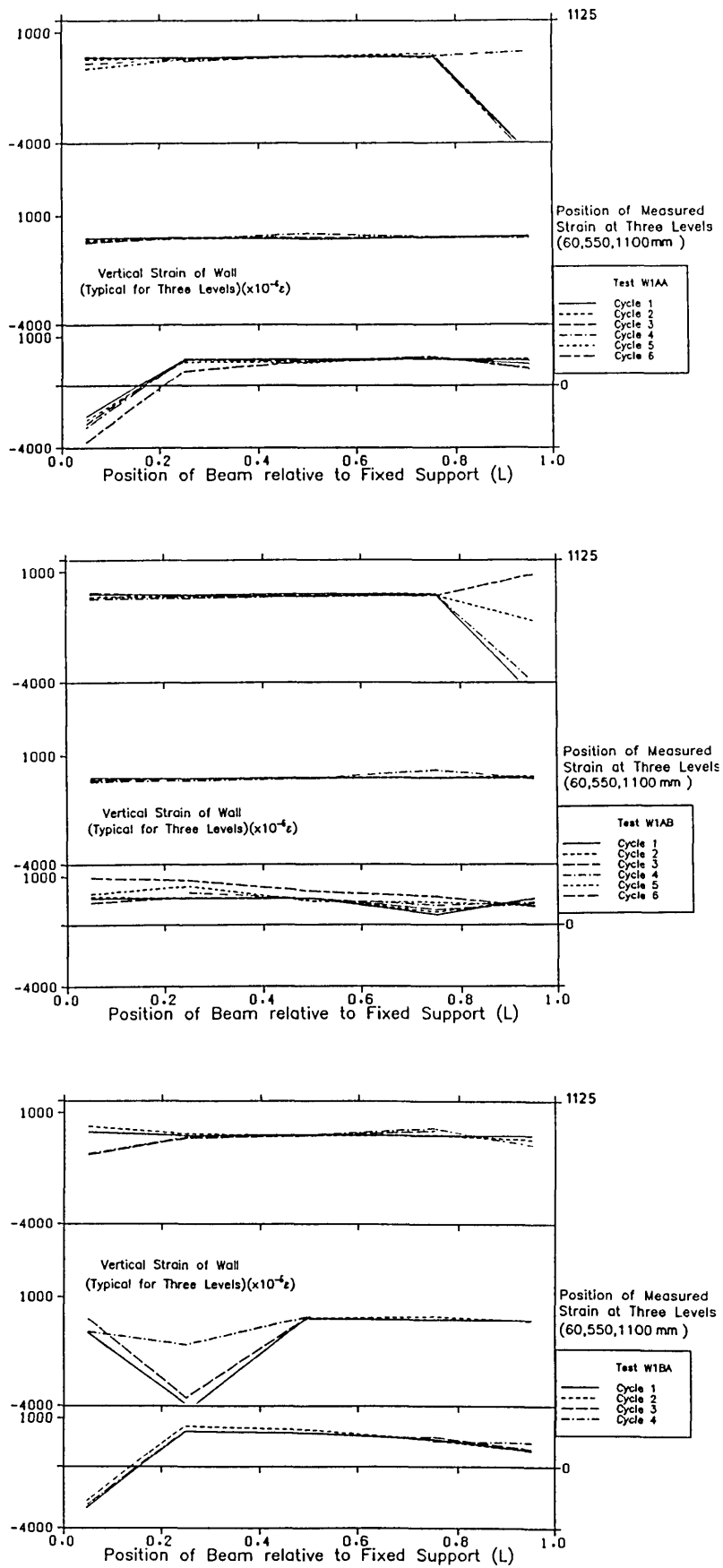


Figure A6.4 Distribution of vertical strain along wall (Test W1).

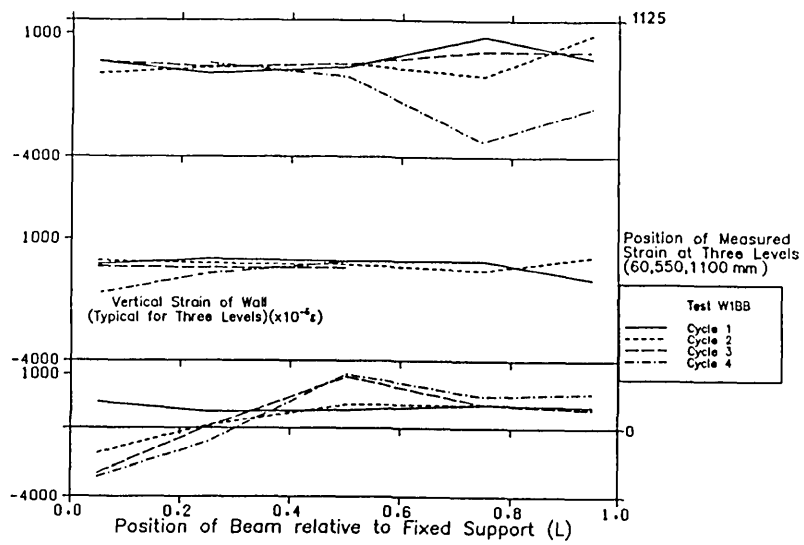


Figure A6.4 Continued.

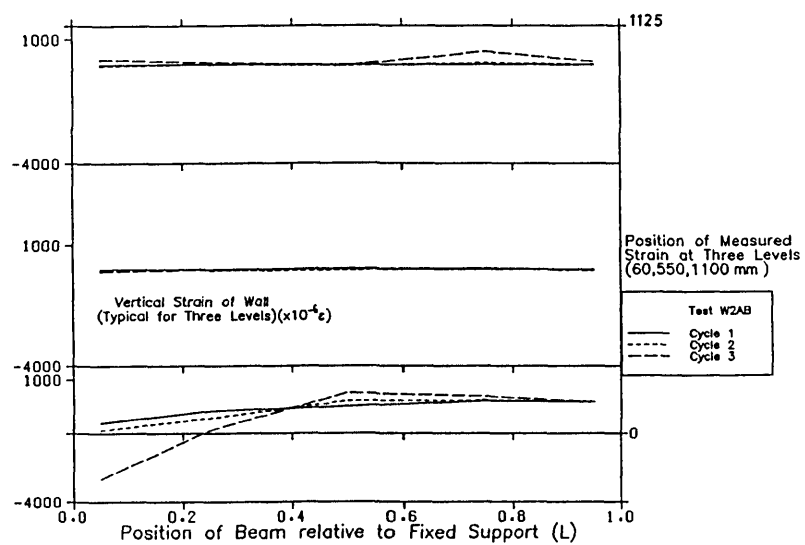
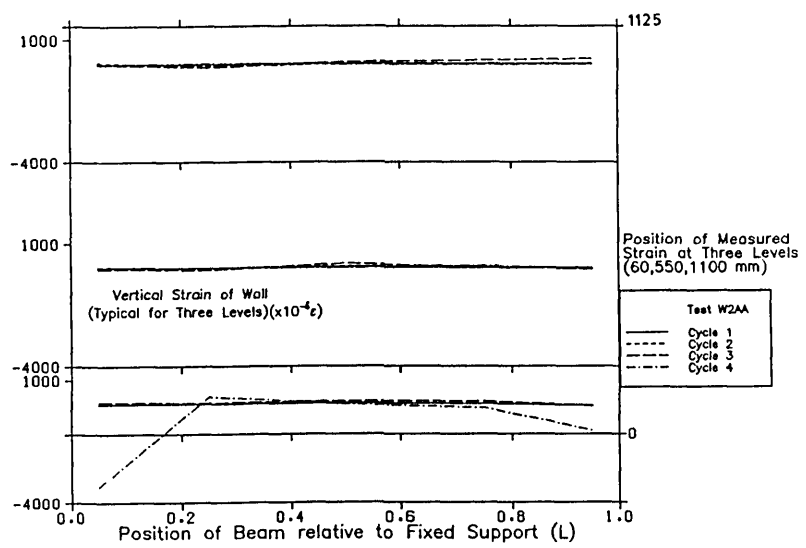


Figure A6.5 Distribution of vertical strain along wall (Test W2).

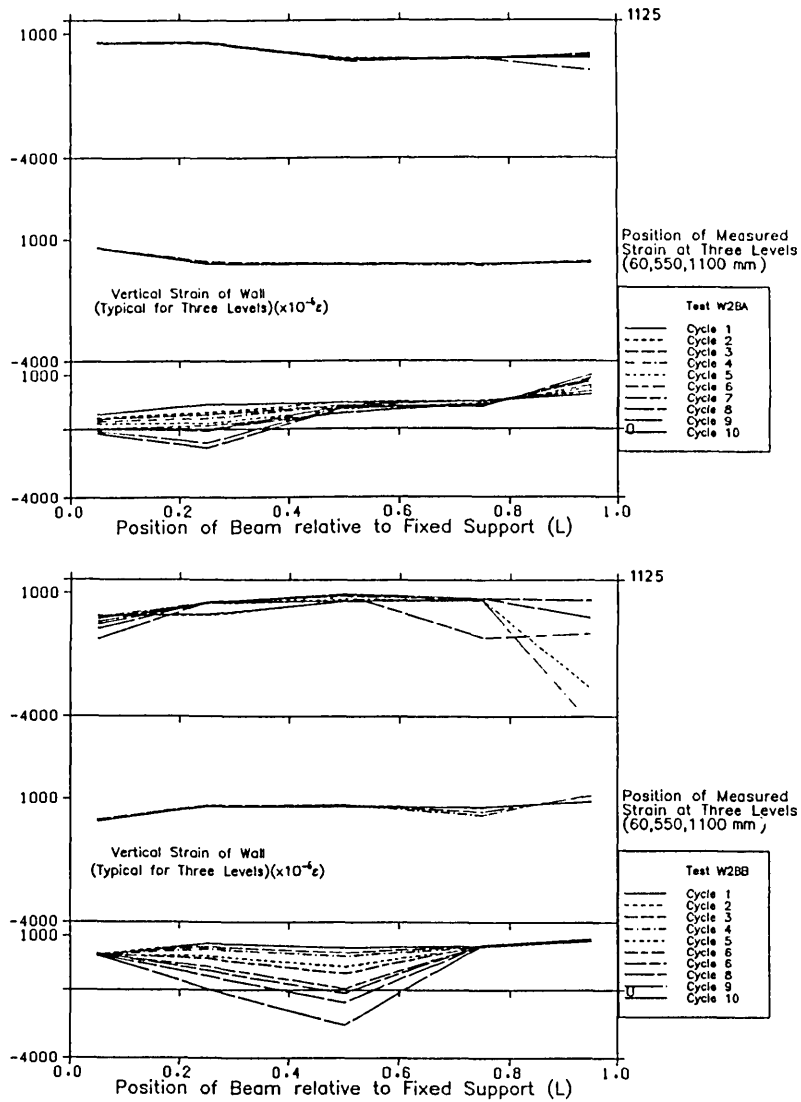


Figure A6.5 Continued.

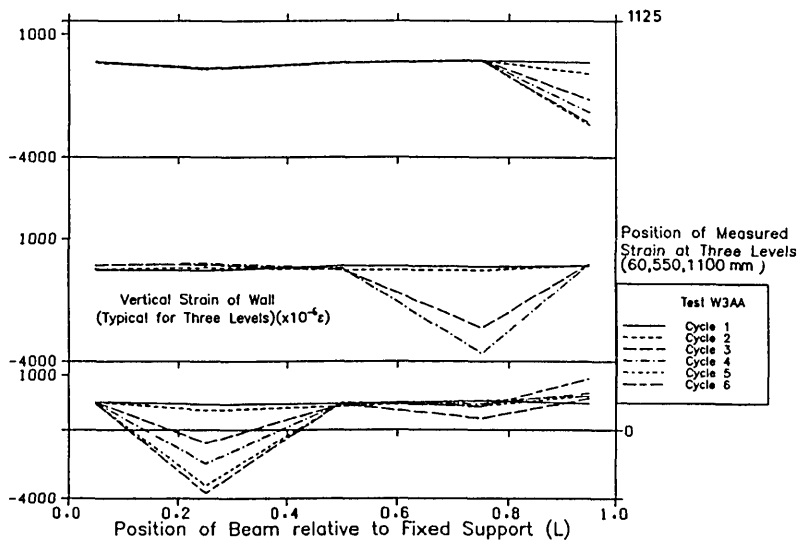


Figure A6.6 Distribution of vertical strain along wall (Test W3).



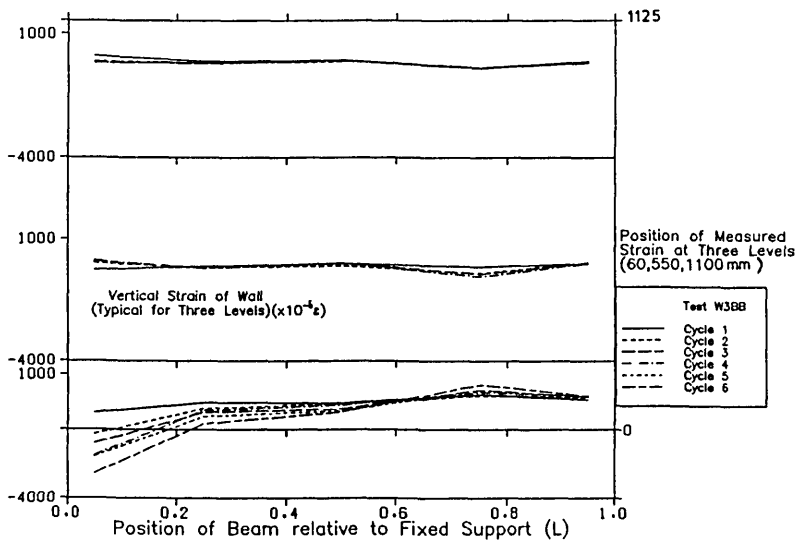
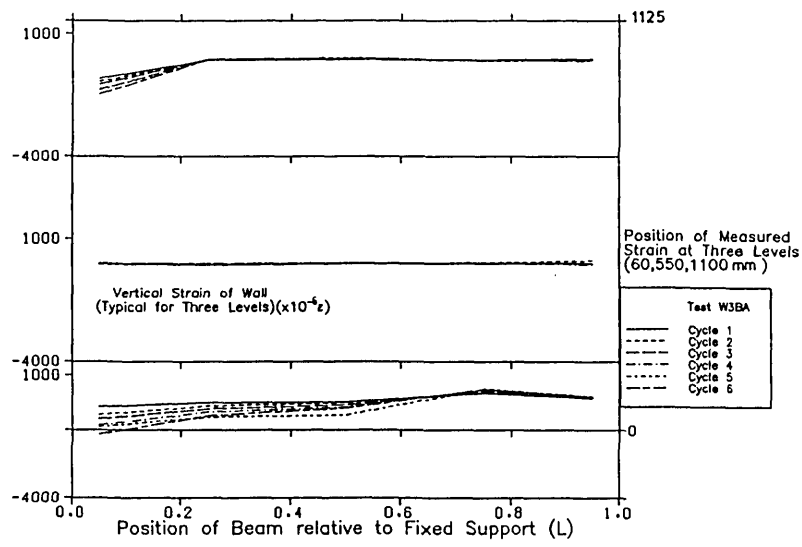
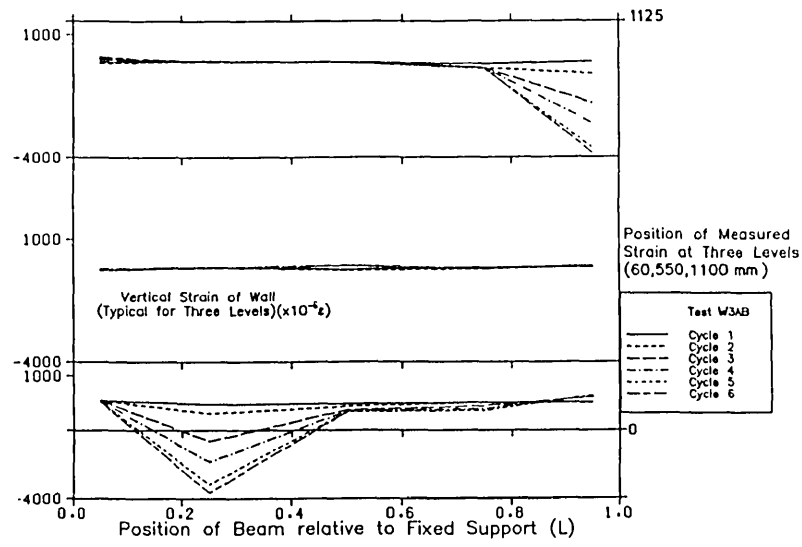


Figure A6.6 Continued.

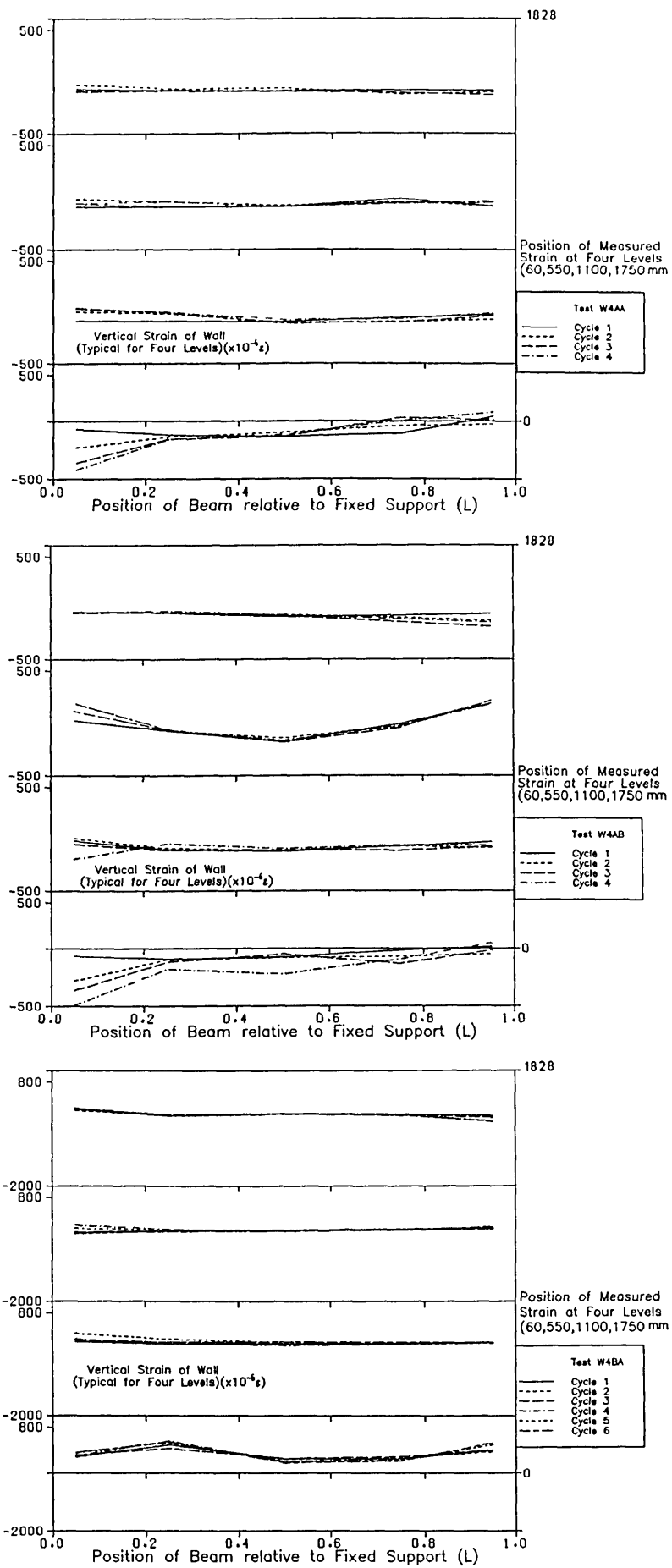


Figure A6.7 Distribution of vertical strain along wall (Test W4).

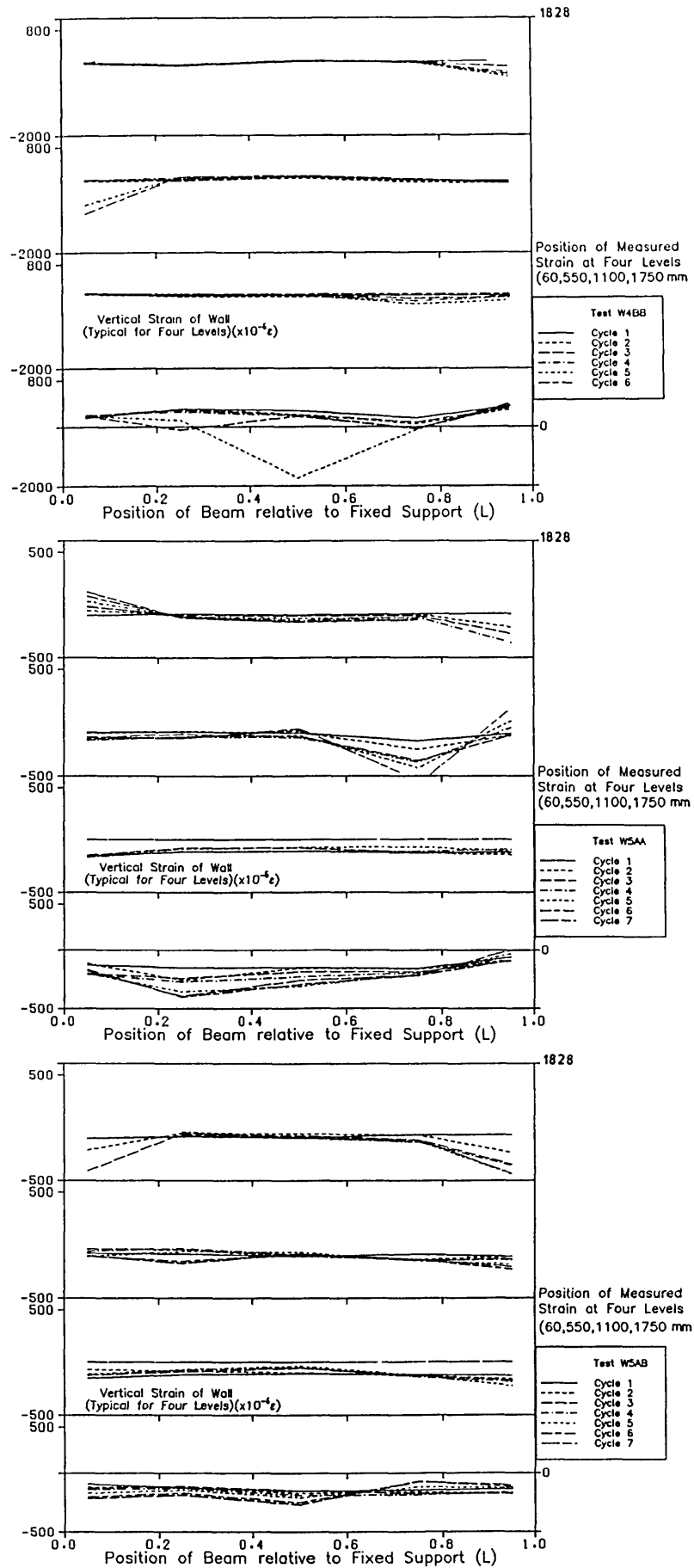


Figure A6.8 Distribution of vertical strain along wall (Test W5).

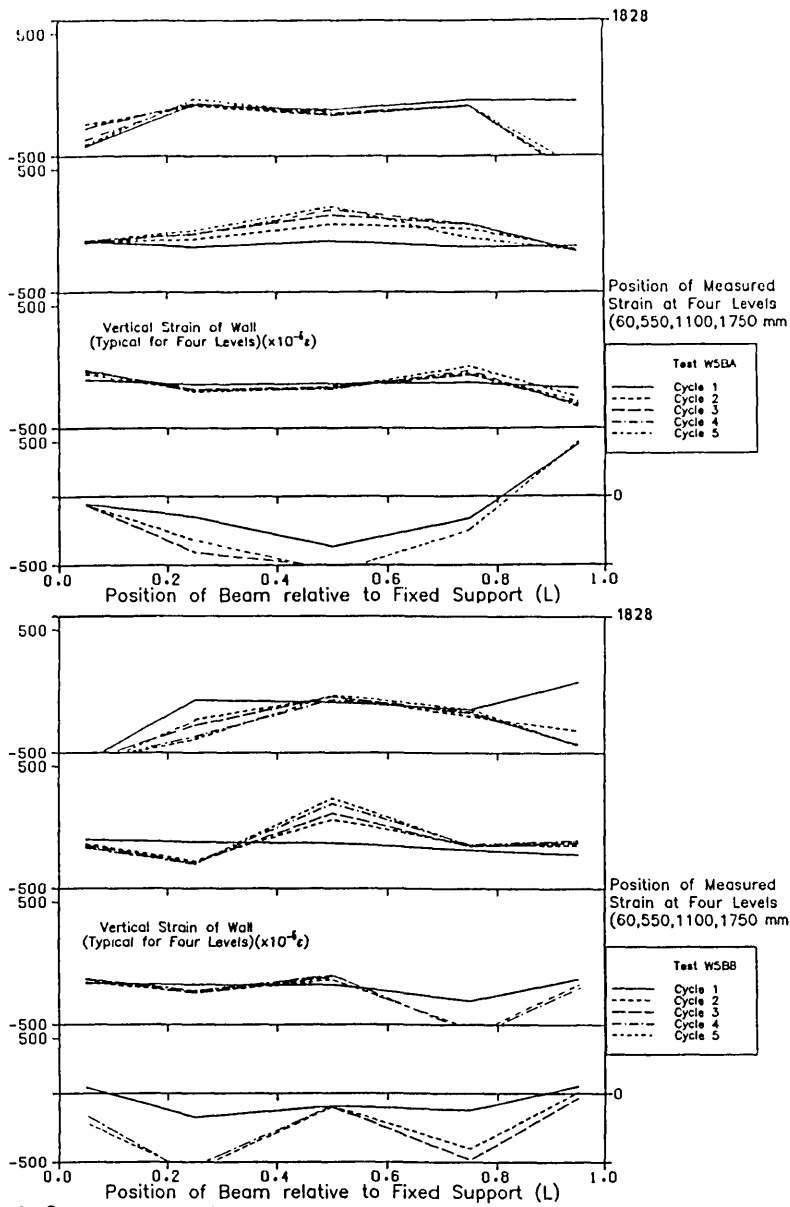


Figure A6.8 Continued.

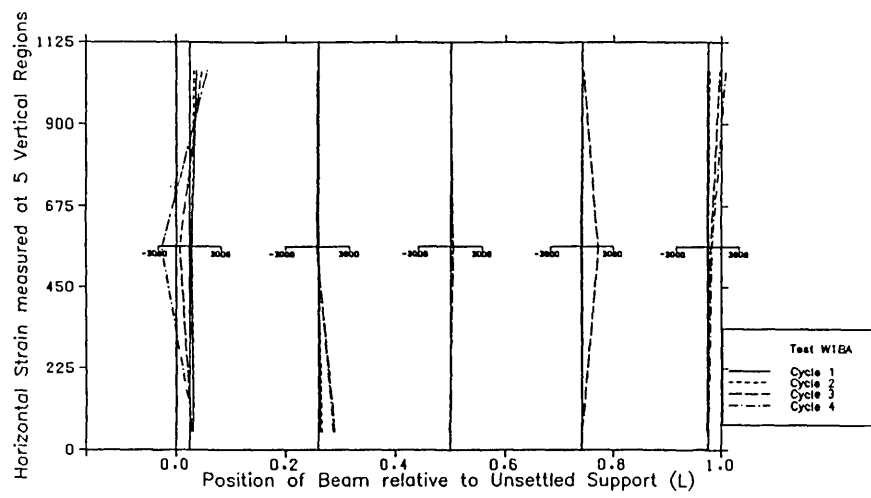
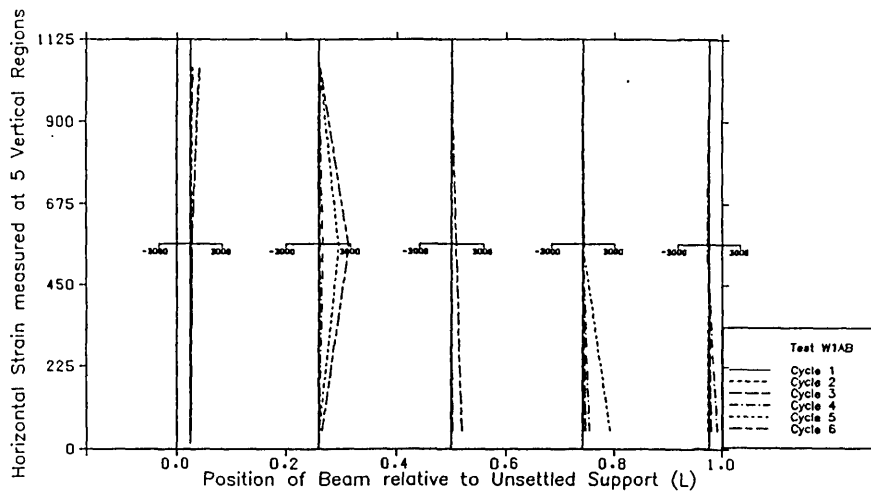
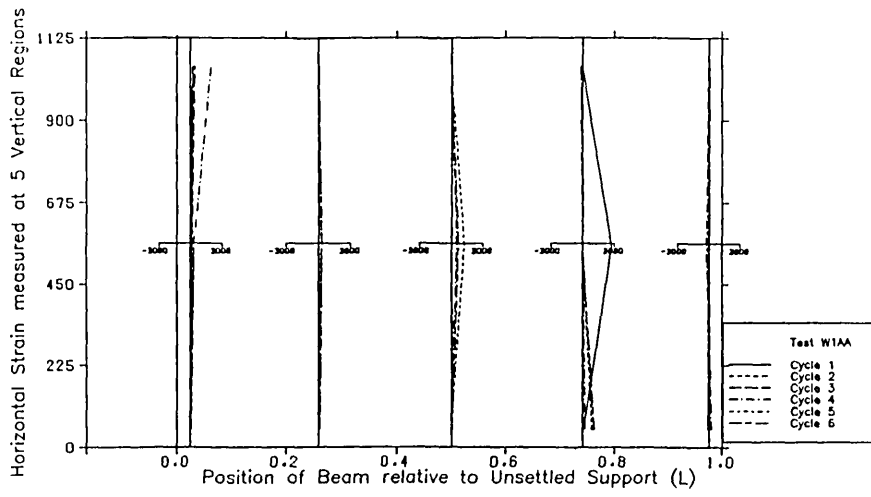


Figure A6.9 Distribution of horizontal strain along wall (Test W1).

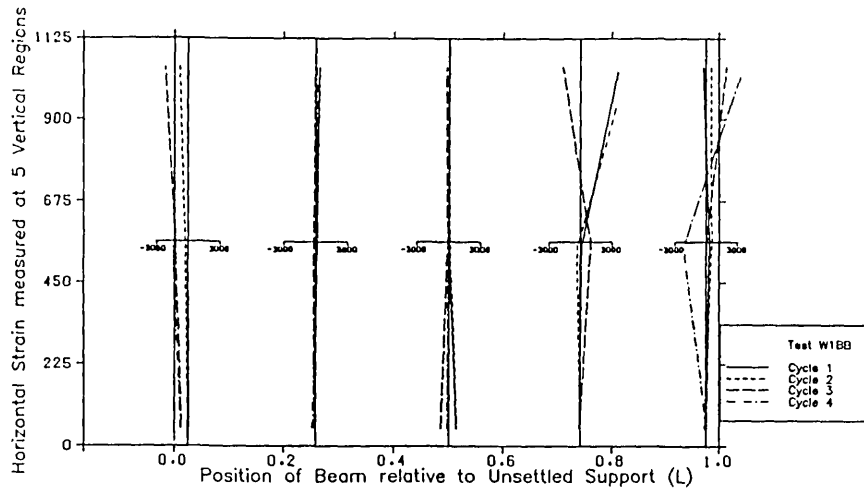


Figure A6.9 Continued.

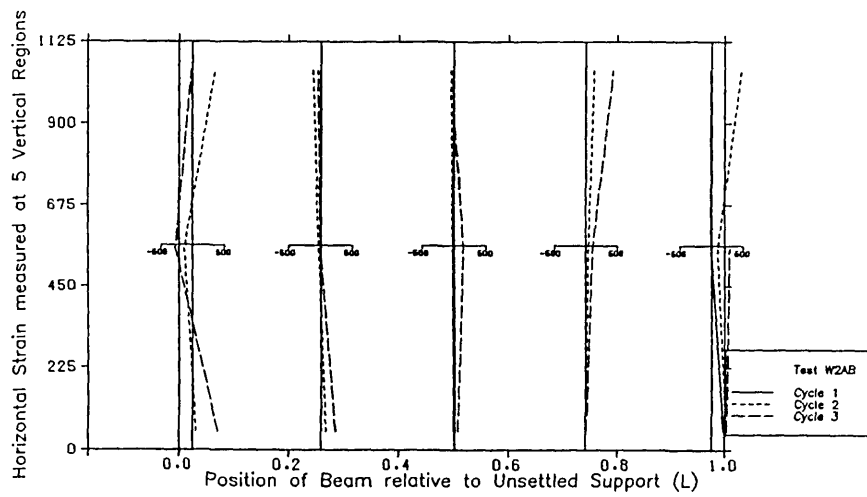
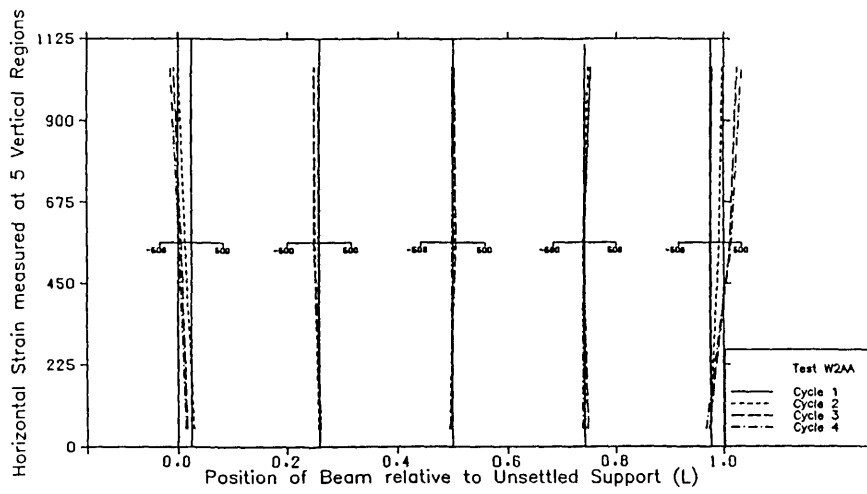


Figure A6.10 Distribution of horizontal strain along wall (Test W2).

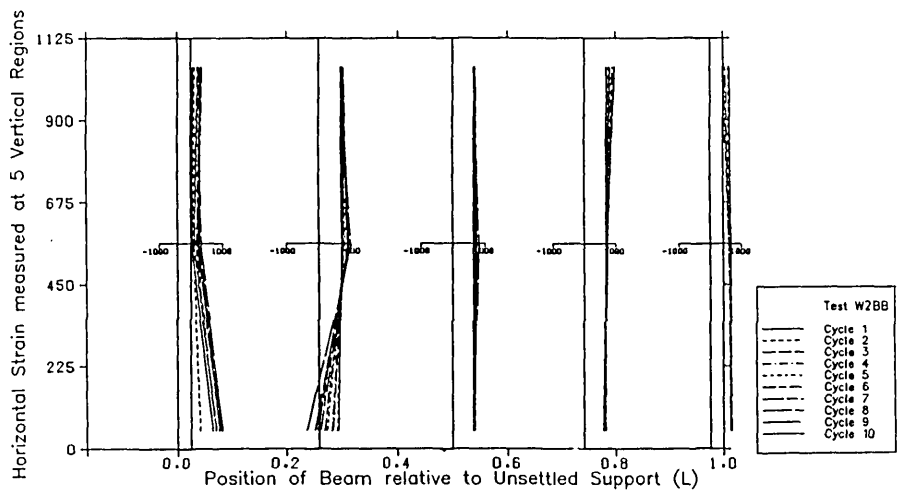
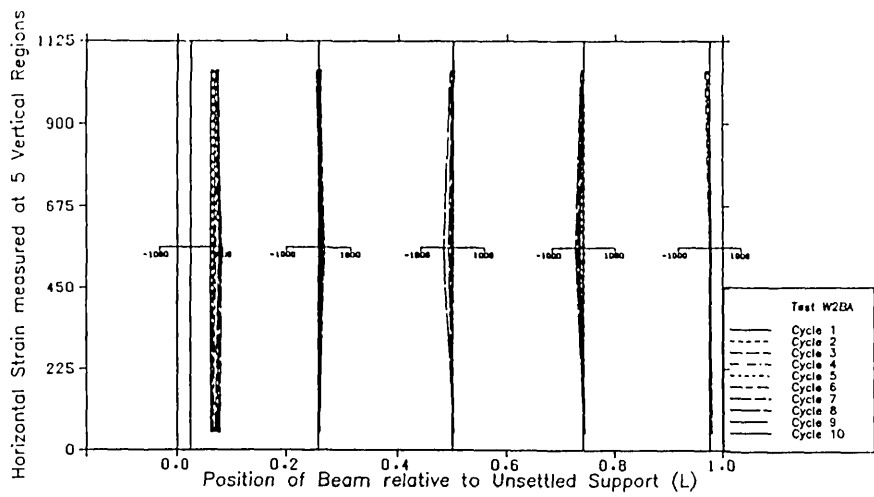


Figure A6.10 Continued.

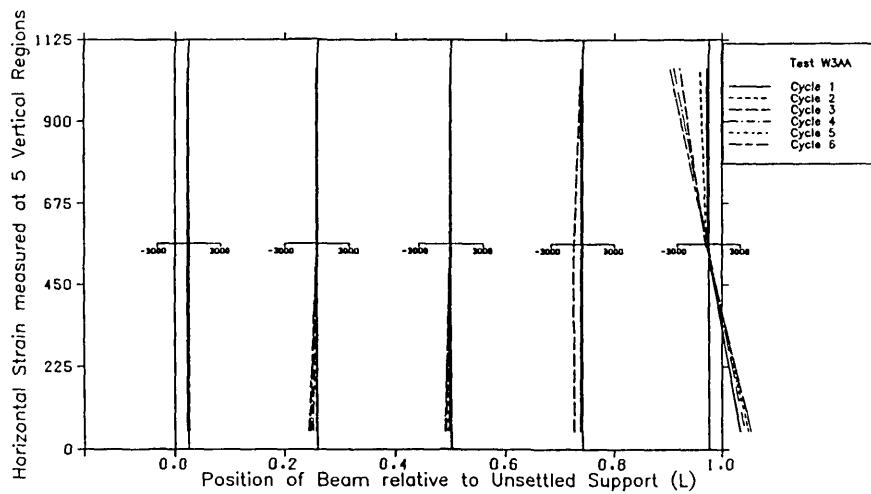


Figure A6.11 Distribution of horizontal strain along wall (Test W3).

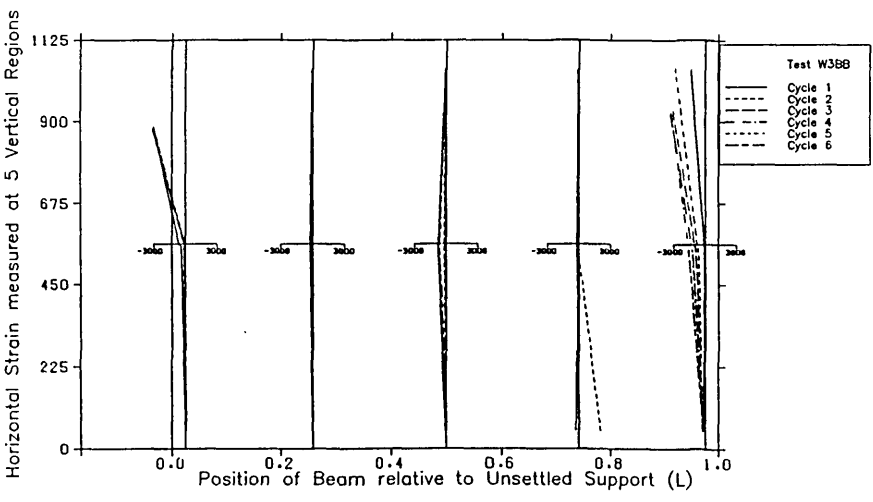
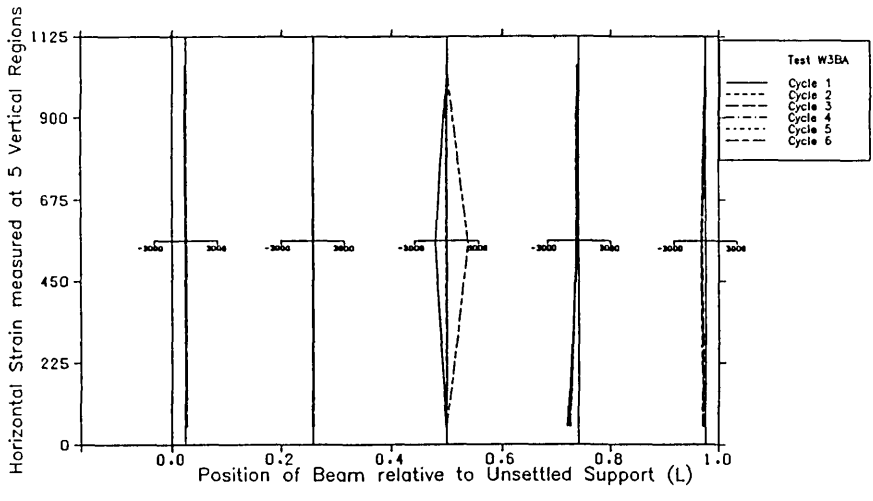
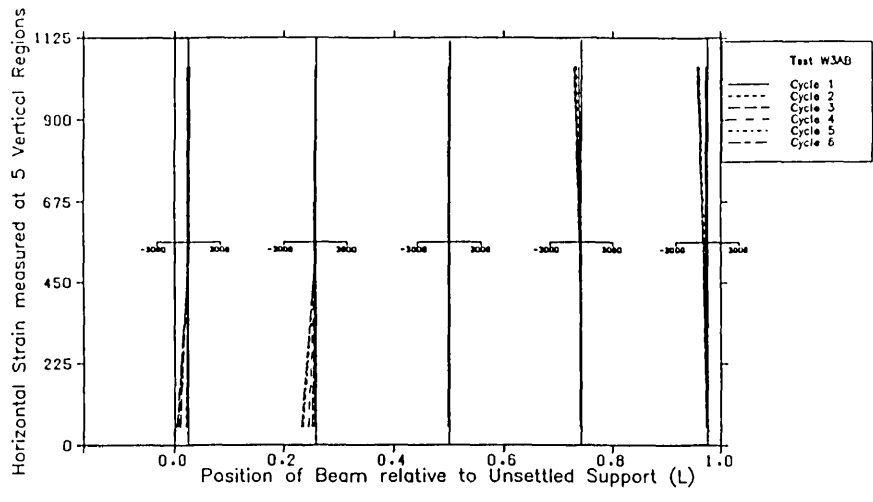


Figure A6.11 Continued.



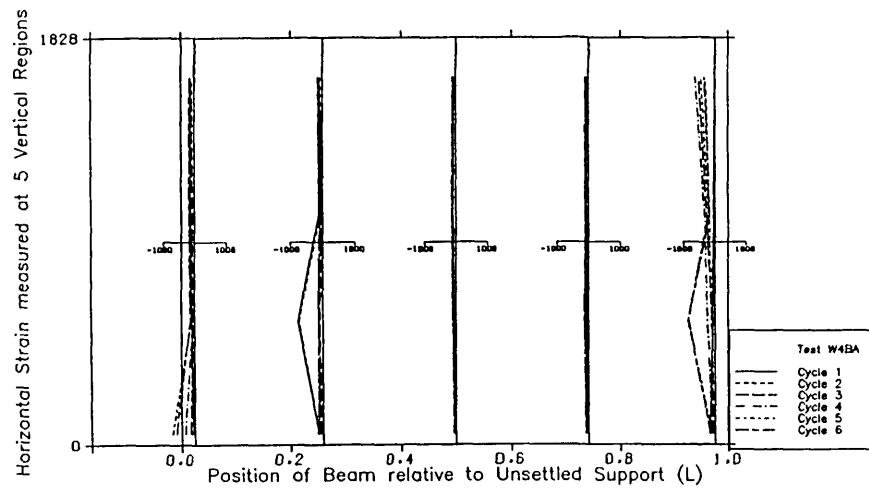
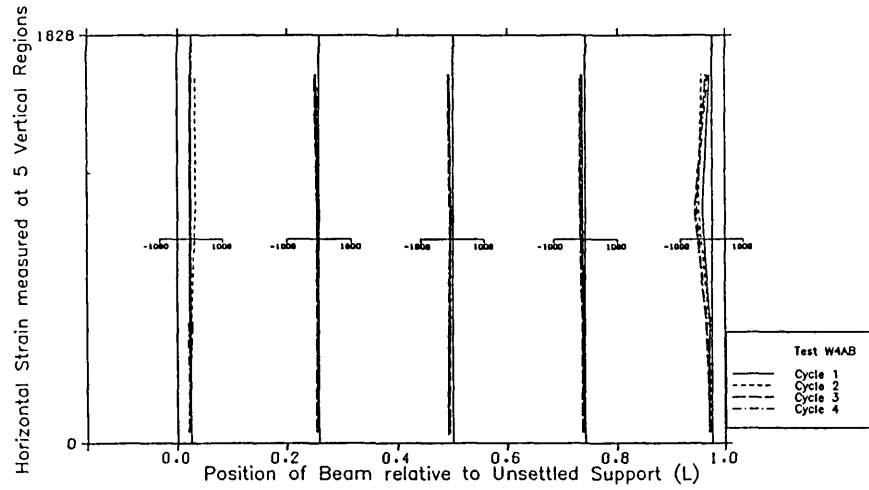
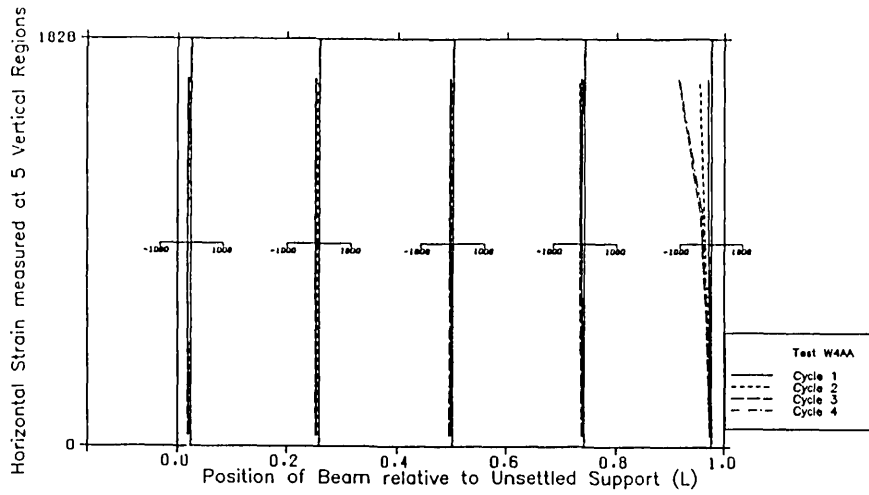


Figure A6.12 Distribution of horizontal strain along wall (Test W4).

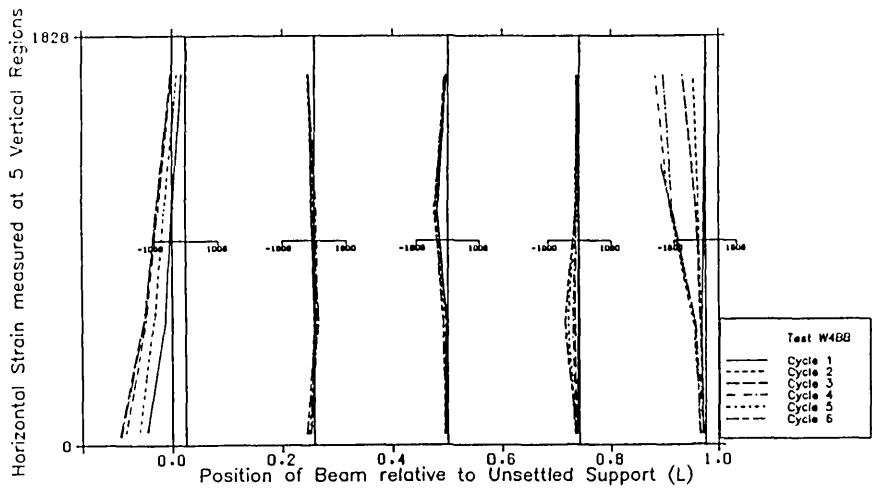


Figure A6.12 Continued.

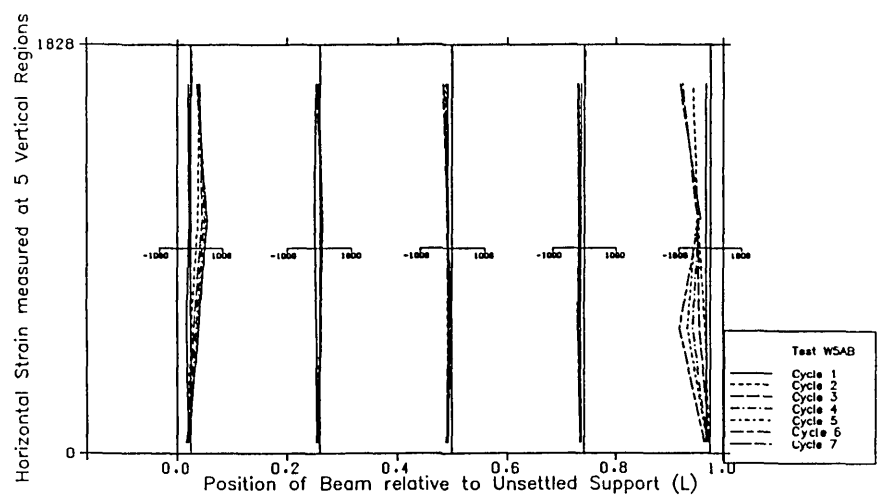
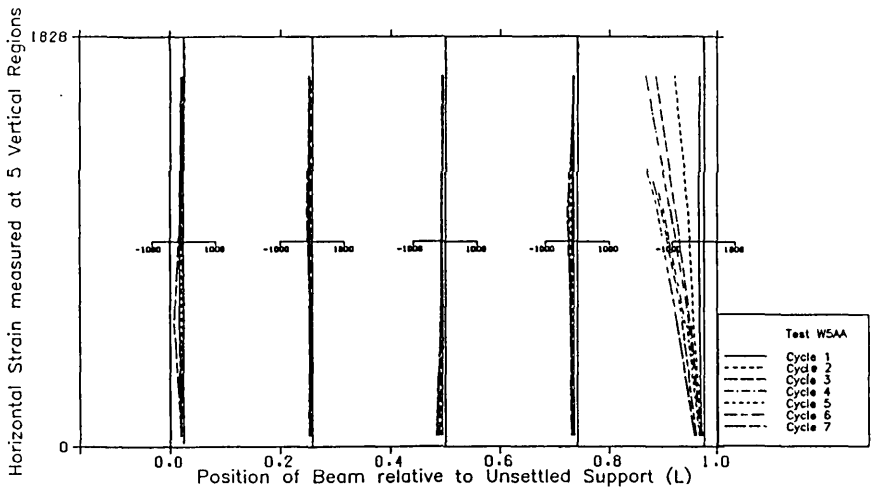


Figure A6.13 Distribution of horizontal strain along wall (Test W5).

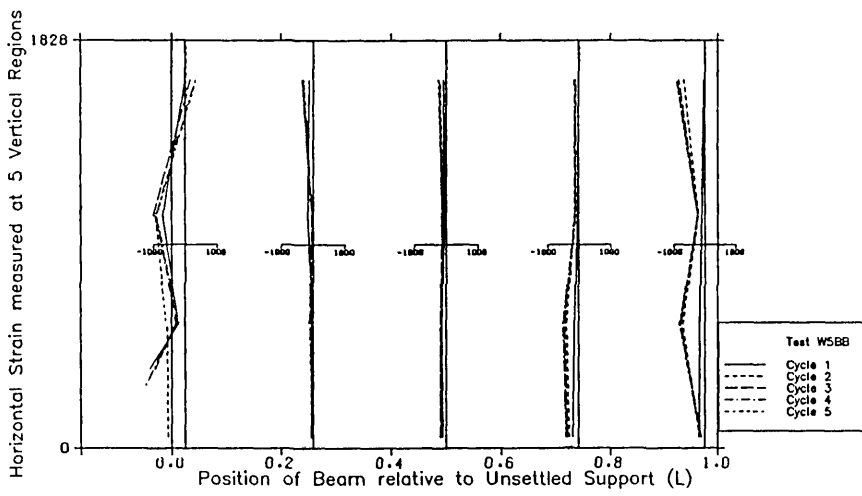
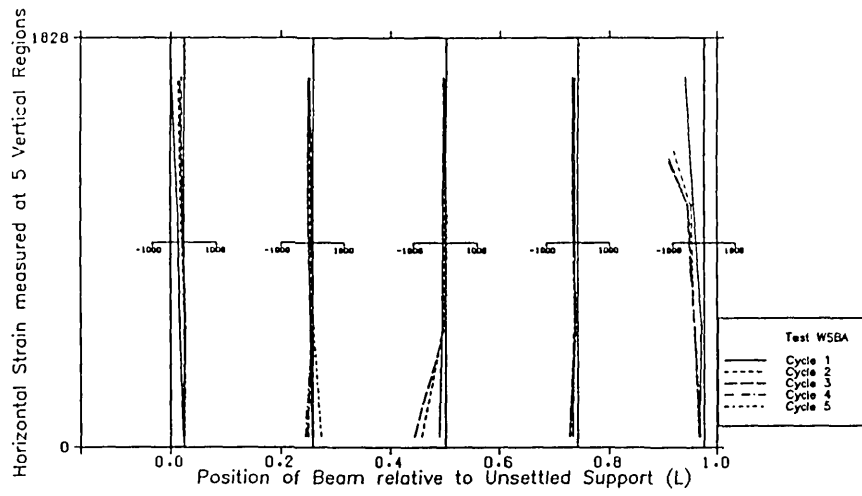


Figure A6.13 Continued.

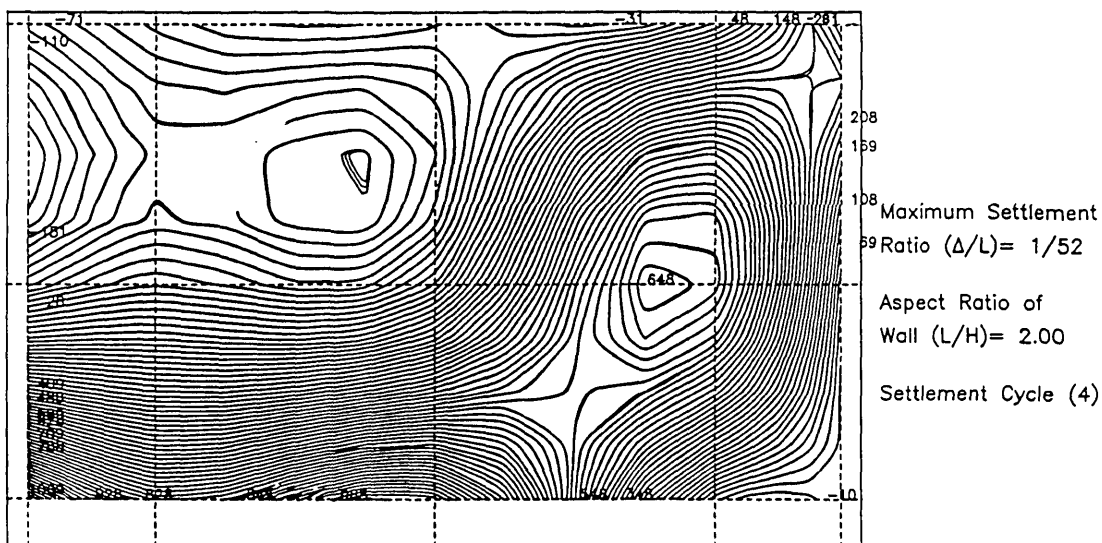
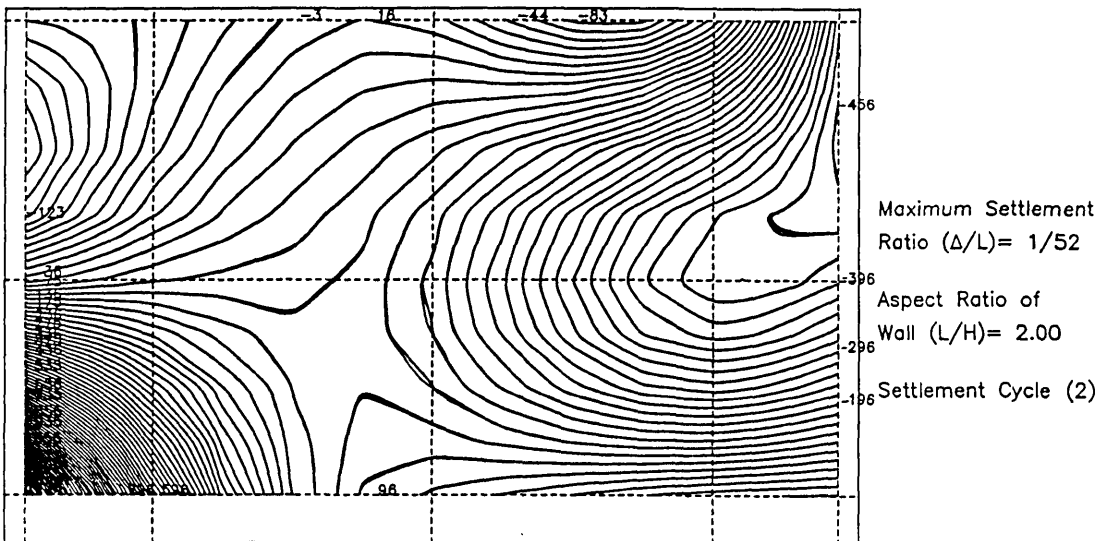
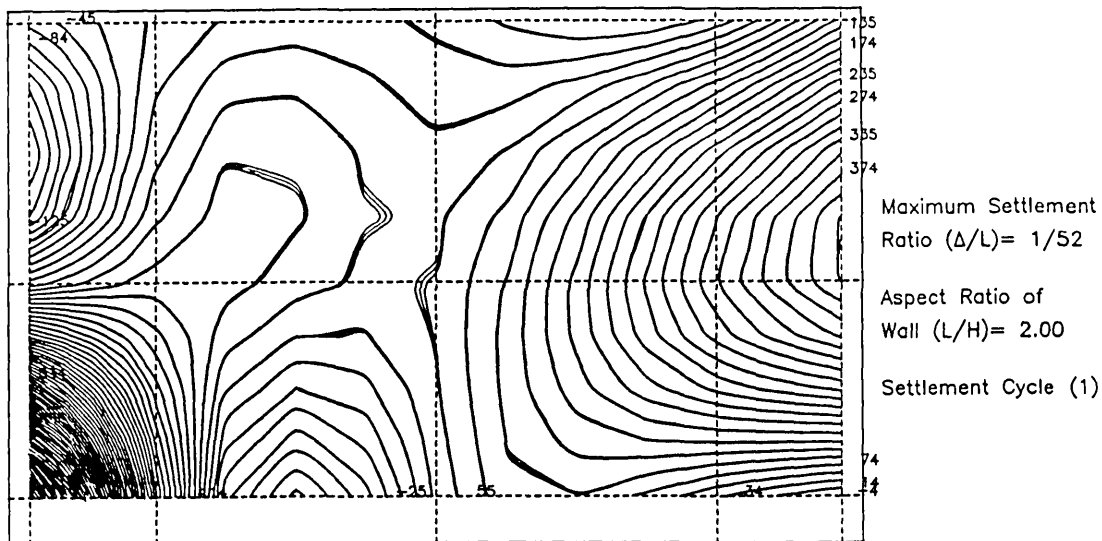


Figure A6.14 Maximum principal strain distribution of wall (Test W1BA).

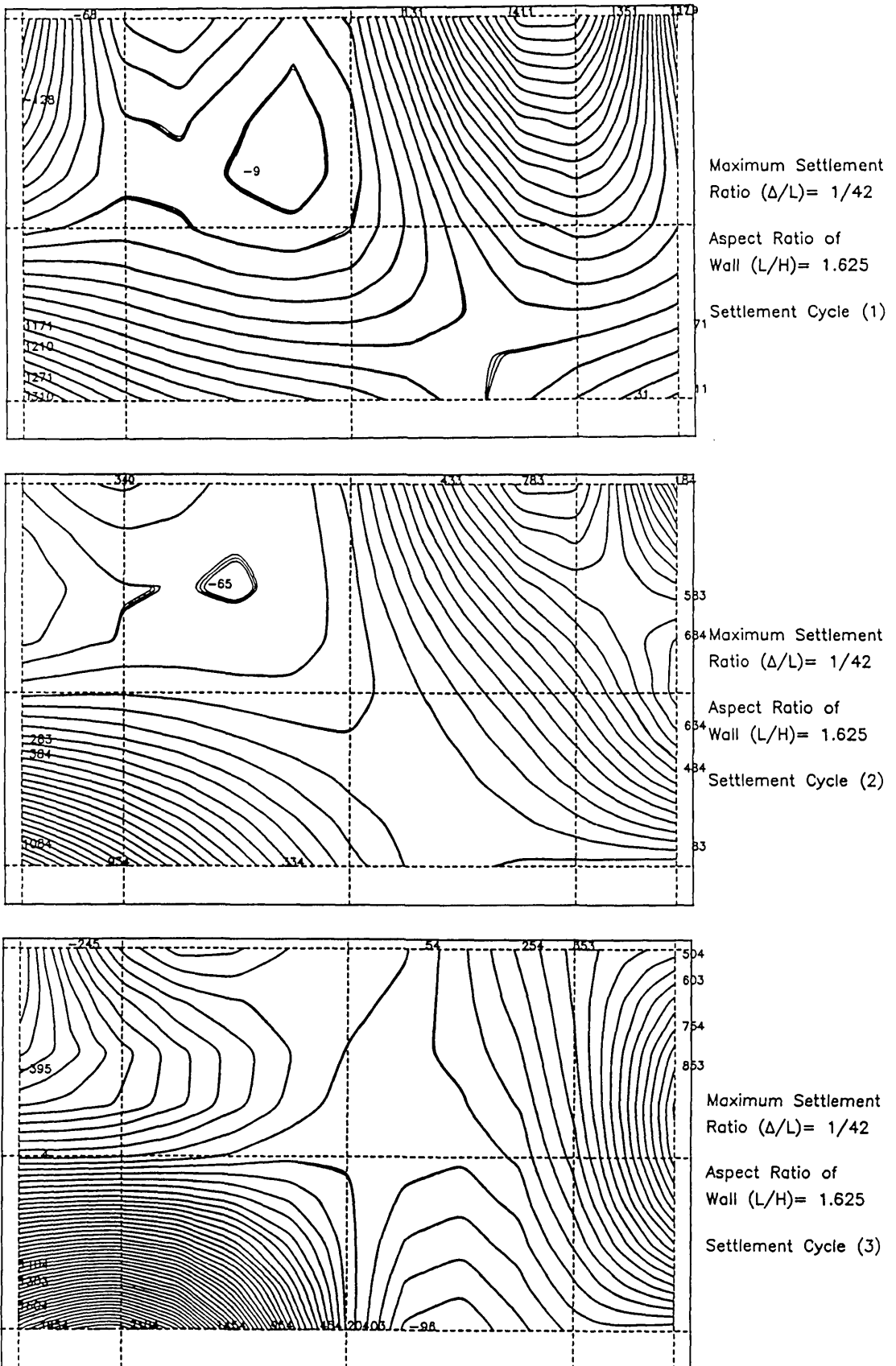


Figure A6.15 Maximum principal strain distribution of wall (Test W1BB).

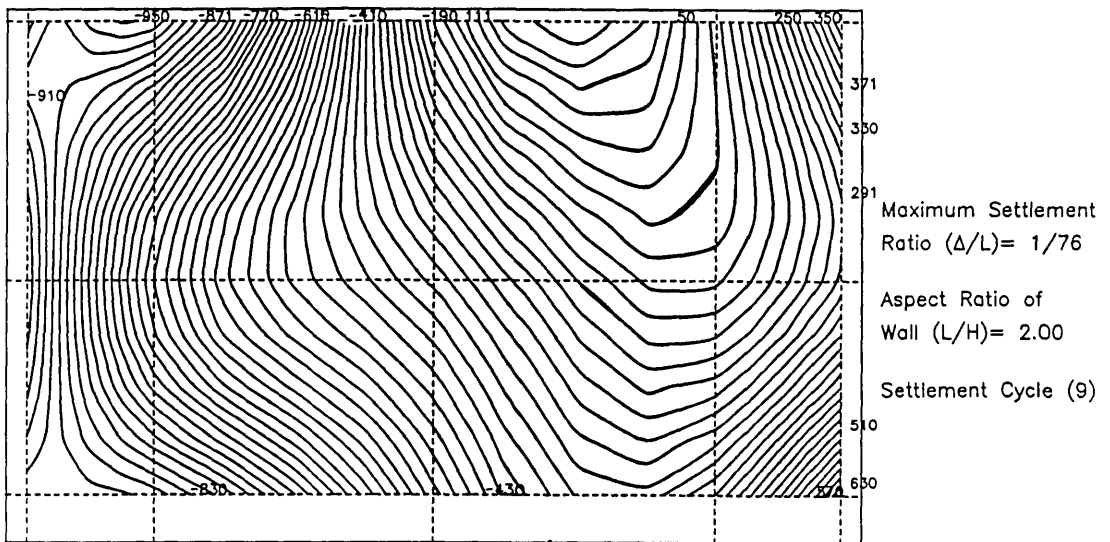
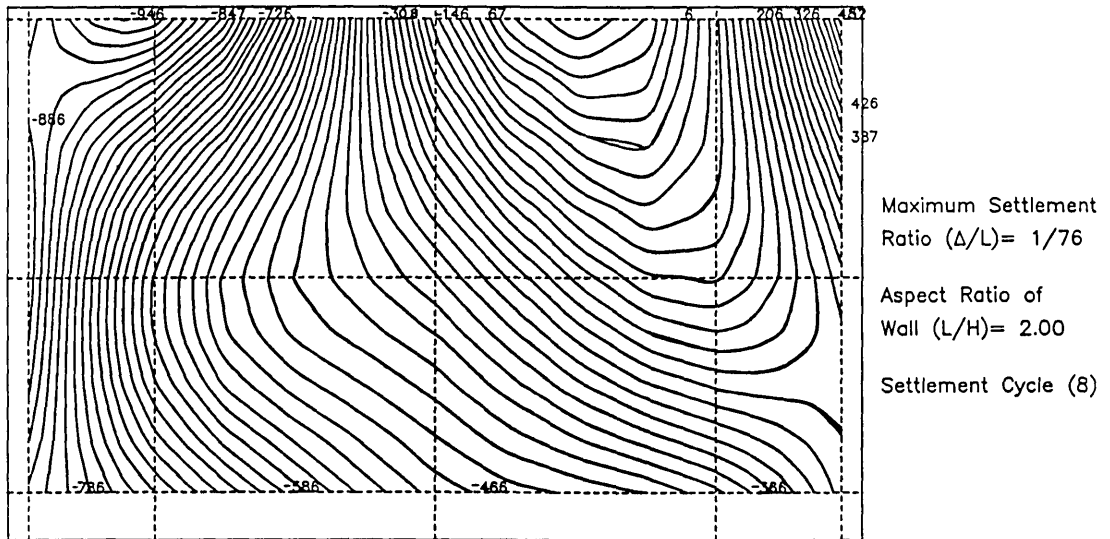
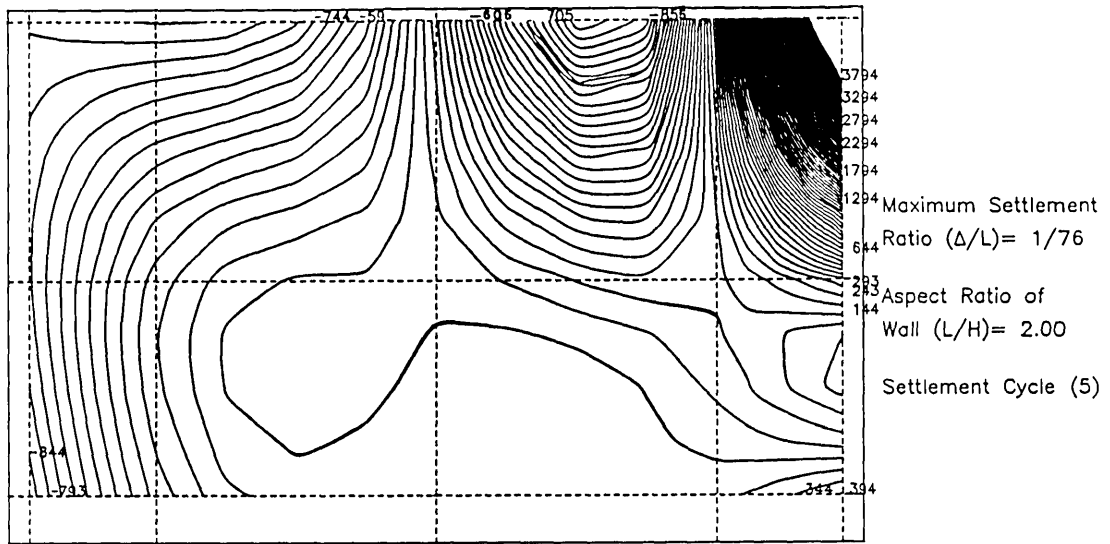


Figure A6.16 Maximum principal strain distribution of wall (Test W2BA).

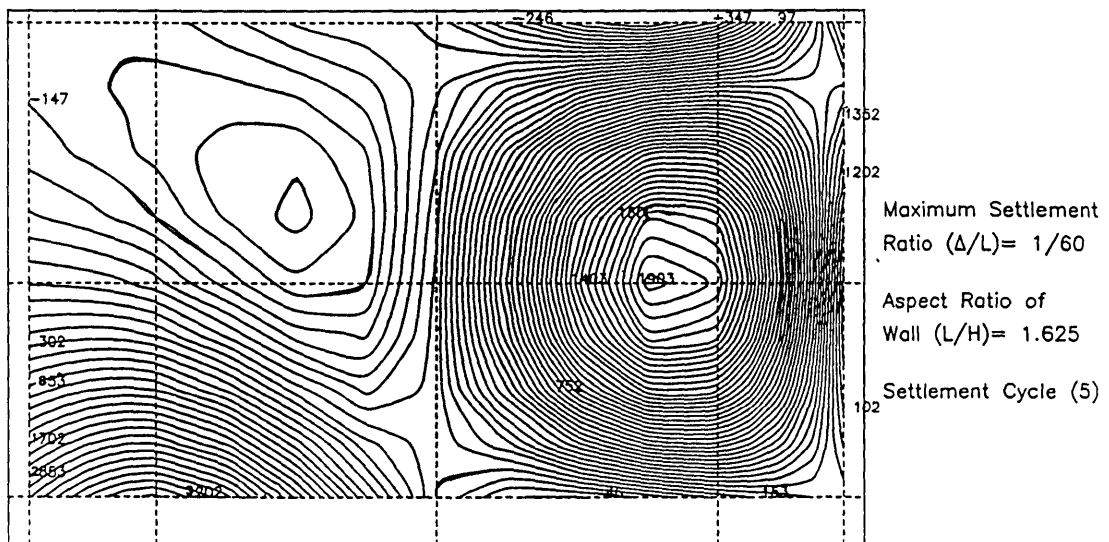
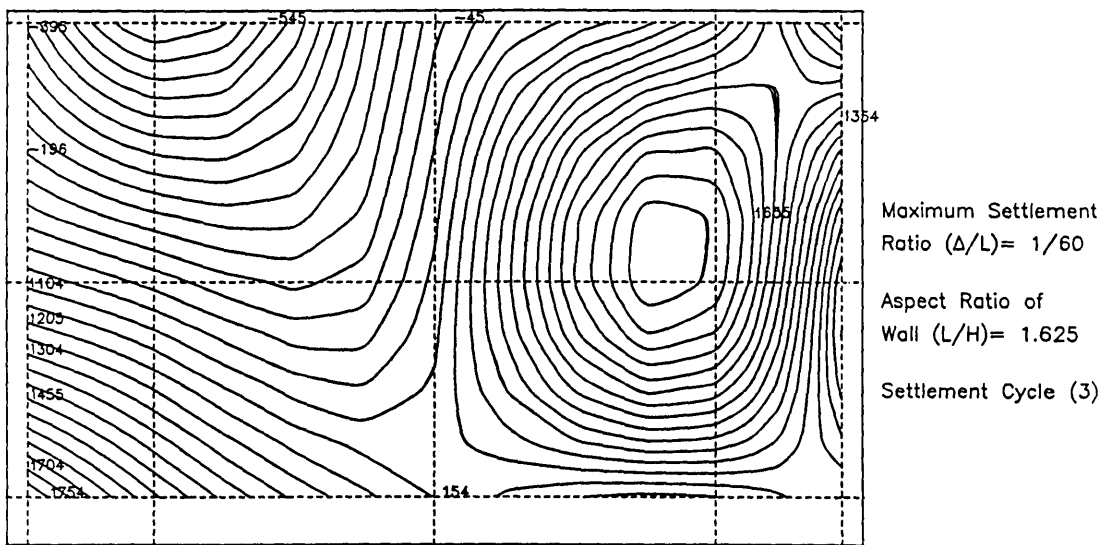
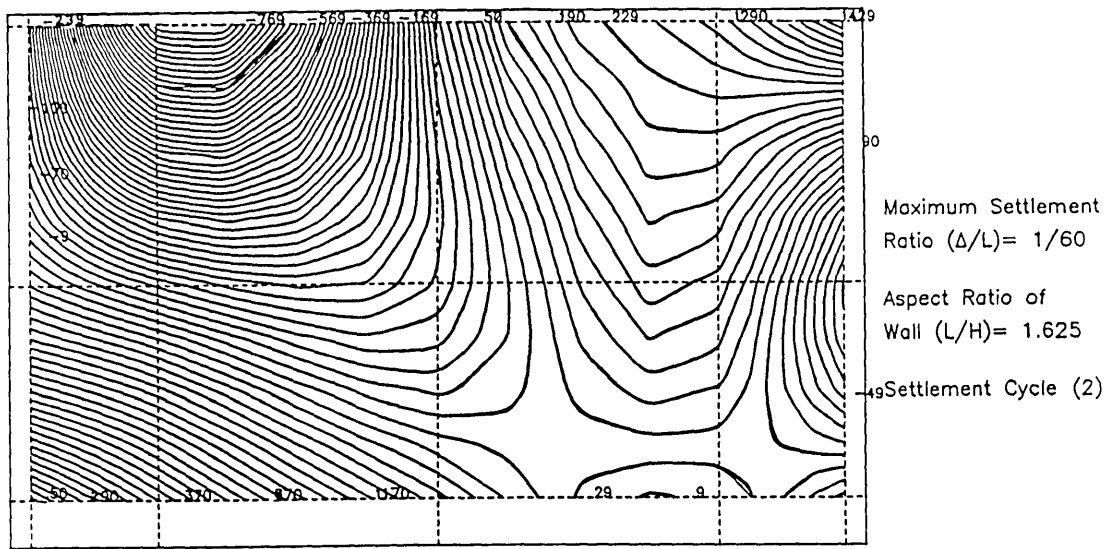


Figure A6.17 Maximum principal strain distribution of wall (Test W3AB).

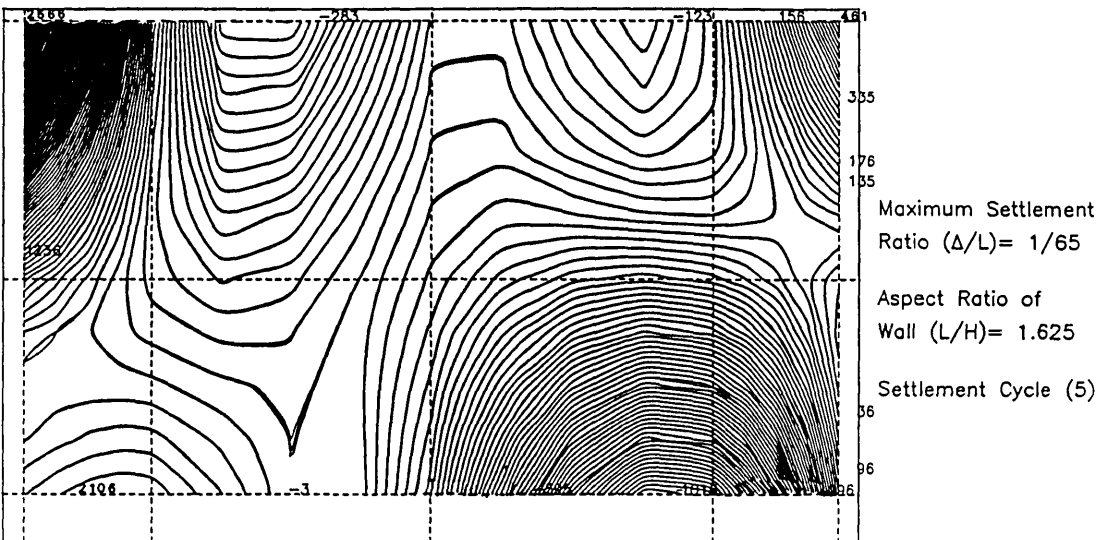
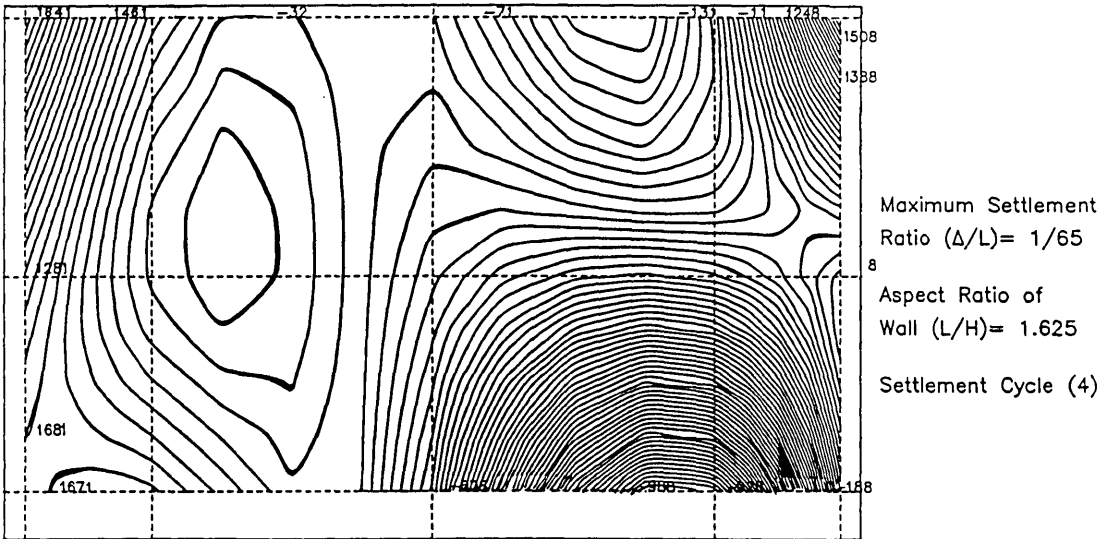
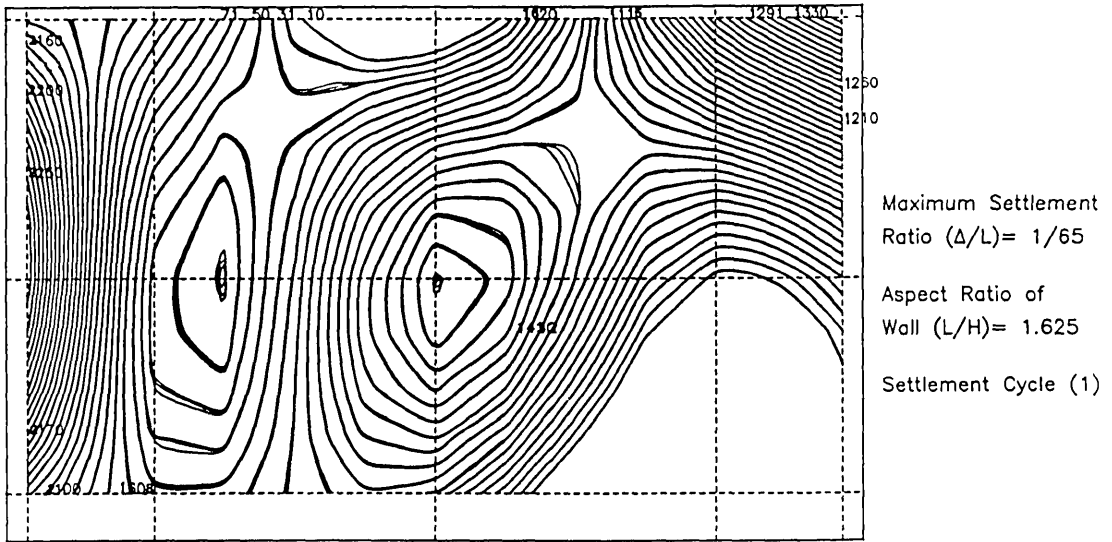


Figure A6.18 Maximum principal strain distribution of wall (Test W3BB).



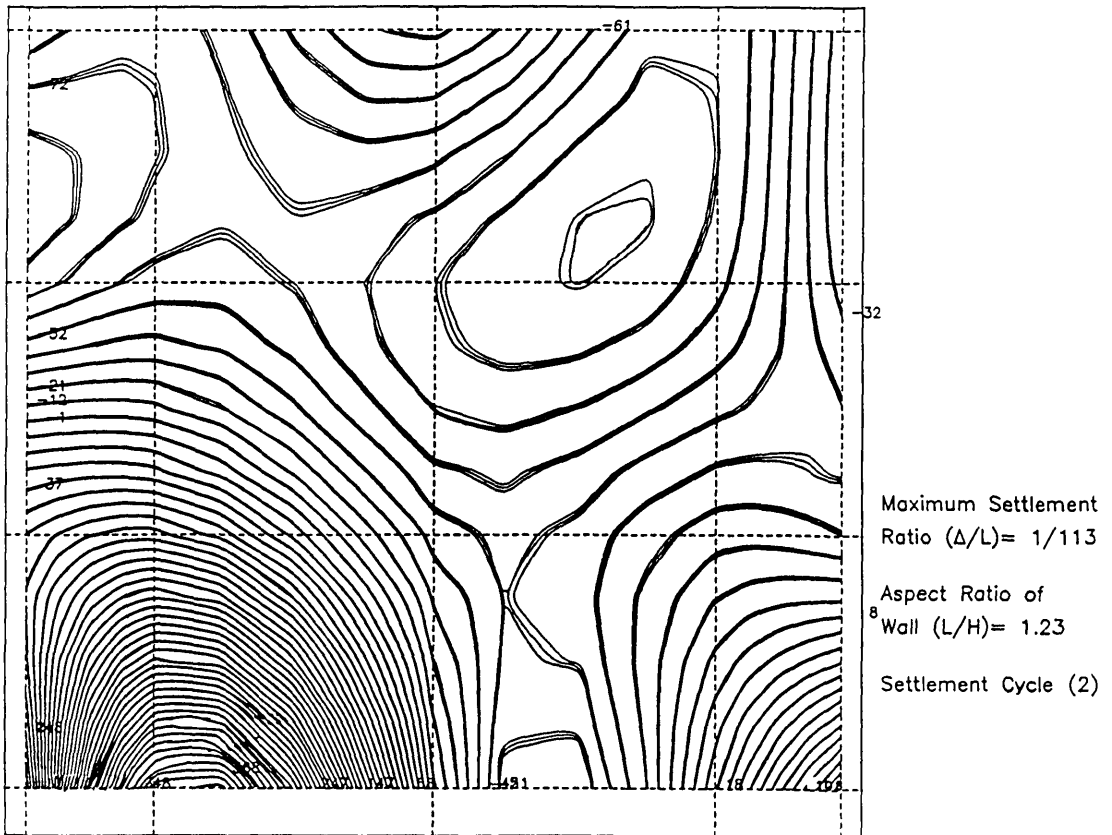
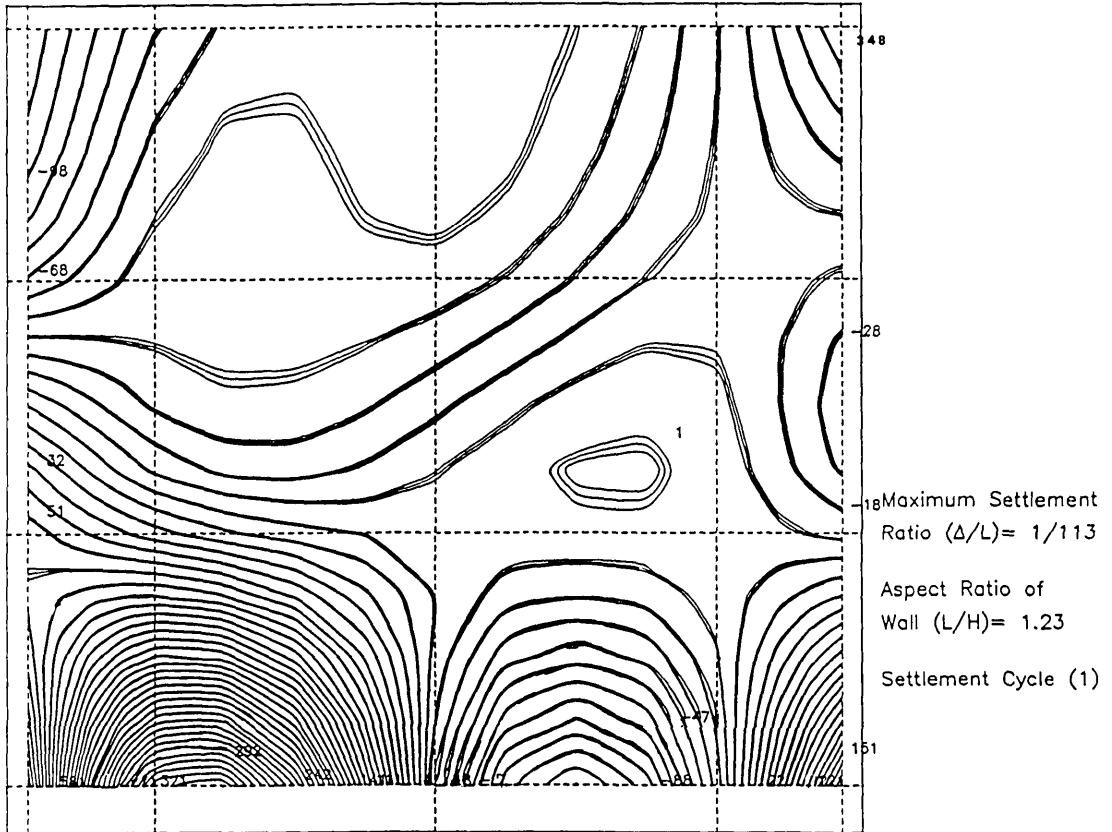


Figure A6.19 Maximum principal strain distribution of wall (Test W4BA).

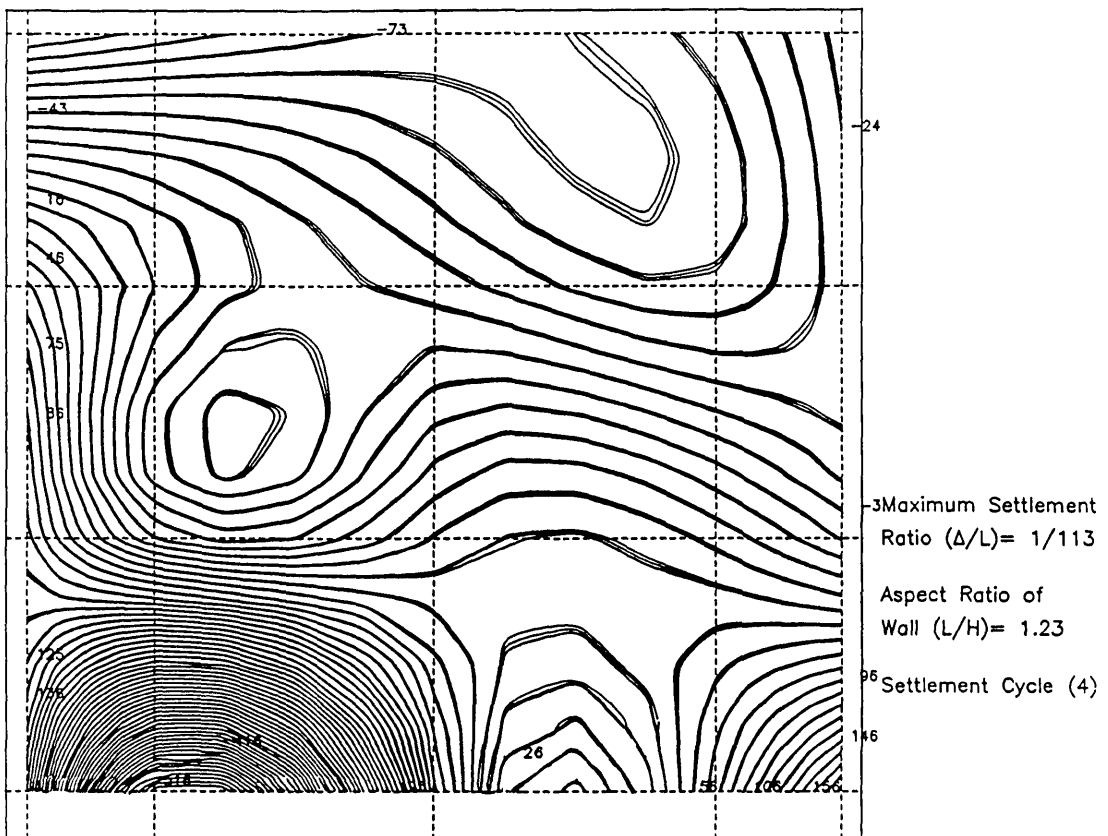
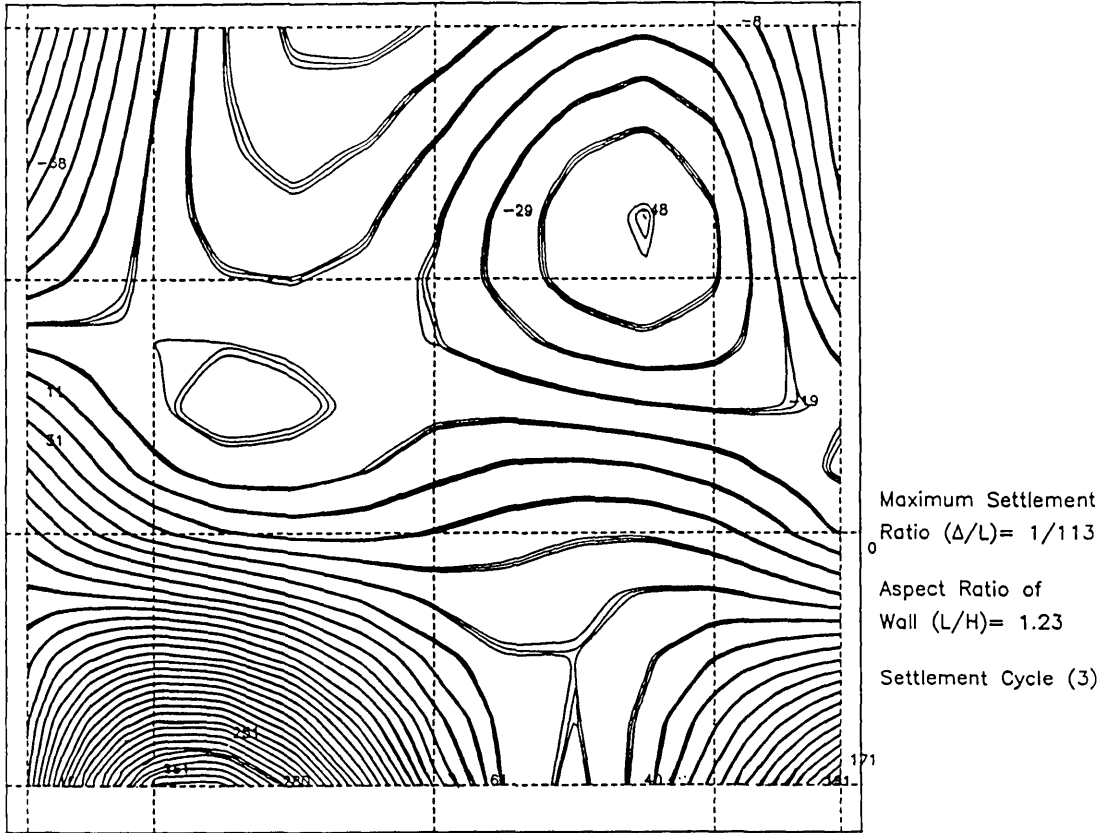


Figure A6.19 Continued.

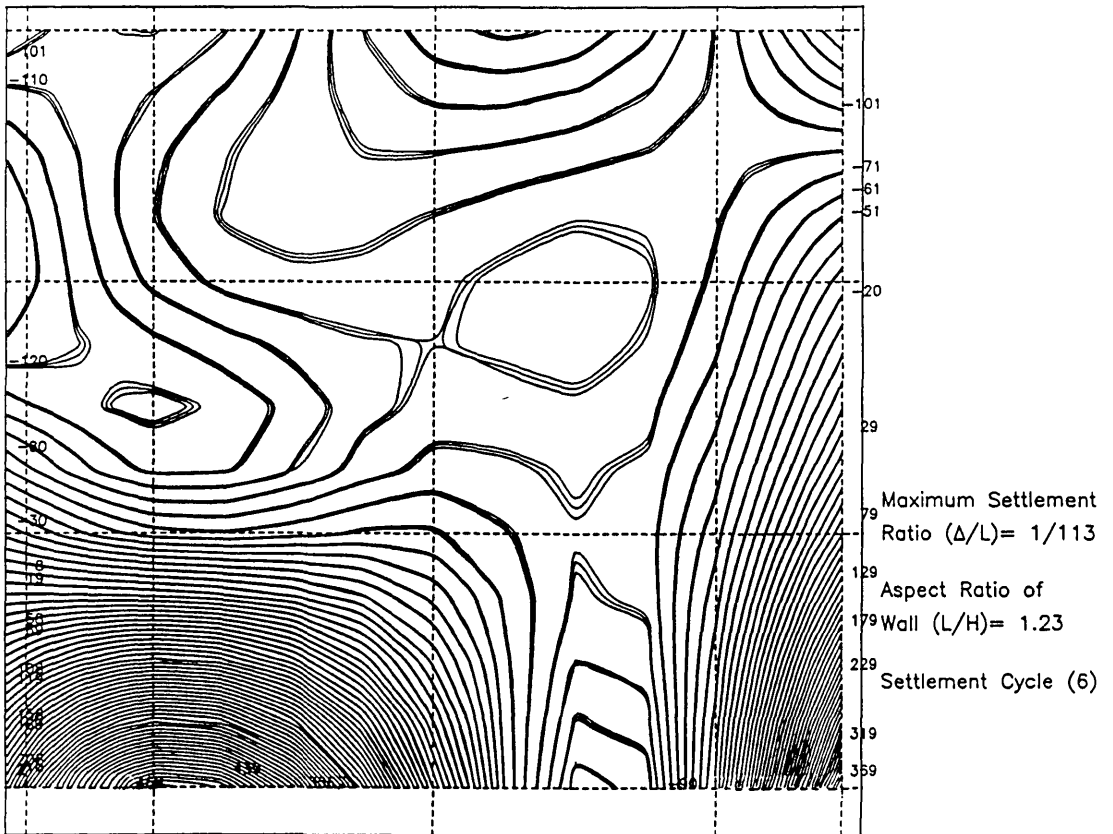
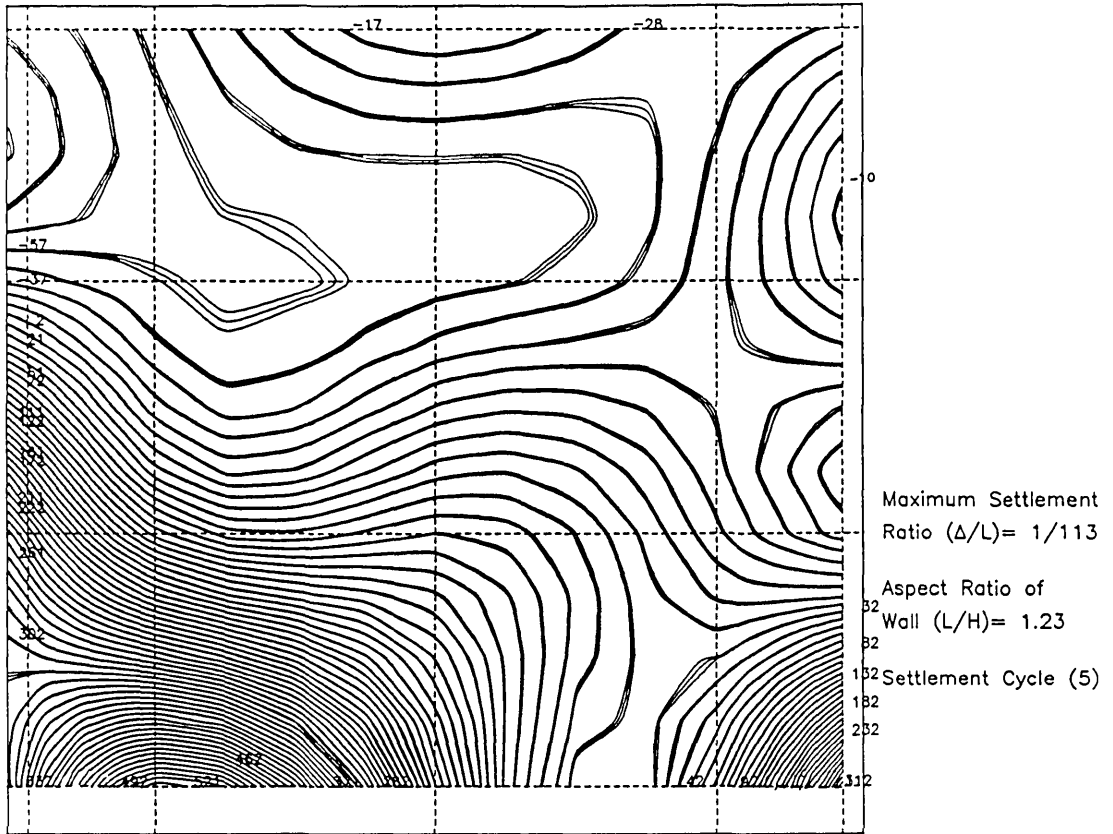


Figure A6.19 Continued.

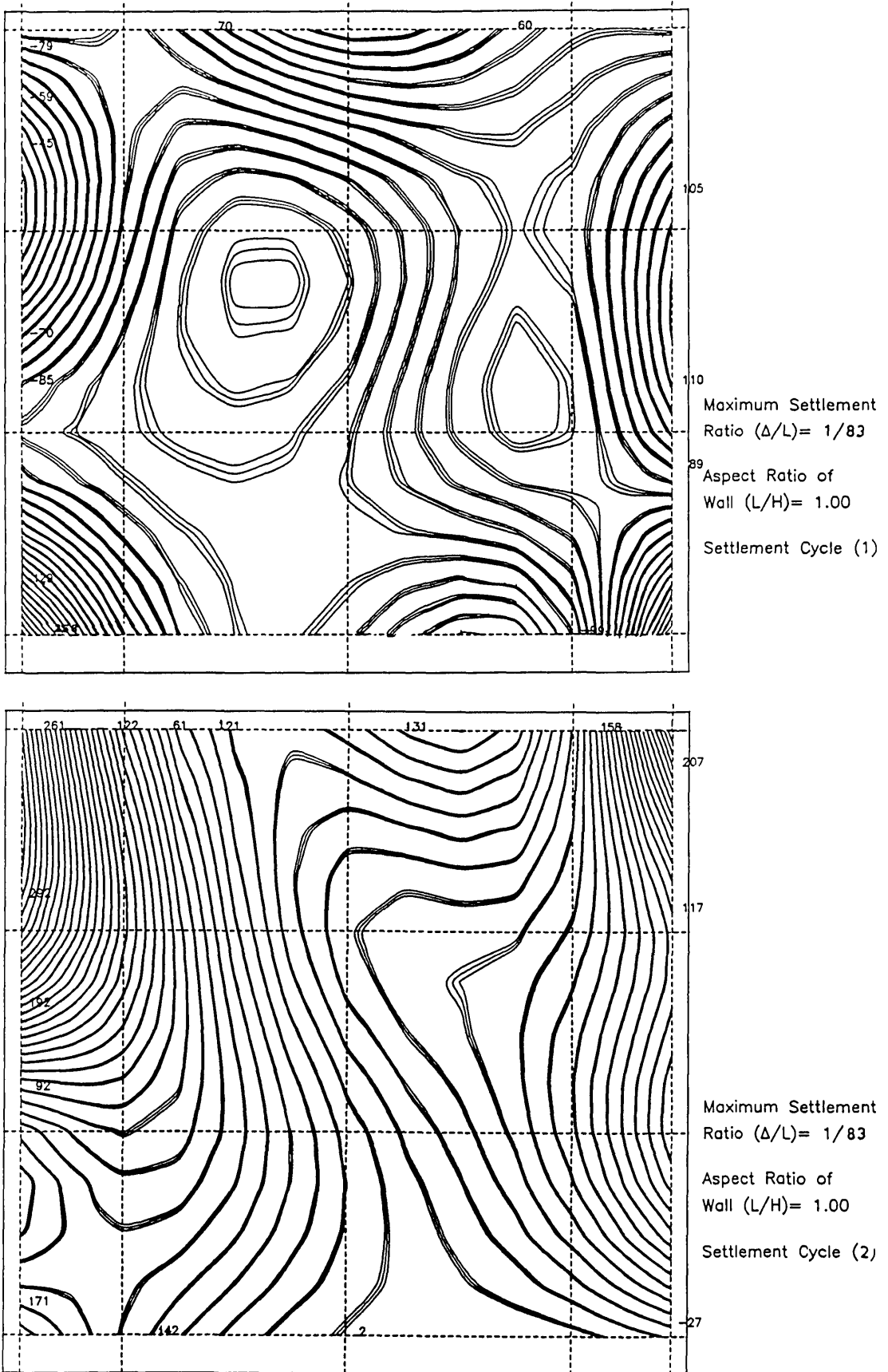


Figure A6.20 Maximum principal strain distribution of wall (Test W5AB).

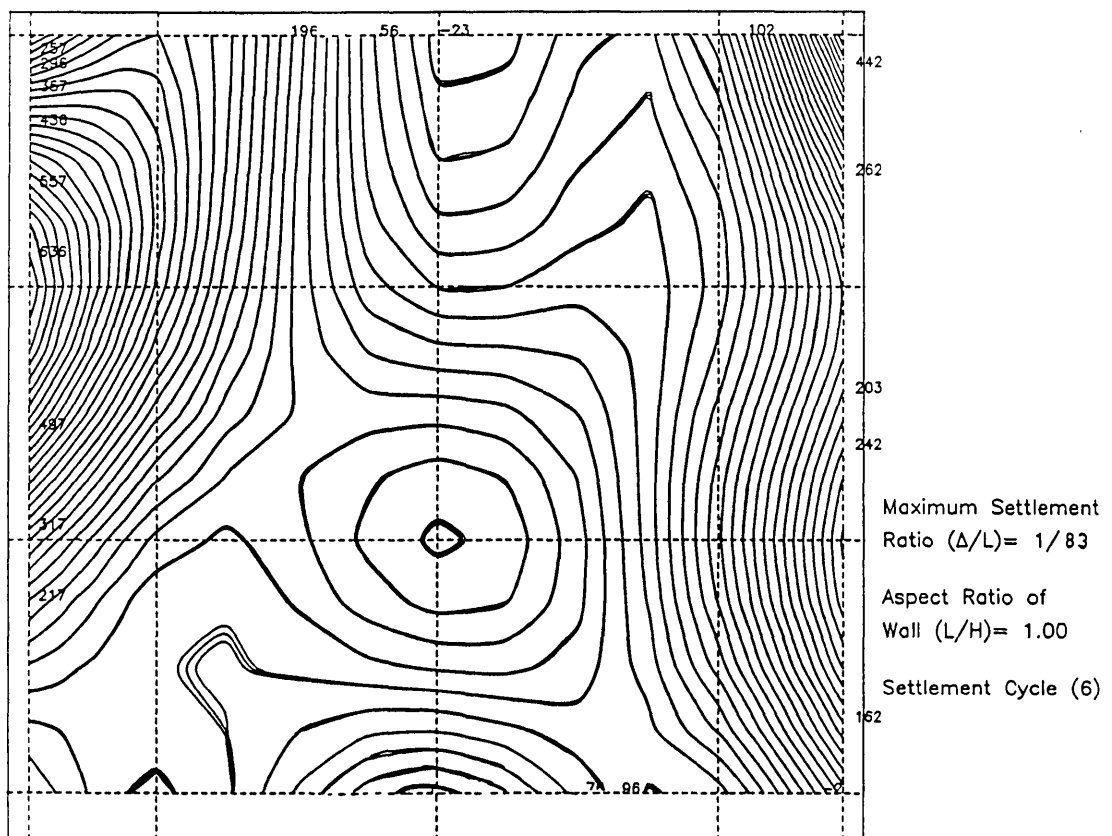
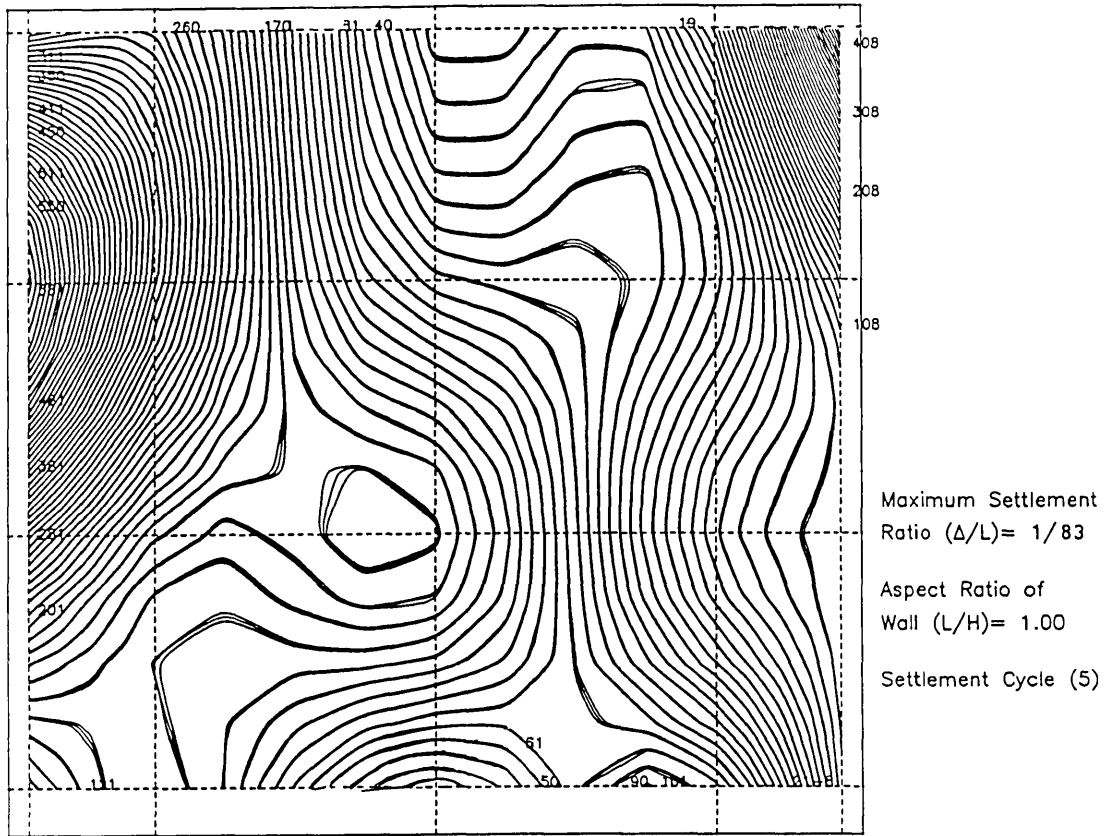


Figure A6.20 Continued.

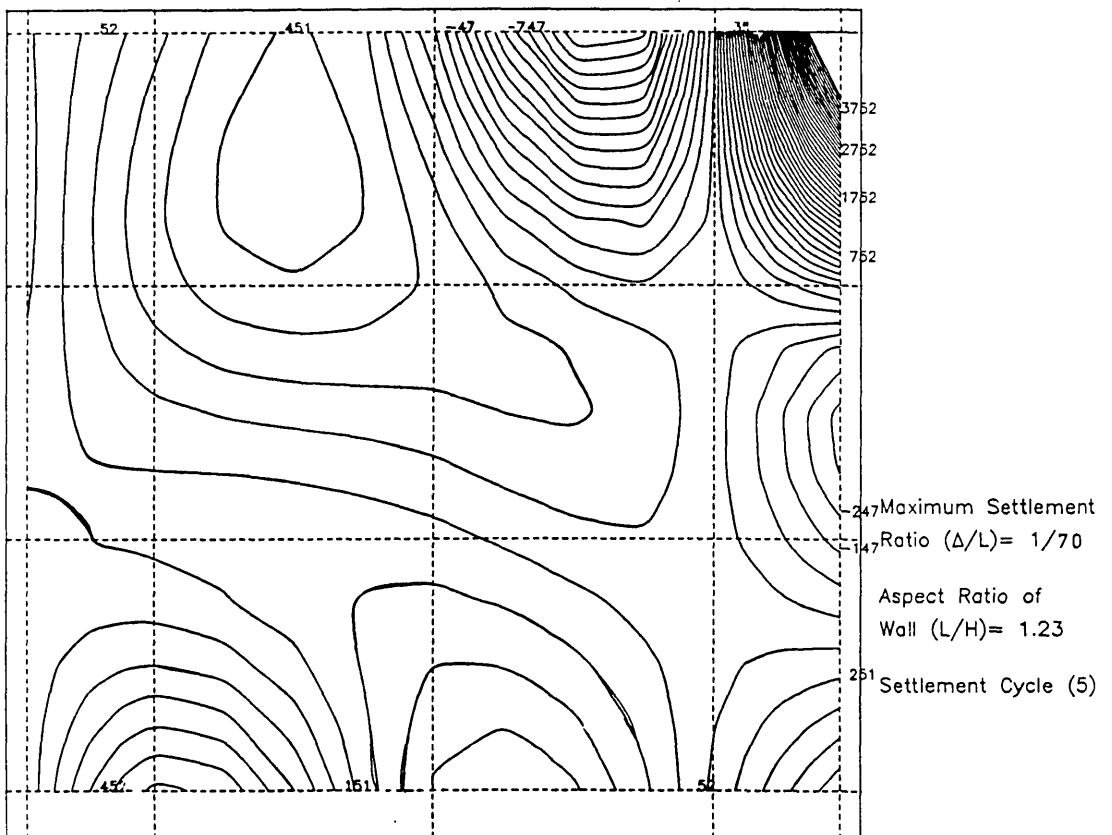
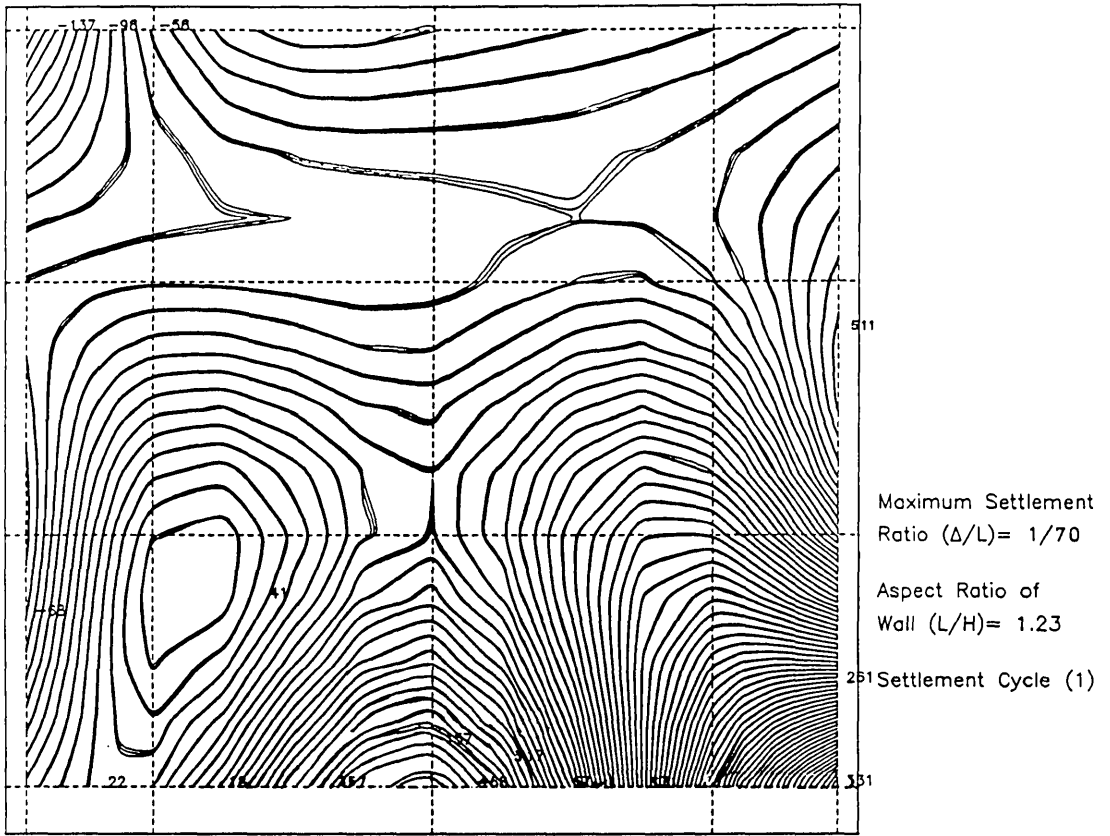


Figure A6.21 Maximum principal strain distribution of wall (Test W5BA).